Atomic Spectra and Oscillator Strengths
for Astrophysics and Fusion Research

Royal Netherlands Academy of Arts and Sciences
P.O. Box 19121, 1000 GC Amsterdam, the Netherlands

Proceedings of the Third International Colloquium.
Amsterdam, 28–31 August 1989

Scientific Committee

J.E. Hansen, Zeeman Laboratory, University of Amsterdam
E. Biémont, Institut d'Astrophysique, Liège
H. Butcher, Kapteyn Astronomical Institute, Roden
L.J. Curtis, University of Toledo, USA
M. Godefroid, Université Libre de Bruxelles
H.F. Henrichs, 'Anton Pannekoek' Institute, University of Amsterdam
A. Hibbert, The Queen's University of Belfast
M. Huber, ESA/ESTEC, Noordwijk
Se. Johansson, University of Lund, Sweden
R. Mewe, SRON-Laboratory for Space Research. Utrecht
R.J. Rutten, Astronomical Institute, Utrecht

ISBN 0 444 85723 0

Koninklijke Nederlandse Akademie van Wetenschappen
Verhandelingen, Afd. Natuurkunde, Eerste Reeks, deel 33

Atomic Spectra and Oscillator Strengths for Astrophysics and Fusion Research

J.E. Hansen, *editor*

North-Holland, Amsterdam/Oxford/New York/Tokyo, 1990

Table of contents

Preface

This volume contains the invited and contributed papers to the Colloquium on Atomic Spectra and Oscillator Strengths for Astrophysics and Fusion, which was held in Amsterdam from August 28 to 31, 1989 as part of the colloquium program of the Royal Netherlands Academy of Arts and Sciences. The colloquium, which was attended by about 70 participants from 12 countries, was the third in a series which was started in Lund, Sweden, 1983 and continued in Toledo, USA, in 1986.

The titles of the lectures reflect the purpose of the meeting: to bring together consumers and producers of atomic data in order to exchange information about what data are most urgently needed and what can be supplied at this point in time. The proceedings includes all the lectures presented at the colloquium as well as extended abstracts of the posters. The astrophysicists were asked to talk about present problems in astrophysics in which atomic data is used or is needed and the atomic physicists about what is known and what can be measured or calculated at the moment and with what precision.

It was clear from the lectures that the astrophysical needs for atomic data at this time, when several new space telescopes and space labs are close to being launched, are very large particularly in the ultraviolet. While considerable advances have been made regarding the computational possibilities for supplying reliable data, it was obvious from the talks that the possibilities for providing the data from so called "traditional analysis of spectra" is rapidly disappearing and several astrophysicists expressed their concern about this development both orally and in their written contributions.

The spirit of cooperation that permeated the colloquium made the organization most rewarding. One small incident during the conference captures something of the atmosphere. During the very witty talk given by Prof. Blackwell, Oxford we were told that the electricity price for one measured gf value in his experiment is about 300 dutch guilders. At this point Prof. Kurucz, Harvard Smithsonian, interrupted and clutching 300 guilders in one hand announced his personal willingness to pay for the next value. It must be hoped that this attitude will spread to the wider community and in particular to the funding agencies before it is too late.

The colloquium was, as mentioned above, part of the colloquium program of the Royal Netherlands Academy of Arts and Sciences. It is a pleasure to thank the Academy for having selected the colloquium for the 1989 program and for the friendly and professional way in which the Academy, in particular in the person of Mrs. A. Muller, helped to run the meeting in the Academy building in Amsterdam.

I am grateful to my colleagues on the Scientific Commitee, especially Se. Johansson, H. Henrichs and R.J. Rutten, for their help and advice in setting up the program, and to the members of the Atomic Physics group at the Zeeman Laboratory for their help with the practical arrangements, in particular to Mrs. I. Brouwer for keeping the paperwork under control, and to Drs. M. Landtman for his help with the collection of the manuscripts.

The colloquium was further sponsored by Control Data Corporation and by the Leids Kerkhoven-Bosscha Fonds and their support is gratefully acknowledged. I would like to thank Mrs. R. Zeippen and Mrs. J. Seaton for adding to the appearance of the proceedings by putting their private sketches from the conference and from Amsterdam at my disposal.

Jørgen E. Hansen
Amsterdam, June 1990


ANNO
1722
Herengracht/Leidsegracht

Astrophysics and atomic data

David S. Leckrone, Sveneric Johansson,
Robert L. Kurucz and Saul J. Adelman

High resolution ultraviolet spectroscopy from space observatories – what atomic physics and astrophysics can do for each other

ABSTRACT

Stellar spectra obtained with the IUE satellite demonstrate the complexity and richness in information of the 1150 -3300 A region. Ultraviolet astrophysical spectroscopy will reach a new plateau of resolution and precision with the launch of the Hubble Space Telescope in 1990. The atomic data base required for the accurate analysis of IUE and HST data lags well behind our observational capabilities in completeness and quality. We describe a project to assess the currently available atomic data, particularly for the lower ionization states of the iron-group and lighter elements. We illustrate the capabilities of the HST/GHRS instrument, and provide examples of transitions of special interest for early HST research.

INTRODUCTION

The sharp-lined, ultraviolet, photospheric absorption spectra of slowly rotating early-type stars contain a wealth of astrophysical information about the cosmic abundances of the elements and about physical processes occurring in the stellar surface layers. The effective temperature range 8500 K to about 20000 K encompasses young, normal A and B-type stars, a variety of chemically peculiar stars, and several types of very old, highly evolved stars. High resolution spectroscopy of these objects in the 1100 to 3000 A range provides access to lines of many atomic species not well represented in ground-based, optical spectra and to intrinsically strong resonance and low excitation lines which are often less susceptible to non-LTE effects than are their more highly excited congeners, observed at optical and near-infrared wavelengths. These spectra are also a rich "laboratory" for the study of atomic spectra, particularly those of the first few ionization states of the iron group and lighter elements. The density of lines of observable strength is great (up to tens of lines per Angstrom) for reasons that are described by Johansson (1984). This creates both opportunities and problems: opportunities to obtain substantial new information about the atomic structure of many species, and problems in obtaining quantitatively accurate astrophysical information from the spectra, because of serious line blending and difficulties in locating the line-free continuum. Thus, ultraviolet spectrum synthesis is hindered by the compounding of three sources of uncertainty related to atomic data: 1. uncertainty in the wavelengths, oscillator strengths and broadening parameters of the primary lines being analysed; 2. uncertainty in the identity and atomic parameters of the lines with which the primary lines are blended; and 3. uncertainty in the position of the reference level relative to which absorption line strengths are measured, the continuum.

Fortunately, the massive, semi-empirical atomic data bases calculated originally by Kurucz and Peytremann (1975) and Kurucz (1981) have provided a rational starting point from which to attack these problems, converting UV spectrum synthesis from the hopeless to the very difficult. Over the past four years Kurucz has recomputed predicted energy levels, wavelengths, oscillator strengths and broadening parameters for the first nine ionization states of elements z = 20 to 28. His preliminary new data base for the first four ions of these elements, of greatest relevance here, now contains data for about 25 million predicted lines. However, only those lines involving transitions to experimentally determined levels have sufficiently accurate wavelengths to be used in spectrum synthesis. This limits the currently applicable data set to about half a million lines. The on-going term analysis of iron-group spectra by Johansson and others, based on laboratory observations, is the critical process which allows the conversion of lines from the predicted category to the "good" (i.e. accurate) category.

Good quality co-added stellar spectra obtained with the International Ultraviolet Explorer satellite at moderate resolution and signal-to-noise ($\lambda/\delta\lambda$ = 12000, S/N = 50,

Leckrone and Adelman, 1989) provide the opportunity to begin to assess the completeness and accuracy of the available atomic data base applicable to the ultraviolet. We report here the initial results of a detailed examination we have undertaken of the spectral content of the normal, A1 V star, omicron Pegasi (o Peg), in five test intervals within 1700 - 1900 A. We compare the IUE observations, line-by-line, with synthetic spectra, calculated using the new Kurucz data base, supplemented with data for the lighter elements from Kurucz and Peytremann and other sources. The match is good enough to indicate that we are on the right track, both observationally and computationally. Each specific discrepancy is then assessed in terms of the accuracy of energy levels and transition probabilities of the theoretically calculated lines, in terms of what is known from laboratory spectra, and in terms of phenomena of atomic physics, such as configuration interactions, which are difficult to predict theoretically.

With the launch of the Hubble Space Telescope (HST) and its Goddard High Resolution Spectrograph (GHRS) next year, UV astrophysical spectroscopy will undergo a quantum jump in precision and resolution ($\lambda/\delta\lambda$ = 25000 to 90000; S/N up to 400 at the lower resolution and up to 80 at the higher). We illustrate in this paper the potential of the GHRS with examples of simulated stellar spectra at this resolution. Currently the state of the atomic data needed to quantitatively analyse GHRS (and IUE) data is lagging well behind our observational capabilities. We face the bleak prospect of attempting to analyse spectra of 1% precision, obtained at great expense, with atomic parameters that can be inaccurate by factors of 2 or 10, if they exist at all. The GHRS will be relentless in highlighting this problem. Two general types of activity are needed: continued development of the very large atomic data bases needed to accurately treat UV line blending and to synthesize wide spectral intervals for continuum placement; and determination of accurate wavelengths, oscillator strengths and broadening parameters for individual UV lines critical to specific astrophysical problems, examples of which are given here. In turn, atomic physics will reap a substantial benefit in terms of the feedback of information about the atomic structure of many species, including those difficult to observe in the laboratory.

ANALYSIS OF TEST INTERVALS IN o PEG SPECTRUM

We have selected five wavelength intervals 12 to 15 A wide for a detailed comparison between IUE observations and synthetic spectra calculated with the new Kurucz iron-group data base. These are listed in table 1. The "quality" designations A through D are very rough indicators of our expectations prior to the study about the completeness and quality of the atomic data within each interval. Currently, we have

Table 1. Test intervals for evaluation of quality and completeness of atomic data base

Wavelength (A)	Quality
1857 - 1872	B
1838 - 1851	A
1751 - 1765	D
1740 - 1752	C
1728 - 1741	C

completed the initial calculations and evaluations with respect to atomic physics for each interval. We have also iterated the calculations once to determine the effect of modifications made, on the basis of these evaluations, to log gf values and wavelengths and the effect of the addition of "new" lines omitted from the initial calculations. This work is still very much in progress, and several additional iterations of the calculations will be necessary before we are satisfied that all possibilities to improve the fit, based on current knowledge, have been exhausted. At that point, the remaining discrepancies between observations and calculations should give an indication of the work remaining to be done on the atomic data base in this wavelength region. Note that the calculations utilize a line-blanketed, LTE model atmosphere, abundances, and microturbulent velocity derived by Adelman (1988) in a very thorough ground-based study of this star. For elements for which the optical region abundances are poorly known, we adopt solar abundances. Some of the discrepancies we find in this comparative study may reflect errors in the assumed abundances, which will later be resolved by abundance work in the UV. In such cases, however, we would expect to find systematic discrepancies in many lines of the same element.

In the following discussion, we illustrate in detail the initial evaluation of one test interval, 1740 - 1752, and present selected results from several others. Figure 1 shows the observed spectrum and figure 2 the initial theoretical calculation, unaffected by instrumental broadening or by the broadening of lines due to the star's rotation. In figure 3 the theoretical spectrum has been broadened to the instrumental resolution of 0.15 A and to a projected stellar rotational velocity of 9 km s^{-1}. The latter is then superposed on the observed spectrum in figure 4. The N I and

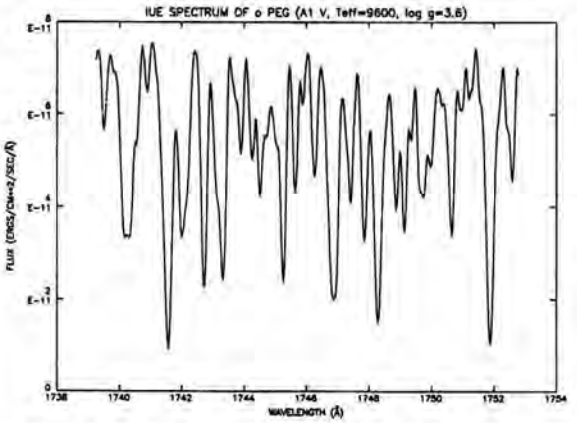

Fig. 1. IUE spectrum of o Peg, obtained by co-addition of nine large-aperture images.

C I lines labeled in figure 3 illustrate lines of particular astrophysical interest, which appear to be reasonably "clean" in the observations. (The N abundance has been adjusted to achieve a good fit, as part of another study, and in fact is about 0.5 dex below solar in these illustrations).

Inspection of figure 4 immediately shows a reasonably good match between calculation and observation for some absorption features, but also numerous examples of missing opacity and discrepant line strengths. The line-by-line investigation of each disparity between observation and calculation revealed three general classes of problems in all the test intervals: missing lines; apparent

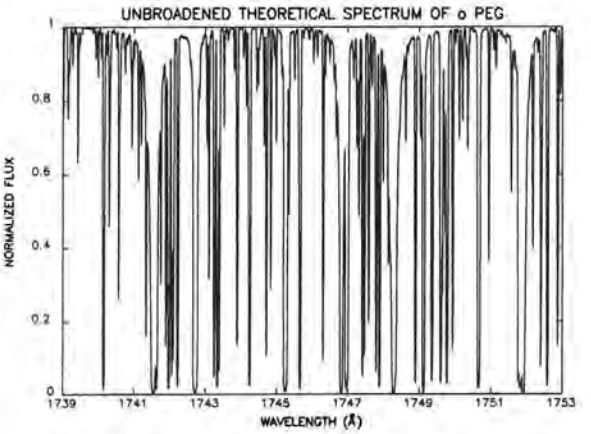

Fig. 2. Theoretical spectrum for o Peg, calculated with new Kurucz atomic data.

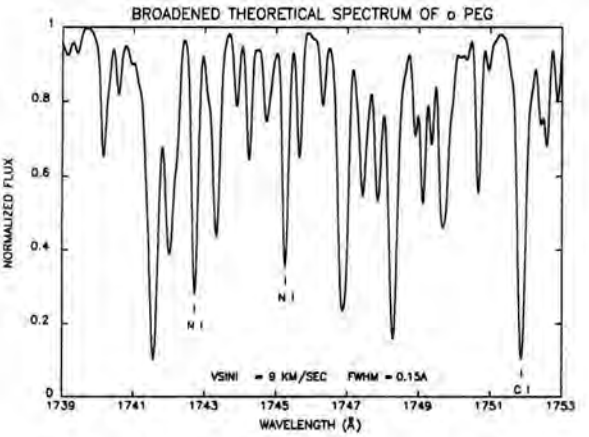

Fig. 3. Theoretical spectrum of figure 2, convolved with instrumental broadening and stellar rotational broadening functions.

discrepancies in the Kurucz oscillator strengths or wavelengths with respect to line strengths or wavelengths observed in laboratory data; and some very interesting examples of the effects of level mixing.

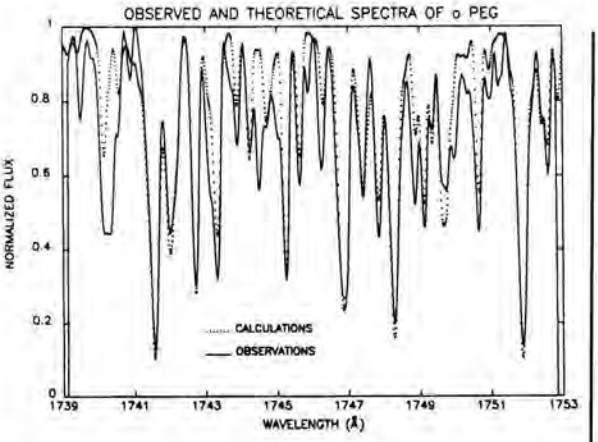

Fig. 4. Observed spectrum normalized to the estimated position of the line-free continuum and superposed on the theoretical spectrum of figure 3.

Lines Missing From The Atomic Data Base

Figure 5 shows a 4 A subsection of a test interval with the positions marked of 15 lines which did not appear in the original set of "good" Kurucz lines and were, therefore not contained in the original calculation. Those labeled "new FeII" are lines found in the set of predicted Kurucz lines, arising in transitions to upper levels which Johansson has recently identified from experimental term analysis. Their wavelengths are now known with good accuracy and Kurucz has already calculated their oscillator strengths and damping parameters, so that they could be included in the first iteration of the spectrum synthesis, labeled "revised calculation" in figure 5. Lines labeled "new FeI" have also been identified in laboratory spectra and their lower level excitation potentials are known. However, we can only estimate their log gf values by similarity to other FeI lines of similar strength. Those rough estimates will be refined in subsequent iterations. The numerous lines labeled "unk" (an abbreviation of "unknown") in figure 5 are known to exist in laboratory spectra of the denoted element, although the ionization state is not always known with certainty. Since their excitation potentials and oscillator strengths are presently not known, they could not be included in the revised calculation. It is encouraging that these "unk" lines correspond in several cases to positions where line opacity is clearly missing from the calculations, suggesting possible identifications for the missing lines. It is also gratifying that several of the "new" lines added to the calculation clearly improved the match to the observations.

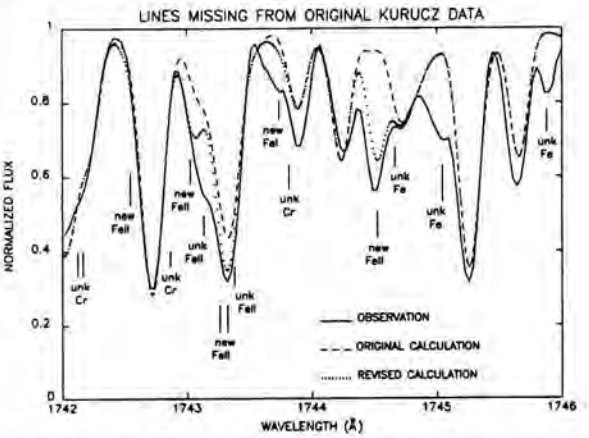

Fig. 5. Examples of lines seen in laboratory spectra which were not included in the original calculation.

"Discrepancies" In The Atomic Data Base

A segment of the 1858 - 1870 test interval shown in figure 6 illustrates the situation where there are apparent disagreements between the relative strengths of lines of similar excitation seen in laboratory spectra and the relative strengths one would infer from Kurucz's log gf values. For example, two FeI lines at 1863.548 and 1865.309 A (labeled "stronger in lab." in figure 6) have calculated log gf's -3.11 and -3.71, respectively. These lines, arising from 0.00 eV, are seen in absorption in laboratory spectra with a strength comparable to other FeI lines for which Kurucz has calculated larger log gf's. Our initial estimate was that log gf for 1863.548 should be in the range -1.5 to -2, while that for 1865.309 should be near -1.0 to -1.5. In both cases the substitution of log gf's in our revised calculation resulted in lines that are stronger than observed in the stellar spectrum. Further iterations will allow us to test how "discrepant" the Kurucz log gf's might be. One expects the calculated log gf's for FeI to have rather large uncertainties because of its complex atomic structure, which has many interacting series converging towards the lowest limit. The majority of FeI lines below 2000 A are unclassified, and the levels from which they arise are unknown.

Thus, stellar and laboratory absorption spectra should, in principle, be especially useful in establishing the relative strengths of FeI lines in the far UV.

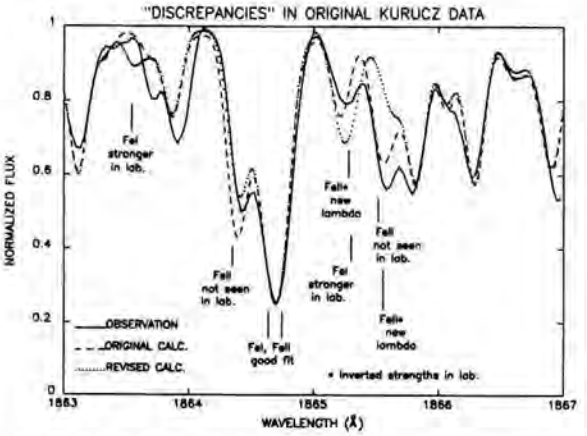

Fig. 6. Examples of apparent "discrepancies" between the Kurucz atomic data base and laboratory data.

Two FeII lines, at 1864.357 and 1865.530 A, are not seen in laboratory spectra, although with the excitation potentials and log gf's given by Kurucz (E.P. = 2.34 and 2.28 eV; log gf = -3.25 and -2.75, respectively) they are calculated to be moderately strong lines in o Peg. The 1864.357 A line is observed to be weaker than calculated in the stellar spectrum (figure 6). Eliminating the line entirely from the synthetic spectrum, as illustrated in the revised calculation, is clearly going too far. A more accurate log gf for this line should be obtainable from further iterations of the spectrum synthesis. Such a refinement of log gf may not be possible for the 1865.530 A line, since it is unresolved in these observations from another FeII line, 1865.545 A, which also has a serious problem, discussed below.

Two FeII lines, at 1865.212 and 1865.545 A, arise from the same upper level and have wavelengths given by Kurucz (1865.221 and 1865.554 A, respectively) that we have revised slightly due to a small revision in the experimental level value. More significantly, in the laboratory data 1865.545 is stronger than 1865.212. The reverse is true in Kurucz's log gf's (-0.65 for 1865.212, -1.83 for 1865.545). We have not attempted to modify the log gf's in the revised calculation in figure 6. The discrepancies in these log gf's, together with unresolved blending with the other problematical lines discussed previously, results in the poor fit to the observed profiles of these lines illustrated. It will require the resolution of the HST/GHRS to disentangle the blended lines and to obtain further astrophysical information about their relative strengths.

To conclude this discussion of examples of "discrepancies" in the Kurucz atomic data base, we note that the observed feature at 1864.70 A, a blend of two FeII lines and one FeI line, is already rather well fit by the original calculations, using the Kurucz data as given. Clearly, the Cowan (1968) code used by Kurucz is capable of providing accurate data, limited primarily by the quality of the input energy level information and by the knowledge of configuration interactions.

Problems of atomic physics

The most remarkable spectral interval that we have investigated is illustrated in the sequence of figures 7 through 9. There are two (and perhaps three) different examples of interesting phenomena of atomic physics affecting the spectrum synthesis here. Figure 7 illustrates the initial calculation. We note that, from 1857 to 1869 A, the computational match to the observations is as good as, or better than, that in any other of the test intervals, with occasional

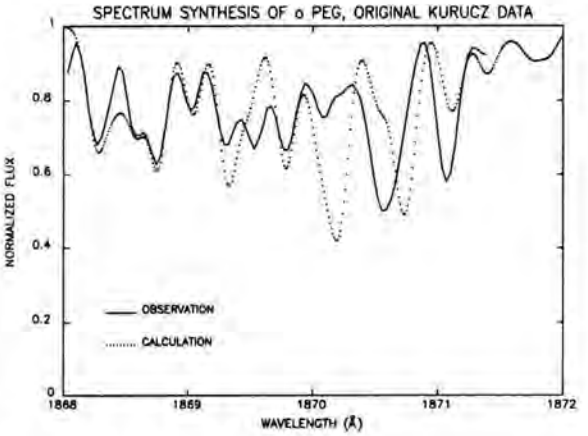

Fig. 7. Initial calculation for a portion of the 1857 - 1872 A test interval.

instances of missing line opacity and other discrepancies as discussed previously. But

from about 1869.1 to about 1871.2 A the quality of the spectrum synthesis becomes especially bad. In iterating the calculation, we first introduced "new" FeI lines at 1869.260 and 1870.352 A, with roughly estimated log gf's, based on relative laboratory intensities. Four "new" FeII lines were added at 1869.553, 1870.534, 1871.004 and 1871.056 A. Only the first of these has a known Kurucz log gf. Classification of the other three FeII lines is not complete, and estimated log gf's were also adopted for them. These lines are labeled in figure 8. Also shown are the positions of four SiII lines, belonging to multiplet UV 9.02, the lower, $3s3p^2\ ^2D$, term of which is known to strongly interact with $3s^23d\ ^2D$ (Froese Fischer, 1968; Artru, et al., 1981). Since Kurucz and Peytremann did not include this configuration interaction in their calculations, their log gf's for these SiII lines are in error by about 2 dex (Lanz and Artru, 1985). Therefore, we substituted the SiII log gf's from Artru, et al., in the revised calculation shown in figure 8.

The quality of the fit between observation and calculation in figure 8 is somewhat better than in figure 7. However, several serious discrepancies remain. Of particular interest is the observed feature at 1870.6 A. In addition to the "new" FeII line,

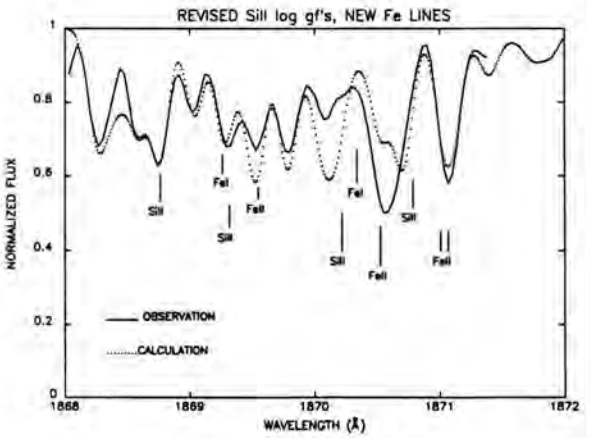

Fig. 8. Spectrum synthesis including "new" Fe lines and SiII log gf's which take account of configuration interactions.

1870.534 A, mentioned previously, two other FeII lines found in the Kurucz data base contribute to this feature - 1870.607 A (b^2P - x^6P) and 1870.697 A (b^2P - w^2P). In the 1950's Edlen found that the accidental coincidence of these two upper levels, separated by 2.4 cm^{-1}, results in a strong mixing between them, even though they are otherwise completely unrelated (Johansson, 1984). If we assume a 50-50 mixture, then the original Kurucz log gf's, -6.50 and -1.76, respectively, become -2.10 for both lines. Substituting this value into the calculation results in the synthetic profile plotted in figure 9. Clearly, the qualitative shape of the calculated profile now more closely resembles the observed profile than in figures 7 and 8. Further adjustments to the total gf-value for the combined transitions, 1870.607 and 1870.697, as well as adjustments to the originally estimated log gf for the "new" FeII line at 1870.534 A might yield an acceptable match to both the shape and strength of the observed feature. However, the preferred course is to attempt to resolve these components with the HST/GHRS.

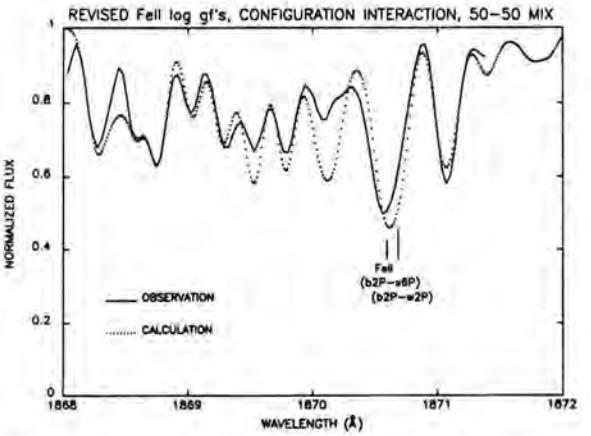

Fig. 9. Spectrum synthesis accounting for mixing due to accidental coincidence of FeII upper levels.

In general, theoretical calculations are not sufficiently accurate to reliably predict mixing due to the accidental coincidence of levels. Laboratory and astrophysical data are essential in finding and evaluating short-range effects of this kind in complex spectra.

One remaining concern about the spectrum synthesis shown in figure 9 is the grossly excessive absorption predicted at 1870.1 A. A major contributor to the feature is FeII 1870.169 A, about which there is a mystery. This line, which in LS coupling should be one

of the strongest members of its multiplet, 4s a^4D-4p y^4F, does not appear at this wavelength in laboratory spectra, but rather another component of the same multiplet, predicted by Kurucz to have a log gf value two orders of magnitude less. From both the calculated log gf's and the relative laboratory intensities for all the lines in the multiplet, we know that LS relative intensities do not apply. Moreover, the agreement between relative calculated log gf's and relative laboratory strengths for many of the lines in the multiplet is not good. Johansson notes that several lines in the multiplet, though not 1870.169, have different log gf's in the new Kurucz calculations than in Kurucz (1981), suggesting that new configuration interactions were included in the more recent calculations. But the configuration interactions directly relevant to this multiplet were included in 1981. He speculates that mixing in the theoretical calculations between the ^4F upper term of this multiplet and a higher lying ^4F term of the same parent configuration may result in changes in predicted log gf's for this multiplet, if the higher lying ^4F term is perturbed by newly included configuration interactions. The simple question for atomic theorists is, is this mixing between terms having the same type of LS parent term ($3d^6\,^3F$ in FeIII) correct or not? The next iteration of our calculations will utilise a log gf = -5.5, rather than the value, -3.64, listed at this wavelength by Kurucz.

We conclude the discussion of the assessment of the test intervals, by illustrating in figure 10 the current theoretical fit (after one iteration) to the observations in our "A-quality" interval, 1838 - 1851. Here the qualitative match to the shapes of some obviously complex blends is remarkably good, and there are numerous features which we come close to matching in absolute quantitative terms as well. On the other hand, even in this the best interval, there are still examples of missing line opacity, discrepancies in line strengths and perhaps even anomalies in transition wavelengths. Note for example the good fit to the detailed profile of the complex feature near 1846.7 A, while next to it, at 1846.0 A, is another blend for which the fit is strangely poor. It is clear from this exercise that the information content of these spectra is high, from both an astrophysical and an atomic physics viewpoint. It will be much higher still in the HST/GHRS spectra.

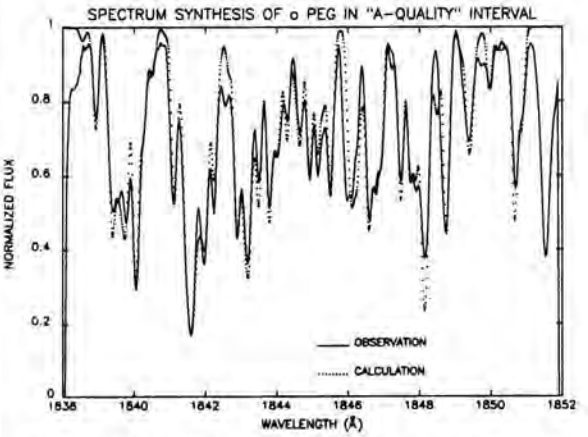

Fig. 10. First iteration of spectrum synthesis of test interval in which atomic data were expected to be relatively complete.

OBSERVATIONAL CAPABILITIES OF THE GHRS

The GHRS, scheduled to be launched on the HST in 1990, will be photometrically superior to the IUE, as well as capable of higher spectral resolution. With its 512-diode digicon detectors, it will provide a highly linear photon counting capability over a very wide dynamic range. Its chief shortcoming will be the time required to cover wide spectral intervals with its one-dimensional detector arrays. In the high resolution mode it will measure wavelength intervals ranging from 5 to 16 A in a single observation. In the IUE observations of o Peg illustrated in this paper, the primary determinant of spectral resolution is the resolving power of the instrument. In GHRS observations of sharp-lined stars, resolution will be limited primarily by the doppler broadening of spectral lines by stellar rotation. For o Peg we have adopted a projected rotational velocity vsini = 9 km s^{-1} (it may actually be a bit lower). Other early-type stars, especially in the chemically peculiar HgMn sequence, have unmeasurably small rotational velocities and will appear exceedingly sharp-lined in GHRS data. Figure 11 shows a five angstrom segment of the theoretical spectrum of o Peg, broadened to the resolution of the IUE. In figure 12 we show the spectrum as it might appear in data obtained with the GHRS, assuming the stellar vsini = 9 km s^{-1}. For a similar star with slower projected rotation

(either because the star is intrinsically slowly rotating or because it is seen pole-on), the spectrum might appear as shown in figure 13. Ambiguities and quantitative inaccuracies in spectrum syntheses, caused by unresolved blending, will at least be improved, if not remedied, by data of this quality. Moreover, one will be able to

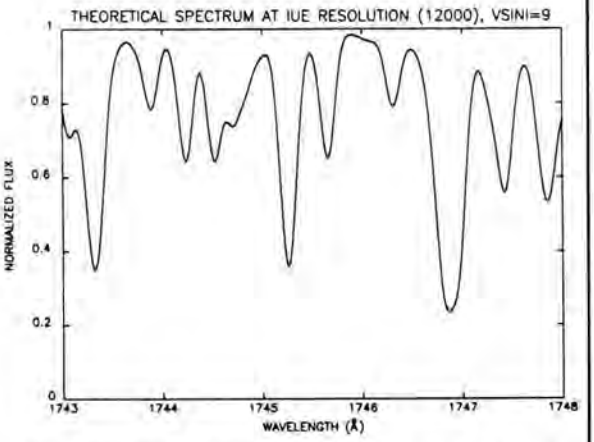

Fig. 11. Calculated o Peg spectrum broadened to the resolution of the IUE.

resolve closely spaced lines, whose relative strengths need to be accurately measured, such as the FeII 1870.607 and 1870.697 A lines discussed previously. Astrophysicists will need atomic data of quality commensurate with the quality of these observations. This

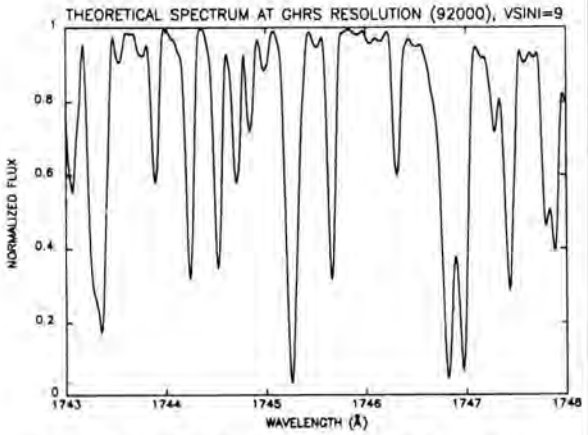

Fig. 12. The same spectrum as in figure 11, broadened to the resolution of the GHRS.

means an atomic data base which is essentially complete with respect to the stronger transitions in the first four ionization states of the more abundant elements, with well determined wavelengths, and log gf values that are accurate to at least 0.1 dex. The process of creating such a data base, however, will be an interactive one, involving direct working relationships among experimental and theoretical atomic physicists and spectroscopic astrophysicists.

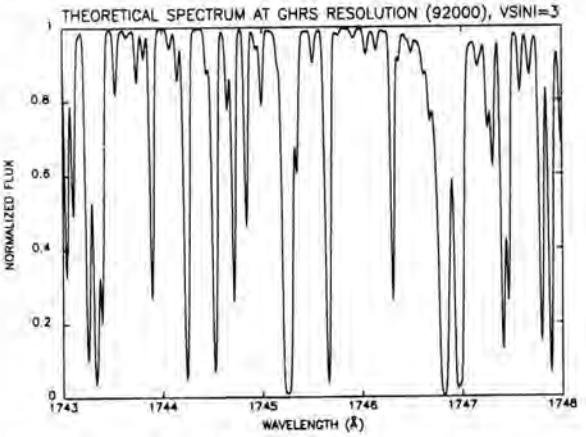

Fig. 13. The same spectrum as in figure 12 with reduced stellar rotation.

NEEDS FOR PRIMARY ATOMIC DATA

Two classes of accurate atomic data are needed for the quantitative analysis of ultraviolet stellar spectra. If we are attempting to derive the abundance of an element from specific, well observed lines, we need wavelengths, oscillator strengths and broadening parameters for those lines. We denote these as "primary" data. Of nearly equal importance, however, are a complete knowledge of what lines of other elements, or what weaker lines of the same element, are contributing significant opacity to the primary line and accurate atomic data for those blending contaminants. We denote these as "secondary" data. Our previous discussion has focused on the large atomic data base needed as the source of secondary data. Here we briefly describe some specific examples of primary data that are needed for the analysis of our own HST/GHRS and IUE data.

N I

A substantial literature exists about the spectrum and oscillator strengths of N I. In a study just completed, Roby, Leckrone and Adelman (1989, in preparation) used IUE spectra (including that of o Peg, illustrated in this paper) to derive nitrogen abundances from the multiplets near 1742.7, 1745.2 and 1411.9 A. When the experimental log gf values were used (e.g. from Wiese et al., 1966, renormalized according to Lawrence and Savage, 1966, or from Dumont et al., 1974) a systematic difference of 0.5 to 1.2 dex was found between abundances from the 1411 A feature and those from 1742 and 1745 A. The situation is complicated by the usual uncertainties in the background blending, which we have treated as carefully as possible.(We believe the random uncertainty in the abundance from a single line to be about ±0.3 dex.) Interestingly, this systematic discrepancy was greatly reduced or went away entirely when we adopted the calculated N I log gf's from Kurucz and Peytremann. Since all recently published oscillator strengths for 1742 and 1745 A, both theoretical and experimental, agree to within 0.1 dex, this result suggests that there is a problem with the expermental log gf's for the lines near 1411. The resolution of this discrepancy is very important, because the astrophysical interpretation hinges on which N abundance we adopt. The 1742/1745 abundances are below solar and below the values derived from high-excitation near infrared lines, while the 1411 values are close to solar and to the near-IR values. On the other hand we view the 1742/1745 abundances as the more reliable and have a ready astrophysical explanation for the disagreement with the near-IR values and solar values.

O I

We have attempted to derive stellar oxygen abundances from the low excitation intersystem lines of O I at 1356, 1359 and 1641 A. Oxygen lines observed in the red or near-IR are either very weak or are susceptible to large non-LTE effects. The lines of the oxygen resonance multiplet, 1302, 1305 and 1306 A, are broad, strongly saturated and difficult to measure accurately in our IUE data. Leckrone and Adelman (1986) reported a preliminary, and somewhat controversial, oxygen abundance for the highly evolved, horizontal branch star HD109995, based on the 1356 A line. But the literature is somewhat ambiguous about whether the log gf for this line from Zeippen, et al. (1977) or from Froese Fischer (1987) should be viewed as the more reliable (they differ by 0.5 dex, an astrophysically critical uncertainty). Moreover, Zeippen et al. did not compute a gf value for the 1641 A transition, a project that would be of great interest for the interpretation of IUE and GHRS observations.

Hg I, II, III, and Au II

Lines of the first three Hg ions will be extensively studied in GHRS spectra of the Hg-rich chemically peculiar stars. These stars exhibit isotope anomalies - the hotter members of the group having a terrestrial isotope mixture and the cooler members being deficient in the lighter Hg isotopes (the Hg lines in the most extreme case, the star chi Lupi, arise from nearly pure ^{204}Hg). The only astrophysical model currently offered to explain this anomaly invokes the diffusion of the lighter isotopes to high stellar atmospheric layers, where they "hide" in the form of Hg III. To test this hypothesis, one has to search for the Hg III lines in the ultraviolet, and hopefully measure abundances from them. They have not been found in IUE spectra. But we do not know their oscillator strengths and cannot predict how strong they should be. Similarly, one wants to measure abundances using lines of Hg I and Hg II for comparison. In a related area, GHRS will be

Table 2. Lines of Hg and Au for which oscillator strengths are needed

Ion	Wavelength (A)
Hg I	2537
	1849
Hg II	1942
	1650
Hg III	2354
	1678
	1379
	1335
	1331
Au II	2082
	1801
	1783
	1740

used to look for ultraviolet lines of Au II in these stars, searching for the abundance pattern as a function of atomic number (the stars are often Pt-rich as well). Extremely weak Au lines have been detected in two or three stars in ground-based spectra, but one would get more positive detections and more accurate abundances from ultraviolet lines. Table 2 lists the Hg and Au lines that we are planning to observe with the GHRS.

ACKNOWLEDGEMENTS

We would like to thank Dara Norman and Keith Feggans of the GHRS Data Analysis Facility at the Goddard Space Flight Center for their help in the preparation of the computer-generated figures for this paper.

REFERENCES

Adelman, S.J., 1988 - Elemental abundance analyses with coadded DAO spectrograms - IV. Revision of previous analyses. In: Mon. Not. R. Astr. Soc., 235, 749.

Artru, M.C., Jamar, C., Petrini D. and Praderie, F., 1981 - Autoionized levels and oscillator strengths for SiII. In: Astron. Astrophys. Suppl. Ser., 44, 171.

Cowan, R.D., 1968 - Theoretical calculation of atomic spectra using digital computers. In: Journ. Opt. Soc. Amer., 58, 808.

Dumont, P.D., Biemont, E. and Grevesse, N., 1974 - Transition probabilities for vacuum ultraviolet lines of N I through N IV. In: J. Quant. Spectrosc. Radiat. Transfer, 14, 1127.

Froese Fischer, C., 1968 - Superposition of configuration results for Si II. In: Astrophys. J., 151, 759.

Froese Fischer, C., 1987 - The 2p-3s transitions in atomic oxygen. In: J. Phys. B: At. Mol. Phys., 20, 1193.

Johansson, S., 1984 - A comparison between the observed and predicted Fe II spectrum in different plasmas. In: Physica Scripta, T8, 63.

Kurucz, R.L., 1981 - Semiempirical calculation of gf values, IV: FeII. Smithsonian Ap. Obs. Spec. Rept., No. 390.

Kurucz, R.L. and Peytremann, E., 1975 - A table of semiempirical gf values. Smithsonian Ap. Obs. Spec. Rept., No. 362.

Lanz, T. and Artru, M.C., 1985 - Compilation of oscillator strengths for singly ionized silicon (Si II). In: Physica Scripta, 32, 115.

Lawrence, G.M. and Savage, B.D. 1966 - Radiative lifetimes of uv multiplets in boron, carbon and nitrogen. In: Phys. Rev., 141, 67.

Leckrone, D.S. and Adelman, S.J., 1986 - The ultraviolet lines of carbon, nitrogen, and oxygen in the IUE spectrum of the field horizontal-branch A star HD 109995. In: New Insights In Astrophysics, ESA SP-263, 65.

Leckrone, D.S. and Adelman, S.J., 1989 - On the signal-to-noise ratio in IUE high dispersion spectra. In: Astrophys. J. Suppl., 71, in press.

Wiese, W.L., Smith, M.M. and Glennon, B.M., 1966 - Atomic Transition Probabilities 1. Hydrogen Through Neon. NSRDS-NBS 4.

Zeippen, C.J., Seaton, M.J. and Morton, D.C., 1977 - Some O I oscillator strengths and the interstellar abundance of oxygen. In: Mon. Not. R. Astr. Soc., 181, 527.

AUTHORS' ADDRESSES

David S. Leckrone
Code 681
NASA Goddard Space Flight Center
Greenbelt, Maryland 20771, USA

Sveneric Johansson
Atomic Spectroscopy, Department of Physics
University of Lund
Solvegatan 14
S-223 62 Lund, Sweden

Robert L. Kurucz
Smithsonian Astrophysical Observatory
60 Garden Street
Cambridge, Massachusetts 02138, USA

Saul J. Adelman
Department of Physics
The Citadel
Charleston, South Carolina 29407, USA

Sveneric Johansson

The iron group elements and the 'missing' opacity in ultraviolet and optical spectra of stars

ABSTRACT

The present knowledge of the spectra of iron group elements - the three lowest stages of ionization - is discussed in view of the needs for atomic data in stellar spectroscopy. Possible contributions from unknown lines in these spectra to the residual line opacity in stars are examined. The likelihood of such an explanation of the "missing" opacity is illustrated by some recent examples of identifications of new kinds. Future work in laboratory astrophysics is outlined.

INTRODUCTION

The strong interaction between atomic and stellar spectroscopy has been natural and obvious ever since the first line spectra of atoms and stars were recorded. Line spectra of atoms provide the data we need to establish the energy levels and they give an insight into dynamic processes of the atom. Line spectra of stars contain indirect information about the chemical composition as well as other properties of a stellar atmosphere. The ultimate goal in these two branches of spectroscopy is that the analysis of the observed spectrum will give unambiguous explanations of all observed features, which have a reasonable emission intensity or absorption depth. However, this goal has been achieved only in a very small number of cases.

The relative cosmic abundance, deduced from stellar spectra, decreases quite rapidly for elements beyond nickel in the periodic table. According to the adopted theory for stellar evolution this is a consequence of the fusion processes active in the creation of the different elements. The 4p-elements, gallium to krypton, are thus about three orders of magnitude less abundant than nickel, and the 4d-elements, the palladium group, another order of magnitude less abundant. Even if there is a great interest in the heavier elements for studies of e.g. chemically peculiar stars, the primary common field of interest in atomic and stellar spectroscopy is the first third of the periodic table. Here, the astrophysical needs require in general more complete term analyses, which include highly excited configurations.

The number of transitions in a given spectrum, for which we set reasonable limits in line strength and excitation energy, depends on the complexity of the structure of the emitting (or absorbing) atom or ion. This complexity is determined by the number of valence electrons, and deviations from pure coupling conditions for these valence electrons further increase the number of lines. This means that the simplest case is the spectrum of hydrogen or hydrogen-like ions having regular spectral series with single lines (observationally), while the most complex and line rich spectra of the astrophysically important elements are due to the iron group members. The high cosmic abundance of iron allows the spectra of its neutral (first spectrum), singly ionized (second spectrum) and doubly ionized (third spectrum) atoms - Fe I, Fe II, and Fe III - to account for the bulk of lines in photospheric spectra of stars and the sun.

In recent years there has been a great progress in the work on laboratory spectra of iron group elements mainly due to developments of the experimental techniques, computerized routines in the data handling and complementary methods in the analysis work. In spite of that, spectra of the iron group elements are still believed to be responsible for most of the unexplained or "missing" opacity in line-rich spectra of stars. In this paper I will discuss the reasons for this suspicion in view of the present knowledge of the atomic structure of the relevant atoms and ions and with reference to current work in laboratory and stellar spectroscopy. I will concentrate on plausible contributions from unknown lines, i.e. transitions to or from energy levels, which are not experimentally known. Rough values of the wavelengths and line strengths for such transitions can be predicted from theoretical calculations or from regularities along iso-ionic or iso-electronic sequences. Missing opacity that may depend on large uncertainties in the values of different atomic parameters for already known transitions will only be mentioned in passing.

THE MISSING OPACITY IN STELLAR SPECTRA

Several astronomers working on spectra of high resolution of the sun and other stars have realized

that atomic data of sufficient quantity and quality are lacking for complete and satisfactory analyses. This will certainly be even more apparent when spectra from the GHRS (Goddard High Resolution Spectrograph) on board the HST (Hubble Space Telescope) will be available for analysis. Missing data in the form of unknown lines or uncertain oscillator strengths due to theoretical or experimental difficulties may be responsible for the residual absorption that sometimes is referred to as the missing opacity. The origin of this missing opacity is probably not the same in all wavelength regions of a stellar spectrum and is certainly different for stars that differ in temperature, i.e. there is not a unique solution or a single missing element.

Information about missing opacity in the sun can be extracted from detailed studies of the solar spectrum, either from matching a synthetic and an observed spectrum or from the long lists with line identifications. These tables give wavelengths and widths of observed absorption features, which are counted and used for statistics. The ratio between the number of unidentified and observed lines gives a very rough estimate of the missing information. It is of course difficult to estimate whether a proposed identification of a solar line is alone responsible for the total absorption - some features may still be blended by unknown lines. One way to check that is to calculate the absorption depth by means of a model atmosphere and relevant atomic data.

The knowledge about the solar spectrum as judged from the statistics of the analysis is still incomplete. In the region 2935-8730 A twenty-seven percent of the 24000 measured absorption features remained unidentified in the analysis by Moore *et al* (1966). In a later analysis (Moore *et al*, 1982), covering the region between 3069 and 2095 A, about 20% of the 6150 solar lines lack identification. As much as 62% of all lines have single identifications, i.e. are unblended. Finally, in the VUV region, 1175 - 1710 A, Sandlin et al (1986) managed to identify only 51% of the 3250 lines by means of the data bank available about five years ago. The analysis of the optical region is based mainly on the data in the Multiplet Tables (Moore, 1962, Moore, 1972) while later analyses in the ultraviolet region also include recent laboratory data, discussed in the next section.

The completeness of an analysis of a stellar spectrum is not easy to assess from the percentage of identified lines. A line list with hundreds of lines and a seemingly complete analysis may result if large line widths, intrinsic or instrumental, or bad wavelengths allow every observed feature to be identified on the basis of wavelength coincidences with laboratory or predicted lines. The frequent departure from LS coupling in excited configurations of the iron-group elements makes the traditional criterion of consistency in form of complete LS multiplets unreliable. Intercombination lines could be as likely as LS-allowed transitions because of serious mixing of different spin states.

A flora of problems with missing data for analyses of stellar spectra has been presented at this meeting and I refer the reader to the papers by e.g. Artru, Kurucz, Leckrone and others.

THE PRESENT KNOWLEDGE OF IRON-GROUP SPECTRA

The present status of the analysis for the spectra of the three lowest ionization stages of the iron group elements has recently been reviewed (Johansson and Cowley, 1988), where the work on these spectra during the past 35 years was emphasized. The reason for that was to stress that much new data have become available since the time when the Multiplet Tables were issued. The progress has been measured by comparing the number of atomic energy levels, reported in the Atomic Energy Levels (AEL) by Moore (1971), with the number of levels given in the new compilation by Sugar and Corliss (1985). Of the total of 24 spectra, Sc I-III to Ni I-III, there are only three, V I, Co I and Ni I, for which no new levels have been reported. The largest relative progress applies to third spectra, where the relative increase in five of them is more than 100 percent. However, we find the largest absolute increase for the second spectra, where nearly 2000 of the presently known 3464 levels are new and therefore not included in AEL. This means that transitions that involve any of these new levels are not present in the Multiplet Tables. As regards first spectra, the number of reported levels is about 3350, and the main part of the about 500 new levels, reported after 1950, belong to Rydberg series, observed in absorption spectra. The standard compilations of atomic data used in stellar spectroscopy, the Multiplet Tables, thus lack a great portion of the atomic transitions, that are presently known in spectra of the iron group elements. There are later compilations that contain these new data, but they are arranged as finding lists and not as tables of LS multiplets. The two sets of tables by Kelly (1979, 1987) in the UV and VUV regions provide complementary laboratory data for the elements hydrogen to krypton, sorted by spectrum in each element and sorted by wavelength in a total finding list. Unfortunately, some lines that were reported as unidentified in the original papers have been given erroneous identifications in these compilations. Another valuable source of wavelengths

for a bulk of lines is the updated tables by Kurucz (1988). Here, the spectral lines are based on transitions between experimentally established levels, and the tables therefore also include predicted lines, that have not been observed in the laboratory. However, the user is here guided by calculated oscillator strengths, which may help to confirm proposed identifications. The uncertainties of the calculated log gf-values are somewhat dependent on the LS purity of the combining levels, which in practice means the excitation potential (E.P.) of the upper level. At high excitation energies the large level density complicates the labelling of the levels and large uncertainties in the level composition can be expected.

The completeness of the analysis of the first three spectra of the iron group elements was also graded in the review mentioned above. The data were arranged in eight different groups according to the different types of one-electron transitions, 3d-4p, 4s-4p, 4p-4d etc, that have been observed in two systems of configurations (see next paragraph). The status today, the presence in the Multiplet Tables, the wavelength region and the excitation potential were given for all eight groups in all spectra. The different groups are of course of different importance in stellar spectroscopy, but most of them are represented in astrophysical spectra, at least for iron. It should be pointed out, however, that even if the progress in the analysis of iron group spectra has been considerable since the time the Multiplet Tables came out, the strongest and most prominent transitions were of course known at that time, particularly in the optical region. For abundance work the strongest lines are not always the most important ones, because of saturation effects.

It is often suitable to divide the electronic configurations in the iron group spectra in two different systems, the singly-excited (SE) system and the doubly-excited (DE) system. The singly excited system, $3d^k nl$, dominates the third spectra, whereas the DE system, $3d^{k-1}4snl$, is dominant in first spectra. In second spectra the two systems overlap to a great extent and are of equal importance. In general, the SE system is well established in second and third spectra but far from complete in first spectra. The analysis of the DE system on the other hand is quite complete in first spectra, fragmentary in second spectra, but, with a few exceptions, completely unknown in third spectra.

The major part of photospheric absorption due to iron group elements can be ascribed to 3d-4p and 4s-4p transitions. Valence electrons in a 3d- or 4s orbital have the largest binding energy and the $(3d+4s)^k$ complex of configurations comprises therefore the ground state in all spectra, discussed here. These transitions appear in the optical region in first spectra, which explains the dominance of Fe I over Fe II in this part of the solar spectrum. From the statistics in Table 12 in (Moore *et al* 1966) we can see that the Fe I/Fe II ratio is almost 10, as regards the number of identified lines. For the second spectra the 4s-4p transitions in the SE system appear in the region 2000-3000 A, whereas the 3d-4p transitions are spread from vacuum-ultraviolet (VUV) to infrared (IR). In the solar spectrum between 2000 and 3000 A the number of identified lines from first and second spectra, of any iron group element, are nearly the same. In third spectra the 3d-4p transitions are most important, since the relatively high excitation potential of the 4s configuration reduces the Boltzmann factor (exp -E/kT) for the 4s-4p transitions. The bulk of the 3d-4p transitions in third spectra appears well below 2000 A. Nearly all data associated with the transitions discussed in this paragraph are known and compiled.

The situation for the DE system in second and third spectra, where a great portion of the fundamental 4s-4p and 3d-4p transitions is unknown, is far from satisfactory. This fact will be discussed in detail below, as these transitions are presumptive candidates for unidentified stellar lines.

The next groups of transitions of astrophysical relevance emanate from the 4p configurations, which are the lowest configuration of opposite parity to the $(3d+4s)^k$ complex. The 4p-*ns* and 4p-*nd* transitions in first spectra appear in the optical region for *ns* = 5s and *nd* = 4d and in the UV region for higher values of n. These are prominent in the solar spectrum and will be discussed later. In second spectra the 4p-4d and 4p-5s transitions in the SE system fall in the line-rich resonance region between 2000 and 3000 A.

The so-called highly-excited lines, i.e. transitions between highly-excited configurations like 4d-4f, 5s-5p, 5p-5d etc, have been observed in the optical and infrared regions of stellar spectra and the solar spectrum. Some examples will be given in the next section.

SOME EXAMPLES OF NEW KINDS OF STELLAR IDENTIFICATIONS

Before I go into a more detailed discussion of where we can expect to find unknown lines, which can explain some of the missing opacity, I will give some examples of recent laboratory analyses that have yielded new stellar identifications. All examples concern absorption spectra and the E.P. we refer to should always be assigned to the lower level in an atomic transition. Highly-excited lines, found in emission in stellar spectra, are often a result of selective excitation processes in the line-forming plasma and can hardly be predicted or foreseen. They are therefore excluded from this

discussion (see e.g. the paper by Jordan).

At the first meeting in this series Baschek (1984) discussed the criteria for observing very faint lines of iron group elements in terms of element abundance, excitation potential and oscillator strength. He emphasized the equal probabilities to find faint lines of Fe II and strong lines of elements with lower abundance in stellar spectra. A couple of years later this was illustrated in new findings of doubly-excited Fe II lines around 1800 A in the IUE spectrum of 21 Peg (Adam *et al* 1987). The E.P for these transitions was as high as 7 eV and the observed absorption depths required, according to model atmosphere calculations, log-gf values of the order of 0 to 1. Independent ab initio calculations of the oscillator strengths yielded values of that order of magnitude, which thereby confirmed the identifications. Similar types of transitions in Fe II are present in the spectra discussed by Leckrone at this meeting.

The first identification of high-level transitions of iron-group elements in absorption spectra of stars was made in the optical spectrum of υ Sgr (Johansson, 1978). The presence of 4d-4f transitions of Fe II indicated that levels with an E.P. of more than 10eV were populated sufficiently to give observable absorption features. That study was later followed up by a closer examination of these transitions in chemically peculiar (CP) stars (Johansson and Cowley, 1984), for which a preliminary check by means of wavelength coincidence statistics gave a positive response. A similar work is in progress on the 4d-4f transitions of Cr II (Johansson *et al*, 1986). They appear clearly in optical spectra of CP stars that have an enhanced abundance of chromium.

Similar high-level transitions have been found in the infrared spectrum of the sun, where newly identified 4d-4f transitions of Fe I appear strongly (Johansson and Learner, 1989). These identifications imply an E.P. of about 6 eV, which is the highest levels found populated in the sun for a neutral iron group element. However, preliminary studies at longer wavelengths show also the presence of 4f-5g transitions of Fe I in the solar spectrum, which means an EP of 7 eV, i.e. 80% of the ionization potential. A similar study in Ni I, including new identifications of solar lines in the infrared, is reported by Litzén at this meeting.

A recent laboratory study of the absorption spectrum of Fe I in the UV region has yielded data, which allow a reasonably complete analysis in this region (Brown et al, 1988). The laboratory plasma source was capable of populating metastable states up to about 2.5 eV, which should be sufficient for the astrophysical needs in the VUV region. The richness of observed lines below 1900 A is due to a mixture of more than 25 different spectral series, which converge towards 9 series limits, located within 0.2 eV. It will be a challenging task to provide accurate oscillator strengths for all these lines.

HOW CAN WE FIND EXPLANATIONS FOR THE REMAINING MISSING OPACITY?

The general conception that the iron-group elements are responsible for the main part of the remaining missing opacity in stellar spectra may be examined in view of our present knowledge of iron-group spectra, discussed in the previous section. In this contribution I prefer to discuss different wavelength regions, with a special emphasis on the satellite ultraviolet.

Satellite ultraviolet, below 2000 A.

It has been shown by Leckrone at this meeting that there is a lot of unexplained absorption in IUE spectra of early-type stars below 2000 A. One of the critical regions seems to be the 1700 - 1800 A interval, which happens to coincide with the interval, where the strongest unidentified lines in the laboratory spectrum of iron occur. Current work on Fe II in this wavelength region (Baschek and Johansson, 1988) leads to the suspicion that many lines can be explained as 4s-4p transitions in the doubly-excited (DE) system between $3d^54s^2$ and $3d^54s4p$, i.e. transitions similar to that of the strong UV 191 multiplet around 1780 A. The five lowest terms of $3d^54s^2$ in Fe II, a^6S, b^4G, d^4P, c^4D and ^2I, have E.P.:s lower than 8 eV. The relative Boltzmann factors for these terms at T=10000 K are 1.00, 0.012, 0.008, 0.005 and 0.003. If we assume that the oscillator strengths are of the same order of magnitude as for transitions from b^4G, which have been observed in *o* Peg (T=9600 K) (in the paper by Leckrone *et al* in these proceedings), there should be a reasonable probability for transitions from higher $3d^54s^2$ terms to appear in the spectrum. No 4s-4p transitions from these higher terms have so far been identified in the laboratory spectrum. It should be noted, that the doubly-excited Fe II lines identified in the region 1750-1900 A by Adam *et al* (1987) in 21 Peg (T = 10,500 K), arise from levels with Boltzmann factors of 0.014 and 0.004 on the scale used above. Similar transitions in other second spectra should also be of astrophysical relevance. They are supposed to occur between 1700 and 2000 A.

The large span of the $3d^{k-1}4s4p$ configuration in most second spectra gives rise to a considerable overlap with the $3d^k np$ series of the SE system.

The interaction between these configurations yields an increased number of transitions, which, depending on the degree of mixing, complicates the analysis of the laboratory and stellar spectra. The level mixing, which affects the calculated gf-values, is very sensitive to the accuracy of the predictions of level values in the calculations. Some accidental coincidences have very low chances to be revealed from calculations but their effect on the spectrum may be drastic (see e.g. Brage *et al*, 1987, and the paper by Leckrone *et al* in these proceedings).

For cooler stars, where the ionization balance favours the neutral elements, the contribution from first spectra to the opacity should primarily be from the 4s-*np* and 3d-*np* series in the SE and DE systems. The ionization potentials of the neutral iron-group elements define the series limits to range from 1900 A (Sc) down to 1430 A (Ni). The Fe I case has been discussed in the previous section.

The contributions from third spectra concern mainly 3d-4p and 4s-4p transitions. According to Johansson and Cowley (1988), all relevant data are known for the SE system, but very little is known for the DE system. The bulk of the 3d-4p transitions in the DE system are predicted to occur below 1000 A for all third spectra. They should be of the same significance in this region as the 4s-4p transitions of the SE system are in the 1000-2500 A region. Thus, the E.P. of the strongest 3d-4p transitions of Fe III at 640 A is the same as for the UV multiplet 34 around 1900 A.

The 4s-4p transition in the DE system of third spectra is only known in Ti III at 1818 A and should go towards shorter wavelengths in the iso-ionic sequence. In Fe III the corresponding lines are predicted at about 1550 A. It should be pointed out that the Boltzmann factor is considerably smaller for the 4s-4p transition than for the 3d-4p transition in the DE system of third spectra.

The 3d-4p transitions in the DE system of second spectra are also very plausible as candidates for unidentified lines in the 1000-2000 A region, where the bulk of lines appears at the short-wavelength side. These transitions are far from completely analysed, as can be seen in Table 2 of the review by Johansson and Cowley (1988). It is important to emphasize the low E.P. for these transitions, which makes them very strong candidates for unidentified lines in stellar spectra.

Satellite ultraviolet, 2000-3000 A.

This is the strong resonance region of second spectra of the iron-group elements, where in principle everything is experimentally known. It is also the region for the 4s-4p transitions in third spectra, where the data are complete as well. The missing opacity may here have two different origins among the iron-group elements, which require quite different stellar conditions.

For solar-type and cooler stars the contribution from first spectra may be considerable. The transitions identified as strong lines in the solar spectrum are of the type 4p-*nl*, where *nl* is 5d,6d...,6s,7s.... The 4p-*n*d,*n*s series terminate at about 2250 A in the DE system and at 3100 A in the SE system. I believe that the majority of the missing opacity in the solar spectrum is due to these spectral series of first spectra, particularly Fe I (see e.g. Johansson, 1984).

For hotter stars the 4p-5s and 4p-4d transitions of second spectra could be possible in this region. The excitation potential of the lowest 4p levels is about 5 eV. In a recent laboratory study of 4p-4d transitions in Fe II, the super-multiplets of most probable astrophysical importance have been studied (Johansson and Baschek, 1988). Since they fall in a region where the spectral response of IUE is quite low, the presence of these lines has not yet been systematically studied.

The optical and infrared regions.

In the ultraviolet part of the optical region of the solar spectrum the dominance of first spectra is overwhelming, in particular Fe I. There are still unidentified lines in this region and many of them can certainly be identified with Fe I and other spectra of neutral iron group elements. The 4p-*nl* transitions discussed both in the previous subsection and the previous section should account for that. The presence of 4d-4f lines of Fe II in stellar spectra (see above) suggests that such transitions from other second spectra could be of relevance as well. They are supposed to appear in the 4000-8000 A region. Other highly-excited lines that could be possible are due to 5s-5p, 5p-5d and 5p-6s transitions in the red and infrared regions. Similar transitions of first spectra dominate the extra-photographic infrared region of the solar spectrum and should also be of importance in stellar spectra. Complementary data are still needed for these types of transitions.

FUTURE WORK ON THE MISSING ATOMIC DATA

In this concluding section I will discuss some possible ways to get hold of some of the missing data for the iron-group elements, particularly in

the VUV region. As concerns term analysis work, the accuracy of wavelength measurements is critical for the level search in complex spectra. The introduction of FTS measurements in this wavelength region is the most important step for future work. The FTS data from Kitt Peak in the infrared and optical regions from stable hollow-cathode lamps have been ideal for analysis of first spectra. The first FTS data on iron in the UV region from Imperial College have already been used for term analysis of Fe II (Johansson and Baschek, 1988). If the wavelength region can be extended down to 1100 A, say, the combined data from these two FTS facilities will be of extreme value for analysis of second spectra. In addition, if it will be possible to run a pulsed light source, the observed spectrum will not be dependent on the selective excitation through charge transfer that now determines the excitation of the ions in the hollow-cathode lamp. The FTS data can also be used for a determination of branching ratios, which, together with accurate life time measurements, will produce a large set of gf-values (discussed by Thorne at this meeting). This method has already been applied to Mo I (Whaling *et al*, 1989) and current work is in progress on Fe I by Whaling and coworkers.

Since the only powerful sources for absorption spectroscopy on ions are the stars, the use of the high-resolution spectrograph (GHRS) on the Hubble Space Telescope will be another instrument to hope for in both stellar and atomic spectroscopy. As has been discussed by Leckrone at this meeting the process of matching synthetic and observed spectra iteratively, where theoretical, experimental and observational data are involved, may eventually give accurate values both for stellar and atomic parameters. Stellar spectra can be used in term analysis as discriminators between lines from different ionization stages and, within an ion, between lines having different excitation energies.

Laser experiments, devoted to particular problems in laboratory astrophysics, can be used for selective excitation of highly-excited states in neutral atoms. The even-parity Rydberg states in neutral atoms can be reached through a two-step excitation by means of one tuned and one scanning laser. The state is found by opto-galvanic detection. Preliminary works on Fe I have been performed (Johansson and Axner, 1988) and all the newly found levels have combinations that give rise to strong lines in the solar spectrum. When this technique is developed further it would also be worth trying on ions either with a frequency-doubled or tripled tuned laser for the first excitation or perhaps by means of monochromatic synchrotron radiation. The obstacle will certainly be to find an ion-source with sufficient ion density.

CONCLUSION

A brief review of the spectra of the three lowest ionization stages of iron group elements implies that there are predicted transitions with sufficiently high intensity to be present in stellar spectra. However, the experimental wavelengths for the corresponding lines are unknown. This means that the atomic data base for stellar spectroscopy still lacks important information even for elements with a high cosmic abundance, which hampers a satisfactory analysis. Plausible explanations of some of the missing opacity can be presented but much experimental and theoretical work has to be performed in order to improve the situation. Some developments on the technical side provide good experimental conditions for data recording but the small number of people working on these problems is still the limiting factor.

ACKNOWLEDGEMENTS

Financial support by the Swedish Natural Science Research Council (NFR) and The Swedish Board for Space Activities (DFR) is gratefully acknowledged.

REFERENCES

Adam, J., B. Baschek, S. Johansson, A. E. Nilsson and T. Brage, 1987 - Ultraviolet doubly excited Fe II lines in the laboratory and in the A-type star 21 Pegasi. In: Astrophys. J., 312, 337-343.

Baschek, B., 1984 - The role of oscillator strengths in modelling and analysing stellar spectra. In: Phys. Scr. T8, 21-24, (Ed. U. Litzén).

Baschek, B. and S. Johansson, 1988 - New laboratory recordings of Fe II in the IUE region. In: Physics of formation of Fe II lines outside LTE. Eds. R. Viotti, A. Vittone and M. Friedjung (Reidel, Dordrecht, The Netherlands) p. 35-39.

Brage, T., A. E. Nilsson, S. Johansson, B. Baschek and J. Adam, 1987 - Accidental degeneracy of doubly excited states in Fe II. In: J. Phys. B: Atom. Mol. Phys. 20, 1153-1160.

Brown, C. M., M. L. Ginter, S. Johansson and S. G. Tilford, 1988 - Absorption spectra of Fe I in the 1550-3215 A region. In: J. Opt. Soc. Am. B5, 2125-2158.

Johansson, S., 1978 - Absorption lines in υ Sgr identified as high-level transitions of Fe II. In: Mon. Not. R. astr. Soc., 184, 593-598.

Johansson, S., 1984 - A comparison between the observed and predicted Fe II spectrum in different plasmas. In: Phys. Scripta, T8, 63-69 (Ed. U. Litzén).

Johansson, S. and C. R. Cowley, 1984 - The identification of high-level transitions of Fe II in stellar spectra. In: Astron. Astrophys., 139, 243-247.

Johansson, S., J. W. Brault, C. R. Cowley, O. Garcia-Riquelme, V. Kaufman and S. Orti-Ortin, 1986 - Analysis of 4d-4f transitions in Cr II with astrophysical applications. In: Atomic spectroscopy annual report (University of Lund, Lund, Sweden) p. 66.

Johansson, S. and O. Axner, 1988 - Optogalvanic detection of highly-excited Fe I levels populated by two-step laser In: Atomic spectroscopy annual report (University of Lund, Lund, Sweden) p. 26.

Johansson, S. and B. Baschek, 1988 - Term analysis of complex spectra: New experimental data for Fe II. In: Nucl. Instr. Meth. Phys. Res., B31, 222-232.

Johansson, S. and C.R. Cowley, 1988 - Complex atoms in astrophysical spectra. In: J. Opt. Soc. Am., B5, 2264-2279.

Johansson, S. and R. C. M. Learner, 1989 -The lowest $3d^64s4f$ subconfiguration of Fe I determined from laboratory and solar Fourier transform spectra. In: Astrophys. J., submitted.

Kelly, R.L., 1979 - Atomic emission lines in the near ultraviolet; hydrogen through krypton. NASA Techn. Mem. 80268: Sects. I and II. (NASA, Goddard Space Flight Center, Greenbelt, Md., U.S.).

Kelly, R.L., 1987 - Atomic and ionic spectrum lines below 2000 angstroms: hydrogen through krypton. Parts I, II and III. In: J. Phys. Chem. Ref. Data 16, Suppl. 1.

Kurucz, R.L., 1988 - Semiempirical calculation of gf-values for the iron group. Private communication.

Moore, C.E., M.G.J. Minnaert and J. Houstgast, 1966 - The solar spectrum 2935 A to 8770 A, Natl. Bur. Stand. (U.S.) Monogr. 61.

Moore, C.E., R. Tousey and C.M. Brown, 1982 - The solar spectrum 3069 A-2095 A, NRL Rep. 8653 (Naval Research Laboratory, Washington, D.C.)

Moore, C.E., 1962 - An ultraviolet multiplet table, Natl. Bur. Stand. (U.S.) Circ. 488, Sec. 1 (1950), Sec. 2 (1952), Secs. 3, 4 and 5 (1962).

Moore, C.E., 1972 - A multiplet table of Astrophysical Interest, revised ed., Natl. Stand. Ref. Data Ser. Natl.Bur. Stand. (U.S.) 40.

Moore, C.E., 1971 - Atomic Energy Levels, Natl. Stand. Ref. Data Ser. Natl. Bur. Stand. 35.

Sandlin, G.D., J.-D.F. Bartoe, G.E.Brueckner, R.Tousey and M.E. VanHoosier, 1986 - The high-resolution solar spectrum, 1175-1710 A. In: Astrophys. J. Suppl. Ser. 61, 801-898.

Sugar, J. and C.R. Corliss, 1985 - Atomic energy levels of the iron-period elements: potassium through nickel. In: J. Phys. Chem. Ref. Data 14, Suppl. 2.

Whaling, W. and J. W. Brault, 1988 - Comprehensive transition probabilities in Mo I. In: Phys. Scripta, 38, 707.

AUTHOR'S ADDRESS:

Atomic Spectroscopy, Department of Physics, University of Lund, Solvegatan 14, S-223 62 Lund, Sweden

Robert L. Kurucz

Why I study the solar spectrum

ABSTRACT

Time and money should be spent to observe the spectra of the sun and bright stars at high resolution and high signal-to-noise. This should have higher priority than observing stars at low signal-to-noise and low resolution because interpreting such spectra is beyond the state of the art. High quality spectra are needed to determine and to test the line data and the physics that go into model atmosphere and spectrum synthesis programs which then can be used to interpret faint spectra. The sun and bright stars should be considered spectroscopic sources for studying atoms and molecules.

THE IMPORTANCE OF STUDYING THE SOLAR SPECTRUM

In the search for new results, the usual observational strategy of astronomers is to minimize signal-to-noise and resolution by observing objects as faint as possible. Whenever a new telescope or a better detector is built it is used to observe fainter objects instead of trying to understand the spectra of objects that can be well-observed. The actual spectra consist of many thousands of lines blended together. Even at infinite resolution and signal-to-noise the blends are difficult to interpret. At low resolution and signal-to-noise a spectrum does not contain enough information for interpretation. Without a priori information from other sources, the analysis of such a spectrum is usually incorrect. A significant fraction of telescope time around the world is wasted on low quality observations.

I believe that the best strategy is to study the brightest stars with the highest possible resolution and signal-to-noise. We can learn more about, say, globular clusters and the evolution of the galaxy by studying the brightest stars well, rather than by numerous poor observations. The sun is the brightest star available to us. It is possible to observe the solar spectrum with a signal-to-noise of 10000 and a resolving power of 1000000 at insignificant cost compared to most space projects. But nobody does. In the sun we can study contributions to blends at the 1 per mil level. Such lines can be better observed in the sun than lines that are 1000 times stronger in a globular cluster star. In stars such lines might be much stronger and affect or dominate a crucial abundance determination, or might appear where you expect a Zeeman component from giant starspots. The sun is also a good spectroscopic source for studying atoms and molecules. There are many cases where lines can be seen in the sun that have been difficult or impossible to see in the laboratory. Below I discuss the solar and stellar atlases that are available. There is very little available compared to what could be easily obtained, and there is very little compared to what is needed. The situation is disgraceful.

To be evenhanded, let me say that the laboratory situation is disgraceful as well. There is not one metal or molecule spectrum that I consider to be well analyzed. By that I mean that there are lines from that spectrum that appear in the sun or stars, and that matter in some way, but that are unidentified or unclassified. Half the lines in the solar spectrum are unidentified or unclassified. For relatively small amounts of money for modern spectrographs, lasers, and computers, one could make the analyses and even measure the oscillator strengths and damping constants along the way. I know there are people at this meeting who would like to try, but who barely receive support. I also know that this research historically has been very labor intensive, but computers are ideal for working with large masses of data, as I am sure I demonstrate below. Why is everyone afraid to be enthusiastic about basic science? Why is everyone a slave to the fads of funding agencies? Do everything. Then when we need data for our project of the moment, they will already have been published.

I have developed computer programs for producing model stellar atmospheres and for synthesizing spectra. I am collecting and computing data on all relevant atomic and molecular lines. I check the line gf values and damping constants by comparing the computed spectra to the observed spectra. Once I can compute realistic spectra for the sun and the brightest stars these programs and data can be used to predict the spectra of stars that are too faint to observe well (or even stars from the early universe that no longer exist). All the stellar parameters can be varied to determine the most sensitive and

easily measurable diagnostics. Then observing programs can be designed to measure those diagnostic features. The integrated spectra of clusters and galaxies can be treated in the same way. Below I discuss these computer projects and the line data.

SPECTRUM SYNTHESIS PROGRAMS

The spectrum synthesis computer programs have been under development since 1965 and have been described by Kurucz and Furenlid (1981) and by Kurucz and Avrett (1981). The algorithms for computing the total line opacity are extremely fast because maximum use is made of temperature and wavelength factorization and pretabulation. On a Cray computer a 500,000 point spectrum can be computed in one run. The same programs run on a VAX only much more slowly. There is no limit to the number of spectrum lines that can be treated in LTE. I currently have 58,000,000. At present I can treat 50,000 lines including non-LTE effects. The line data are described below.

The spectrum calculations require a pre-existing model atmosphere that can be empirical, such as the Vernazza, Avrett, and Loeser (1981) solar models, or theoretical, such as the ones I describe below. The "model atmosphere" does not have to be stellar. It can be a disk, a planetary atmosphere, a laboratory source, etc. Quantities that need be computed only once for the model atmosphere are pretabulated. There can be a depth-dependent microturbulent velocity or a depth-dependent Doppler shift.

Line data are divided into two groups for treatment. In the first group, the lines must have a source function that is either the Planck function or some function that approximately accounts for non-LTE effects in the outer layers. The first group of lines is processed to produce a summed line absorption coefficient for the wavelength interval of interest, including radiative, Stark, and van der Waals broadening. The line center opacity is also saved for each line for subsequent computation of the central depth.

In the second group of lines, each line has its individual source function, which is taken to be the Planck function if the calculation is LTE, and which is determined from the departure coefficients in the model in a non-LTE calculation. This group of lines is processed by directly computing the line opacity and source function at every wavelength point.

The spectrum is computed with a version of the model atmosphere program ATLAS (Kurucz 1970) in which departure coefficients have been inserted in the partition functions, in the Saha and Boltzmann equations, and in the opacities. Departure coefficients for levels that are higher than have been computed are assumed to be the same as those for the ground state of the next higher stage of ionization. If the model atmosphere is in LTE the departure coefficients are all set to unity. The program computes the non-LTE opacity and source function, adds in the LTE opacity and source function, adds the continuum opacity and source functions, and then computes the intensity or flux at each wavelength point and for each line center. Photoionization continua are put in at their exact positions, each with its own cross-section and with the series of lines that merge into each continuum included so that there are no discontinuities in the spectrum.

Hydrogen line profiles are computed using a routine from Peterson (1979) that approximates the Vidal, Cooper, and Smith (1973) profiles, works to high n, and includes Doppler broadening, resonance broadening, van der Waals broadening, and fine-structure splitting. Autoionization lines have Shore-parameter Fano profiles. Other lines have Voigt profiles that are computed accurately for any value of the parameter a. A few strong lines can be treated with approximate partial redistribution effects but the computer cost increases dramatically.

To compute a rotationally broadened flux spectrum I first compute intensity spectra at 17 angles and then pass them through the rotation program. A grid of points is defined on the disk and, for the given V sin i, the Doppler shift and angle are computed for each point. The intensity spectra are interpolated and summed over the disk to obtain the flux. In the rigid-body spherical approximation, symmetries are used to reduce the number of calculations, but the method works in the case of differential rotation as well.

To compute macroturbulent or instrumental broadening the broadening function is defined at integral values of the point spacing. Then the spectrum is read in, one wavelength at a time, redistributed among neighboring wavelengths, and added to a buffer for the new spectrum.

I also have a series of programs for computing the transmission of the spectrum through the Earth's atmosphere.

The most important step in the spectrum synthesis work is the final preparation of plots because I can display enough information to study the spectrum as a whole, to compare with one or more observed spectra, to study individual features in detail, and to identify lines and the relative composition of blends.

ATLASES

I have made a considerable effort to obtain observed spectra of the sun and bright stars for testing my calculations. I have all the published atlases. Fortunately Delbouille and Roland for the sun and the Griffins for the bright stars are committed to producing high quality atlases. I have many solar FTS spectra from James Brault at Kitt Peak. In many cases I have had to take or reduce the spectra myself (Kohl, Parkinson, and Kurucz 1978; Kurucz and Avrett 1981; Kurucz and Furenlid 1981; Kurucz, Furenlid, Brault, and Testerman 1984), and projects are now underway for Sirius, Vega, and the sun with a number of collaborators. Here I will describe a few of these atlases to give an impression of what is available. In every case the wavelength coverage is incomplete and higher quality is possible and needed.

The solar flux spectrum is important for its effects on other objects and on us, rather than for solar physics. In the flux spectrum much of the spatial and Doppler information about the solar atmosphere has been integrated away leaving a spectrum broadened and blended by the 2 km/s solar rotation. The flux spectrum is quite important for stellar physics, however, because the sun serves as the "standard star". We can determine its properties much better than those of any other star. Solar flux spectra are required for planning and interpreting stellar and planetary observations because they have the resolution and signal-to-noise to show what is actually being observed.

Observations made from ground-based observatories include the atmospheric transmission spectrum so it is necessary to consider blending and blocking by terrestrial lines and to have resolution high enough to resolve their profiles. A solar flux spectrum observed from the ground is useful for indicating these problems. The spectrum should have a resolving power greater than 1000000 and a signal-to-noise greater than 10000. For atmospheric chemistry and planetary and cometary atmospheres, and for space-based stellar observations, however, the true flux spectrum above the atmosphere is required.

The solar flux atlas by Kurucz, Furenlid, Brault, and Testerman (1984) plots residual flux for 296 to 1300 nm and also gives a table to convert to the absolute irradiance calibration by Neckel and Labs (1984). The spectrum was observed at Kitt Peak using the Fourier Transform Spectrograph on the McMath telescope. The resolving power is 522000 in the red and infrared and 348000 in the ultraviolet. The resolution is not high enough to resolve the terrestrial lines so there is some ringing. The atlas was fitted together from 8 overlapping scans that have reasonable signal-to-noise at the center but fall off in the region of overlap. In the final spectrum the signal-to-noise varies from 2000 to 9000. Ideally an atlas should be made from many more overlapping scans so that only near maximum regions need be used. The wavelength scale was set from a terrestrial O2 line. The continuum level was estimated from high points and it is uncertain, especially in the ultraviolet. There are also problems caused by broad structures in the atmospheric transmission produced by ozone and O2 dimer.

The flux spectrum has been poorly observed. The existing atlas covers only the ground based spectrum in the visible. It is very high quality by astronomical standards but still leaves considerable room for improvement. There are no high resolution flux atlases covering other wavelength regions or above the atmosphere. I do not expect there to be any improvement this century. In the meantime there are three approaches to approximating the flux spectrum. The first is to model the atmospheric transmission and then to divide the ground based spectrum by it. This should work quite well as long as the signal-to-noise is very high and the transmission is not near zero. The second method is semiempirical: fitting a central intensity spectrum computed from a model to the observed central intensity spectrum and then using the derived line parameters to generate the flux spectrum. The problem is that a significant fraction of the lines in the spectrum have not been identified so they would have to be guessed. The third method is to compute a purely theoretical flux spectrum from the existing line data. At present computing a realistic spectrum is beyond the state of the art.

Intensity spectra are better for spectroscopy because there is no rotational broadening and so less blending. They are better for solar physics because they are determined by conditions in only a small region of the disk. Spectro-spectraheliograms show the spectrum at each resolution element, but they give almost too much information because they emphasize the instantaneous velocity field. The existing intensity atlases are space and time averages over a small area on the disk.

The best central intensity spectrum in the visible is the Jungfraujoch atlas by Delbouille, Roland, and Neven (1973). The spectrum was observed in small wavelength sections from 300 to 1000 nm using a rapid-scanning double-pass monochrometer. The resolving power is about 750000 at 500 nm and the signal-to-noise is about 10000 by my guess. The wavelengths were set from Pierce and Breckinridge's (1973) line list. The wavelengths are not accurate in the 900 nm region

because of lack of wavelength standards. I am reducing Brault's FTS spectra that will provide good wavelengths in this region.

The Kitt Peak infrared central intensity atlas by Delbouille, Roland, Brault, and Testerman (1981) is the best available spectrum in the infrared. It is the combination of 9 FTS scans on the McMath telescope with resolving power about 400000 at 1 um decreasing to about 130000 at 5 um. The signal-to-noise varies from 3200 to 5200. Delbouille and Roland are redoing the atlas from Jungfraujoch to improve the resolution and signal-to-noise and especially to reduce the water vapor which is very bad on Kitt Peak. They will also produce a limb spectrum.

The JPL ATMOS experiment (Farmer 1987) was flown on the shuttle to obtain infrared FTS spectra of the atmosphere at sunset from which to measure trace molecules. Before sunset, solar intensity spectra were recorded. Wavelength coverage is 2 to 16 um, resolution is 0.0147 cm-1, and signal-to-noise varies from 1000 to 3000. Breckinridge and Dumont are preparing an atlas of the solar spectrum that will be available this fall.

The central intensity spectra taken by the Ultraviolet Spectrometer and Polarimeter on the Solar Maximum Mission spacecraft (SMM/UVSP) are the best in the ultraviolet but will not be ready for publication until some time in 1990. Richard Shine et al. at Lockheed have reduced the region from 129 to 177 nm. I am working on the region from 180 to 350 nm. The instrument failed before the spectrum was completely scanned so there is a gap between the two sections. The resolution and signal-to-noise are low by visible standards but are still much better than previous work in the ultraviolet. Better spectra are not likely to be produced this century.

I plan to publish or republish atlases for the sun and bright stars with the lines labelled, including terrestrial lines from the AFGL HITRAN line list (Rothman et al. 1987). I am synthesizing each spectrum and should be able eventually to deconvolve the blends and to deconvolve the atmospheric transmission where it is not near zero.

MODEL ATMOSPHERES

I and my coworkers have developed techniques for statistically including the opacity of millions of lines in model atmosphere calculations (Strom and Kurucz 1966; Kurucz 1970; Kurucz, Peytremann, and Avrett 1975, Kurucz 1979a,b). The inclusion of line opacity brought about a tremendous improvement in the quality of the models. Systematic errors in the determination of stellar effective temperatures, gravities, and abundances have been greatly reduced, although further improvement is still required. The fluxes computed from these models can be compared directly to stellar observations, or can be convolved with various photometric bandpasses to calibrate the photometric systems in common use (Relyea and Kurucz 1978; Buser and Kurucz 1978). The models I have been able to compute thus far have been based upon the atomic line data computed by Kurucz and Peytremann (1975). These include solar abundance models for temperature ranging from 5500 K to 50000 K and 1/10 and 1/100 solar abundance (of elements heavier than helium) models for temperatures 5500 K to 10000 K (Kurucz 1979a), and newer grids of models for A and B stars (8000 K to 20000 K) with enhanced (3 and 10 times solar) and reduced (1/3 and 1/10 solar) abundances and a comprehensive grid for the temperature range 5500 K to 8500 K for abundances 10, 3, 1, 1/3, 1/10, 1/30, 1/100, 1/300, 1/1000, and 0 times solar. As all these models have been computed with scaled solar abundances and assuming a 2 km/s microturbulent velocity, they can be used only as a first guess for peculiar-abundance Am and Ap stars, and for stars with enhanced turbulence. These models have been widely distributed; I can now supply a tape with data for 1200 models. I have also supplied numerous copies of the model atmosphere programs, the line opacities, the line lists, colors, programs for computing abundances, line profiles, and spectra.

Unfortunately, there are systematic errors in the cooler models because molecular line opacity was not included. My theoretical model for the solar photosphere has several per cent error in the flux in the red and, of course, cannot reproduce the molecular features in the ultraviolet. There are also systematic errors in the models at all temperatures caused by missing atomic line opacity.

I have been working to improve atomic and molecular line data as described below. In late 1988 I used these line data to compute new solar abundance opacity tables for use in my modelling. The calculations involved 58,000,000 lines, 3,500,000 wavelength points, 56 temperatures, 21 pressures, and 5 microturbulent velocities, and took a large amount of computer time. The opacity is tabulated both as 12-step distribution functions for intervals on the order of 1 to 10 nm, and as opacity sampling where, simply, every hundredth wavelength point in the calculation was saved.

I have rewritten my model atmosphere program to use the new line opacities, additional continuous opacities, and an approximate treatment of convective overshooting. It will soon be ready for distribution. The opacity calculation was checked by computing a

solar model which is a tremendous improvement over my earlier calculations. It matches both the observed irradiance and the observed continuum limbdarkening. I am beginning to compute a whole grid of solar abundance models for a range of microturbulent velocities.

I have now completed calculations for 1/100 and 1/10 solar abundance opacities. Each abundance takes two to three months (100 to 125 Cray hours). I plan to compute opacities for abundances ranging from 1/10000 solar to 10 times solar. For each abundance I will compute a grid of models for temperatures ranging from K stars to O stars, for gravities down to the radiation pressure limit, for a range of microturbulent velocities. I will compute fluxes for each model and predict the colors in all photometric systems. This should allow calibrations consistent for both cool and hot stars. I expect to be able to compute a complete, full-resolution spectrum for any of the models which can be compared directly to high resolution observations, or degraded to low resolution, say, 1 A.

Additional projects are computing model atmospheres for metallic line and peculiar stars with self-consistent abundances, and computing models for cool stars with abundance and isotopic variations. Grids of models will also be produced that go to very large optical depths so that they can provide surface boundaries for stellar interior models.

ATOMIC AND MOLECULAR DATA

All the calculations described above depend on having reliable gf values and damping constants for atomic and molecular lines, photoionization cross-sections, and, for non-LTE problems, collision cross-sections.

My earlier model calculations used the distribution-function line opacity computed by Kurucz (1979a,b) from the line data of Kurucz and Peytremann (1975). We had computed gf values for 1.7 million atomic lines for sequences up through nickel using scaled-Thomas-Fermi-Dirac wavefunctions and eigenvectors determined from least squares Slater parameter fits to the observed energy levels. That line list has provided the basic data and has since been combined with a list of additional lines, corrections, and deletions. The line data are being constantly, but slowly, improved. I collect all published data on gf values and include them in the line list whenever they appear to be more reliable than the current data. I have prepared lists for H_2, CO (Kurucz 1977), SiO (Kurucz 1980), and Fe II (Kurucz 1981). Lucio Rossi of the Istituto Astrofisica Spaziale in Frascati, John Dragon of Los Alamos, and I have computed line lists for electronic transitions of CH, NH, OH, MgH, SiH, CN, C_2, and TiO. In addition to lines between known levels, these lists include lines whose wavelengths are predicted and are not good enough for detailed spectrum comparisons but are fine for statistical opacities. Work is continuing on other molecules, and molecular ions, and on the infrared vibration-rotation spectra. I also have data for terrestrial atmospheric molecules.

In 1983 I recomputed the opacities using the additional atomic and molecular data described above. These new opacities were used to produce improved empirical solar models (Avrett, Kurucz, and Loeser 1984), but were found to still not have enough lines. For example, there are several regions between 200 and 350 nm where the predicted solar intensities are several times higher than observed, say 85% blocking instead of the 95% observed. The integrated flux error of these regions is several per cent of the total. In a flux constant theoretical model this error is balanced by a flux error in the red. The model predicts the wrong colors. In detailed ultraviolet spectrum calculations half the intermediate strength and weak lines are missing. After many experiments, I determined that this discrepancy is caused by missing iron group atomic lines that go to excited configurations that have not been observed in the laboratory. Most laboratory work has been done with emission sources that cannot strongly populate these configurations. Stars, however, show lines in absorption without difficulty. Including these additional lines will produce a dramatic increase in opacity, both in the sun and in hotter stars. A stars have the same lines as the sun but more flux in the ultraviolet to block. In B stars and in O stars there will be large effects from third, fourth, and fifth iron group ions. Envelope opacities that are used in interior and pulsation models will also be strongly affected.

I was fortunate to have been granted a large amount of computer time at the San Diego Supercomputer Center by NSF to carry out new calculations. To compute the iron group line lists I determined eigenvectors by combining least squares fits for levels that have been observed with computed Hartree-Fock integrals (scaled) for higher configurations including as many configurations as I can fit into a Cray. My computer programs have evolved from Cowan's (1968) programs. All configuration interactions are included. The following table is an example for Fe II,

```
                even
d6 4s   d6 4d          d5 4s2   d5 4s4d
   5s      5d    d6 5g    4s5s     4s5d
   6s      6d       6g    4s6s     4s6d
   7s      7d       7g
   8s      8d                d5 4p2
   9s                          d7

22 Configurations    5723 levels
largest Hamiltonian  1102 x 1102
Slater parameters 729
(many fixed at scaled Hartree-Fock)

                odd
 d6 4p   d6 4f   d5 4s4p   d5 4s4f
    5p      5f      4s5p
    6p      6f      4s6p
    7p              4s7p
    8p              4s8p
    9p                    d4s2 4p

16 Configurations  5198 levels
largest Hamiltonian 1049 x 1049
Slater parameters 541
(many fixed at scaled Hartree-Fock).
```

The laboratory data are from the computer tapes that NBS uses to print its energy level compilations (Sugar and Corliss 1985). Transition integrals are computed with scaled-Thomas-Fermi-Dirac wavefunctions and the whole transition array is produced for each ion. The forbidden transitions are computed as well. Radiative, Stark, and van der Waals damping constants and Lande g values are automatically produced for each line.

The least squares fits to determine the energy levels are now complete for the first 10 ions of the Fe group. The most complex spectra were done first before moving toward the simpler Ca end of the iron group. Fe II has been redone several times in collaboration with Sveneric Johansson from Lund (Johansson and Baschek 1988). We have added many more known levels, so the line lists will include many more Fe II lines with accurate positions. Johansson has given me revised levels for Fe I (Brown et al. 1988) so I will also redo those calculations.

The following table shows the line lists completed at the present time with the number of electric dipole lines saved for each ion,

	I	II	III	IV	V
Ca	48573	4227	11740	113121	330004
Sc	191253	49811	1578	16985	130563
Ti	867399	264867	23742	5079	37610
V	1156790	925330	284003	61630	8427
Cr	434773	1304043	990951	366851	73222
Mn	327741	878996	1589314	1033926	450293
Fe	789176	1264969	1604934	1776984	1006385
Co	546130	1048188	2198940	1569347	2032402
Ni	149926	404556	1309729	1918070	1971819

	VI	VII	VIII	IX
Ca	217929	125560	30156	22803
Sc	456400	227121	136916	30587
Ti	155919	356808	230705	139356
V	39525	160652	443343	231753
Cr	10886	39668	164228	454312
Mn	79068	14024	39770	147442
Fe	475750	90250	14561	39346
Co	1089039	562192	88976	15185
Ni	2211919	967466	602486	79627.

The forbidden lines have not yet been tabulated. The files fill 28 tapes. Most of these lines have uncertain wavelengths because they go to predicted levels. I have produced a single tape edition of these data that has all the lines with reliable wavelengths between laboratory determined energy levels.

In general the calculations are greatly improved over my earlier work and show considerably less scatter. Some of the calculated lifetimes agree perfectly with the best measurements. Fe II lifetimes are about 15% shorter than observed. There can still be considerable scatter for lines that occur only because of configuration interactions. I found a few typographical errors in the input energy data because the output line list had lines in the wrong positions. Those spectra were recomputed.

Several of these calculations have already been revised. I have already redone Ti I using the thesis by Forsberg (1987). This process will continue into the future. I will recompute the energy levels and line lists when new analyses become available and I will make the predictions available to laboratory spectroscopists. I plan to continue on with the heavier and lighter elements as a background project.

Diatomic molecules are also poorly analyzed. Stars are very high temperature sources by laboratory standards. High V and high J levels are populated and produce significant opacity, but in current laboratory studies only low V and low J levels have been observed. Many excited electronic states that could produce significant opacity have not been analyzed at all. Thorough laboratory analyses are required. I have obtained James Brault's FTS CN spectra but have not yet reduced them. They will provide a tremendous advance in our knowledge of CN and should account for many weak features in the solar spectrum (stronger in cool stars). I have the Air Force atmospheric line list, but there are many weak atmospheric lines that are clearly present in our high quality solar spectra but that are not in the line list. I am also trying to get all the old Los Alamos molecular line data into shape for use in opacity calculations.

I eventually need line lists for the tria-

tomic molecules so that I can work on M stars, but I hope that other people will do the work before I have to learn the physics. I am working on the low temperature bands now, however, for atmospheric transmission.

I plan to distribute my computed line data on tapes. I am setting up a print-on-demand system for the atomic data where I will provide tables of all laboratory measurements, usually a meager amount, together with my computed energy levels, damping constants, Lande g values, branching ratios, and line gf values. These should be of useful to both laboratory and astronomical spectroscopists.

ACKNOWLEDGEMENTS

This work is supported in part by NASA grants NSG-7054, NAG5-824, and NAGW-1486, and has been supported in part by NSF grant AST85-18900. The most important contribution to this work is a large grant of Cray computer time at the San Diego Supercomputer Center.

REFERENCES

Avrett, E.H., Kurucz, R.L., and Loeser, R., 1984 - New models of the solar temperature minimum region and low chromosphere. Bull. Amer. Astron. Soc., 16, 450.

Brown, C.M., Ginter, M.L., Johansson, S., and Tilford, S.G., 1988 - Absorption spectra of Fe I in the 1550-3215 A region. Journ. Opt. Soc. Amer. B., 5, 2125-2158.

Buser, R. and Kurucz, R.L., 1978 - Theoretical UBV colors and the temperature scale for early-type stars. Astron. Astrophys., 70, 555-563.

Cowan, R.D., 1968 - Theoretical calculation of atomic spectra using digital computers. Journ. Opt. Soc. Amer., 58, 808-818.

Delbouille, L., Roland, G., Brault, J., and Testerman, L., 1981 - Photometric Atlas of the Solar Spectrum from 1850 to 10000 cm-1. Kitt Peak National Observatory, Tucson, 189 pp.

Farmer, C.B., 1987 - High resolution infrared spectroscopy of the sun and the earth's atmosphere from space. Mikrochimica Acta, III, 189-214.

Forsberg, P., 1987 - The spectrum and term system of neutral titanium, Ti I. Thesis. University of Lund.

Johansson, S. and Baschek, B., 1988 - Term analysis of complex spectra: new experimental data for Fe II. Nucl. Instr. and Methods in Phys. Res., B31, 222-232.

Kohl, J.L., Parkinson, W.H., and Kurucz, R.L., 1978 - Center and Limb Solar Spectrum in High Spectral Resolution: 225.2 to 319.6 nm. Harvard-Smithsonian Center for Astrophysics,Cambridge, Mass., 365 pp.

Kurucz, R.L., 1970 - ATLAS: A computer program for computing model stellar atmospheres. Smithsonian Astrophys. Obs. Spec. Rep. No. 309, 291 pp.

Kurucz, R.L., 1974 - A preliminary theoretical line-blanketed model solar photosphere. Solar Phys., 34, 17-23.

Kurucz, R.L., 1977 - The Fourth Positive system of carbon monoxide. Smithsonian Astrophys. Obs. Spec. Rep. No. 374, 170 pp.

Kurucz, R.L., 1979a - Model atmospheres for G,F,A,B, and O stars. Astrophys. Journ. Suppl., 40, 1-340.

Kurucz, R.L., 1979b - A progress report on theoretical photometry. Dudley Obs. Rep. No. 14, ed. A.G. Davis Philip, pp. 363-382.

Kurucz, R.L., 1980 - SiO in the ultraviolet solar spectrum (abstract). Bull. Amer. Astron. Soc., 11, 710.

Kurucz, R.L., 1981 - Semiempirical calculation of gf values, IV: Fe II. Smithsonian Astrophys. Obs. Spec. Rep. No. 390, 319 pp.

Kurucz, R.L. and Avrett, E.H., 1981 - Solar spectrum synthesis. I. A sample atlas from 224 to 300 nm. Smithsonian Astrophys. Obs. Spec. Rep. No. 391, 145 pp.

Kurucz, R.L. and Furenlid, I.,1981 - A sample spectral atlas for Sirius. Smithsonian Astrophys. Obs. Spec. Rep. No. 387, 142 pp.

Kurucz, R.L., Furenlid, I., Brault, J., and Testerman, L., 1984 - Solar Flux Atlas from 296 to 1300 nm. National Solar Obs., Sunspot, 240pp.

Kurucz, R.L., and Peytremann, E, 1975 - A table of semiempirical gf values. Smithsonian Astrophys. Obs. Spec. Rep. No. 362 (in 3 parts), 1219 pp.

Kurucz, R.L., Peytremann, E. and Avrett, E.H., 1975 - Blanketed Model Atmospheres for Early-Type Stars. Smithsonian Institution Press, Washington, D.C., 189 pp.

Neckel, H. and Labs,D., 1984 - The solar radiation between 3300 and 12500 A. Solar Physics, 90, 205-258.

Peterson, D.M., 1979 - Personal communication.

Pierce, A.K. and Breckinridge, J.B., 1973 - The Kitt Peak table of photographic solar spectrum wavelengths. Kitt Peak National Obs. Contribution No. 559.

Relyea, L.J. and Kurucz, R.L., 1978 - A theoretical analysis of uvby photometry. Astrophys. Journ. Suppl., 37, 45-69.

Rothman, L.S., Gamache, R.R., Goldman, A., Brown, L.R., Toth, R.A., Pickett, H.M., Poynter, R.L., Flaud, J.-M., Camry-Peyret, C., Barbe, A., Husson, N., Rinsland, C.P., and Smith, M.A.H., 1987 - The HITRAN database: 1986 edition. Applied Optics, 26, 4058-4097.

Strom, S.E. and Kurucz, R.L., 1966 - A statistical procedure for computing line-blanketed model stellar atmospheres with appli-

cations to the F5 IV star Procyon. Journ. Quant. Spectrosc. Radiat. Trans., 6, 591-607.
Sugar, J. and Corliss, C., 1985 - Atomic Energy Levels of the Iron-Period Elements: Potassium through Nickel., Journ. of Phys. and Chem. Ref. Data, vol. 14, Supplement 2.
Vernazza, J.E., Avrett, E.H., and Loeser, R., 1981 - Structure of the solar chromosphere. III. Models of the EUV brightness components of the quiet sun. Astrophys. Journ. Suppl., 45, 635-725.
Vidal, C.R., Cooper, J., and Smith, E.W., 1973 - Hydrogen Stark broadening tables. Astrophys. Journ. Suppl., 25, 37-136.

AUTHOR'S ADDRESS

Harvard-Smithsonian Center for Astrophysics
60 Garden Street
Cambridge, Massachusetts 02138, USA

Keith Butler

Atomic data requirements for stellar atmospheres: work in Munich on hot star atmospheres and winds

ABSTRACT

Recent work on hot stars in Munich is discussed with particular emphasis on the atomic data requirements necessary.

INTRODUCTION

The great improvements in the quality of spectra in recent years are amply illustrated in fig. 1 where optical observations of two B stars from Gehren et al. (1985) are shown. Although

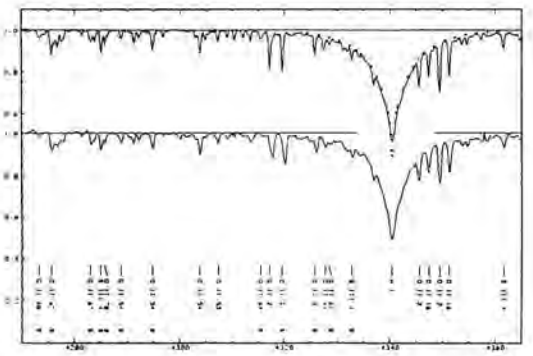

Fig.1 Optical Spectra for two B stars, BS 2928 (upper), S 285-6 (lower). Gehren et al (1985)

the signal to noise ratios are comparable, the object in the lower plot is more than 100 times fainter than that in the upper one. Similar advances have been made in other spectral regions. To make adequate use of such good quality material it has become necessary to construct theoretical models of similar accuracy, firstly to determine astrophysical stellar parameters (temperatures, densities, number fractions) as well as possible and secondly to put tighter constraints on the models themselves. In the case of stellar atmospheres this requires a large amount of atomic data as will be seen from the examples that follow, taken from recent work in Munich.

'STANDARD' MODEL NON-LTE LINE FORMATION CALCULATIONS

'Standard' means that the atmospheres are plane-parallel and are in hydrostatic and radiative equilibrium. While the run of temperature and density with depth is held fixed (line formation), the number densities of the ions in question are allowed to adjust freely to this structure and are not fixed to their thermodynamic values (non-LTE). All of the reported calculations were carried out using the DETAIL, SURFACE, ANALYS suite of programs written by Giddings (1981), the advantage being that the computer time scales linearly with the number of frequency points in the grid so that a large number may be included in the model.

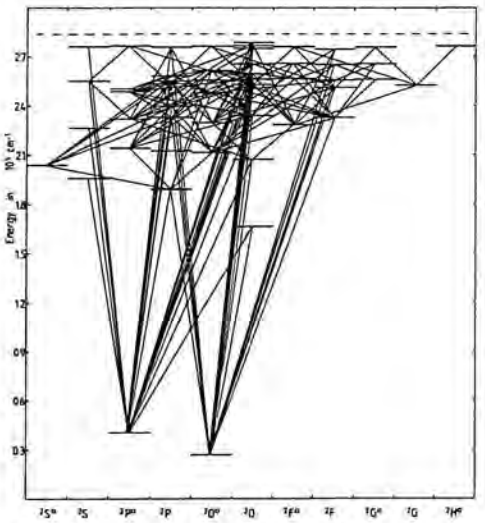

Fig. 2 Model atom for OII calculations (Becker and Butler (1988a). NB. The quartet system was also included in the model.

There are many lines belonging to O II to be seen in fig. 1. Becker and Butler (1988a,b) performed calculations for this ion using the model atom shown in fig. 2. To do this f-values, photoionisation cross sections, collisional excitation and ionisation rates for ALL the levels shown were needed, plus additional data for a few levels of O I and O III. To synthesise the final spectra radiative and collisional damping parameters were also required. The success of the calculation is shown by the fact that the new results show (almost) no sensitivity to the value of the 'microtur-

bulence' adopted. 'Microturbulence' is an ad hoc additional broadening usually necessary to make LTE calculations match the observations. Further details may be found in the cited papers. A similar picture was found for N II (see Becker and Butler 1988c,1989) where again a large amount of atomic data was input.

There has long been a problem with the abundance derived in LTE from the C II 4267 A line, it was consistently much below solar. Our new calculations (Eber and Butler 1988) removed this discrepancy. The atomic model was once more on the same scale as shown previously but in addition it was found that dielectronic recombination also plays a significant role. This was incorporated in the models in the manner suggested by Mihalas and Hummer (1973) whereby the resonances are treated as pseudo-bound states. Oscillator strengths were therefore required in this approximation. The solid curve in fig 3. shows the good agreement obtained with the observed points when solar abundance is assumed.

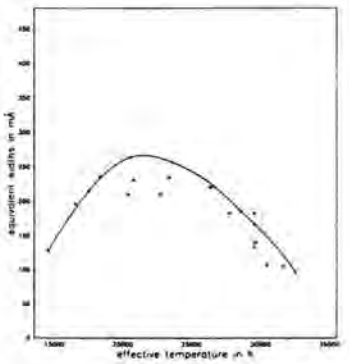

Fig. 3 Comparison of CII calculations (full curve) with observations (points). (Eber and Butler (1988)

These calculations were all designed to allow the abundances in hot stars to be determined with some accuracy. Of course before this can be done it is essential that the other stellar parameters, temperature and density (gravity) also be known accurately. The gravity is usually determined from the shape of the wings of the hydrogen lines which are density sensitive as they are Stark- broadened. On the other hand, the temperature in the range of interest (15000- 35000K) is usually found from the ratios of strengths of the lines of ions of Si. Unfortunately, these lines also depart from the LTE predictions. Becker and Butler (1990) have managed to obtain a consistent picture through similarly extensive calculations to those described above except that this time Si II/III and IV are all treated simultaneously in the same thorough fashion. This consistency is demonstrated in fig. 4. where all the curves cross in a small region. The smallness of this region determines how good a fit may be obtained.

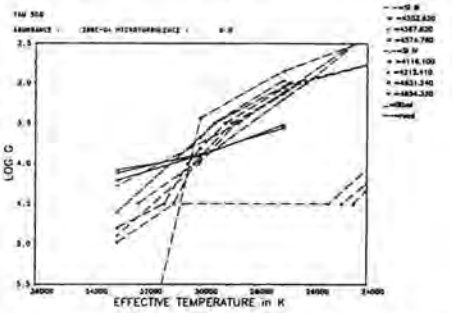

Fig. 4 Fit for various Si (broken) and H (full) lines for Tau Sco (Becker and Butler 1990)

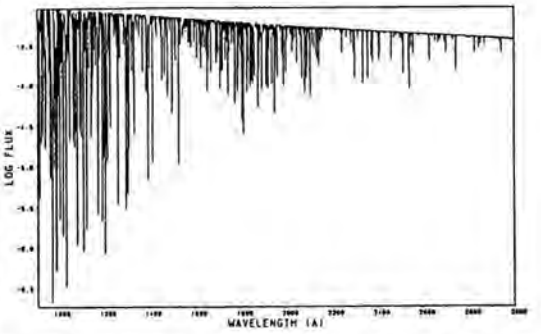

Fig. 5 LTE line blanketing for the B star BS 2928

Admittedly not all the problems have been solved. Some lines are still troublesome. One idea as to where improvements might still be made was the observation that the ionisation thresholds of the levels involved all lie between 1000 and 3000 A. There are many spectral lines in this range that might be expected to affect the lines of interest (see fig. 5). Tests so far indicated that this is not the case but the atomic data (f-values, damping parameters) are of dubious quality.

As a final example, we have just started gathering data for a non-LTE calculation of Fe in order to determine the iron abundance in stars with temperatures of 40000K and upwards. As a first step we have used relatively inaccurate data to generate the spectrum shown in fig. 6. This might give some indication of the magnitude of the problem.

While only line formation calculations have been described here, progress in radiative transfer techniques (Anderson 1989, Werner 1986) makes it likely that models of similar complexity (with the same demanding use of atomic data) will soon be

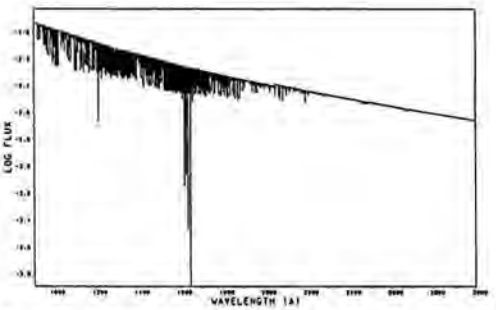

Fig. 6 A synthesised Fe IV/V/VI spectrum for a 60000 K, log g = 6 star

made in which the temperature and density are also allowed to react to this additional opacity (non-LTE line blanketing).

APPLICATIONS

The main goal of the calculations just described was to provide tools to determine accurate stellar parameters. These tools have been put into action in a number of cases. For example, Schoenberner et al. (1988) analysed a number of hot stars which had been designated as being strong in nitrogen. The analysis showed this to be correct, quantified the overabundance and showed helium and carbon to be also overabundant, thus demonstrating that nuclear processed material has been brought to the surface of these stars in conflict with current stellar evolution theories. This point is fully discussed in the paper.

The supernova in the Large Magellanic Cloud in 1987 caused a great deal of excitement. In particular, the spectral type of the pre-cursor was not at all what had been expected. The group in Munich had been studying similar objects (though unfortunately not the SN itself) as part of a program to look at abundances in the LMC (and SMC) and since the tools were at hand, were able to obtain the abundances shown in Table 1 (Kudritzki et al. 1987). Again there is clear evidence

Table 1 Log abundances relative to the sun for two B supergiants and H II regions in the LMC. (Kudritzki et al 1987)

element	Sk 21-65	Sk 41-68	LMC/HII
He	+0.41±0.05	+0.28±0.05	-0.07
C	≤ -0.9	≤ -0.7	-0.77±0.15
N	+0.5±0.2	+0.2±0.1	-1.02±0.1
O	-0.7±0.2	0.0±0.2	-0.49±0.08
CNO	≤ -0.4	≤ -0.2	-0.59
Si	-0.6±0.2	+0.1±0.2	
Mg	-1.1±0.2	-0.9±0.2	
Al	≤ -0.7	≤ -0.6	

for the presence of nuclear processed material, once more showing some disagreement with stellar evolution time scales.

In fact, all of the models had been developed to re-analyse the spectra obtained by Gehren et al. (1985) an example of which is shown in fig. 1. Their LTE analysis showed no evidence for a galactic abundance gradient as can be seen for nitrogen and oxygen in fig. 7. This disagrees with results for H II regions (Shaver et al 1985) where an abundance gradient is observed. If confirmed by the proposed non-LTE investigation this means that theoreticians considering galactic evolutionary models must reconsider their results.

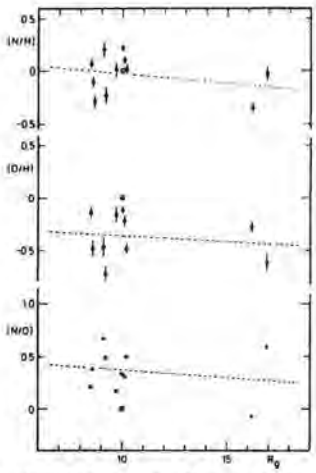

Fig. 7 Log abundances for O and N as a function of galactocentric distance. Note the lack of a gradient. (Gehren et al 1985)

STELLAR WINDS AND UNIFIED MODELS

In the previous section only successful calculations were described. Butler (1984) made calculations for N III which were also in agreement with observation for stars of high gravity (see fig. 8). However, Butler and Simon (1985) using the identical model found a nitrogen overabundance of a factor of six in rough agreement with theoretical estimates but this result must be treated with some scepticism. In particular the value of the microturbulence used is supersonic for a star of this temperature and gravity. This, together with the pattern of the deviations in the line strengths shows the need for stellar wind calculations, in fact for 'unified' models in which the wind and photosphere are treated simultaneously.

The success of the stellar wind calculations alone may be seen from fig. 9 taken from Puls (1987). The fit is almost perfect but there are no adjustable parameters involved. Another beautiful

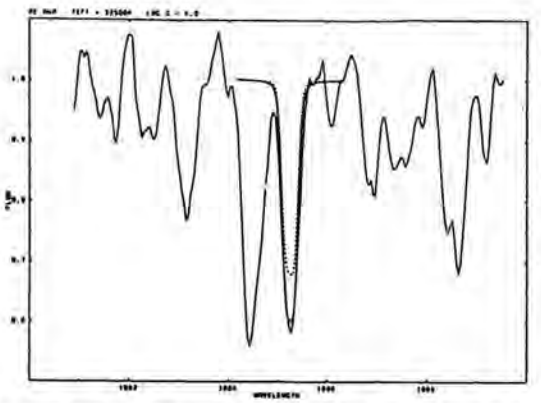

Fig. 8 Fit for the N III 1885 line in AE Aur. Full curve - three times solar abundance, broken - solar. (Butler 1984)

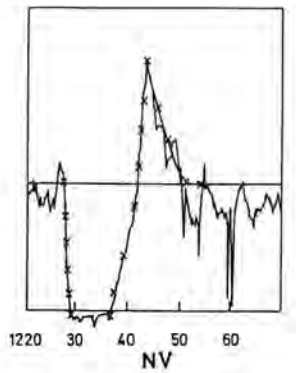

Fig. 9 Fit for the N V resonance line in Zeta Pup (Puls 1987)

example is to be seen in the work of Pauldrach et al. (1989). Walborn and Panek (1984a,b,1985) had observed strong trends in the strengths of the Si IV UV resonance lines with gravity while lines of other ions showed no similar effects. The calculations show exactly the same trends as observed. The reader is referred to the cited papers for details.

Gabler et al (1989) have recently obtained 'unified' photospheric and wind models in which the change in H alpha from a strong absorption line to a very strong emission line can be clearly seen and understood as a consequence of the velocity field. The models may also be able to explain the 'Zanstra discrepancy' in Planetary Nebula as they produce orders of magnitude more flux shortward of the He II Lyman edge than do plane-parallel models.

In making these wind models, non-LTE calculations have been made for a very large number of ions (see Pauldrach 1987 for details) the data for which have been begged, borrowed and generally acquired by every means possible. In addition the winds are assumed to be radiatively driven, i.e. ions absorb photons thereby gaining momentum with a net component away from the star thus forming the wind. To derive the force given to the matter by the radiation integrations over spectra similar in complexity to that shown in fig 6. are necessary throughout the wind. For this once more a huge number of f-values and damping parameters are needed. The current data have been taken from the work of Abbott (1982) but this was intended for temperatures less than 50000K. To extend the wind calculations to higher temperatures f-values and energy levels in particular are needed for Fe, Mn, Ni, Ti, Cr, Cu, Zn for all ionisation stages but especially for those with more than four electrons removed. The data need only have statistically good accuracy but should not be in LS-coupling.

SUMMARY

I hope that it is clear from these few examples that any atomic data you may calculate will always find a good (and useful) home in Munich. There is relatively urgent need for the oscillator strength data described in the last paragraph and all data on iron, preferably not in LS-coupling, would be greatly appreciated.

ACKNOWLEDGEMENTS

I would like to thank the Deutsche Forschungsgemeinschaft for their continuing support of this research under grant Ku 474/13-2, my colleagues for being such avid users of atomic data of all flavours and Dr. Hansen and his crew for their very kind attention to details.

REFERENCES

Abbott, D.C., 1982, Ap. J., 259, 282.
Anderson, L.S., 1989, Ap. J., 339, 558.
Becker, S.R. and Butler, K., 1988a, Astron. Astrophys., 201, 232.
Becker, S.R. and Butler, K., 1988b, Astron. Astrophys. Supp., 74, 211.
Becker, S.R. and Butler, K., 1988c, Astron. Astrophys. Supp., 76, 331.
Becker, S.R. and Butler, K., 1989, Astron. Astrophys., 209, 244.
Becker, S.R. and Butler, K., 1990, Astron. Astrophys. to be submitted.
Butler, K., 1984, Ph.D. Thesis, University of London.
Butler, K. and Simon, K.P., 1985, in ESO Conference and Workshop proceedings No. 21, ed. I.J. Danziger, F. Mateucci, K Kjar.

Eber, F. and Butler, K., 1988, Astron. Astrophys., 202, 153.
Gabler, R., Gabler, A., Kudritzki, R.P., Puls, J. and Pauldrach, A.W.A., 1989, Astron. Astrophys., in press.
Gehren, T, Nissen, P.E., Kudritzki, R.P. and Butler, K., 1985, in ESO Conference and Workshop proceedings No. 21, ed. I.J. Danziger, F. Mateucci, K. Kjar.
Giddings, J.R., 1981, Ph.D. Thesis, University of London.
Kudritzki, R.P., Groth, H.G., Butler, K., Husfeld, D., Becker, S.R., Eber, F., and Fitzpatrick, E, 1987, in Proceedings of the ESO workshop on SN 1987a.
Mihalas, D and Hummer, D.G., 1973, Ap. J., 179, 827.
Pauldrach, A.W.A., 1987, Astron. Astrophys., 183, 295.
Pauldrach, A.W.A., Kudritzki, R.P., Puls, J. and Butler, K., 1989, Astron. Astrophys., in press.
Puls, J., 1987, Astron. Astrophys., 184, 227.
Schoenberner, D., Herrero, A., Butler, K., Becker, S.R., Eber, F., Kudritzki, R.P. and Simon, K.P., 1988, Astron. Astrophys., 197, 209.
Shaver, P.A., McGee, R.X., Newton, L.M., Danks, A.C. and Pottasch, S.R., 1983, MNRAS, 204, 53.
Walborn, N.R. and Panek, R., 1984a, Ap. J., 280, L27.
Walborn, N.R. and Panek, R., 1984b, Ap. J., 286, 718.
Walborn, N.R. and Panek, R., 1985, Ap. J., 291, 806.
Werner, K., 1986, Astron. Astrophys., 161, 177.

AUTHOR'S ADDRESS

Universitaetssternwarte Muenchen
Scheinerstr 1, 8000 Muenchen 80.

B. Baschek

How many lines make a model atmosphere?

ABSTRACT

Present line lists contain of the order of 10^6 to 10^7 lines to be included in model atmospheres. On the other hand, this number is far too large to be considered in the quantitative analysis of atmospheres of supernovae and accretion disks which exhibit differential motions. The question of how many lines are needed to construct reliable model atmospheres is discussed using the distribution of Fe II lines in the ultraviolet as typical example. Estimates of the completeness of line lists are desirable.

LINE ABSORPTION IN MODEL ATMOSPHERES

Most of the information about stellar atmospheres, nebulae etc. is based upon the analysis of spectral lines. The role of the lines is twofold (see e.g. Baschek, 1984): On the one hand, the detailed comparison of observed with synthetic spectra requires the treatment of many individual lines. Accurate atomic data as well as a good model atmosphere are vital e.g. to the determination of reliable element abundances. Since lines usually are blended, complete knowledge of all possible contributors and their atomic data to the line considered is needed. On the other hand, the lines contribute to the absorption coefficient and hence determine the atmospheric stratification. For the bulk of lines (of the order of 10^6 to 10^7) only modest accuracy of their wavelength positions and atomic data is required, but completeness of the line lists (down to a given line strength) is essential.

The twofold role of lines in the model analysis of a spectrum leads to a conflict of interests regarding the need for atomic data. As has been emphasized in many contributions to this Colloquium, clearly more identifications of line transitions, oscillator strengths and other atomic parameters are needed, in particular in the ultraviolet spectral range. On the other hand the question arises how far the enormous number of lines can be reduced to keep the computational effort feasible.

While the modelling e.g. of compact static stellar atmospheres in LTE with 10^6 to 10^7 lines poses no serious problem, the analysis of differentially moving media in particular leads to involved radiative transfer problems. Model atmospheres e.g. of supernovae (Hauschildt et al., 1989 a,b) and of accretion disks (Baschek et al., 1988) require considerable numerical effort which makes the inclusion of a very large number of lines prohibitive. A model maker's nightmare would be to go on revising his models whenever a new, more extended line list should become available.

In this contribution, I would like to address the question of how many lines are needed to construct model atmospheres, not systematically but rather by discussing some relevant aspects on the basis of the distribution of the ultraviolett Fe II lines.

A discussion of the pros and cons of the various methods to deal with larger numbers of spectral lines, the direct approach and statistical methods such as opacity sampling and opacity distribution functions, is given e.g. by Mihalas (1978). In this context, it should be pointed out that opacity distribution functions cannot be utilized for differentially moving atmospheres since here not only information on the line strengths but also on the line distances (Doppler shifts) is required.

DISTRIBUTION OF LINE STRENGTHS

As a typical example we consider the Fe II spectrum in the resonance region 2200-2600 Å. Photographic laboratory spectra of hollow-cathode discharges obtained at the National Bureau of Standards, Gaithersburg, which are used for the term analysis of Fe II contain about 1800 Fe II lines and 800 as yet unidentified lines, i.e. at most 2600 Fe II lines of reliably measurable strength. This corresponds to a line density $\Lambda = 4.5$ or ≤ 6.5 lines $Å^{-1}$, respectively, in the resonance region. The recent line list of Kurucz (1988), utilizing the laboratory analysis by Johansson and Baschek (1988), contains altogether 1265000 Fe II lines of which 71800 are in the resonance range, yielding $\Lambda = 180$ lines $Å^{-1}$.

A simple expression for the strength of an absorption line is $\zeta = gf \exp(-\chi/kT)$ where f

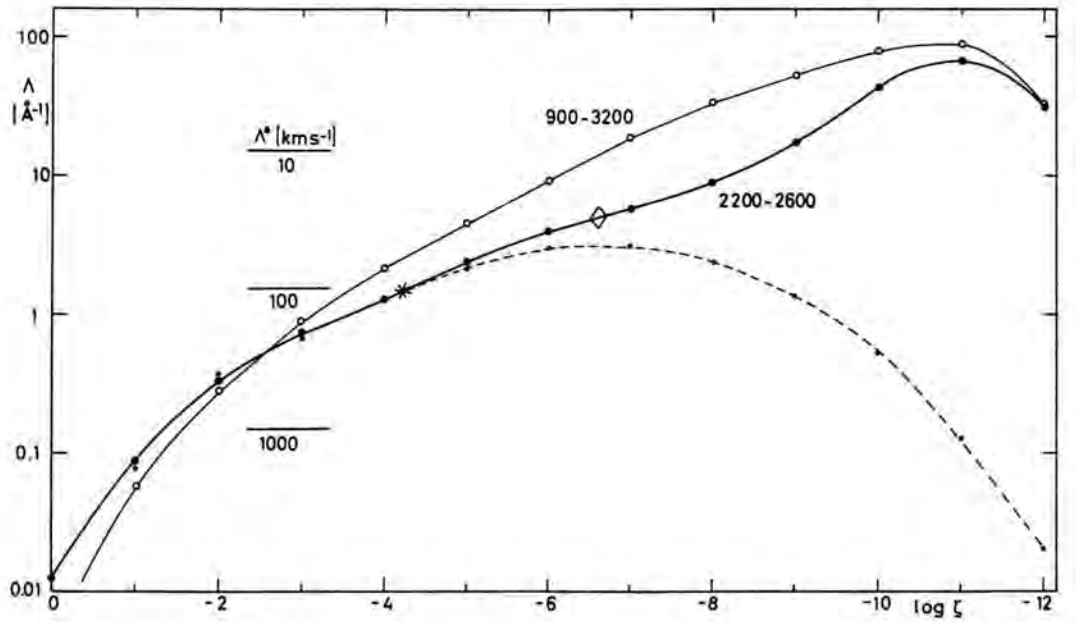

Fig. 1. Line density Λ of Fe II lines in the ultraviolet as function of the "strength factor" $\zeta = gf \exp(-\chi/kT)$ for $T = 10^4$ K according to the line lists of Kurucz (1988; solid curves) and Kurucz and Peytremann (1975; broken curve). Λ refers to the interval of line strengths between 10ζ and ζ.

is the oscillator strength, g the statistical weight, and χ the excitation energy of the lower level. The distribution of the Fe II lines in the resonance range as a function of ζ is shown in Fig. 1 for a temperature $T = 10^4$ K. Comparison of the recent list of Kurucz (1988) with that of Kurucz and Peytremann (1975) demonstrates the progress for lines fainter than $\zeta \simeq 10^{-6}$.

In their calculation of supernova spectra Spies et al. (1989) use an opacity sampling method taking into account lines for which the ratio η of line absorption coefficient in the center to continuous absorption exceeds a given value η_o. η is proportional to ζ and inversely proportional to the Doppler width $\Delta\lambda_D$. Typical parameters, e.g. for SN 1987 A during the first days after outburst, are $T \simeq 10^4$ K and an electron density $n_e \simeq 2.10^{10}$ cm^{-3}. For the microturbulent velocity which determines $\Delta\lambda_D$ a value of 1000 km s^{-1}, i.e. about 1/10 of the expansion velocity, had been adopted. For the model analysis of this supernova spectrum 4700 Fe II lines in the resonance region had been included, corresponding to a (cumulative) density of 12 lines Å^{-1} ('diamond' in fig. 1). Note that the sum over the "strength factor" ζ is determined by the stronger lines, already at $\zeta \simeq 10^{-4}$ convergence to within 1 per cent of its value is reached ('asterisk' in fig. 1). This emphasizes the need to achieve complete lists for lines with large ζ.

In order to estimate how many lines can be resolved in the spectrum we define a saturation line density $\Lambda^* = 1/\delta\lambda$ by setting the separation δλ of lines (considering a group of comparable strength) equal to their half half-widths. For Gaussian profiles

$$\Lambda^* = (\sqrt{\ln 2}\ \Delta\lambda_D)^{-1} \simeq 1.2/\Delta\lambda_D$$

with $\Delta\lambda_D = \lambda_o \cdot v/c$, v being the most probable thermal plus microturbulent velocity. The characteristic order of magnitude for stellar atmospheres, novae and supernovae is v = 10, 100, and 1000 km s^{-1}, respectively. At λ_o = 2400 Å this corresponds to $\Delta\lambda_D$ = 0.08, 0.8, and 8 Å or to Λ^* = 15, 1.5, and 0.15 lines Å^{-1}.

As long as the actual line density $\Lambda < \Lambda^*$, the lines have to be treated individually. On the other hand, if $\Lambda > \Lambda^*$ the lines form a quasi-continuum which may be added to the other continuous opacities. The fluctuating part of this quasi-continuum is proportional to the square root of the line density, with amplitudes and wavelength positions showing little resemblance to the individual lines.

The comparison of Λ^* with the Fe II line distribution (fig. 1) indicates that e.g. supernova models for a microturbulent velocity of 1000 km s^{-1} would not need very many lines (of Fe II in the resonance region) to be included. Stellar model atmospheres with $v \lesssim 10$ km s^{-1}, however, require consideration of the lines almost to the present limit of Kurucz' list. A systematic study of the dependance of the line distribution with wavelength for all relevant atoms and ion would be desirable.

The above estimates of the contribution of lines in terms of ζ (or η) and $\Delta\lambda_D$ are too simplified. Besides these parameters the atmospheric structure influences the line strengths, e.g. via temperature or velocity gradients, and hence the detectability of lines.

How can now atomic spectroscopy provide information on bulk line strengths and their completeness in accord with the astrophysical criteria? A systematic evaluation e.g. of the sums over gf $\exp(-\chi/kT)$ for all important elements and ionization stages in a set of wavelength intervals would be very valuable, possibly using f sum rules and the dependence of f on the quantum number n. It may be helpful to divide the level diagram into series with the same ionization limit in order to extrapolate from the known lines of lower n towards the limit. The confluence of lines before the limit to an effective continuum is determined either by the Doppler width or by the Stark broadening. In this context, it should also be realized that the continua of more complex atoms are not smooth functions (as is frequently assumed in model atmosphere codes) but exhibit marked structure due to resonances, e.g. in the case of Fe I (Hansen et al., 1977). Some of these structures might be observable, e.g. in the ultraviolet continua of neutral atoms in A stars, in spite of the crowding of lines.

CONCLUSION

Quantitative analysis of atmospheres with differential motions, e.g. of supernovae and accretion disks, involves considerable effort for the construction of models and the treatment of radiative transfer. This raises the question to what extent the number of lines contributing to the opacity can be reduced. This problems deserves a systematic investigation of line distributions and their completeness by combining astrophysical criteria with methods of atomic physics.

ACKNOWLEDGEMENT

I would like to thank R.L. Kurucz for putting his line list at our disposal, and M. Best and P.H. Hauschildt for information on Fe II lines in supernova models.

REFERENCES

Baschek, B., 1984 - The Role of Oscillator Strengths in Modelling and Analysing Stellar Spectra. In: Physica Scripta, T8, 21-24.

Baschek, B., J. Adam, R. Plate, H. Störzer and R. Wehrse, 1988 - Line radiation from accretion discs:Spatially resolved distribution. In: Adv. Space Res. 8, (2) 315-(2)319.

Hansen, J.E., B. Ziegenbein, R. Lincke and H.P. Kelly, 1977 - Observation and interpretation of the photoionization cross section of the neutral iron atom (Fe I). In: J. Phys. B: Atom. Molec. Phys. 10, 37-45.

Hauschildt, P.H., G. Shaviv and R. Wehrse, 1989a - Theoretical models for the continuum and colors of SN 1979C and SN 1980K. In: Astron. Astrophys. 210, 262-272.

Hauschildt, P.H., G. Shaviv and R. Wehrse, 1989b - An atlas of calculated continuum energy distributions for supernovae of type II. In: Astron. Astrophys. Suppl. Ser. 77, 115-123.

Johansson, Se. and B. Baschek, 1988 - Term analysis of complex spectra: New experimental data for Fe II. In: Nucl. Instr. Methods Phys. Res. B 31, 222-232.

Kurucz, R.L., 1988 - private communication.

Kurucz, R.L. and E. Peytremann, 1975 - A Table of Semiempirical gf Values. Smithsonian Astrophys. Obs. Special Report 362.

Mihalas, D., 1978 - Stellar Atmospheres. W.H. Freeman, San Francisco.

Spies, W., P.H. Hauschildt, R. Wehrse, M. Best, G. Shaviv, A. Cassatella, R. Gilmozzi, L. Sanz Fernandez de Cordoba, W. Wamsteker and N. Panagia, 1989 - Model atmospheres for SN 1987 A during the first days after outburst. In: Astron. Astrophys., submitted.

AUTHOR'S ADDRESS

Institut für Theoretische Astrophysik
der Universität Heidelberg
Im Neuenheimer Feld 561
D-6900 Heidelberg
Federal Republic of Germany

Fiorella Castelli and Piercarlo Bonifacio

A computed spectrum for the normal star ι Her (B3 IV) in the Region 1228–1950 Å

ABSTRACT

We have compared high resolution IUE and Copernicus spectra of the sharp-lined normal star ι Her (B3 IV) in the region 1228-1950 A with an LTE synthetic spectrum, in order to investigate to what extent we are able to reproduce observations of B stars in far UV with the available line data and models. We have found that in spite of the great number of lines used for computing the spectrum, more lines must be added. Furthermore, we have obtained a large scatter in the abundances for nearly all the elements investigated, in agreement with the results of Peters and Polidan (1985) for the same star.

THE DATA AND THE DATA ANALYSIS

The observational data used for this study are the following: a) The Copernicus ultraviolet spectral Atlas by Upson and Rogerson (1980) from 1228 to 1467.7 A. b) The IUE HR images SWP5720 from 1228 to 1950 A and SWP3243 from 1467.7 to 1950 A, taken from the IUE archive. SWP5720 was reprocessed with the new software IUESIPS2.

We have compared the spectra in the whole range studied by superimposing two different images normalized to the continuum. This comparison, as well as the comparison with the synthetic spectrum, have shown that the resolution of the reprocessed IUE image SWP5720 is comparable with that of the second order Copernicus spectrum (nominal resolution 0.05 A from 999.3 to 1422.2 A), while the FWHM in SWP3243 is larger.

The model parameters Teff=17180±110 K and log g=3.43±0.02 for ι Her have been derived with a fit of the observed Strömgren indices c_0=0.290 and β=2.661 to the computed ones of the grid of Lester et al. (1986). The index c_1=0.294 has been dereddened by means of the UVBYBETA code (Moon, 1985), which makes use of empirical calibrations. The values of the observed indices c_1 and β have been taken from Hauck and Mermilliod (1980).

A model computed with the ATLAS8 code (Kurucz,1970) and the atomic line lists provided by Kurucz (1988) have been used in the SYNTHE code (Kurucz and Avrett,1981) to obtain a synthetic spectrum. We have made some changes in the log gf of CI, CII, SiII, SiIII of Kurucz's line lists.

The input line lists for computing the synthetic spectrum in the region 1228-1950 A have a total number of about 76000 lines.

As a first step we have adopted, for all elements, the photospheric solar abundances of Anders and Grevesse (1989).

SOME RESULTS FROM THE COMPARISON

1) Broadening Velocities: By comparing large regions of the observed spectrum with spectra computed with different values of macrovelocity V (rotational +macroturbulent+ instrumental) and microturbulence ξ, we have found that the best agreement is given by ξ= 0 Km/s and V= 15 Km/s for Copernicus and IUE SWP5720 spectra and V =20 Km/s for the IUE SWP3243 image.

2) Identification: A very high number of the observed features can be readily identified, and at first glance the agreement between observed and computed spectra seems good. However, some strong features are still unidentified and several blends require either more predicted components or different log gf for the predicted lines. We have compared our identification with those made by Upson and Rogerson (UR)(1980) for ι Her and by Artru et al. (1989) for the B stars π Ceti and ν Capricorni. We have found that some lines are missing in Kurucz's lists. Furthermore, the SiII lines identified by Artru (1986), some lines of Moore's tables (1950), and all the CuIII lines are also missing. However,numerous lines correctly predicted by using our line data and model are not considered by Upson and Rogerson (1980) and by Artru et al. (1989). We have inserted in Kurucz's lists the lines for which we have found the corresponding atomic data in the literature; the most important are the lines of Ga III at 1495 and 1534 A.

3) Abundances: To determine the abundances we have compared, for each image, the observed profiles of several lines with the profiles computed by changing the starting solar abundance at steps of about 0.25 dex. Nearly always the abundances derived from the same lines of different images agree remarkably well. We have found that different ionisation states of the same element and different lines of the same ionisation state can yield different abundances.

In Table 1 we compare our results with those of Peters and Polidan (PP)(1985), who analysed both the UV and visual spectra of ι Her. The solar abundances from Anders and Grevesse (AG) (1989), relative to the total number of atoms, are also given for comparison. The large errors in the derived abundances given by Peters and Polidan confirm the scatter found by us. However, for PII, PIII and SiIV, our results clearly disagree with those of Peters and Polidan (1985).

Table 1: Abundances logϵ for some elements.

	Sun (AG)	ι Her(This paper)		ι Her (PP)
B	-9.44	BII	-10.00	
C	-3.48	CI	-4.75 to -4.00	
		CII	-3.75	-3.62±0.46
		CIII	-3.48	-3.13
N	-3.99	NI	-4.50 to -5.00	
		NII		-4.15±0.39
O	-3.11	OI	$\geq$-3.11	-3.05±0.15
		OII		-3.38±0.44
Mg	-4.46	MgII	-4.46	-4.62±0.09
Al	-5.57	AlII	-5.75 to -6.0	
		AlIII	-5.75	-5.62±0.24
Si	-4.49	SiII	-4.49 to -4.75	-5.00±0.47
		SiIII	-4.49	-4.63±0.44
		SiIV	-4.00	-4.65
P	-6.59	PII	-7.5 to -6.59	-5.67±0.55
		PIII	$\geq$-6.59	-7.02±0.60

The close analogy with the results of an abundance analysis performed by Castelli et al.(1985) from the UV spectrum of the peculiar Bp star HR 6000 seems to indicate that the scatter in the abundances is probably due to the model and to the atomic data available, rather than to the quality of the data and to stellar peculiarities.

REFERENCES

Anders,E.,Grevesse,N.:1989, Geochimica et Cosmochimica Acta 53, 197.

Artru,M.C.: 1986,Astron. Astrophys. 168,L5-L6

Artru,M.C.,Borsenberger,J.,Lanz,T.:1989, Astron. Astrophys. Suppl., in press.

Castelli,F. Cornachin,M., Hack,M., Morossi,C.:1985, Astron. Astrophys. Suppl. 59,1.

Hauck,B.,Mermilliod,M.:1980, Astron. Astrophys. Suppl.40, 1.

Kurucz,R.L.:1970, SAO Special Report 309.

Kurucz,R.L.:1988,private communication.

Kurucz,R.L.,Avrett,E.H.:1981, SAO Special Report 391.

Lester,J.B.,Gray,R.O.,Kurucz,R.L.:1986, Astrophys.J. Suppl.61, 509.

Moon,T.T.:1985, "Stellar Parameters from Strömgren Photometry: Fortran Programs", Comm. Univ. of London Obs. No. 78.

Moore, C.E.:1950, NBS Circular 488.

Peters,G.J.,Polidan,R.S.:1984, IAU Symp. 111, 121.

Upson II,W.L.,Rogerson,Jr.,J.B.: 1980, Astrophys. J. 42, 175.

AUTHOR'S ADDRESS

Osservatorio Astronomico di Trieste,
Via G.B. Tiepolo 11, 34131 Trieste, Italy.

Marie-Christine Artru

Atomic data and stellar chemical peculiarities for the elements Z=6 to 20

ABSTRACT

Current studies of main-sequence stars showing chemical anomalies, are briefly presented from the point of view of their connection with atomic spectroscopy. Analysis of their observed spectra and theoretical interpretation of their chemical peculiarities are shown to be strongly dependent on the amount of available atomic data and, to a lesser extent, on the accuracy of these data. We review the recent compilations available for laboratory wavelengths and transition probabilities of the elements Z=6 to 20. It is pointed out that some incompleteness may occur even for these light elements. A few examples concerning Si II are detailed to stress the astrophysical importance of progress in the study of high-excitation transitions and autoionisation.

1. INTRODUCTION

Investigation of stellar atmospheres requires a lot of atomic data from laboratory physics and, conversely, the stellar plasmas allow to observe experimental conditions that can not be reached in experiments. We will review some aspects of current studies of chemical peculiarities in main-sequences stars.

The scope of this paper is limited to the elements Z=6 to 20, from carbon to calcium. This avoids questions which are specific to the lighter elements and the severe problems raised by the heavier elements. The intermediate elements have generally well-established spectroscopic properties and they are favourable cases for constructing refined astrophysical models about stellar atmospheres, such as non-LTE transfer, abundance inhomogeneity, macroscopic movements and radiative diffusion. We will consider main-sequence stars of spectral types A and B (effective temperatures from about 7000 to 20000 K), with emphasis on those (about 20%) which show chemical anomalies by reference to a "normal" composition, close to the solar one. The proceedings of Cowley et al. (1986) review recent progress in understanding these peculiar stars. A great variety of chemical anomalies are found, often varying with time according to the stellar rotational phases. Therefore they offer the opportunity of differential studies, and, thanks to the continuous improvement of the observational performances, they may even appear as natural spectroscopic experiments.

Section 2 presents some astrophysical problems which are closely connected to atomic data. We give some details concerning the identification of the numerous observed lines in the UV spectra of hot stars. Then we briefly review the determination of elemental abundances and the theoretical computation of radiative forces acting on atoms and ions. These two steps are important to develop models of radiative diffusion to explain the chemical separation of elements. Section 3 recalls the available updated compilations of basic spectrocopic data and discuss some recent progress. Section 4 reports a few examples from our studies about Si II in stellar spectra, in order to illustrate their connexion with atomic physics.

2. ASTROPHYSICAL QUESTIONS ABOUT CHEMICALLY PECULIAR STARS

Identification of ultra-violet lines in stellar spectra

The ultra-violet spectra of A and B stars contains numerous absorption lines of atoms and ions, their density being much larger than in the visible range at similar wavelength dispersion. High-resolution spectral observations in the ultra-violet have already been obtained by the Copernicus satellite and by the International Ultraviolet Explorer (IUE), much more is expected soon from the Hubble Space Telescope (see the contribution of Leckrone et al, in these proceedings). Since its launch in 1978, the IUE satellite has recorded thousands of stellar spectra covering the range 115-320 nm, with a resolution of 10^4. Therefore it has already contributed greatly to extend the observational basis for many detailed investigations of physical processes in stellar atmospheres (see Kondo et al., 1987).

To interpret the new ultra-violet stellar spectra, one must correctly identify the species which account for the observed lines or features. This task is often difficult because of the large number of observed lines and the frequent occurrence of blends. For example there is a controversy about the appearance of the C IV and Si IV resonance lines in the UV spectra of some B stars: if present they may reveal superionization processes in the stellar atmospheres, but Hubeny et al (1985) have pointed out the risk of erroneous identifications due to blending lines, underlining the importance of careful identification work. In Ap stars the enhancement of rare elements may be detected by observing ultra-violet resonance lines of their ions, but these are generally weak and often blended: a correct identification is crucial and generally requires that all the lines of abundant elements have previously been recognized in the studied range.

A detailed line identification is also an important preliminary step when studying low dispersion spectra, especially to determine the origin of observed absorption features. An illustration is given in Fig. 1 which shows the rotational variation observed in a low-dispersion ultra-violet spectrum of a peculiar star (Artru and Freire, 1988): several absorption features appear to vary differently from

one phase to the other. This reveals inhomogenous surface abundances of the corresponding absorbers. At low resolution, single resonance lines (C II, Si II, Ga II) are readily recognized, but other features are not easily identified when they correspond to a local accumulation of medium lines from a complex spectrum. For instance, a large variation occurs at 142 nm (Fig.1) which can be attributed to titanium, since four Ti III lines has previously been identified at this wavelength by inspecting high-resolution spectra. These lines appears on the spectra of two stars with similar effective temperature (see Fig.2).

Much work has already been done to provide extensive lists of identified ultra-violet lines in various types of stellar spectra. Several published atlases of A and B stars are based on observations from the Copernicus satellite (one of Sirius by Rogerson, 1987, others are referenced therein). The IUE spectra displayed in Fig.2 are taken from our recent atlas of two normal B stars (Artru et al, 1989). It gives an identification for about 80% of 1460 lines measured in the short spectral range (125-198 nm). Most of the listed transitions (about 75%) belong to elements heavier than Z=20 (Fe II and Fe III being preponderant) and this proportion is expected to be even larger in the long wavelength range of IUE.

Systematic procedures of line identification must be based on a suitable list of laboratory wavelengths, including the most complete up-to-date data, but restricted to the atomic transitions which have a reasonable chance to give an observable stellar line. Because of the high probability of fortuitous wavelength coincidences in the ultra-violet, it is necessary to use other criteria of identification, usually based on predicted line intensities. This would require the knowledge of all oscillator strengths in the line list, which is generally far from being the case.

Methods of wavelength coincidence statistics (see Cowley and Merritt, 1987 and references therein) overcome the difficult identification of each individual line of complex spectra. They allow an objective and quick detection of rare elements from the crowded ultra-violet stellar spectra. However they also require complete atomic line lists, at least for the studied species, and even oscillator strengths in their most sophisticated versions.

Abundance determination

The quantitative abundance studies have always provided the basic observational constraints on the theoretical interpretation of chemical anomalies in stars. They must be further developped to fully benefit from numerous recent progress: modern detectors, ultra-violet observations, refined atmosphere models and accurate atomic data.

A review of abundances in A stars, including the Am and Ap peculiar stars, was given by Wolf (1983). Also Cowley and Adelman (1983) have discussed the different techniques to increase the accuracy of stellar abundance

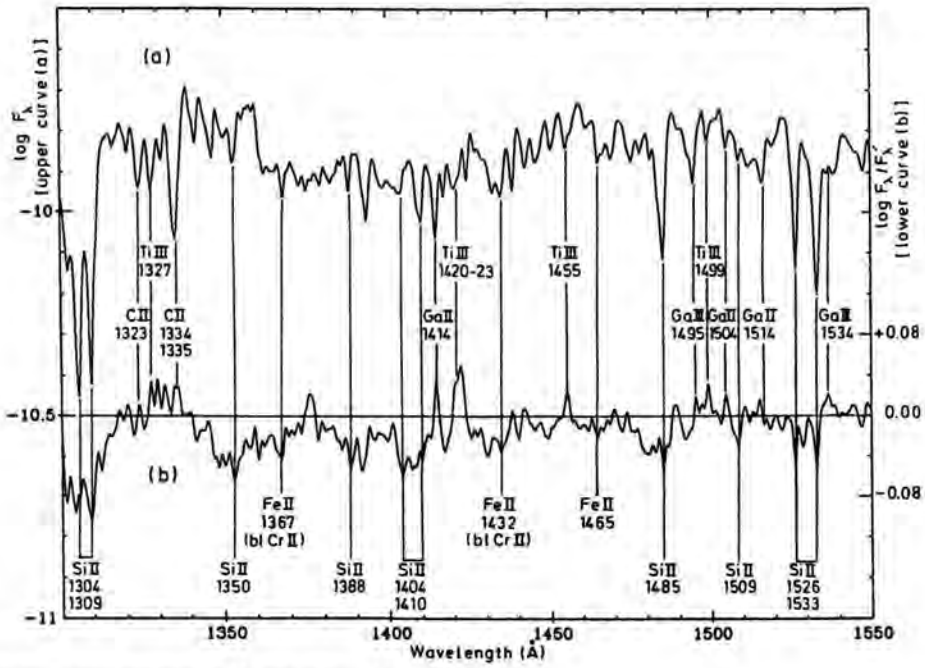

Fig. 1. Low-resolution spectrum of the star HD25823 (upper curve a) and ratio of two spectra recorded at different phases (lower curve b). From Artru and Freire-Ferrero (1988)

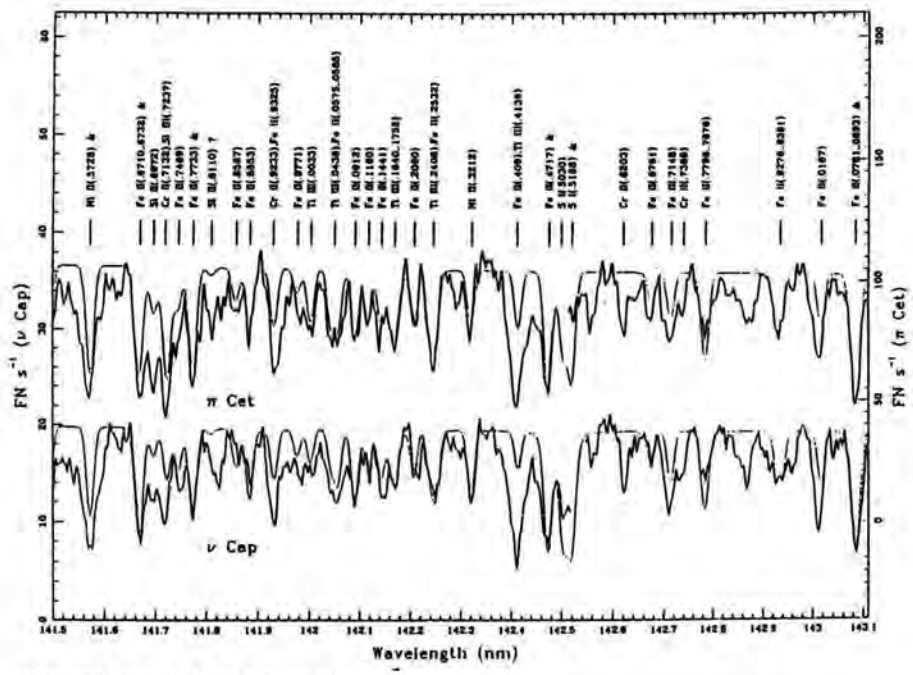

Fig .2. High-resolution spectra of two B stars: IUE observation (solid line) and LTE synthetic calculation (dotted lines). From Artru et al (1989)

determinations. Recent results are summarized in the proceedings of Cowley et al (1986) by Sadakane for hot stars (p.369), by Dworetsky for Hg-Mn stars (p.397), and by Boyarchuk and Savanov for Am stars (p.433). There is still a need for collecting reliable abundances for many elements in extended samples of peculiar and comparison stars. Such a study was done for Hg-Mn stars by Guthrie (1984). Series of consistent data are available from systematic abundance determinations in A and B stars by Adelman (1988) and Kocer et al (1987), earlier references being given therein. A recent workshop (Adelman and Lanz, 1988) achieved a decisive step towards clarifying the difficulties of this task, by means of a thorough comparison between independent elemental analyses of the same observational data (co-added visible spectra of two peculiar stars, o Peg and ϕ Her). Abundance of the elements C, Mg, Al, Si, S and Ca were determined with basically the same set of atomic data and the largest discrepancies obtained were typically about 0.2-0.3 dex.

The interpretation of ultra-violet spectra by synthetic computation requires preliminary reliable abundances. For instance Sadakane and Ueta (1989) have carefully redetermined abundances of 14 elements in Sirius from photographic spectra. Conversely, some ultra-violet lines, especially the strong resonance ones, can be used to determine abundances. This has been done for aluminum by Sadakane et al (1983) who confirm the general underabundance of this element in Ap star. Because of the heavy line blending in the ultra-violet, abundances must be derived by means of synthetic computations, often done in the LTE approximation. Then one or several abundances are adjusted as parameters to fit the observed spectrum. Such an exhaustive study of IUE spectra was done by Castelli et al (1985) for the He-weak star HR6000.

A number of abundances have been derived by Lanz (1987) in a sample of silicon stars,both from visible and ultra-violet spectra. The study of silicon in the ultra-violet is detailed by Artru and Lanz (1987). The silicon overabundances were found significantly smaller (2 to 5 times) than those deduced from the visible lines. These discrepancies are only partly explained by underestimates of the line damping in the visible (Lanz et al, 1988) and a strong departure from the LTE populations is expected.

The abundant elements, carbon, nitrogen and oxygen suffer from a severe lack of reliable abundance data although their study is of special importance in the context of the diffusion theory (Michaud, 1976, 1987). In the optical range they have been observed mainly by red or infra-red high-excitation transitions of the neutral atoms (Lambert et al, 1982; Faraggiana et al, 1988; Roby, 1987), while their stronger blue or UV lines may be affected by non-LTE effects (Lennon 1983, Lanz 1987). These elements are also essential in many stellar investigations related to the chemical history of the galactic material. For instance, Adelman et al (1986) have studied them in horizontal-branch stars.

Computation of radiative forces

The theory of radiative diffusion of elements gives a convincing explanation of chemical peculiarities observed in main-sequence stars: as a result of the competition between stellar gravity and radiative acceleration, a given element may be pushed up and accumulate on the stellar surface. Michaud (1976) gives the basic equations which allow to evaluate radiative accelerations. Further developments of the diffusion theory have been reviewed in Cowley et al (1986): in particular Alecian (p.381) discuss the role of magnetic fields and Michaud (p.459) the effects of stellar hydrodynamics, such as mass loss.

The first step of any diffusion model is the calculation of radiative accelerations: it involves the probabilities of all photoabsorption processes (lines and photoionisation) for every populated states of every ion, at each depth of the stellar atmosphere. Moreover the radiative acceleration due to a saturated line depends strongly on the broadening effects and on possible blends with other strong lines. Therefore, as recently pointed out by Michaud (1987), there are important needs for atomic data (up to high ionization stages) to calculate the radiative accelerations with sufficient accuracy (typically 30%).

Although the light elements are favourable cases, detailed calculations of their radiative acceleration in stellar atmospheres are still scarce. Complete non-LTE computations have been performed by Borsenberger et al (1981, 1984) for some of the alkaline-earths. The radiative diffusion of silicon has been calculated by Alecian and Vauclair (1981) who found that its accumulation is sensitive to the magnetic field.

3. Sources of basic atomic data

A great number of atomic lines should be introduced in any refined calculation concerning the stellar atmospheres of normal and peculiar stars. Therefore all exhaustive up-to-date compilations of basic atomic data are invaluable tools to insure the completeness and the quality of the astrophysical interpretations. Compared with heavier elements, those we consider here (Z= 6 to 20) are favourable cases, since their spectra have relatively simple structures and most of them have already been thoroughly studied.

Compilations of energy-levels and multiplet tables

C I to VI	Moore, 1970 (sect.3)
N I to III	Moore, 1975 (sect.5)
N IV to VII	Moore, 1970 (sect.4)
O I	Moore, 1976 (sect.7)
O III	Moore, 1985 (sect.11)
O IV	Moore, 1983 (sect.10)
O V	Moore, 1980 (sect.9)
O VI to VIII	Moore, 1979 (sect.8)
Na I to XI	* Martin and Zalubas, 1981
Mg I to XII	* Martin and Zalubas, 1980
Al I to XIII	* Martin and Zalubas, 1979
Si I	Moore, 1967 (sect.2)
Si II to IV	Moore, 1965 (sect.1)
Si I to XIV	* Martin and Zalubas, 1983
P I to XV	* Martin et al, 1985
K I to XIX	* Corliss and Sugar, 1979
Ca I to XI	* Sugar and Corliss, 1979

* compilations of energy-levels only

The original NBS tables of atomic energy levels and multiplets still provide a basic source of spectroscopic data, thanks to the exceptionally good quality of these early data. They have been up-dated for a number of light elements as summarized in the following table. A finding list has been prepared by Adelman et al (1985).

Fairly complete data in the ultra-violet range are now available thanks to the new publications of Kelly (1979, 1987) who provides invaluable lists of classified lines (with convenient access to the original references, updated to 1977 and 1981) and their finding lists including all spectra of elements up to Z=36. Therefore at the moment the main need for updated finding lists is actually in the optical region. The NBS report from Reader and Corliss (1980) has the advantage of covering the whole spectral range and of including all heavy elements, but it gives a limited list of lines, selected on the basis of their intensity in emission spectra, and it does not provide any classification or excitation energy of the transitions.

Compiling transition probabilities is quite a difficult task because there is a wide variety of methods of determination and the true accuracy of published results is often hard to estimate. The NBS compilations of Wiese et al (1966,1969) are still widely used. A new list of critically evaluated transition probabilities has been published by Wiese and Martin (1980) for selected atomic and ionic transitions. Other compilations exist for the Li-like spectra (Martin and Wiese, 1976) and for Si II (Lanz and Artru, 1985). One is in preparation for the Be-like ions of carbon, nitrogen and oxygen (Allard et al, 1989). For example, to compile the gf-values of C III published since 1966, 45 new references were found with theoretical results, and 13 with lifetime measurements, allowing us to list oscillator strengths for one hundred new multiplets.

The NIST (NBS) bibliographical data base is a major help in extracting the best updated results from the literature. Commission 14 of the IAU gives regular lists of references, selected for their usefulness in astrophysics: the last one (Swings, 1988) contains hundreds of new publications from 1984 to 1987; a large part of them is still devoted to extended spectral analyses or new oscillators strengths, even for light elements.

Extensive computations of theoretical atomic data are very promising for many stellar applications. Their importance has been proved by the continuing use of the early data of Kurucz and Peytremann (1975) by astrophysicists. The international collaboration on the OPACITY project of Seaton (1987) is producing a lot of very accurate data (see his contribution to this colloquium).

4. Examples concerning Si II in the spectra of Ap stars

The Si II spectrum is an important contributor to the opacity in the photosphere of A and B stars and all its features are enhanced in the case of peculiar silicon stars. From our studies related to this spectrum, we will borrow some illustrative examples showing the close interaction between stellar and atomic spectroscopy.

The Si II lines appear so strongly in the IUE ultra-violet

spectra of A and B stars, even with normal abundance, that we can identify additional transitions which were not previously listed, neither in the laboratory lists (Kelly, 1987), nor in the list due to Kurucz and Peytreman (1975). For instance the stellar spectra shows a new doublet ($3s3p^2\ ^2D$--$3s^210f\ ^2F^o$) for which wavelengths can be predicted from known levels. A few such identifications have been made in our stellar atlas (Artru et al, 1989) for Si II and Ca II; others may still be missing for very abundant species. A new Si II identification in IUE spectra of Ap stars was given by Artru (1986, Fig.1): in this case the upper levels $3s3p(^1P)3d\ ^2D^o$ were previously unknown and we have established the identification simultaneously on laboratory and stellar spectra.

Our second Si II example concerns the autoionising transition $3s^23d^2D$ -$3s3p(^1P)\ ^2F^o$ which explains the wide depression, observed at 140 nm in silicon stars (Artru, 1986). This transition comes from a known excited level ($3s^23d\ ^2D$ at 9.84 eV) to an upper level which is theoretically predicted as strongly autoionising. Figure 3 shows its effect on the calculated spectrum of a silicon star. This identification was confirmed by synthetic calculations applied to several peculiar stars and compared to the IUE

Fig. 3. Synthesis of the Si II autoionizing line (lower spectrum, solid line) and observed IUE spectrum of the silicon star HD34452 (upper spectrum). From Artru (1986)

observations (Artru and Lanz, 1987). It is also consistent with the new theoretical energies of the $3s3p(^1P)3d$ states, computed by Le Dourneuf et al (1989). Nevertheless there exists no laboratory measurement of this photoionisation resonance which has actually been located at 140 nm by means of stellar observations.

In Fig.3 the strong observed Si II blend at 148.5 nm is badly reproduced by the calculation. This has been corrected later, as detailed in Artru and Lanz (1987), by revising the autoionisation width of the high-excitation transition to $3s3p(^3P)3d\ ^2F^o$. In a cooler star this blend is dominated by the other Si II transition of lower excitation (3d-7f) and, taking this into account, we have obtained a satisfactory interpretation by correctly re-evaluating the Stark broadening. This underlines the importance of correctly introducing line broadening in the synthesis of strong stellar lines.

AKNOWLEDGMENTS

I thank J. Hansen for improvement of this contribution.

REFERENCES

Adelman, S. J.: 1988, Mon. Not. R. astr. Soc. 235, 749 and 763

Adelman, S. J., Lanz, T., eds: 1988, " Elemental Abundance Analyses", Publ. Institut Astronomie de Lausanne

Adelman, C.J., Adelman S. J., Fischel, D., Warren, W.H.: 1985, Astron. Astrophys. Suppl. Ser. 60, 339

Adelman, S.J., Hayes, D.S., Davis Philip, A.G.: 1986, Publ. Astr. Soc. Pacific 98, 783

Alecian, G., Vauclair, S.: 1981, Astron. astrophys. 101, 16

Allard, N., Artru, M.-C., Lanz, T., Le Dourneuf, M.: 1989, to be submitted to Astron. Astrophys. Suppl. Ser.

Artru, M.-C.: 1986, Astron. Astrophys. 168, L5

Artru M.-C., Lanz, T.: 1987, Astron. Astrophys. 182, 273

Artru M.-C., Freire Ferrero R.: 1988, Astron. Astrophys. 203, 111

Artru M.-C., Borsenberger, J., Lanz, T.: 1989, Astron. Astrophys. Suppl. Ser., in press

Borsenberger, J., Michaud, G., Praderie, F.: 1981, Astrophys J. 243, 533 and 1984,139,147

Castelli, F., Cornachin, M., Hack, M., Morossi, C.: 1985, Astron. Astrophys. Suppl. Ser. 59, 1

Corliss, C., Sugar, J.: 1979, J. Phys. Chem. Ref. Data 8, 1109

Cowley C.R., Adelman, S.J.: 1983, Quaterly J. Roy. Astr. Soc. 24, 393

Cowley C.R., M.M., Mégessier, C., eds, 1986, "Upper Main Sequence Stars with Anomalous Abundances", Proceedings of the 90th colloq. IAU, Reidel Publ.

Cowley C.R., Merritt D.R.: 1987, Astrophys. J. 321, 553

Faraggiana, R., Gerbaldi, M., van't Verr, C., Floquet, M.: 1988, Astron. Astrophys. 201, 259

Guthrie, B.N.G.: 1984, Mon. Not. R. astr. Soc. 206, 85

Hubeny, I., Stefl, S., Harmanec,P.: 1985, Bull Astron. Inst. Czechosl. 36, 214

Kelly, R.L.: 1979, " Atomic Emission Lines in the Near Ultraviolet. Hydrogen through Krypton", Techn. Mem. 80268, NASA

Kelly, R.L.: 1987, "Atomic and Ionic Spectral Lines Below 2000A: Hydrogen through Krypton", J. Phys. Chem. Ref. Data 16, Suppl. 1

Kocer, D., Bolcal, C., Inelmen, E., Adelman, S.J.: 1987, Astron. Astrophys. Suppl. Ser. 70, 49

Kondo, Y., Wamsteker, W., Boggess, A., Grewing, M., de Jager, C., Lane, A.L., Linski, J.L., Wilson, R., eds, 1987, "Exploring the Universe with the IUE Satellite", Reidel Publ.

Kurucz, R.L., Peytremann, E.: 1975, SAO Special Report 362

Lambert, D.L., Roby, S.W., Bell, R.A.: 1982, Astrophys. J. 254, 663
Lanz, T.: 1987, Ph D Thesis, Geneva Observatory
Lanz, T., Artru M.-C.: 1985, Physica Scripta 32, 115
Lanz, T., Dimitrijevic, M.S., Artru M.-C.: 1988, Astron. Astrophys. 192, 249
Le Dourneuf, M., Vo Ky Lan, Zeippen, C.: 1989 (private communication)
Lennon, D.J.: 1983, Mon. Not. R. Astr. Soc. 205, 829
Martin, G.A., Wiese, W.L.: 1976, J. Phys; Chem. Ref. Data 5, 537
Martin, W.C., Zalubas, R.: 1979, J. Phys. Chem. Ref. Data 8, 817
Martin, W.C., Zalubas, R.: 1980, J. Phys. Chem. Ref. Data 9, 1
Martin, W.C., Zalubas, R.: 1980, J. Phys. Chem. Ref. Data 10, 153
Martin, W.C., Zalubas, R.: 1983, J. Phys. Chem. Ref. Data 12, 323
Martin, W.C., Zalubas, R. , Musgrove, A.: 1985, J. Phys. Chem. Ref. Data 14, 751
Michaud, G., Charland, Y., Vauclair, S., Vauclair G.: 1976, Astrophys. J. 210, 447
Michaud, G.: 1987, Physica Scripta 36, 112
Moore, C.E.: 1965 to 1985, NSRDS-NBS 3, sections 1 to 11
Reader, J., Corliss, C.H.: 1980, "Wavelengths and Atomic Transition Probabilities for Atoms and Atomic Ions", part I, NSRDS-NBS 68
Roby, S.W.: 1989, Bull. Am. Astr. Soc. 19,1024
Sadakane, K., Takada, M., Jugaku, J.: 1983, Astrophys. J. 274, 261
Sadakane, K., Ueta, M.: 1989, Publ. Astron. Soc. Japan 41, 279
Rogerson, J.B. Jr: 1987, Astrophys. J. Suppl. Ser. 63, 369
Seaton, M.J.: 1987, J. Phys. B 20, 6363
Sugar, J., Corliss, C.: 1979, J. Phys. Chem. Ref. Data 8, 865
Swings, J.-P., ed: 1988, Transact. of the IAU, Kluwer Acad. Publ.
Wiese, W.L., Martin, G.A: 1980, "Wavelengths and Atomic Transition Probabilities for Atoms and Atomic Ions", part II, NSRDS-NBS 68
Wiese, W.L., Smith, M.W., Glennon, B.M.: 1966, "Atomic Transition Probabilities", Vol. I, hydrogen through neon, NSRDS-NBS 4
Wiese, W.L., Smith, M.W., Miles, B.M.: 1969, "Atomic Transition Probabilities", Vol. II, sodium through calcium NSRDS-NBS 22
Wolf, S.C.: 1983," The A-Stars : Problems and Perspectives, NASA-SP 463

AUTHOR'S ADDRESS
Observatoire de Paris-Meudon (DAMAP)
92190 Meudon, France
present address:
Ecole Normale Supérieure de Lyon
46 Allée d'Italie, 69364 Lyon Cedex 07, France

F.P. Keenan, P.J.F. Brown, P.L. Dufton and D.E. Holmgren

Determination of stellar and interstellar abundances from weak absorption lines

ABSTRACT

In this paper we discuss how accurate interstellar gas phase element abundances may be derived using weak absorption lines in the spectra of early-type stars, providing both the interstellar line strength and the corresponding f-value have been reliably determined. We also discuss an analogous method for estimating cosmic abundances using weak *stellar* absorption lines in the spectra of main sequence early-type stars. Such stellar atmospheres should be uncontaminated by the products of interior nuclear reactions. As the stars will also have short lifetimes, the stellar abundances should reflect the current chemical composition of the solar neighborhood.

INTRODUCTION

A major area of astronomical research for several decades has been the study of the diffuse interstellar medium (see, for example, Cowie and Songaila 1986, Harris 1988 and references therein), which consists of gas and dust grains. One important method for observing the gas phase material is through the absorption lines it produces in the optical and UV spectra of early-type stars (Bohlin *et al.* 1983, Joseph *et al.* 1985). Of particular interest is the chemical composition of the dust, which may be inferred from the *depletions* of the elements observed in the gas phase (see, for example, York *et al.* 1983). The depletion d_i of an element is defined by (Shull 1986):

$$\log d_i = \log(N_i/N_H) - \log (N_i/N_H)_\odot$$

where (N_i/N_H) and $(N_i/N_H)_\odot$ are the relative abundance of element i to hydrogen in the interstellar medium, and the cosmic abundance, respectively. Values of N_H can be determined to an accuracy of approximately 10% from Lα and H_2 absorption lines (Bohlin *et al.* 1978, Savage *et al.* 1977, Shull and Van Steenberg 1985). In this paper we discuss how reliable interstellar and cosmic (stellar) abundances may be estimated through the analysis of absorption lines with small oscillator strengths.

INTERSTELLAR ABUNDANCES

Interstellar abundances are normally estimated using a curve of growth with a single Maxwellian velocity distribution, in which the derived abundance depends on the absorption line strength (denoted by the equivalent width W_λ), the velocity distribution of the line of sight interstellar material (characterised by a Doppler width b), and the oscillator strength f of the transition under consideration (Spitzer 1978). However for absorption lines with small oscillator strengths ($f \leq 10^{-2}$), the derived element abundance for most sightlines depends exclusively on the measured interstellar absorption line strength and f-value and not on the adopted b-value. To determine accurate abundances one therefore needs reliable estimates of these two quantities.

Bohlin *et al.* (1983) have published a survey of ultraviolet interstellar absorption lines in the spectra of 88 early-type stars, obtained with the Princeton high resolution (~0.05Å FWHM) spectrometer on board the *Copernicus* satellite (Rogerson *et al.* 1973). These observations cover the wavelength range 950–1370Å, and include highly reliable equivalent widths for many weak absorption lines in species such as N I and O I. For example, for the N I 1161Å line in the line of sight to β^1Sco, Bohlin *et al.* find $W_\lambda = 3.2\pm0.5$mÅ, while for O I 1356Å towards κ Ori, $W_\lambda = 3.1\pm0.3$mÅ. More recently, Van Steenberg and Shull (1988a) have extended the work of Bohlin *et al.* by publishing a survey of interstellar line strengths in the wavelength range 1097–2605Å towards 261 early-type stars, obtained with the lower resolution (~0.2Å FWHM) spectrographs on board the *International Ultraviolet Explorer* (IUE) satellite (Boggess *et al.* 1978). Although the IUE observational data are not as good as those from *Copernicus*, due to lower resolution and signal-to-noise capabilities, IUE can observe much fainter stars. Moreover in the future very high quality observations of faint stars should be available from the very high resolution (~0.01Å FWHM) spectrometers on board the *Space Telescope* (see Gull *et al.* 1986 and references therein).

Over the past few years there have been several studies of interstellar abundances using the absorption lines in the Bohlin *et al.* (1983) *Copernicus* and Van Steenberg and Shull (1988a) IUE surveys. These include York *et al.* (1983) for the elements N and O, Harris and Bromage (1984) for Cl, Jenkins *et al.* (1986) for Mg, P, Cl, Mn, Fe, Cu and Ni, Harris and Mas Hesse (1986) for S, Harris (1987) for Fe, P and S, and Van Steenberg and Shull (1988b) for Si, Mn, Fe, S and Zn. However in general these authors used oscillator strengths taken from the literature (and particularly the compilation of Morton and Smith 1973). In many cases, the wavefunc-

tion had not been optimised for the transition of interest and hence the corresponding f-value was not reliable. At Queen's University Belfast we therefore embarked on an extensive project in 1983 to calculate accurate f-values using the CIV3 code of Hibbert (1975) for the transitions observed by Bohlin *et al.* (The methods employed by Hibbert to determine f-values are discussed by him elsewhere in these proceedings). To date, interstellar abundances accurate to normally ±0.1 dex have been derived for magnesium (Murray *et al.* 1984), nitrogen (Hibbert *et al.* 1985), oxygen (Keenan *et al.* 1985) and phosphorous (Dufton *et al.* 1986), while work on chlorine is in progress. Our results are significantly different from those of previous authors, and imply effectively zero depletions for low density sightlines, consistent with such sightlines generally having little interstellar dust content (Keenan *et al.* 1986).

In the future we intend to extend our work to calculate f-values for other species in the Bohlin *et al.* (1983) survey, including Fe II, Cu II and Ni II. We also plan to produce atomic data relevant to *Space Telescope* observations.

COSMIC ABUNDANCES

As noted in the previous Section, the combination of high quality interstellar absorption line strengths and accurate f-values allows extremely reliable interstellar abundances to be derived. For example, towards ζ Oph the oxygen abundance is known to ±0.04 dex (Keenan *et al.* 1985). However as pointed out in the Introduction, an important quantity in interstellar medium studies is the element *depletion*, as from this the grain composition is inferred. Hence an accurate knowledge of the *cosmic abundance* value of the element under consideration is also required. Unfortunately, cosmic abundances employed in interstellar work are usually determined from the sun and meteorites, and are often uncertain (Grevesse 1984, Meyer 1985a,b), thereby vitiating the accuracy of the interstellar depletions. Furthermore, cosmic abundances determined in this way apply to the interstellar medium as it was in the solar neighbourhood some 5×10^9yrs ago, and hence are not necessarily appropriate to studies of current depletions.

At Queen's we have therefore recently undertaken a programme to derive accurate *contemporay* cosmic abundances using a similar approach to that employed in the interstellar work described above. Weak *stellar* absorption lines (with typical equivalent widths of 5mÅ) are observed in the spectra of main sequence early-type stars. Due to their weakness, these lines have equivalent widths which are very sensitive to the element abundance, but not to the assumptions made in the model atmosphere analysis.

We have initially observed weak lines of argon as as the cosmic abundance of this element is particularly uncertain (Grevesse 1984, Meyer 1985a,b), and it has been extensively detected in the interstellar medium through absorption lines of A I at 1066.7 and 1048.2Å (see Duley 1985 and references therein). Observational data were obtained using the coudé spectrograph with a CCD detector on the Coudé Feed Telescope at the Kitt Peak National Observatory in December 1988 (see Keenan *et al.* 1990 for more details). For γ Peg, δ Cet and HR 1765 the 4587–4611Å wavelength region was observed, which includes the A II line at 4589.98Å. In addition, spectra covering the wavelength interval 4647–4672Å (which contains the A II line at 4657.94Å) were obtained for γ Peg. In Figure 1 we show the spectrum of γ Peg from 4585–4605Å to illustrate the high quality of the observational data. The equivalent widths found for the A II 4590 and 4658Å lines were in the range 5–7mÅ, with errors of typically ±0.5mÅ.

The observational data were analysed by comparing measured stellar Strömgren colours (effective temperature indicators), β indices (surface gravity indicators) and A II equivalent widths with those predicted by local thermodynamic equilibrium (LTE) model atmosphere codes. All theoretical results were deduced using the line blanketed grid of models of Kurucz (1979), or new models calculated with Kurucz's program. The derivation of effective temperatures and surface gravities have been discussed in detail by Keenan *et al.* (1990).

Using the stellar atmospheric parameters, argon abundances were deduced by comparing the observed A II line strengths with those predicted from LTE model atmosphere calculations (see Brown *et al.* 1986 for more details). A microturbulent velocity $V_t = 5 \pm 5 \mathrm{kms}^{-1}$ was adopted for the all the stars, as this value has been found to be appropriate for LTE analyses of near main sequence early-type stars (see, for example, Hardorp and Scholz 1970; Kodaira and Scholz 1970); however for the programme stars the derived A II abundances are effectively independant of the choice of V_t (see below). Oscillator strengths for the A II 4590 and 4658 Å transitions were taken from Garcia and Campos (1985), who measured A II lifetimes (and hence f-values) to an accuracy of better than 10% using the delayed-coincidence method.

In Table 1 the derived argon abundances log [A] (on the scale log [H] = 12) are summarised, along with the changes in log [A] (Δlog [A]) found when *all* the observational uncertainties (equivalent widths *and* atmospheric parameters) are taken into account. An inspection of the table shows that the results are relatively insensitive to the observational uncertainties, and the derived values of log [A] should be accurate to approximately ±0.05 dex. Support for this comes from the fact that for the three stars the derived argon abundances are in excellent agree-

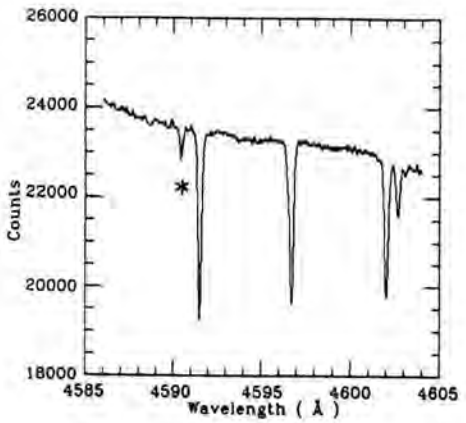

Fig. 1. The spectrum of γ Peg from 4585–4605Å, which clearly shows the weak A II line at 4590Å (marked with an asterisk). This feature has an equivalent width of W_λ = 6.3±0.5mÅ.

ment, with discrepancies of typically 0.05 dex, while for γ Peg the values of log [A] estimated from the two A II lines differ by only 0.07 dex.

For the three stars we obtain a mean abundance of log [A] = 6.49±0.04, where the error bar refers to the sample standard deviation. There is also an uncertainty in log [A] which arises from possible non-LTE effects. However very recent non-LTE calculations for A II performed by us (Holmgren *et al.* 1990) indicate that these effects should be small ($\leq$0.02 dex) for the transitions under consideration. In view of this, and the fact that there is a possible 10% uncertainty in the adopted A II f-values (Garcia and Campos 1985), we therefore conclude that our mean argon abundance should be accurate to ±0.05 dex.

Table 1. Derived stellar argon abundances, on the scale log [H] = 12

Star	Line (Å)	log [A]	Δlog [A]
γ Peg	4590	6.50	±0.03
γ Peg	4658	6.43	±0.09
HR 1765	4590	6.53	±0.08
δ Cet	4590	6.49	±0.03

As the stars under consideration are on or near the main sequence, their atmospheres should be uncontaminated by the products of interior nuclear reactions (Brown *et al.* 1986), and hence any derived abundances should reflect those of the interstellar material from which the stars formed some 10^6–10^7yrs ago. During these short lifetimes it is unlikely that the stars have moved significantly from their places of origin, and as they lie within typically 500pc of the sun (Savage *et al.* 1985), our result of log [A] = 6.49±0.05 therefore represents an *accurate* evaluation of the *current cosmic* abundance value of argon in the solar neighborhood.

As argon is not present in the solar photospheric spectrum (see, for example, Grevesse 1984), previous estimates of the cosmic abundance value have been determined from emission lines formed in the solar corona, which are detected in the X-ray region of the spectrum. In these analyses most authors have calculated argon abundance *ratios* (for example A/Fe; Doschek *et al.* 1985), and used the solar abundance of the denominator to infer that for argon. Using this method, Withbroe (1971), Walker *et al.* (1974) and Doschek *et al.* have determined values for log [A] of 6.65, 6.78 and 6.44, respectively, with error estimates of approximately ±0.2–0.3 dex. According to Meyer (1985b), the only *absolute* argon abundance determination is that of Veck and Parkinson (1981), who found log [A] = $6.38^{+0.18}_{-0.30}$ from an analysis of solar flare data from the OSO-8 satellite. These authors were able to measure the absolute abundance as they analysed not only the A XVII line emission at ~4Å, but also the continuum emission, which is dominated by free-free and free-bound processes in hydrogen. We note that our result is in good agreement with that of Veck and Parkinson, and also with the recent measurement by Doschek *et al.* However the error estimate in our argon abundance is 12% or less, as opposed to the $\simeq$75% uncertainty in those of Veck and Parkinson and Doschek *et al.*

It is interesting to note that although up to now the most reliable cosmic argon abundance estimate is the log [A] = 6.38 of Veck and Parkinson (1981), many workers have adopted the Withbroe (1971) value of log [A] = 6.65 in interstellar depletion studies of argon (see, for example, York 1983, Duley 1985). For the sightlines to λ Sco and α Vir, York (1983) and York and Kinahan (1979) found argon depletions of ~0.20 and ~0.15 dex, respectively, using the Withbroe cosmic abundance value. However adoption of the present result implies that argon is effectively undepleted in these sightlines, which is to be expected as they are unreddened and hence contain few interstellar grains (see Keenan *et al.* 1986).

In the future we plan to extend our work by observing weak absorption lines of P II in early-type stellar spectra, as this species is extensively observed in the interstellar medium (Dufton *et al.* 1986), and accurate oscillator strength calculations performed at QUB are available (Hibbert 1988).

ACKNOWLEDGEMENTS

F. P. Keenan, P. J. F. Brown and D. E. Holmgren acknowledge financial support from the SERC.

REFERENCES

Boggess, A. *et al.* 1978, *Nature*, **275**, 372.
Bohlin, R.C. *et al.* 1983, *Ap. J. Suppl.*, **51**, 277.
Bohlin, R.C., Savage, B.D., and Drake, J.F. 1978, *Ap. J.*, **224**, 132.
Brown, P.J.F., Dufton, P.L., Lennon, D.J., and Keenan, F.P. 1986, *M.N.R.A.S.*, **220**, 1003.
Cowie, L.L., and Songaila, A. 1986, *Ann. Rev. Astr. Ap.*, **24**, 499.
Doschek, G.A., Feldman, U, and Seely, J.F. 1985, *M.N.R.A.S.*, **217**, 317.
Dufton, P.L., Keenan, F.P., and Hibbert, A. 1986, *Astr. Ap.*, **164**, 179.
Duley, W.W. 1985, *Ap. J.*, **297**, 296.
Garcia, G., and Campos, J. 1985, *J. Quant. Spectrosc. Rad. Tranfs.*, **34**, 85.
Grevesse, N. 1984, *Phys. Scr.*, **T8**, 49.
Gull, T.R. *et al.* 1986, *New Insights in Astrophysics*, ESA SP-263, p653.
Hardorp, J., and Scholz, M. 1970, *Ap. J.*, **154**, 1111.
Harris, A.W. 1987, *Ap. J.*, **322**, 368.
Harris, A.W. 1988, *A Decade of UV Astronomy with IUE*, ESA SP-281, p3.
Harris, A.W., and Bromage, G.E. 1984, *M.N.R.A.S.*, **208**, 941.
Harris, A.W., and Mas Hesse, J.M. 1986, *Ap. J.*, **308**, 240.
Hibbert, A. 1975, *Comp. Phys. Commun.*, **9**, 141.
Hibbert, A. 1988, *Phys. Scr.*, **38**, 37.
Hibbert, A., Dufton, P.L., and Keenan, F.P. 1985, *M.N.R.A.S.*, **213**, 721.
Holmgren, D.H., Brown, P.J.F., Dufton, P.L., and Keenan, F.P. 1990, *Ap. J.*, submitted.
Jenkins, E.B., Savage, B.D., and Spitzer, L. 1986, *Ap. J.*, **301**, 355.
Joseph, C.L., Snow, T.P., and Morrow, C. 1985, *Ap. J.*, **296**, 213.
Keenan, F.P., Bates, B., Dufton, P.L., Holmgren, D.E., and Gilheany, S. 1990, *Ap. J.*, in press.
Keenan, F.P., Dufton, P.L., Hibbert, A., and Murray, M.J. 1986, *M.N.R.A.S.*, **222**, 143.
Keenan, F.P., Hibbert, A., and Dufton, P.L. 1985, *Astr. Ap.*, **147**, 89.
Kodaira, K., and Scholz, M. 1970, *Astr. Ap.*, **6**, 93.
Kurucz, R.L. 1979, *Ap. J. Suppl.*, **40**, 1.
Meyer, J.-P. 1985a, *Ap. J. Suppl.*, **57**, 151.
Meyer, J.-P. 1985b, *Ap. J. Suppl.*, **57**, 173.
Morton, D.C., and Smith, W.H. 1973, *Ap. J. Suppl.*, **26**, 333.
Murray, M.J., Dufton, P.L., Hibbert, A., and York, D.G. 1984, *Ap. J.*, **282**, 481.
Rogerson, J.B. *et al.* 1973, *Ap. J. (Letters)*, **181**, L97.
Savage, B.D. *et al.* 1977, *Ap. J.*, **216**, 291.
Savage, B.D. *et al.* 1985, *Ap. J. Suppl.*, **59**, 397.
Shull, J.M. 1986, *New Insights in Astrophysics*, ESA SP-263, p511.
Shull, J.M., and Van Steenberg, M.E. 1985, *Ap. J.*, **294**, 599.
Spitzer, L. 1978, *Physical Processes in the Interstellar Medium*, New York: Wiley.
Van Steenberg, M.E., and Shull, J.M. 1988a, *Ap. J. Suppl.*, **67**, 225.
Van Steenberg, M.E., and Shull, J.M. 1988b, *Ap. J.*, **330**, 942.
Veck, N.J., and Parkinson, J.H. 1981, *M.N.R.A.S.*, **197**, 41.
Walker, A.B.C., Rugge, H.R., and Weiss, K. 1974, *Ap. J.*, **188**, 423.
Withbroe, G.L. 1971, *The Menzel Symposium*, NBS SP-353, p127.
York, D.G. 1983, *Ap. J.*, **264**, 172.
York, D.G. *et al.* 1983, *Ap. J. (Letters)*, **266**, L55.
York, D.G., and Kinahan, B.F. 1979, *Ap. J.*, **228**, 127.

AUTHORS' ADDRESS

Department of Pure and Applied Physics, The Queen's University of Belfast, Belfast BT7 1NN, Northern Ireland.

Emile Biémont[§]

Oscillator strength determination for heavy elements

ABSTRACT

Some important developments during the years 1980-1989 concerning the determination of atomic oscillator strengths for the heavy elements (Z > 28) are presented. More particularly, we focus attention here on the progress concerning f value determination in the copper to krypton sequences and also concerning lifetime measurements for neutral and singly ionized refractory elements. Astrophysical implications are also mentioned.

INTRODUCTION

Calculations of atomic structure and radiative transition rates for heavy atoms and ions (Z > 28) have become more tractable during recent years mostly due to the advent of large supercomputers which make the simultaneous consideration of correlation and relativistic effects more feasible and more realistic. The calculation of transition probabilities have also benefited from the increase in experimental data concerning the atomic structure of moderately or highly ionized elements (laser produced plasmas - Tokamak devices - beam-foil spectroscopy) which often makes the use of semi-empirical methods for calculating oscillator strengths more reliable.

During the past decade, a significant change of orientation in the experimental determination of oscillator strengths for heavy elements has consisted in the fact that the activities in this field, which were previously concentrated upon the use of absorption and emission techniques, have progressively moved to radiative lifetime measurements and to branching ratio determinations. This change is related directly to the intensive and general use of pulsed dye lasers for selective excitation and to the development of powerful beam-laser techniques.

It is not the purpose of this limited review to discuss all the aspects of the progress realized in the whole field but we want to focus here on two specific subfields. In the first section of this paper, we will concentrate upon the oscillator strength determination along the copper to krypton sequences and spotlight some specific characteristics of these results. The second section will present a summary of lifetime and branching ratio measurements for heavy refractory elements (neutral or singly ionized) which remain of major interest in astrophysics for the determination of the chemical composition of the sun.

THE COPPER TO KRYPTON SEQUENCES : STATE OF THE ART

The knowledge of the atomic structure of moderately or strongly ionized elements along the Cu to Kr sequences has progressed substantially in the recent past. The state of the analysis of atomic spectra for the elements Cu to W is illustrated in Table 2. This table updates a previous compilation of Cowan (1981a). These developments have given an important impulse to the determination of transition probabilities (or related quantities), although the available data remain very fragmentary. The main references containing f values (or related quantities) are summarized in Table 1. They concern allowed (E1) or forbidden (M1, E2) transitions.

Table 1 - Recent progress in f value or lifetime determinations along the Cu to Kr sequences (period 1980-1989).

Ions	Type	Reference Cu Sequence
Cu	E1	Bezuglov et al. (1982)
Cu to Mo	E1	Curtis (1981)
Cu	E1	Hannaford and Lowe (1983a)
Cu	E1	Osherovich et al. (1981)
Cu	E1	Kono and Hattori (1982)
Cu	E1	Cederquist et al. (1984)
Cu	E1	Carlsson et al. (1987)
Cu	E1	Carlsson (1988)
Cu	E1	Carlsson et al. (1987)
Cu	E1	Zettl et al. (1984)
Ga	E1	Lindgård et al. (1982)
Ga,Ge	E1	Ryabtsev and Wyart (1987)
Ge	E1	Pinnington et al. (1981a)

As	E1	Pinnington et al. (1981b)
As to Br	E1	Ryabtsev et al. (1984)
Ge to Mo	E1	Wyart et al. (1984)
Se	E1	Bahr et al. (1982)
Cu to Mo	E1	Victor and Taylor (1987)
Cu to In	E1	Lindgård et al. (1980)
Cu to Kr	E1	Pinnington et al. (1982)
Kr	E1	Livingston et al. (1980)
Y to Ag	E1	Klapisch et al. (1981)
Mo	E1	Denne and Poulsen (1981)
Sr to Nd	E1	Biémont (1988)
I	E1	Johnson et al. (1985)
Xe	E1	Breton et al. (1988)
Pr	E1	Finkenthal et al. (1986)
Tm to Pt	E1	Mandelbaum et al. (1983)
Cu to Bi	E1	Curtis (1989)
Cu to U	E1	Curtis and Theodosiou (1989)

Zn Sequence

Zn	E1	Afaneseva (1982)
Zn	E1	Bruneau (1984)
Zn to U	E1,M1, E2	Anderson and Anderson (1983)
Zn	E2	Beck (1981)
Zn	E1	Ueda et al. (1981)
Zn to Mo	E1	Victor and Taylor (1987)
Mo, Ag	E1	Träbert (1989)
Mo	E1	Finkenthal et al. (1981)
Zn to Kr	E1	Pinnington et al. (1982)
Zn to W	E1	Biémont and Godefroid (1980)
As	E1	Pinnington et al. (1981b)
Kr	E1	Pinnington et al. (1984)
Rb to Xe	E1	Biémont et al. (1989a)
Xe	E1	Breton et al. (1988)
Pr	E1	Finkenthal et al. (1986)
Rb to W	E1	Biémont (1989)
Tm to Pt	E1	Mandelbaum et al. (1983)

Ga Sequence

Ga to Kr	E1	Aashamar et al. (1983)
Ga	E1	Brage et al. (1987)
Ga	E1	Tursunov and Eshkobilov (1984)
Ga	E1	Lindgård et al. (1982)
Ge	E1	Miller and Bengtson (1980)
As	E1	Pinnington et al. (1981b)
Ga to Se	E1	Migdalek (1983)
Br to In	E1	Biémont and Quinet (1989)
Mo	E1	Finkenthal et al. (1981)
Xe	E1	Breton et al. (1988)
Ga to Xe	M1,E2	Biémont and Hansen (1987)

Ge Sequence

Ge to Ag	M1,E2	Biémont and Hansen (1986b)
Kr	E1	Fawcett and Bromage (1980)
Rb	E1	O'Sullivan (1989)
Sr	E1	O'Sullivan and Maher (1989)
Zr	E1	Chaghtai et al. (1980)
Ru to Pd	E1	O'Sullivan et al. (1988a)
Xe	E1	Breton et al. (1988)

As Sequence

As to Ag	M1,E2	Biémont and Hansen (1986b)
As	E1	Lotrian et al. (1980)
Kr	E1	Fawcett and Bromage (1980)
Sr	E1	O'Sullivan and Maher (1989)
Zr	E1	Khan et al. (1980)
Br to Mo	E1	O'Sullivan (1989)
Xe	E1	Breton et al. (1988)
Ru,Rh	E1	O'Sullivan and Kane (1989)

Se Sequence

Se to Ag	M1,E2	Biémont and Hansen (1986a)
Kr	E1	Coetzer et al. (1982)
Xe	E1	Breton et al. (1988)
Ru,Rh,Pd	E1	O'Sullivan et al. (1988b)

Br Sequence

Br to Xe	M1,E2	Biémont et al. (1988)
Kr	E1	Blagoev (1981)
Kr	E1	Brandt et al. (1982)
Kr	E2	Fonseca and Campos (1982)
Kr	E1	Ward et al. (1985b)
Kr	E1	Schade et al. (1989)
Cd	E1	Costello and O'Sullivan (1984)
Xe	E1	Breton et al. (1988)

Kr Sequence

Kr	E1	Brandt et al. (1982)
Kr	E1	Fonseca and Campos (1980)
Kr to Mo	E1	Sureau et al. (1984)
Rb	E1	Ceyzeriat et al. (1980)
Cd	E1	Costello and O'Sullivan (1984)
Xe	E1	Breton et al. (1988)
Pr,Dy	E1	Finkenthal et al. (1986)

A) The experimental results

Although the experimental determination of oscillator strengths mostly concerns the first ionization degrees (up to 8), some results have been obtained by beam-foil spectroscopy for Mo XIV (Denne and Poulsen, 1981) and for I XXV (Johnson et al., 1985) in the copper sequence. In fact, the Cu, Zn and Ga sequences have been investigated mostly by beam-foil spectroscopy up to Kr VIII (Pinnington et al., 1981a,b; 1982, 1984; Bahr et al., 1982; Cederquist et al., 1984; Livingston et al., 1980). Some laser excitation results have been reported by Hannaford and Lowe (1983a) (Cu I) and by Ward et al. (1985b) (Kr II). Results obtained by different "classical" techniques (hook method, wall-stabilized arcs, shock tube,

Table 2. Status of the analysis of atomic spectra (July 1989)

Key : A : Analysis essentially complete; B : the lowest configurations and portions of some higher ones known; C : two dozens or so levels known; D : about a dozen levels known; E : very fragmentary analysis, 2 to 5 levels known. Due to limited space available, the references used for preparing this table are not quoted here.

	1	2	3	4	5	6	7	8	9	10	11	12	13	14	15	16	17	18	19	20
Cu	A																			
Zn	A	B																		
Ga	A	A	B																	
Ge	A	A	C	B																
As	A	A	C	C	B															
Se	A	B	C	C	C	B														
Br	A	B	C	D	D	C	B													
Kr	A	A	B	C	C	D	C	B												
Rb		A	A	D	C	C	C	C	C											
Sr			A	A	B	C	C	C	C	A										
Y				B	C	B	B	C	C	C	A									
Zr					A	B	B	B	C	C	C	A								
Nb						B	B	B	B	C	C	C	C							
Mo							B	B	B	B	C	C	C	A						
Tc																				
Ru									D	D	C	C	D		C	C				
Rh										D	D			D	E	C	C			
Pd											D	D	C		D	E	C	C		
Ag												D	C	D			E	C	C	
Cd													E	D				E	C	C
In																				

	39	40	41	42	43	44	45	46
Er	E	C						
Tm		D	C					
Yb			C	C				
Lu				E	C			
Hf					D	C		
Ta						D	C	
W							D	C

	19	20	21	22	23	24	25	26	27	28	29	30	31	32	33	34	35	36	37	38
In	E	C	C																	
Sn			C	C																
Sb				E	C															
Te					E	C														
I						E	C													
Xe	E	E	E	E	E	E	E	C												
Cs								E												
Ba									E	C										
La										E	C									
Ce											E	C								
Pr												E	C							
Nd													E	C						
Pm																				
Sm															E	C				
Eu																E	C			
Gd																	E	C		
Tb																			C	
Dy																			E	C
Ho																				

delayed coincidences,...) have been reported for Cu I, Cu II, Zn I, Ge II, Kr I, Kr II, As I (see e.g. Miller and Bengston, 1980; Lotrian et al., 1980; Ueda et al., 1981; Kono and Hattori, 1982, Fonseca and Campos, 1980, 1982; Blagoev, 1981; Zettl et al., 1984).

B) The theoretical results

The choice of a theoretical method for performing calculations of atomic structure in heavy elements is essentially determined by a compromise between the wanted accuracy and the computer time needed.

Large MCDF codes (e.g. Desclaux, 1975; Grant et al., 1980) are available and allow a "fully" relativistic treatment of the heavy atoms or ions but their use is, in practice, limited by the "complexity" and the number of configurations to be introduced in the calculations. Nevertheless, extensive results have been obtained recently along the zinc sequence (Biémont, 1989) and more limited data along the Ge, As and Se sequences (O'Sullivan et al., 1988a,b; O'Sullivan, 1989; O'Sullivan and Maher, 1989; O'Sullivan and Kane, 1989).

The model potential (PM) techniques look also promising and their potential has been discussed recently by Hibbert (1989). Among the recent results obtained by such techniques, let us quote here the data published by Migdalek (1983), by Aashamar et al. (1983) (Ga sequence) and by Victor and Taylor (1987) (Cu and Zn sequences).

The parametric potential method of Klapisch et al. (1977) in its relativistic version (RPPT) has been used frequently as support for experiments concerning moderately or highly ionized elements (see e.g. Mandelbaum et al., 1983; Wyart et al., 1984; Finkenthal et al., 1986; Ryabtsev and Wyart, 1987).

The relativistic Hartree-Fock (HXR, HFR) method of Cowan (1981b) is among the techniques widely used both for allowed (see e.g. Biémont, 1988; Biémont and Quinet, 1989; Biémont et al., 1989a) and for forbidden transitions (see e.g. Biémont and Hansen, 1986a,b; 1987; 1988) while the non relativistic MCHF technique has provided results for zinc-like (Biémont and Godefroid, 1980) and gallium-like atoms (Brage et al., 1987).

A limited comparison between the HFR, MCDF, and PM results obtained along the zinc isoelectronic sequence is presented in Table 3.

Table 3 - Comparison between recently reported f values along the zinc sequence; HFR : Biémont et al. (1989a); PM : Victor and Taylor (1987); MCDF-EAL : this work (Babushkin Gauge).

$4s^2\ {}^1S - 4s4p\ {}^1P^o$

	Rb VIII	Y X	Mo XIII	Sn XXI	Xe XXV
HFR	1.718	1.629	1.510	1.282	1.205
PM	1.722	1.718	1.489	-	-
MCDF	1.692	1.615	1.509	1.291	1.217

$4s4p\ {}^1P^o - 4p^2\ {}^1S$

HFR	0.211	0.199	0.185	0.164	0.155
PM	0.213	0.207	0.185	-	-
MCDF	0.210	0.199	0.186	0.165	0.160

$4s4p\ {}^1P^o - 4p^2\ {}^1D$

HFR	0.169	0.171	0.166	0.136	0.115
PM	0.262	0.255	0.316	-	-
MCDF	0.169	0.168	0.162	0.131	0.115

$4s4p\ {}^1P^o - 4s4d\ {}^1D$

HFR	1.659	1.527	1.361	1.061	0.975
PM	1.683	1.630	1.384	-	-
MCDF	1.656	1.540	1.386	1.095	1.006

$4s4p\ {}^3P^o - 4s4d\ {}^3D$

HFR	1.038	0.974	0.884	0.708	0.639
PM	1.010	0.936	0.880	-	-
MCDF	1.020	0.963	0.878	0.705	0.648

$4s4p\ {}^3P^o - 4p^2\ {}^3P$

HFR	0.465	0.432	0.339	0.344	0.315
PM	0.577	0.576	0.502	-	-
MCDF	0.343	0.344	0.332	0.299	0.287

The agreement between MCDF and HFR data is excellent for the ions Rb VIII to Xe XXV. Larger differences are observed between MCDF (or HFR) and PM data particularly for the $4s4p\ {}^1P^o - 4p^2\ {}^1D$ transition.

We shall now briefly spotlight some general characteristics which are encountered when calculations of atomic structure and intensities are carried out along isoelectronic sequences. These general considerations will be illustrated by some specific examples chosen among recent HXR and MCDF results reported along the zinc sequence for the ions Rb VIII to W XLV (Biémont, 1989; Biémont et al., 1989a) :

- change of the percentage compositions (and the corresponding difficulties for the designation of the levels) when Z increases along the sequence. The HXR composition is illustrated for three specific cases on

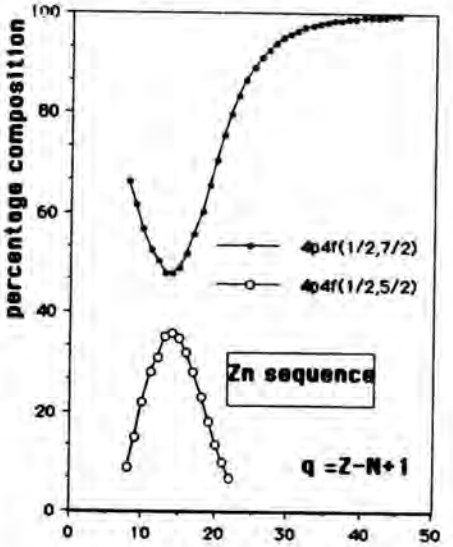

Fig. 1. Percentage composition (jj coupling) of the 4p4f(1/2, 7/2)$_3$ levels along the zinc isoelectronic sequence.

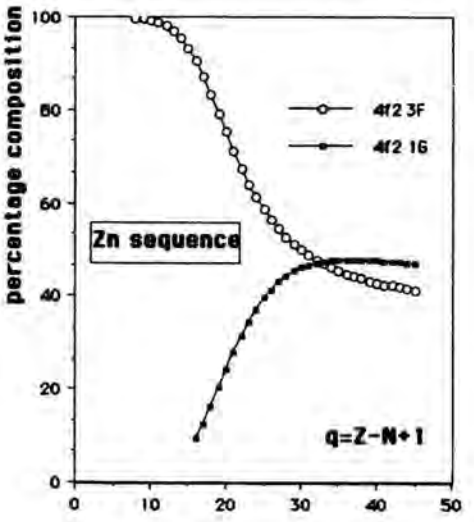

Fig. 2. Same as Fig. 1 for the $4f^2\ ^3F_4$ level. 4f2 3F is written for $4f^2\ ^3F$.

Figures 1 to 3 which show respectively the strong interaction between 4p4f(1/2, 7/2)$_3$ and 4p4f(1/2, 5/2)$_3$ at around q = Z-N+1 $\simeq$ 15 (Fig. 1), the smooth change of composition for the $4f^2\ ^3F_4$ level (Fig. 2) (more correctly designated as $4f^2\ ^1G_4$ at q $\simeq$ 30) and the sudden change of composition for 4p4f(3/2, 5/2)$_4$ (which is better designated as $4d^2\ ^3F_4$ at q $\simeq$ 16 (Fig. 3);

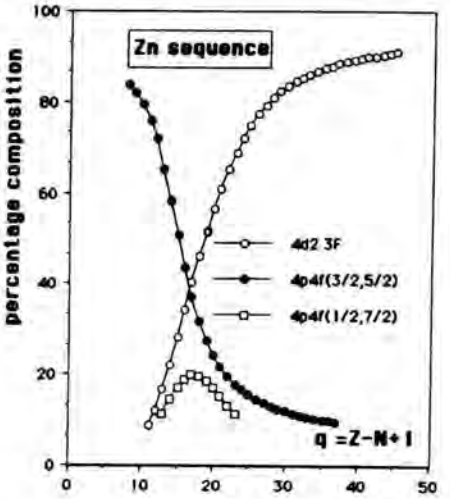

Fig. 3. Same as Fig. 1 for the 4p4f(3/2, 5/2)$_4$ or ($4d^2\ ^3F_4$) level. 4d2 3F is written for $4d^2\ ^3F$.

- the increasing importance of relativistic effects when Z and the ionization degree increase along the sequence and, consequently, the need for a "fully" relativistic approach for very high electric charges. This is illustrated on Figures 4 and 5 which show the differences (in %) between MCDF-EAL and HXR ab initio values for the even levels belonging to the configurations $4s^2 + 4p^2 + 4d^2 + 4f^2 + 4s4d + 4p4f$ in In XX and Tm XL respectively. It appears (Figure 5) that the differences tend to become systematically positive for Tm XL due to the fact that the relativistic effects are considered in a more accurate way in the MCDF approach than in the HXR method;

- the appearance of level crossings. This is illustrated on Fig. 6 in the case of the $4d^2 + 4p4f$ configurations for the ions Rb

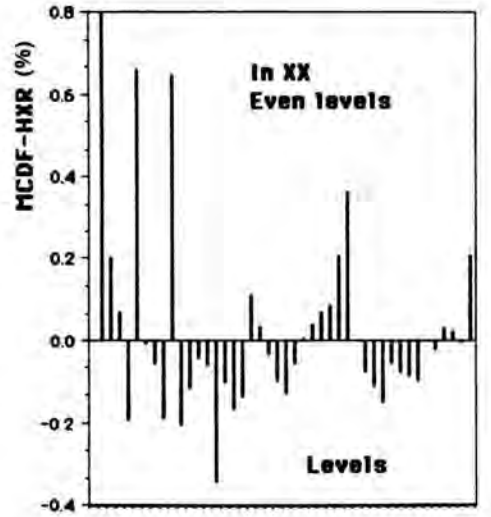

Fig. 4. Comparison between MCDF-EAL and HXR ab initio values of the even parity energy levels of In XX (configurations $4s^2 + 4p^2 + 4d^2 + 4f^2 + 4s4d + 4p4f$).

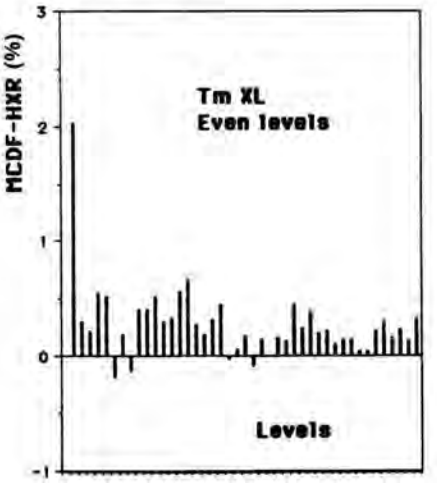

Fig. 5. Same as Fig. 4 for Tm XL.

VIII to Cs XXVI. The level crossings are frequently responsible for noticeable irregularities appearing in the curves showing the behaviour of f values as a function of Z. Some examples have been illustrated recently by Biémont and Quinet (1989) in the case of the gallium sequence.

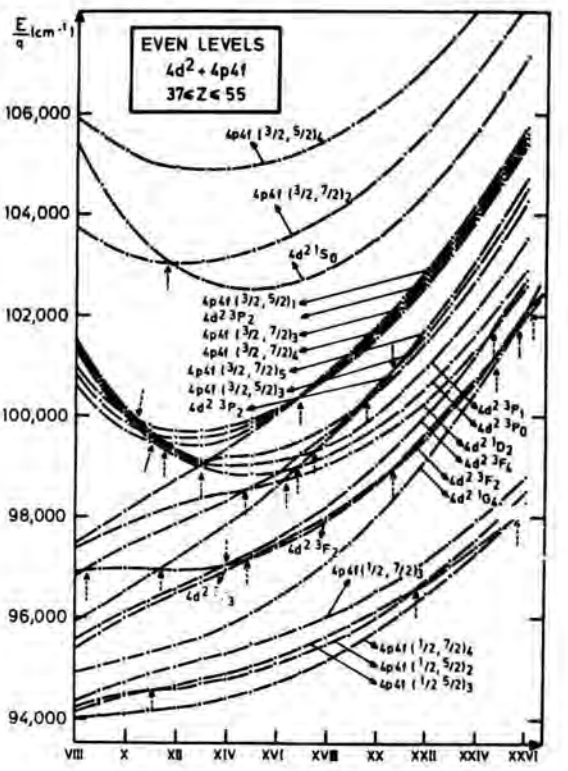

Fig. 6. Zinc isoelectronic sequence : theoretical energy level values divided by q = Z = N + 1 as a function of q.

RADIATIVE LIFETIMES AND OSCILLATOR STRENGTHS FOR HEAVY REFRACTORY ELEMENTS (Z > 39)

It has appeared, in the beginning of the eighties, that our knowledge of the radiative transition probabilities for the heavy refractory elements was still very incomplete. This situation was essentially related to the fact that it is very difficult by conventional thermal means to produce a vapour pressure sufficient for the measurement of radiative lifetimes and, on the other hand, that the calculation of accurate theoretical data for these neutral and singly ionized elements requires a detailed consideration of correlation and of relativistic effects.
The use of selective laser excitation by different groups (Clayton, Berlin, Kiel, Wisconsin, Aarhus, ...) combined with branching ratio measurements (mostly by

Fourier transform spectroscopy) has given a definitive boost to the determination of accurate transition probabilities for these elements.

We have summarized in Table 4 the different lifetime measurements concerning neutral or singly ionized elements present in the solar photospheric spectrum obtained with techniques based on laser excitation . These elements have been classified as refractory or siderophile according to the classification adopted for the meteorites. This table updates a review published by Richter (1984) a few years ago.

Table 4 - Heavy refractory (and siderophile) elements : lifetime and branching ratio determinations (period 1980-1989). In the last column, are given the solar abundances as derived from the lifetime measurements (starred reference) and the difference (Δ) between photospheric and meteoritic abundances (in the usual logarithmic scale where the hydrogen abundance is = 12.00).

A) Refractory

Reference	Solar abundance
Y I-YII	
*Hannaford et al.(1982)	*2.18±0.12 (Y I)
Hannaford and Lowe (1982)	*2.25±0.03 (Y II)
Rudolph and Helbig (1982b)	Δ = 0.03
Hannaford and Lowe (1983a)	
Gorshkov and Komarovskii (1986)	
Wännström et al. (1988)	
Zr I-Zr II	
* Biémont et al. (1981)	*2.57±0.07 (Zr I)
Hannaford and Lowe (1981)	*2.56±0.05 (Zr II)
Poulsen et al. (1981)	Δ = 0.04
Duquette et al. (1982a)	
Poulsen et al. (1982)	
Rudolph and Helbig (1982a)	
Hannaford and Lowe (1983a)	
Nb I-Nb II	
Duquette and Lawler (1982)	*1.42±0.06 (Nb II)
Kwiatkowski et al. (1982a)	Δ = 0.02
Rudolph and Helbig (1982c)	
*Hannaford et al. (1985)	
Mo I-Mo II	
Duquette et al. (1981b)	*1.92±0.05 (Mo I)
Kwiatkowski et al. (1981)	Δ = 0.04
Rudolph and Helbig (1982c)	
*Biémont et al. (1983)	
Hannaford and Lowe (1983a)	
Hannaford and Lowe (1983b)	
Schnehage et al. (1983)	
Whaling et al. (1984)	
Pleklotkina and Verolainen (1985)	
Whaling et al. (1986)	
Whaling and Brault (1988)	
Ru I	
*Biémont et al. (1984)	*1.84±0.07 (Ru I)
Salih and Lawler (1985)	Δ = 0.02
Rh I	
*Kwiatkowski et al.(1982a)	*1.12±0.12 (Rh I)
Salih et al. (1983)	Δ = 0.03
Duquette and Lawler (1985)	
Ba II	
Gaillard et al. (1982)	
Nd I - Nd II	
Marek and Stahnke (1980)	*1.47±0.07 (Nd II)
*Ward et al. (1984)	Δ = 0.00
Ward et al. (1985a)	
Sm I - Sm II	
Brand et al. (1980)	*1.01±0.06 (Sm II)
Vogel et al. (1988)	Δ = 0.04
*Biémont et al. (1989b)	
Eu I - Eu II	
Klimkin and Prokofiev(1980)	*0.51±0.08(Eu II)
Meyer et al. (1981)	Δ = 0.03
*Biémont et al. (1982b)	
Karner et al. (1982)	
Arnesen et al. (1983)	
Gd I - Gd II	
Marek and Stahnke (1980)	*1.12±0.04 (Gd II)
*Bergström et al. (1988)	Δ = 0.05
Er I - Er II	
Marek and Stahnke (1980)	*0.93±0.06 (Er II)
Gorshkov and Komarovskii (1981)	Δ = 0.02
Bentzen et al. (1982)	
*Biémont and Youssef (1984)	
Lu I	
Kwiatkowski et al. (1980)	
Hf I	
Duquette et al. (1982b)	
W I - W II	
Duquette et al. (1981a)	*1.11±0.15 (W I)
Kwiatkowski et al. (1982b)	Δ = 0.43
*Holweger and Werner (1982)	
Obbarius and Kock (1982)	
Kwiatkowski et al. (1984a)	
Pleklotkina and Verolainen (1985)	
Den Hartog et al. (1987)	
Os I	
*Kwiatkowski et al.(1984b)	*1.45±0.10 (Os I)
	Δ = 0.07
Ir I	
*Gough et al. (1983)	*1.38±0.05 (Ir I)
Hannaford and Lowe (1983a)	Δ = 0.01
*Youssef and Khalil (1988)	
Pt I	
*Gough et al. (1982)	*1.74±0.05 (Pt I)
Hannaford and Lowe (1983a)	Δ = 0.06
*Youssef and Khalil (1987)	

B) Siderophile

Pd I	
*Biémont et al. (1982a)	*1.69±0.04 (Pd I)
	Δ = 0.30

Au I	
*Hannaford et al. (1981)	*1.3±0.12 (Au I)
Bezuglov et al. (1982)	$\bar{\Delta}$= 0.30
Hannaford and Lowe (1983a)	

From the numerous comparisons performed with the different sets of lifetimes, it has appeared that :

- the results obtained with laser excitation are much more accurate than those published previously (i.e. basically before 1980) and they differ sometimes considerably from them;
- the different sets of lifetimes published after 1980 are generally consistent within a few percent.

These two conclusions are illustrated on Figures 7 and 8 where we have plotted the ratio between different sets of lifetimes for a number of selected elements. As seen on Fig. 7, this ratio is close to unity when comparing two sets of measurements obtained from laser experiments while the dispersion of the results is much greater (Fig. 8) when comparing these lifetimes with those obtained by different techniques.

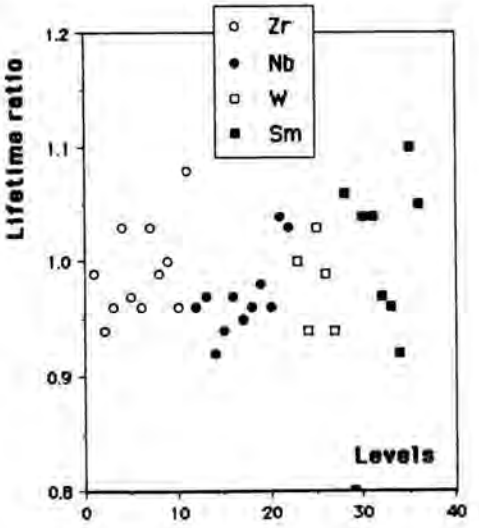

Fig. 7. Ratio of lifetime measurements for different refractory elements. We have plotted τ(HL)/τ(DL) for Zr I, τ(KZ)/τ(DS) for Nb I, τ(KM)/τ(DU) for W I and τ(BG)/τ(VE) for Sm II.
The symbols have the following meaning : KZ : Kwiatkowski et al. (1982a); DS : Duquette and Lawler (1982); KM : Kwiatkowski et al. (1982b):DL : Duquette et al. (1982a); BG : Biémont et al. (1989b); VE : Vogel et al. (1988); HL : Hannaford and Lowe (1981); DU : Duquette et al. (1981a).

We give in the last column of Table 4 the solar photospheric abundances as they have been deduced on the basis of the lifetime measurements quoted in the same table (starred references) and also the difference (Δ, on the logarithmic scale) between photospheric and meteoritic abundances, the meteoritic results being taken from a recent compilation by Anders and Grevesse (1989).

As appears from Table 4, there is now, on the basis of the new atomic data, agreement within the respective error bars between the carbonaceous chondrites and the photosphere for all the heavy refractory elements if we except W and Au. Though the large difference observed for W could be real according to the careful solar analysis carried out by Holweger and Werner (1982), it is more probable that W is only a small contributor to the two weak absorption lines used for the solar analysis. Similar conclusions are valid for Au.

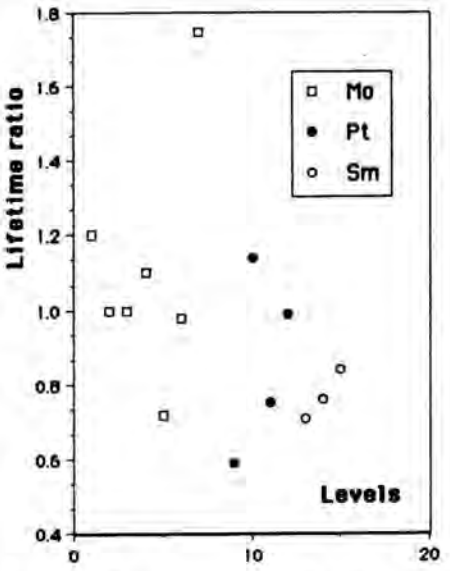

Fig. 8. Same legend as for Fig. 7. Here are plotted : τ(KM)/τ(BL) for Mo I, τ(RA)/τ(GH) for Pt I and τ(BG)/τ(B) for Sm II, where :
KM : Kwiatkowski et al. (1981); BL : Baumann et al. (1978); RA : Ramanujam and Andersen (1978); GH : Gough et al. (1983); BG : Biémont et al. (1989b); B : Blagoev (1978).

The overall agreement sun-meteorites, which is now observed for all these elements, was hidden until recently because large uncertainties were affecting the atomic data (mostly the oscillator strengths) used for the solar analyses.

AUTHOR'S ADDRESS

Institut d'Astrophysique - Université de Liège, B-4200 Cointe-Liège (Belgique)

(§) Senior Research Associate of the belgian National Fund for Scientific Research (FNRS)

REFERENCES

Aashamar, K., Luke, T.M., Talman, J.D., 1983, J.Phys. **B16**, 2695.
Afaneseva, N.V., 1982, Opt.Spectr. **52**, 465.
Anders, E. and Grevesse, N., 1989, Geochim. Cosmochim. Acta **53**, 197.
Anderson, E.K., Anderson, E.M., 1983, Opt. Spectr. **54**, 567.
Arnesen, A., Hallin, R., Nordling, C., Staaf, Ö, Vogel, O., Ward, L., 1983, Z.Phys. **A310**, 251.
Bahr, J.L., Pinnington, E.H., Kernahan, J.A., O'Neil, J.A., 1982, Can.J.Phys. **60**, 1108.
Baumann, M., Liening, H., Lindel, H., 1978, Phys.Lett. **68A**, 319.
Beck, D.R., 1981, Phys.Rev. **A23**, 159.
Bentzen, S.M., Nielsen, U., Poulsen, O., 1982, J.Opt.Soc.Am. **72**, 1210.
Bergström, H., Biémont, E., Lundberg, H., Persson, A., 1988, Astron.Astrophys. **192**, 335.
Bezuglov, N.N., Gorshov, V.N., Osherovich, A.L., Plekhotkina, G.L., 1982, Opt.Spectr. **53**, 239.
Biémont E., 1988, At.Data Nucl.Data Tables **39**, 157.
Biémont E., 1989, At.Data Nucl.Data Tables (in press).
Biémont E., Hansen, J.E., 1986a, Phys.Scr. **34**, 116.
Biémont E., Hansen, J.E., 1987, Nucl.Instr. Methods **B23**, 274.
Biémont E., Hansen, J.E., 1986b, Phys.Scr. **33**, 117.
Biémont E., Cowan, R.D., Hansen, J.E., 1988, Phys.Scr. **37**, 850.
Biémont E., Godefroid, M., 1980, Phys.Scr. **22**, 231.
Biémont E., Quinet, P., Fawcett, B.C., 1989a, Phys.Scr. **39**, 562.
Biémont E., Quinet, P., 1989 (to be published).
Biémont E., Grevesse, N., Hannaford, P., Lowe, R.M., 1981, Astrophys.J. **248**, 867.
Biémont, E., Grevesse, N., Kwiatkowski, M., Zimmermann, P., 1982a, Astron. Astrophys. **108**, 127.
Biémont, E., Grevesse, N., Kwiatkowski, M., Zimmermann, P., 1984, Astron. Astrophys. **131**, 364.
Biémont, E., Karner, C., Meyer, G., Träger, F., zu Putlitz, G., 1982b, Astron. Astrophys. **107**, 166.
Biémont, E., Grevesse, N., Hannaford, P., Lowe, R.M., 1989b, Astron. Astrophys. (in press).
Biémont, E., Grevesse, N., Hannaford, P., Lowe, R.M., Whaling, W., 1982, Astrophys. J. **275**, 889.
Biémont, E., Youssef, N.Y., 1984, Astron. Astrophys. **140**, 177.
Blagoev, K.B., 1978, Opt.Spectrosc. **44**, 17.
Blagoev, K.B., 1981, J.Phys. **B14**, 4743.
Brage, T., Froese Fischer, C., Carlsson, J., Wahlström, C.-G., 1987, Phys.Rev. **A35**, 1113.
Brand, H., Drake, K.H., Lange, W., Mlynek, J., 1980, Phys. Lett. **75A**, 345.
Brandt, T., Helbig, V., Nick, K.-P., 1982, J.Phys. **B15**, 2139.
Breton, C., DeMichelis, C., Hecq, W., Mattioli, M., Ramette, J., Saoutic, B., Bauche-Arnoult, C., Bauche, J., Wyart, J.-F., 1988, Phys.Scr. **37**, 33.
Bruneau, J., 1984, J.Phys. **B17**, 3009.
Carlsson, J., 1988, Phys.Rev. **A38**, 1702.
Carlsson, J., Dönszelmann, A., Lundberg, H., Persson, A., Sturesson, L., Svanberg, S., 1987, Z.Phys. **D6**, 1251.
Cederquist, H., Mannervik, S., Kisielinski, M., Forsberg, P., Martinson, I., Curtis, L.J., Ramanujam, P.S., 1984, Phys.Scr. **T8**, 104.
Ceyzeriat, P., Pegg, D.J., Carré, M., Druetta, M., Gaillard, M.L., 1980, J.Opt. Soc.Am. **70**, 901.
Chaghtai, M.S.Z., Khan, Z.A., Rahimullah, K., 1980, J.Phys. **B13**, 2523.
Coetzer, P.J., Kotze, P.B., Van der Westhuizen, P., 1982, Z.Phys. **A306**, 19.
Costello, J.T., O'Sullivan, G., 1984, J.Phys. **B17**, 4477.
Cowan, R.D., 1981a, Phys.Scr. **24**, 615.
Cowan, R.D., 1981b, The Theory of Atomic Structure and Spectra, Univ. of California Press.
Curtis, L.J., 1981, J.Opt.Soc.Am. **71**, 566.
Curtis, L.J., 1989, Phys.Scr. **39**, 447.
Curtis, L.J. and Theodosiou, C.E., 1989, Phys.Scr. **39**, 317.
Denne, B., Poulsen, O., Phys.Rev. **A23**, 1229.
Den Hartog, E.A., Duquette, D.W., Lawler, J.E., 1987, J.Opt.Soc.Am. **B4**, 48.
Desclaux, J.-P., 1975, Comp.Phys.Comm. **9**, 31.

Duquette, D.W., Salih, S., Lawler, J.E., 1982a, Phys.Rev. **A25**, 3382.
Duquette, D.W., Salih, S., Lawler, J.E., 1982b, Phys.Rev. **A26**, 2623.
Duquette, D.W., Salih, S., Lawler, J.E., 1981a, Phys.Rev. **A24**, 2847.
Duquette, D.W., Salih, S., Lawler, J.E., 1981b, Phys.Lett. **83A**, 214.
Duquette, D.W., Lawler, J.E., 1982, Phys.Rev. **A26**, 330.
Duquette, D.W., Lawler, J.E., 1985, J.Opt. Soc.Am. **B2**, 1948.
Fawcett, B.C., Bromage, G.E., 1980, J.Phys. **B13**, 2711.
Finkenthal, M., Lippman, A.S., Huang, L.K., Yu, T.L., Stratton, B.C., Moos, H.W., Klapisch, M., Mandelbaum, P., Bar-Shalom, A., Hodge, W.L., Phillips, P.E., Price, T.R., Porter, J.C., Richard, B., Rowan, W.L., 1986, J.Appl.Phys. **59**, 3644.
Finkenthal, M., Bell, R.E., Moos, H.W., Bhatia, A.K., Marmar, E.S., Terry, J.L., Rice, J.E., 1981, Phys.Lett. **88ZA**, 123.
Fonseca, V., Campos, J., 1982, J.Phys. **B15**, 2349.
Fonseca, V., Campos, J., 1980, J.Phys. **B13**, 3957.
Gaillard, M.L., Pegg, D.J., Bingham, C.R., Carter, H.K., Mlekodaj, R.L., Cole, J.D., 1982, Phys.Rev. **A26**, 1975.
Gorshkov, V.N., Komarovskii, V.A., 1981, Opt. Spectr. **50**, 853.
Gorshkov, V.N., Komarovskii, V.A., 1986, Opt. Spectr. **60**, 541.
Gough, D.S., Hannaford, P., Lowe, R.M., 1983, J.Phys. **B16**, 785.
Gough, D.S., Hannaford, P., Lowe, R.M., 1982, J.Phys. **B15**, L431.
Grant, I.P., McKenzie, B.J., Norrington, P.H., Mayers, D.F., Pyper, N.C., 1980, Comp.Phys.Comm. **21**, 207.
Hannaford, P., Lowe, R.M., 1981, J.Phys. **B14**, L5.
Hannaford, P., Lowe, R.M., 1982, J.Phys. **B15**, 65.
Hannaford, P., Lowe, R.M., 1983a, Opt.Eng. **22**, 532.
Hannaford, P., Lowe, R.M., 1983b, J.Phys. **B16**, 4539.
Hannaford, P., Lowe, R.M., Grevesse, N., Biémont E., Whaling, W., 1982, Astrophys. J. **261**, 736.
Hannaford, P., Lowe, R.M., Biémont, E., Grevesse, N., 1985, Astron.Astrophys. **143**, 447.
Hannaford, P., Larkins, P.L., Lowe, R.M., 1981, J.Phys. **B14**, 2321.
Hibbert, A., 1989, Phys.Scr. **39**, 574.
Holweger, H., Werner, K., 1982, Sol.Phys. **81**, 3.
Johnson, B.M., Jones, K.W., Gregory, D.C., Ekberg, J.O., Engström, L., Kruse, T.H., Cecchi, J.L., 1985, Phys.Scr. **32**, 210.
Karner, C., Meyer, G., Träger, F., zu Putlitz, 1982, Astron.Astrophys. **107**, 161.
Khan, Z.A., Chaghtai, M.S.Z., Rahimullah, K., 1980, J.Phys. **B13**, 2517.
Klapisch, M., Mandelbaum, P., Schwob, J.L., Bar-Shalom, A., Schweitzer, N., 1981, Phys.Lett. **84A**, 177.
Klapisch, M., Schwob, J.L., Fraenkel, B.S., Oreg, J., 1977, J.Opt.Soc.Am. **67**, 148; see also Luc, E., 1972, Physica **62**, 393.
Klimkin, V.M., Prokopev, V.E., 1980, Opt. Spectr. **49**, 1081.
Kono, A., Hattori, S., 1982, J.Quant.Spectr. Radiat.Transfer **28**, 383.
Kwiatkowski, M., Zimmermann, P., Biémont, E., Grevesse, N., 1982a, Astron.Astrophys. **112**, 337.
Kwiatkowski, M., Teppner, U., Zimmermann, P., 1980, Z.Naturforsch. **35A**, 370.
Kwiatkowski, M., Neuman, F., Werner, K., Zimmermann,P., 1984a, Phys.Lett. **A103**, 49.
Kwiatkowski, M., Micali, G., Werner, K., Zimmermann, P., 1981, Phys.Lett. **85A**, 273.
Kwiatkowski, M., Zimmermann, P., Biémont, E., Grevesse, N., 1984b, Astron.Astrophys. **135**, 59.
Kwiatkowski, M., Micali, G., Werner, K., Schmidt, M., Zimmermann, P., 1982b, Z.Phys. **A304**, 197.
Lindgård, A., Curtis, L.J., Martinson, I., Nielsen, S.E., 1980, Phys.Scr. **21**, 47.
Lindgård, A., Mannervik, S., Jelenkovic, B., Veje, E., 1982, Nucl.Instrum.Methods **202**, 59.
Livingston, A.E., Curtis, L.J., Schectman, R.M., Berry, H.G., 1980, Phys.Rev. **A21**, 771.
Lotrian, J., Guern, Y. Cariou, J., 1980, J. Phys. **B13**, 685.
Mandelbaum, P., Klapisch, M., Bar-Shalom, A., Schwob, J.L., Zigler, A., 1983, Phys.Scr. **27**, 39.
Marek, J., Stahnke, H.J., 1980, Z.Phys. **A298**, 81.
Meyer, G., Ruland, W., Sahm, A., zu Putlitz, G., 1981, Astron.Astrophys. **95**, 278.
Migdalek, J., 1983, J.Quant.Spectr.Radiat. Transfer **30**, 169.
Miller, M.H., Bengtson,R.D., 1980, Astrophys. J. **235**, 294.
Obbarius, H.U., Kock, M., 1982, J.Phys. **B15**, 527.
Osherovich, A.L., Plekhotkina, G.L., Obidin, V.R., 1981, Opt.Spektr. **50**, 1046.
O'Sullivan, G., Costello, J.T., Kane, M., Carroll, P.K., 1988a, J.Phys. **B21**, L195.
O'Sullivan, G., Maher, M., 1989, J.Phys. **B22**, 377.
O'Sullivan, G., Kane, M., 1989, Phys.Scr. **39**, 317.

O'Sullivan, G., Kane, M., Costello, J.T., 1988b, J.Phys. **B21**, 2399.
O'Sullivan, G., 1989, J.Phys. **B22**, (in press).
Pinnington, E.H., Ansbacher, W., Kernahan, J.A., 1984, J.Opt.Soc.Am. **B1**, 30.
Pinnington, E.H., Bahr, J.L., Irwin, D.J.G., 1981a, Phys.Lett. **84A**, 247.
Pinnington, E.H., Bahr, J.L., Irwin, D.J.G., Kernahan, J.A., 1982, Nucl.Instrum. Methods **202**, 67.
Pinnington, E.H., Bahr, J.L., Kernahan, J.A., Irwin, D.J.G., 1981b, J.Phys. **B14**, 1291.
Pleklotkina, G.A., Verolainen, Y.F., 1985, Opt.Spectrosc. **58**, 447.
Poulsen, O., Andersen, T., Bentzen, S.M., Nielsen, U., 1981, Phys.Rev. **A24**, 2523.
Poulsen, O., Andersen, T., Bentzen, S.M., Koleva, I., 1982, Nucl.Instrum.Methods, **202**, 139.
Ramanujam, P.S., Andersen, T., 1978, Astrophys.J. **226**, 1171.
Richter, J., 1984, Phys.Scr. **T8**, 70.
Rudolph, J., Helbig, V., 1982a, Z.Phys. **A306**, 93.
Rudolph, J., Helbig, V., 1982b, J.Phys. **B15**, L1.
Rudolph, J., Helbig, V., 1982c, Phys.Lett. **89A**, 339.
Ryabtsev, A.N., and Wyart, J.-F., 1987, Phys. Scr. **36**, 255.
Ryabtsev, A.N., Wyart, J.F., van Kleef, T.A.M., Joshi, Y.N., 1984, Phys.Scr. **30**, 407.
Salih, S., Lawler, J.E., 1985, J.Opt.Soc.Am. **B2**, 422.
Salih, S., Duquette, D.W., Lawler, J.E., 1983, Phys.Rev. **A27**, 1193.
Schade, W., Helbig, V., 1986, Phys.Lett. **A115**, 39.
Schade, W., Stryla, Z.W., Helbig, V., Langhans, G., 1989, Phys.Scr. **39**, 246.
Schnehage, S.E., Danzmann, K., Kock, M., 1983, J.Quant.Spectr.Radiat.Transfer **29**, 507.
Träbert, E., 1989, Phys.Scr. **39**, 722.
Tursunov, A.T., Eshkobilov, N.B., 1984, Opt. Spectr. **56**, 241.
Ueda, K., Imura, H., Karasawa, M., Fukuda, K., 1981, J.Phys.Soc.Japan **50**, 3545.
Victor, G.A., Taylor, W.R., 1987, At.Data Nucl. Data Tables **28**, 107.
Vogel, O, Edvardsson, B., Wännström, A., Arnesen, A., Hallin, R., 1988, Phys.Scr. **38**, 567.
Wännström, A., Vogel, O., Arnesen, A., Hallin, R., 1988, Phys.Scr. **38**, 564.
Ward, L., Vogel, O., Arnesen, A., Hallin, R., Wännström, A., 1985a, Phys.Scr. **31**, 161.
Ward, L., Wännström, A., Arnesen, A., Hallin, R., Vogel, O., 1985b, Phys.Scr. **31**, 149.
Ward, L., Vogel, O., Ahnesjö, A., Arnesen, A., Hallin R., McIntyre, L., Nordling, C., 1984, Phys.Scr. **29**, 551.
Whaling, W., Chevako, P., Lawler, J.E., 1986, J.Quant.Spectr.Radiat.Transfer **36**, 491.
Whaling, W., Brault, J.W., 1988, Phys.Scr. **38**, 707.
Whaling, W., Hannaford, P., Lowe, R.M., Biémont, E., Grevesse, N., 1984, J.Quant. Spectr.Radiat.Transfer **32**, 69.
Wyart, J.-F., Van Kleef, T.A.M., Ryabtsev, A.N., Joshi, Y.N., 1984, Phys.Scr. **29**, 319.
Youssef, N.H., Khalil, N.M., 1988, Astron. Astrophys. **203**, 378.
Youssef, N.H., Khalil, N.M., 1988, Astron. Astrophys. **186**, 333.
Zettl, F., Neger, T., Jaeger, H., 1984, J. Phys. **B17**, 1755.

E. Biémont, C. Froese Fischer,
M. Godefroid, N. Vaeck and A. Hibbert

Accurate f values for N I and astrophysical implications

ABSTRACT

Two independent and accurate theoretical methods have been used (CIV3 and MCHF) for firmly establishing the oscillator strength scale of the infrared $\Delta n = 0$ transitions of N I. A refined value of the solar abundance of nitrogen is deduced from the CIV3 results: A(N) = 7.99 ± 0.04, in the usual logarithmic scale where the H abundance is 12.00.

INTRODUCTION

An accurate knowledge of CNO abundances in the sun is important for several reasons. Beside of the fact that they constitute a critical test of stellar evolution, the solar abundances remain the primary source of information for cosmic abundances and are often considered as standards for stellar composition. Moreover, due to the fact that these elements are basically volatile and incompletely condensed in meteorites, the sun remains the only source of information for the solar system abundances. The abundance value of nitrogen deduced in previous investigations (Lambert, 1968, 1978) suffered from the lack of an accurate scale of oscillator strengths. The main aim of this study is to provide such an accurate scale of f values for the $\Delta n = 0$ transitions of solar interest and hence to assess definitely the solar abundance value derived from allowed N I transitions.

CIV3 CALCULATIONS

The 12 lines used for the solar analysis (see Table 1) involve the 3 configurations $2s^22p^2n\ell$ ($n\ell$ = 3s,3p,3d). The CI calculations have been performed using an orthogonal basis set (1s,2s,3s,4s,5s, 2p,3p,4p,3d,4d,5d,4f,5f,5g) which, except for the Slater type orbitals 4p,5f, had already been obtained previously (Hibbert *et al.*, 1985). Configuration interaction has been considered for the configurations $2s^22p^2ns$, $2s^22p^2nd$, $2s^22p3pns$,$2p^4nd$ (n=3-5), $2s^22p^25g$, $2p^4ns$ (n=2-5), $2s2p^3np$ (n=3,4) and $2s2p^34f$ for the even parity. For the odd parity, the configurations $2s^22p^3$, $2s^22p^2np$, $2p^4np$ (n=3,4), $2s^22p^2nf$ (n=4,5), $2s2p^3ns$, $2s2p^3nd$ (n=3-5) and $2p^5$ have been retained. This gives rise to 157 and 151 CSF's respectively including all the coupling schemes. Another approach allowed in CIV3 and adopted here consists in making adjustments to the diagonal matrix elements to achieve an accurate energy spitting between the energy states. The inclusion of relativistic effects is done in the Breit-Pauli approximation including the spin-orbit, spin-other-orbit, spin-spin, mass correction and Darwin terms, and keeping the same adjustments as those found in the LS coupling.

MCHF RESULTS

The wave functions obtained with the CIV3 code include near-degeneracy and semi-internal correlation but do not retain external correlation effects. With the MCHF package, we used the notion of "reference set" for generating the wave function expansion, considering all possible single and double excitations which can be generated from the (2p,3s,3p,3d,4s,4p,4d,4f, 5s,5p,5d) virtual orbital basis set. The expansion sizes are quite large reaching 1333 CSF's for the $3p\ ^2D^o$ wave functions. Another major difference with CIV3 lies in the form of the radial distributions defining the one-electron orbitals, which are numerical (instead of analytical) and found by solving the MCHF equations. The Breit-Pauli calculations (MCHF+BP) of the transition probabilities will be performed in the near future and more details about the CIV3 and MCHF calculations themselves will be published at that time.

SOLAR ANALYSIS

The sample of the 12 infrared lines which was retained for the solar analysis is presented in Table 1 together with the relevant atomic (CIV3 *gf* values in the length and velocity formalisms) and solar data. For the 7 lines blended with CN, the CN weak contributions as calculated by Lambert (1978) were deduced from the center-of-disk equivalent widths. A classical LTE method of direct integration of the profiles was used for the analysis (see e.g. Biémont *et al.*, 1981) with the Holweger and Müller (1974) solar model. The mean abundance result, A(N) = 7.99 ± 0.04, corresponding to the mean of the length and velocity CIV3 f values, does agree very well with the abundance value reported by Lambert (1978) but with the basic difference that the scale of oscillator strength is now firmly established. This mean abundance result is slightly, though significantly lower than the result proposed by Anders and Grevesse (1989) (A(N) = 8.05 ± 0.04) and deduced from molecular lines.

REFERENCES

Anders,E., Grevesse,N., 1989 - Geochim. Cosmochim. Acta **53**, 197

Biémont,E., Grevesse,N., Hannaford,P., Lowe,R.M., 1981 - Astrophys.J. **248**, 67

Delbouille,L., Neven,L., Roland,G., 1973 - Photometric Atlas of the Solar Spectrum λ 3000 to λ 10000 - Institut d' Astrophysique - Université de Liège

Hibbert,A., Dufton,P.L., Keenan,F.P., 1985 - Mon. Not. R. Astr. Soc. **213**, 721

Table 1 : N I transitions used for the solar analysis.

λ_{lab} (a)	λ_{sun} (b)	transition	E_{low} (c)	Weight	W_λ (d)	log $gf^{(e)}$ L	V	A_N (f)
7442.293	.23+	$3s\,^4P_{3/2} - 3p\,^4S^o_{3/2}$	10.33	2	2.7*	−0.387	−0.463	7.97
7468.307	.27+	$3s\,^4P_{5/2} - 3p\,^4S^o_{3/2}$	10.33	2	4.9	−0.171	−0.248	8.04
8216.345	.31	$3s\,^4P_{5/2} - 3p\,^4P^o_{5/2}$	10.34	1	8.7	0.146	0.089	7.96
8683.401	.39	$3s\,^4P_{3/2} - 3p\,^4D^o_{5/2}$	10.33	2	8.1*	0.115	0.102	7.89
8718.726	.77	$3s\,^4P_{5/2} - 3p\,^4D^o_{5/2}$	10.34	1	4.3*	−0.338	−0.347	8.02
9392.789	.78	$3s\,^2P_{3/2} - 3p\,^2D^o_{5/2}$	10.69	2	9.5*	0.328	0.378	7.97
8629.238	.17	$3s\,^2P_{3/2} - 3p\,^2P^o_{3/2}$	10.69	1	4.6*	0.090	0.078	7.91
8655.887	.86	$3s\,^2P_{3/2} - 3p\,^2P^o_{1/2}$	10.69	1	1.5	−0.603	−0.616	8.06
8594.005	3.99	$3s\,^2P_{1/2} - 3p\,^2P^o_{1/2}$	10.69	1	2.6*	−0.320	−0.332	8.04
10112.483	.53	$3p\,^4D^o_{5/2} - 3d\,^4D_{7/2}$	11.76	1	3.6	0.622	0.600	8.00
10114.644	.66	$3p\,^4D^o_{7/2} - 3d\,^4D_{9/2}$	11.76	2	5.4	0.778	0.755	8.05
10108.893	-	$3p\,^4D^o_{3/2} - 3d\,^4D_{5/2}$	11.75	2	2.5	0.443	0.420	7.99

(a) Laboratory wavelength (in Å) from Moore (1975)
(b) Solar wavelength (in Å) from Moore *et al.* (1966) (+) or from Swensson *et al.* (1970)
(c) Lower excitation potential (in eV)
(d) Equivalent width (in mÅ as measured on the Jungfraujoch spectra (Delbouille *et al.*, 1973); ⋆ CN contribution deduced (see text)
(e) log gf as obtained in this work in the length (L) or velocity (V) formalisms
(f) Abundance in the logarithmic scale ($A_N = \log \frac{N_N}{N_H} + 12.00$) calculated with the HM model and the mean of gf_L and gf_V.

Holweger,H., Müller,E.A., 1974 - Solar Phys. **39**, 19

Lambert,D.L., 1968 - Mon. Not. R. Astr. Soc. **138**, 143

Lambert,D.L., 1978 - Mon. Not. R. Astr. Soc. **182**, 249

Moore,C.E., 1975 - Selected Tables of Atomic Spectra - NSRDS - NBS 3, Section 5

Moore,C.E., Minnaert,M.G.J., Houtgast,J., 1966, The Solar Spectrum 2935 Å to 8770 Å - NBS Monograph 61

Swensson,J.W., Benedict,W.S., Delbouille,L., Roland,G., 1970, - The Solar Spectrum from λ 7498 to λ 12016 - Mem. Soc. Roy. Sci. Liège - Spec. Vol. 5

AUTHORS' ADDRESSES

E.Biémont (Senior Research Associate of the belgian FNRS)
Institut d'Astrophysique , Université de Liège, Liège - Belgique

C.Froese Fischer
Department of Computer Science, Vanderbilt University, Nashville, USA

M. Godefroid (Research Associate of the Belgian FNRS) and

N.Vaeck (IRSIA Fellowship)
Laboratoire de Chimie Physique Moléculaire, Université Libre de Bruxelles - Bruxelles, Belgique

A.Hibbert
Department of Applied Mathematics and Theoretical Physics, Queen's University of Belfast - Northern Ireland

Carole Jordan

The spectra of cool stars in the ultraviolet region

ABSTRACT

The spectra of cool stars in the wavelength region from 1200 Å to 3000 Å are now well known after eleven years of operation of the International Ultraviolet Explorer (IUE). The solar spectrum provides a detailed guide to the spectra of other main sequence stars from type ~ F5 V to M5 V. Photo-excitation processes become relatively more important in cool giants and supergiants and control much of the emergent spectrum in low gravity stars cooler than ~ K1. Photo-ionization cross-sections and oscillator strengths are required in the interpretation of these spectra.

INTRODUCTION

Observations from rockets and space vehicles have provided a wealth of detail about the solar uv and X-ray spectrum. (See reviews by Tousey, 1988; Feldman, Doschek and Seely, 1988; and Jordan, 1988). Apart from a few lines, the emission from ionized species is controlled predominantly by collisional excitation by electrons. Emission from neutral lines can also be the result of radiative recombination. A full line list for the region 1175 Å - 1710 Å can be found in Sandlin et al. (1986).

The IUE satellite, which has now operated successfully for over 11 years, has led to a substantial amount of information concerning the spectra of other late-type stars, in the wavelength region from ~ 1200 Å to 3000 Å. It has become clear that the uv spectra of main-sequence (dwarf) stars, later than ~ F5 V, are very similar to the solar spectrum, although differences in the structure of the chromosphere and transition region lead to changes in relative line intensities.

On the other hand, there are distinct differences between the solar spectrum and the spectra of giants and supergiants. The late F and type G to K0 III giants still show emission from lines formed in a 'transition region', at temperatures between ~ 2×10^4 and 2×10^5 K, but emission in the O I resonance lines around 1304 Å is relatively stronger. Figure 1 shows a low resolution IUE spectrum of β Cet (G9.5 III), illustrating typical transition region lines and the strong O I resonance lines. (From Eriksson et al., 1983). This strong O I emission was discovered from rocket spectra of α Boo (K2 III) (McKinney et al., 1976) and is caused by fluorescent excitation of the 3d $^3D^0$ term in O I by the strong H Ly β line at 1025.72 Å. (Haisch et al. 1977). Observations with IUE have shown that this process is occurring in virtually all cool low gravity stars.

Giant and supergiant stars cooler than K 1 III or mid-G I have spectra which below ~ 2000 Å are dominated by radiative processes, with lines excited by ion-electron collisions being relatively weaker. Since most of the requirements for further atomic data arise from these observations of cool low gravity stars the rest of this review will concentrate on their spectra, and how they relate to the conditions in the stellar chromospheres. The potential use of future observations from space will be briefly mentioned.

UV SPECTRA OF COOL GIANTS AND SUPERGIANTS

In the IUE short-wavelength region, (SWR) ~ 1200 Å - 2000 Å, the spectra of cool giant stars (later than ~ K1 III) are dominated by H Ly α (1216 Å) and the O I resonance lines (uv 2) at ~ 1304 Å. Figure 2 shows a low resolution spectrum of β Gru (M5 III), taken from Johansson and Jordan (1984). At high resolution (~ 0.07 Å), it becomes apparent that the blend at ~ 1816 Å contains both Si II (uv 1) and the three lines of S I (uv 2), and that the intensities of the S I lines increase relative to those of Si II as the surface temperature of the star decreases. (Brown and Jordan, 1980; Carpenter and Wing, 1979). The lines of Si II are excited by ion-electron collisions, but as discussed further below, the S I lines depend on the H Ly α radiation field and the consequences of high line opacities.

High resolution observations also show that the strong feature at ~ 1304 Å in the low resolution spectra is a blend of O I (uv 2) and of S I (uv 9). This is illustrated in Figure 3, which shows the lines in α Boo (K2 III), from Ayres et al.

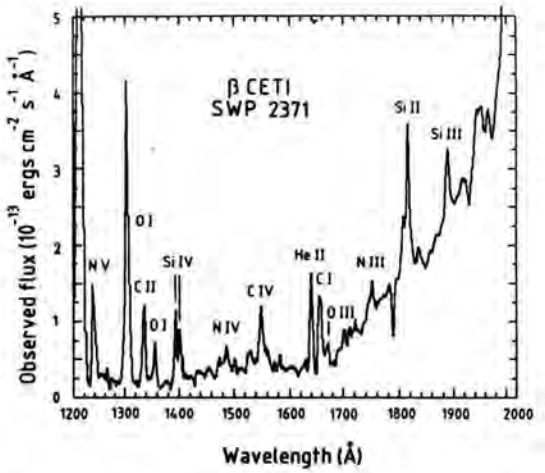

Fig. 1. A low resolution IUE spectrum of β Cet (G9.5 III). From Eriksson et al. (1983).

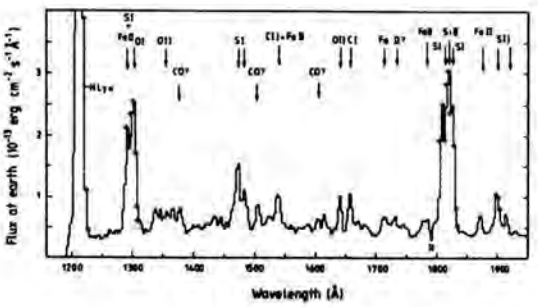

Fig. 2. A low resolution IUE spectrum of β Gru (M5 III). From Johansson and Jordan (1984).

(1986). The O I lines, which are themselves excited via H Ly β fluorescence, have two wavelength coincidences with members of S I uv 9, and cause the observed S I emission, again by fluorescence.

Of the remaining lines, only those of C II (uv 1) and Fe II originate from singly charged ions. The rest of the spectrum is made up of several multiplets of S I, lines of C I and further O I transitions. Also, weaker features which appear systematically in the cool giant spectra can be identified as lines of CO, in the fourth positive

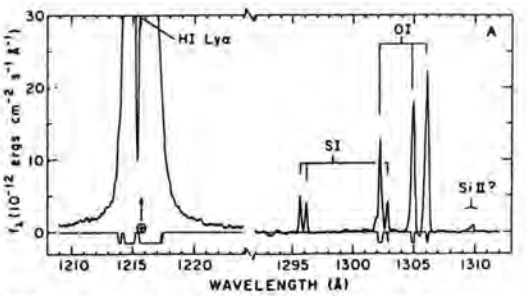

Fig. 3. Part of a high resolution spectrum of α Boo (K2 III), showing S I (uv 9), excited by O I (uv 2). From Ayres et al. (1986).

system, again excited by fluorescence by the strong O I resonance lines. (Ayres et al., 1981). High resolution observations (Ayres et al. 1986) suggest that the transitions are from excited V=9 levels to the lower V=1,2,5 and 9 levels, with the excitation by O I taking place in the 0-9 band.

In the IUE long wavelength region (LWR), from ~ 2000 Å to 3000 Å, the Mg II resonance lines are usually the strongest feature. Inter-system lines of C II (uv 0.01), Si II (uv 0.01) and Al II are also present but the majority of the emission lines are from Fe II. Wing, Carpenter and Wahlgren (1983) have prepared a very useful atlas of high resolution IUE spectra from low gravity stars.

Many of the Fe II lines are from the strong resonance multiplets (uv 1 to 5) and from multiplets terminating on low lying even terms, (eg uv 35, 36, 62, 63, 64), and these are probably excited by ion-electron collisions. However, a number of multiplets are present which would not be strong without some additional source of excitation. Two types of process occur. First, multiplets which have low transition probabilities (eg uv 32-34, uv 60, 61 and uv 78) but which share a common upper level with a strong, optically thick multiplet have their intensity enhanced by 'line leakage' (Brown, Ferraz and Jordan, 1981). Secondly, the strong H Ly α line causes fluorescent excitation of levels around 10 eV, which decay through multiplets such as uv 380, 391 and 399 around 2800 Å to 2900 Å, and in transitions to a^4P and c^4F around 1289-1300 Å and 2507-2509 Å, respectively. (Johansson and Jordan, 1984). A number of other fluorescent routes exciting lines in Fe II, Cr II and Ni II have recently been discussed by Carpenter et al. (1988), in the context of γ Cru (M3.4 III).

Other fluorescent processes also lead to

lines observable in the LWR region. The most striking example is the excitation of the Fe I y^5G^0 J=3 level, from a $^5F_4$, by the Mg II (uv 1) line at 2795.5 Å, which produces two strong emission lines in Fe I at 2843.98 Å and 2823.28 Å (Gahm 1974; Van der Hucht et al., 1979). The lines are seen in a wide variety of giants and supergiants cooler than ~ mid K.

At the sensitivity of IUE few well - resolved emission lines remain unidentified in the SWR spectra and the weaker lines or contributors to blends cannot be observed at high resolution. A relatively small number of weak lines remain unidentified in the high resolution LWR spectra, and these are likely to be due to transitions in singly charged ions. In the solar spectrum, apart from weak lines (see Sandlin et al. 1986), most lines of any strength have acceptable identifications, but there are a few exceptions. The first is at 1318.99 Å, and is usually attributed to N I (uv 12), but the line is significantly stronger than expected from the rest of the multiplet. The spatial behaviour of the line suggests a neutral atom is the origin and as Chipman and Bruner (1975) point out it behaves like the S I line at 1300.91 Å. This is a line from a level above the first ionization limit. Muller (1968) reports an unidentified line of S I at 1319.0 Å, and Berry et al. (1970) also list an unidentified line of S I at 1318.0 Å in their beam foil spectra. A re-examination of the S I spectrum in this region would be of value. A similar line appears at 1351.66 A, and has been attributed to Cl I, photoexcited by the strong line of C II at 1335.17 Å (Shine, 1983). However the spatial behavour of this line makes the identification dubious and it may also be from an unknown level above the first ionization limit in C I, S I or Si I. The line is also observed in the spectra of cool giants, which suggests that recombination might be the excitation mechanism.

EXCITATION PROCESSES AND PLASMA DIAGNOSTICS

The relative decrease in the importance of collisional excitation and increase in radiative excitation can be understood in terms of the lower surface gravities of cool giants and supergiants. The electron density is lower than in main-sequence stars or hotter giants, scaling roughly as $g_*^{1/2}$, while the opacity in strong lines increases roughly as $g_*^{-1/2}$ (Ayres, 1979), owing to the greater extent of the atmosphere in hydrostatic equilibrium. The fluorescent excitation processes are aided by the large opacities of the strong lines that cause the photoexcitation.

Judge (1986) has discussed the effects of the H Ly α radiation on the photoionization of neutral species such as S I, from the $3p^4$ ^1D level; C I, from the $2p^2$ ^1D level ; and of Si I, from the ground ^3P term. The radiation resulting from radiative recombination in C I also photoionizes S I (Judge, 1988). Although recent calculations are available for the photoionization cross sections of the ground states of Si I and S I, (Mendoza and Zeippen, 1988), calculations of comparable accuracy are required for cross sections out of the excited terms of the ground configurations in C I and S I.

In S I the excitation by H Ly α occurs to several high levels with n ~ 12, 13. But because of a strong series perturbation (with $3d'$ $^3D^0$), the oscillator strength for the most important excitation, in $3p^4$ - $3p^3 12d$ $^3D^0$ is not well known. Also, the emergent spectrum depends on the transition probabilities for the decay routes and these too require further attention. (See Judge, 1988, for details). Judge concludes that the emission in S I uv 2 is produced by the H Ly α excitation, but that emission in uv 1 and uv 3 is formed by radiative and low temperature di-electronic recombination, respectively. Improved values for the radiative and autoionizing decay rates for levels above the first ionization limit are thus also needed. In multiplet uv 1 the observed relative intensities of the two transitions from $3p^3 4s$ $^5S^0$ do not agree with the calculated branching ratio, but this could be due to opacity effects.

The fluorescent excitation of O I by H Ly β has been discussed by Skelton and Shine (1982), in the context of the solar atmosphere. They used an observed branching ratio for the decays from $2p^3 3d$ $^3D^0$, (Christensen and Cunningham, 1978), and an experimental f-value from Brooks et al. (1977) for the pumping transition, $2p^4$ ^3P - $2p^3 3d$ $^3D^0$. However, these values differ significantly from the results of the close-coupling calculations by Pradhan and Saraph (1977), and in view of the importance of the O I lines in understanding stellar chromospheres these differences need to be resolved. Work is in progress at Oxford (Munday, private communication), on calculating the O I fluorescence in cool, low gravity stars.

The first calculations of the excitation of the Fe I $y\ ^5C^0_3$ level by the Mg II k line at 2795.5 Å have recently been made by Harper (1988, 1989) for ι Aur (K3 II) and several

cool giants. He finds agreement between observed and calculated fluxes to within a factor of two, depending on the details of the models adopted. The Fe I lines are potentially a valuable diagnostic of the mid chromosphere in cool giants, between the regions where the Ca II H and K and Mg II h and k lines are predominantly formed. However, the fluorescence occurs where iron is mostly in the form of Fe II, and the results are sensitive to the Fe I/Fe ion population ratio. Further work on the relative photoionization cross sections from Fe I levels would be of value.

The f-value of the pumped transition is small and the y $^5G^0_3$ level is strongly mixed with z $^5H^0_3$ (Fawcett, 1987), but Harper finds that the calculated line fluxes are more sensitive to the ion balance than this f-value.

Lines which are interlocked through a common upper level are particularly useful when one of the lines is optically thick and the other is optically thin. Two cases occur in the IUE SWR spectra; C I (uv 2) at $\lambda \sim 1656$ Å, shares a common upper level with C I (uv 32), at 1993.62 Å. Mult. uv 2 is optically thick, while uv 32, $2p^2\ ^1D_2$ - $2p3s\ ^3P^0_1$, being an intercombination line is optically thin. The ratio of the line fluxes then yields the optical depth, and hence the mass-column-density in uv 2. (Jordan,1967). This is a valuable quantity when modelling stellar chromospheres and the method has been applied by Judge (1986) to α Boo.

A similar pair of lines occurs in O I, where uv 146, at 1641.30 Å, is pumped by the resonance lines (uv 2). Multiplet uv 146, $2p^4\ ^1D_2$ - $2p^33s\ ^3S_1$, is a common feature in the spectra of cool low gravity stars (see Fig.2) and the identification is confirmed by high resolution observations. (Brown and Jordan, 1980). The branching ratio from $2p^33s\ ^3S_1$ has recently been calculated by Froese-Fischer (1987), since the 1641.30 Å line has also been discovered in day-glow spectra observed from satellites. The O I lines now provide a good method of determining the resonance line opacities. Other examples of this type are discussed by Jordan (1988).

Methods of determining the electron density directly from suitable line ratios, usually involving intersystem lines, are also important and many of the atomic data are now available. However, there remains a systematic discrepancy between calculated and observed line ratios within the Si II multiplet $3s^23p\ ^2P$ - $3s3p^2\ ^4P$, around 2334-2350 Å. (Fig. 4). This occurs in both high density chromospheres, like the Sun, and in cool giants and bright giants (Judge, 1986; Harper 1988). The observed ratio of the transitions $(^4P_{\frac{1}{2}} - ^2P_{\frac{1}{2}} + ^4P_{5/2} - ^2P_{3/2})/(^4P_{\frac{1}{2}} - ^2P_{3/2})$ is lower than calculated and the observations suggest that the calculated branching ratio from $^4P_{\frac{1}{2}}$ (Nussbaumer, 1977) is too large by an order of magnitude. Recent calculations by Huang (1987) give an even smaller ratio than required by the observations.

FUTURE WORK

The operation of the Hubble Space Telescope,

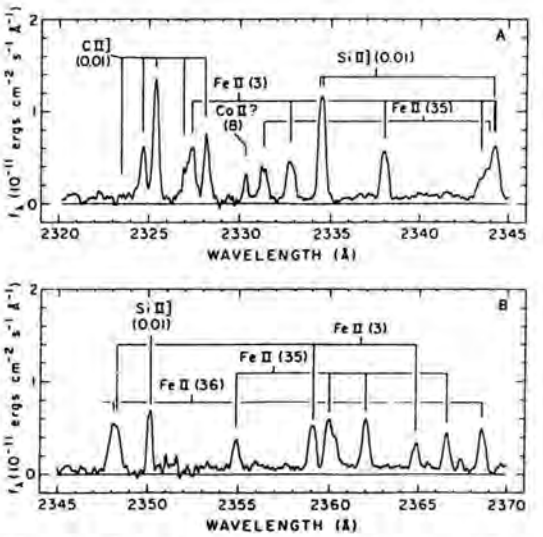

Fig. 4. Part of a high resolution spectrum of α Boo (K2 III), showing lines of C II], Si II] and Fe II. From Ayres et al. (1986).

with its higher spectral resolution than IUE, should lead to further line identifications in features currently suspected to be blends. Depending on the actual sensitivity achieved there is hope that the high resolution and medium resolution spectra will show features which at present can only be observed as blends at low ($\sim$ 6 Å) resolution with IUE. This will undoubtedly lead to further problems in spectroscopy and further demands for atomic data. The improved wavelength resolution should allow the profiles of strong lines to be measured more accurately, particularly in regions near line centre where self-reversals occur. These profiles contain much information concerning the details of chromospheric structure in cool stars.

The extension of observations to below $\sim$ 1200 Å, to at least the H Lyman continuum,

will provide data which, apart from some spectra obtained with Copernicus, have not been available for cool stars. The flux in the H Ly β line and in members of the O I uv 4 multiplet, in which H Ly β pumping occurs, would be directly observable. A considerable number of resonance lines occur in this region which will be of value in modelling the chromospheres and transition regions of late-type stars.

REFERENCES

Ayres, T.R., 1979 - Chromospheric scaling laws, width luminosity correlations, and the Wilson-Bappu effect. In: Astrophys. J., 228, 509-520.

Ayres, T.R., Moos, W. and Linsky, J.L., 1981 - Far ultraviolet fluorescence of carbon monoxide in the red giant Arcturus. In: Astrophys. J. Lett., 248, L137-L140.

Ayres, T.R., Judge, P.G., Jordan, C., Brown., A. and Linsky, J.L., 1986 - High dispersion observations of Alpha Bootis (K1 III) with the International Ultraviolet Explorer. In: Astrophys. J., 311, 947-959.

Berry, H.G., Schectman, R.M., Martinson, I., Bickel, W.S. and Bashkin, S., 1970 - Beam foil spectra of sulphur 600-4000 Å. In: J. Opt. Soc. Am., 60, 333-344.

Brown, A. and Jordan, C., 1980 - S I emission in EUV spectra of late-type stars. In: Mon. Not. R. astr. Soc., 191, 37P-41P.

Brooks, N.H., Rohrlich, D. and Smith. W.H., 1977 - Transition probabilities and absolute oscillator strength for transitions of C I, O I and N I observed in absorption in H I regions. In: Astrophys. J., 214, 328-330.

Brown, A., Ferraz, M.C. de M. and Jordan, C., 1981 - The structure of chromospheres around late-type giants and supergiants. In: The Universe at Ultraviolet Wavelengths: the first two years of IUE. (R.D. Chapman Ed.). NASA CP-2171, 297-302.

Carpenter, K.G. and Wing, R.F., 1979 - Survey of the ultraviolet spectra of late-type stars. In: Bull. Am. Astr. Soc., 11, 419.

Carpenter, K.G., Pesce, J.E., Stencel, R.E., Brown, A., Johansson, S. and Wing, R.F., 1988 - The ultraviolet spectrum of noncoronal late-type stars: the Gamma Crucis (M3.4 III) reference spectrum. In: Astrophys. J. Suppl., 68, 345-369.

Chipman, E. and Bruner, E.C., 1975 - The solar spectrum from 1173 to 1324 Å. In: Astrophys. J., 200, 765-772.

Christensen, A.B., and Cunningham, A.J., 1978 - Laboratory study of O I (7900 Å) branching ratio. In: J. Geophys. Res., 83, 4393 - 4396.

Eriksson, K., Linsky, J.L., Simon, T., 1983 - Outer atmospheres of cool stars. XIV. A model for the chromosphere and transition region of Beta Ceti (G9.5 III). In: Astrophys. J., 272, 665-667.

Fawcett, B.C., 1987 - A study of theoretical computations of oscillator strengths for Fe I. RAL Report 87-114.

Feldman, U., Doschek, G.A. and Seely, J.F., 1988 - Solar spectroscopy in the far-ultraviolet-X-ray wavelength regions: status and prospects. In: J. Opt. Soc. Am. B., 5, 2237-2251.

Froese-Fischer,C., 1987 - The 2p-3s transitions in atomic oxygen. In: J. Phys. B., 20, 1193-1202.

Gahm, G.F., 1974 - A finding list for fluorescing lines in stars with strong emission lines of H, Mg II and Ca II. In: Astron. Astrophys. Suppl., 18, 259-266.

Haisch, B.M., Linsky, J.L., Weinstein, A. and Shine, R.A., 1977 - Analysis of the chromospheric spectrum of O I in Arcturus. In: Astrophys. J., 214, 785-797.

Harper, G., 1988 - The outer atmospheres of hybrid giants. D. Phil Thesis, University of Oxford.

Harper, G., 1989 - Fe I - Mg II k line fluorescence in K giant and bright giant stars. Submitted to Mon. Not. R. astr. Soc.

Huang, K-N., 1986 - Energy-level scheme and transition probabilities of the Al-like ions. In: Atomic Data and Nuclear Data Tables, 34, 1-77.

Johannson, S. and Jordan, C., 1984 - Selective excitation of Fe II in the laboratory and late-type stellar atmospheres. In: Mon. Not. R. astr. Soc., 210, 239-256.

Jordan, C., 1967 - The relative intensities of C I lines in the solar EUV spectrum. In: Sol. Phys., 2, 441-450.

Jordan, C., 1988 - Ultraviolet spectroscopy of cool stars. In: J. Opt. Soc. Am. B., 5, 2252-2263.

Judge, P.G., 1986 - Constraints on the outer atmospheric structure of late-type giant stars with IUE: methods and applications to Arcturus (α Boo K2 III). In: Mon. Not. R. astr. Soc., 221, 119-153.

Judge, P.G., 1988 - The excitation of S I emission lines in chromospheres of late-type giant stars. In: Mon. Not. R. astr. Soc., 231, 419-444.

McKinney, W.R., Moos, H.W. and Giles, J.W., 1976 - The far-ultraviolet (1180-1950 Å) emission spectrum of Arcturus. In:

Astrophys. J. 205, 848-854.
Mendoza, C. and Zeippen, C.J., 1988 - Photoionisation cross sections of the ground states of neutral Si, P and S. In: J. Phys. B. 21, 259-266.
Müller, D., 1968 - Measurements of absorption oscillator strengths of S I and S II lines in the region 1100-2000 Å. In: Z. Naturforsch 23a, 1707-1716.
Nussbaumer, H., 1977 - The Si II spectrum in quasi-stellar objects. In: Astron. Astrophys., 58, 291-293.
Pradhan, A.K. and Saraph, H.E., 1977 - Oscillator strengths for dipole transitions in neutral oxygen. In: J. Phys. B., 10, 3365-3374.
Sandlin, G.D., Bartoe, J-D.F., Brueckner, G.E., Tousey, R. and VanHoosier, M.E., 1986 - The high resolution solar spectrum. In: Astrophys. J. Suppl., 61, 801-898.
Shine, R.A., 1983 - Formation of the Cl I line at 1351 Å in the solar chromosphere. In: Astrophys. J., 266, 882-888.
Skelton, D.L. and Shine, R.A., 1982 - Formation of the O I resonance triplet and intercombination doublet in the solar chromosphere. In: Astrophys. J., 259, 869-879.
Tousey, R., 1988 - The solar spectrum from Fraunhofer to Skylab - an appreciation of the contributions of Charlotte E. Moore Sitterly. In: J. Opt. Soc. Am. B., 5, 2230-2236.
Van der Hucht, K.A., Stencel, R.E., Haisch, B.M. and Kondo, Y., 1979 - A comparision of emission lines in the ultraviolet spectra of α Boo (K2 IIIp), α Tau (K5 III), α Ori (M1-2 Ia-b) and α Sco (M1.5 Iab + B 2.5 V). In: Astron. Astrophys. Suppl., 36, 377-394.
Wing, R.F., Carpenter, K.G. and Wahlgren, G.M., 1983 - An atlas of high resolution IUE spectra of late-type stars: 2500-3230 Å. Perkins Obs. Spec. Publ. 1 (Perkins Observatory Columbus, Ohio).

AUTHOR'S ADDRESS

Department of Theoretical Physics,
University of Oxford,
1, Keble Road, Oxford, OX1 3NP, UK.

R. Mewe

High-resolution X-ray spectroscopy in astrophysics

ABSTRACT

The detection of X-rays from astrophysical sources has provided evidence for the existence of a large variety of stellar, interstellar and extragalactic plasmas with temperatures above one million Kelvin. High-resolution X-ray spectroscopy of such plasmas will allow a detailed study of the physical processes that release the energy and maintain these plasmas. In particular the spectroscopic space missions near the end of the century, viz. NASA's Advanced X-ray Astrophysics Facility (*AXAF*) and ESA's X-ray Multi-Mirror Mission (*XMM*) give astronomers the opportunity to measure many emission and absorption features with a resolution of ~ 0.05 Å in the wavelength range $\sim$ 1–300 Å, allowing them to interpret much better the origins of the different spectral components. To illustrate the diagnostic capabilities of such observations spectral simulations are shown for various types of cosmic sources.

1. INTRODUCTION

Traditionally X-ray spectroscopic results in astrophysics were obtained with instruments used for photometry, viz. proportional counters which have only a limited resolving power, allowing merely to determine the overall shape of the spectrum. Typically, one characterized the X-ray spectrum of a cosmic source by indicating whether it was best fit by simple blackbody, thermal bremsstrahlung, or power law models. In recent years, the introduction of solid state and transmission grating spectrometers on the *EINSTEIN* and *EXOSAT* satellites with somewhat higher spectral resolution (e.g. $\lambda/\Delta\lambda = 10$–100) has provided a taste of detailed spectroscopy of cosmic plasmas and motivated the use of more sophisticated emission models, which include the line emission expected from hot optically thin plasmas in collisional ionization equilibrium (e.g. Raymond and Smith 1977, Mewe *et al.* 1985, 1986). However, since most of the lines are not explicitly spectrally resolved, the spectral constraints derived are still highly model-dependent.

High-resolution spectroscopy in the soft X-ray wavelength region ($\sim$ 2–140 Å) such as will be possible with the next generation of spectroscopic X-ray satellites *AXAF* (Weisskopf 1987) and *XMM* (Barr *et al.* 1988) will allow astronomers to individually detect and identify many of the expected discrete soft X-ray spectral features for many different classes of cosmic sources.

Some of the spectrometers that are currently foreseen on these missions are: the High-Energy Transmission Grating (*HETG*) on *AXAF* (Canizares *et al.* 1987) (with a spectral range $\lambda\lambda \simeq$ 2–30 Å, a spectral resolution $\Delta\lambda \sim 0.02$ Å, and an effective area A of up to ~ 200 cm^2 between 4–10 Å), the Low-Energy Transmission Grating Spectrometer (*LETGS*) on *AXAF* (Brinkman *et al.* 1987) ($\lambda\lambda \simeq$ 4–140 Å, $\Delta\lambda \simeq 0.05$ Å, and A up to ~ 30 cm^2 between 6–50 Å), and the Reflection Grating Spectrometer (*RGS*) on *XMM* ($\lambda\lambda \simeq$ 5–35 Å, $\Delta\lambda \simeq 0.05$ Å, and A up to ~ 250 cm^2 between 10–20 Å).

Contained in the above wavelength regions are a multitude of prominent features from nearly all ion stages of many abundant elements, including the K-shell line and continuum transitions of C, N, O, Ne, Mg, and Si, and the L-shell transitions of Si, S, Ar, Ca, Ni, and Fe. Many of these features will be detected either in emission or absorption for a large variety of different astrophysical plasmas including: stellar coronae, isolated hot white dwarfs, cataclysmic variables, X-ray binaries, supernova remnants, the interstellar medium, normal galaxies, clusters of galaxies, and active galactic nuclei. The detection of emission and absorption features allows to uniquely determine the most important physical parameters for these plasmas including the electron temperature and density distributions, the ion and elemental abundances, mass motions, and the nature of the ambient radiation field. The spectroscopic data we expect to obtain will provide the most direct insight into the physical phenomena that drive the X-ray energy release and will likely provide an enormously important new tool for the study of virtually all known cosmic X-ray sources. Thus high-resolution X-ray spectroscopy represents one of the final observational frontiers for high-energy astrophysics.

In the following sections I briefly discuss the physics determining the formation of X-ray spectra in various types of plasmas, present a few observational results and focus specifically on a number of simulations of spectral observations with the *AXAF* and *XMM* spectrometers for various types of cosmic sources.

2. SPECTRA FORMATION IN PLASMAS

The spectral properties of the emitted radiation will greatly vary with the different physical conditions of spectral line formation in various kinds of astrophysical plasmas. Rather than attempt to include all we know about the physics of X-ray sources, I consider a limited number of highly simplified models (once we have gained a better understanding of the source structure and of the importance of various physical processes, we may synthesize such models into successively more sophisticated approximations of the source model). I distinguish between three categories of plasma models applicable to the cosmic sources which are expected to exhibit soft X-ray spectra (for reviews see e.g. Holt and McCray 1982, McCray 1982, 1984, Mewe 1984, Barr *et al.* 1988): optically thin plasmas, nebular-type photo-ionized plasmas, and optically thick plasmas.

2.1. *Optically thin thermal plasmas*

In a hot optically thin plasma that is sufficiently transparent that the transfer of radiation can be neglected the emergent X-ray spectrum faithfully represents the microscopic emission processes in the plasma and therefore is directly linked to the physical conditions in the plasma. This is the standard *coronal model* that was first applied by Elwert (1952) to the solar corona. It assumes a tenuous plasma in a steady state in which electron collisions control the ionization state and emissivity of the gas. The gas is in a state of statistical equilibrium both for the bound atomic states and for the ionization balance and the plasma electrons and the ions are relaxed to Maxwellian energy distributions with a common temperature, T, a free parameter controlled by external processes. Examples of such plasmas are stellar coronae, supernova remnants, and the hot gas in the interstellar medium and in galaxies and clusters, and possibly also the low-density intercloud medium that pervades most of the central broad-line region in active galactic nuclei.

2.1.1. Ionization state. Much of the temperature sensitivity of the soft X-ray spectrum is associated with the ionization structure which is determined by a balance between electron impact ionization (including sometimes a contribution from autoionization) and radiative plus dielectronic recombination.

As an example Figure 1 shows the iron ionization structure as a function of temperature as calculated by different authors (Arnaud and Rothenflug (1985) (AR) and Raymond and Smith (1977), Raymond (1988) (RS)). As can be seen, it varies dramatically with temperature throughout the range 0.1–100 MK. On the basis of the estimated uncertainties (20–40%) in both ionization and recombination rates (for a discussion see e.g. Raymond 1988, 1989, Mewe 1989), we can expect the predicted ratio of ion concentrations of adjacent ionization stages to be off by a factor, say ~1.5–2. Fortunately, the ionization and recombination rates for the H- and He-like ions, which emit the lines that are among the strongest from hot astrophysical plasmas, are known more accurately than most of the other rates. In the case of ions which have a closed outer electron shell (e.g. He- and Ne-like ions) it doesn't matter very much because such ions cover a broad plateau in dependence of temperature (see Figure 1). This is caused by the fact that this ionization stage can easily be reached from the Li-like stage (only one outer electron with low binding energy) and persists long since the next ionization step towards the H-like stage suddenly needs a much (~4 times) higher ionization energy. This implies that the adjacent Li-like stage is quite critically dependent on temperature. But such ions can still exist when the plasma is not isothermal, but instead has a broad distribution of temperatures (as is often the case, e.g. in stellar coronae or in supernova remnants).

Comparing the AR and RS results, we notice that the overall shapes of the curves are quite similar and that the shifts of the ion peaks are generally limited to within about $\Delta\log T \approx 0.1$. However, the peak values may differ by about 10–30% and sometimes up to ~ 50%. The differences often result from different dielectronic recombination rates (cf. Raymond 1988). The discrepancies are worst for the lower stages of ionization (e.g. Fe VIII and Fe IX), but nearly vanish for the simpler and more thoroughly studied ions of the He- and H-like sequences. Generally, the discrepancy is ~ 10–20% in T, which for many diagnostic purposes is good enough. On the other hand, for a given temperature, the ion abundances may differ by a factor up to about two, especially for the ions just around the He-like and Ne-like "plateaus". For diagnostics of tenuous plasmas the AR ionization balance computations can be used with reasonable accuracy.

However, a few words may be said about possible effects of electric fields on dielectronic recombination (DR) rates. Experimental breakthroughs occurred about five years ago when DR cross sections could be measured for a few singly ionized atoms (e.g. Mg^+ and Ca^+) in crossed-beam experiments (e.g. Hahn 1985, Müller *et al.* 1987 and Dunn 1986). The measured cross-section values were a factor ~ 5–10 larger than predicted ones. A possible explanation of this strong discrepancy was given in terms of the effect of an electric field that causes Stark mixing of different ℓ levels of a given n state. In the experiment, a magnetic field $B \sim 200$ Gauss was used to focus the electron beam. The ions which cross the electron beam with velocities $v \sim 10^7$ cm/s then experience in their rest frame a Lorentz field $E = 10^{-8} vB \approx 20$V/cm, sufficient to produce full Stark mixing. The explanation is as follows. As A_a decreases rapidly with ℓ and as DR rates scale $\propto A_a A_r/(A_a + A_r)$ (A_a, A_r are probabilities for autoionization and radiative decay, resp.) the contribution of resonant states is limited to $\ell \lesssim \ell_c$ (for which $A_a \gtrsim A_r$). The result of mixing high and low ℓ levels is that A_a is increased for high ℓ and decreased for low ℓ, thus flattening the $A_a(\ell)$ versus ℓ curve, so that more states effectively participate in the recombination process, and the DR cross section is increased. In the actual plasma environment the mean thermal drift of ions across a magnetic field of a few hundred Gauss may well generate such Lorentz electric fields (e.g. in solar or stellar coronal loop structures).

Though the effects of electric fields are yet to be fully incorporated into future DR rate calculations, it is interesting to visualize this effect on the hand of a simple model (see Müller *et al.* 1987). The typical enhancement factor for the DR recombination of ion $Z^{+(z+1)}$ due to full Stark mixing I approximate by $f = 1+10\,(z+1)^{-1.15}$. (We note that the effects are biggest for the lower ions as here many n states take part in the DR process). Figure 2 compares the results for the AR oxygen and iron ionization balance without and with correction for the DR rates. This illustrates that this effect can be important for the lowly ionized atoms that are formed e.g. in cool ($\lesssim$ 2 MK) coronal or photoionized plasmas.

2.1.2. Line excitation and spectra. The spectral lines that dominate the soft X-ray spectrum and the cooling of astrophysical plasmas at temperatures up to ~ 10 MK are mainly excited by electron collisional excitation from the ground state, followed by spontaneous radiative decay from the upper line level. The formation of a particular spectral line transition $2 \rightarrow 1$ emitted by ion Z^{+z} from element of atomic number Z is as follows. The total depopulation rate of the upper level (2) is equal to $N_2 \sum_i A_{2i}$, where N_2 is the density (cm^{-3}) of ions in the upper level 2 and A_{2i} is the probability (s^{-1}) of a spontaneous radiative transition from level 2 towards a lower level i (collisional de-excitation is neglected here). This will be balanced by electron collisional excitations from the ground state (g) at a rate $n_e N_g S_{g2}$, so that the volume emissivity P_{21} (phot cm^{-3} s^{-1}) is given by

$$P_{21} = N_2 A_{21} = n_e N_g B S(T) = (N_H/n_e) A_Z n_e^2 \eta_z B S(T), \quad (1)$$

where n_e is the plasma electron density (cm^{-3}), $S(T)$ is the rate coefficient ($cm^3\ s^{-1}$) for collisional excitation $g \rightarrow 2$ (dependent on electron temperature T), $B = A_{21}/\sum_i A_{2i}$ is the radiative branching ratio, N_g the ground state population (cm^{-3}) of ion Z^{+z}, $A_Z = N_Z/N_H$ the abundance of element Z relative to hydrogen (H), η_z the fraction of ions from element Z in ionization stage z and N_H/n_e is of the order unity ($\simeq$ 0.85) for a plasma with cosmic abundances. The excitation rate coefficient can be written as:

$$S(T) = 8.62\ 10^{-6}\ \frac{\bar{\Omega}(y)}{\omega T_{[K]}^{1/2}} \exp(-y)\ (cm^3\ s^{-1}), \quad (2)$$

where $y = E_0/kT$, E_0 is the excitation threshold energy, ω is the statistical weight of the initial (usually ground) level and $\bar{\Omega}(y)$ is the collision strength averaged over the Maxwellian electron energy distribution. Some time ago I have introduced (e.g. Mewe 1972, Mewe and Schrijver 1978, Mewe 1988) a parametrized interpolation formula for Ω that represents the correct behaviour near threshold and asymptotically at high energies and that can be integrated analytically over the Maxwellian electron energy distribution. We have used such an expression to fit to many available theoretical and experimental data for excitation cross sections or rates. When no data are available one can make use, for a rough estimate, in the case of optically allowed dipole transitions, of the Gaunt factor formula:

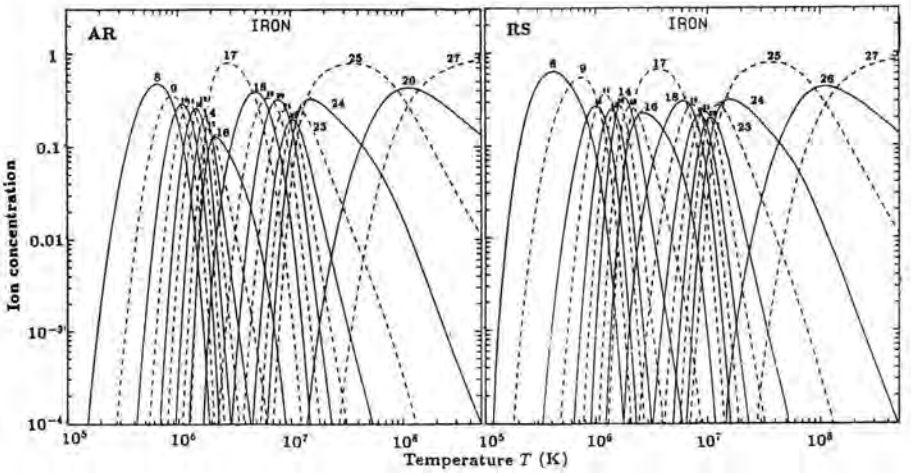

Fig. 1. Ion fractions as a function of temperature for iron as calculated by AR and RS (see text). Ion stages are designated by numbers, e.g. 8 indicates ion Z^{+7} (Fe VIII), etc.

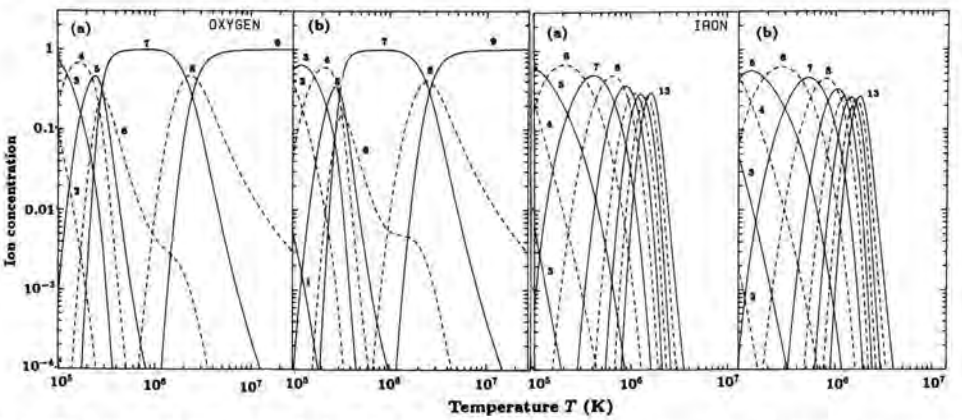

Fig. 2. Ion fractions for O and Fe as calculated for the AR ionization balance without (a) and with (b) correction for ℓ level Stark mixing.

$$\tilde{\Omega} = \frac{8\pi}{\sqrt{3}} \frac{E_H}{E_0} \omega f \bar{g} = 197.3\, \omega f \bar{g} E_{0[\mathrm{eV}]}^{-1}, \qquad (3)$$

where f is the absorption oscillator strength and $\bar{g} \equiv \bar{g}(y)$ the average Gaunt factor. With an accuracy of a factor of two or so typically $\bar{g} \sim 0.2$ for $\Delta n \neq 0$ transitions and ~ 1 for $\Delta n = 0$ transitions.

Though in a number of cases the Gaunt factor approximation method gives reasonably accurate results, more accurate values are needed, especially for the weaker lines and optically forbidden transitions. Raymond (1988) gives a brief discussion of the accuracy of several computational methods such as Coulomb-Born (CB) and Distorted Wave (DW) approximations, and the more accurate Close Coupling (CC) method, which properly takes into account the dominant resonances near the threshold of excitation (for a review of theory see Seaton (1975), of crossed-beam experiments see Dolder and Peart (1986), and of plasma measurements of atomic rates see Griem (1988)). CB tends to overestimate the collision strength near threshold by $\sim$ 20–50%, while DW gives better results, especially for high-Z ions. Few accurate CC results are available for He-like ions (Kingston and Tayal 1983). Recent compilations of excitation collision strengths are reported by Aggarwal *et al.* (1985) and by Gallagher and Pradhan (1985). For many of the strongest X-ray lines, e.g. from H- and He-like ions and Li- to Ne-like ions, the collision strengths are known with better than 20% accuracy. Near threshold, the strong resonances may spoil the accuracy. However, for applications of rate coefficients in plasma diagnostics, we should not worry too much about this, because in averaging the cross section over the electron energy distribution we smooth out these resonances for a great deal.

Furthermore, there is an additional contribution to the X-ray spectrum from continuum emission due to bremsstrahlung, recombination, and two-photon emission from H- and He-like ions (Mewe *et al.* 1986).

The overall appearance of the X-ray spectra will be dominated by the ionization structure. Therefore, in a wide temperature range (0.01–10 MK) the X-ray spectra of optically thin sources are rich in emission lines from many ions of a number of cosmically abundant elements in different ionization stages. In extremely hot ($\gtrsim$ 100 MK) plasmas all abundant elements are nearly fully ionized and the X-ray emission is dominated by continuum radiation. The emission line and continuum X-ray spectra have been reasonably accurately calculated (e.g. Raymond and Smith 1977, Mewe *et al.* 1985, 1986). From a comparison between different calculations Raymond (1988) concludes that for the strongest X-ray lines, e.g. those of the H- and He-like ions, the agreement generally approaches about 20% (which is important because the He-like lines can be used for density diagnostics), whereas for other cases (e.g. iron lines around 10–12 Å and silicon and sulphur lines around 40–50 Å) discrepancies of a factor of two may exist due to the uncertainties in the atomic rates for excitation

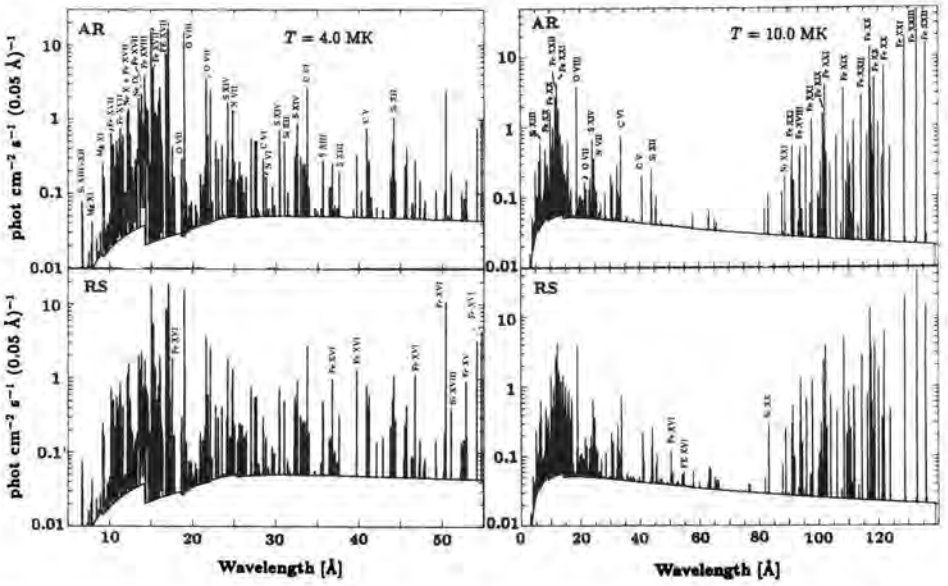

Fig. 3. Comparison of various optically thin X-ray spectra calculated for different ionization balances (AR: Arnaud and Rothenflug, RS: Raymond and Smith) for temperature $T = 4$ MK and 10 MK, reduced emission measure $\varepsilon/d^2 = 10^{50}$ cm^{-3} pc^{-2} (d is source distance), and wavelength regions 5–55 Å and 3–140 Å, respectively. The intrinsic spectral lines are assumed to be Doppler-broadened corresponding to the temperature T. The most prominent lines are labelled with the corresponding ion species. The spectra are binned in 0.05 Å intervals. The most prominent lines are labelled with the corresponding ion species. The contribution from the continuum radiation is separately indicated by a solid line. In all calculations excitation rates from Mewe *et al.* (1985) are used.

and ionization. A comparison in Figure 3 of theoretical spectra derived using two different ionization balance calculations (AR vs. RS) for isothermal, cosmic abundance plasmas at $T = 4$ and 10 MK, respectively, confirms the above conclusions. Figure 3 also illustrates that the X-ray spectrum is very sensitive to the electron temperature, so that a measurement of the spectrum provides an extremely sensitive temperature diagnostic. Substantial differences are observed for the two cases, not only in the overall shape of the spectral energy distribution, but also in the detailed line structure in virtually every narrow wavelength band. In some cases the line strengths are sensitive to the electron density and in certain circumstances also to deviations from the ionization equilibrium (e.g. transient plasmas in supernova remnants or solar flares) or to deviations from Maxwellian electron energy distributions (e.g. solar flares).

2.1.3. Differential emission measure modelling. Eq. (1) shows that for an optically thin isothermal plasma with cosmic abundances the line intensity integrated over the whole source volume V (cm^3) is proportional to the well-known total *emission measure* $\varepsilon \equiv \int n_e^2 dV$ (cm^{-3}) of the source, but for a general (and more realistic) multi-temperature structure in the plasma the situation is more complicated. In this case we can make use in the analysis of optically thin spectra of the concept of a differential emission measure (DEM) distribution, which is defined as follows. For a multi-temperature plasma the line strength can be expressed as $\propto \int S(T) n_e^2 dV \equiv \int S(T)\varphi(T)dT$, where $\varphi(T) = n_e^2 \frac{dV}{dT}$ (cm^{-3} K^{-1}) is the so called *differential emission measure* (which also can be used to describe the continuum emission). Note that the total emission measure is given by $\varepsilon = \int n_e^2 dV = \int \varphi(T) dT$. The differential emission measure distribution can be derived from the observed spectrum by deconvolving $\varphi(T)$ from the measured spectral intensities, using known emission functions for the individual wavelength bins. For this deconvolution we can apply an iterative technique which uses an initial form for the differential emission measure, $\varphi_0(T)$, to calculate theoretical line intensities, i.e. the Withbroe-Sylwester iteration scheme based on a method proposed by Withbroe (1975) and modified by Sylwester *et al.* (1980). Lemen *et al.* (1989) have applied this technique to analyze the *EXOSAT* X-ray spectra of stellar coronae, but this method can be applied equally well to investigate the temperature structures of other kinds of optically thin plasmas such as supernova remnants and cooling flows in clusters of galaxies.

2.1.4. Electron density diagnostics. Determination of electron densities n_e in hot cosmic plasmas provides another challenge for X-ray astronomy. In combination with a determination of the emission measure $\varepsilon = \int n_e^2 dV$ from spectral fits a value derived for the electron density will provide direct information about the emitting source volume V. In order to test current theoretical models of the X-ray source, it is very important to establish its size. Electron densities can be measured using density-sensitive spectral lines originating from metastable levels or using innershell excitation satellites to resonance lines (e.g. Mewe 1988). In the first case the He-like $2 \rightarrow 1$ triplet system lines are particularly important (Gabriel and Jordan 1969, Pradhan and Shull 1981, Pradhan 1982, 1985, Mewe *et al.* 1985). The intensity ratio of the forbidden (f) to intercombination (i) lines varies with electron density due to the collisional coupling between the metastable 2^3S upper level of the forbidden line and the 2^3P upper level of the intercombination line. The f/i line intensity ratio in the wavelength region 5–42 Å of He-like ions from C through S can be used to diagnose coronal plasmas in the density range $n_e = 10^8$–10^{15} cm^{-3} and corresponding temperature range $T \sim$ 1–20 MK. Figure 4 shows the expected O VII line strengths with 0.05 Å resolution, for a coronal plasma with a temperature of 2 MK and densities of 10^{10}, 10^{11}, and 10^{12} cm^{-3}, respectively.

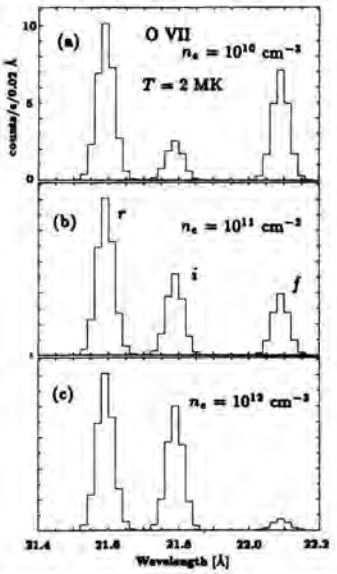

Fig. 4. O VII triplet at 22 Å as observed with the *XMM-RGS* for $T = 2$ MK, $n_e = 10^{10}$, 10^{11} and 10^{12} cm^{-3} and $\varepsilon/d^2 = 10^{52}$ cm^{-3} pc^{-2}. Symbols r,i,f indicate the resonance, intercombination, and forbidden line, respectively.

2.1.5. Deviations from the coronal approximation. Apart from the uncertainties of the basic atomic parameters (typically ~ 30–50%), other uncertainties can arise from the simplifying assumptions made in the coronal model. Raymond (1988) and Mewe (1989) have discussed several effects of relaxing the restrictions by considering optical depth and high-density effects, and deviations from a Maxwell distribution or from ionization equilibrium in transient plasmas.

2.1.6. Examples of spectra from optically thin sources. Because the emission line spectra and continua from optically thin plasmas are fairly well known, high-resolution X-ray spectroscopy has its most obvious application in the measurement of optically thin sources such as the *coronae of stars*. X-ray observations with the *EINSTEIN* observatory have demonstrated that soft X-ray emitting coronae are a common feature among stars on the cool side of the Hertzsprung-Russell diagram. Observations with the transmission grating spectrometers (*TGS*) aboard *EINSTEIN* (Mewe *et al.* 1982) and *EXOSAT* (Schrijver 1985, Lemen *et al.* 1989, Schrijver *et al.* 1989) and with the solid state spectrometer (*SSS*) on *EINSTEIN* (Swank *et al.* 1981) have shown that data of even modest spectral resolution

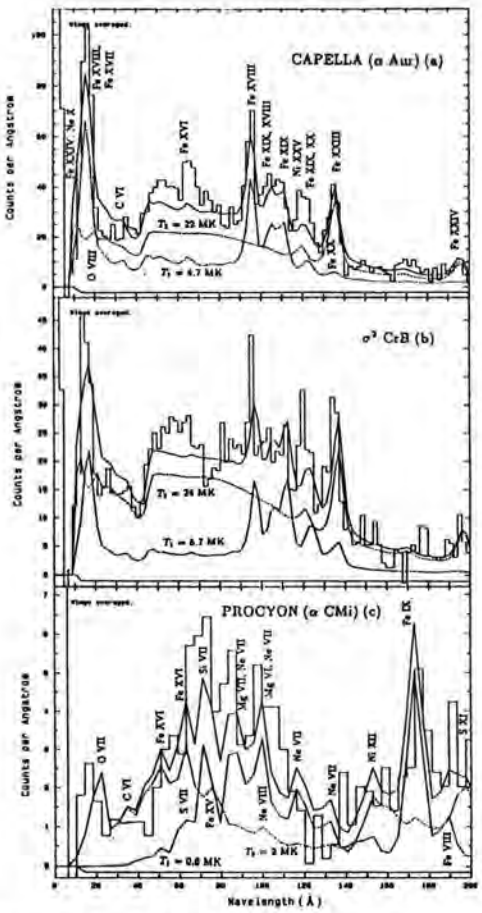

Fig. 5. *EXOSAT* 500 lines/mm *TGS* spectra of Capella (a), σ^2 CrB (b) (binned in 2 Å bins), and Procyon (c) (binned in 4 Å bins), compared with the best-fit two-temperature spectrum (continuous line). The two temperature components 1 and 2 are shown separately by a dotted or a dash-dotted line, respectively. The most prominent lines are labelled with the corresponding ion species.

($\lambda/\Delta\lambda$= 10-100) allows the identification of coronal material at different temperatures whose existence may relate to a range of possible magnetic loop structures in the outer atmospheres of these stars. Comparison of measured line fluxes with known theoretical emissivities yields the DEM distribution with temperature, which is an essential first step in building a model for a stellar corona and assessing the important terms in the coronal energy balance. Figure 5 shows the results obtained with the *EXOSAT-TGS* with $\sim$ 3 Å resolution for three different late-type stars. Some interesting points readily emerge from an identification of the spectral lines and line complexes in these spectra. The active stars Capella and σ^2 CrB show a prominent Fe XXIII line at 133 Å which is typical for hot plasmas with temperatures T of about 10–20 MK, such as observed in solar flares (e.g. Mason *et al.* 1984). This line is absent in the spectrum of the much cooler corona ($T \simeq 0.6$ MK) of the star Procyon, which contains instead a strong blend of lines around 170 Å, that can be identified as a group of spectral lines from Fe IX–XI ions (formed at T in the range 0.6–2 MK). On the other hand, this 170 Å emission feature is not present in the spectra of Capella and σ^2 CrB which implies that only relatively little plasma cooler than 2 MK can be present in the coronae of these stars. This conclusion is supported by the narrowness of the Fe XVII–XVIII line complex at 15 Å: if much plasma with temperatures below 2 MK were present, this complex would be broadened by O VII lines at 21.6 Å and 22.1 Å. The intensity ratio of the 15 Å Fe XVII-XVIII line complex and the Fe XVIII–XXIII line complex between 90–140 Å demonstrates that the spectra cannot be emitted by an isothermal plasma, but instead requires at least a two-temperature interpretation. On the basis of a detailed DEM analysis Lemen *et al.* (1989) confirm that the emission of the corona of each of these stars is dominated by plasma in two relatively narrow temperature intervals: 5 MK and 25 MK for Capella and σ^2 CrB, and 0.6 MK and $\sim$ 2 MK for Procyon. By analogy with the Sun, the outer atmospheres of cool stars with a convection zone are generally assumed to consist of magnetic loop structures filled with hot plasma, which connect opposite polarities in the photosphere. The DEM distributions as provided by such loop models suggest model coronae comprising two distinct ensembles of quasi-static magnetic loops with maximum temperatures around the dominant temperatures given above (Schrijver *et al.* 1989).

The improved spectral resolution of the next generation of spectrometers aboard *XMM* and *AXAF* is needed to fully resolve the temperature structure of stellar coronae, as is shown in Figure 6 which compares between simulations for transmission grating spectra from *AXAF* and *EXOSAT*.

Another important class of thin X-ray sources are the *remnants of supernova explosions*, which play a dominant role in the heating and the replenishment (hence the enrichment by heavy elements) of matter in the surrounding interstellar medium. Supernova explosions, dramatic events in themselves, have also profound and long lasting effects on the appearance and future evolution of the galaxies in which they occur. Following a stellar explosion a substantial fraction of the star's mass is ejected at high velocity into the surrounding interstellar medium and the visible manifestations of such an event are collectively described by the term supernova remnant (SNR). For young remnants (i.e. those with age $\lesssim 10^4$ years) the associated high-temperature plasma is mostly comprised of ejected material, whereas for the old remnants the plasma results from the ambient interstellar gas that has been heated by the passage of the shock wave from the explosion. In either case, plasma temperatures are in the range above 1 MK and hence observations of spectrally resolved X-ray emission lines provide the most useful information about this hot gas.

The detection and analysis of the X-ray emission spectra of recently detected extragalactic supernovae will be of particular importance. The recent observation of hard X-rays from the supernova SN1987A raises the very interesting possibility

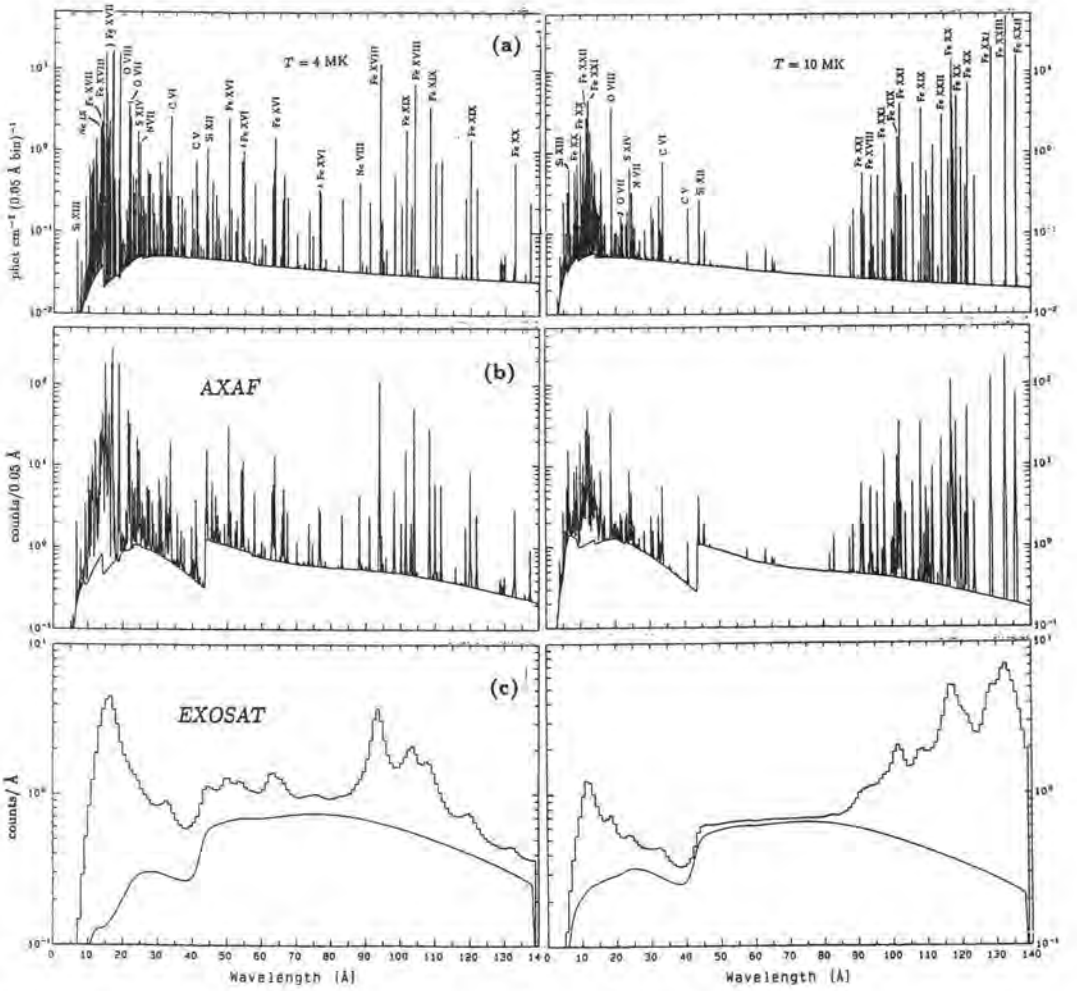

Fig. 6. Panel a: incident photon flux spectra between 3–140 Å, integrated over 10^4 s, calculated for an optically thin plasma with temperature $T = 4$ and 10 MK, reduced emission measure $\varepsilon/d^2 = 10^{50}$ cm^{-3} pc^{-2}. The most prominent lines are labelled with the corresponding ion species. Panels b and c: Incident spectra convolved with the response of *AXAF–LETGS* and *EXOSAT-TGS*, respectively. The upper curves in panels c are the total line plus continuum spectra, whereas the bottom curves represent the contribution from the continuum radiation only.

of detecting soft X-rays from the remnant during the lifetime of *XMM*. An indication of the power of future X-ray spectroscopy for these studies is provided by Figure 7 which exhibits a simulation of a two-component spectrum of a Puppis A type SNR placed at a distance of 55 kpc in the Large Magellanic Cloud.

Finally, I consider the *clusters of galaxies* which are prominent X-ray sources due to the presence of hot intracluster gas. The discovery of iron line emission at $\sim$ 6.7 keV has demonstrated that such intracluster gas must have been processed in stars within the galaxies, since it is enriched with heavy elements. An accurate determination of the temperature of this gas (10-100 MK) provides the opportunity to measure the gravitational cluster potential, since the gas must be close to hydrostatic equilibrium. This gives an indication of the "hidden" mass in the cluster which appears to be a common constituent of our Universe. The gas density within the core of a cluster is generally so high that radiative cooling is important and an inflow of gas takes place onto the central galaxy. The mass flow of the cooling gas is estimated to reach sometimes very large values of up to 400 solar masses per year, which implies that the total accumulation of matter can be comparable to the mass ($10^{12} M_\odot$) of a whole large galaxy. The simple presence or

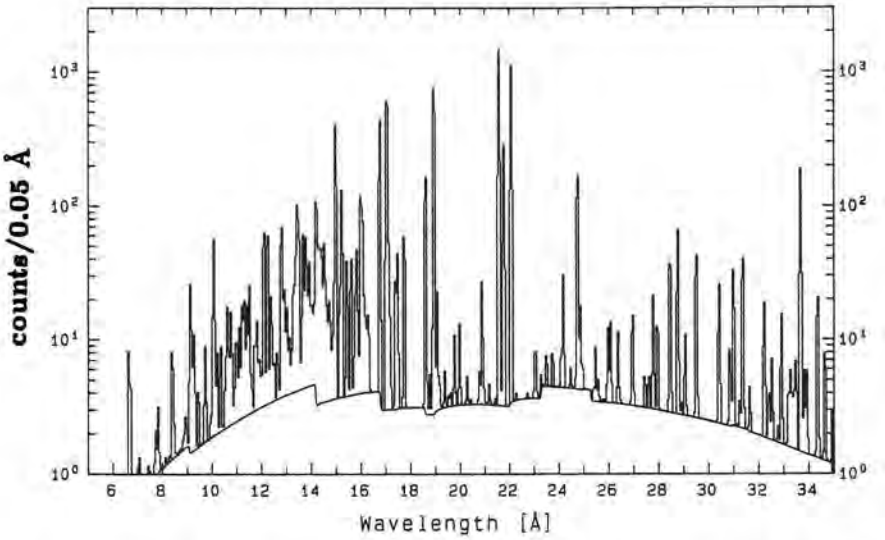

Fig. 7. A simulation of the spectrum of the Puppis A supernova remnant as seen through the *XMM-RGS* in 10^4 s for the case where the source is placed at the distance (55 kpc) of the Large Magellanic Cloud. At this distance, the finite source extent does not appreciably degrade the instrument spectral resolution. Assumed parameters: temperatures T_1=2 MK, T_2=7 MK, emission measures ε_1=1.8 10^{59} cm^{-3}, ε_2=4 10^{58} cm^{-3} and a correction for the interstellar absorption with a hydrogen column density N_H=5 10^{20} cm^{-2}.

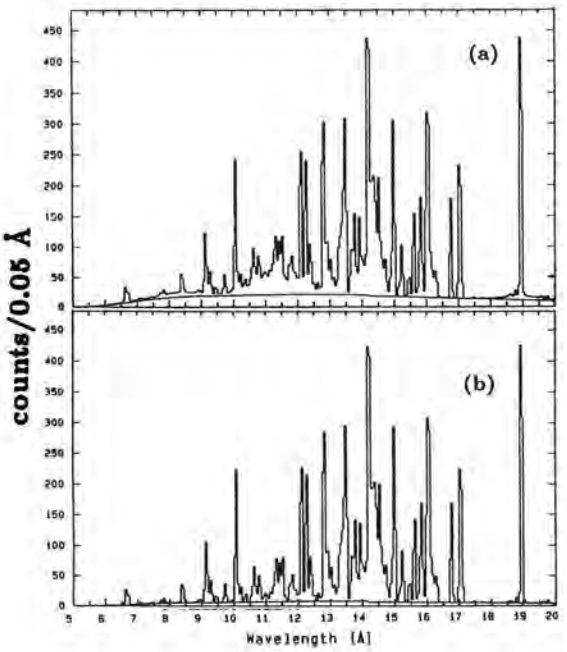

Fig. 8. Two-temperature spectrum of the cooling flow onto M87 in the Virgo cluster, folded through the response of the *XMM-RGS* for an observation time of 10^4 s. Top panel (a) shows the total spectrum of cooling flow (T_1=7 MK) and hot cluster gas (T_2=20 MK), bottom panel (b) shows the (dominant) contribution of the cooling flow only. Interstellar hydrogen column density $N_H = 10^{21}$ cm^{-2}. At the distance of 20 Mpc the cooling flow can be considered as a point source, but the finite extent of the hot gas component appreciably degrades the instrumental resolution and efficiency.

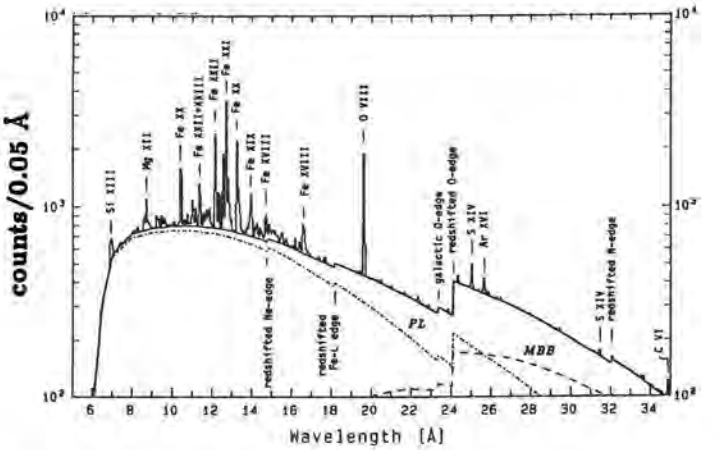

Fig. 9. Typical AGN spectrum as observed with the *XMM-RGS* in 10^5 s. The contributions from power law (PL) and modified black body (MBB) spectra are separately plotted (for details see text). O I absorption edge from our galaxy and various redshifted absorption edges and prominent emission lines from the source are indicated.

absence of certain spectral lines defines the temperature distribution in the source. Figure 8 shows the simulated *XMM-RGS* spectrum of the cooling flow onto the massive galaxy M87 at the core of the Virgo cluster. A simple two-temperature model has been used (parameters from Lea *et al.* (1982)). With a relatively short (10^4 s) exposure the emission lines of the cooling flow are bright and well resolved, whereas the lines from the hot component are smeared out due to the finite source extent and give only a minor contribution.

The most efficient energy sources known occur in *active galactic nuclei* (AGN). It is generally considered that accretion onto a supermassive black hole is the basic underlying process, which can be more than an order of magnitude more efficient in converting restmass to energy than is nuclear fusion. Detailed X-ray spectral studies are essential in understanding the accretion of matter onto such huge compact objects. Clearly this is of primary importance for testing the laws of physics under extreme conditions.

Current models of the X-ray emission of AGN distinguish between a hard X-ray power-law component and a soft excess above $\sim$ 25 Å. The hard component is usually attributed to non-thermal radiation from the central source that is inverse Compton scattered by very energetic electrons. The soft component is associated with the hotter parts of the accretion disk and described by a modified blackbody spectrum or it may be thermal bremsstrahlung of tenuous gas, in both cases with temperatures in the range 0.3–1 MK. Hence the absence or presence of spectral lines will show the true nature of this soft X-ray excess.

In some AGN there is evidence for another soft component of which the origin is presently unknown. Optical measurements show that the central region (radius $\sim$ 0.3 pc) contains dense ($\sim 10^9$ cm^{-3}) blobs of cool ($\sim$ 0.01 MK) gas with velocities $\sim 10^4$ km/s, the so called broad line region (BLR). It may be possible that the soft X-rays are emitted by a hot ($\sim$ 10 MK) tenuous ($\sim 10^6$ cm^{-3}) and *optically thin* gas that is in pressure equilibrium with these clouds and that pervades most of this central volume. High-resolution X-ray spectroscopy with the possibility to detect lines will be the ultimate tool to probe the physical conditions in the cores of AGN. To illustrate this I show in Figure 9 an example of a typical AGN spectrum folded through the *XMM-RGS* response (Kaastra *et al.* 1989). Three components are included: a power law with photon index -1.7 (average parameters from 3C 120, cf. Petre *et al.* (1984)), thermal line and bremsstrahlung with temperature 10 MK and emission measure 2 10^{66} cm^{-3} (parameters from 3C 120) and modified blackbody emission with temperature 1 MK (parameters from NGC 5548, cf. Kaastra and Barr (1989)). The system is placed at a redshift of 0.033 (i.e. distance 198 Mpc). Due to the redshift several absorption edges (e.g. from O I) due to absorption in our galaxy (column density $N_H = 2\ 10^{20}$ cm^{-2}) and at the source ($N_H = 10^{21}$ cm^{-2}) can be resolved, as well as many thermal emission lines. At long wavelengths the modified blackbody component dominates, at shorter wavelengths the power law. The *redshifted* O VIII line at 19.6 Å can be detected within 10^4 s at the 5σ level for AGN's with a spectrum as shown in Figure 9.

2.2. *Nebula-type photoionized plasmas*

The nebular model is applicable to an important class of cosmic X-ray sources involving photoionized nebulae. Examples include accretion-powered sources like X-ray binaries, cataclysmic variables, and active galactic nuclei, where a central X-ray emitting region is surrounded by a cooler, partially ionized medium. Other examples are early-type stars in which X-rays produced in a hot corona must be transferred outward through a stellar wind, and stellar sources located near the nucleus of normal galaxies which are surrounded by the local interstellar medium.

In all these cases photoelectric absorption edges will substantially modify the emergent X-ray spectrum particularly at

longer wavelengths. High-resolution spectral measurements of the strength of K-shell absorption edges in combination with emission lines produced by recombination, provide information on the geometry of the medium surrounding the source along the line of sight. The nebular model (e.g. Holt and McCray 1982, McCray 1982, 1984, Kallman and McCray 1982) is the X-ray analogue of a planetary nebula, in which a central continuum source ionizes the surrounding gas. The gas may be optically thick to photoabsorption but not to electron scattering. The ionization and temperature structure of the gas are established by a stationary balance between photoionization (collisional ionization can be neglected) and heating due to the central X-ray source and, on the other hand, (radiative plus dielectronic) recombination and charge exchange and cooling of the gas. When the gas is optically thin, the local radiation field is determined by geometrical dilution of the source spectrum. Then the local state of the gas (at radius R from the central X-ray source) can be parametrized in terms of the scaling parameter $\xi = L/nR^2$ (L is the total luminosity of the central source, n is the local gas density).

The model can be applied to a wide variety of astrophysical X-ray sources and ranges from optically thin to optically thick in the photoionization continuum of abundant elements. In the latter case, the transfer of continuum radiation should be taken into account.

It may be instructive to contrast the nebular model with the coronal model. In the latter model the mechanism for heating the gas is not specified, but the heat input is coupled directly to the ions and free electrons. The parameters characterizing this model are electron temperature, element abundances, and emission measure. At a given temperature only one or two ionization stages of a given element are abundant. In the nebular model the temperature of the gas is not a free parameter, but instead is determined by absorption and emission of radiation in the gas. The elements are primarily ionized by innershell photoionization. As a result a wider range of ionisation stages of a given element can simultaneously occur

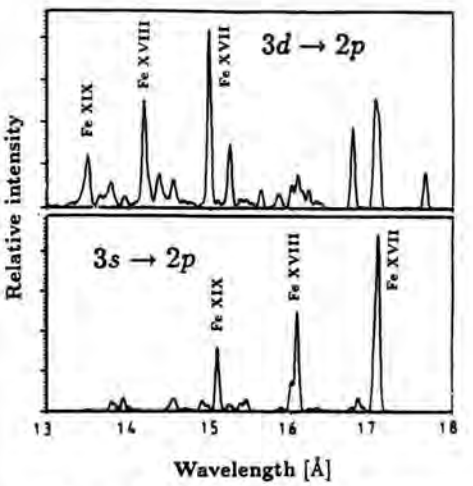

Fig. 10. Model spectra of Fe XVII–XIX from 13–18 Å with 0.052 Å resolution calculated by Liedahl *et al.* (1989). Both spectra are plotted on the same scale, wavelength in Å, intensity in arbitrary units. *Top:* Collisional equilibrium with T = 5.75 MK for the electron temperature. The strong lines at 13.5, 14.2, and 15.0 Å (from Fe XIX, XVIII, and XVII, respectively) are collisionally excited $3d$ lines. *Bottom:* Recombination-dominated spectrum at T=0.11 MK and ionization structure appropriate to an X-ray photoionized nebula. The prominent lines at 15, 16, and 17 Å (from Fe XIX, XVIII, and XVII) are all recombination-cascade-populated $3s$ lines, which cannot be excited by electron collisions at this low electron temperature. The electron density is in each case 10^{11} cm^{-3}.

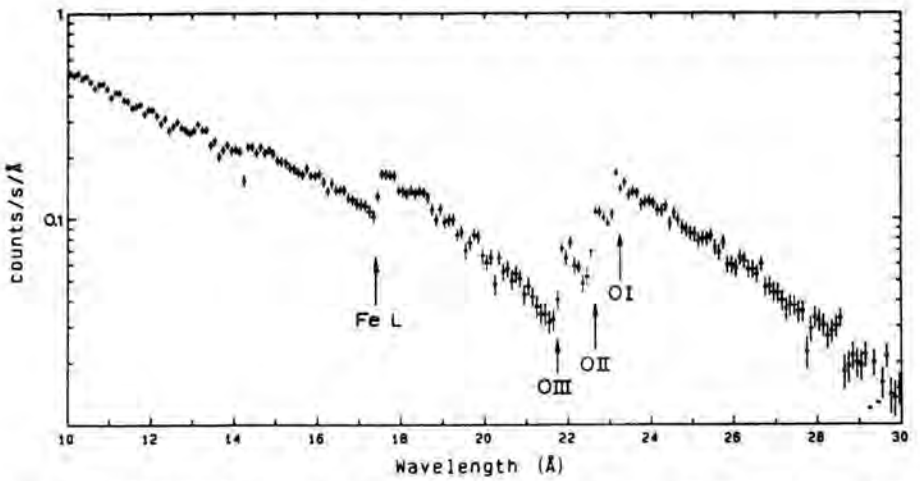

Fig. 11. Simulated *AXAF–LETGS* spectrum of a strong compact X-ray source, observed for 10^4 s with a resolution of 0.1 Å. Interstellar hydrogen column density $N_H = 3\ 10^{21}$ cm^{-2}.

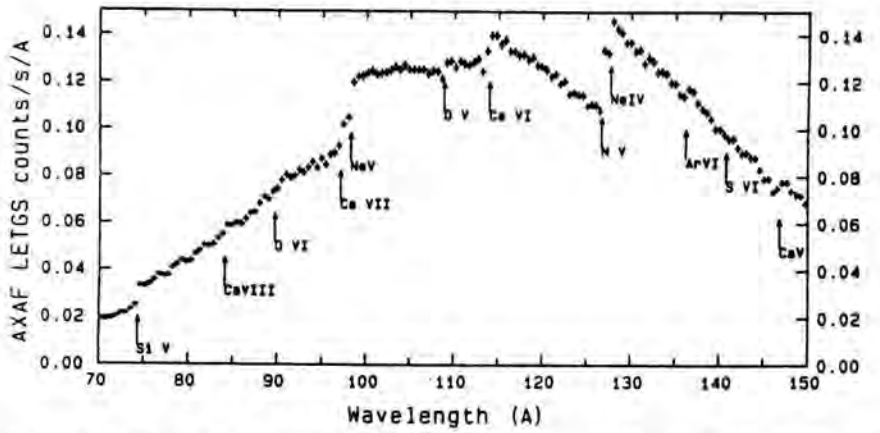

Fig. 12. A hot DA white dwarf (effective temperature 0.065 MK, magnitude V=15) observation simulation for the *AXAF-LETGS* with an integration time of 10^5 s. Traces of metal abundances are assumed a factor of $\sim$ 10 below the observed abundances in the DA dwarf Feige 24 and slightly above the upper limits observed in the hot DA dwarf HZ 43 (Paerels *et al.* 1986). Interstellar column density $N_H = 3\ 10^{19}$ cm^{-2}.

and the elements are more highly ionized ("overionized") at a given temperature than they would be in the coronal model. The emergent X-ray spectrum consists of the central continuum with a low-energy cutoff due to photoabsorption and emission lines due to recombination and fluorescence (in the latter case e.g. K-shell lines from ions with nearly stripped L-shells with reasonable radiative yields such as Li-, Be- and B-like ions (Chen 1986, Chen and Crasemann 1987)) in the nebula, typically near the continuum absorption cutoff.

X-ray photoionized plasmas can differ from collisionally ionized plasmas with similar ion concentrations. Because the photoionized plasma is *overionized* relative to the electron temperature, the excitations of important lines are dominated by recombination, photoexcitation, and cascades as opposed to collisional excitation and dielectronic recombination. This has a drastic effect on the emergent spectrum, as illustrated in Figure 10, where I have plotted spectra calculated for Fe XVII - XIX ions assuming coronal and photoionized conditions respectively (Liedahl *et al.* 1989). As can be seen, it will be straightforward to distinguish photoionized plasmas from coronal plasmas with such spectra. The relative line intensities detected in the photoionized case can be shown to be sensitive functions of the density and geometry of the emission regions and of the spectral shape of the photoionizing continuum.

Another means to distinguish the two types of plasma models is density diagnostics (see Figure 4). Deviations from coronal equilibrium can alter this diagnostics through different recombination and ionization effects, but the line intensity ratios remain density-sensitive also for these cases (Pradhan 1985). The *f/i* ratio does not depend on the model because its density dependence is determined only by the collisional coupling between the upper levels of the two lines, but the ratio *(f+i)/r* does. E.g., for the O VII triplet it is $\sim$ 1 in the coronal model (where the lines are excited by electron collisions from the ground) and $\sim$ 3 in the photoionized nebular model (where population occurs through recombination, directly or via cascades). Hence this diagnostic tool can be quite generally applied to many astrophysical and laboratory sources, while the singlet/triplet ratio can be used as an indication of the model conditions.

2.3. *Optically thick plasmas*

In the extreme case of very dense plasmas, e.g. those present in the inner regions of accretion flows on compact objects such as very hot white dwarfs (in cataclysmic variables) and neutron stars (in hard X-ray binaries) and in the centre of AGN, the source is optically thick to both continuum and line radiation. The spectrum will resemble, at very high optical depths, blackbody emission or a superposition of blackbody type spectra (cf. also Figure 9). However, at intermediate optical depths, the spectral formation is influenced by complicated radiation transfer effects as well as by fundamental atomic processes. Discrete spectral structure is expected which can provide much information about the source (Ross 1979). For X-ray emitting plasmas, Compton scattering plays a significant role as well where transfer through the scattering plasma will broaden and shift line profiles (in addition to thermal broadening) and alter the continuum distribution, depending on temperature and column density (Lightman *et al.* 1981). The spectral resolving power of the future spectrometers is sufficient to resolve the X-ray spectral features that are indicative of the nature of the Compton scattering processes as well as of the structure of the accretion disk corona or the magnetosphere of the neutron star. Emission features observed from X-ray binaries lie in the wavelength region 9–20 Å and are probably from L-transitions from partially ionized iron atoms (e.g. Vrtilek *et al.* 1986).

The spectrum not only contains information on the primary X-ray source itself, but will be modified by fluorescent emission lines and absorption edges produced by the cooler, surrounding medium. The depth of an absorption edge is a measure of the element responsible for this edge and since the

energy of an edge moves towards higher values with increasing ionization, in this way the population of various ionization stages of the constituents of the circumstellar material can be measured. With high spectral resolution one is able to determine the element abundances of the interstellar medium towards many strong galactic and extragalactic X-ray sources. Figure 11 shows a simulation of the X-ray spectrum of a strong accreting compact X-ray source (integrated X-ray flux at Earth $\sim 3\ 10^{-9}$erg cm^{-2}s^{-1}) with a column density of intervening matter of N_H=3 10^{21}cm^{-2}, observed with the *AXAF-LETGS*. The spectrum shows the possible identification of various ionization stages of oxygen.

Finally, another important class of objects to be studied at very soft X-rays are *isolated* hot white dwarfs with optically thick (in visible and UV) photospheric plasmas with effective temperatures in the range $\sim$ 0.03–0.2 MK. At high gravity all hydrogen is pressure-ionized and the outer layers of the photosphere are transparent to the soft X-ray radiation of hotter and deeper layers which become optically thick to the X-rays. The shape of the X-ray spectra is very sensitive to photospheric parameters like effective temperature, gravity and element abundances (for a review e.g. Heise 1988). Trace amounts of highly ionized metals may produce a variety of absorption edges that can be detected in high-resolution X-ray spectra at long wavelengths and which allows one to accurately determine effective temperatures and element abundances for objects as hot DA and very hot DO white dwarf stars. Figure 12 shows a simulation for an observation of a hot DA white dwarf with very low metal abundances ($\sim 10^{-7}$) at a distance $\sim$ 100 pc (magnitude $V = 15$).

3. SUMMARY

High-resolution X-ray spectroscopy has applications to a wide range of hot astrophysical plasmas. Its significance as a tool in understanding the physics of such sources will depend much on the reliability of theoretical models to interpret the spectra. In this paper I have considered various models used in describing the characteristics of hot plasmas and discussed several examples of the emergent X-ray spectrum to illustrate some of the problems of interpretation. It is clear that the complexity of plasma physics and the atomic parameters involved are such that a sound verification of plasma theories and atomic physics which are applied will be required and that for instance better model calculations with improved collisional excitation and ionization rates for the complex ions will be needed for the interpretation of future *AXAF* and *XMM* X-ray spectra.

ACKNOWLEDGEMENTS

This work has been supported by the Space Research Organization of the Netherlands (SRON).

REFERENCES

Aggarwal, K., Berrington, K., Eissner, W., Kingston, A.: 1986, *"Report on Recommended Data"*, Atomic Data Workshop, Daresbury Lab.

Arnaud, M., Rothenflug, R.: 1985, *Astron. Astrophys. Suppl. Ser.* **60**, 425

Barr, P., *et al.*: 1988, *The High-Throughput X-Ray Spectroscopy Mission: The Mission Science Report*, ESA SP-1097

Brinkman, A.C. *et al.*: 1987, *Astro. Lett. and Communications* **26**, 73

Canizares, C.R. *et al.*: 1987, *Astro. Lett. and Communications* **26**, 87

Chen, M.H.: 1986, *Atom. Data Nuc. Data Tab.* **34**, 301

Chen, M.H., Crasemann, B.: 1987, *Phys. Rev. A* **35**, 4579

Dolder, K., Peart, B.: 1986, *Adv. At. Mol. Phys.* **22**, 197

Dunn, H.: 1986, in *At. Proc. in Electron-Ion and Ion-Ion Collisions*, (ed. F. Brouillard), Plenum Publ. Co., p. 93; in *Electronic and At. Collisions* (ed. D.C. Lorents, W.E. Meyerhof, J.R. Peterson), Elsevier Sc. Publ., p. 23

Elwert, G.: 1952, *Z. Naturf.* **7a**, 432

Gabriel, A.H., Jordan, C.: 1979, *MNRAS* **145**, 241

Gallagher, J.H., Pradhan, A.K.: 1985, JILA Data Center Report No. 30, JILA, Univ. of Colorado, Boulder

Griem, H.R.: 1988, *J. Quant. Spectr. Rad. Transf.* **40**, 403

Hahn, Y.: 1985, *Adv. At. Mol. Phys.* **21**, 123

Heise J.: 1988, in *X-ray Astronomy with EXOSAT* (eds. R. Pallavicini, N.E. White), Memorie della Società Astronomica Italiana **59**, p. 53

Holt, S., McCray, R.: 1982, *Ann. Rev. Astron. Astrophys.* **20**, 323

Kaastra, J.S., Barr, P.: 1989, submitted to *Astron. Astrophys.*

Kaastra, J.S., Mewe, R., Brinkman, A.C.: 1989, to be published

Kallman, T.R., McCray, R.: 1982, *Astrophys. J. Suppl.* **50**, 263

Kingston, A.E., Tayal, S.S.: 1983, *J. Phys. B.* **16**, 3465

Lea, S., Mushotzky, R., Holt, S.S.: 1982, *Astrophys. J.* **262**, 24

Lemen, J.R., Mewe, R., Schrijver, C.J., Fludra, A.: 1989, *Astrophys. J.* **341**, 474

Liedahl, D.A., Kahn, S.M., Osterheld, A.L., Goldstein, W.H.: 1989, in preparation.

Lightman, A.P., Lamb, D.Q., Rybicki, G.B.: 1981, *Astrophys. J.* **248**, 738

Mason *et al.*: 1984, *Solar Phys.* **92**, 199

McCray, R.: 1982, in *Galactic X-ray Sources* (ed. P. Sanford, Wiley & Sons, Chicester), p. 71

McCray, R.: 1984, *Physica Scripta* **T7**, 73

Mewe, R.: 1972, *Astron. Astrophys.* **20**, 215

Mewe, R.: 1984, *Physica Scripta* **T7**, 5

Mewe, R.: 1988, in *Astrophysical and Laboratory Spectroscopy* (eds. R. Brown, J. Lang), Scottish Univ. Summer School in Phys. Publ., p. 129

Mewe, R.: 1989, in *Physical Processes in Hot Cosmic Plasmas* (ed. W. Brinkmann), Kluwer Acad. Publ., in press

Mewe, R. *et al.*: 1982, *Astrophys. J.* **260**, 233

Mewe, R., Gronenschild, E.H.B.M., van den Oord, G.H.J.: 1985, *Astron. Astrophys. Suppl. Ser.* **62**, 197

Mewe, R., Lemen, J.R., van den Oord, G.H.J.: 1986, *Astron. Astrophys. Suppl. Ser.* **65**, 511

Mewe, R., Schrijver, J.: 1978, *Astron. Astrophys.* **65**, 99

Müller *et al.*: 1987, *Phys. Rev. A* **36**, 599

Paerels, F.B.S. *et al.*: 1986, *Astrophys. J.* **308**, 190; **309**, L33

Petre, R., Mushotzky, R.F., Krolik, J.H., Holt, S.S.: 1984, *Astrophys. J.* **280**, 499
Pradhan, A.K.: 1982, *Astrophys. J.* **263**, 477
Pradhan, A.K.: 1985, *Astrophys. J.* **288**, 824
Pradhan, A.K., Shull, J.M.: 1981, *Astrophys. J.* **249**, 821
Raymond, J.C.: 1988, in *Hot Thin Plasmas in Astrophysics* (ed. R. Pallavicini), Kluwer Acad. Publ., Dordrecht, p. 3
Raymond, J.C.: 1989, in *High Resolution X-ray Spectroscopy of Cosmic Plasmas* (eds. P. Gorenstein, M.V. Zombeck), Proc. IAU Coll. 115, Cambridge, U.S.A., Reidel Publ. Co.
Raymond, J.C., Smith, B.W.: 1977, *Astrophys. J. Suppl.* **35**, 419
Ross, R.R.: 1979, *Astrophys. J.* **233**, 334
Schrijver, C.J.: 1985, *Space Sci. Rev.* **40**, 3
Schrijver, C.J., Lemen, J.R., Mewe, R.: 1989, *Astrophys. J.* **341**, 484
Seaton, M.J.: 1975, *Adv. At. Mol. Phys.* **11**, 83
Sylwester, J., Schrijver, J., Mewe, R.: 1980, *Solar Phys.* **67**, 285
Swank, J.H., White, N.E., Holt, S.S., Becker, R.H.: 1981, *Astrophys. J.* **246**, 208
Vrtilek, S.D. *et al.*: 1986, *Astrophys. J.* **307**, 698; **308**, 644
Weisskopf, M.C.: 1987, *Astro. Lett. and Communications* **26**, 1; see also other articles in this volume
Withbroe, G.L.: 1975, *Solar Phys.* **45**, 301

AUTHOR'S ADDRESS

SRON-Laboratory for Space Research, Utrecht
Beneluxlaan 21
3527 HS Utrecht, The Netherlands

Harvey R. Butcher

Age of the elements via stellar spectroscopy: Struggles with atomic spectra and transition probabilities

ABSTRACT

A program to develop a stellar cosmochronometer based on radioactive decay is described, with emphasis on the laboratory data needed to remove remaining incertainties.

INTRODUCTION

It should be possible in principle to explore the origin of the elements as well as the chemical evolution of the Galaxy by observing the abundances of various species in stellar spectra. It is believed that dwarf stars like the Sun exhibit surface compositions identical to that of the interstellar gas from which they formed. Study of stars of this type as a function of stellar age should, therefore, yield a detailed picture of the chemical history of the Galaxy. And to the extent that nucleosynthesis has been an on-going phenomenon in the Galaxy, this history may provide clues to the actual sites of element synthesis.

To develop these possibilities requires observation and interpretation of absorption lines in stellar spectra. To estimate abundances, knowledge of the physical state of stellar atmospheres must be combined with the relevant atomic and molecular line parameters measured in the laboratory. Over the past several decades a great deal of preliminary work has been done in this field. It has become clear on the one hand that the basic idea of using stellar observations for these purposes is sound, but on the other that the situation is complex and unlikely to be unravelled easily. So for example, in the disc of the Galaxy one sees gradients in the abundances of C, N, and O, which are almost certainly due to hydrogen burning reaction products from inside stars. But one also finds at any given age significant variations in the absolute abundance levels of the heavier elements -- arguing for inefficient mixing of the interstellar gas together with continuing element production, but at the same time no detectable variation of relative abundances of elements which would be expected to show large variations -- that is, unless mixing is very efficient or only small amounts of synthesis have occurred since early epochs. No convincing explanation is available for such apparent contradictions.

It has also become clear that many of the key elements to be analyzed have only weak lines occurring in crowded regions of stellar spectra, which cannot be studied without excellent laboratory data on all lines present in their vicinity.

A good example of the latter situation is the subject of this contribution. Butcher (1987) has proposed that the techniques of radioactive decay chronometry might be extended to the whole Galaxy, by observing the abundances of the long lived but radioactive element thorium (14 Gyr half-life) in stars of various ages. There are three or four potentially unblended lines of thorium in stellar spectra (Hauge and Sørli 1973; Holweger 1980), but only the strongest -- at 4019.129 Å -- has reliable enough laboratory data on its expected strength to warrant detailed study. To circumvent the many difficulties in analyzing the atmospheres of solar type dwarf stars, it was proposed that a nearby line of neodymium be used to normalize the thorium abundance. The figure displays the 4019 Å region in a typical solar type star. Both the thorium and neodymium lines are unsaturated and derive from the dominant ion throughout the atmospheres of these stars. The lines also have nearly identical excitation potentials. The ratio of their line strengths is therefore proportional to the Th/Nd abundance ratio to within 2% over a stellar temperature range of 4500 to 6500 K.

A reliable Th/Nd stellar cosmochronometer would provide constraints on galactic evolution and nucleosynthesis complementary to the existing Solar System chronometers (primarily the uranium and thorium isotope ratios). The observed Th/Nd ratio in a given star results from an integration of destruction and production processes in the Galaxy, as well as radioactive decay, up to the epoch of the stellar birth. Therefore, even though one has only a single decay to use, examination of stars of different ages effectively samples these processes at several points in the history of the Galaxy. Such

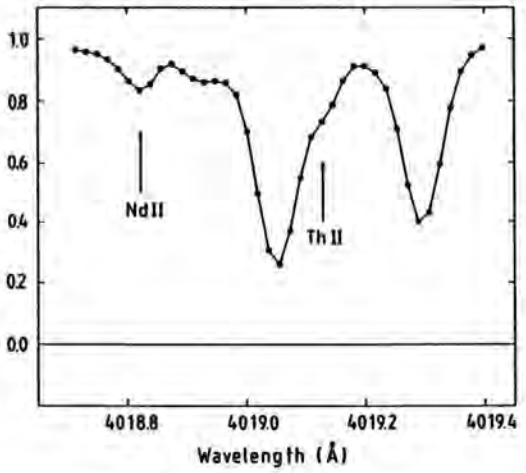

The 4019 Å region in a solar type star.

effects as astration (causing loss of matter to the system via incorporation in low mass, long lived stars; also the modification of abundances by nuclear processes in successive generations of stars) and infall of extra-galactic material (which effectively dilutes in later epoch stars the quantity of material synthesized early in the life of the Galaxy, perhaps to the point even that it cannot be detected in Solar System matter) can be directly examined by investigating very old and very young stars, and requiring that the Solar System uranium and thorium isotopic data and the Th/Nd stellar data yield consistent results. In particular, because the Solar System data do not effectively constrain evolutionary models having large ages (Meyer and Schramm 1986; Fowler and Meisl 1986), whereas the Th/Nd stellar data are especially sensitive in this case, it seems very important that the proposed Th/Nd chronometer be developed to the point where it can provide reliable information on the age and evolution of the Galaxy.

First observations of the Th/Nd ratio in stars of all ages were also presented by Butcher (1987). As shown in the figure, no variation of the ratio was detected within the experimental errors in that data. This result was then combined with Solar System data to constrain the age of the Galaxy to no more than 11 or 12 Gyr, independently of whether synthesis occurred in a more or less single event at early epochs or over an extended period lasting the entire history of the Galaxy.

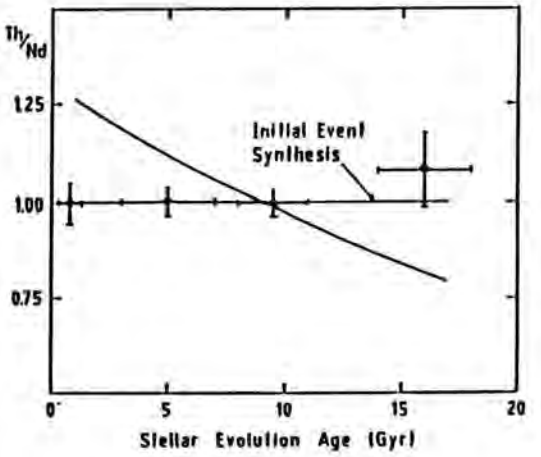

Mean values of Th/Nd vs. stellar age. The horizontal solid line is the predicted behavior for element production concentrated at early epochs. The sloping solid line is the predicted relation for continuous synthesis at a constant rate throughout the lifetime of the Galaxy. The horizontal error bars indicate the spread in ages of stars in the point.

This age disagrees, however, with our best estimates for the ages of the globular clusters as based on stellar evolution theory (e.g. VandenBerg 1983). The most metal poor clusters should have the most reliable age estimates (because they are least susceptible to errors in the opacity parameters), but they also yield the largest ages, and one must naturally suspect that there might be something wrong with the Th/Nd analysis.

The various problems which could be compromising that analysis are summarized in the following section. Then, that laboratory data which at present seem most necessary for the analysis are listed.

MAJOR UNCERTAINTIES

Four likely areas for error in the Th/Nd analysis may be cited:

(1) The relative r- and s-process contributions at element synthesis to the abundances of Nd and Th.

Thorium is thought to be synthesized only in the r-process, while in the Solar System neodymium has roughly equal contributions from the r- and

s-processes (Howard etal 1986). Because the s-process appears to require the presence of seed nuclei, whereas the r-process does not (but see also Clayton 1988, and Malaney and Fowler 1989), one naturally expects the relative contributions from the two processes to evolve systematically with epoch in the Galaxy (cf Clayton 1987; Mathews and Schramm 1988). That they do not, at least in the disc of the Galaxy (Lambert 1987; Butcher 1975; Butcher 1988), is a puzzle of the first order, but fortunate for the Th/Nd analysis. For extremely metal deficient stars in the galactic halo, s-process abundances do seem to vary between stars (Spite and Spite 1978; Sneden and Parthasarathy 1983; Sneden and Pilachowsky 1985). The Th and Nd lines in these stars will be exceedingly weak, but if they are ever measured, it will be possible to correct for non-solar s-process contributions to Nd by also measuring other s- and r-process abundances similar to Nd in atomic mass (eg, Ba, Eu, Gd, etc). Similarly, one can, at least in principle, measure high and low mass r-process species (eg, Eu and Os) in stellar spectra, to test and correct for evolutionary variation in the shape of the r-process abundance curve. This uncertainty, therefore, is unlikely to be a serious one, unless the derivation of the required abundances cannot be made because of inadequate laboratory data on the spectra in question.

(2) The stellar age estimates.

If the largest ages used in the Th/Nd analysis are overestimated, then the derived total age of the Galaxy may be underestimated. This possibility is potentially a serious one, because at present the only stars which can be studied have relatively strong lines and orbits characteristic of stars confined to the disc of the Galaxy. They cannot therefore be said to belong to the halo population, which is generally agreed to contain the oldest stars.

The stars in the analysis do, however, have rather large and apparently reliable trigonometric parallaxes, and can be placed on the H-R diagram with some confidence. When this was done, the three stars HR 1136, HR 3018, and HR 5699 all have ages above 15 Gyr. The first object has a perfectly normal disc-like galactic orbit as well as solar abundances, and is also cool enough that the theoretical isochrones are converging as they approach the Hayashi limit; its age is clearly uncertain at the 25% level. The remaining two stars, however, are each moderately metal poor and have high enough space motions that they must be considered as being intermediate between the disc and halo populations. And they are not so evolved that they cannot be reliably placed in the H-R diagram. Taking conservative error estimates on their parallax measurements, on their photometry, and on their overall heavy element abundances, one can only conclude that they are indeed as old as the halo proper. On the other hand, with only two stars of this type, even though they were not selected primarily on the basis of their age (rather because they were the most metal poor dwarfs having some chance of yielding a result with present equipment), one cannot yet be entirely confident that they are representative of the earliest epochs of the Galaxy.

(3) The detailed spectrum model used to fit to the observational data and derive the Th and Nd line strengths.

Because the Th line used in the analysis is located in the wing of a blended line of Fe and Ni, its precise measurement depends on having very accurate wavelengths for those lines. In addition, its strength is influenced, at roughly the two percent level, by the damping parameter for the Fe line in the blend. Inconsistencies in the reported wavelengths for these lines lead to an uncertainty in the equivalent width of the Th line in the solar spectrum of some 20%. Investigation of any potential contamination of the Th line by comparing its expected and measured strengths cannot therefore be made yet. Fortunately, Learner, Thorne and colleagues at Imperial College, London, report elsewhere at this conference that they have made the necessary measurements, so it is now possible to repeat the analysis with much improved wavelengths. A quantitative estimate of the precision required for the Fe line's damping parameter will also be derivable as part of this re-analysis.

(4) The purity of the Th line.

If the Th line is contaminated by some line of a stable element of unknown strength, its variation due to radioactive decay will be diluted and a young age will be incorrectly inferred. A contamination of 10% was assumed in the original analysis, but several workers have proposed a higher contamination (Holweger 1980; Aldering 1987; Whaling and Lawler 1988), of up to 30% and by a weak line of Co I at 4019.13 Å.

Aldering has kindly calculated synthetic spectra for the region around 4019 , with and without a 30% contamination by Co I, and covering a temperature

range of 4000 - 7000 K. Over the temperature range of the stars studied to date (4700 - 6300 K), he predicts for zero contamination a 2% variation of Th/Nd, but over 40% for a contribution from the Co I line to the measured equivalent width in the solar spectrum of 30%. The observed scatter of the data, with one caveat and excepting that for HR 3018 (which has a substantially higher estimated error), is well explained by a constant Th/Nd ratio with an 8% standard deviation. It therefore seems highly unlikely that the contamination of the Th line equivalent width measurement in the Sun is as much as 30%. A value of 10% is certainly permitted, however, and the numbers of stars at the extremes of temperature are few, so the matter cannot be said yet to have been resolved in a completely satisfactory way.

The caveat mentioned above is that there is in the data as they now stand a dependence of the Th line strength on the stellar velocity width parameter. That is, the stars with the narrowest lines, HR 509 and HR 5460, yielded slightly larger Th/Nd ratios than the rest of the sample. Because they are neither the oldest, youngest, hottest, or coolest stars in the sample, these points have simply been corrected in a plausible manner for the subsequent analysis. The best fit model spectrum to the data for these stars also showed deviations significantly above the noise, however, from which one can only conclude that the model spectrum needs improvement, especially as regards the relevant wavelengths. Now that this can be done, it will soon be possible to comment more reliably on the likely contamination, at least as estimated from the variation of the Th/Nd ratio with stellar temperature.

LABORATORY DATA NEEDED

The discussion above indicates that the following atomic line data will be essential, or at the least very helpful, in establishing a reliable Th/Nd chronometer.

(i) Precise relative wavelengths for the Th II, Ni I, Fe I, and Nd II lines. With this information it should be possible to improve the model spectrum for fitting to the stellar spectra, thereby to derive a reliable equivalent width for the Th line in the solar spectrum and test for the level of contamination, and to eliminate the increased Th/Nd ratio at small velocity broadenings. Luckily, the ICL group has reported greatly improved values for some of these wavelengths at this meeting.

(ii) The damping parameter for the Fe I 4019.04 Å line, which is expected to be larger than that for any other line in the vicinity. If this parameter is as large as or larger than estimated from the calculations of Warner (1967; 1969), accurate knowledge of its value will significantly improve the resulting chronometer.

(iii) The transition probability of the Th II 4019.129 Å line. The Aarhus group (Simonsen et al 1988) have measured the lifetime of the upper level of this transition to very high accuracy, but the relevant branching ratio from this level remains uncertain at the 10% or more level. A convincing comparison of the predicted and measured equivalent widths of the line in the Sun cannot be made, and hence the contamination estimated, until this measurement is pinned down.

(iv) Transition probabilities for three other measurable absorption lines of Th II in the solar spectrum, at 3675, 3741, and 4086 Å (Hauge and Sørli 1973; Holweger 1980). Predicted strengths for these lines, together with accurate wavelengths relative to nearby stronger features, would make it possible to include them in the analysis, and thereby strengthen confidence in the final conclusions.

(v) An accurate transition probability for the potential contaminator line, Co I 4019.126 Å, relative to another Co I line nearby in wavelength and unblended in stellar spectra. A good candidate line for this purpose is Co I 4011.08 Å, although the Co I blend 4019.29 + 4019.30 Å might also be a possibility. Both of these lines, as well as any others proposed, should be examined carefully for blending, of course, before the proposed test is made (the 4019.3 Å blend has been difficult to fit in some of the author's stellar spectra without inclusion of a blend of unknown origin in the spectrum model). If an appropriate Co I line can be found, it should be possible to ascertain the contamination by Co I 4019.13 Å, independently of uncertainties in the absolute equivalent width of the Th line.

(vi) Line strength determinations for other potential blends at the position of Th II 4019.129 Å. Kurucz and Peytremann (1975) give numerous

possible contaminators. Most of these can be ruled out by the Th/Nd vs stellar temperature test, or by the ratio in s-process enhanced stars (cf Butcher 1987). The only remaining serious candidate for an undetected contaminator is Tb II 4019.12 Å, which, being from a predominantly r-process element, may not have been detected in any of the tests carried out so far. Unfortunately, the spectrum of Tb II has never been fully analyzed, so that the term classification and lower level of 4019.12 Å are not known. Prof Klinkenberg reported privately at this meeting that the line of terbium at 4019.12 Å in his spectra is in fact a blend of a Tb I and Tb II line. The suggestion, therefore, is that the Tb II line is unlikely to be of significant strength in stellar spectra.

REFERENCES

Aldering, G.S. 1987, unpublished.

Butcher, H. 1975, *Ap.J.* **199**, 710.

Butcher, H. 1987, *Nature* **328**, 127.

Butcher, H. 1988, *ESO Messenger*, Nr 51, p 12.

Clayton, D.D. 1987, *Nature* **329**, 397.

Clayton, D.D. 1988, *Mon.Not.Rast.Soc.* **234**, 1.

Fowler, W.A., and Meisl, C.C. 1986, in "Cosmological Processes," p 83, Arnett et al eds. VNU Science Press, Utrecht.

Hauge, Ø., and Sørli, H. 1973, *Solar Physics* **30**, 301.

Holweger, H. 1980, *Observatory* **100**, 155.

Howard, W.M., Mathews, G.J., Takahashi, K. and Ward, R.A. 1986, *Ap.J.* **309**, 633.

Kurucz, R.L., and Peytremann, E. 1975, SAO Special Report, no. 362.

Lambert, D. 1987, *Astrophys.Astr.* **8**, 103.

Malaney, R.A. and Fowler, W.A. 1989, *Mon.Not.Rast.Soc.* **237**, 67.

Mathews, G.J. and Schramm, D.N. 1988, *Ap.J.* **324**, L67.

Meyer, B.S. and Schramm, D.N. 1986, *Ap.J.* **311**, 406.

Simonsen, H., Worm, T., Jessen, P., and Poulsen, O. 1988, *Physica Scripta* **38**, 370.

Sneden, C. and Parthasarathy, M. 1983, *Ap.J.* **267**, 757.

Sneden, C. and Pilachowski, C.A. 1985, *Ap.J.* **288**, L55.

Spite, M. and Spite, F. 1978, *Astr.Astrophys.* **67**, 23.

VandenBerg, D.A. 1983, *Ap.J.Suppl.* **51**, 29.

Warner, B. 1967, *Mon.Not.Rast.Soc.* **136**, 381.

Warner, B. 1969, *Observatory* **89**, 11.

Whaling, W., and Lawler, J.E. 1988, unpublished.

AUTHOR'S ADDRESS

Kapteyn Astronomical Institute
P.O. Box 800
9700 AV Groningen
The Netherlands

Michael R. Rosa[+)]

Atomic data for and from the analysis of gaseous nebulae

ABSTRACT

The need for cross-checks between observations of emission line strengths in gaseous nebulae, and theoretical predictions of transition probabilities and collision strengths for forbidden lines is discussed. Observed line ratios of transitions in the ions N^+, O^{+2} and S^+ are compared with theoretical predictions. It is concluded that inconsistencies are apparent, which need to be resolved in order to achieve the accuracies in derived astrophysical data that can be expected from modern observational techniques and calculations of atomic data.

INTRODUCTION

Substantial improvements in accuracy have been made over the last decade in both, the observational determination of emission line ratios in gaseous nebulae, and in theoretical computations of transition probabilities and collision strengths for the ions of interest. In addition observations can now be compared with detailed models of H II regions treating the radiative transfer in the presence of inhomogeneities and dust (Mathis 1982).

As a result, the fine analysis of real objects in terms of chemical abundances and of the energy distribution in the ionizing source becomes feasible on the 10% accuracy level for an increasing number of objects. This opens up new ways to investigate elemental abundance variations in galaxies within and between H II regions, rather than on kpc scales. This will have impacts on our understanding of the history of star formation and chemical evolution. The access to the otherwise unobservable FUV continua of hot stars will put constraints on input physics and parameters of stellar model atmospheres. Ions of particular interest in such studies are O^+, O^{+2}, S^+ and S^{+2} because they can be used profitably to map the the ionization structure without reference to total elemental abundances (Mathis 1982).

CONSISTENCY CHECKS

In order to achieve this goal, a close interaction between observations and theory is required. Observers in trying to approach higher accuracies on ever fainter lines need reliable theoretical predictions of line emissivities in order to cross-check the calibration procedures. On the other hand, theoretical predictions of forbidden line collision strengths and transition probabilities can only be tested against observations of real astronomical objects. What is required from time to time, are consistency checks similar to those of eg. Liller an Aller (1954), Seaton and Osterbrock (1957) and Saraph and Seaton (1970).

THE O^{+2} $\lambda\lambda$ 5007,4959 RATIO

The intensity ratio of these strong ^1D-^3P transitions in the $2p^2$ ground configuration of O^{+2} is essentially independent of T_e and n_e. It is the ratio of transition probabilities and energy differences, and could provide an ideal check on the linearity of detectors and on the external accuracy of the data analysis.

Theoretical predictions have remained almost unchanged, converging from an early value of 2.93 in 1951 to 2.89 ± 0.02 today. Liller and Aller (1954) obtained 3.03 ± 0.11 from photoelectric observations; at that time not in contradiction with theory. The analysis of more than 600 modern data, which takes into account detector non-linearities and blends with faint He I lines, leads to a most probable observed ratio of 3.03 with a formal 3σ uncertainty of 0.005. Theoretical predictions therefore are off by about 10%, at least a 10σ effect. A similar discrepancy exists for the iso-electronic ion N^+; 2.92 ± 0.03 predicted versus 3.06 ± 0.01 observed.

These discrepancies are significant. They are disturbing, because they are consistent in the iso-electronic sequence (i.e. not likely to be observational inaccuracies), and because prediction as well as observation have remained at essentially unchanged values, despite the several orders of magnitude improvements in input physics and observational techniques. As a user of atomic data one might ask the question: how large are the margins for more important line ratios in that sequence ?

THE PROBLEMATIC S^+ ION - ELECTRON DENSITIES

The S^+ ion plays a dominant role in plasma diagnostics for most of the observations of gaseous nebulae. The ''said to be'' density sensitive ^2D-^4S nebular type transitions are easily observed and resolved even in faint objects at low spectral resolution. Usually, they

provide the only electron density estimator available in chemical abundance studies.

The comparison by Saraph and Seaton (1970) of densities obtained from several such n_e sensitive emission line ratios of O^+ and the iso-electronic ions S^+, Cl^{+2} and Ar^{+3} led to the conclusion, that corrections had to be applied (mainly to S^+ density values) in order to achieve consistency.

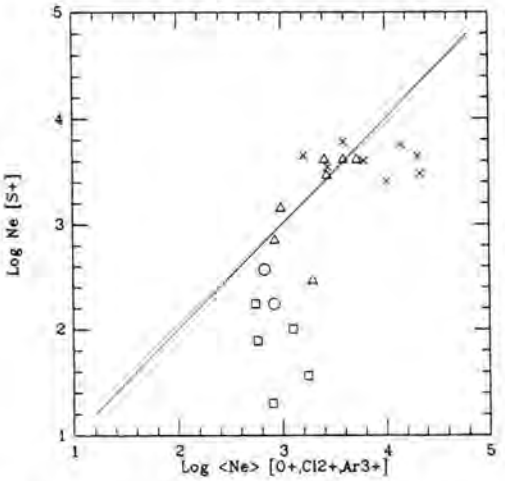

Fig. 1. Comparison of logarithmic densities derived from the S^+ ^2D-^4S transitions with averaged densities obtained from other ions.

Eissner and Zeippen (1981) resolved a long standing discrepancy between predicted and observed asymptotic densities for the O^+ ion (Seaton and Osterbrock 1957), later followed up along the $2p^3$ and $3p^3$ sequences, altering the transition probability sets. Also the new calculations of collision strengths for these sequences have led to significant changes (cf. Butler and Zeippen 1989 and references therein). How do these modern atomic data sets compare with new observations ?

In Fig. 1 logarithmic densities from the nebular S^+ ^2D-^4S transitions are compared with electron densities obtained from O^+, Cl^{+2} and Ar^{+3} (average if applicable) for the planetary nebulae (crosses) of Saraph and Seaton (1970), the Orion nebula (triangles), the 30 Doradus H II region (circles) and several other galactic and extragalactic nebulae (squares). S^+ density values are large underestimates almost everywhere in the diagram, especially in the low and high density regimes. In other words, observationally S^+ has only a very narrow density sensitive region. If this holds true, i.e. if something is amiss in the atomic data set of S^+, this would be particularly disturbing, because most of the electron densities obtained for extragalactic objects are based on S^+ observations. A direct consequence would be that filling factors have to be lowered by considerable amounts.

THE S^+ ION - MISSING INTERNAL CONSISTENCY

This seems not to be the only trouble with S^+. The ratio of the transauroral to nebular lines ($\lambda\lambda$ 6718 + 6731)/($\lambda\lambda$ 4069 + 4076) might be used to obtain T_e and n_e simultaneously for the same ion, a unique possibility. But determinations of either of the two parameters for a large sample of observations in low S^+ density objects are not in satisfactory agreement with values derived from plasma diagnostics of other ions.

In addition, the predicted line emissivity ratio of the two transauroral lines remains almost constant 3.0-3.2 over the T_e, n_e range covered by observational data. Yet, the available data are: 0.3-2.3 (giant H II regions), 2.1 (Orion nebula), 2.3 (Jupiter's plasma ring in the orbit of Io), and 0.9-7.5 (supernova remnants). There is a clear dependence of the observed ratio on T_e and n_e simultaneously.

It seems that the density sensitivity absent in the S^+ ^2D-^4S transitions is found again in the (^2D-^4S)/(^2P-^2D) emissivity ratio. Both sets, that of collision strengths and that of transition probabilities, seem to require improvements to reach consistency.

CONCLUSIONS

In summary it is comforting that the large set of atomic data available today for analysis of gaseous nebula spectra is consistent enough in general to show the presence of a few marked discrepancies. Earlier work on gaseous nebulae (cf. Saraph and Seaton (1970) or Pequinot et al (1978)) discussed differences found between plasma temperatures or densities determined from different ionic species, or problems in obtaining model nebulae consistent with observations in terms of real astrophysical effects (eg. density gradients, temperature structure) Although some of those interpretations might be valid, historically the development of the atomic data sets used has made most of those object related explanations obsolete.

While the small discrepancies between observation and prediction for the N^+ and O^{+2} ^1D-^3P transitions do not necessarily influence the astrophysical interpretation of the data, they might carry important information about atomic physics. On the other hand, a careful inspection of the S^+ ion, both from obser-

vations and from theoretical calculations, is highly desirable.

Besides the understanding in atomic physics to be gained from improved calculations, the astrophysical interpretation of nebular data depends strongly on accurate atomic data for this particular ion. Not only provide S^+ n_e estimates the sole source of this plasma parameter for a large majority of interesting astronomical objects. Reliable sulphur abundances require accurate collision strengths and transition probabilities for S^+, because S^+ is the second most abundant ionization stage in the bulk of gaseous nebulae. The continuation of the long standing, excellent interaction between atomic physics and observational astrophysics of gaseous nebulae should be fruitful for both sides in the areas discussed.

REFERENCES

Butler, K. and Zeippen, C.J.: 1989 - Astron.Astrophys., 208, 337

Eissner, W. and Zeippen, C.J.: 1981 - J.Phys.B. 14, 2125

Liller, W. and Aller, L.H.: 1954 - Astrophys.J. 120, 48

Mathis,J.S.: 1982 - Astrophys.J., 261, 195

Pequinot, D., Aldrovani, S.M.V., Stasisnka, G.: 1978 - Astron.Astrophys., 63, 313

Saraph, H.J. and Seaton, M.J.: 1970 - Month. Not.Roy.Astr.Soc. 148, 367

Seaton, M.J. and Osterbrock, D.E.: 1957 - Astrophys.J. 125, 66

AUTHOR'S ADRESS

Space Telescope European Coordinating Facility
European Southern Observatory, D-8046 Garching
+)Affiliated to the Astrophysics Division,
Space Science Department, European Space Agency

Donald C. Morton

The astrophysical importance of resonance lines

ABSTRACT

This paper outlines the astrophysical situations in which absorption lines from ground states dominate spectra, the instruments expected to be available to study these spectra, and the gaps in the atomic data where new laboratory or theoretical studies would be very useful.

INTRODUCTION

There are several astrophysical situations where absorptions from the ground states of atoms, i.e. resonance lines, dominate the spectra. In gaseous regions where both the particle and radiation density are low, almost all the atoms will be in their ground states, or at most excited by a few hundredths of an electron volt if a low lying fine-structure level is present. The absorption spectra from such regions thus consist of only resonance lines. With the exception of a few transitions of Na I, K I, Ca I, Ca II, Ti II and Fe I, all these lines occur at wavelengths shortward of the atmospheric cutoff at 3000 Å.

The most familiar example of such a low density region is the interstellar medium, which produces resonance lines in absorption against stars shining through it. The quasi-stellar objects (QSOs) typically have absorption lines, which in many ways resemble ultraviolet interstellar spectra redshifted to visible wavelengths. Thus the QSO lines usually are attributed to low density gas either in intervening galaxies or in clouds in the intergalactic medium.

The ultraviolet spectra of all luminous hot stars show that they have winds which eject material back into the interstellar gas at velocities up to 3500 km s^{-1} (Snow and Morton, 1976). These winds usually are revealed by the ultraviolet resonance transitions of Mg II, C IV, Si IV, N V and O VI, which have emission lines near their expected positions and broad absorption lines extending to shorter wavelengths.

Finally, some ten percent of all QSOs have broad absorption lines blueshifted from the emission lines by as much as 35 000 km s^{-1} (Hazard et al, 1984). The shifted lines are attributed to mass flow from the QSO, by analogy with the hot stars.

OBSERVATIONAL OPPORTUNITIES

Table I summarizes the major space facilities, past and future, that will be suitable for observations shortward of the atmospheric cutoff at 3000 Å. Ground-based telescopes also can observe the UV resonance lines in redshifted QSOs, including lines shortward of the Lyman limit.

WAVELENGTH DATA REQUIRED

The available data on resonance lines have increased considerably since the tabulation by Morton and Smith (1973) and the revisions listed by Morton (1978). Morton, York and Jenkins (1989) summarized the latest data on the stronger transitions which are likely to appear in QSO spectra and noted several cases where improvements were necessary. Since then Kaufman and Martin (1989) have added new wavelength measurements of the O VI resonance lines.

However, as indicated in Table 2, many important transitions still lack sufficiently accurate wavelengths. For brevity only the strongest line from the ground level of each multiplet is given. Although we would like wavelengths to 1 part in 10^6 to take full advantage of the Hubble Space Telescope, in many cases 3 or even 10 parts in 10^6 would be useful improvements on existing data.

In addition, any information on hyperfine structure or isotope shifts for resonance lines with separations exceeding 1 part in 10^6 would be useful. Wayte, Wynne-Jones and Blades (1978) detected the Na I hyperfine structure towards α Cygni, demonstrating that there are regions of the interstellar gas where the line-of-sight velocity dispersion is as small as $\sigma = 0.27$ km s^{-1}. When lines are this narrow, isotope effects also may contribute to the line widths. For example, according to the estimates by Clark (1989), C^{12}-C^{13} = 0.015 Å for C II λ1335 and N^{14}-N^{15} = 0.010 Å for N II λ1085.

Table 1. Observational Opportunities

Telescope	Wavelength Range (Å)	Resolution	Date
Space Observatories			
Copernicus	710-3185	$2x10^4$, $6x10^3$	1972-1984
International UV Explorer	1150-3200	300, 12000	1978-Now
Hubble Space Telescope	1150-3200	$2x10^3$, $2x10^4$, 10^5	1990 MAR
Hopkins UV Telescope	450-1850	500	1990 APR
Extreme UV Explorer	70- 760	260	1991 AUG
Lyman Far UV Explorer	910-1250	$1.5x10^4$, $3x10^4$	~1996
(awaiting approval)	400-1600	$4x10^3$	
	100- 350	130-900	
Ground-Based Observatories			
10 major Telescopes 3 to 5m	>3000	$<3x10^5$	Now
Redshifted QSOS (z>4)	> 600	"	"
Keck Telescope 10m	>3000	10^5	~1992
ESO Very Large Telescope 4x8m	>3000	$3x10^5$	1995-2000

Table 2. Lines Requiring Better Wavelengths

Ion	Resonance Line Wavelengths (Å)	Year of Latest Publication
A. Lines Longward of 912 Å		
P II	1532.51, 1301.87, 1152.81, 963.81	1959
S III	1190.21, 1012.50	1929
Cl III	1015.02	1928
Cl IV	973.21	1928
B. Lines Shortward of 912 Å		
S III	698.73, 681.50, 677.75, 484.19	1929, 1937
S IV	657.34, 551.17	1925
S V	786.48	1932
S VI	248.99	1937
Cl III	572.69, 557.12	1928, 1934
Cl IV	831.43, 607.09, 599.73, 549.22, 534.73	1928, 1934
Cl V	883.13, 681.92, 633.19, 538.03	1928
Cl VI	671.37	1925
Ar III	878.73, 637.28, 529.90, 488.45, 475.71, 467.39	1935
Ar IV	850.60, 452.91, 396.87	1935
Ar V	705.35, 511.89, 458.12, 337.56	1941
Ar VI	754.93, 588.92, 548.91, 457.48, 292.15	1941, 1961
Ar VII	585.75	1941

TRANSITIONS REQUIRING IMPROVED OSCILLATOR STRENGTHS

An accuracy of 10% or 0.04 dex is very desirable, but 25% or 0.10 dex still would be useful. Weak transitions are particularly important because they often do not need any saturation correction in the analysis. The desired weakness usually is a result of significant cancellation in a dipole transition, or an intersystem change in the spin state. In either case, experiments are difficult and theoretical calculations require many terms. Nevertheless, perseverance with both tactics is well worthwhile until theory and experiment agree.

C II

These weak intersystem transitions from 2323 to 2328 Å are preferred over the saturated lines at shorter wavelengths. However, the calculated values of Cowan, Hobbs and York (1982) and Nussbaumer and Storey (1981) have deviations up to 0.5 dex.

N I

Lugger et al (1978) derived f-values for 18 lines of N I from 1161 to 951 Å using the observed strengths of interstellar lines and experimental values for multiplets 1 and 2. Further experiments to check these results are very desirable, particularly the weak intersystem line at 1159.814 Å.

O I

Zeippen, Seaton, and Morton (1977) published theoretical f-values for many O I lines from 1039 to 919 Å. A few experimental determinations would be very useful to check these calculations. Further theoretical and experimental work on the weak intersystem line at 1355.598 Å should improve our confidence in its use.

Mg II

The determination of the interstellar abundance of this important ion depends on the weak dipole doublet at 1240.395 and 1239.925 Å. At present the best oscillator strength is the theoretical value by Hibbert et al (1983); it is smaller than an earlier calculation of Black, Weisheit and Laviana (1972) by 0.56 dex. An experimental check here is most desirable.

Si II

Recent calculations by Luo, Pradhan and Shull (1989) agree reasonably well with those of Dufton et al (1983) except for the weak dipole transition at 1808.013 Å. Both calculations also give acceptable agreement with the oscillator strengths of λλ1304, 1260, 1193, and 1190 adopted by Morton, York and Jenkins (1989) from lifetime measurements. However, the observed interstellar strength of λ1526 seems systematically too large for the calculated f. Experimental determinations for λλ1526, 1020, 989 and especially 1808 are needed and would provide a reliable curve of growth which could be used for other ions.

Ti III

Measurement of this ion is necessary to determine the titanium abundance in regions where the hydrogen is ionized. Martin, Fuhr, and Wiese (1988) adopted the theoretical value of Kurucz and Peytremann (1975) for λ1291.624, but the accuracy is low.

Cr II

The column density of Cr II relative to Zn II is a useful indicator of condensation on to grains. The lines at 2065.501, 2061.575 and 2055.596 are present in some stellar and QSO spectra. Currently the best oscillator strengths are from the calculations of Kurucz and Peytremann (1975).

Fe II

Like Si II, this ion has many lines accessible to IUE and the Space Telescope, so that the complete curve of growth should be derivable, but the atomic data are not yet reliable enough. Measurements by Moity (1983) and Kroll and Kock (1987) have confirmed the f-values that Morton and Smith (1973) derived from the lifetimes of Assoussa and Smith (1972). However, the careful calculations of Nussbaumer, Pettini and Storey (1981) are larger by amounts ranging from 0.025 to 0.17 dex. Consequently the best f-values at present for the shorter wavelength lines probably are those which Shull, Van Steenberg and Seab (1983) determined from interstellar lines. More laboratory measurements are needed.

Fe III

The iron abundance in H II regions depends on this ion. At present the only oscillator strengths for the lines at 1122.526, and several multiplets shortward of 912 Å are the calculations of Kurucz and Peytremann (1975).

Ni II

Several resonance lines between 1752 and 1308 Å have been seen in stars or QSOs, but the only source of f-values is Kurucz and Peytremann (1975).

Finally, since many experimental and theoretical results on transition probabilities are transformed from multiplets to individual lines under the assumption of LS coupling, it is important to watch for evidence for deviations. Goldbach and Nollez (1987) have presented experimental evidence for deviations in some C I multiplets.

AUTHOR'S ADDRESS

Herzberg Institute of Astrophysics, National Research Council of Canada, 100 Sussex Drive, Ottawa, Ontario, Canada, K1A OR6.

REFERENCES

Assoussa, G.E. and W.H. Smith, 1972 - Ap. J. 176, 259.
Black, J.H., J.C. Weisheit and E. Laviana, 1972 - Ap. J. 177, 567.
Clark, C.W., 1989 - Ap. J. 285, 322.
Cowan, R.D., L.M. Hobbs and D.G. York, 1982 - Ap. J. 257, 373.
Dufton, P.L., A. Hibbert, A.E. Kingston, J.A. Tully, 1983 - Mon. Not. R. astr. Soc. 202, 145.
Goldbach, C. and G. Nollez, 1987 - Astron. Ap. 181, 203.
Hazard, C., D.C. Morton, R. Terlevich, and R. McMahon, 1984 - Ap. J. 282, 33.
Hibbert, A., P.L. Dufton, M.J. Murray and D.G. York, 1983 - Mon. Not. R. astr. Soc. 205, 535.
Kaufman, V. and W.C. Martin, 1989 - J.O.S.A. in press.
Kroll, S. and M. Kock, 1987 - Astron. Ap. Suppl. 67, 225.
Kurucz, R.L. and E. Peytremann, 1975 - Smithsonian Ap. Obs. Spec. Rept. No. 362.
Lugger, P.M., D.G. York, T. Blanchard and D.C. Morton, 1978 - Ap. J. 224, 1059.
Luo, D., A.K. Pradhan and J.M. Shull, 1989 - Ap. J. (in press).
Martin, G.A., J.R. Fuhr, and W.L. Wiese, 1988 - J. Phys. Chem. Ref. Data 17, Suppl. 3.
Moity, J., 1983 - Astron. Ap. Suppl. 52, 37.
Morton, D.C., 1978 - Ap. J. 222, 863.
Morton, D.C. and W.H. Smith, 1973 - Ap. J. Suppl. 26, 333.
Morton, D.C., D.G. York and E.B. Jenkins, 1989 - Ap. J. Suppl. 68, 449.
Nussbaumer, H., M. Pettini and P.J. Storey, 1981 - Astron. Ap. 102, 351.
Nussbaumer, H. and P.J. Storey, 1981 - Astr. Ap. 96, 91.
Shull, J.M., M. Van Steenberg and C.G. Seab, 1983 - Ap. J. 271, 408.
Snow, T.P. and D.C. Morton, 1976 - Ap. J. Suppl. 32, 429.
Wayte, R.C., I. Wynne-Jones and J.C. Blades, 1978 - Mon. Not. R. astr. Soc. 182, 5p.
Zeippen, C.J., M.J. Seaton and D.C. Morton, 1977 - Mon. Not. R. astr. Soc. 181, 527.

E.A. Gurtovenko, R.I. Kostik and
R.J. Rutten

New solar oscillator strengths from Kiev

ABSTRACT

We briefly review the Kiev program for determining oscillator strengths of Fraunhofer lines from the optical solar spectrum. It has recently resulted in a new compilation of *gf*-values for nearly two thousand lines (Gurtovenko and Kostik 1989).

THE SOLAR PHOTOSPHERE AS A FURNACE

The solar photosphere may be regarded as a natural furnace from which Fraunhofer lines originate in order to enable the measurement of their oscillator strength. As such a furnace, the photosphere provides important advantages:

- the number of measurable lines is large;
- the measurable lines are often precisely the ones needed in composition studies of other stars;
- the furnace properties are rather well known.

In contrast, laboratory measurements used to have very large errors until the precise Oxford measurements became available (*e.g.* Blackwell *et al.* 1982), while such high-precision data exist for only a few lines which mostly are less suitable for stellar abundance determinations, being too strong or located in the overly crowded blue and violet spectral regions (see Grotrian diagrams in Rutten 1983 or Rutten and Kostik 1988).

The disadvantage of the solar photospheric furnace is that all errors in the employed modelling of the solar line formation propagate into the derived *gf*-values. *A priori*, one would expect such modelling errors to be quite large. Firstly, decades of solar radiative transfer research have resulted in detailed understanding of solar line formation, indicating that departures from LTE are non-negligible but difficult to quantify for many lines and spectral species (see Mihalas 1978 and Vernazza *et al.* 1981). Second, the solar photosphere is obviously inhomogenous. It displays granulation as a result of vigorous convective overshoot (see Rutten and Severino 1989), producing large variations on small spatial and short temporal scales. It bounces up and down in an intricate small-scale pattern of appreciable amplitude set by the tens of thousands of global *p*-modes which interfere together. It is pervaded by magnetic fields, largely confined in very slender kilogauss "fluxtubes" which contain an internal photosphere distinctly different from the surrounding plasma. Larger-scale organization exists also, both for the velocity patterns and for magnetic activity phenomena—again contributing to lateral inhomogeneity. Third, atomic parameters necessary in the modelling (even if that delivers the unknown radiative transition probability) are woefully lacking: bound-free probabilities, collision cross-sections, damping "constants" *etc.* are mostly unknown.

Surprisingly, solar *gf*-determination employing simple standard plane-parallel modelling assuming the validity of LTE and using "microturbulent", "macroturbulent" and "damping enhancement" fudge parameters to take care of the inhomogeneities and atomic unknowns works astonishingly well. The classical example was set by Holweger (1967); it has been followed in many studies since—including the Kiev ones.

THE KIEV PROGRAM

A program of determining empirical oscillator strengths from the optical solar spectrum was started at Kiev in the early eighties. Its first results were two extensive lists of Fe I *gf*-values (Gurtovenko and Kostik 1981a, 1981b). They were found to be of good quality, both in comparisons with laboratory data (Wiese 1983, Cowley and Corliss 1983) and in studies of their internal consistency (Rutten and Kostik 1982, Rutten and Zwaan 1983, Rutten and Van der Zalm 1984, Rutten and Kostik 1988).

The latter studies have also led to understanding of why such simplistic fits are actually so good (typically better than 0.1 dex or 25%); see the review by Rutten (1988b) for explanation, Rutten and Van der Zalm (1984) for recipes and Rutten (1988a) for examples. In fact, they are so good that the issue can be turned around: patterns in the internal consistency of such fits can be useful diagnostics of solar line formation.

THE NEW KIEV COMPILATION

The success of these earlier Fe I lists have led to continued effort at Kiev. Very recently, Gurtovenko and Kostik (1989) have published a new compilation of solar *gf*-values, specifying oscillator strengths for 1958 lines from 40 chemical elements. Diagnostical analysis is in progress; first results are given in Gurtovenko *et al.* 1989.

References

Blackwell, D. E., Petford, A. D., Shallis, M. J., and Simmons, G. J.: 1982, *Monthly Notices Roy. Astron. Soc.* **199**, 43

Cowley, C. R. and Corliss, C. H.: 1983, *Monthly Notices Roy. Astron. Soc.* **203**, 651

Gurtovenko, E. A. and Kostik, R. I.: 1981a, *Astron. Astrophys. Suppl.* **46**, 239

Gurtovenko, E. A. and Kostik, R. I.: 1981b, *Astron. Astrophys. Suppl.* **47**, 193

Gurtovenko, E. A. and Kostik, R. I.: 1989, *Fraunhofer Spectrum and the System of Solar Oscillator Strengths*, Naukova Dumka, Kiev

Gurtovenko, E. A., Kostik, R. I. and Rutten, R. J.: 1989, in J.-O. Stenflo (Ed.): *The Solar Photosphere: Structure, Convection and Magnetic Fields*, Proc. Symposium Int. Astron. Union 136, Kluwer Acad. Pub., Dordrecht

Holweger, H.: 1967, *Zeitschr. f. Astrophysik* **65**, 365

Lites, B. W.: 1972, *Observation and Analysis of the Solar Neutral Iron Spectrum*, NCAR Cooperative Thesis No. 28, High Altitude Observatory, Boulder

Mihalas, D.: 1978, *Stellar Atmospheres*, W.H. Freeman and Comp., San Francisco

Rutten, R. J.: 1983, in R.M. West (Ed.): *Highlights of Astronomy*, **6**, Reidel, Dordrecht, p. 801

Rutten, R. J.: 1988a, in Cayrel de Strobel, G. and Spite, M. (Eds.), *The Impact of Very High S/N Spectroscopy on Stellar Physics*, p. 367, IAU Symposium 132, Reidel, Dordrecht

Rutten, R. J.: 1988b, in Viotti, R., Vittone, A., and Friedjung, M. (Eds.), *Physics of Formation of FeII Lines Outside LTE*, p. 185, IAU Colloquium 94, Reidel, Dordrecht

Rutten, R. J. and Kostik, R. I.: 1982, *Astron. Astrophys.* **115**, 104

Rutten, R. J. and Kostik, R. I.: 1988, in Viotti, R., Vittone, A., and Friedjung, M. (Eds.), *Physics of Formation of FeII Lines Outside LTE*, p. 83, IAU Colloquium 94, Reidel, Dordrecht

Rutten, R. J. and Severino, G. (Eds.): 1988, *Solar and Stellar Granulation*, NATO ASI Series C263, Kluwer Acad. Publ., Dordrecht

Rutten, R. J. and Van der Zalm, E. B. J.: 1984, *Astron. Astrophys. Suppl.* **55**, 143

Rutten, R. J. and Zwaan, C.: 1983, *Astron. Astrophys.* **117**, 21

Vernazza, J. E., Avrett, E. H., and Loeser, R.: 1981, *Astrophys. J. Suppl. Ser.* **45**, 635

Wiese, W. L.: 1983, in West, R. M. (Ed), *Highlights of Astronomy*, **6**, 795

AUTHOR ADDRESSES

Ernest A. Gurtovenko and Roman I. Kostik:
Main Astronomical Observatory
Academy of Sciences of the Ukrainian S.S.R.
252127 Kiev, U.S.S.R.

Robert J. Rutten:
Sterrekundig Instituut
Postbus 80 000
NL-3508 TA Utrecht
The Netherlands

Theoretical calculations of atomic data


3d →
2p

Charlotte Froese Fischer

The challenge of theoretical predictions of oscillator strengths and lifetimes

ABSTRACT

The prediction of the lifetime of *one* excited state may require the calculation of *many* transition probabilities and possibly also autoionization rates. Some of the important concepts for performing multiconfiguration Hartree-Fock calculations for a portion of a spectrum and for highly accurate results for few electron systems are reviewed. Transitions in C I are used as an example as well as the $1s2s2p^2\ ^5P - 1s2p^3\ ^5S$ transition in Li^-.

INTRODUCTION

There are many challenges to the theoretical prediction of oscillator strengths and lifetimes.

As interest shifts from resonance transitions to transition probabilities for excited states, the amount of needed information increases rapidly. The challenge, in effect, is to perform a calculation for a portion of the spectrum, predicting many transition probabilities along with lifetimes in a single calculation. Such calculations are not "fine tuned" calculations for transitions between a specific pair of levels, but they can provide large amounts of reasonably accurate information. Among the *ab initio* methods, the Energy_Average_Level (EAL) calculations of the General Relativistic Atomic Structure Package (GRASP) (Dyall et al., 1989) can be used to provide such information, but the restriction of a single orthonormal basis for the initial and final state, in effect, limit the code to a study of ionized systems. In this paper, the multiconfiguration Hartree-Fock method with Breit-Pauli corrections for the relativistic effects will be applied to the study of excited state transitions in Carbon.

Another challenge is the prediction of lifetimes for the levels of a Rydberg series. In an unperturbed Rydberg series, the lifetimes increase smoothly as $(n^*)^3$, where n^* is the effective quantum number, but the presence of a perturber may cause an irregular behaviour (Brage et al., 1987). In some instances, the mixing with the perturber causes cancellation in the transition matrix element, resulting in a minimum in the lifetime trend. The correct prediction of the minimum is sensitive to both correlation and relativistic shift effects. Intuitively, one would not think of relativistic effects as being important in Rydberg series, but they may shift the perturber relative to the Rydberg series, thereby affecting the mixing of the perturber with the series and hence the transition probabilities that define the lifetime.

With the availability of supercomputers, it is also a challenge to improve on the accuracy of f-value predictions. Johnson *et al.*(1988) have applied many-body perturbation theory (MBPT) to third order to the study of transitions in alkali atoms: five hours of Cray X-MP/24 time were required for the calculations they describe.

Many other difficult problems remain. In core excited states, a level may decay by a variety of mechanisms, including autoionization to the continuum, as was the case for the core excited $2p^5 3s3d\ ^4L$ states of Na I (Froese Fischer, 1986). An accurate prediction of the lifetime requires not only accurate radiative transition probabilities, but also reliable autoionization rates. Transition probability calculations are rarely performed for the transition metals where the open *d*-shells greatly magnify the correlation problem. Even correlation studies have not yet been performed in all atomic systems. For example, the ground configuration of U^{+4} is $5f^2$. A relativistic MCDF (EAL) calculation produces results for which a number of levels are inverted. As in Pr^{+3} (Morrison and Rajnak, 1971), important correlation contributions are expected to arise from the interaction of $5d^{10}5f^2$ with $5d^8 5f^4$. With only those two non-relativistic configurations in the wave function expansion, the total number of $j-j$ coupled configuration states is 123, 297, 482, 555, 611, 561, and 505 for J=0 to J= 6, respectively, or 3134 configuration states for an EOL calculation. For many *ab initio* approaches, atomic structure codes need to be revised to deal with wave function expansions 10 - 100 times larger than those presently employed.

Let me now describe how the MCHF Atomic Structure Program has been used to meet some of these challenges.

SPECTRUM CALCULATIONS

Consider the problem of predicting transition data for $3s \rightarrow 3p$, $4p$, $3p \rightarrow 3d$, $4s$, and $4d$, and $3d \rightarrow 4p$ transitions in C I, transitions of interest in astrophysics. In this case, the remaining electrons are in the configuration $1s^2 2s^2 2p$; in the description of the calculation we will omit reference to the $1s^2$ shell and treat the problem as a four electron problem. Our calculation will be one in which a basis of radial functions is obtained from a series of MCHF calculations, and the total energies and wave function expansions will be obtained from a Breit-Pauli interaction matrix. Thus our calculation is essentially non-relativistic but with relativistic corrections that include spin-orbit interaction and non fine-structure effects such as the mass correction, one- and two-body Darwin terms, and spin-spin contact.

For an *ab initio* calculation, several principles need to be kept in mind.

The Complex

The set of configuration states of the same parity, the same LS term, and for which the orbitals all have the same set of principal quantum numbers, form a *complex*. In non-relativistic theory, these are the configu-

ration states which may exhibit substantial configuration mixing in the expansion of a wave function. In a calculation like the one for C I, where all terms are of interest, one may simply classify the configuration states into odd and even configuration states. For example, for the $2s^22p3l$ states, the odd and even configurations are the following:

Odd	$2s^22p3s$, $2p^33s$, $2s^22p3d$, $2p^33d$, $2s2p^23p$
Even	$2s^22p3p$, $2p^33p$, $2s2p^23s$, $2s2p^23d$

A similar set defines the $2s^22p4l$ complex. For the Carbon problem under consideration, the two sets should be combined.

The Upper Bound Principle

Experience with many calculations has shown that results are more reliable when the lower lying complex is also included in a wave function expansion. Then, by the Hylleraas-Undheim-MacDonald (1930, 1933) theorem, the n^{th} eigenvalue of the interaction matrix for a given LS term is an upper bound to n^{th} exact energy for that term. For Carbon, this required the inclusion of the following configuration states:

Odd	$2s2p^3$
Even	$2s^22p^2$, $2p^4$

In neutral atoms, not all of the levels of the lower complex lie below those of the excited complex. In Carbon, the $2s2p^3$ LS levels lie above those of the $2s^22p3s$ levels, except for $2s2p^3\ ^5S$, and play an important role in the interactions.

Term Dependence

The radial functions of orbitals in a given configuration may exhibit considerable LS term dependence, as was shown by Hansen (1973). Such term dependence can readily be checked by performing a series of Hartree-Fock calculations for each term. Table 1. shows the mean radii of $3l$ orbitals for different terms of the same configuration. Note that term dependence is negligible for $3s$ and $3d$ (though not all terms were checked), but considerable for $3p$. The term dependence here, to a large extent,

Table 1: Term Dependence of $3l$ orbitals for the configurations $2s^22p3l$ in Carbon.

$3l$	Term	$< r_{3l} >$	$3l$	Term	$< r_{3l} >$
$3s$	^3P	5.941	$3d$	^3P	10.597
	^1P	6.213		^1P	10.770
$3p$	^3D	7.338	$3p$	^1D	9.041
	^1P	7.135		^3P	8.500
	^3S	7.651		^1S	9.581

can be classified according to whether the corresponding $2s^22p^2$ configuration state is allowed. When the state is *not* allowed, the mean radius of $3p$ is more contracted than when it *is* allowed.

Optimization of Orbitals

If no term dependence were present, radial functions could be determined from an MCHF calculation for any term, but when term dependence is present, the LS terms need to be chosen carefully. Term dependence can be incorporated into a calculation like the one being described, by including additional configurations in the expansion to represent this dependence and by carefully selecting the LS term (or calculation) that determines a particular radial function, $P_{nl}(LS;r)$. For example, we could define

$$P_{3p}(^1S) = aP_{3p}(^1P) + bP_{np}(^1S), \quad < 3p|np >= 0.$$

Clearly the radial basis could be defined in a number of ways. Generally, the radial basis should include the most contracted orbital as well as a more diffuse orbital so that the term dependence can be represented by a linear combination of these orbitals. In the present case, since the calculations include the $2s^22p4p$ configuration states, we will allow the $4p$ orbital to play the role of the diffuse orbital. This keeps the size of the interaction matrix to a minimum, but may not provide the best possible results. In particular, since there is no radial basis for the representation of the diffuse $4p$, the configuration states for the latter will not be represented well. This will be shown to be the case later.

A limitation in the prediction of transition probabilities and lifetimes by the MCHF Atomic Structure Package (MCHF_ASP) that needs to be kept in mind, is the fact that the codes for performing the angular integrations for the transition operator can deal only with a limited amount of non-orthogonality between the initial and final state. Most angular momentum theories for operators assume a common, orthonormal basis for the initial and final state. The MCHF multipole program (Godefroid *et al.* 1989) allows for some non-orthogonality but restricts the non-orthogonality in such a way that the number of overlap integrals arising from non-orthogonality be at most two. In the present calculation, it is desirable to have the $\{1s,\ 2s,\ 2p\}$ set of orbitals be the same in the initial and final state. Because of the strong interaction between $2s^22p\ ^2P$ and $2p^3\ ^2P$, these orbitals were obtained from a 2x2 MCHF calculation for C^+ with a wave expansion over these two configuration states.

Separate calculations were performed for the odd and even configurations states.

For the odd configuration states, the $3s$, $4s$, $3d$ and $4d$ orbitals were obtained from MCHF calculations for

$$\{2s^22p3l,\ 2p^33l\}\ ^3P.$$

The $3p$ correlation orbital was obtained from an MCHF calculation for the $2p3s\ ^3P$ state with an expansion over the $n = 3$ odd complex plus the $2s2p^3$ and $2s2p^23p$ configuration state. In this calculation, only the $3p$ orbital was varied. A similar calculation was performed for the $4p$ correlation orbital, replacing the $n = 3$ complex by the $n = 4$ complex.

For the even configuration states, the $3p$, $3s$, and $3d$ orbitals were obtained from an MCHF calculation for the $2p3p\ ^1P$ state with a wave function expansion over

$$\{2s^22p3p,\ 2s2p^23s,\ 2s2p^23d\}\ ^1P.$$

Table 2: Theoretical total energies (in au) and energies relative to $2s^22p^2\ ^3P$ (in cm^{-1}) along with lifetimes for levels from part of the spectrum of Carbon.

nl	LS	J	Energy (a.u.)	Energy (cm-1)	Tau (ns)
3s	3P	0	-37.48573433	48373.1	3.08e+00
		1	-37.48564648	48392.3	3.07e+00
		2	-37.48546322	48432.6	3.07e+00
	1P	1	-37.47725779	50233.4	3.01e+00
3p	1P	1	-37.44554150	57194.0	1.11e+02
	3D	1	-37.44182530	58009.5	4.92e+01
		2	-37.44173242	58029.9	4.92e+01
		3	-37.44158809	58061.6	4.92e+01
	3S	1	-37.43676923	59119.2	3.78e+01
3p	3P	0	-37.42830544	60976.7	2.38e+01
		1	-37.42825069	60988.7	2.38e+01
		2	-37.42815282	61010.2	2.38e+01
	1D	2	-37.41684581	63491.6	2.40e+01
	1S	0	-37.41074219	64831.2	2.78e+01
3d	1D	2	-37.40530094	66025.3	1.38e+01
4s	3P	0	-37.40521870	66043.4	6.84e+00
		1	-37.40514206	66060.2	6.75e+00
		2	-37.40496105	66099.9	6.57e+00
	1P	1	-37.40361248	66395.9	7.58e+00
3d	3F	2	-37.40355209	66409.1	7.44e+00
		3	-37.40350664	66419.1	5.90e+00
		4	-37.40328547	66467.7	3.73e+01
	3D	1	-37.40347043	66427.1	3.41e+00
		2	-37.40339878	66442.8	4.69e+00
		3	-37.40332174	66459.7	5.56e+00

The $n = 4$ orbitals were obtained from a similar calculation for the $2p4p\ ^1P$ state, but now both the $n = 4$ and $n = 3$ complexes were included in the wave function expansion, though only the $n = 4$ orbitals were varied. The $3p$ and $4p$ orbitals had mean radii of 6.843 and 15.231, respectively. If better accuracy is desired, more p orbitals should be introduced and optimized on the ^1S state.

Once the radial functions have been determined, a configuration interaction, Breit-Pauli calculation can be performed for each of the odd and even configuration states, for a series of J values, and E1 transition probabilities computed for all possible transitions. Table 2. summarizes some of the energy levels and lifetime data from this calculation.

Table 2. immediately shows that there is not a great deal of J-dependence in the lifetimes, the only exception being the levels of the $2pnd\ ^3F$ states and to a lesser extent also the ^3D state. For the ^3F states there is considerable mixing with the ^3D states, and in the $^3D_1$ case, also with $2s^22p4s\ ^1P_1$. Thus for most of this spectrum, a non relativistic calculation is expected to be adequate.

Table 3. compares the theoretical term energies relative to the $2p3s\ ^3P$ term with similar observed values, where the observed terms energies are obtained from statistically weighted LSJ levels. With the exception of the of the $2p3p$ and $2p4p\ ^1D$, ^3P, ^1S LS terms the predicted and observed levels are in reasonably good agreement.

But such broad brush calculations, unless considerably refined, can only present the general picture. To confirm the accuracy of some of the transition probabilities,

Table 3: Comparison of LSJ-averaged, MCHF+BP term energies with similarly averaged observed values, relative to the $2p3s\ ^3P$ energy, in cm^{-1}.

nl	LS	Energy (cm-1) theory	Obs.	Diff
3s	3P	0	0	0
	1P	1820	1609	211
3p	1P	8782	8485	297
	3D	9628	9349	279
	3S	10707	10371	336
	3P	12587	11002	1585
	1D	15079	12238	2841
	1S	16418	13603	2816
3d	1D	17614	17307	307
4s	3P	17668	17760	-91
	1P	17986	17965	21
3d	3D	18022	17937	85
	3F	18035	17853	182
	1F	18279	18158	121
	1P	18462	18355	107
	3P	18721	18942	-221
4p	1P	20223	20190	33
	3D	20489	19829	661
	3S	20880	20732	148
	3P	21993	20961	1032
4d	1D	23285	23127	158
	3F	23443	23388	55
	3D	23451	23467	-16
	1F	23573	23576	-3
	1P	23606	23689	-83
	3P	23667	23733	-66
4p	1D	25915	21397	4518
	1S	31987	21879	10108

Table 4: Comparison of theoretical Breit-Pauli (LSJ) and MCHF (LS) wavelengths (in air) and line strengths with critically evaluated data.

	λ (Å)	S_l	S_v
$3s\ ^3P \rightarrow 3p\ ^3D$			
LSJ	10383	168.0	
LS	10873	170.0	173.9
NBS[1)]	10695	160.0	
$3p\ ^3D \rightarrow 4s\ ^3P$			
LSJ	12434	107.0	
LS	12059	67.4	67.1
NBS	11886	85.	

non-relativistic MCHF calculations using non-orthogonal orbitals were performed for three states over all couplings of the configurations as indicated below:

$3s\ ^3P$ $\{2s^22p_13s_1,\ 2p_1^33s_1,\ 2s^22p_33d_3,\ 2p_1^33d_2,$
$2s^23d_14f_1,\ 2p_1^23d_14f_1,\ 2s2p_1^3,\ 2s2p_13p_1\}$

$3p\ ^3D$ $\{2s^22p_13p_1,\ 2p_1^33p_1,\ 2s2p_1^23d_1,$
$2s2p_1^23s_1,\ 2s^23d_24d_2,\ 2p_1^23d_24d_2,\}$

$4s\ ^3P$ $\{2s^22p_14s_1,\ 2p_1^34s_1,\ 2s^22p_33d_3,\ 2p_1^33d_2,$
$2s^23d_14f_1,\ 2p_1^23d_14f_1,\ 2s2p_1^3,\ 2s2p_13p_1\}$

Thus, in the calculation for $4s\ ^3P$, for example, the $3d$ orbitals are correlation orbitals. Table 4. compares the LSJ averaged data for two multiplets, the LS values from the non-orthogonal, non-relativistic calculation, and the compiled data included in the NBS publication, derived from both theory and experiment. In order to separate the energy prediction from the prediction of the transition matrix element, the line strength, S, is compared rather than the oscillator strength. Clearly evident is the fact that the non-relativistic MCHF calculations, which have included more correlation effects, yield the better wavelengths: indeed, relativistic shift effects would improve agreement with observation. In the non-relativistic scheme, the length and velocity values of the line strength are also compared. In the case of the $3s\ ^3P \rightarrow 3p\ ^3D$ transition, the line strength is essentially unchanged, yet for the $3p\ ^3D \rightarrow 4s\ ^3P$ transition it has reduced substantially, with length and velocity values coming into good agreement. In this case there is extensive mixing of $2s^22p4s$ and $2s^22p3d$, mixing which is more accurately represented in the variational MCHF calculation.

ACCURATE FEW-ELECTRON CALCULATIONS

Unlike MBPT, where open shell cases may pose difficult problems, the MCHF method can be used in such cases and, with sufficient CPU time and memory, some accurate results can be obtained for few-electron systems. This was demonstrated by Brage and Froese Fischer (1988) who predicted the wavelengths of the $1s2s2p^2\ ^5P \rightarrow 1s2p^3\ ^5S$ transition in Be I-like ions to spectroscopic accuracy. In such calculations, systematically larger and larger expansions are used until "convergence" is obtained. Several concepts are used in generating the expansions.

1. *reference set*
   Configurations for which a configuration state forms a major component in the wave function expansion define the reference set.

2. *active set*
   In a combinatorial approach in which *all* configuration states are generated that can be constructed from orbitals for a given set of electrons, the latter is called the "active set".

3. *single and double replacements*
   Configurations will interact with some members of the reference set only if they differ by no more than two electrons from some member. The single and/or double replacement procedure systematically replaces one and/or two electrons in each configuration of the reference set.

4. *virtual set*
   The electrons that are used in the single and double replacement of electrons are electrons from a virtual set.

In the Be I-like calculations, the initial active set consisted of $1s$, $2s$, $2p$, $3s$, $3p$, $3d$ and $4f$ electrons. Orbitals for the first three were obtained from a Hartree-Fock calculation, and the others from a variational calculation for an expansion over the configuration states generated by the active set. Then $4s$, $4p$ and $4d$ orbitals were obtained by adding to the expansion those configuration states that were obtained by single and double replacements from the previous set. Finally, all electrons were placed in the active set and a CI calculation performed with and without relativistic shift effects.

Since these calculations have been performed, it has been found that better accuracy can be obtained by varying *all* (or almost all) orbitals rather than only the new orbitals. This was done in the study of the binding energies of negative alkaline earths. However, with an active set, a rotation of the radial basis is a transformation that does not change the total energy and so, for uniqueness and stability, it is desirable to delete certain configurations. The best candidates are those for which Brillouin's theorem should hold. Table 5. reports the results from a study of the $1s2s2p^2\ ^5P \rightarrow 1s2p^3\ ^5S$ transition of Li^-, a case not included in the earlier study. The first part of the table shows the convergence of the total energies for the two states, the wavelength (in air) for the transition, and the length and velocity values of the line strength (the observed transition energy was used for the computation of the latter) for a calculation that ignores correlation with the $1s$ electron. Note that the converged wavelength deviates from the observed by 42 Å. The next set of calculations, is for a fully correlated wave function. It was found that the s-orbitals play a much more important role in the ^5P state, that the contribution of the $5s$ was considerably larger than the contribution from the highest nl for other l-values, and so a $6s$ was added to the active set for the ^5P state. The resulting wavelength

Table 5: Convergence of total energy (in a.u.), wavelength, length and velocity forms of the line strength for the $1s2s2p^2\ ^5P \rightarrow 1s2p^3\ ^5S$ transition in Li^- as the active set is increased. The latter consists of all electrons with $n \leq N$. The symbols s and p are used to indicate an additional s or p electron, respectively.

N	E(^5P)	E(^5S)	λ(Å)	S_l, S_v
Outer Correlation Only				
3	−5.381345	−5.248208	3421.6	39.2, 40.0
4	−5.383501	−5.251369	3447.6	37.2, 38.9
5	−5.383820	−5.251675	3447.2	36.7, 39.1
Full correlation				
3,p	−5.382850	−5.251602	3470.8	
4,p	−5.385691	−5.255043	3486.8	
5,p	−5.386225	−5.255744	3491.2	
5,sp	−5.386251		3491.5	
With relativistic shift effects			3489.4	
Bunge (1980)				
Non-relativistic			3491.1	
With empirical corrections			3489.8 ± 0.9	
Exp. (Bromander *et al.* 1973)			3489.7 ± 0.2	

from the final energies, when corrected for a relativistic shift effect is 3489.4 Å, which deviates from the observed value by about 0.3 Å. The results are also compared with those reported by Bunge (1980).

It should be mentioned that, at each stage, new orbitals for outer correlation were determined and those configuration states retained with a mixing coefficient larger than 0.00005 in magnitude. A subset with mixing coefficients greater than 0.0005 was used as a zero-order set for a first-order perturbation like calculation for the many remaining configuration states. Again, the new orbitals were varied and the new configuration states with mixing coefficients larger than 0.00005 added to the earlier set. Finally, a variational calculation was performed. In this way, very large calculations could be avoided. In the case of the first-order MCHF calculation, where only a few percent of the matrix elements are non-zero, a sparse version of MCHF was used. The expansion lengths of the final wave functions were 604 and 345 configuration states, respectively, for ^5P and ^5S reflecting the greater difficulty of the calculation for the ^5P state.

CONCLUSION

For few electron systems, MCHF calculations for some transition energies can be performed that are close to experimental accuracy. But many challenges remain. One problem that is of particular concern in the MCHF approach is the evaluation of matrix elements *between* different states. In the MCHF method, orbitals are optimized for a given state and though they may be orthonormal *within* a state, they are not orthonormal between states. Thus the evaluation of the transition operator becomes more difficult and no general solution to this problem has been developed.

ACKNOWLEDGEMENTS

This research was supported by the U.S. Department of Energy, Office of Basic Energy Sciences.

REFERENCES

Brage, T., Froese Fischer, C., Carlsson, J. and C.-G. Wahlström 1987 Lifetimes and oscillator strength trends for the $4s^2nd\ ^2D$ series of Ga I In: Phys. Rev. A , **35** 1113–1118.

Brage, T. and Froese Fischer, C. 1988 the $1s2s2p^2\ ^5P - 1s2p^3\ ^5S$ transition in Be I-like ions In: J. Phys. B: Atom. Molec. Phys. **21** 2563 – 69.

Bromander, J., Hultberg, S., Jelenkovic, B., Liljeby, L. and Mannervik, S. 1979 A beam-foil study of lithium In: J. Physique, Colloque Suppl. **40** C1 10 – 13.

Bunge, C.F. 1980 Core-excited bound states of negative lithium In: Phys. Rev. A **22** 1 – 8.

Dyall, K.G., Grant, I.P., Johnson, C.T., Paria, F.A., Plummer, E.P. 1989 - GRASP A General Purpose Relativistic Atomic Structure Program. In: Comput. Phys. Commun. (in press)

Froese Fischer, C. 1986 Energy levels and lifetimes for some core-excited quartet states in Na I and Mg II In: Phys. Rev. A **34** 1667 –76.

Froese Fischer, C. 1988 Accurate oscillator strengths In: Nucl. Instr. Meth. Phys. Res. B**31** 265 – 272.

Froese Fischer, C. 1989 The MCHF atomic structure package In: Comput. Phys. Commun. (in preparation).

Godefroid, M.R., Froese Fischer, C. and Hibbert, A. 1989 A program for performing angular integrations for transition operators In: Comput. Phys. Commun. (in preparation).

Hansen, J.E. 1973 *LS*-term dependence of Slater integrals in $p^n p'$ configurations In: J. Phys. B: Atom. Molec. Phys. **6** 1387 –96; 1751 – 60; 1967 – 74.

Hibbert, A. 1982 Model Potentials in Atomic Structure In: Adv. Atomic Molecular Phys., **18** 309–340.

Hylleraas, E.A. and Undheim, B. 1930 Numerische berechnung der 2S-Terme von ortho- und par-Helium In: Z. Phys. **65** 759 (1930); MacDonald, J.K.L. 1933 Successive approximations by the Rayleigh Ritz variation method In: Phys. Rev. **43** 830.

Johnson, W.J., Saperstein, J. and Idrees, M. 1987 Second-order energies and third-order matrix elements of alkali metal atoms In: Phys. Rev. A **35**, 3218.

Morrison, J. and Rajnak K. 1971 Many-body calculations for the heavy atoms In: Phys. Rev. A **4** 536.

Wiese, W.L., Smith, M.W. and Glennon, B.M. 1966 - *Atomic Transition Probabilities*, Vol. 1, NSRDS-NBS 4, U.S. Government Printing Office, Washington, D.C. 20402

AUTHOR'S ADDRESS

Department of Computer Science, Box 6035B
Vanderbilt University
Nashville, TN 37235 USA

Alan Hibbert

Calculation of weak lines

ABSTRACT

We describe the situations which give rise to small oscillator strengths, particularly those which are unusually small as a result of some form of cancellation. We discuss through specific examples the type of calculation which is needed to give accurate results.

INTRODUCTION

The importance of weak absorption lines in the determination of stellar and interstellar abundances has been described by Keenan *et al.* (1989) in these proceedings. We discuss in this article the theoretical situations which give rise to weak lines and the calculation of the corresponding small oscillator strengths (or alternatively transition probabilities).

The most obvious division which separates transition probabilities into "large" and "small" is between "allowed" (i.e. electric dipole or E1) transitions and "forbidden" (i.e. electric quadrupole (E2) or higher multipole (Eλ) and magnetic multipole (Mλ)) transitions. The formula for transition probabilities of Eλ or M(λ-1) transitions contains the factor $\alpha^{2\lambda+1}$ where α ($\simeq 1/137$) is the fine structure constant. The presence of this factor implies that for "forbidden" transitions, the transition probabilities are normally several orders of magnitude smaller than for "allowed" transitions. A discussion of "forbidden" transitions is given by Zeippen(1989) in these proceedings, so we shall not consider them in this article. Instead, we shall investigate situations in which oscillator strengths of "allowed" transitions are small - that is, smaller than the norm for "allowed" transitions.

METHOD OF CALCULATION

In principle, the oscillator strength of a transition can be expressed in an infinite number of different but (for exact calculations) equivalent forms. In practice, at most two forms are calculated:

$$\text{length}: f_l = \frac{2\Delta E}{3g} | < \Psi_1 | \mathbf{r} | \Psi_2 > |^2 \qquad (1)$$

$$\text{velocity}: f_v = \frac{2}{3g\Delta E} | < \Psi_1 | \nabla | \Psi_2 > |^2 \qquad (2)$$

where ΔE is the transition energy (in atomic units), Ψ_1 and Ψ_2 are the initial and final state wave functions and g is the multiplicity of the state with lower energy (either $(2L+1)(2S+1)$ in LS coupling or $(2J+1)$ in intermediate coupling). Of course, neither Ψ_1 nor Ψ_2 is known exactly, so in general the two forms f_l and f_v give different values. The extent of the agreement gives *some* measure of the accuracy of the results, even though complete agreement between them does not in itself guarantee their correctness. Some convergence of that agreement as the wave functions are improved is also necessary.

For atomic systems with more than one electron, the wave functions cannot be determined exactly. In practice, they are usually expanded in infinite series of basis functions. For systems with several electrons, the most common expansion method is known as configuration interaction (CI) of which MCHF (Multi-Configurational Hartree-Fock) and SOC (Superposition Of Configurations) are specific, important classes. In this method, we expand

$$\Psi_1 = \sum_i a_i \phi_i \qquad (3)$$

$$\Psi_2 = \sum_j b_j \psi_j \qquad (4)$$

so that, for example,

$$f_l = \frac{2\Delta E}{3g} | \sum_i \sum_j a_i b_j < \phi_i | \mathbf{r} | \psi_j > |^2 \qquad (5)$$

Each of $\{\phi_i\}$, $\{\psi_j\}$ is a *configuration state function*. For many transitions for which $f_l \geq 0.1, a_1 \gg a_i (i = 2, 3, \ldots)$ and $b_1 \gg b_j (j = 2, 3, \ldots)$ where ϕ_1 and ψ_1 refer to the Hartree-Fock (HF) configurations of the two states (i.e. those associated with the normal labelling of the states). In such cases, the expansions (3) and (4) can be truncated after a fairly small number of terms and still result in quite accurate values for f_l (and similarly for f_v). In the next section, we shall consider situations where f_l is, for a number of different reasons, much smaller than 0.1. In these cases, the expansions (3) and (4) have to be much longer and the configurations chosen much more carefully in order to achieve a level of accuracy which gets even the first significant figure in f_l correct.

CAUSES OF SMALL OSCILLATOR STRENGTHS

We first discuss how abnormally small oscillator strengths occur.

Cancellation in the transition integral

The dipole matrix element $< \phi_i|r|\psi_j >$ in (5) contains the radial integral

$$\int_0^\infty r P_{n_i l_i}(r) P_{n_j l_j}(r) dr \qquad (6)$$

as a factor. In certain cases, this integral is approximately zero because the positive and negative parts of the integrand almost cancel. If also the coefficients of ϕ_i and ψ_j are close to unity in the expansions (3) and (4) respectively, so that all others are small, then the entire oscillator strength will be small.

Two specific instances of this situation are the 2s ^{2}S - 3p ^{2}P^o transition in Li (Weiss 1963) and the 3s ^{2}S - 4p ^{2}P^o transition in Mg II (Hibbert *et al.* 1983). The states of these alkali-like ions are well represented by the HF approximation so that the expansions (3) and (4) are each dominated by a single term. For both ions, the radial integral is close to zero. Although that means that the oscillator strength will be close to zero, it also means that the contributions from other terms in (3) and (4), while being small in absolute terms, are of comparable magnitude to the HF contribution. We shall discuss the Mg II transition in some detail later.

Cancellation due to CI

In the examples of the previous section, all the states are nearly 100% pure; in many other cases, the states are at least 90% pure (i.e. one coefficient in (3), say a_1, dominates the rest, with $a_1^2 \geq 0.9$). But in some states, there is strong CI mixing so that although one coefficient is larger in magnitude than the rest, there are two and sometimes more which are fairly large, say with $a_i^2 \geq 0.2$. We have investigated astrophysically important transitions involving such states for a number of singly ionised species of second row elements. For example, in the case of the $3s^23p^2\ ^3$P - $3s3p^3\ ^3$P^o transition in P II (Hibbert 1986), the ground state ^{3}P is over 90% pure, but the ^{3}P^o state has an expansion (4) of the form

$$\Psi(^3\mathrm{P}^o) = 0.81\ \psi_1(3s3p^3) + 0.50\ \psi_2(3s^23p3d) + \ldots$$

so that $b_1^2 = 0.66$, $b_2^2 = 0.25$ and the remaining terms are each fairly small.

This is a widely occurring situation. Other instances include the $2s^22p\ ^2$P^o - $2s2p^2\ ^2$D transition in C II (Weiss 1967) where there is strong mixing between $2s2p^2\ ^2$D and $2s^23d\ ^2$D; also the $3s3p\ ^1$P^o - $3p^2\ ^1$D transitions in Mg-like ions (Froese Fischer and Godefroid 1982, Tayal and Hibbert 1984, Baluja and Hibbert 1985); the $3s^23p^3\ ^4$S^o - $3s3p^4\ ^4$P in S II (Ojha and Hibbert 1989); the $3s^23p\ ^2$P^o - $3s3p^2\ ^2$D transition in Si II (Dufton *et al.* 1983); the $3s^23p^5\ ^2$P^o - $3s3p^6\ ^2$S transition in Ar II (Hibbert and Hansen 1987). In all these transitions of the form $3s^23p^n$ - $3s3p^{n+1}$, the upper state exhibits strong CI mixing of the form

$$b_1\psi_1(3s3p^{n+1}) + b_2\psi_2(3s^23p^{n-1}3d) \qquad (7)$$

with $b_1, b_2 \gg b_i, (i \geq 3)$, (Bauche *et al.* 1987). Moreover, as Bauche *et al.* discuss, the CI mixing (7) leads to small oscillator strengths because

$$b_1 < \phi_1|r|\psi_1 > + b_2 < \phi_1|r|\psi_2 > \simeq 0 \qquad (8)$$

Neither of the two matrix elements in (8) is small, but the combination (8) *is*. The two contributions almost cancel each other out.

When this cancellation due to CI occurs, the contributions from the remaining configurations play proportionally a more significant rôle than they would in the absence of such cancellation. We shall discuss specific cases later.

Intercombination lines

The situations described above assumed *LS* coupling of angular momentum. The selection rules for transitions in *LS* coupling require $\Delta S = 0$ and $\Delta L = 0$ or 1 with $L = 0 \rightarrow L' = 0$ excluded. In that approximation, E1 transitions of the form ^{1}S - ^{3}P^o are forbidden; i.e. their oscillator strengths are identically zero. If the fine structure of the ^{3}P^o state is taken into account, then although the oscillator strength of the $^1S_0$ - $^3P_0^o$, $^3P_2^o$ E1 transitions remain zero, that of the $^1S_0$ - $^3P_1^o$ transition becomes non-zero. Even in the approximation of one configuration per *LS* symmetry, we can write

$$\Psi_1(^1\mathrm{S}_0) = a_1\phi_1(^1\mathrm{S}_0) + a_2\phi_2(^3\mathrm{P}_0) \qquad (9)$$

$$\Psi_2(^3\mathrm{P}_1^o) = b_1\psi_1(^3\mathrm{P}_1^o) + b_2\psi_2(^1\mathrm{P}_1^o) \qquad (10)$$

so that

$$< \Psi_1|r|\Psi_2 > = a_1b_2 < \phi_1|r|\psi_2 > + a_2b_1 < \phi_2|r|\psi_1 > \qquad (11)$$

Although a_2 and b_2 are generally small, they are non-zero so that the oscillator strength is non-zero, but normally small. We shall discuss important special cases in the next section.

EXAMPLES OF SMALL OSCILLATOR STRENGTHS

In this section, we discuss the calculation of a number of oscillator strengths in which we have used the general CI code CIV3 (Hibbert 1975, Glass and Hibbert 1978), which is of SOC type.

$3s\ ^2S - 4p\ ^2P^o$ *in Mg II*

An extensive CI calculation of the oscillator strength of this transition was undertaken by Hibbert *et al.* (1983). Results were presented at different levels of approximation which we display in Table 1.

Table 1. Oscillator strengths of the 3s ^{2}S - 4p ^{2}P° transition in Mg II.

	Hibbert *et al.* (1983)		Other calculations	
	f_l	f_v	f_l	f_v
A :	0.00028	0.00033	0.00033[a]	
B :	0.00123	0.00101	0.00097[b]	0.00095
C :	0.00038	0.00037		

Notes - a : Biémont (1975); b : Froese Fischer (1976)

The single configuration (HF) approximation gives oscillator strengths (calculation A) in close agreement with the work of Biémont (1975): the values are small, and length and velocity forms agree quite closely. The introduction of configurations describing the polarisation of the core - particularly $2p^5 3d4p\ ^2S$ and $2p^5 3d3s\ ^2P^o$ - increase the oscillator strength by a factor of three or four (calculation B). Again the values of Hibbert *et al.* are in general agreement with an MCHF calculation of Froese Fischer (1976) which similarly includes the effect of core polarisation. Again the length and velocity values agree satisfactorily. This shows that agreement between length and velocity forms is not in itself a guarantee of accuracy.

It is interesting to consider how such a substantial change arises. If we consider the expression

$$F_{ij} = \left(\frac{2\Delta E}{3g}\right)^{\frac{1}{2}} a_i b_j < \phi_i|r|\psi_j > \qquad (12)$$

then (5) becomes

$$f_l = \left(\sum_i \sum_j F_{ij}\right)^2 \qquad (13)$$

In the velocity form, the equivalent F_{ij} associated with the two core polarising configurations given above are -0.052 and 0.060. Their combined effect is itself only 0.008, but because the interactionF_{11} between the HF configurations is only 0.018, the proportionate effect is substantial. Other F_{ij} also contribute to the considerable increase in f_l.

Hibbert *et al.* went further than this, and added other configurations, the most significant of which were $2p^6ns\ ^2S$ and $2p^6np\ ^2P^o$, especially $2p^64s\ ^2S$ (calculation C). The effect was to reduce once again the oscillator strength to around 0.0004. It is particularly interesting that the inclusion of $2p^64s\ ^2S$ should be so striking. In the approximation which includes only $2p^6ns\ ^2S$ configurations in the ground state wave function, its coefficient a_i would be zero, (Brillouin's theorem) : the Hamiltonian matrix element between 3s ^{2}S and ns ^{2}S is zero. These matrix elements remain zero as more configurations are added, but the expansion coefficients a_i change to albeit small non-zero values and the F_{ij} associated with the 4s ^{2}S and 4p ^{2}P° configurations has the value -0.017.

For this transition, all these values of F_{ij} are small. For an oscillator strength in the range 0.1 to 1.0, such as for the 3s ^{2}S - 3p ^{2}P° transition, the non-HF contributions F_{ij} have only a small influence on the value obtained. In many calculations, the corresponding configurations could probably be omitted. But because the oscillator strength is so small in this case, it is crucial that they are included, and an extensive CI calculation be undertaken, if accurate results are to be achieved.

The implications for interstellar magnesium abundances using these accurate results are discussed by Murray *et al.* (1984).

$3s^23p^2\ ^3P - 3s3p^3\ ^3P^o$ *in P II*

We remarked earlier that the $^3P^o$ state is dominated not just by the $3s3p^3$ configuration but by a linear combination of $3s3p^3$ and $3s^23p3d$, as in (7). It is important to realise that the variationally optimum 3d function for this linear combination is not the same as that for the $3s^23p3d\ ^3P^o$ state. In fact, the $3s3p^3$ configuration interacts strongly with the $3s^23pnd$ Rydberg series: the wave function for each member contains a substantial contribution of $3s3p^3$, (though decreasing with n). Alternatively, if spectroscopic radial functions $P_{nd}(r)$ are used in the configurations in the expansion of the $3s3p^3$ state :

$$\Psi(3s3p^3) = b_1\psi_1(3s3p^3) + \sum_n b_n\psi_n(3s^23pnd) \qquad (14)$$

then the summation will need to contain many terms. Even then it will not be complete : it should also include the continuum (Hansen 1977). This problem can be overcome by replacing (14) by

$$\Psi(3s3p^3) = b_1\psi_1(3s3p^3) + b_2\psi_2(3s^23p\overline{3d}) \qquad (15)$$

in which the radial function $P_{\overline{3d}}(r)$ is optimised on the lowest energy eigenvalue of the Hamiltonian matrix $< \phi_i|H|\phi_j >$, using the variational principle directly as in the SOC method (e.g. Hibbert 1975) or via MCHF equations (e.g. Froese Fischer 1978).

Hibbert(1986) discussed a set of calculations of the oscillator strength for this transition, with different levels of approximation. In all cases the oscillator strength is small. It is sufficient to look at the simplest of his calcula-

Table 2. Oscillator strengths of the $3s^23p^2\ ^3P$ - $3s3p^3\ ^3P^o$ transition in P II.

	f_l	f_v	$\Delta E(3s3p^3$ - $3s^23p3d)$
A	0.0255	0.0304	0.1407
B	0.0192	0.0227	0.1282
C	0.0110	0.0113	0.1227
Expt	0.017 ± 0.005[a]		0.1227

Notes - a : Livingstone *et al.* (1975) ; energies in atomic units.

tions to see how the smallness arises. In terms of (12) and (15), $F_{11} = 0.440$, $F_{12} = -0.280$. The sum is 0.160. Hence by (13) an oscillator strength which would be 0.194 without the CI in (15) has been reduced to 0.026, a change of almost an order of magnitude (see calculation A of Table 2). The addition of further configurations reduced the oscillator strength still more (calculation B).

Although we noted above that P_{3d} differs considerably from the 3d radial function appropriate to the $3s^23p3d\ ^3P^o$ state, it transpires that it is important that at least the $3s^23p3d\ ^3P^o$ state is as accurately represented as is $3s3p^3\ ^3P^o$, if the $3s^23p^2\ ^3P$ - $3s3p^3\ ^3P^o$ oscillator strength is to be calculated accurately. The two states interact strongly, over and above (15), and the extent of their mixing influences the coefficients b_i for each state and thence the oscillator strength. A crucial measure of how accurately the mixing has been calculated is the energy splitting $\Delta E(3s3p^3$ - $3s^23p3d)$. It can be seen from Table 2 that in this regard calculation B represents a substantial improvement over calculation A, but the splitting is still not small enough (so the mixing is not strong enough). Calculation B is an extensive CI calculation, and a final refinement can be made by making *small* adjustments to the diagonal Hamiltonian matrix elements, so that the eigenvalue separation correponds to the associated experimental energy separation. A justification for this process has been given by Brage and Hibbert (1989). It is necessarily approximate, but this fine tuning generally leads to results which are more accurate than the *ab initio* results from which they are derived. We give the resulting values as calculation C in Table 2. They are in good agreement with the best and most recent experimental values obtained using beam-foil spectroscopy. The results of calculation C were used by Dufton *et al.* (1986) to determine the abundance of phosphorus in the interstellar medium.

Again, as in our first example, an extensive CI calculation is necessary to obtain results which are at all accurate. It is worth pointing out that results based on CI expansions such as (14), where "spectroscopic orbitals" or "real state orbitals" are used, may indeed exhibit cancellation effects, but they will normally not be reliable because they do not treat the interaction with the continuum. Indeed, a finite CI treatment necessitates a proper variational treatment of the form of (15). Semi-empirical methods for handling such cases will not normally be adequate.

$3s^2\ ^1S_0 - 3s3p\ ^3P_1$ in Si III

This transition was discussed by Ojha *et al.* (1988) following a similar calculation for Al II by Hibbert and Keenan (1987). This intercombination line has a non-zero oscillator strength because of the fine-structure mixing of $3s3p\ ^3P^o_1$ and $^1P^o_1$, and to a lesser extent $3s^2\ ^1S_0$, $3p^2\ ^1S_0$ and $3p^2\ ^3P_0$. To get that mixing right, it is necessary to obtain wave functions for all these states which give accurately the energy separations.

We compare in Table 3 the value of the associated emission transition probability calculated by Ojha *et al.* with that from experiment and those obtained by other theorists. All three calculations lie within a few per cent of the experimental value. Each involves extensive CI though the details of the calculations are different. Nussbaumer (1986) used the SUPERSTRUCTURE code (Eissner *et al.* 1974) which is of SOC type with the radial functions obtained using a scaled-Thomas-Fermi potential. Laughlin and Victor (1979) used a model potential approach which incorporates core polarisation (see Laughlin 1989 - these proceedings - for further discussion of this method). Ojha *et al.* (1988) used CIV3, together with the fine-tuning which we discussed above.

Table 3. Transition probabilities of the $3s^2\ ^1S_0$ - $3s3p\ ^3P^o_1$ transition in Si III : Comparison of results.

Source	Nature of Work	A-value (s^{-1})
a	CI with model potential	1.78×10^4
b	Large-scale CI	1.8×10^4
c	Large-scale CI with core polarisation	1.672×10^4
d	Lifetime measurement using ion-trap	1.67×10^4

Notes - a : Laughlin and Victor (1979); b : Nussbaumer (1986); c : Ojha *et al.* (1988); d : Kwong *et al.* (1983).

It is this fine-tuning which leads to such good agreement with experiment. We display in Table 4 a series of calculations using CIV3, both in *ab initio* form ("uncorrected") and with the fine-tuning added ("corrected"). The three calculations consisted of :

A : valence-shell correlation only
B : A + core polarisation treated by model potentials (similar to the scheme of Laughlin and Victor)

C : A + extra *configurations* to allow for the explicit polarisation of the core

Table 4. Transition probabilities of the $3s^2\ ^1S_0$ - $3s3p\ ^3P^o_1$ transition in Si III: Convergence of calculations. (Ojha *et al.* 1988)

Calculation	Uncorrected	Corrected
A[a]	1.368×10^4	1.642×10^4
B	1.799×10^4	1.683×10^4
C	1.649×10^4	1.672×10^4

Note - a : see text.

The "uncorrected" transition probabilities vary quite substantially. This is mainly because the $^3P^o_1$ - $^1P^o_1$ energy splitting is over-estimated by 5% in calculation A, underestimated by 3% in calculation B, whereas in calculation C it is correct to within 0.2%. On the other hand, the "corrected" results, obtained by adjusting diagonal matrix elements so that the eigenvalue differences agree with the experimental energy differences, are much more consistent. This demonstrates that this process of fine-tuning an already good calculation can lead to rather accurate transition probabilities, especially for intercombination lines.

CONCLUSIONS

We have described in this article a variety of situations which give rise to small oscillator strengths . Their common feature is that, for a reliable value to be obtained theoretically, a careful and extensive calculation is necessary, and preferably one which gives special attention to those particular transitions. Values of small oscillator strengths which arise from simpler calculations, or from calculations which consider simultaneously a wide range of transitions, must be treated with caution, because it is unlikely that the values so obtained will have converged with respect to the addition of further configurations.

REFERENCES

Baluja, K.L. and Hibbert, A., 1985 - Energies and oscillator strengths for allowed transitions in S V, Cl VI and Fe XV. In Nucl. Inst. Meth. **B9**, 477-86.

Bauche, J., Bauche-Arnoult, C., Klapisch, M., Mandelbaum, P. and Schwob, J-C., 1987 - Quenching of transition arrays through configuration mixing. In J. Phys. B. **20**, 1443-50.

Biémont, E., 1975 - Systematic trends of Hartree-Fock oscillator strengths along the sodium isoelectronic sequence. In J. Quant. Spect. Rad. Transf. **15**, 531-42.

Brage, T. and Hibbert A., 1989 - Plunging configurations and J-dependent lifetimes in Mg-like ions. In J. Phys. B. **22**, 713-26.

Dufton, P.L., Hibbert, A., Kingston, A.E. and Tully, J.A., 1983 - Wave functions and oscillator strengths for Si III. In Mon. Not. R.A.S. **202**, 145-50.

Dufton, P.L., Keenan, F.P. and Hibbert, A., 1986 - The abundance of phosphorus in the interstellar medium. In Astron. Astrophys. **164**, 179-83.

Eissner, W., Jones, M. and Nussbaumer, H., 1974 - Techniques for the calculation of atomic structures and radiative data including relativistic corrections. In Comp. Phys. Commun. **8**, 270-306.

Froese Fischer, C., 1976 - Correlation effects and f-values in the sodium sequence. In *Beam-Foil Spectroscopy*, Vol. 1., (Plenum : New York), pp. 69-76.

Froese Fischer, C., 1978 - A general multi-configurational Hartree-Fock program. In Comp. Phys. Commun. **14**, 145-53.

Froese Fischer, C. and Godefroid, M.R., 1982 - Short-range interactions involving plunging configurations of the n=3 singlet complex in the Mg sequence. In Phys. Scr. **25**, 394-400.

Glass, R. and Hibbert, A., 1978 - Relativistic effects in many-electron atoms. In Comp. Phys. Commun. **16**, 19-34.

Hansen, J.E., 1977 - Multiconfiguration Hartree-Fock study of the interaction between sp^6 and s^2p^4d in the Cl I, Br I and I I isoelectronic sequences with particular emphasis on the neutral halogen. In J. Opt. Soc. Am. **67**, 754-60.

Hibbert, A., 1975 - A general program to calculate configuration interaction wave functions and oscillator strengths of many-electron atoms. In Comp. Phys. Commun. **9**, 141-72.

Hibbert, A., 1986 - Oscillator strengths of ^3P - $^3P^o$ transitions in P II. In J. Phys. B. **19**, L455-9.

Hibbert, A., Dufton, P.L., Murray, M.J. and York, D.G., 1983 - Oscillator strengths for Mg^+ transitions. In Mon. Not. R.A.S. **205**, 535-41.

Hibbert, A. and Hansen, J.E., 1987 - Accurate wave functions for ^2S and $^2P^o$ states in Ar II. In J. Phys. B. **20**, L245-51.

Hibbert, A. and Keenan, F.P., 1987 - Oscillator strengths for intercombination and forbidden transitions amongst the $3s^2$ and 3s3p levels in Al II. In J. Phys. B. **20**, 4693-7.

Keenan, F.P., Brown, P.J.F., Dufton, P.L. and Holmgren, D.E., 1989 - Determination of stellar and interstellar abundances from weak absorption lines. In these proceedings.

Kwong, H.S., Johnson, B.C., Smith, P.L. and Parkinson, W.H., 1983 - Transition probability of the Si III 189.2 - nm intersystem line. In Phys. Rev. A. **27**, 3040-3.

Laughlin, C., 1989 - Accurate model-potential methods for the prediction of energy spectra and oscillator strengths in one- and two-valence-electron atomic systems. In these proceedings.
Laughlin, C. and Victor, G.A., 1979 - Intercombination line oscillator strengths for the Mg I isoelectronic sequence. In Astrophys. J. **234**, 407-9.
Livingstone, A.E., Kernahan, J.A., Irwin, D.J.G. and Pinnington, E.H., 1975 - Beam-foil studies of phosphorus in the vacuum ultraviolet. In Phys. Scr. **12**, 223-9.
Murray, M.J., Dufton, P.L., Hibbert, A. and York, D.G., 1984 - Interstellar magnesium abundances. In Astrophys. J. **282**, 481-4.
Nussbaumer, H., 1986 - Temperature and density determination from Si III lines. In Astron. Astrophys. **155**, 205-9.
Ojha, P.C. and Hibbert, A., 1989 - Oscillator strengths for transitions among the low-lying energy levels of S II. In J. Phys. B. **22**, 1153-62.
Ojha, P.C., Keenan, F.P. and Hibbert, A., 1988 - Oscillator strengths for transitions among the $3s^2$ and 3s3p levels of Si III. In J. Phys. B. **21**, L395-401.
Tayal, S.S. and Hibbert, A., 1984 - Oscillator strengths and series perturbations in Al II. In J. Phys. B. **17**, 3835-45.
Weiss, A.W., 1963 - Wave functions and oscillator strengths for the lithium isoelectronic sequence. In Astrophys. J. **138**, 1262-76.
Weiss, A.W., 1967 - Superposition of configurations and atomic oscillator strengths - Carbon I and II. In Phys. Rev. **162**, 71-80.
Zeippen, C. J., 1989 - Calculations of forbidden lines. In these proceedings.

AUTHOR'S ADDRESS

Department of Applied Mathematics and Theoretical Physics, The Queen's University of Belfast, Belfast BT7 1NN, N. Ireland.

Cecil Laughlin

Accurate model-potential methods for the prediction of energy spectra and oscillator strengths in one- and two-valence-electron atomic systems

ABSTRACT

Model-potential methods which include long-range polarisation terms are briefly reviewed. Transition wavelengths and oscillator strengths for dipole allowed transitions in some one- and two-valence-electron ions are presented. An alternative form of the dipole operator for use with the Coulomb approximation is introduced. Fine-structure splittings and intercombination transitions are also considered.

INTRODUCTION

Transition wavelengths and oscillator strengths are fundamental quantities in atomic spectroscopy and are essential for the interpretation of solar and stellar spectra and for diagnostic spectroscopy of fusion plasmas. Accurate experimental measurements of oscillator strengths are not usually available, and thus there is a great need for precise theoretical values.

Model-potential methods, in which the effects of the core electrons of an atomic system are represented by effective operators, present an attractive approach for describing the valence-electron properties (such as energy spectra and transition rates) of few-valence-electron systems. By explicitly including only the optical electrons in the calculations they simplify the computational tasks dramatically and, in favourable cases, they provide highly accurate results. They also provide a simple physical picture of the system.

An extensive number of model-potential approaches have been employed and it is not our intention to review these here (see Hibbert (1982) and Laughlin and Victor (1988) for recent reviews). Instead we concentrate on our approach to the problems of predicting transition wavelengths and oscillator strengths in alkali- and alkaline-earth-like systems and illustrate the high accuracy that may be achieved. But first we revisit the simplest model-potential method, the Coulomb approximation, which has been widely used to calculate oscillator strengths since the early applications to lithium and sodium by Trumpy (1930) and to a variety of one- and two-electron systems by Bates and Damgaard (1948).

THE COULOMB APPROXIMATION FOR OSCILLATOR STRENGTHS

For a one-valence-electron ion consisting of a nucleus of charge Z and $N+1$ electrons, the optical electron is considered to move in the Coulomb potential $(Z-N)/r$ with energy E, where $-E$ is the experimental ionisation potential. Because the wave functions thus determined are irregular at the origin, they are set equal to zero close to the nucleus, say $0 \leq r \leq r_c$, and the length form $\mathbf{r}$ of the electric dipole operator is used to emphasise the asymptotic region far from the nucleus where the approximation should be good. For the method to be successful in practice it is clear that dipole matrix elements should not be sensitive to the choice of r_c. An interesting question is: can we find a form of the electric dipole operator which has longer range than the length form $\mathbf{r}$? One such form may be derived quite simply from the commutator

$$[H, r^2\mathbf{r}] = -2\mathbf{r} - r\nabla r - 2\mathbf{r}\frac{\partial}{\partial r}r \tag{1}$$

which gives (Laughlin, 1989a)

$$\langle\psi_1|\mathbf{r}|\psi_2\rangle = \langle r\psi_1|\mathbf{b}|r\psi_2\rangle, \tag{2}$$

where

$$\mathbf{b} = -\tfrac{1}{2}\left[(E_1-E_2)\mathbf{r} + \nabla + 2\hat{\mathbf{r}}\frac{\partial}{\partial r}\right]. \tag{3}$$

When ψ_1 and ψ_2 are approximate wave functions, $\langle\psi_1|\mathbf{r}|\psi_2\rangle$ will *not* be equal to $\langle r\psi_1|\mathbf{b}|r\psi_2\rangle$ and the latter expression apparently provides an attractive alternative long-range form of the dipole operator for use with Coulomb wave functions. In practice, however, no real advantage seems to be gained with this formulation. In fig. 1 we show how the 3d–4p transition matrix element for the sodium atom varies with r_c. Generally, there is little to choose between $\mathbf{r}$ and $r\mathbf{b}r$ as far as sensitivity to r_c is concerned. A problem with $r\mathbf{b}r$ is that it is not Hermitian and, in fact, the mean of $\langle r\psi_1|\mathbf{b}|r\psi_2\rangle$ and $\langle r\psi_2|\mathbf{b}|r\psi_1\rangle^*$ is $\langle\psi_1|\mathbf{r}|\psi_2\rangle$, even for approximate (differentiable) wave functions ψ_1 and ψ_2.

FORM OF THE MODEL POTENTIAL

Many forms of model potential have been used in practice (see, for example, Hibbert (1982) and Szasz (1985), and references therein). Our formulation (Laughlin *et al*, 1978, Fairley and Laughlin, 1984) is based on a core potential derived from Hartree-Fock orbitals plus long-range polarisation terms. For a 1-valence-electron system the model Schrödinger equation is

$$\left(-\tfrac{1}{2}\nabla^2 + V_M\right) = \varepsilon_{nl}\phi_{nl}, \tag{4}$$

where, in atomic units,

$$V_M = -\frac{Z}{r} + V_{HF} - \frac{\alpha_d}{2r^4}W_1\left(\frac{r}{r_c}\right) + U(r). \tag{5}$$

Here, α_d is the static dipole polarisability of the core (quadrupole and dynamical correction terms may also be

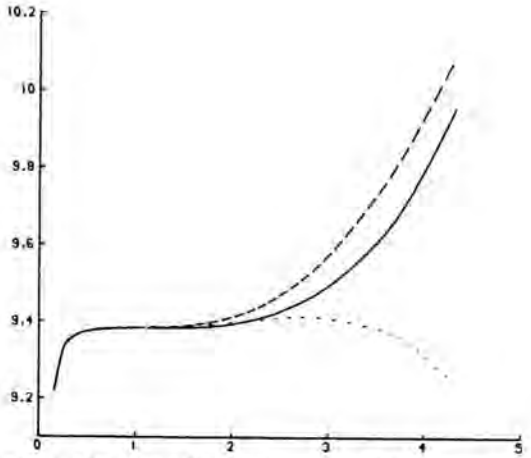

Fig. 1. Variation of the sodium atom 3d–4p transition matrix element (vertical axis) with the cut-off radius r_c for the Coulomb wave functions (horizontal axis) calculated with various dipole operators: ———— $\mathbf{r}$; - - - - - - - $r\mathbf{b}r$; ———— $r\mathbf{b}^{\dagger}r$.

included; see, for example, Peach (1983)) and the polarisation potential $\alpha_d/2r^4$ is cut off for small r by the function $W_1(r/r_c)$, where r_c is an effective core radius. $U(r)$ is a short-range correction chosen empirically so that the eigenvalues ε_{nl} of equation (1) give very precise values for the observed ionisation energies. If the Hartree-Fock core potential V_{HF} contains only the static interactions with the fixed Hartree-Fock core orbitals then V_M is a local potential, whereas if exchange terms are included in V_{HF} then V_M will be non-local. Higher accuracy is achieved when a non-local potential is employed.

For a 2-valence-electron system we adopt the equation

$$\left[-\tfrac{1}{2}\nabla_1^2-\tfrac{1}{2}\nabla_2^2+V_M(1)+V_M(2)+\frac{1}{r_{12}} - \frac{\alpha_d}{r_1^2 r_2^2}P_1(\hat{\mathbf{r}}_1\cdot\hat{\mathbf{r}}_2)W_2\left(\frac{r_1}{r_c},\frac{r_2}{r_c}\right)\right]\Psi = E\Psi, \qquad (6)$$

where the final term in the square brackets is the so-called "dielectric" term (Chisholm and Öpik, 1964) modified by a cut-off function W_2. The eigenfunctions Ψ and eigenvalues E of equation (6) are calculated variationally by expanding Ψ in terms of properly antisymmetrised and angular-momentum coupled products of the 1-electron functions ϕ_{nl} of equation (4).

POLARISATION CORRECTIONS TO THE DIPOLE OPERATOR

Consider an electric dipole transition between 2 states with model-potential wave functions Ψ_a and Ψ_b, each of which satisfy equation (6). In lowest order in the valence electron–core electron interaction, the dipole matrix element is $\langle\Psi_a|\mathbf{r}_1+\mathbf{r}_2|\Psi_b\rangle$. Since a dipole moment is induced on the core by the valence electrons a corrected dipole operator $\mathbf{d}_1+\mathbf{d}_2$ replaces $\mathbf{r}_1+\mathbf{r}_2$, where

$$\mathbf{d} = \mathbf{r}\left(1-\frac{\alpha_d(\omega)}{r^3}\right), \qquad (7)$$

$\alpha_d(\omega)$ being the dipole polarisability of the core at the transition frequency $\omega = |E_a - E_b|$ (Bersuker, 1957; Hameed *et al*, 1968). It has recently been shown (Laughlin, 1989b) that the next correction to $\mathbf{r}$ is of order r^{-6} and can be written in terms of the dipole-quadrupole interaction $\nabla\frac{1}{r}\cdot\nabla\nabla\frac{1}{r}$. This latter correction has not yet been included in any actual calculations.

OSCILLATOR STRENGTH RESULTS

Rather few oscillator strengths are known to high accuracy, even for the relatively simple alkali-like systems. For Li and Na, however, Gaupp *et al* (1982) have carried out precise beam-laser measurements on the resonance transitions and we can use these experimental values as a check on the accuracy of the model-potential calculations. Some comparisons are presented in Table 1. It may be observed that the model-potential values calculated with the corrected form of the dipole operator (equation (7)) are very close to the measured values, though they fall outside the experimental error bars of Gaupp *et al* (1982). We note that this discrepancy also exists for other recent theoretical values (Froese Fischer, 1988). The Coulomb approximation also provides reliable values.

Accurate data are also available in the helium isoelectronic sequence of ions (Schiff *et al*, 1971; Kono and Hattori, 1984). The excited states of these systems may be treated in the model-potential framework by constructing an effective potential to represent the K-shell electron and it has been found that model-potential oscillator strengths for triplet transitions in ions up to Ne IX agree to better than 1% with the very extensive *ab initio* calculations of Schiff *et al* (1971) and Kono and Hattori (1984), even for weak transitions. Some specimen results are also included in Table 1.

Turning now to 2-valence-electron systems, where accurate solution of equation (6) is more difficult, the situation is less favourable. However, the evidence suggests that reliable oscillator strength values can be obtained with model-potential methods without undue computational effort. As examples, we present some specimen results for beryllium sequence ions in Table 2. Results are also available for the magnesium sequence (Victor *et al*, 1976a), the calcium sequence (Victor *et al*, 1976b) and the copper and zinc sequences (Victor and Taylor, 1983).

In the case of the $2s^2\,{}^1S-2s2p\,{}^1P^o$ resonance transitions in the beryllium sequence, agreement between the model-potential values and the results of Reistad and Martinson (1986), obtained by an isoelectronic smoothing of available reliable experimental data, is good. The largest discrepancy (5%) occurs for B II and only for this ion does the predicted value lie outside the error bars derived

Table 1. Comparison of model-potential oscillator strengths with other values.

System	Transition	Oscillator strength			
		Model potential†		Other	Coulomb approximation
		(1)	(2)		
Li	$2s\ ^2S - 2p\ ^2P^o$	0.7536	0.7471	$0.7416 \pm 0.0012^a, 0.7480^b$	0.763
Na	$3s\ ^3S - 3p\ ^3P^o$	0.9784	0.9572	$0.9536 \pm 0.0016^a, 0.9714^b$	0.981
Li^+	$2s\ ^3S - 2p\ ^3P^o$	0.3091	0.3083	0.3080^c	0.303
Li^+	$2p\ ^3P^o - 3d\ ^3D$	0.6258	0.6241	0.6247^d	0.618
Be^{2+}	$2s\ ^3S - 3p\ ^3P^o$	0.2505	0.2517	0.2526^c	0.248
C^{4+}	$2p\ ^3P^o - 3s\ ^3S$	0.06730	0.06789	0.06784^c	0.0671
C^{4+}	$2p\ ^3P^o - 4s\ ^3S$	0.01377	0.01395	0.01396^c	0.0144

† Column (1) is calculated with the dipole length operator r; column (2) includes a core polarisation correction (see equation (7) of text).
[a] Gaupp *et al* (1982); [b] Froese Fischer (1988); [c] Schiff *et al.* (1971); [d] Kono and Hattori (1984).

Table 2. Wavelengths and oscillator strengths for beryllium-like ions.

Ion	Transition	Wavelength (Å)	Oscillator strength	
			Model potential	Experiment
Be I	$2s^2\ ^1S - 2s2p\ ^1P^o$	2349.3	1.372	1.341 ± 0.047^a
B II	$2s^2\ ^1S - 2s2p\ ^1P^o$	1362.5	1.012	0.965 ± 0.020^a
C III	$2s^2\ ^1S - 2s2p\ ^1P^o$	977.0	0.764	0.754 ± 0.014^a
	$2s2p\ ^1P^o - 2s3s\ ^1S$	690.5	0.021	0.022 ± 0.002^b
N IV	$2s^2\ ^1S - 2s2p\ ^1P^o$	765.1	0.614	0.620 ± 0.014^a
	$2s2p\ ^3P^o - 2s3d\ ^3D$	283.5	0.625	0.602 ± 0.060^c
	$2s3p\ ^3P^o - 2s3d\ ^3D$	7117.0	0.143	0.127 ± 0.041^c
	$2s2p\ ^1P^o - 2s3d\ ^1D$	335.1	0.541	0.477 ± 0.052^c
	$2s3s\ ^3S - 2s3p\ ^3P^o$	3481.0	0.578	0.125 ± 0.048^c
O V	$2s^2\ ^1S - 2s2p\ ^1P^o$	629.7	0.513	0.527 ± 0.014^a
	$2s^2\ ^1S - 2s3p\ ^1P^o$	172.2	0.406	0.373 ± 0.041^c
	$2s2p\ ^3P^o - 2s3d\ ^3D$	192.9	0.657	0.576 ± 0.075^c
	$2s3p\ ^1P^o - 2s3d\ ^1D$	3144.7	0.227	0.469 ± 0.122^c
	$2s2p\ ^1P^o - 2s3d\ ^1D$	220.4	0.544	0.510 ± 0.066^c
	$2s3s\ ^1S - 2s3p\ ^1P^o$	5114.1	0.210	0.318 ± 0.079^c
Ne VII	$2s3s\ ^3S - 2s3p\ ^3P^o$	1987.0	0.380	0.781 ± 0.063^c

[a] Reistad and Martinson (1986); [b] Ishii *et al* (1985); [c] Lang *et al* (1987).

by Reistad and Martinson (1986). We observe that the model-potential and configuration-interaction (Hibbert (1974), Serrão (1986)) oscillator strengths for this transition are in harmony and are discrepant with Reistad and Martinson's value.

A comparison of our N IV, O V and Ne VII results with the experimental results of Lang *et al* (1987) reveals some puzzling features. For some transitions there is good agreement, whilst for others there are large discrepancies. The experimental method measured branching ratios and employed beam-foil lifetime measurements of the common upper level to deduce transition probabilities. Errors in the lifetime measurements would clearly lead to unreliable transition probabilities, and this may partly explain some of the discrepancies. However, there are situations where experimental and theoretical branching ratios differ significantly, for example, the experimental and theoretical branching ratios for the 2s3p ^{1}P^o – 2s3d ^{1}D and 2s2p ^{1}P^o – 2s3d ^{1}D transitions in O V are, respectively, $4.41.10^{-3}$ and $2.05.10^{-3}$. The discrepancy here does not arise from cancellation effects in the dipole matrix elements (neither oscillator strength is small) and, in fact, all recent theoretical calculations are in good accord.

Relative oscillator strengths for lines of neutral calcium absorbed from the 4s4p ^{1}P^o level have recently been measured by Smith (1988) and in Table 3 we compare these with the model-potential values. The agreement between the two sets of results is, on the whole, reasonable. A large discrepancy occurs for the weak 4s4p ^{1}P^o – 4s6s ^{1}S transition which is severely affected by cancellation effects in the dipole matrix element. This transition has also been studied by Froese Fischer and Hansen (1985) and their oscillator strength, 0.001, does not agree with either of the values in Table 3, though it is intermediate between them.

Table 3. Absorption oscillator strengths from the level 4s4p ^{1}P^o of neutral calcium.

	Oscillator strength	
Upper level	Model potential	Experiment[a]
4s5s ^{1}S	0.143	0.160
4s6s ^{1}S	0.0003	0.0089
4p^2 ^{1}S	0.113	0.115
4s7s ^{1}S	0.0152	0.0133
4s4d ^{1}D	0.254	0.207
4p^2 ^{1}D	0.594	0.580
4s5d ^{1}D	0.353	0.281

[a] Smith (1988).

QUARTET LEVELS OF LITHIUM-LIKE IONS

Core-excited 1s2s*nl* ^4L and 1s2p*nl* ^4L levels of 3-electron ions have been actively investigated by both experimental and theoretical groups in recent years. These levels are readily populated by foil excitation and, as they are metastable against Coulomb autoionisation, optical emission spectra can readily be observed and radiative lifetime measurements may be performed. Various theoretical approaches have been employed, including model-potential (see, for example, Laughlin (1988) and references therein). The quartet term system of N V has recently been investigated by beam-foil spectroscopy (Blanke *et al*, 1987; Garnir *et al*, 1988) and by charge exchange in a gas cell (Bouchama *et al*, 1988) but there is a paucity of theoretical data, so we now present some results in Table 4 for this system.

The identifications proposed by Blanke *et al* (1987), Garnir *et al* (1988) and Bouchama *et al* (1988) for wavelengths shorter than 230 Å are confirmed by the present model-potential calculations and the wavelength predictions of Chung (Baudinet-Robinet *et al*, 1986). Garnir *et al* (1988) observed a line at 633.18 Å which they assigned to the 1s2p3d ^{4}F^o – 1s2p4f ^{4}G transition in N V. However, our wavelength for this transition is 675.01 Å, and we would therefore propose that the observed line arises from 1s2p3p ^{4}D – 1s2p4d ^{4}F^o. Garnir *et al* (1988) also observed a line of medium intensity at 672.88 Å which they assigned to 1s2p3d ^{4}F^o – 1s2p4f ^{4}F, and a weak blended line at 673.90 Å which they assigned to 1s2s3d ^{4}D – 1s2s4f ^{4}F^o. Our results (Table 4) suggest that these assignments should be interchanged. If this suggestion is correct then it is puzzling that the 1s2p3d ^{4}F^o – 1s2p4f ^{4}G line has not been observed in the beam-foil spectrum. The model-potential transition probabilities indicate that the 445.60 Å line should probably be assigned to 1s2s3p ^{4}P^o – 1s2s5d ^{4}D, rather than to 1s2p3p ^{4}D – 1s2p5d ^{4}D^o.

FINE-STRUCTURE SPLITTINGS AND INTERCOMBINATION TRANSITIONS

We parameterise the spin-orbit interaction $V_{so}^{(1)}$ as

$$V_{so}^{(1)} = \tfrac{1}{2}\alpha^2 Z_f \frac{\boldsymbol{l}\cdot\boldsymbol{s}}{r^3}, \qquad (8)$$

where α is the fine-structure constant and Z_f is determined empirically so that $V_{so}^{(1)}$ reproduces the observed fine-structure splittings of the $j = l \pm \frac{1}{2}$ levels of the 1-electron ion. The effective nuclear charge Z_f depends on the angular momentum l but, for fixed l, it varies very little with the principal quantum number n (Weisheit and Dalgarno, 1971). For 2-valence-electron ions we also include the spin-own-orbit and spin-spin interactions (Bethe and Salpeter, 1971) in the fine-structure Hamiltonian H_1. For ions near the neutral end of an isoelectronic sequence, H_1 is small and may be treated as a perturbation. Some calculated and observed fine-structure splittings for triplet terms of 2-valence-electron ions are presented in Table 5. It may be observed that the errors

Table 4. Wavelengths and transition probabilities in the quartet spectrum of N V.

Transition	Wavelength (Å)					Transition probability (10^{-8} s^{-1})
	Model potential	Chung	Garnir *et al* (1988)	Blanke *et al* (1987)	Bouchama *et al* (1988)	
1s2s2p ^{4}P° – 1s2s4d ^{4}D	151.4	151.43	151.50	151.58	151.5	238.4
1s2p^2 ^{4}P – 1s2p4d ^{4}D°	160.0	159.84	159.84	159.82	159.7	293.8
1s2s2p ^{4}P° – 1s2s3d ^{4}D	193.4	193.52	193.54	193.50	193.6	760.9
1s2p^2 ^{4}P – 1s2p3d ^{4}P°	202.5	202.38	202.40	202.41	202.4	412.1
1s2s2p ^{4}P° – 1s2s3s ^{4}S	211.0	211.13	211.10	211.11	211.1	177.5
1s2p3p ^{4}D – 1s2p5d ^{4}D°	445.4		445.60			5.6
1s2s3p ^{4}P° – 1s2s5d ^{4}D	445.6					21.8
1s2s3s ^{4}S – 1s2s4p ^{4}P°	555.1				555.4	17.1
1s2p3s ^{4}P° – 1s2p4p ^{4}D	595.0		594.96			18.4
1s2s3p ^{4}P° – 1s2s4d ^{4}D	626.0	625.43	626.01			45.1
1s2p3p ^{4}D – 1s2p4d ^{4}F°	633.7					46.4
1s2s3d ^{4}D – 1s2s4f ^{4}F°	673.1	673.01	673.90			92.8
1s2p3d ^{4}F° – 1s2p4f ^{4}F	673.5	672.61	672.88			14.4
1s2p3d ^{4}F° – 1s2p4f ^{4}G	675.0		633.18			84.9

in the predicted values are usually less than 5%, thus validating our representation of H_1.

Table 5. Calculated (Δ^c) and observed (Δ^o) fine-structure splittings (cm^{-1}) for triplet terms of 2-valence-electron ions.

Ion	Term	0 — 1		1 — 2	
		Δ^c	Δ^o	Δ^c	Δ^o
C III	2p3s ^{3}P°	33.4	33.3	68.1	68.6
C III	2p3d ^{3}P°	−14.3	−14.5	−25.4	−26.3
O V	2p^2 ^{3}P	159.8	155.7	279.6	268.8
Mg I	3s3p ^{3}P°	20.3	20.1	41.3	40.7
Mg I	3s4p ^{3}P°	3.46	3.30	7.03	6.75
Si III	3s3p ^{3}P°	132.1	128.6	267.2	261.7
Si III	3p^2 ^{3}P	132.0	133.5	261.5	258.5
S V	3p^2 ^{3}P	383.0	362.0	775.0	767.0
Ca I	4s4p ^{3}P°	53.2	52.2	106.6	105.9
Ca I	4s4d ^{3}P°	4.14	3.67	6.24	5.58

Intercombination transitions, such as 3s^2 ^{1}S$_0$ – 3s3p ^{3}P$_1^o$ in magnesium-like ions, arise from the mixing of singlet and triplet levels, for example, 3s3p ^{3}P$_1^o$ with 3s3p ^{1}P$_1^o$ and 3s^2 ^{1}S$_0$ with 3p^2 ^{3}P$_0$, by the fine-structure Hamiltonian H_1. The model-potential results for 3s^2 ^{1}S$_0$ – 3s3p ^{3}P$_1^o$ transitions in selected ions of the magnesium sequence (Laughlin and Victor, 1979) are compared with recent theoretical and experimental values in Table 6.

Table 6. 3s^2 ^{1}S$_0$ – 3s3p ^{3}P$_1^o$ intercombination transition wavelengths (λ) and oscillator strengths (f) for magnesium sequence ions.

Ion	λ (Å)	f (10^{-5})		
		Model potential	Other theory	Experiment
Mg I	4572.4	0.211		0.206 ± 0.029[a]
Al II	2669.2	1.10	1.12[b]	1.07 ± 0.07[c]
Si III	1892.0	2.85	2.67[d]	2.67 ± 0.16[e]
S V	1204.4	10.6	11.1[f]	

[a] Kwong *et al* (1982); [b] Hibbert and Keenan (1987); [c] Johnson *et al* (1986); [d] Ojha *et al* (1988); [e] Kwong *et al* (1983); [f] Dufton *et al* (1986).

The agreement obtained is most satisfactory. For Si III,

the model-potential value lies just outside the experimental error bars of Kwong *et al* (1983). It has been pointed out by Ojha *et al* (1988) that our oscillator strength is probably too large by approximately 4.6% since we overestimate the fine-structure splitting in this case by about 2.3%. We have used experimental singlet-triplet energy separations in our perturbation calculations of $^3P_1^o - {}^1P_1^o$ and $^1S_0 - {}^3P_0$ mixings, but have preferred to use without modification the prescription given by equation (8) for $V_{so}^{(1)}$, with Z_f determined as described previously.

REFERENCES

Bates, D.R. and Damgaard, A., 1949. *Phil. Trans. Roy. Soc.(London)* **A242**, 101.

Baudinet-Robinet, Y., Dumont, P.D. and Garnir, H.P., 1986. *Phys. Scr.* **33**, 73.

Bersuker, L.B., 1957. *Opt. Spectrosc.* **3**, 97.

Bethe, H.A. and Salpeter, E.E., 1971. *Quantum Mechanics of One- and Two-Electron Atoms*. Springer-Verlag, Berlin.

Blanke, J.H., Heckmann, P.H., Träbert, E. and Hucke, R., 1987. *Phys. Scr.* **35**, 780.

Bouchama, T., Denis, A., Désesquelles, M., Farizon, M. and Martin, S., 1988. *Nucl. Instr. and Meth.* **B31**, 367.

Chisholm, C.D.H. and Öpik, U., 1964. *Proc. Phys. Soc.* **83**, 541.

Dufton, P.L. Hibbert, A., Keenan, F.P., Kingston, A.E. and Doschek, G.A., 1986. *Astrophys. J.* **300**, 448.

Fairley, N.A. and Laughlin, C., 1984. *J. Phys. B* **17**, 2757.

Froese Fischer, C., 1988. *Nucl. Instr. and Meth.* **B31**, 265.

Froese Fischer, C. and Hansen, J.E., 1985. *J. Phys. B* **20**, 4031.

Garnir, H.P., Baudinet-Robinet, Y., Dumont, P.-D., Träbert, E. and Heckmann, P.H., 1988. *Nucl. Instr. and Meth.* **B31**, 161.

Gaupp, A., Kukse, P. and Andrä, H.J., 1982. *Phys. Rev.* **A26**, 3351.

Hameed, S., Herzenberg, A. and James, M.G., 1968. *J. Phys. B* **1**, 822.

Hibbert, A., 1974. *J. Phys. B* **7**,1417.

Hibbert, A., 1982. *Adv. At. Mol. Phys.* **18**, 309.

Hibbert, A. and Keenan, F.P., 1987. *J. Phys. B* **20**, 4693.

Ishii, K., Suzuki, M. and Takahashi, J., 1985. *J. Phys. Soc. Japan* **54**, 3742.

Johnson, B.C., Smith, P.L. and Parkinson, W.H., 1986. *Astrophys. J.* **308**, 1013.

Kono, A. and Hattori, S., 1984. *Phys. Rev.* **A30**, 2093.

Kwong, H.S., Smith, P.L. and Parkinson, W.H., 1982. *Phys. Rev.* **A25**, 2629.

Kwong, H.S., Johnson, B.C., Smith, P.L. and Parkinson, W.H., 1983. *Phys. Rev.* **A27**, 3040.

Lang, J., Hardcastle, R.A., McWhirter, R.W.P. and Spurrett, P.H., 1987. *J. Phys. B* **20**, 43.

Laughlin, C., 1988. *Z. Phys. D* **9**, 273.

Laughlin, C., 1089a. Submitted for publication.

Laughlin, C., 1989b. *J. Phys. B* **22**, L21.

Laughlin, C. and Victor, G.A., 1979. *Astrophys. J.* **234**, 407.

Laughlin, C. and Victor, G.A., 1988. *Adv. At. Mol. Phys.* **25**, 163.

Laughlin, C., Constantinides, E.R. and Victor, G.A., 1978. *J. Phys. B* **11**, 2243.

Müller, W., Flesch, J. and Meyer, W., 1984. *J. Chem. Phys.* **80**, 3297.

Ojha, P.C., Keenan, F.P. and Hibbert, A., 1988. *J. Phys. B* **21**, L395.

Peach, G., 1983. In: *Atoms in Astrophysics* (P. G. Burke, W. B. Eissner, D. G. Hummer and I. C. Percival, eds.) p. 115. Plenum, New York.

Reistad, N., and Martinson, I., 1986. *Phys. Rev.* **A34**, 2632.

Schiff, B., Pekeris, C.L. and Accad, Y., 1971. *Phys. Rev.* **A4**, 885.

Serrão, J.M.P., 1986. *J. Quant. Spectrosc. Radiat. Transfer* **35**, 265.

Smith, G., 1988. *J. Phys. B* **21**, 2827.

Szasz, L., 1985. *Pseudopotential Theory of Atoms and Molecules*. John Wiley, New York, New York.

Trumpy, B., 1930. *Z. Physik.* **61**, 54.

Victor, G.A. and Taylor, W.R., 1983. *Atom. Data and Nuc. Data Tables* **28**, 107.

Victor, G.A., Stewart, R.F. and Laughlin, C., 1976a. *Astrophys. J. Suppl. Series*, **31**, 237.

Victor, G.A., Stewart, R.F. and Laughlin, C., 1976b. In: *Beam-Foil Spectroscopy* (I. A. Sellin and D. J. Pegg, eds.), p. 43. Plenum, New York.

Weisheit, J.C. and Dalgarno, A., 1971. *Phys. Rev. Lett.* **27**, 701.

AUTHOR'S ADDRESS

Department of Mathematics,
University of Nottingham,
Nottingham NG7 2RD, England.

C.J. Zeippen

Calculations of radiative transition probabilities for forbidden lines

ABSTRACT

A review is presented of some typical results illustrating the level of accuracy reached in recent theoretical calculations of radiative transition probabilities for forbidden lines. The emphasis of the present paper is put on results obtained with the computer program SUPERSTRUCTURE, but comparisons with other studies allow for an assessment of the data and comments are made on the present state of the art. Most of the transitions considered here are between levels in the ground configurations $2p^{2,3,4}$ and $3p^{2,3,4}$, but some other cases are mentioned briefly.

INTRODUCTION

It has been known for some time that well-chosen forbidden lines arising through electric quadrupole (E2) and magnetic dipole (M1) transitions can be used as a basis for electron temperature and/or density diagnostics both in astrophysics and fusion research (see, for example, Seaton, 1968, Osterbrock, 1974 & 1989, or Hinnov & Suckewer, 1980). For these diagnostics to be meaningful, there are two obvious requirements : good observations and accurate atomic data, such as collision strengths and radiative transition probabilities. I shall be looking at the latter in the present paper. To treat the subject exhaustively would take a much longer talk. Many reviews and compilations exist, which have been widely consulted by users of atomic data and by atomic physicists who want to decide which case to tackle next (see, for example, Wiese et al, 1966 & 1969, Garstang, 1968, Eidelsberg et al, 1981, Mendoza, 1983, Kaufman & Sugar, 1986). Biémont & Zeippen (1989) have started an extended review of recent developments. Here, although some other cases will be mentioned very briefly, we shall mainly content ourselves with the important transitions in the ground configurations $2p^{2,3,4}$ and $3p^{2,3,4}$ for comparatively light elements. Indeed, the importance of relativistic effects increases and that of correlation effects decreases as Z becomes larger. All calculations then tend to converge in the middle-Z range until the Breit-Pauli approximation ceases to hold and only fully-relativistic structure programs give reasonable data. Here, the emphasis will be on values obtained with the code SUPERSTRUCTURE, but comparisons will of course be made with other theoretical findings. It should be noted that very few experimental results exist in this field, which makes all the more crucial the need for assessing various sets of theoretical data yielded by methods and codes as different as possible.

THE METHODS

The code SUPERSTRUCTURE (Eissner et al, 1974) has been used extensively to produce accurate transition probabilities. It is a configuration-interaction (CI) computer program which accounts for fine-structure and other relativistic effects in the low-Z Breit-Pauli approximation. The one-electron radial orbitals P_{nl} are computed using a Thomas-Fermi statistical model (SM) potential (Eissner & Nussbaumer, 1969), or are obtained from the Coulomb potential. In the version of the code modified by Nussbaumer & Storey (1978), there is one scaling parameter per (n,1), allowing for much flexibility in building the orbitals. Those scaling parameters are determined through term energy minimization procedures. The Breit-Pauli Hamiltonian is treated as a perturbation and the expansion of the relativistic wavefunctions may be improved by means of the term energy correction (TEC) procedure described by Zeippen et al (1977).

The probability for a transition between levels i and j, forbidden for electric dipole (E1) radiation but not for E2 and M1 radiation is taken to be

$$A_{ij} = A_{ij}(E2) + A_{ij}(M1) \qquad (1)$$

with (2)

$$A_{ij}(E2) = 2.6733\ 10^{3}\ (E_i-E_j)^5\ 1/g_i\ S_{ij}(E2)\ s^{-1}$$

and (3)

$$A_{ij}(M1) = 3.5644\ 10^{4}\ (E_i-E_j)^3\ 1/g_i\ S_{ij}(M1)\ s^{-1}$$

S_{ij} is the line strength and energies are expressed in Rydbergs and lengths in Bohr radii.

Relativistic corrections to the M1 operator are included, i.e.

$$S_{ij}(M1) = |\langle i|\mathbf{Q}|j\rangle|^2 \qquad (4)$$

where

$$\mathbf{Q} = \mathbf{Q}^{\circ} + \mathbf{RC} = \sum_{m=1}^{N} \{\boldsymbol{\ell}(m)+\sigma(m)\} + \mathbf{RC} \qquad (5)$$

$\mathbf{Q}^{\circ}$ is the usual lowest-order M1 operator, corresponding to the magnetic moment and the sum runs over all N electron coordinates. Expression (5) is implemented in DIPOLE, a program complementary to SUPERSTRUCTURE and written by Eissner & Zeippen (1981). The expressions for the operators labelled **RC** can be found in Drake (1971) or Sucher (1978).

Another CI code which has been used extensively to compute transition probabilities is CIV3 (Hibbert, 1975). It calculates Slater-type orbitals using Hartree-Fock functions like those of Clementi & Roetti (1974), together with correlation orbitals, to provide initial estimates. The parameters defining the orbitals are obtained through minimization procedures similar to the ones in SUPERSTRUCTURE. There is a relativistic version of the code (Glass & Hibbert, 1978) incorporating the Breit-Pauli Hamiltonian.

Combining the Hartree-Fock, Breit-Pauli and CI formalisms is the computer program MCHF-BP (Froese Fischer, 1978 & 1983). Firstly, a non-relativistic MCHF calculation produces a set of radial functions for a given LS term, providing the basis for an interaction matrix to be determined in the BP approximation for a wavefunction expansion over a large set of configurations which may interact electrostatically or through relativistic corrections, for one or more J-values of interest.

The semi-empirical framework of HXR and HFR self-consistent-field methods have been implemented in the Cowan-Zealot suite of programs (Bromage, 1978) which are used in connection with Cowan's (1981) atomic structure codes. The self-consistent-field method with relativistic corrections is used to set up the radial wavefunctions. Energies and spectra are then computed with the help of conventional Slater-Condon theory with configuration mixing.

The relativistic equivalent to the MCHF code described above is the multiconfiguration Dirac-Fock program written by Desclaux (1975). The MCDF computer program is based on a more rigorous theory than the codes incorporating the Breit-Pauli formalism. It does not introduce adjustable parameters in building the wavefunctions and it treats the leading correlation and relativistic effects on an equal level. Note that the variational principle gives a stationary solution in this case and not a minimum, as the Dirac equations have two solutions.

Finally, among many other methods, I shall also mention the non-closed-shell-many-electron theory (NCMET) of atomic structure developed by Sinanoglu et al (see, for example, Sinanoglu, 1969) or the FOTOS formalism (see, for example, Nicolaides & Beck, 1978).

THE ASTROPHYSICAL IMPORTANCE OF THE DIAGNOSTICS BASED ON FORBIDDEN LINES

Rosa (1989) explains in detail the importance of atomic data in the study of gaseous nebulae. Suffice to say here that some forbidden line intensity ratios are sensitive to electron temperature and/or density and that some of those are powerful tools to analyze the spectra from nebulae, on condition that the quality of observations is matched by that of atomic data and vice versa.

For instance, the ratio I(3729 Å)/I(3726 Å) in O II is of great importance (see, for example, Seaton & Osterbrock, 1957, Canto et al, 1980, O'Dell & Castaneda, 1984, Zeippen, 1980 & 1987). A good illustration of the interplay between observations and atomic data is the high-density limit $r(N_e=\infty)$ of the ratio I(3729 Å)/I(3726 Å) which is equal to $3/2\ A(^2D_{5/2}\text{-}^4S_{3/2})/A(^2D_{3/2}\text{-}^4S_{3/2})$, thus allowing for a "direct" check of consistency between observed intensities and atomic data : the theoretical value for $r(\infty)$ must never be superior to the one observed in nebulae with high electron density. This is but one example where one may consider, with great caution (after all, there are still many uncertainties in our knowledge of nebulae...), the universe as a large laboratory.

Another ratio of interest is I(4741.5 Å)/I(4712.7 Å) in Ar IV (see the recent study by Zeippen et al, 1987), which is a good companion to the equivalent ratio in O II, as their ranges of sensitivity complement one another.

Finally, it is worth mentioning the work recently completed by Stanghellini & Kaler (1989) who analyzed 146 planetary nebulae and showed, in particular, how new atomic data change the conclusions drawn.

FORBIDDEN LINES IN THE $2p^2$ CONFIGURATION

The most complete SUPERSTRUCTURE calculation to date is by Nussbaumer & Rusca (1979) who considered all the members of the isoelectronic sequence up to Ni XXIII. There is good

agreement with the work of Nicolaides & Sinanoglu (1971 & 1973). In the case of O III, the values obtained by Baluja & Doyle (1981), using CIV3, and by Nussbaumer & Storey (1981), using SUPERSTRUCTURE, agree rather well with each other and with the earlier work of Nussbaumer & Rusca (1979). Based on a smaller configuration basis set, the values computed with SUPERSTRUCTURE by Kastner et al (1977) differ markedly from the latter. Recent MCHF +BP calculations were performed by Froese Fischer & Saha (1985) who also present a detailed comparative discussion of the main sets of probabilities available in the literature for this case. Using a large number of configurations, Froese Fischer & Saha (1985) obtained good agreement with the relativistic MCDF results of Cheng et al (1979) and the data computed by Fawcett (1978) using the Cowan-Zealot package. However, the discrepancies with the SUPERSTRUCTURE or CIV3 results can be important for some E2 transitions. For the M1 transitions, there is reasonable agreement between all main studies. In view of this situation, a new and more ambitious effort using SUPERSTRUCTURE might be timely.

FORBIDDEN LINES IN THE $2p^3$ CONFIGURATION

The ground configuration $2p^3$ of N-like ions is a tricky case because it has a half-filled outer shell. In this case, the first-order spin-orbit interaction vanishes and second-order effects become important (see the discussion in Eissner & Zeippen, 1981). Trying to solve the inconsistencies between observed and calculated values for $r(\infty)$ pointed out by Seaton & Osterbrock (1957) in their study of O II forbidden lines, Zeippen (1980) showed that the usual lowest-order M1 transition operator was not adequate to treat the most "sensitive" transitions and that the inclusion of relativistic corrections (**RC** in formula (5) above) was required. Eissner & Zeippen (1981) confirmed this viewpoint and proposed new forbidden transition probabilities which yielded, in particular, a value for $r(\infty)$ close to the one observed in nebula NGC 7027 for the high-density limit of the ratio I(3729 Å)/I(3726 Å). Zeippen (1982) extended the calculation to the first twenty members of the isoelectronic sequence. A detailed comparison with previous work (including Garstang, 1972, Fawcett, 1978, Cheng et al, 1979, Bhatia & Mason, 1980a & 1980b) was also carried out by this author. Using a larger configuration basis set in the MCHF+BP code, Godefroid & Froese Fischer (1984) were able to show that some important correlation effects had been neglected so far and published improved probabilities, with the qualification that the **RC** operators were not included in their expression for the M1 transition operator. Taking full advantage of the progress in computing facilities and of the findings of all the previous studies, Butler & Zeippen (1984), Zeippen (1987) and Becker et al (1989) have now produced what should be the most accurate transition probabilities to date for this sequence up to Fe XX, with an estimated uncertainty within 10%. Note that the agreement between the new SUPERSTRUCTURE results and the MCHF+BP values for the same quantities has now reached a good level. Finally, it should be said that the theoretical value for $r(\infty)$ is now smaller than the one observed in nebulae with high electron density, which is not inconsistent.

FORBIDDEN LINES IN THE $2p^4$ CONFIGURATION

For this isoelectronic sequence, no extended SUPERSTRUCTURE calculation has been reported, apart from the preliminary results of Mendoza & Zeippen quoted by Mendoza (1983). There are calculations by Kastner et al (1977) and Bhatia et al (1979) but those are based on a limited number of configurations. A study of the sequence has been performed by Baluja & Zeippen (1988) who used CIV3, including the intrashell correlations within the n=2 complex and the intershell correlations between the n=2 and the n=3 complexes. They calculated E2 and M1 transition probabilities for 17 species, obtaining good agreement with two experimental results for O I (McConkey et al, 1966, Corney & Williams, 1972). In this paper, a detailed comparison is made with the MCHF+BP results of Froese Fischer & Saha (1983) who include the n=2, n=3 and n=4 complexes in their calculations, and with the relativistic data of Cheng et al (1979). The agreement between the three sets of results is generally good, although some discrepancies can be seen. The differences between the MCHF+BP and the CIV3 data are smaller than the ones with the MCDF values. Other studies include the work of Garstang (1951), Nicolaides & Sinanoglu (1971) and Fawcett (1978). It could be worthwhile to perform a large-scale SUPERSTRUCTURE calculation for this sequence, as the preliminary results of Mendoza & Zeippen (see Mendoza, 1983) tend to agree rather well with the most reliable data available.

FORBIDDEN LINES IN THE $3p^2$ CONFIGURATION

The three main recent calculations performed for this case will be considered here. The SUPERSTRUCTURE study of the isoelectronic sequence up to Ni XV is by Mendoza & Zeippen (1982b) who used a 7-configuration basis set and improved over earlier work by Czyzak & Krueger (1963) or McKim-Malville & Berger (1965). Biémont & Bromage (1983) produced results for alternate ions from S III to Sn XXXVII with the help of the HXR self-consistent-field method and Slater-Condon theory. The agreement between the SUPERSTRUCTURE and HXR results is good, which is significant as the two methods and physical models differ markedly. A relativistic MCDF computation has been done by Huang (1985) who takes all the configurations in the n=3 complex into account. Unfortunately, this author included no comparison with previous work in his paper. A quick assessment shows the usual trend of some discrepancies at the neutral end of the isoelectronic sequence and converging results as Z increases. Only a more detailed comparative study will tell if there is a need for further work on this case.

FORBIDDEN LINES IN THE $3p^3$ CONFIGURATION

Again, as in the case of $2p^3$, second-order effects play an important rôle, but to a smaller extent as Z is higher for n=3 than for n=2 and the higher-order corrections decrease as Z increases (see the discussion in Eissner & Zeippen, 1981). The first "modern" computation was performed by Mendoza & Zeippen (1982a) using a 7-configuration basis set in SUPERSTRUCTURE and its companion DIPOLE. They obtained some sizeable changes as compared to previous work (Czyzak & Krueger, 1963 & 1965, Garstang, 1968 & 1972). Biémont & Hansen (1985) provided a check on those new results with the help of the HXR and HFR self-consistent-field methods. They found reasonable agreement but noted that the discrepancies were more substantial for this isoelectronic sequence than in the case of $3p^2$, which is not surprising in view of the more complex problem in hand. Froese Fischer & Godefroid (1986) published some MCHF+BP results, in particular for S II and Ni XIV. Their detailed comparison with the work of Mendoza & Zeippen (1982a) and with the MCDF results of Huang (1984) shows a reasonable agreement between the three studies. The general conclusion here must be that there seems to be room for improvement of at least some of the forbidden transition probabilities available in the literature for the $3p^3$ isoelectronic sequence.

FORBIDDEN LINES IN THE $3p^4$ CONFIGURATION

Mendoza & Zeippen (1983) based their SUPERSTRUCTURE calculation on an 8-configuration basis set, obtaining reasonable agreement with previous work by Czyzak & Krueger (1963) and McKim-Malville & Berger (1965). The HXR/HFR results were obtained by Biémont & Hansen (1986b) and their values were found to be in satisfactory agreement with the SUPERSTRUCTURE data, although there are some sizeable discrepancies. Very recently, a relativistic MCDF computation was performed by Saloman & Kim (1989). These authors compare their results with the two previous sets of data and they conclude that the differences can be explained by the approximations and adjustments used in the HXR/HFR and SUPERSTRUCTURE studies and by the limitation of their own calculations at low Z (small number of configurations in the physical model). It should be noted that the values of Biémont & Hansen (1986b) and those of Mendoza & Zeippen (1983) tend to agree better with one another than with the MCDF results.

SOME OTHER CASES

Due to the narrow scope of this talk, it will be impossible to describe in detail many other studies of interest, such as the recent application of the HXR/HFR method to configurations $4p^2$, $4p^3$ and $4p^4$ by Biémont & Hansen (1986a & 1986b), or the attempt of Nussbaumer & Storey (1980), using SUPERSTRUCTURE for treating the forbidden lines of Fe II. All this will have to be assessed in further surveys.

I will conclude by mentioning the forbidden lines between the $3p^6 4s\ ^2S_{1/2}$ and the $3p^6 3d\ ^2D_{3/2,5/2}$ levels in K-like elements. These lines are of astrophysical interest in Ca II (see, for example, Hobbs et al, 1988). There have been two recent calculations by Ali & Kim (1988), using a single-configuration approximation in the MCDF code, and Zeippen (1989), using some amount of CI in SUPERSTRUCTURE. The agreement between the two sets of results is good, even though more sophistication seems necessary to reach a definitive conclusion. The experimental result for K by Hertel & Ross (1969) looks too large, but reasonable agreement is obtained with the theoretical result of Langhoff et al (1985) for the same atom. The earlier transition probabilities of Osterbrock (1951) for Ca II are most probably overestimated.

CONCLUSION

In this necessarily limited review, while providing a sample of references which could be of practical use to the reader, I hope I have shown how much effort by many teams goes into supplying accurate data to astrophysicists and fusion specialists. In this presentation, I have tried to illustrate the idea that detailed comparisons between different sets of results is essential in assessing the accuracy of the data proposed to the user, but also in understanding (and perhaps attenuating) the weaknesses of the various theoretical methods. Saloman & Kim (1989) state that these approximations which include adjustable parameters require experience and judgment on the part of physicists in order to yield reliable results. I would happily extend their view to most methods, as none of them, however rigorous and foolproof in principle, can be treated in practice as a "black box". We all suspect that human beings are still needed in the age of computers : it is certainly true of forbidden line transition probability calculations!

ACKNOWLEDGEMENTS

I am grateful to Pr. M.J. Seaton for his guidance while I was making my very first steps into the field. Friendly thanks are due to my colleagues W. Eissner, C. Mendoza, K. Butler, K.L. Baluja and S.R. Becker (in order of appearance) for excellent collaboration in calculating hundreds of forbidden line transition probabilities over the years.

AUTHOR'S ADDRESS

Observatoire de Paris, UPR 261 du CNRS et DAMAp, 92190 Meudon, France.

REFERENCES

Ali M.A., Kim Y.K. (1988) Phys. Rev. A 38, 3992.

Baluja K.L., Doyle J.G. (1981) J. Phys. B 14, L11.

Baluja K.L., Zeippen C.J. (1988) J. Phys. B 21, 1455.

Becker S.R., Butler K., Zeippen C.J. (1989) Astron. Astrophys. 221, 375.

Bhatia A.K., Feldman U., Doscheck G.A. (1979) Astron. Astrophys. 80, 22.

Bhatia A.K., Mason H.E. (1980a) Mon. Not. R. Astr. Soc. 190, 925.

Bhatia A.K., Mason H.E. (1980b) Astron. Astrophys. 83, 380.

Biémont E., Bromage G.E. (1983) Mon. Not. R. Astr. Soc. 205, 1085.

Biémont E., Hansen J.E. (1985) Phys. Scr. 31, 509.

Biémont E., Hansen J.E. (1986a) Phys. Scr. 33, 117.

Biémont E., Hansen J.E. (1986b) Phys. Scr. 34, 116.

Biémont E., Zeippen C.J. (1989) in preparation for the Third Atomic Data Workshop, Observatoire de Paris, DAMAp, Meudon.

Bromage G.E. (1978) The Cowan-Zealot Suite of Computer Programs for Atomic Structure (Report AL-R3, Rutherford Appleton Laboratory).

Butler K., Zeippen C.J. (1984) Astron. Astrophys. 141, 274.

Canto J., Elliot K.H., Meaburn J., Theokas A.C. (1980) Mon. Not. R. Astr. Soc. 193, 911.

Cheng K.T., Kim Y.K., Desclaux J.P. (1979) Atom. Data Nucl. Data Tables 24, 111.

Clementi E., Roetti C. (1974) Atom. Data Nucl. Data Tables 14, 177.

Corney A., Williams O.M. (1972) J. Phys. B 5, 686.

Cowan R.D. (1981) The Theory of Atomic Structure and Spectra (University of California Press).

Czyzak S.J., Krueger T.K. (1963) Mon. Not. R. Astr. Soc. 126, 177.

Czyzak S.J., Krueger T.K. (1965) Mon. Not. R. Astr. Soc. 129, 103.

Desclaux J.P. (1975) Comput. Phys. Commun. 9, 31.

Drake G.W.F. (1971) Phys. Rev. A 3, 908.

Eidelsberg M., Crifo-Magnant F., Zeippen C.J. (1981) Astron. Astrophys. Suppl. Ser. 43, 455.

Eissner W., Jones M., Nussbaumer H. (1974) Comput. Phys. Commun. 8, 270.

Eissner W., Nussbaumer H. (1969) J. Phys. B 2, 1028.

Eissner W., Zeippen C.J. (1981) J. Phys. B 14, 2125.

Fawcett B.C. (1978) Atom. Data Nucl. Data Tables 22, 473.

Froese Fischer C. (1978) Comput. Phys. Commun. 14, 145.

Froese Fischer C. (1983) J. Phys. B 16, 157.

Froese Fischer C., Godefroid M. (1986) J. Phys. B 19, 137.

Froese Fischer C., Saha H.P. (1983) Phys. Rev. A 28, 3169.

Froese Fischer C., Saha H.P. (1985) Phys. Scr. 32, 181.

Garstang R.H. (1951) Mon. Not. R. Astr. Soc. 111, 115.

Garstang R.H. (1968) in Planetary Nebulae,

eds. Osterbrock & O'Dell (Reidel, Dordrecht) p.143.
Garstang R.H. (1972) Opt. Pura Apl. 5, 192.
Glass R., Hibbert A. (1978) Comput. Phys. Commun. 16, 19.
Godefroid M., Froese Fischer C. (1984) J. Phys. B 17, 681.
Hertel I.V., Ross K.J. (1969) J. Phys. B 2, 285.
Hibbert A. (1975) Comput. Phys. Commun. 9, 141.
Hinnov E., Suckewer S. (1980) Phys. Lett. 79A, 298.
Hobbs L.M., Lagrange-Henri A.M., Ferlet R., Vidal-Madjar A., Welty D.E. (1988) Astrophys. J. 334, L41.
Huang K.N. (1984) Atom. Data Nucl. Data Tables 30, 313.
Huang K.N. (1985) Atom. Data Nucl. Data Tables 32, 503.
Kastner S.O., Bhatia A.K., Cohen L. (1977) Phys. Scr. 15, 259.
Kaufman V., Sugar J. (1986) J. Phys. Chem. Ref. Data 15, 321.
Langhoff S.R., Bauschlicher C.W., Partridge H. (1985) J. Phys. B 18, 13.
McConkey J.W., Burns D.J., Moran K.A., Emeleus K.G. (1966) Phys. Lett. 22, 416.
McKim-Malville J., Berger R.A. (1965) Planet. Space Sci. 13, 1131.
Mendoza C. (1983) in Planetary Nebulae, ed. Flower (Reidel, Dordrecht) p.143.
Mendoza C., Zeippen C.J. (1982a) Mon. Not. R. Astr. Soc. 198, 127.
Mendoza C., Zeippen C.J. (1982b) Mon. Not. R. Astr. Soc. 199, 1025.
Mendoza C., Zeippen C.J. (1983) Mon. Not. R. Astr. Soc. 202, 981.
Nicolaides C.A., Beck D.R. (1978) in Excited States in Quantum Chemistry, ed. Nicolaides & Beck (Reidel, Dordrecht) p.143.
Nicolaides C.A., Sinanoglu O. (1971) Phys. Rev. A 4, 1400.
Nicolaides C.A., Sinanoglu O. (1973) Solar Phys. 29, 17.
Nussbaumer H., Rusca C. (1979) Astron. Astrophys. 72, 129.
Nussbaumer H., Storey P.J. (1978) Astron. Astrophys. 64, 139.
Nussbaumer H., Storey P.J. (1980) Astron. Astrophys. 89, 308.
Nussbaumer H., Storey P.J. (1981) Astron. Astrophys. 99, 177.
O'Dell C.R., Castaneda H.O. (1984) Astrophys. J. 283, 158.
Osterbrock D.E. (1951) Astrophys. J. 114, 469.
Osterbrock D.E. (1974) Astrophysics of Gaseous Nebulae (Freeman, San Francisco).
Osterbrock D.E. (1989) Astrophysics of Gaseous Nebulae and Active Galactic Nuclei (University Science Books, Mill Valley, california).
Rosa M. (1989) Invited talk in this volume.
Saloman E.B., Kim Y.K. (1989) Atom. Data Nucl. Data Tables 41, 339.
Seaton M.J. (1968) Adv. Atom. Molec. Phys. 4, 331.
Seaton M.J., Osterbrock D.E. (1957) Astrophys. J. 125, 66.
Sinanoglu O. (1969) in Atomic Physics, eds. Bederson, Cohen, Pichanick (Plenum Press, New York) p.131.
Stanghellini L., Kaler J.B. (1989) Astrophys. J. 343, 811.
Sucher J. (1978) Rep. Prog. Phys. 41, 1781.
Wiese W.L., Smith M.W., Glennon B.M. (1966) Atomic Transition Probabilities, Vol. 1, NSRDS-NBS 4 (Washington DC : National Bureau of Standards).
Wiese W.L., Smith M.W., Miles B.M. (1969) Atomic Transition Probabilities, Vol. 2, NSRDS-NBS 22 (Washington DC : National Bureau of Standards).
Zeippen C.J. (1980) J. Phys. B 13, L485.
Zeippen C.J. (1982) Mon. Not. R. Astr. Soc. 198, 111.
Zeippen C.J. (1987) Astron. Astrophys. 173, 410.
Zeippen C.J. (1989) Astron. Astrophys. in press.
Zeippen C.J., Butler K., Le Bourlot J. (1987) Astron. Astrophys. 188, 251.
Zeippen C.J., Seaton M.J., Morton D.C. (1977) Mon. Not. R. Astr. Soc. 181, 527.

M.J. Seaton

Mass production of accurate atomic data

ABSTRACT

The Opacity Project involves collaborators in France, Germany, the U.K., the U.S.A. and Venezuela. Energy levels, f-values and photoionisation cross sections are being calculated for all cosmically abundant elements, in all ionisation stages. All levels are included for which the least tightly bound electron is significantly non-hydrogenic and has a principal quantum number $n \leq 10$.

OPACITIES

Let $I(\nu, s)$ be the intensity of radiation with frequency ν, where s is a measure of distance in a direction $\hat{\mathbf{s}}$. The equation of radiative transfer is

$$\frac{dI}{ds} = -\kappa(\nu) I + j(\nu)$$

where $\kappa(\nu)$ is the monochromatic opacity and $j(\nu)$ the emissivity. If $j(\nu)=0$ and $\kappa(\nu)$ is independent of s, the solution is $I(\nu, s) = I(\nu, 0)\exp(-\kappa(\nu)s)$. Many processes contribute to κ : bound-free absorption, spectrum lines, free-free, electron scattering, *etc*. Let $\kappa(\nu, i)$ be the contribution to κ due to processes involving an initial level i. Then $\kappa(\nu, i) = N(i)\sigma(\nu, i)$ where $N(i)$ is the number-density of atoms and σ is a cross section. For bound-free transitions, σ is the photo-ionisation cross-section (multiplied by a correction factor for stimulated emission). For a spectrum line,

$$\sigma = \frac{\pi e^2}{mc} f \phi(\nu),$$

(again times a correction factor) where f is the oscillator strength and $\phi(\nu)$ the line profile normalised to

$$\int \phi(\nu) d\nu = 1.$$

For a black-body enclosure, $I(\nu) = B(\nu, T)$, the intensity of black-body radiation, and $j(\nu) = \kappa(\nu) B(\nu, T)$, which is Kirchhoff's law. For conditions in stellar interiors this law can be assumed, but $I(\nu, s)$ is not exactly equal to $B(\nu, T)$ because there is a net outward flux of radiation, $\mathbf{F}$. An approximate solution of the transfer equation gives $\mathbf{F} = -K \nabla T$ where K is proportional to $(1/\kappa_R)$ and κ_R is the Rosseland mean opacity defined by

$$\frac{1}{\kappa_R} = \left\{ \int \frac{1}{\kappa(\nu)} \dot{B}(\nu, T) d\nu \right\} \left\{ \int \dot{B}(\nu, T) d\nu \right\}^{-1}$$

with $\dot{B} = dB/dT$. This mean is an essential quantity for calculations involving the structures and evolution of the stars.

Huge amounts of atomic data are required for the calculation of κ_R . Although hydrogen and helium are the most abundant cosmic elements, at higher temperatures they are fully ionised and the dominant contribution to κ_R come from heavier elements (what the astronomers call the "metals"). Earlier studies go back to the work of Kramers and there has been a lot of more recent work, although still using atomic data which are not very accurate. Simon (1982) showed that a number of discrepancies between theory and observations of pulsating stars could be resolved by assuming that the "metal" opacities had been under-estimated by factors of about two or three, and this prompted a number of us to make new calculations using much more accurate data. The work involves collaborators in Belfast, Boulder, Caracas, Columbus, London, Munich, Nice, Paris and Urbana and we refer to it as The Opacity Project

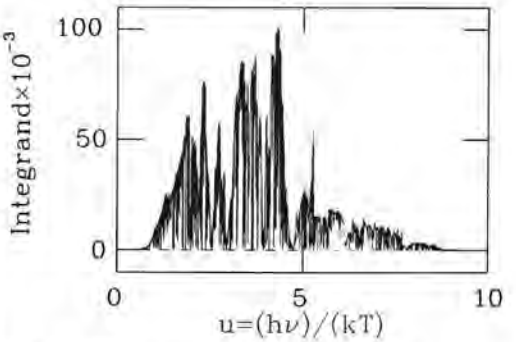

Fig. 1. The integrand for the calculation of the Rosseland mean for carbon, $\log(T) = 4.5$, $\log(\rho) = -8$. The normalisation is such that the area under the curve gives $(1/\kappa_R)$ with κ_R in atomic units per atom

MASS PRODUCTION

We require f-values and profiles for some 10^6 lines, and at least 10^5 photo-ionisation cross sections. We would not claim our data to be more accurate than the best results which have been obtained for individual transitions, using high levels of optimisation, but we do believe them to be more accurate than most of the data in the literature, and much more extensive. How can one achieve such accuracy in mass-production work ?

Our techniques (described by Berrington *et al.*, 1987) are based on those of collision theory. For atomic systems containing $(N+1)$ electrons we need to consider only

states for which not more than one electron is loosely bound, or is not bound at all (final states for photo-ionisation). We use conventional CI methods to calculate functions $\psi_i(N)$ for states containing N electrons which are all more-or-less tightly bound, and for the $(N+1)$ systems we use expansions

$$\Psi(N+1) = A\sum_i \psi_i(N)\theta_i(1) + \sum_j \Phi_j(N+1)c_j$$

where the $\theta_i(1)$ are one-electron orbitals, and A is an operator for anti-symmetrisation and vector-coupling. The functions $\Phi_j(N+1)$ are constructed using the orbitals employed in the functions $\psi_j(N)$. *An essential feature of our method is that the functions θ_i and coefficients c_j are fully optimised.* Efficiency is achieved using the Belfast R-matrix method together with a number of new features.

The orbital functions θ_i contain radial functions $F_i(r)$. A first step is to obtain non-physical functions $\Psi^{(n)}$ for an inner region $r<R$, having radial functions $F_i^{(n)}$ satisfying

$$\frac{dF_i^{(n)}}{dr} = 0 \text{ for } r = R .$$

The $F_i^{(n)}$ are expanded in terms of basis functions which satisfy the boundary condition. For each combination of angular momenta and parity only one matrix diagonalisation is required to obtain the functions $\Psi^{(n)}$. The functions Ψ for any energy E are expanded in terms of the $\Psi^{(n)}$,

$$\Psi_E = \sum_n \Psi^{(n)} C_{n,E} .$$

The Ψ_E are then matched to solutions for the outer region, $r>R$.

RESULTS FOR A SIMPLE "METAL"

Carbon, the simplest of the astronomers' "metals", has provided our first test case. Figure 1 shows the Rosseland integrand for the case of pure carbon, $\log(T) = 4.5$ and $\log(\rho) = -8$, where T is temperature in K and ρ is the density in gm cm^{-2}. Since κ_R is a weighted harmonic mean, the dips in the integrand correspond to maxima in the monochromatic opacity. There are a number of broad dips, features which had not been anticipated before the calculations were made. They are due to what Yu Yan and Seaton (1987) call *PEC resonances* (photo-excitation of the core). Their nature is illustrated in Figure 2 (from Tully, Seaton and Berrington, 1989), which shows cross sections, on logarithmic scales, for photoionisation of C III *2s5d* levels. The cross sections have series of resonances converging to the *2p* limit, and the most pronounced of these are due to processes

$$2s\,5d + h\nu \rightarrow 2p\,5d \rightarrow 2s + e$$

which give maxima at frequencies close to that for the $2s \rightarrow 2p$ transition.

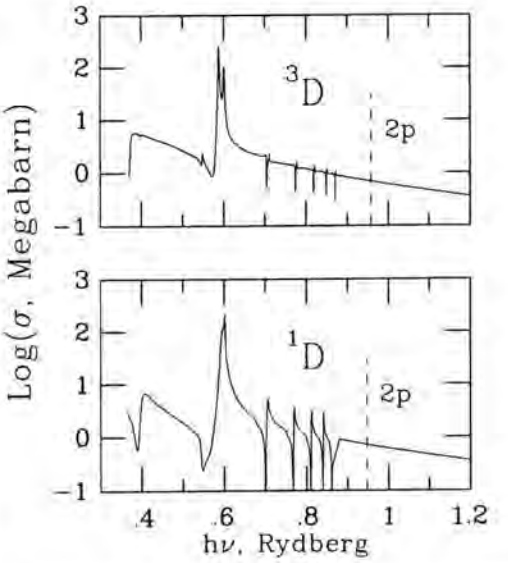

Fig. 2. Calculated photoionisation cross sections for C III *5d* levels. Note the use of logarithmic scales for σ. The features giving large maxima in the cross sections are PEC resonances (see text).

The spectrum lines also make important contributions to the mean opacity. For carbon, at temperatures and densities of interest for the stellar structure problems, our opacities are about two to three times larger than the values available at the time when Simon's paper was written. It seems likely that, when all the elements are included, we will obtain factors similar to those which he postulated.

LEVELS AND LINES

We make calculations for all cosmically abundant elements in all ionisation stages. We calculate levels for all states having an outer electron which is significantly non-hydrogenic and has a principal quantum number $n \leq 10$. Our results for energy levels may be of value for systemmatic studies of trends along iso-electronic sequences and in making identifications.

Following the notation of collision theory, we refer to the ψ_i as *target states*. For $N=1$ the targets included are $1s$, $2s$, $2p$ together with two states to allow for the polarisability of $1s$ (Fernley, Taylor and Seaton, 1987), and for $N=2$ allowance is made for the polarisability of $1s^2$ (Peach, Saraph and Seaton, 1988). For N between 3

and 10 we include all target states with configurations $1s^2 2s^x 2p^y$. For $N > 10$ the calculations become much more difficult. An example of the problems which arise is given at this meeting by H.E. Saraph and P.J. Storey who, as a part of the Opacity Project, have tackled the case of Fe VII with ground configuration $3s^2 3p^6 3d$.

I am sometimes asked whether we make much use of experimental data for the opacity work. The short answer is that we do not have experimental results for some 10^6 f-values or 10^5 photoionisation cross sections. It is, nevertheless, very important to use what experimental data are available to check the accuracy of the calculations. A recent careful compilation of all available data for f-values and lifetimes in C III, N IV and OV has been made by Allard *et al.* (1989), including all available experimental results for lifetimes. Figure 3 compares calculated lifetimes τ for 33 transitions in C III with adopted values from experimental measurements. With the exception of three "rogue" values (for which the experimental results are probably in error) the *r.m.s.* deviation is 12 per cent. Whether that gives a guide to the accuracy of the calculations or of the measurements would be hard to say: in either case the result is not too bad.

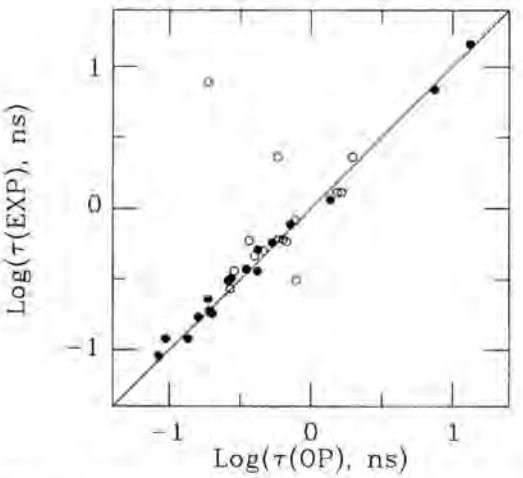

Fig. 3. Lifetimes for transitions in C III. Opacity Project results (OP) from Tully, Seaton and Berrington (1989). Experimental results (EXP) from the compilation of Allard *et al.* (1989). The filled circles are from recent measurements and cases for which several independent determinations have been made. The open circles are cases for which only one older determination is available.

PLASMA PERTURBATIONS

Stellar interiors comprise envelopes and cores. Our opacity calculations are for envelopes, the outer regions for which it is not a bad approximation to assume that atoms exist. They do not, of course, exist for states of indefinitely high excitation. In order to calculate equations of state (giving the level populations $N(i)$) it is necessary to allow for the plasma perturbations which lead to *dissolution* of the high states.

The line profiles, $\phi(\nu)$, are also determined by the perturbations of atoms by the surrounding plasma. Consider, again, the case of a transition such as $2s \rightarrow 2p$ in C IV. The profile is mainly determined by electron impacts,

$$2s + e + h\nu \rightarrow 2p + e$$

The perturbation by the added electron, which broadens the line, is similar to the perturbation which gives the PEC resonances (the only essential difference being that for the resonances the perturbing electron is initially in a bound state). The R- matrix method has been used to calculate line-profile parameters for 42 transitions in positive ions (Seaton, 1988) and the results have been used to obtain a simple approximate formula. For neutral atoms, extensive calculations have been made using semi-classical methods (Griem, 1974) and give results in good agreement with measurements (Konjevic, Dimitrijevic and Wiese, 1984). Again, we fit to a simple empirical formula (Seaton, 1989).

For systems which are hydrogenic, or nearly-hydrogenic, it is necessary to allow for the perturbations by the ion micro-field, which gives Stark shifts. Techniques have been developed for the efficient calculation of profiles in hydrogenic systems, paying particular attention to the line wings.

PUBLICATIONS

The main results from the Opacity Project are being published in two series of papers, one concerned with equations of state and the other with atomic data. More complete tabulations of numerical results will be given in a separate publication of the U.K. Institute of Physics. It is planned that all data will eventually be made available through data banks.

ACKNOWLEDGEMENTS

I thank Drs. N. Allard, M.-C. Artru, T. Lanz and M. Le Dourneuf for permission to quote from their unpublished work.

REFERENCES

Allard, N., M.-C. Artru, T. Lanz and M. Le Dourneuf, 1989. *Private communication.*

Griem, H.R., 1974. Spectral line broadening by plasmas. Academic Press.

Konjević, K., M.S. Dimitrević and W.L. Wiese, 1984. J. Phys. Chem. Ref. Data, **13**, 649.

Simon, N., 1982. Astrophys. J., **260**, L87.

Papers in the series "The equation of state for stellar envelopes", Astrophysical Journal :-

I. Hummer, D.G. and D. Mihalas 1988 - An occupation probability formalism for the truncation of the internal partition function. **331**, 794.

II Mihalas, D, W. Däppen and D.G. Hummer 1988.- Algorithms and selected results. **331**, 815.
III Däppen, W., D.Mihalas, D.G. Hummer and B.Weibel Mihalas, 1988 - Thermodynamic quantities. **332**, 261.
IV Mihalas, D., D.G. Hummer, B.Weibel Mihalas and W. Däppen, 1989 - Thermodynamic quantities and selected ionization fractions for six element mixes. *In press*.

Papers in the series "Atomic data for opacity calculations", J. Phys. B., Atom. Mol. Opt. Phys :-

I Seaton, M.J., 1987 - General description. **20**, 6363.
II Berrington, K.A., P.G. Burke, K. Butler, M.J. Seaton, , P.J. Storey, K.T. Taylor and Yu Yan, 1987 - Computational methods. **20**, 6379
III Yu Yan, K.T. Taylor and M.J. Seaton, 1987 - Oscillator strengths for C II. **20**, 6399
IV Yu Yan and M.J. Seaton, 1987 - Photoionisation cross-sections for C II. **20**, 6409.
V Seaton, M.J., 1987 - Electron impact broadening of some C III lines. **20**, 6431.
VI Thornbury, J.F. and A. Hibbert, 1987 - Static dipole polarisabilities of the ground states of the helium sequence. **20**, 6447.
VII Fernley, J.A., K.T. Taylor and M.J. Seaton, 1987 - Energy levels, f-values and photoionisation cross sections for He-like ions, **20**, 6457.
VIII Seaton, M.J., 1988 - Line profile parameters for 42 transitions in Li-like and Be-like ions. **21**, 3033.
IX Peach, G., H.E. Saraph and M.J. Seaton, 1988 - The lithium iso-electronic sequence. **21**, 3669.
X D. Luo, A.K.Pradhan, H.E. Saraph, P.J. Storey, and Yu Yan, 1989 -Oscillator strengths and photoionisation cross-sections for O III. **22**, 389.
XI Luo, D and A.K. Pradhan, 1989 - The carbon iso-electronic sequence. *Submitted.*
XII Seaton, M.J., 1989 - Line-profile parameters for neutral atoms of He, C, N and O. *Submitted.*
XIII Tully, J.A., M.J. Seaton and K.A. Berrington, 1989 - The beryllium iso-electronic sequence. *To be submitted.*

AUTHOR'S ADDRESS

Department of Physics and Astronomy,
University College London,
Gower St., London WC1E 6BT, England.

K. Butler[1], C. Mendoza[2] and C.J. Zeippen[3]

Radiative data for ions in the Mg isoelectronic sequence

ABSTRACT

A large number of energy levels, f-values and photoionisation cross sections have been calculated for ions of astrophysical interest in the Mg isoelectronic sequence. This work is part of an international collaboration which is aimed at computing stellar envelope opacities (the Opacity Project). Statistical comparisons of quantum defects, f-values and radiative lifetimes are carried out with experiment and with previous theoretical work in order to assess the accuracy of the results. We conclude that the present dataset is as accurate as those calculated using elaborate methods.

METHOD

Bound states with electronic configurations $3lnl'\ ^{1,3}L$ ($l \leq 2$, $l' \leq 4$, $n \leq 10$, $L \leq 4$) were calculated within the close-coupling formalism (Burke and Seaton 1971) for astrophysically abundant ions in the Mg sequence, namely: Mg I, Al II, Si III, S V, Ar VII, Ca IX and Fe XV. Full use was made of the recently developed Opacity Project R-matrix package described by Berrington *et al* (1987). A seven-state approximation ($3s\ ^2S$, $3p\ ^2P^0$, $3d\ ^2D$, $4s\ ^2S$, $4p\ ^2P^0$, $4d\ ^2D$, $4f\ ^2F^0$) was adopted for all target ions except Mg II where the $5s\ ^2S$ state was also included. Target representations were obtained in a similar fashion to Butler *et al* (1984) and Mendoza and Zeippen (1987), but core polarisation effects were neglected throughout. Oscillator strengths and photoionisation cross sections were calculated for all possible optically allowed transitions, and radiative lifetimes could then be easily estimated from the bound-bound data using theoretical wavelengths.

COMPARISON WITH PREVIOUS WORK

Members of the Mg sequence, particularly the neutral and lowly ionised species, have been extensively studied both theoretically and experimentally. Instead of reviewing this work, and considering the volume of data generated in the present calculation, we will attempt to assess the accuracy of the data by carrying out statistical comparisons with experiment and with representative sets of calculations which emphasise both quality and quantity.

Following Yu Yan *et al* (1987) the comparison of two datasets, for instance length/velocity f-values or theoretical/experimental quantum defects, will be carried out in terms of an average percentage difference defined as

$$\Delta = 100 \times \left[\sum_i (a_i - b_i)^2\right]^{1/2} \left[\sum_i a_i \times b_i\right]^{-1/2}$$

where a_i and b_i are corresponding values in the two sets.

Term energies

We have calculated a total of 1247 bound states, and a comparison with experimental quantum defects for 368 observed multiplets gives an average percentage difference of $\Delta = 2.4$ %. Experimental values were taken from Moore (1971), Martin and Zalubas (1979, 1980, 1983), Sugar and Corliss (1979, 1982), Joelsson *et al* (1981), Litzén and Redfors (1987) and Redfors (1988). From this comparison we have excluded 6 states with questionable experimental assignments: $3p4p\ ^1D$ and $3s7d\ ^1D$ of Si III; $3p3d\ ^1P^0$ and $3p3d\ ^1F^0$ of S V; $3s5f\ ^1F^0$ and $3s6f\ ^1F^0$ of Fe XV.

Oscillator strengths

We have computed weighted oscillator strengths, gf-values, for 17041 possible bound-bound transitions. Comparisons of gf-values in the length and velocity formulations for each ion gives $\Delta = 1.8\%$ for Mg I, increasing along the sequence up to $\Delta = 3.1\%$ in Fe XV. This is caused by the effects of series perturbers which become more conspicuous for higher Z.

In Table 1 we compare present absorption oscillator strengths with four other sets of calculations. In set MCHF we have excluded four transitions involving the strongly mixed $3p3d\ ^1P^0$ and $3s6p\ ^1P^0$ states of Si III which show fairly large f-values very different from the present ones. For similar reasons we have not included two transitions in set CIV3 involving the strongly mixed $3p4p\ ^1D$ and $3s5d\ ^1D$ states of S V; the transition $3s3p\ ^3P^0 \rightarrow 3s4s\ ^3S$ in S V is also excluded from this set since we think that the f-value given by Baluja and Hibbert (1985) has been misquoted. The agreement with set MCHF is particularly good; however, the excellent agreement with set MS is not representative of the sequence since only Mg I was considered.

Radiative lifetimes

A comparison of present radiative lifetimes (calculated

Table 1. Comparison of f-value (length formulation) average percentage differences between present results and representative sets of values calculated previously for ions in the Mg sequence. VSL: Model potential method of Victor *et al* (1976). MCHF: Multiconfiguration Hatree-Fock results of Froese Fischer (1975, 1979) and Froese Fischer and Godefroid (1982). CIV3: Configuration interaction calculations by Baluja and Hibbert (1980, 1985), Tayal and Hibbert (1984) and Tayal (1986). MS: L^2 method of Moccia and Spizzo (1988).

Set	No. Trans.	Δ (%)
VSL	615	8.3
MCHF	219	2.2
CIV3	337	4.8
MS	429	1.9

in the length formulation and theoretical wavelengths) with those given for 25 states of Mg I by Moccia and Spizzo (1988) shows an agreement well within 15%. Furthermore, the differences with the lifetimes calculated by Froese Fischer and Godefroid (1982) for 57 singlet states of the ions considered here are not larger than 20%, if one excludes the long-lived $3p^2\ ^1D$ state of Al II and the strongly mixed $3p3d\ ^1P^0$ and $3s6p\ ^1P^0$ states of Si III. The agreement could perhaps be improved if the radiative lifetimes were corrected with observed wavelengths. A comparison with measured lifetimes is not conclusive due to the wide scatter in the experimental results.

COMMENTS

This level of agreement increases our confidence in the accuracy of the present radiative data for this sequence within the context of opacity calculations. Although significant differences can always be found in computed f-values when states mix strongly or for transitions where there is a lot of cancellation, we have shown here that the present data are in general as accurate as those calculated previously for this sequence using detailed methods.

REFERENCES

Baluja K.L and Hibbert A., 1980, *J. Phys. B*, **13**, L327.

Baluja K.L. and Hibbert A., 1985, *Nucl. Instr. Meth.*, **B9**, 477.

Berrington K.A., Burke P.G., Butler K., Seaton M.J., Storey P.J., Taylor K.T. and Yu Yan, 1987, *J. Phys. B*, **20**, 6379.

Burke P.G. and Seaton M.J., 1971, *Meth. Comput. Phys*, **10**, 1.

Butler K., Mendoza C. and Zeippen C.J., 1984, *MNRAS*, **209**, 343.

Froese Fischer C., 1975, *Can. J. Phys.*, **53**, 184; **53**, 338.

Froese Fischer C., 1979, *J.O.S.A.*, **69**, 118.

Froese Fischer C. and Godefroid M., 1982, *Nucl. Instr. Meth.*, **202**, 307.

Joelsson L., Zetterberg P.E. and Magnusson C.E., 1981, *Physica Scripta*, **23**, 1087.

Litzén U. and Redfors A., 1987, *Physica Scripta*, **36**, 895.

Martin W.C. and Zalubas R., 1979, *J. Phys. Chem. Ref. Data*, **8**, 817.

Martin W.C. and Zalubas R., 1980, *J. Phys. Chem. Ref. Data*, **9**, 1.

Martin W.C. and Zalubas R., 1983, *J. Phys. Chem. Ref. Data*, **12**, 323.

Mendoza C. and Zeippen C.J., 1987, *Astron. Astrophys.*, **179**, 339.

Moccia R. and Spizzo P., 1988, *J. Phys. B*, **21**, 1133.

Moore C.E., 1971, *Atomic Energy Levels*, Nat. Stand. Ref. Data Ser., Nat. Bur. Stand (USA), **35/V.I**.

Redfors A., 1988, *Physica Scripta*, **38**, 702.

Sugar J. and Corliss C., 1979, *J. Phys. Chem. Ref. Data*, **8**, 865.

Sugar J. and Corliss C., 1982, *J. Phys. Chem. Ref. Data*, **11**, 135.

Tayal S.S., 1986, *J. Phys. B*, **19**, 3421.

Tayal S.S. and Hibbert A., 1984, *J. Phys. B*, **17**, 3835.

Victor G.A., Stewart R.F. and Laughlin C., 1976, *Ap. J. Suppl. Ser.*, **31**, 237.

Yu Yan, Taylor K.T. and Seaton M.J., 1987, *J. Phys. B*, **20**, 6399.

AUTHORS' ADDRESSES

1. Institut für Astronomie und Astrophysik der Universität München, Scheinerstrasse 1, 8000 München 80, FRG.
2. IBM Venezuela Scientific Center, P.O. Box 64778, Caracas 1060A, Venezuela.
3. UPR 261 du CNRS et DAMAp, Observatoire de Paris, 92190 Meudon, France.

C. Mendoza

Radiative data for $3p^q$ Fe ions

ABSTRACT

A large number of bound states, oscillator strengths and photoionisation cross sections have been calculated for Fe ions with ground configurations $3p^q$, $q = 1 \rightarrow 6$. This has been carried out as part of an international collaboration, known as the Opacity Project, which is concerned with computing improved stellar envelope opacities. Some of the difficulties encountered in calculating radiative data for such ions are discussed, and present results are compared with recent compilations in order to estimate the accuracy of the data.

METHOD

In the close-coupling (CC) approximation the complete wavefunction for a bound or a free state of a system composed of an N-electron ionic target + electron takes the form

$$\Psi = \mathcal{A} \sum_{i=1}^{I} \chi_i \theta_i + \sum_{j=1}^{J} \Phi_j c_j \qquad (1)$$

where $\mathcal{A}$ is an antisymmetrisation operator; χ_i and θ_i are the ith free-channel target and electron wavefunctions respectively; the Φ_j, often referred to as "bound" channels, are square-integrable functions for the entire system, built up from target orbitals and introduced to compensate for orthogonality conditions imposed on the θ_i (Burke and Seaton 1971). Recent developments concerning the calculation of bound states and radiative data from such wavefunctions within the R-matrix formalism (Burke *et al* 1971) are described by Berrington *et al* (1987), and constitute what could be called the Opacity Project R-matrix Package.

The inclusion of all the ionic thresholds in the CC expansion which give rise to bound states for the Fe $3p^q$ ions, plus the target configuration interaction necessary to attain a reasonable degree of accuracy, would lead to huge calculations. Moreover, in many cases the spectroscopic data available for these ions are not sufficient to attempt such computations. Taking these three points into account, we have adopted "modest size" targets which nevertheless lead to involved computational efforts.

Target representations were obtained with the program SUPERSTRUCTURE (Eissner *et al* 1974); each target state was expressed in a configuration interaction expansion involving single and double excitations within the $n = 3$ complex. The following target approximations were employed.

Fe XV: $3s^2\ ^1S$, $3s3p\ ^3P^0$, $^1P^0$, $3p^2\ ^3P$, ^1D, ^1S, $3s3d\ ^3D$, ^1D.

Fe XIV: $3s^23p\ ^2P^0$, $3s3p^2\ ^4P$, ^2D, ^2S, ^2P, $3s^23d\ ^2D$, $3p^3\ ^2D^0$, $^4S^0$, $^2P^0$.

Fe XIII: $3s^23p^2\ ^3P$, ^1D, ^1S, $3s3p^3\ ^5S^0$, $^3D^0$, $^3P^0$, $^1D^0$, $^3S^0$, $^1P^0$.

Fe XII: $3s^23p^3\ ^4S^0$, $^2D^0$, $^2P^0$, $3s3p^4\ ^4P$, ^2D, ^2P, ^2S.

Fe XI: $3s^23p^4\ ^3P$, ^1D, ^1S, $3s3p^5\ ^3P^0$, $^1P^0$.

Fe X: $3s^23p^5\ ^2P^0$, $3s3p^6\ ^2S$.

We have calculated bound states of the $(N + 1)$-electron systems with effective quantum numbers $\nu \leq 10$, active electron orbital angular momenta $l \leq 4$ and for total orbital angular momenta $L \leq 4$. Although bound states belonging to spectroscopic series converging to neglected target thresholds will be missing, many doubly and triply excitated states with $n = 3$ will appear as "bound channel states" arising from the second expansion in equation (1). This presents a problem: the target threshold energies are usually adjusted empirically with observed energies, and therefore bound states arising from the first expansion in equation (1) will reflect these corrections; on the other hand, this is not the case for the bound channel states, and consequently series perturbations, which strongly affect radiative properties, in some situations may be inaccurately represented.

Further inaccuracies can arise by the neglect of relativistic effects which are important for these ions. Under the present framework, whereby radiative data are obtained consistently for a large number of both bound-bound and bound-free transitions, the inclusion of relativistic effects would rapidly lead to intractable computations. Relativistic effects within the context of the opacity work have been discussed by Fernley *et al* (1987) for the case of He-like ions.

Table 1. Number of bound states, number of transitions and average percentage difference between length and velocity gf-values calculated in the present work for $3p^q$ Fe ions.

Ion	No.States	No.Trans	$\Delta(gf_l, gf_v)$
Fe XIV	467	17271	6.7
Fe XIII	817	38286	10
Fe XII	903	58983	17
Fe XI	1156	77187	23
Fe X	765	45369	21
Fe IX	409	13029	26

RESULTS

Following Yu Yan *et al* (1987) we will compare datasets in terms of an average percentage difference defined as

$$\Delta(a,b) = 100 \times \left[\sum_i (a_i - b_i)^2\right]^{1/2} \left[\sum_i a_i \times b_i\right]^{-1/2} \quad (2)$$

where a_i and b_i are corresponding values in two sets.

In Table 1 we give a summary for each ion regarding the number of levels, number of transitions and the average percentage difference between length and velocity gf-values (weighted oscillator strengths) calculated in the present work. It can be seen that the $\Delta(gf_l, gf_v)$ for these ions are much larger than those found for Mg-like ions (< 4%) by Butler *et al* (1989); they grow from from a reasonable ~ 7% for Fe XIV to a high ~ 26% for Fe IX. This is mainly due to transitions involving bound channel states which come in large numbers as one moves towards lower stages of ionisation. Some of these states are found to have large gf-values bearing large differences in the length and velocity results. Large differences are also found for strongly mixed states, particularly when one of them is a bound channel state.

A comparison of present results with 127 experimental multiplets compiled by Corliss and Sugar (1982) for these ions gives a term energy (relative to the ground state of each ion) average percentage difference of $\Delta(E_{NBS}, E_{OP}) = 1.5\%$, and for those states for which a quantum defect can be defined (103) it leads to $\Delta(\mu_{NBS}, \mu_{OP}) = 7.3\%$. It is worth mentioning that due to the complexity of the term structure of these ions, to theoretical shortcomings and the scanty spectroscopic data available, a fair agreement in the quantum defect between theory and experiment does not always imply unambiguous term assignments.

We also compare radiative data for 61 multiplet transitions compiled by Fuhr *et al* (1981). We find the agreement in the transition wavelength to be within 6%, except for the transitions $4s\ ^2S \rightarrow 4p\ ^2P^0$ and $4p\ ^2P^0 \rightarrow 4d\ ^2D$ of Fe XIV where it is ~ 20%. Furthermore, $\Delta(f_{NBS}, f_{OP})$ is found to be ~ 16%.

COMMENTS

We have briefly discussed some of the problems that are found in the calculation of radiative data for Fe $3p^q$ ions. The lack of experimental data, particularly radiative lifetimes, inhibits us from being more precise regarding the accuracy of present datasets. In order to estimate the importance of relativistic effects on multiplet oscillator strengths, we will compare with the extensive work on f-values for Fe ions by Fawcett (1989, and references therein) and Froese Fischer and Liu (1986). Results will be reported elsewhere.

REFERENCES

Berrington K.A., Burke P.G., Butler K., Seaton M.J., Storey P.J., Taylor K.T. and Yu Yan, 1987, *J. Phys. B*, **20**, 6379.

Burke P.G., Hibbert A. and Robb W.D., 1971, *J. Phys. B*, **4**, 153.

Burke P.G. and Seaton M.J., 1971, *Meth. Comput. Phys*, **10**, 1.

Butler K, Mendoza C. and Zeippen C.J., 1989, this volume.

Corliss C. and Sugar J., 1982, *J. Phys. Chem. Ref. Data*, **11**, 135.

Eissner W., Jones M. and Nussbaumer H., 1974, *Comput. Phys. Commun.*, **8**, 270.

Fawcett B.C., 1989, *Atomic Data and Nuclear Data Tables*, **41**, 181.

Fernley J.A., Taylor K.T. and Seaton M.J., 1987, *J. Phys. B*, **20**, 6457.

Froese Fischer C. and Liu B., 1986, *Atomic Data and Nuclear Data Tables*, **34**, 261.

Fuhr J.R., Martin G.A., Wiese W.L. and Younger S.M., 1981, *J. Phys. Chem. Ref. Data*, **10**, 305.

Yu Yan, Taylor K.T. and Seaton M.J., 1987, *J. Phys. B*, **20**, 6399.

AUTHOR'S ADDRESS

IBM Venezuela Scientific Center, P.O. Box 64778, Caracas 1060A, Venezuela.

Hannelore E Saraph and Peter J Storey

Calculation of bound states and oscillator strengths for Fe VII

ABSTRACT

Data for radiative transitions between all bound and free states of elements with significant stellar abundances are required for opacity calculations that are discussed by Seaton in these proceedings. In the iron ions, valence electron states are interspersed with those of excited configurations. The large spread in energy of these core-excited configurations makes theoretical and experimental analysis very difficult. Recent developments of computer codes and exploitation of modern computer power have made this first attempt at a comprehensive study for Fe VII possible. Our results are not definitive, discrepancies with experimental data are still large, but we hope that they will form a sound basis for future work. A full account of this work is in preparation for submission to Journal of Physics B.

THE CALCULATION

The Fe^{7+} target states

Of the seven configurations $3s^23p^63d,4s,4p,4d,4f$, and $3p^53d^2$, $3s3p^63d^2$ all 31 terms are retained to serve as target states. In addition, the $3p^43d^3(^2D)$ states provide correlation with the ground state $3p^63d$. The ionic orbitals 1s to 4f are optimised in a statistical model potential (Nussbaumer and Storey, 1978, 1988).

The Fe^{6+} bound and free states

In the close coupling expansion the wave function for Fe^{6+} is given by

$$\Phi^{SL\pi} = A\Sigma_i\phi_i F_i + \Sigma_j c_j \Phi_j \qquad (1)$$

where A is an antisymmetrisation operator, ϕ and F are vector-coupled functions for target and added electrons, and Φ are wave functions for additional configurations of Fe^{6+} formed from target orbitals only. Free variation of the radial part of F and the configuration mixing coefficients c leads to a set of coupled integro differential equations for each $SL\pi$. For the solution we use the opacity version of the RMATRX code described by Berrington *et al.*, 1987.

Restrictions

SL-coupling is used throughout. The angular momenta of the added electron are restricted to ℓ=0 to 4. The equations are solved for S= 0,1, and 2 and L=0 to 8. All bound states with energies such that the principal quantum number of the lowest channel is less than 11 are obtained and stored; 515 such states are below the first ionisation limit. We calculate oscillator strengths for all dipole allowed transitions between these terms and photoionisation cross sections from 0 to 10 Rydberg from all these bound states.

SPECIAL FEATURES OF Fe VII

Configuration mixing in bound states

Experimental energies are known for only 8 terms of Fe^{7+}, (Corliss and Sugar, 1985) out of the 31 terms included here. For these, our target term energies differ by .20 to .46 Ryd (increasing with energy). In a similar way they differ from results by Fawcett, 1989 who has calculated energies for levels $J=\frac{1}{2}$ to $3\frac{1}{2}$ of configuration $3p^53d^2$ using configuration interaction and Slater parameters to fit to the experimental data. Core-excited configurations $3p^x3d^y$ cover wide bands of the energy, as illustrated in fig. 1. The valence electron states $3dnl$ couple strongly with core-excited states and this affects their quantum defects, (Ekberg, 1981). Our close coupling expansion takes account of these effects, but, as a consequence of the shortcomings of our target energies our calculation for Fe^{6+} does not reproduce the perturbations between the principal series and the excited configurations quite accurately. In particular, terms with open core parent configurations are shifted to higher energies. Table 1 shows the difference between calculated and experimental energies for seven configurations. A table of term energies is available.

Oscillator strengths

Calculated oscillator strengths are very sensitive to the composition of the wave functions. The earlier data as compiled by Fuhr *et al.*, 1988 did not include configuration mixing between core-excited states and valence electron states that we include. But they do include spin-orbit coupling effects that we neglect. Fuhr *et al.* assign accuracy D^- to

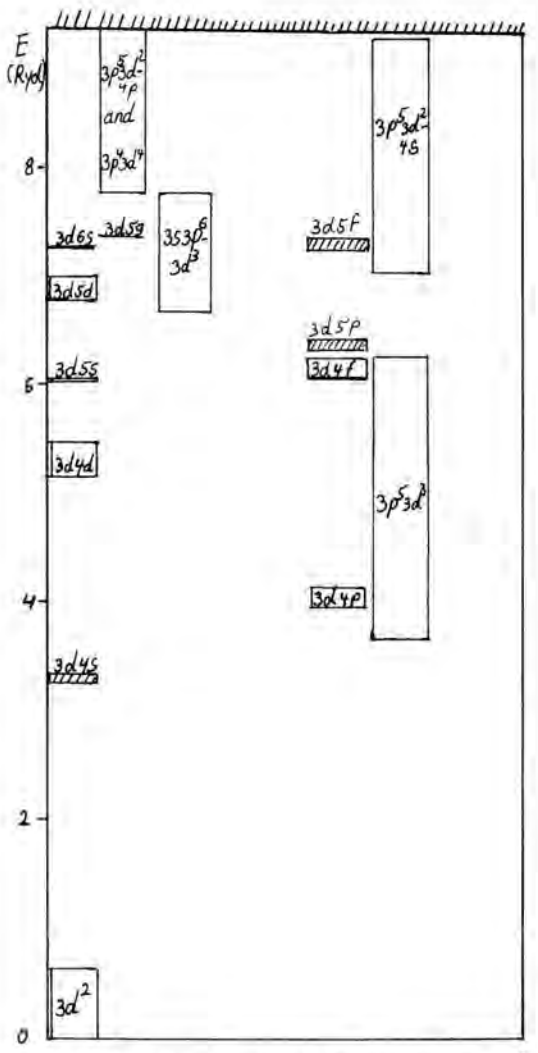

Fig. 1. Energy ranges spanned by config. of Fe^{6+}.

Table 1. Differences (in Ryd) between calculated and experimental ionisation energies.

configuration	error range	exceptions
$3p^6 3d^2$	-0.10 to -0.11	^1S: -0.05
$3p^6 3d4s$	0.04	
$3p^6 3d4p$	0.00 to 0.01	
$3p^6 3d4f$	0.01 to 0.03	
$3p^6 3d5f$	0.00 to 0.01	$^3H^o$:-0.01
$3p^5 3d^3$	0.10 to 0.32	$(^4F)^3D^o$:.39
		$(^4P)^3S^o$:.48
$3p^5 3d^2 4s$	0.23 to 0.30	

the old data. Comparison with the present results illustrates both, the 'sharing' of oscillator strengths between configuration-mixed terms, and the deviations from LS coupling see table 2. Algebraic transformations are used to transform our LS-coupling results to intermediate coupling for the comparison.

No experimental data exist for transitions between quintets. These occur at λλ 170...350Å between terms of core excited configurations, and all have f-values smaller than 0.1.

Table 2. Fe VII: Comparison of our oscillator strengths with data from Fuhr *et al.*, (NBS). λ are the multiplet wavelengths in Å.

c	c'	T	T'	J	J'	λ_{NBS}	λ_{OP}	f_{NBS}	f_{OP}
$3d^2$	$3p^5 3d^3(^2H)$	^1G	$^1G^o$	4	4	173	166	1.6	.80
	$3p^6 3d4f$		$^1G^o$	4	4	159	155	.09	.56
	$3p^5 3d^3(^4F)$	^3F	$^3F^o$	4	4	177	179	1.2	.68
				3	3			1.1	.61
				2	2			.69	.64
	$3p^6 3d4f$		$^3F^o$	4	4	152	150	.08	.45
				3	3			.13	.40
				2	2			.18	.42
	$3p^6 3d4p$		$^3F^o$			232	248	.06	.07
	$3p^5 3d^3(^4F)$	^3F	$^3D^o$	4	3	166	152	.95	.89
				3	2			.85	.79
	$3p^6 3d4f$		$^3D^o$	4	3	150	147	.02	.00
	$3p^6 3d4p$		$^3D^o$			234	249	.09	.12

REFERENCES

Berrington KA, Burke PG, Butler K, Seaton MJ, Storey PJ, Taylor KT, and Yu Yan 1987 J Phys B 20 Atom Mol Opt Phys 6379

Corliss C and Sugar J 1985 *Atomic data for controlled fusion research* Vol IV (edit. W L Wiese, ORNL-6089/V4)

Ekberg JO 1981 Physica Scripta 23 7

Fawcett BC 1989 private comm and At Nucl Data Tables, 1989 *in press*

Fuhr JR, Martin GA and Wiese WL 1988 *Atomic transition probabilities iron through nickel* J Phys Chem Ref Data 17 Suppl 4, 169

Nussbaumer H and Storey PJ 1978 Astron Astrophys 64 139

Nussbaumer H and Storey PJ 1988 ibid. 193 327

Seaton MJ 1989 *these proceedings*.

AUTHORS' ADDRESS

Department of Physics and Astronomy,
University College London, London WC1E 6BT UK

Gediminas Žukauskas

An alternative method of investigation of radiative lifetimes in atoms and ions

ABSTRACT

A method for theoretical investigation of radiative lifetimes, which does not require knowledge of the transition probabilities between the level under investigation and all the possible lower lying levels is proposed. The method is based on the analytical summation of the transition probabilities with the use of the averaged transition energy (method A), or with the correct transition energy (method B). The numerical results obtained are compared with the experimental and other theoretical data.

DESCRIPTION

The radiative lifetime τ of the level LSJ of the excited configuration, π, under investigation is given by the expression

$$\tau_{\pi LSJ}=(A_{\pi LSJ})^{-1} = \Big| \sum_{\pi'L'S'J'} A_{\pi LSJ\to\pi'L'S'J'} \Big|^{-1}. \quad (1)$$

In practice the total transition probability is influenced only by electric dipole (E1) transitions (the numerical values of the higher multipole transition probabilities are much smaller). The direct application of (1) requires knowing the energy of lower levels, and the numerical summation of all possible transition probabilities.

METHOD A

When the configuration under investigation is highly excited one can substitute for the correct transition energy $\Delta E_{\pi LSJ\to\pi'L'S'J'}$ the average energy $\Delta\overline{E_{\pi\to\pi'}}$ as was suggested by Rajnak and Wybourne (1963) in their study of correlation effects in the term structure of configurations. In the present case use of the same approximation simplifies the expression for the total transition probability and leads to the following definition of the matrix element of the effective transition operator:

$$A_{\pi LSJ\to\pi'L'S'J'} = \overline{(\Delta E_{\pi\to\pi'})^3}(\pi LSJ|T_{eff}|\pi LSJ) =$$

$$\overline{(\Delta E_{\pi\to\pi'})^3}(\pi LSJ|Q_tQ_t|\pi LSJ) =$$

$$\overline{(\Delta E_{\pi\to\pi'})}\ (\pi LSJ|Q_vQ_v|\pi LSJ). \quad (2)$$

An explicit expression for the radiative lifetime of the configuration under investigation $\pi\equiv(n_1l_1)^{N_1}(n_2l_2)^{N_2}$ was obtained by the use of the technique of electron creation and annihilation operators (Judd, 1967) and has the following form (units ns) (Bogdanovich et al. 1985, 1986):

$$\tau_{\pi LS} = \{21.42\ [\overline{(\Delta E_{\pi\to\pi'})^3}(\ g_2((l_1)^{N_1}(l_2)^{N_2}\ LS) +$$

$$N_2(2l_2+1)^{-1}(l_2\|C^{(k)}\|l_1)^2)\langle n_1l_1|r|n_2l_2\rangle^2 +$$

$$\Sigma\overline{(\Delta E_{\pi\to\pi''})^3}\ N_2(2l_2+1)^{-1}(l_2\|C^{(k)}\|l_3)^2 *$$
$$\pi''$$

$$\langle n_2l_2|r|n_3l_3\rangle^2]\}^{-1}\ , \quad (3)$$

where $\pi'\equiv(n_1l_1)^{N_1+1}(n_2l_2)^{N_2-1}$ and $\pi''\equiv(n_1l_1)^{N_1}(n_2l_2)^{N_2-1}\ n_3l_3$. This expression can easily be written in the velocity form by replacing the radial integral and the power of the transition energy $\overline{\Delta E^3}\to\overline{\Delta E}$.

METHOD B

In the general case of two open shells the summation can be performed without any approximation for the transition energy, but the corresponding expressions are much more complicated and contain the matrix elements of 2-,3-, and 4-body effective operators, if the transition operator in the velocity form is used ($H_{eff}=Q_vQ_v$). Particular expressions for the radiative lifetimes of the configuration $(n_1l_1)^{N_1}\ n_2l_2$ (the transitions to the lower configuration $(n_1l_1)^{N_1}\ n_3l_3$ are included) have been published by Bogdanovich et al. (1988). The corresponding expression for the case of the configuration $(n_1l_1)^{N_1+1}$ being the lower one has been obtained by the author and will be published elsewhere.

RESULTS

From the comparison of the numerical results (table I) we conclude that the method proposed allows one to obtain radiative lifetimes which are in good agreement with experiment and with other theoretical data.

The formulas for the radiative lifetimes expressed in terms of the few-body effective operators allow us to apply a least-squares fitting procedure to the radiative lifetime calculations.

Table I. Comparison of the lifetimes (ns) obtained by various methods.

Ar II $3p^4(^3P)4d\ ^4P_{5/2}$

This work		Meth.(A)	ref. 1	ref. 2
Q_L	Q_V		exp.	exp.
3.7	4.1		3.9±0.4	4.4

Kr II $4p^4(^3P)5p\ ^4D_{5/2}$

This work(A)		ref.3	ref.4	ref.2	ref.5	ref.6
Q_L	Q_V	exp.	exp.	exp.	theo.	exp.
9.89	11.19	11.2 ±0.80	10.18 ±0.40	7.6	9.6	9.55 ±0.31

Ne II $2p^4(^3P)3p\ ^4P_{5/2}$, $^4D_{7/2}$

This work(B)		ref. 2	ref. 5	ref. 7
Q_L	Q_V	exp.	theo.	exp.
7.20	6.62	7.4	6.95	6.3
5.64	6.12	5.2	5.05	5.5

References

1: Blagoev 1983
2: Fink et al. 1970
3: Blagoev 1981
4: Donnelly et al. 1975
5: Koozekanani and Trusty 1969
6: Ward et al. 1985
7: Luyken 1971

REFERENCES

Bogdanovich, P.O., G. Žukauskas, A. Momkauskaitė and V. Tutlys, 1985, Liet. Fiz. Rink. (Soviet Phys. Coll.) 6, 43-53.

Bogdanovich, P.O., G. Žukauskas, A. Momkauskaitė and V. Tutlys, 1986, Izvestija Akad. Nauk SSSR, Phys. Series, 50, no. 7, 1298-1302.

Bogdanovich, P.O., G. Žukauskas and A. Momkauskaitė, 1988, Optika i Spektrosk., 64, no. 4, 715-720.

Blagoev, K.B., 1981, J. Phys. B, 14, 5743.

Blagoev, K.B., 1983, J. Phys. B, 16, 33.

Donnelly, K.E., P.J. Kindlmann and W.R. Bennett, 1975, JOSA, 65, 1359.

Fink, U., S. Bashkin and W.S. Bickel, 1970, JOSA, 10, 1241.

Judd, B.R., 1967, Second Quantization and Atomic Spectroscopy (The Johns Hopkins Press, Baltimore).

Koozekanani, S.H. and G.L. Trusty, 1969, JOSA, 59, 1281.

Luyken, B.F., 1971, Physica, 51, 445.

Rajnak, K. and G.B. Wybourne, 1963, Phys. Rev., 132, 280-290.

Ward, L., A. Wännström, A. Arnesen, R. Hallin and O. Vogel, 1985, Phys. Scripta, 31, 149-158.

AUTHOR'S ADDRESS

Institute of Physics of the Academy of Sciences of the Lithuanian SSR, K. Požėlos 54, Vilnius, 232600, Lithuanian SSR, USSR.

M.-J.E. Vilkas, G.A. Gaigalas, G.V. Merkelis, and Z.B. Rudzikas

Application of many-body perturbation theory to the investigation of energy spectra of atoms and ions with open shells

ABSTRACT

Un till now accurate calculations of energy spectra of many-electron atoms have usually been carried out using the superposition-of-configurations method or the multi-configurational Hartree-Fock approach. Perturbation theory (PT) has been applied to relatively simple systems with few electrons outside closed shells. This is explained by the absence of a well developed PT in the case of quasi-degenerate states as well as by considerable computational difficulties. In this paper, an efficient PT is described, which is suitable for atoms with several open shells. The carbon isoelectronic sequence is considered as an example of the application of the method.

DESCRIPTION

Merkelis et al. (1986) proposed the original graphical method for constructing a stationary PT series, when its spin-angular part is expressed in terms of irreducible tensorial products of electron creation and annihilation operators (a^+ and a).

The diagrams employed represent (Fig. 1) sums of Feynman diagrams (F.d.) over one-electron magnetic quantum numbers.

Using this method, expressions for H_{eff} in second order of PT have been obtained for the case of an extended model space (Lindgren and Morrison, 1982). The computer programmes to generate radial and spin-angular parts of matrix elements of H_{eff} have been worked out for two open shells $(n_1l_1)^{N_1}(n_2l_2)^{N_2}$.

Fig. 1

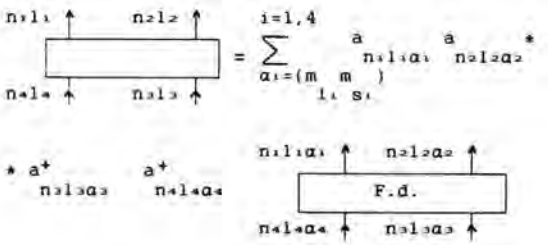

RESULTS

Energy spectra in the carbon isoelectronic sequence were calculated to illustrate the application of the method and the use of the developed programmes. The energy levels of the configurations $1s^22s^22p^2$, $1s^22p^4$ and $1s^22s2p^3$ were calculated. The united basis of one-electron functions, found in the Hermitian potential, proposed by Morrison (1972), was used. The first order relativistic corrections were taken into account in the Breit-Pauli approximation. The energy levels of the configurations considered were calculated in an extended model space. The calculations were carried out for C I, O III, Ne V, P X, Ca XV and Fe XXI. Table I contains the energy values for P X (second column: this work; third: multi-configurational Hartree-Fock calculations due to Froese Fischer and Saha (1985); fourth: multiconfigurational Dirac-Fock calculations due to Cheng, Kim and Desclaux (1979); fifth: experiment of Kasyanov, Kononov, Korobkin, Koshelev and Serov (1973) and the sixth column: Hartree-Fock calculations using the potential proposed by Morrison (1972)). σ_M denotes the root-mean-square deviation.

Table 1. The energy levels (in cm^{-1}) of the configurations $1s^22s^22p^2$, $1s^22s2p^3$ and $1s^22p^4$ in P X.

	this work	theo.[a]	theo.[b]	exp.[c]	HF[d]
$1s^22s^22p^2$					
$^3P_0$	0	0	0	0	0
$^3P_1$	3588	3679	3685	3681	3598
$^3P_2$	9170	9044	9024	9033	9187
$^1D_2$	59336	61397	62393	59679	62310
$^1S_0$	119670	120399	116287	119963	116322
σ_M	215	770	2046		2010
$1s^22s2p^3$					
$^5S_2$	167896	166526	154918	167730	153285
$^3D_2$	321786	326886	325592	323195	324561
$^3D_1$	321859	327099	325762	323405	324646
$^1D_3$	322273	326930	325605	323222	325055
$^3P_0$	378772	383719	381358	379932	380874
$^3P_1$	378934	383697	381474	379907	381052
$^3P_2$	379258	383915	381691	380139	381378
$^1D_2$	483808	492937	499680	484741	502163
$^3S_1$	490401	498368	502137	490584	506970
$^1P_1$	540767	550518	555441	541968	558447
σ_M	1035	5351	8522		10309
$1s^22p^4$					
$^3P_2$	739889		754251	742605	754932
$^3P_1$	746184		760585	749020	761151
$^3P_0$	748665		762938	751420	763667
$^1D_2$	789179		812516	793057	813909
$^1S_0$	898734		922664	902341	927807
σ_M	3196		15451		17507

[a] Froese Fischer and Saha (1985)
[b] Cheng et al. (1979)
[c] Kasyanov et al. (1973)
[d] HF with Morrison potential

The analysis of the calculations shows that our approach leads to the most accurate results for the ions Ne V, P X, and Ca XV. For C I and O III it is necessary to take higher orders in the Coulomb interaction into account, whereas for Fe XXI one has to account for the correlation corresponding to relativistic operators. Let us notice that correlation effects considerably lowers the upper levels of the ground and excited configurations.

REFERENCES

Cheng, K.T., Y.-K. Kim and J.P. Desclaux, 1979, At. Dat. Nucl. Dat. Tables, 24, 111.

Froese-Fischer, C. and H.P. Saha, 1985, Phys. Scripta, 32, 181.

Kasyanov, Yu.S., E.Ya. Kononov, V.V. Korobkin, K.N. Koshelev and R.V. Serov, 1973, Optics and Spectrosc., 35, 586.

Lindgren, I. and J. Morrison, 1982, Atomic Many-Body Theory (Springer series in Chemical Physics, Vol. 13, Springer, Berlin).

Merkelis, G.V., G.A. Gaigalas, J.M. Kaniauskas and Z.B. Rudzikas, 1986, Izvest. Acad. Nauk SSSR, Phys. Series 50, 1403.

Morrison, J.C., 1972, Phys. Rev. A, 6, 643.

AUTHOR'S ADDRESS

Institute of Physics of the Academy of Sciences of the Lithuanian SSR, K. Požėlos 54, Vilnius, 232600, USSR.

Lorenzo J. Curtis

Semiempirical formulations of line strengths using singlet-triplet mixing angles

ABSTRACT

Results are presented in which singlet-triplet mixing angles for two valence electron (or hole) isoelectronic sequences are determined from energy level data. These are utilised together with transition moments obtained from other sequences and from LS coupling and hydrogenic formulae to specify E1 and M1 oscillator strengths.

INTRODUCTION

For systems with two out-of-shell electrons, singlet-triplet and L-state mixing within a given configuration manifests itself in the energy splittings, line strengths, and g-factors of the constituent levels. In intermediate coupling, the wave functions of levels with common J are an admixture of LS basis states not subject to the ΔL and ΔS selection rules that restrict the constituent amplitudes. In *ab initio* calculations this is implicitly included in the wave function. It is also possible to empirically determine the mixing amplitudes explicitly from energy level data, to combine these with transition moments obtained by semiempirical methods, and thereby to specify line strengths (and g-factors) for two-electron systems.

MIXING ANGLES

The nsn'ℓ, nsn'p^5, np^2 and np^4 configurations are particularly apt examples, since they contain no more than two levels of the same J, so that intermediate coupling connects the LS basis states only pairwise. Specification is given by two-by-two off-diagonal matrices **M** and diagonalisation is achieved by a basis transformation $\mathbf{T}^{-1}\mathbf{M}\,\mathbf{T}$, where

$$\mathbf{T} = \begin{pmatrix} \cos\vartheta_J & \sin\vartheta_J \\ -\sin\vartheta_J & \cos\vartheta_J \end{pmatrix}$$

Here ϑ_J is the mixing angle, given by

$$\sin\vartheta_J = \left[1 + \left(W_J \pm \sqrt{1 + W_J^2} \right)^2 \right]^{-1/2} .$$

Using Slater energy relationships which relate the levels within a configuration, the quantity W_J can be specified in terms of their J centroid energies ε_J.

For the nsn'ℓ configuration, the $J=\ell$ levels are mixed and W_J is given by

$$W_\ell = - \frac{\ell\varepsilon_{\ell+1} - (2\ell+1)\varepsilon_\ell + (\ell+1)\varepsilon_{\ell-1}}{\sqrt{\ell(\ell+1)}\,(\varepsilon_{\ell+1} - \varepsilon_{\ell-1})}$$

For ℓ=1 this describes both the nsn'p and the nsn'p^5 configurations, and the mixing is between the $^3P_1$ and $^1P_1$ levels.

For the np^2 and np^4 configurations there are two mixing angles. For J=0, the mixing between the $^3P_0$ and $^1S_0$ is given by

$$W_0 = - \frac{10\,\varepsilon_2 - 21\,\varepsilon_1 + 11\,\varepsilon_0}{4\sqrt{2}\,(5\,\varepsilon_2 - 3\,\varepsilon_1 - 2\,\varepsilon_0)}$$

whereas for J=2, the mixing between the $^3P_2$ and ^1D is given by

$$W_2 = - \frac{5\,\varepsilon_2 + 3\,\varepsilon_1 - 8\,\varepsilon_0}{2\sqrt{2}\,(5\,\varepsilon_2 - 3\,\varepsilon_1 - 2\,\varepsilon_0)}$$

LINE STRENGTHS

In terms of these mixing angles, the line strengths for the resonance and intercombination lines in an ns^2-nsn'p or an np^5-nsn'p^5 transition is

$$S_{E1}(^1S_0, {}^1P_1') = k\cos^2\vartheta_1 \left|\langle ns|r|n'p\rangle\right|^2$$

$$S_{E1}(^1S_0, {}^3P_1') = k\sin^2\vartheta_1 \left|\langle ns|r|n'p\rangle\right|^2$$

where the factor k accounts for the number of equivalent electrons (k=2 for ns^2-nsn'p; k=6 for n'p^6-nsn'p^5).

Fig.1 presents an application to the $3s^2$-

Figure 1

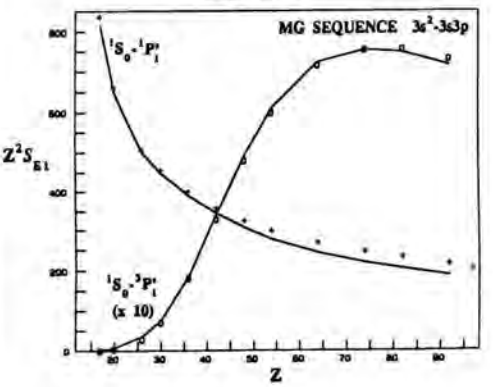

3s3p transition in the Mg sequence, using the transition moments obtained from the Na sequence (Kim & Cheng, 1978), adjusted by an overall factor 1.25. In all figures to follow, solid lines trace semiempirical values and symbols denote *ab initio* calculations (Cheng & Johnson, 1977).

Fig. 2 presents a similar example for the $2p^6$-$2p^5 3s$ transition in the Ne sequence (Ivanova & Glushkov, 1986), using a fully screened hydrogenlike transition moment, adjusted by an overall factor 0.73. (*Ab initio* values, Biémont & Hansen, 1987.)

Figure 2

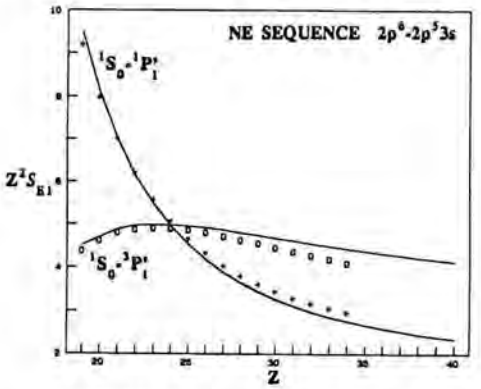

The M1 line strengths within an nsn'p configurations are given by (Curtis,1989)

$$S_{M1}(^3P'_1, {}^3P_0) = 2\cos^2\theta_1$$
$$S_{M1}(^3P_2, {}^3P'_1) = (5/2)\cos^2\theta_1$$
$$S_{M1}(^1P'_1, {}^3P_0) = 2\sin^2\theta_1$$
$$S_{M1}(^1P'_1, {}^3P'_1) = (3/2)\cos^2\theta_1 \sin^2\theta_1$$
$$S_{M1}(^1P'_1, {}^3P_2) = (5/2)\sin^2\theta_1$$

and for the np^2 and np^4 configurations by

$$S_{M1}(^3P_1, {}^3P'_0) = 2\cos^2\theta_0$$
$$S_{M1}(^3P'_2, {}^3P_1) = (5/2)\cos^2\theta_2$$
$$S_{M1}(^1D'_2, {}^3P_1) = (5/2)\sin^2\theta_2$$
$$S_{M1}(^1D'_2, {}^3P_2) = (135/2)\cos^2\theta_2 \sin^2\theta_2$$
$$S_{M1}(^1S'_0, {}^3P_1) = 2\sin^2\theta_0$$

Fig. 3 displays applications of these formulae to the Si sequence (Huang,1985).

Figure 3

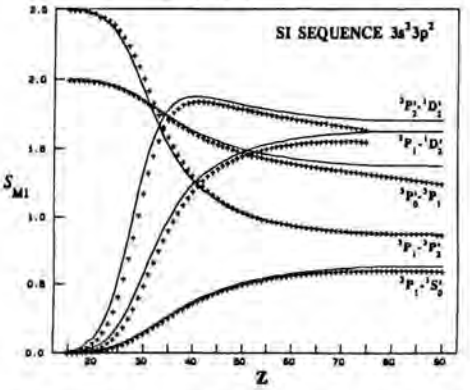

This semiempirical exposition provides a useful means for comparison of theoretical and experimental results, and characterises and separates intermediate coupling effects.

ACKNOWLEDGEMENT

The work was supported by the US Dept.of Energy, Office of Basic Energy Sciences, Division of Chemical Sciences, under Grant number DE-FG05-88ER13958.

REFERENCES

Biémont,E.& Hansen,J.E., 1987 At.Data Nucl. Data Tables **37**, 1-15.

Cheng,K.T.& Johnson,W.R. 1977 Phys.Rev.A**16**, 263-272.

Cheng,K.T *et al*, 1979 At.Data Nucl.Data Tables.**24**, 111-189

Curtis,L.J., 1989 J.Phys.B**22**, L267-271.

Huang,K.N. 1985 At.Data Nucl.Data Tables **32**, 503-566.

Ivanova,E.P.& Glushkov,A.V. 1986 JQSRT **36**, 127-145.

Kim,Y.K.& Cheng,K.T. 1978 JOSA **68**, 836-842.

AUTHOR'S ADDRESS: Dept.Physics and Astronomy, Univ.of Toledo, Toledo Ohio 43606 USA

K. Aashamar+, T.M. Luke, and J.D. Talman

Oscillator strengths for sextet transitions in Cr II

Oscillator strengths for transitions among low-lying sextet terms of singly ionized Chromium have been calculated using two different methods: the Multi-configuration Optimized Potential Model (MCOPM) and an R-matrix model based on target MCOPM wave functions. Estimates of numerical cancellation effects in the MCOPM calculation as well as direct comparison of the sets of independently calculated results, indicate an accuracy of 10% or better in the oscillator strengths reported. Exceptions, where relativistic effects not included in this work may be important, are noted. Comparison with available observations is given.

The transition or iron series elements are important in both terrestrial and astrophysical plasmas. However, even a nonrelativistic treatment of these elements is likely to encounter computational difficulties resulting in part from the occurrence of near degeneracies among terms of the same L and S coming from different configurations. A feature of the Cr II sextet system is that the low-lying terms are relatively widely spaced so we do not generally encounter such problems. Consequently, despite the substantial storage and speed demands caused by the importance of correlation effects, rather reliable calculations on present computers can be performed.

The Cr II sextet transitions considered in the present work are the following: $3d^4 4s$ - $3d^4 4p$, $3d^4 4d$ - $3d^4 4p$, $3d^4 5s$ - $3d^4 4p$, plus the one from the $3d^4 4p$ $^6P^o$ to the $3d^5$ ^6S ground state. There are - to our knowledge - no other reliable calculations for the sextets, and there are few experimental data as well.

We have performed the calculations in two completely independent ways and present the results of both. A brief description of the two methods is given in the next paragraphs. Following that, we present comparison and discussion of the different sets of results.

The MCOPM approach proceeds basically in two stages (Aashamar et al, 1981). In the first, with only a moderate set of configurations, we perform a variational calculation in which a weighted energy average over selected spectroscopic terms is minimized with respect to variations in the potentials in which the orbitals are calculated. This gives a set of "best potentials" to be used in the second stage to calculate orbitals for a CI calculation involving an enlarged set of 41 configurations. This set includes configurations of the form $3d^5$, $3d^4nl$, $3d^3nln'l'$ ($n, n' \leq 7$; $l,l' \leq 4$).

In applications of the R-matrix method to bound state problems (Seaton, 1985, Berrington et al, 1988) low-lying states of the atom or ion considered are treated as bound states in the collision of an electron with the corresponding ionized system. Wave functions for the Cr II states are thus taken to be properly symmetry-projected close coupling expansions over terms built from bound states of the N-1 electron core coupled to different "free channel" states of an electron bound to said core. Since the "free channel" functions are orthogonal to the orbitals used to construct the core, a sum over "bound channel" N electron functions is added for completeness. The expansion coefficients of the latter and the "free channel" wave functions are fully optimized for each state, being determined by the coupled integro-differential equations arising from the energy variational principle. Results are presented for two different sets of orbitals for the target ion core. The first set is a subset of the orbitals obtained in the MCOPM calculation for Cr II. The other set was obtained in a 6-configuration MCOPM calculation on Cr III using 50% weight on the ground state and 50% equally distributed on the 18 excited states. These sets are similar except for the 3d and 4d orbitals which are more compact in the Cr II optimization for reasons involving their dual spectroscopic/correlation roles. In the present R-matrix calculation we include free channels with s, p, and d waves associated with $3d^4$, $3d^3 4s$, 4p, 4d, and 5s target states, as well as bound channels needed for completeness.

Table 1 gives the three sets of oscillator strengths obtained for the transitions of present interest. They have been corrected for wavelengths differing from observation, the corrections being less than 10% in all cases. The three sets, being obtained using different combinations of methods and potentials, are seen to be very consistent, and the gf_l-gf_v differences are generally reasonable. The gf_l values are the more reliable. Estimates of cancellation effects in the MCOPM calculation suggest errors in the gf_v values of roughly twice the errors in the gf_l values from this source alone. The quite different MCOPM and R-matrix calculations give gf_l values with a spread of less than 10% except for the single transition involving the ground state.

There are few experimental results available, and we report these too in Table 1, as listed by Sugar and Corliss (1985) from the work of Musielok and Wujec (1979). The three values quoted have likely uncertainties of 50%, and do not serve to distinguish among the present calculations with a view to preferred method.

The 4p $^6D^o$, 4d ^6D, and 4d ^6F terms lie very close

in energy to certain other terms of different L and S. Admixtures of these through relativistic effects may alter corresponding oscillator strengths significantly. We have not attempted to estimate this mixing in the present work.

Table 1. Oscillator strengths for sextet transitions in Cr II in MCOPM and R-matrix calculations. (See text for descriptions.) Observed oscillator strengths are obtained from the observations of Musielok and Wujec (1979) assuming L-S coupling.

	MCOPM		R-matrix			
			Cr II		Cr III	
Transition (gf_{obs})	gf_l	gf_v	gf_l	gf_v	gf_l	gf_v
4d ^{6}G-4p ^{6}F^o	31.9	28.2	33.4	-	33.0	31.1
4d ^{6}F-4p ^{6}F^o	7.52	7.51	8.21	6.53	8.01	-
4d ^{6}F-4p ^{6}D^o	16.4	14.9	17.1	15.1	16.7	15.5
4s ^{6}D-4p ^{6}F^o (10.4)	13.2	9.94	14.5	-	14.6	12.4
5s ^{6}D-4p ^{6}F^o	6.76	6.05	6.64	6.03	6.33	6.24
4d ^{6}D-4p ^{6}F^o	1.11	1.21	1.00	0.97	1.01	-
4s ^{6}D-4p ^{6}D^o (4.8-5.5)	9.04	8.58	10.0	8.04	9.89	7.47
5s ^{6}D-4p ^{6}D^o	4.60	4.30	4.58	-	4.33	4.26
4d ^{6}D-4p ^{6}D^o	10.5	10.3	11.2	9.08	10.9	9.28
4s ^{6}D-4p ^{6}P^o (6.4)	6.00	6.35	6.61	4.84	6.62	4.55
5s ^{6}D-4p ^{6}P^o	3.26	3.23	3.21	-	3.07	3.00
4d ^{6}D-4p ^{6}P^o	5.42	5.20	5.77	5.17	5.63	5.26
4d ^{6}P-4p ^{6}D^o	2.83	2.94	2.81	2.44	2.76	2.50
4d ^{6}P-4p ^{6}P^o	8.18	8.15	8.50	7.53	8.50	7.71
3d^5 ^{6}S-4p ^{6}P^o	1.84	1.38	1.98	1.84	2.24	1.35
4d ^{6}S-4p ^{6}P^o	2.65	2.51	2.79	2.22	2.64	-

ACKNOWLEDGEMENTS

This work was carried out with the support of the Norwegian Research Council for Science and the Humanities and the Natural Sciences and Engineering Research Council of Canada.

REFERENCES

Aashamar, K., Luke, T.M. and Talman, J.D. (1981) J. Phys. B: At. Mol. Phys. 14, 803-810 (and references therein).

Berrington, K.A., Burke, P.G., Butler, K., Seaton, M.J., Storey, P.J., Taylor, K.T. and Yu Yan (1988) J. Phys. B: At. Mol. Opt. Phys. 20, 6379-6397.

Musielok, J. and Wujec, T. (1979) Astron. Astrophys. Suppl. 38, 119-129.

Seaton, M.J. (1985) J. Phys. B: At. Mol. Phys. 18, 2111-2131.

Sugar, J. and Corliss, C. (1985) J. Phys. Chem. Ref. Data 14, Suppl. No. 2.

AUTHORS' ADDRESSES

†Institute of Physics, University of Oslo, P.O.Box 1048 Blindern, 0316 Oslo 3, Norway;
Department of Applied Mathematics, University of Western Ontario, London, Ontario, Canada.

Emile Biémont and Pascal Quinet

Oscillator strengths for the gallium-like ions Br V – In XIX

ABSTRACT

Electric dipole oscillator strengths have been calculated for the $n = 4, \Delta n = 0$ transitions of the ions Br V to In XIX along the gallium isoelectronic sequence. Results are reported here for the $4s^24p$-$4s^24d$ and $4s^24p - 4s4p^2$ transitions. The Relativistic Hartree-Fock approach of Cowan (1981) combined with a least-square-fitting procedure of the hamiltonian eigenvalues to the observed energy levels has been used for the calculations. Analytical expressions have also been applied for interpolation or extrapolation of the Slater parameter values.

INTRODUCTION

The transition probabilities for strongly or moderately ionized gallium-like ions (Z>35) are very sparse. The only results available for the E1 transitions have been published by Aashamar et al. (1983). Some radiative lifetime values obtained by BFS have been reported for Br V by Pinnington et al.(1977) and for Kr VI by Irwin et al.(1976), by Livingston(1976) and by Pinnington(1976).

In view of this lack of transition probabilities, we report here the first extensive set of f values for the ions Br V to In XIX.

RESULTS

All the odd configurations (except $4p4f^2$ and $4f^3$) and all the even configurations (except $4d4f^2$) in the $n = 4$ complex have been considered in the calculations i.e. $4s^24p + 4s^24f + 4s4p4d + 4s4d4f + 4p^3 + 4p^24f + 4p4d^2 + 4d^24f$ and $4s^24d + 4s4p^2 + 4s4p4f + 4s4d^2 + 4s4f^2 + 4p^24d + 4p4d4f + 4d^3$.

The experimental energy levels used for the fitting procedure were due to Budhiraja and Joshi (1971) for Br V, Druetta and Buchet (1976) for Kr VI, Litzén and Reader (1989) for the ions Rb VII to Mo XII, Reader et al. (1986) for the ions Ru XIV to In XIX and Denne et al.(1985) for Ag XVIII.

Moreover, in order to interpolate or extrapolate the parameter values of E_{AV}, F^k, G^k, α and ζ along the sequence, we have used q-expansions of the type:

$E_{AV} = A + Bq + Cq^2 + Dq^3 + E/q$,

$F^k, G^k, \alpha = A + Bq + C/(q+1)$ and

$\zeta = \zeta_0 + \zeta_1 q + \zeta_2 q^2 + \zeta_3 q^3 + \zeta_4 q^4$, where

$q = Z - N + 1$ and where A,B,C,D,E and ζ_i were determined by least-square optimization of the parameter values for the 6 elements Rb to Mo.

The final oscillator strengths obtained with the fitted parameters for the $4s^24p - 4s^24d$ and $4s^24p - 4s4p^2$ transitions are presented in Table 1. They agree well (within a few percent) with the results of Aashamar et al. (1983) except for the $4s^24p\ ^2P^o - 4s4p^2\ ^2S$ transition but our results for that transition are compatible with the f values reported by Bahr et al. (1982) for Se IV. The f values obtained in this work for the $4s^24p\ ^2P^o - 4s4p^2\ ^2D$ transition agree reasonably well with the results reported by Pinnington et al.(1977) for Br V and by Irwin et al. (1976) for Kr VI. They are larger for the $4s^24p\ ^2P^o - 4s^24d\ ^2D$ transition but this discrepancy between theory and experiment has been discussed in detail by Aashamar et al. (1983).

AUTHORS' ADDRESSES

E.Biémont – Institut d'Astrophysique
Université de Liège – B-4200 Cointe-Liège -Belgique
Senior Research Associate of the belgian FNRS

P.Quinet - Faculté des Sciences - Université de Mons - B-7000 Mons Belgique.
IRSIA Fellowship

REFERENCES

Aashamar,K.,Luke,T.M.,Talman,J.D.,1983, Oscillator strengths in the gallium sequence. In : J.Phys. B16,2695

Bahr,J.L., Pinnington,E.H., Kernahan,J.A., O'Neil,J.A.,1982 - Beam-foil spectroscopy of Se IV,V and VI. In : Can.J. Phys. 60,1108

Budhiraja,C.J., Joshi,Y.N., 1971 - Spectrum of Br V. In : Can.J.Phys.49,391

Cowan R.D.,1981 - The Theory of Atomic Structure and Spectra - University of California Press.

Denne,B., Hinnov,E., Cohen,S.,Timberlake, J., 1985 - Ground configurations of

highly ionized silver. In : J.Opt.Soc. Am. B2,1661.
Druetta,M., Buchet,J.P., 1976- Beam-foil Study of krypton between 400 and 800 Å. In : J.Opt.Soc.Am. 66,433
Irwin,D.J.G., Kernahan,J.A.,Pinnington,E.H. Livingston,A.E.,1976. Beam-foil mean-life measurements in Krypton. In : J.Opt.Soc. Am. 66,1396
Litzén,U., Reader,J.,1989, Spectra and energy levels of the galliumlike ions Rb VII-Mo XII. In : Phys.Scr. 39,73
Livingston,A.E., 1976, New identifications in the spectra of Kr IV-Kr VII. In : J.Phys. B9, L215
Pinnington,E.H.,Kernahan,J.A.,Donnelly,K.E., 1977 - Beam-foil spectroscopy of bromine from 450 to 1000A. In: J.Opt.Soc.Am.67,162
Pinnington,E.H.,1976 - Beam-foil spectroscopy at the University of Alberta - In: Beam-foil spectroscopy - Vol.1,235-250
Reader,J.,Acquista,N.,Goldsmith,S.,1986, $4s^24p$-$4s4p^2$ and $4s^24p$-$4s^25s$ transitions of galliumlike ions from Rb VII to In XIX In: J.Opt.Soc.Am.B3,874

Table I - Calculated oscillator strengths (log gf) for the $4s^24p - 4s^24d$ and $4s^24p - 4s4p^2$ transitions of gallium-like ions.

Trans.	2J-2J'	Br V	Kr VI	Rb VII	Sr VIII	Y IX	Zr X	Nb XI
				$4s^24p - 4s^24d$				
2P-2D	1-3	0.46	0.45	0.43	0.42	0.40	0.39	0.38
2P-2D	3-3	-0.17	-0.20	-0.22	-0.23	-0.25	-0.26	-0.27
2P-2D	3-5	0.71	0.70	0.68	0.66	0.65	0.63	0.62
				$4s^24p - 4s4p^2$				
2P-2P	1-1	-0.19	-0.27	-0.36	-0.45	-0.54	-0.62	-0.71
2P-2P	1-3	-0.18	-0.22	-0.24	-0.27	-0.29	-0.32	-0.34
2P-2S	1-1	-0.09	-0.06	-0.03	-0.01	0.00	0.01	0.02
2P-2D	1-3	-0.57	-0.48	-0.43	-0.39	-0.36	-0.33	-0.31
2P-4P	1-1	-2.61	-2.46	-2.32	-2.19	-2.08	-1.97	-1.87
2P-4P	1-3	-4.18	-3.97	-3.80	-3.66	-3.54	-3.43	-3.33
2P-2P	3-1	-0.01	-0.01	-0.01	-0.02	-0.03	-0.04	-0.05
2P-2P	3-3	0.48	0.47	0.46	0.45	0.44	0.43	0.42
2P-2S	3-1	-1.09	-1.36	-1.69	-2.16*	-2.99*	-3.82*	-2.58*
2P-2D	3-3	-1.99	-2.01	-2.11	-2.27*	-2.51*	-2.89*	-3.71*
2D-2D	3-5	-0.42	-0.35	-0.31	-0.29	-0.27	-0.27	-0.27
2P-4P	3-1	-2.95	-2.84	-2.74	-2.66	-2.58	-2.52	-2.47
2P-4P	3-3	-2.86	-2.72	-2.59	-2.49	-2.39	-2.31	-2.23
2P-4P	3-5	-2.19	-2.00	-1.84	-1.70	-1.58	-1.46	-1.36

Trans.	2J-2J'	Mo XII	Ru XIV	Rh XV	Pd XVI	Ag XVII	Cd XVIII	In XIX
				$4s^24p - 4s^24d$				
2P-2D	1-3	0.36	0.34	0.32	0.31	0.30	0.29	0.28
2P-2D	3-3	-0.28	-0.30	-0.31	-0.31	-0.31	-0.31	-0.31
2P-2D	3-5	0.60	0.57	0.56	0.55	0.53	0.52	0.51
				$4s^24p - 4s4p^2$				
2P-2P	1-1	-0.79	-0.95	-1.03	-1.10	-1.18	-1.25	-1.32
2P-2P	1-3	-0.36	-0.40	-0.42	-0.44	-0.46	-0.48	-0.49
2P-2S	1-1	0.02	0.01	0.01	0.01	0.00	-0.00	-0.01
2P-2D	1-3	-0.29	-0.26	-0.25	-0.24	-0.22	-0.21	-0.20
2P-4P	1-1	-1.78	-1.61	-1.54	-1.47	-1.40	-1.34	-1.29
2P-4P	1-3	-3.25	-3.09	-3.02	-2.96	-2.90	-2.84	-2.79
2P-2P	3-1	-0.06	-0.08	-0.10	-0.11	-0.12	-0.13	-0.14
2P-2P	3-3	0.42	0.40	0.39	0.38	0.37	0.36	0.35
2P-2S	3-1	-2.13*	-1.69	-1.56	-1.46	-1.38	-1.31	-1.25
2P-2D	3-3	-4.13*	-2.50*	-2.20*	-1.97	-1.79	-1.65	-1.53
2P-2D	3-5	-0.27	-0.29	-0.31	-0.32	-0.34	-0.36	-0.37
2P-4P	3-1	-2.42	-2.36	-2.33	-2.32	-2.31	-2.31	-2.31
2P-4P	3-3	-2.16	-2.04	-1.99	-1.94	-1.89	-1.85	-1.81
2P-4P	3-5	-1.26	-1.10	-1.03	-0.97	-0.92	-0.87	-0.83

* Cancellation effects present.

T.M. Luke

Corrected oscillator strengths in the neon sequence: $Z \leq 26$

Oscillator strengths for transitions among the $2p^6$, $2p^5 3s$, 3p, 3d levels of ions in the neon sequence have been calculated using the Multi-configuration Optimized Potential Model (MCOPM) (Aashamar et al, 1979). Following this ab initio calculation, many of the levels have been corrected by solving an inverse eigenvalue problem using the observed spectrum as input. This correction may result in improved coefficients for the LS coupled terms that are mixed by spin-orbit and other relativistic contributions in the Breit-Pauli hamiltonian. Results for lifetimes are in reasonable agreement with recent calculations of Fawcett (1984) and others but differences between theory and beam foil experiments remain. Some details follow.

The ab initio MCOPM calculation expands the terms of interest using the following 13 configurations: $2s^2 2p^6$; $2s^2 2p^5 3s$, 3p, 3d, 4s, 4p, 4d; $2s2p^6 3s$, 3p, 3d, 4s, 4p, 4d. In this model, the orbitals are calculated in l-dependent central potentials that are varied to minimize a weighted set of LS coupled term energies. The variational principle leads to integral equations for the potentials which are solved iteratively along with the secular equation for the configuration interaction mixing coefficients. These optimized potentials are used as input to the program SUPERSTRUCTURE of Eissner et al (1974) in which the Breit-Pauli hamiltonian matrix is calculated and diagonalized. Rates for transitions among the resulting fine structure levels are then calculated.

The levels thus obtained frequently have mixing coefficients of comparable size for the terms coupled by relativistic effects and these coefficients can be in significant error if there are small errors in the energies of the non-relativistically calculated terms. These will be apparent if the level spectrum is not correctly reproduced in the calculation.

A scheme has been developed to correct for these errors (Luke,1988). It works as follows: Suppose a given level is predominantly a mixture of four terms (whose wave functions have been obtained in the nonrelativistic CI calculation as mixtures of whatever configurations have been included in the study). The Breit-Pauli hamiltonian matrix can be calculated in the subspace of these four terms and its diagonalization accurately reproduces the spectrum obtained in a full SUPERSTRUCTURE calculation. If this does not however reproduce the observed spectrum, one can invert the problem: Use the observed spectrum as input and calculate a corrected set of diagonal matrix elements that yield this observed spectrum. Corrections to the diagonal elements of the Breit-Pauli hamiltonian used in SUPERSTRUCTURE can then be obtained and hence corrected relativistic term-mixing coefficients and transition rates.

Earlier work has been published for the Neon sequence up to Si V. The present calculations have continued along the sequence with the ions Cl VIII, Ar IX, Ti XIII, Cr XV and Fe XVII selected on account of the availability of sufficient experimental data on the required spectra.

Three outcomes resulted from these calculations. Most commonly, the raw uncorrected calculation using these 13 configurations was quite satisfactory. Corrections had little effect and were not required.

In a number of cases, corrections in the mixing coefficients leading to shifts of the order of 15% in the transition rates occurred.

In a small number of cases the inverse eigenvalue problem has no solution. This may not be surprising: Inverse problems usually lead to difficulties. Among these is the fact that the solution is not unique. The corrected set of diagonal matrix elements results from solving a set of nonlinear algebraic equations and there can be up to $n!$ sets of diagonal matrix elements leading to a given set of eigenvalues. In the present method of solution, the set that evolves smoothly from solving the inverse problem with raw calculated spectrum as input (leading to the known raw calculated solution) to solving with the observed spectrum as input is taken to be the correct solution set.

Occasionally this procedure of numerical continuation doesn't work. At some point in the continuation from raw to observed eigenvalue input, the equations cease to have a solution, in the neighbourhood of earlier

solutions at least. It is likely that the difficulty in these cases is that the equations are especially sensitive to small errors in the off-diagonal elements. This has been found to be true in some cases. Slight perturbations in the off-diagonal elements restore the solution. In the cases where this has been found to occur so far, the mixing coefficients have been rather stable so that the corrections have been very modest anyway. There is no reason to believe this will always be the situation and the remaining cases of non-existence of solution to the inverse eigenvalue problem are still being investigated.

The poster accompanying this abstract gives examples of the various outcomes just described as well as some comparisons with observations and other calculations. Except for some high accuracy laser observations of transition rates in Ne I by Hartmetz and Schmoranzer (1983, 1984), only lifetimes appear to be available from experiment at present and these do not give a very sensitive test of transition rates. Nevertheless some comparisons between theory and experiment are given, illustrating cases of both systematic agreement and discrepancy.

ACKNOWLEDGEMENT.

This work was supported by the Natural Sciences and Engineering Research Council of Canada.

REFERENCES.

Aashamar,K.,Luke,T.M.,and Talman,J.D.(1979) J.Phys.B:Atom.Molec.Phys.12,3455-3464.
Eissner,W., Jones,M., and Nussbaumer,H.(1974) Comput.Phys.Commun.8,270-306.
Fawcett,B.C.(1984)Physica Scripta 30,326-334.
Hartmetz,P. and Schmoranzer,H.(1983)Phys. Lett.93A,405-408.
Hartmetz,P. and Schmoranzer,H.(1984)Z.Phys. A317,1-8.
Luke,T.M.(1988)Phys.Rev.A37,1872-1884.
(And references therein.)

AUTHOR'S ADDRESS

Department of Applied Mathematics,
University of Western Ontario,
London, Canada.N6A 5B9

Hannelore E Saraph

The lifetime of Mg^-: $3p^3\ ^4S^o$

ABSTRACT

The decay of Be^- $2p^3\ ^4S^o$ was observed by Gaardsted and Andersen (1989) and the decay of Mg^- $3p^3\ ^4S^o$ is under investigation by Andersen (1989). Accurate theoretical data can help with the detection of this process. Preliminary analysis of the experimental data disagreed for the lifetime with calculations by Beck, 1984. Beck (1989) has since improved on his earlier work. This paper presents an entirely independent approach to a lifetime calculation. The results are in excellent agreement with those of Beck, 1989.

THE CALCULATION

The close coupling approximation is used on two different target models. In both models atomic orbitals are optimised for the weighted sum of the energies of the lowest ten terms of magnesium. The MCHF program by Froese-Fischer, 1978 with modifications by Trefftz, 1988 is used. Model A includes configurations $3s^2$,3s4s,3s5s,3s3d,3s4d,$3p^2$,$3d^2$,$4s^2$,3p4p,3d4d, 3s3p,3s4p,3p3d, and 3p4s. This model gives poor energies for the higher terms of odd parity, see table 1. Model B uses in addition configurations $2p^5$3s3p3d,$2p^5$$3s^2$5s,$4p^2$,3p4d. This model gives a better representation of the higher terms. Tne target models were developed for a scattering calculation, where one aims for a reasonably good representation of *all* the lowest 'closely coupled' terms. Only few of these terms contribute to scattering channels for compound states ^4P and $^4S^o$ and these are listed in table 1. The compound system Mg+e^- is described by the wavefunction

$$\Psi^{SL\pi} = A\Sigma\phi_i F_j + \Sigma c_j \Phi_j \qquad (1)$$

Where A is an antisymmetrisation operator, ϕ and F are vector coupled functions for target and added electron states, and the Φ describe compound states using only target orbitals. Allowing the radial part of F and the configuration mixing coefficients c to vary freely one obtains a set of coupled integro-differential equations for each $SL\pi$. The program COLALG by Eissner, 1972 is used for the algebraic part and the program IMPACT by Crees *et al.*, 1978 for the radial part of the solutions. With these wavefunctions and the coefficients for radiative transitions produced by the program RADALG (Jones, 1974, Eissner and Jones, 1989) oscillator strengths and photoionisation cross sections can be calculated, Saraph, 1987. Spin-orbit coupling is neglected throughout.

Table 1
Term energies (in Ryd) for Mg. Experimental data are from Moore, 1949.

term	exp	model A	model B
$3s^2\ ^1S$	0.0	0.0	0.0
$3s3p\ ^3P^o$	0.1995	0.1890	0.1857
$3s4p\ ^3P^o$	0.4360	0.4714	0.4295
$3s3d\ ^3D$	0.4370	0.4315	0.4332
$3p^2\ ^3P$	0.5272	0.5111	0.5069

RESULTS

Table 2 presents electron affinities for the Mg^- bound states ^4P and $^4S^o$ obtained using the two target models. It also lists the LS-coupling results by Beck, 1989.

Table 2
Electron affinities in Rydberg for Mg^-, relative to the calculated energies of the parent terms $3s3p\ ^3P^o$ and $3p^2\ ^3P$ respectively.

term	model A	model B	Beck(LS)
$3s3p^2\ ^4P$	.0277	.0288	.0236
$3p^3\ ^4S^o$	.0395	.0347	.0394

The present electron affinities differ considerably from those of Beck, 1989. This discrepancy disappears when the wavelength is calculated. Table 3 compares wavelengths and oscillator strengths with the results by Beck 1984 and 1989. The present wavelengths are obtained from the difference of the total energies. Beck's wavelengths are obtained by subtracting the difference of the electron affinities from the inverse observed wavelength of the threshold transition. Beck includes relativistic effects and shows these to be small. It appears that the transition data are fairly stable with respect to improvements in these sophisticated calculations.

Table 3
Wavelengths and oscillator strengths for the process $3s3p^2\ ^4P - 3p^3\ ^4S^o$ (length form.)

	model A	model B	Beck, 1984	Beck, 1989
λ(Å)	2936	2909	2880	2921
f_{abs}	.310	.297	.295	.309

The agreement between the present calculation and that of Beck is very good indeed.

The term $^4S^o$ can also decay directly by radiative detachment. The cross section for this process could be calculated with the present setup. It has a broad maximum around λ=3551 Å that contributes to the decay rate by $.102*10^8\ s^{-1}$, while the decay rate to the bound state is $A=.702*10^9\ s^{-1}$. Hence, the final result for the lifetime of $3p^3\ ^4S^o$ is

$$\tau(^4S^o)=1.40\text{ns},$$

with an error estimate of 5%. The challenge is now with the experimentalists.

REFERENCES

Andersen T 1989, private communication.
Beck DR 1984 Phys Rev A 30 3305
Beck DR 1989 Phys Rev A 40 (Sept.15)
Crees MA, Seaton MJ and Wilson PMH 1978 Comp Phys Commun 15 23
Eissner W 1972 Progr Rep Proc 7th Internat. Confer. on the Physics of Electronic and Atomic Collisions. (Edit. T R Govers and F J de Heer, North Holland) p 460.
Eissner W and Jones M 1989 to be submitted.
Froese-Fischer Ch 1978 Comp Phys Comm, 14 145
Gaardsted JO and Andersen T 1989 J Phys B: At Mol Opt Phys 22 L51
Jones M 1974 Comp Phys Commun 7 353
Moore CE 1949 *Atomic Energy levels* NBS Circular No 467 vol 1 (US Govt Pr.Office)
Saraph HE 1987 Comp Phys Commun 46 107
Trefftz E 1988 J Phys B: At Mol Opt Phys 21 1761.

AUTHOR'S ADDRESS

Department of Physics and Astronomy,
University College London, London WC1E 6BT UK

M. Wilson

Calculation of radiative decay rates and branching ratios in Hg^+

ABSTRACT

Pseudo-relativistic wavefunctions have been used to calculate E1, E2 and M1 radiative decay rates and branching ratios connecting levels of the three lowest lying electron configurations of Hg^+ and compared with recent accurate results obtained from fluctuations (quantum jumps) of laser-induced flourescence studies of a single ion held in an ion trap.

INTRODUCTION and METHOD

The development of ion traps, lasers and photon counting methods have allowed the determination (to within a reasonably high degree of accuracy) of experimental decay rates linking different energy levels from the observed fluctuations in laser-induced flourescence of a single transition in Hg^+ (Itano et al 1987). Referring to Fig 1 the five lowest energy levels of Hg^+ are shown. Itano et al deduced the decay rates for the allowed transition $6p\ ^2P_{1/2}$ - $6s\ ^2S_{1/2}$ and the configuration interaction (CI) induced transition $6p\ ^2P_{1/2}$ - $d^9s^2\ ^2D_{3/2}$. In addition they also determined the forbidden decay rates from the two ^2D levels back to the ground level.

Using the pseudo-relativistic Hartree-Fock model (HFR), (see eg. Cowan 1981), we first obtained single-configuration wavefunctions for the configurations: $5d^{10}6s$, $5d^96s^2$ and $5d^{10}6p$, $5d^96s6p$. These were then used to calculate the usual interaction integrals used to obtain the single and mixed-configuration structures together with the necessary transition integrals required for the appropriate E1 and E2 transitions of interest here. The mixed-configuration energy matrices were diagonalized and the resulting eigenvalues compared with the experimental data. At this stage adjustments were made to the ab initio values of the centre of gravity energies in order to give somewhat closer agreement between calculated and experimental levels. This procedure helps obtain a more realistic degree of CI mixings than that produced entirely by ab initio methods. Finally the resulting CI eigenvectors were combined with the appropriate ab initio transition integrals to calculate the E1, E2 and M1 transition rates, A, between all possible levels of interest.

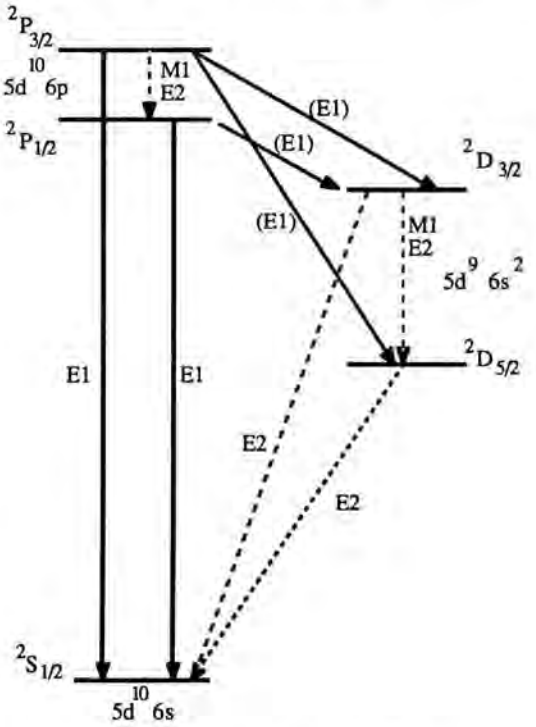

Fig. 1 Low level scheme of Hg^+

RESULTS and DISCUSSION

A selection of our results is presented in Table 1 together with the experimental data. It should be noted that in this preliminary study we have used unscaled values of the HFR transition and interaction integrals. Not unexpectedly the calculated E1 decay rate from the $^2P_{1/2}$ to the $^2S_{1/2}$ is somewhat larger than the experimental value. The weaker CI induced E1 decay to the metastable $^2D_{3/2}$ occurs due to mixing of a ^2P component of the d^9sp configuration for which we found

$5d^{10}6p\ ^2P_{1/2}> \sim 0.992\ 6p\ ^2P> + 0.127\ d^9sp\ ^2P>$ lending some of its 6p - 6s strength to the otherwise forbidden transition. Our calculated rate is is good accord with the experimental value (and an unpublished theoretical estimate quoted by Itano et al.). However, this rate is extremely sensitive to the degree of mixing as indicated

by large changes in the calculated decay rate with small changes in level positions. We also considered the effects of including additional perturbers, of both parities, which might influence this induced transition (see below).

From the results given in Table 1 we may also obtain the total radiative decay rate from $^2D_{3/2}$ being due to both an M1 and E2 contribution of comparable size ie. (55.3 + 71.9) ~ 127 s^{-1} which may be compared with the value 109 ± 5 obtained by Itano et al. Similarly we find the total radiative decay rate from the $^2D_{5/2}$ due to an E2 transition as 12.3 s^{-1} compared to (11.6 ± 0.4) found by Itano et al. Denoting the probabilities for the $^2D_{3/2}$ level to decay to the $^2S_{1/2}$ level or the $^2D_{5/2}$ level as f_1 and f_2 ($f_1 + f_1 = 1$) we obtain from the results in Table 1 f_1 ~ 0.55 whereas Itano et al found $f_1 = 0.491 \pm 0.015$. Our calculated estimate of this branching ratio could be modified to lie closer to the experimental value either by a suitably large decrease in the E2 rate from the $^2D_{5/2}$ or by some even parity mixture not yet included. We investigated the degree of modification on the E2 transition integral by re-calculating our radial wavefunctions using the usual HFR potential but augmented by an approximate correlation potential based on a free electron correlation energy, ie. the function e_c given by eqn (7.71) of Cowan (1981). Although such functions produced transition integrals of slightly smaller magnitudes the effect on the E2 rate was insufficient to account for the observed difference. We are examining the effects of including $5d^{10}6d$, $5d^9 6p^2$, $5d^8 6s 6p^2$ and $5d^8 6s^2 6p$, $5d^9 6p 6d$ but preliminary findings show that these are found to have little influence on the results obtained (with the noteable exception of the CI induced transitions) from our more restricted set of configurations. Bearing in mind the simple model used here the present calculations are gratifyingly close to the empirical values derived from a most beautifully ingenious experiment.

Table 1. Decay rates A(s^{-1}) for Hg^+

Transition				A(s^{-1}) Theory (this work)	Expt (Itano et al)
$5d^{10}6p\ ^2P_{3/2}$ -	$5d^96s^2$	$^2D_{3/2}$	(E1)	1.25×10^4	
-		$^2D_{5/2}$	(E1)	2.89×10^6	
-	$5d^{10}6p$	$^2P_{1/2}$	M1	6.85	
-		$^2P_{1/2}$	E2	0.29	
-	$5d^{10}6s$	$^2S_{1/2}$	E1	8.74×10^8	
$5d^{10}6p\ ^2P_{1/2}$ -	$5d^96s^2$	$^2D_{3/2}$	(E1)	57.7	52 ± 16
-	$5d^{10}6s$	$^2S_{1/2}$	E1	5.74×10^8	$(3.8 \pm 0.6)10^8$
$5d^96s^2\ ^2D_{3/2}$ -	$5d^96s^2$	$^2D_{5/2}$	M1	55.3 ←┐	
-		$^2D_{5/2}$	E2	0.04 127.2	109 ± 5
-	$5d^{10}6s$	$^2S_{1/2}$	E2	71.9 ←┘	
$5d^96s^2\ ^2D_{5/2}$ -	$5d^{10}6s$	$^2S_{1/2}$	E2	12.3	11.6 ± 0.4

ACKNOWLEDGEMENTS

I would like to thank Dr R D Cowan, of the Los Alamos National Laboratory, for many interesting discussions and his invaluable and generous help in implementing the codes used here on the Rutherford-Appleton Laboratory XMP/48. I would also like to thank Dr H A Klein, of the National Physical Laboratory Teddington, for drawing my attention to ion-trap work.

REFERENCES

Cowan, R.D , 1981- The Theory of Atomic Structure and Spectra (Berkeley: University of California Press).

Itano,W.M,J.C.Bergquist,R.G.Hulet and D.J.Wineland, 1987-Phys Rev Lett 59, 2732-2735.

AUTHOR'S ADDRESS

Department of Physics, Royal Holloway and Bedford New College (University of London), Egham, Surrey TW20 OEX, England.

W.H. Goldstein, A. Osterheld, J. Oreg and A. Bar-Shalom

Resonant excitation rates for the $2p^5 3s$ and $2p^5 3p$ levels in Ne-like Fe XVII

The 17Å 2p-3s X-ray emission lines of neon-like Fe XVII are observed in astrophysical settings as diverse as the solar corona (e.g., Loulergue and Nussbaumer 1973), supernova remnants (e.g., Hamilton, Sarazin and Chevalier 1983), and accretion disks (e.g., Kahn et al. 1984). Their intensities in the solar corona have been extensively studied and used as temperature diagnostics (e.g., Rugge and McKenzie 1985, Raymond and Smith 1986). Resonant excitation makes a significant contribution to the population of the $2p^6 3s$ levels at temperatures below threshold for their direct collisional excitation (Smith, Raymond, Mann and Cowan 1985; Raymond 1978). In this regime, the 2p-3s line intensities are very sensitive to resonant excitation, and their utility as a diagnostic depends on accurately accounting for this process. Previous calculations of resonant excitation in Fe XVII adopted a non-relativistic, LS configuration average approach (Omar and Hahn 1988), or extrapolated the results of a subset of detailed calculations to determine the contribution of each autoionizing series (Smith et al. 1985). Configuration average energies were apparently used to determine energetically allowed autoionization channels. This is a gross approximation for energetically broad configurations, and easily leads to incorrect results.

We present the results of a new calculation, in a detailed level accounting scheme, of the resonant excitation rate of $2p^6 3s$ and $2p^5 3p$ levels of Fe XVII. These rates are significantly lower than those in the literature. The present results are similar to those recently reported by Chen and Reed (1989), who also use a detailed level accounting scheme, but a different, multi-configurational Dirac-Fock (MCDF), atomic model.

In the isolated resonance approximation rate coefficients for resonant excitation is given by,

$$\alpha^{res.exc.}(\text{final}) = \sum_{C_{auto}} \sum_{lev \in C_{auto}} R^{capt.}(2p^6 \rightarrow lev) \times \frac{A^{auto.}(lev \rightarrow final)}{\sum_j [A^{auto.}(lev \rightarrow j) + A^{rad.}(lev \rightarrow j)]} \qquad (1)$$

where "final" is a neon-like level and the sodium-like "lev" belongs to the autoionizing configuration C_{auto}. $R^{capt.}$ is obtained by detailed balancing the corresponding autoionization rate, $A^{auto.}$, and the last factor is the branching ratio for "lev". The atomic data for Eq. (1) was calculated in the relativistic, multiconfigurational parametric potential model of Klapisch (1971, 1977) and Bar-Shalom and Klapisch (1988).

Table I The set of autoionizing configurations included in the present calculation, with the autoionization and radiative decay branches for each.

C_{auto}	C_{Ne} (autoion. channels)	C_{Na} (rad.channels)
$2s2p^6 3l5l'$, $l\le2, l'\le4$	$2p^6$, $2p^5 3l$, $2s2p^6 3l$	$(2s2p)^8 nl'(E1)$, $(2s2p)^7 3l''nl'(E1)$, including 2p-2s cascade followed by autoionization.
$(2s2p)^7 3lnl'$, $l\le2, l'\le4$, $6\le n\le10$		
$2p^5 3dnl$, $l\le4$, $11\le n\le15$	$2p^6$, $2p^5 3l$,	$2p^6 nl(E1)$, $2p^6 3d(E1)$
$2p^5 3pnl$, $l\le4$, $11\le n\le20$	$2p^6$, $2p^5 3l$,	$2p^6 3p(E1)$, $2p^6 nl(E1,E2)$, $2p^5 3snl(E1)$
$(2s2p)^7 4l4l'$, $l,l'\le3$	$2p^6$, $2p^5 3l$, $2s2p^6 3l$	$(2s2p)^8 4l(E1)$, $(2s2p)^7 3l4l'(E1)$ including 2p-2s cascade followed by autoionization.
$2p^5 4lnl'$, $l\le3, l'\le4$ $n=5,6,7$ $2s2p^6 3l$	$2p^6$, $2p^5 3l$,	$2p^6 nl(E1)$, $2p^5 3lnl'(E1)$,

The autoionizing configurations included in the outer summation in Eq.(1), and the radiative and autoionization channels included in the branching ratios, are listed in Table I. Our calculations are in intermediate coupling, and for given n, configuration interaction (CI) among the different values of l is included. All CI within the $(2s2p)^7 4l4l'$ configurations was included since they were treated in a single structure calculation. For the $2p^5 4lnl'$ series, CI was included for fixed l and n; i.e., the 4snl', 4pnl', 4dnl' and 4fnl' were treated independently. All CI among neon-like levels was included.

The importance of accounting explicitly for each level (both "final" and "lev") in Eq. (1) has been noted previously, and large errors have been shown to result from the use of average, rather than detailed level-by-level weighted, fluorescence yields in the calculation of resonant processes (Chen and Craseman 1974; Chen, Craseman and Matthews 1975; Bhalla 1975a, 1975b; Chen 1985, 1989). Inaccuracies can be traced to neglecting, in the average treatment, the effect of selection rules on branching ratios for Auger and X-ray processes.

The results of the present calculation, at an electron temperature of 200 eV, are summarized in Table II, along with total rates for ≈200 eV reported by Smith et al. (1985)

and Chen and Reed (1989). The discrepancies with the former calculation have been remarked on previously (Goldstein 1988), and have been confirmed by the independent calculations of the latter.

Table II. Total resonant excitation rate coefficients (units of 10^{-13} cm^3 sec^{-1}) for the $2p^53s$ and $2p^53p$ levels of FeXVII. Levels are listed in energy order. Values for this calculation are at an electron temperature of 200 eV, while those of Smith *et al.* (1985) are at 217 eV and include an extrapolation of n to 100. The results of Chen and Reed (1989) are for T_e=200 eV and were extrapolated beyond n=15 to n=200 for the $2p^53l'nl'$ configurations.

final state	TOTAL RATE ($\times 10^{-13}$ cm^3 sec^{-1}) @ 200 eV *this calc.*	*Smith* et al.	*Chen & Reed*
$[(2p^5)_{3/2}3s]_2$	12.97	50.0	12.2
$[(2p^5)_{3/2}3s]_1$	16.11	38.0	14.4
$[(2p^5)_{1/2}3s]_0$	2.48	11.0	1.9
$[(2p^5)_{1/2}3s]_1$	15.12	48.0	14.2
All $2p^53s$	46.68	147.0	42.7
$[(2p^5)_{3/2}3p_{1/2}]_1$	5.17	5.7	
$[(2p^5)_{3/2}3p_{1/2}]_2$	4.09	4.8	
$[(2p^5)_{3/2}3p_{3/2}]_3$	5.07	6.9	
$[(2p^5)_{3/2}3p_{3/2}]_1$	3.75	3.1	
$[(2p^5)_{3/2}3p_{3/2}]_2$	4.08	5.0	
$[(2p^5)_{3/2}3p_{3/2}]_0$	3.36	2.8	
$[(2p^5)_{1/2}3p_{1/2}]_1$	3.61	3.5	
$[(2p^5)_{1/2}3p_{3/2}]_1$	4.25	13.0	
$[(2p^5)_{1/2}3p_{3/2}]_2$	4.39	12.0	
$[(2p^5)_{1/2}3p_{1/2}]_0$	2.98	1.7	
All $2p^53p$	40.75	58.5	

The overall reduction in the excitation rate for $2p^53s$ levels of Fe XVII implied by the present results suggests that the 3s/3d line ratio observed in solar active regions and flares (Rugge and McKenzie 1985) ought to be reconsidered. A modeling effort is presently underway that apparently succeeds in matching the observed ratios when dielectronic recombination of Fe XVIII is included (Liedahl et al. 1989).

Work performed under the auspices of the U.S. Dept. of Energy by Lawrence Livermore National Laboratory under Contract No. W-7405-ENG-48.

REFERENCES

Bar-Shalom, A. and M. Klapisch, 1988, Comput. Phys. Commun., 50, 375 (1988).
Bhalla, C.P. 1975a, Phys. Rev. A 12, 122; 1975b, J. Phys. B 8, 1200.
Chen, M.H. and K.J. Reed, 1989, "Direct and Resonance Contributions to Electron Impact Excitation on n=2-3 Transitions in Neon-like Ions", UCRL-100304, Jan. 20, 1989, submitted to Phys. Rev. A.
Chen, M.H. and B. Craseman, 1974, Phys. Rev. A 10, 2232.
Chen, M.H. B. Craseman and D.L. Matthews, 1975, Phys. Rev. Lett. 34, 1309.
Chen, M.H. 1985, in "Atomic Inner-Shell Physics" ed. B. Craseman (Plenum, New York, 1985).
Chen, M.H. 1989, "Effective L-Shell Fluorescence Yields for Sodium-like and Neon-like Low-lying Autoionizing States", UCRL-100468, Feb., 1989, submitted to Phys. Rev. A.
Goldstein, W.H. 1988, "Recent Advances in Atomic Modeling" to appear in the proceedings of IAU Colloq. 115, Cambridge, MA, Aug. 22-25, 1988.
Hamilton, A.J.S., C.L. Sarazin and R.A. Chevalier 1983, Ap. J. Suppl., 51, 115.
Kahn, S.M., F.D. Seward and T. Chlebowski 1984, Ap. J., 283, 286.
Klapisch, M. 1971, Comput. Phys. Commun., 2, 239.
Klapisch, M. et al. 1977, J. Opt. Soc. Am., 61, 148.
Liedahl, D., S. Kahn, A.L. Osterheld and W.H. Goldstein 1989, in preparation.
Loulergue, M. and H. Nussbaumer, 1973, Astr. Ap., 24, 209.
Omar, G. and Y. Hahn 1988, Phys. Rev. A, 37, 1983.
Raymond, J.C. 1978, Ap. J., 222, 1114.
Raymond, J.C. and B.W. Smith 1986, Ap. J. 306, 762.
Rugge, H.R. and D.L. McKenzie 1985, Ap. J. 297, 338.
Smith, B.W., J.C. Raymond, J.B. Mann and R.D. Cowan 1985, Ap. J., 298, 898.

AUTHOR'S ADDRESS

Lawrence Livermore National Laboratory,
P. O. Box 808, Livermore CA 94450 U.S.A.

C.P. Bhalla[+], K.R. Karim[++] and M. Wilson[+++]

Comparison of theoretical satellite line intensity factors for dielectronic satellites of Li-like ions

ABSTRACT

Wavelengths, satellite line intensity factors and the resonance energies are presented for Be-like nickel. Comparison is made between the present calculations, performed with the Hartree-Fock model, and those based on the scaled Thomas-Fermi model. Significant differences are found in the line intensity factors for many cases.

DESCRIPTION

There have been rather few calculations of atomic parameters of Be-like ions (TFR Group et al. 1985, Bitter et al. 1985, Chen 1985 Bombarda et al. 1989, Bhalla et al. 1989). One atomic model which has been used extensively is the scaled Thomas-Fermi (TF) model. We report here a comparison of our calculations performed with the Hartree-Fock (HF) model with those with TF, and present the results of our calculations for Be-like nickel. The satellite line intensity factor, F_2^* (s-f) is defined as

$$F_2^*(s\text{-}f) = \frac{(2J_s+1)}{(2J_f+1)} \frac{A_a(s)\, A_r(s\text{-}f)}{\Sigma A_a + \Sigma A_r} . \qquad (1)$$

Table I contains the percentage differences of TF values (Bombarda et al. 1989, TFR Group et al. 1985) from HF values for selected cases.

We find that there is a reasonable agreement between HF and TF results for many strong lines, but significant deviations exist between the two calculations for a large number of lines, in particular for the 1s2s2p3p configuration.

Table 1. Percentage differences between the values of F_2^* (s-f) obtained with TF and HF models for initial configuration $1s2s2p^2$ leading to final configuration $1s^22s2p$ for nickel and argon.

Z = 28					
|s>	|f>	%	|s>	|f>	%
$^1D_2$	$^1P_1$	-13	$^1S_0$	$^1P_1$	10
$^3D_3$	$^3P_2$	3	$^3P_1$	$^3P_2$	12
$^3P_2$	$^1P_1$	18	$^3D_2$	$^3P_2$	6
$^3P_2$	$^3P_1$	2	$^1P_1$	$^1P_1$	15
$^3D_2$	$^3P_1$	7	$^3P_2$	$^3P_1$	40
$^3P_1$	$^3P_0$	3	$^1D_2$	$^3P_2$	16
$^3D_1$	$^3P_1$	3	$^3S_1$	$^3P_2$	16
Z = 18					
$^3D_1$	$^3P_0$	48	$^3S_1$	$^3P_1$	-7
$^3D_1$	$^3P_2$	-60	$^3S_1$	$^3P_2$	-6
$^3D_2$	$^3P_1$	1	$^1D_2$	$^1P_1$	-18
$^3D_3$	$^3P_2$	1	$^3P_2$	$^1P_1$	78
$^3D_2$	$^3P_2$	-34	$^1S_0$	$^1P_1$	7

Tables 2 and 3 contain our results for strong dielectronic satellite lines for nickel. The notation used in the description of the autoionization state |s> and final state |f> is as follows. 5D3 represents $^5D_3$ in the spectroscopic notation. E_s is the energy of the autoionizing state relative to the ground state, $1s^22s\ ^2S$, of the recombining ion.

ACKNOWLEDGEMENTS

It is a pleasure to thank Dr. R.D. Cowan for many helpful discussions. This work was supported by the Division of Chemical Sciences, Office of Basic Energy Sciences, Office of Energy Research, U.S. Department of Energy and in part by the SERC Rutherford Appleton Laboratory.

Table 2. X-ray wavelengths (in Å), line intensity factors, F_2^*, (in units of 10^{12}/s) and E_s (in keV) for the 1s2s2p3p configuration of nickel. Entries with $\lambda \approx 1.59$ and $\lambda \approx 1.37$ represent respectively 2p to 1s and 3p to 1s x-ray transitions.

|s>	|f>	λ	F_2^*(s-f)	E_s
5D3	3P2	1.6088	6.62	6.737
3D2	1P1	1.6077	3.39	6.745
3D1	1P1	1.6073	5.39	6.747
3D2	3P1	1.6060	2.81	6.745
3P2	3P2	1.6042	5.15	6.759
3S1	3P2	1.6026	3.04	6.767
3D2	1P1	1.6007	7.50	6.779
3D2	3P2	1.6001	10.82	6.779
3D2	3P1	1.5990	6.97	6.779
1D2	1P1	1.5984	6.42	6.790
1D2	3P2	1.5978	3.05	6.790
3D3	3P2	1.5974	62.00	6.792
3P2	1P1	1.5972	11.05	6.795
1P1	1P1	1.5972	8.55	6.796
1S0	1P1	1.5969	3.06	6.798
3P1	3P0	1.5968	3.05	6.789
1D2	3P1	1.5967	47.88	6.790
3P2	3P2	1.5966	8.47	6.796
1P1	3P2	1.5966	2.83	6.796
3D2	1P1	1.5950	13.65	6.807
3D2	3P2	1.5944	18.19	6.807
3P2	1P1	1.5641	3.94	6.811
3D1	3P1	1.5940	20.20	6.804
3D3	3P2	1.5938	3.89	6.809
3D1	3P0	1.5938	10.22	6.804
3P2	3P2	1.5935	5.55	6.811
3S1	3P2	1.5932	11.09	6.813
5P2	3P2	1.3805	3.40	6.751
5P3	3P2	1.3801	15.78	6.754
3P2	3P2	1.3793	19.79	6.759
3P1	3P0	1.3790	9.69	6.739
3D2	3P1	1.3789	22.82	6.745
3D1	3P1	1.3786	17.23	6.747
3D3	3P2	1.3785	78.15	6.764
3S1	3P2	1.3780	7.71	6.767
3P2	1P1	1.3772	3.89	6.811
1D2	1P1	1.3761	28.60	6.819
1S0	1P1	1.3749	4.29	6.827
1D2	3P2	1.3746	2.80	6.790
3D3	3P2	1.3742	4.32	6.792
3D2	3P1	1.3737	2.79	6.779

Table 3. X-ray wavelengths (in Å), line intensity factors (in units of 10^{13}/s) and E_s (in keV) for the $1s2s2p^2$ configuration of nickel.

|s>	|f>	λ	F_2^*(s-f)	E_s
5P2	3P2	1.6184	0.262	5.431
5P1	3P1	1.6173	0.236	5.420
5P3	3P2	1.6163	2.217	5.441
3D2	1P1	1.6162	0.303	5.480
3D1	1P1	1.6151	0.202	5.485
3P2	1P1	1.6132	0.535	5.494
3P1	1P1	1.6117	0.441	5.501
1D2	1P1	1.6090	8.080	5.514
3P1	3P2	1.6089	1.177	5.476
3D2	3P2	1.6081	1.901	5.480
3D1	3P2	1.6071	2.494	5.485
3P0	3P1	1.6069	0.220	5.469
3D3	3P2	1.6065	33.760	5.488
3P2	1P1	1.6058	4.048	5.530
3P1	3P1	1.6055	0.695	5.476
3D1	3P1	1.6037	10.620	5.494
3D1	3P1	1.6048	20.680	5.480
3P1	3P0	1.6044	4.094	5.476
3D1	3P1	1.6037	10.130	5.485
3P1	3P1	1.6036	1.140	5.501
1P1	1P1	1.6034	0.815	5.541
3D1	3P0	1.6026	0.219	5.485
1S0	1P1	1.6020	1.705	5.548
3P2	3P1	1.6017	0.530	5.494
1D2	3P2	1.6009	7.500	5.514
3P1	3P1	1.6003	0.572	5.501
3S1	3P2	1.5995	3.634	5.522

REFERENCES

Bhalla, C.P., K.R. Karim and M. Wilson, 1989 - Nucl. Inst. Methods B40/41, 369.

Bitter et al., 1985 - Phys. Rev. A32, 3011.

Bombarda et al., 1988 - Phys. Rev. A37, 504.

Chen, M.H., 1985 - Phys. Rev. A31, 1449.

TFTR Group et al., 1985 - Phys. Rev. A32, 2374.

AUTHORS ADDRESSES

+ Kansas State University, Department of Physics, Manhattan, KS 66506, USA

++ Illinois State University, Department of Physics, Normal, IL 61761, USA

+++ Royal Holloway and Bedford New College (University of London) Egham, Surrey, U.K.

Laboratory measurements of atomic data

Indrek Martinson

Experimental determinations of oscillator strengths in ions

ABSTRACT

Recent measurements of radiative lifetimes and transition probabilities in singly and multiply ionized atoms, by means of beam-foil and beam-laser spectroscopy, are reviewed. The spectra discussed include Ca II and ions of the iron-group and rare-earth elements.

INTRODUCTION

Experimental studies of lifetimes and oscillator strengths (f-values) have been discussed at the two previous meetings in this series. In Lund, six years ago, Richter (1984) reviewed results for neutral and singly ionized atoms, whereas Curtis (1984) also included data for higher charge states. Three years later, in Toledo, Ohio, Wiese (1987) summarized progress and challenges in this field of research. These three reviews, together with several other papers presented at the two previous symposia, contain much useful material of current interest.

The present article concentrates on recent accelerator-based studies of transition rates and lifetimes for ions. After a survey of experimental problems, results for systems of interest to astrophysics and the spectroscopy of fusion plasmas will be briefly surveyed.

EXPERIMENTAL ASPECTS

Most experimental methods used to determine lifetimes and f-values are normally limited to neutral and singly ionized atoms. For detailed discussions of various techniques two excellent reviews (Imhof and Read, 1977, Huber and Sandeman, 1986) can be consulted.

In the case of higher charge states only ion-beam methods, in particular beam-foil spectroscopy (Bashkin, 1976), are generally applicable. With this method the intensities $I(t)$ of the spectral lines of interest are measured as a function of the time t after excitation in the foil. From such data the lifetimes τ of the excited levels may be deduced, in the simplest case by using the relation $I(t) = I(0)\exp(-t/\tau)$, where $I(0)$ is the intensity close to the foil.

In practice many levels in a given ion can be excited. The observed decay curves are thus sums of exponentials. Unless properly accounted for, such cascading may complicate data analyses and introduce systematic errors. However an efficient technique for cascade corrections (ANDC, i.e. arbitrarily normalized decay curves), introduced by Curtis et al. (1971), has essentially eliminated this drawback. Recent experience has shown that modern beam-foil data, analyzed by means of ANDC, compare favorably with the results of elaborate theoretical studies of oscillator strengths (Martinson, 1988, Engström, 1989).

Whenever the spectra are line-rich (e.g. in the case of 3d- and 4f-elements), blending of lines complicates lifetime studies. Careful spectral studies are now necessary before decay measurements can be untertaken. It should further be realized that the available information on spectra is normally far from complete, and unexpected line blends may thus occur. Furthermore, the ion-foil excitation process strongly populates hydrogen-like states (high n and l quantum numbers) as well as doubly-excited levels, transitions from which are very weak or even absent in most other light sources (sparks, laser-produced plasmas, tokamaks, etc.).

The beam-laser method of Andrä et al. (1973), constitutes an important development of the beam-foil concept. The fast ions are now excited by monochromatic laser light (instead of by the foil) into the levels of interest. There is no distorsion of the data due to cascades or line blends. Furthermore, the velocity of the ions (and thus the time scale after excitation) is more precisely known than in the beam-foil case where corrections for energy loss and straggling in the foil must be made. At low ion energies these effects are fairly large.

The beam-laser method is unfortunately limited by the presently available lasers to transitions with wavelengths longer than 2000 Å. In spectra such as C I, N I, O I, S I and in multiply ionized atoms, the most important spectral transitions (in particular the resonance lines) lie well below this limit. In practical beam-laser work several factors must be carefully investigated, for instance stray light from the laser.

SINGLY IONIZED CALCIUM

In the important spectrum Ca II the f-value of the 4s ^2S - 4p ^2P multiplet (the famous H and K lines at 3933 and 3968 Å) has been theoretically studied by many authors, usually by means of single-configuration approximations. There have also appeared lifetime results, e.g. a beam-foil study in which ANDC corrections were included (Emmoth et al. 1975). A typical decay curve which explicitly shows the cascading situation is depicted in fig. 1.

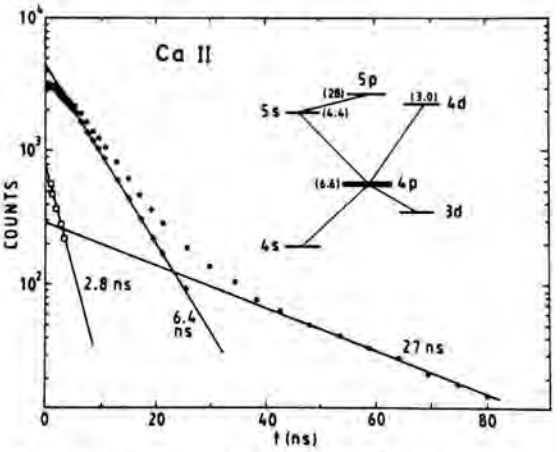

Fig. 1. Decay curve of the 4p ^2P (J = 3/2) level in Ca II (Emmoth et al., 1975), showing both the primary decay and some important cascades. The theoretical lifetimes of are also indicated.

More recently, an accurate beam-laser study has been reported (Gosselin et al., 1988), resulting in improved error limits. A very interesting method, introduced by Masterson and Stoner (1973) and later developed by Becker and Andrä (1985), has been applied to Ca^+ by Becker (1985). The method involves measurement of photon-photon coincidences on foil-excited ions. This apparently highly effective way of eliminating the influence of cascading unfortunately suffers from the fact that the coincidence rates are very low in optical measurements. In the case of Ca II, the preliminary 4p ^2P lifetime, as given in Becker's thesis (1985), is much shorter than most earlier data. Since the final result has not appeared yet, no detailed conclusions can be drawn, however. These facts prompted a new configuration interaction (CI) calculation of Ca II lifetimes (Cowan and Martinson 1988). The CI results (table 1) are in agreement with the beam-foil and beam-laser data. A new, careful beam-foil study of Ca II lifetimes is meanwhile being concluded (Haar 1989). Because of various technical developments, modern beam-foil results are normally much more accurate than the data obtained in the 1970's and earlier.

Table 1. Lifetimes (ns) in Ca II

Level	Without CI	With CI	Experiment
4p $^2P_{1/2}$	6.22	6.75	6.96 (18)[a]
$^2P_{3/2}$	6.05	6.57	6.87 (18)[a]
			6.4 (7)[b]
4d $^2D_{3/2}$	2.94	2.98	
$^2D_{5/2}$	2.99	3.03	2.9 (3)[b]
5s $^2S_{1/2}$	4.62	4.40	3.4 (4)[b]
5p $P_{1/2}$	30.7	27.7	29 (5)[b]

[a]Gosselin et al. (1988) [b]Emmoth et al. (1975)

IRON-GROUP ELEMENTS

Several of the iron-group elements are of great astrophysical significance, because of their high solar, stellar and interstellar abundances. Metals such as Ti, Cr, Fe, Ni and their alloys are used as materials for the first wall, limiters and divertors in tokamaks and other fusion devices. Astrophysical and laboratory (fusion) plasmas thus produce lines belonging to the 3d-elements in various degrees of ionization. However, the spectra and f-values for these elements are of great interest to atomic structure physics as well, presenting challenging problems but also providing insights into many-electron effects for complex atoms and ions.

In this paper some results for Ti, Fe and Ni will be mentioned. This task has been facilitated by the recent appearance of two valuable compilations of atomic transition probabilities, for Sc-Mn (Martin et al., 1988) and Fe-Ni (Fuhr et al., 1988).

Titanium

The beam-laser method has recently been extended to Ti II (Gosselin et al., 1987). A beam of Ti^+ ions was excited from the level a ^4F (J = 7/2) to z $^4D^o$ (J = 5/2) by means of laser radiation and the decay of the upper level was measured. In this way a very

accurate $^4D^o$ lifetime was obtained, 4.01 ± 0.06 ns. This value is in good agreement with a previous result τ = 4.5 ± 0.6 ns (Roberts et al., 1975), based on a combination of emission and beam-foil data (Roberts et al., 1973), but the accuracy has been improved by a factor of ten. By means of the beam-foil method, decay times for transitions in Ti IV - Ti VII (400 - 800 Å) were determined some years ago (Dumont et al. 1981). Typical uncertainties were in the 10 - 20% range. Much interest has recently been focussed on the structure of highly ionized Ne-like ions, largely because of their applications in VUV and soft x-ray laser schemes (Matthews and Rosen 1988). The laser transitions occur between $2p^5 3s$ and $2p^5 3p$ levels. For Ne-like Ti XIII extensive beam-foil measurements of lifetimes of many $2p^5 3p$ and $2p^5 3d$ levels have been reported (Träbert 1986). The results nicely confirm theoretical predictions.

Iron

The spectra and f-values of Fe in various charge states have been studied by many authors, but much important information is still missing. According to Fuhr et al. (1988) there exist very few experimental data points (lifetimes, f-values) for Fe III and higher spectra. However, two beam-foil lifetime papers have appeared, one dealing with Fe II and Fe III (Dolby et al., 1979) and the other with Fe V and Fe VI (Dumont et al., 1979) which were not listed by Fuhr et al. (1988). Dolby et al. investigated three multiplets in Fe II and one in Fe III. For the latter, the a ^5D - z $^5P^o$ resonance multiplet, 1122 - 1132 Å, an experimental mean lifetime of τ = 0.88 ± 0.04 ns was found, whereas a very recent calculation predicts 1.40 ns (Fawcett, 1989). The reason for this rather substantial disagreement is not known. Beam-foil data have been reported for some other Fe III multiplets (Andersen et al., 1977), but here Fawcett (1989) notes that the experimental lifetimes are longer than the theoretical ones. This trend is indeed more common in complex spectra. On the other hand, the experimental data for Fe V and Fe VI (Dumont et al.,1979) agree well with the Thomas-Fermi calculations of Abbott (1978).

Additional experimental work, with careful monitoring of cascades and blends, should be undertaken for many Fe ions. We may also note that the spectrum of Dumont et al. (1979) shows about 20 Fe V lines between 1350 and 1450 Å, whereas there are 140 classified lines in the spark spectrum of Fe V in this region (Ekberg 1975). The two spectra are compared in fig. 2. However, since Dumont et al. (1979) concentrated on strong lines, blending was apparently not too serious.

Nowadays, beam-foil work at higher spectral resolution, by using a large UV spectrometer and a multichannel detector, should be carried out for Fe III - Fe X and perhaps additional

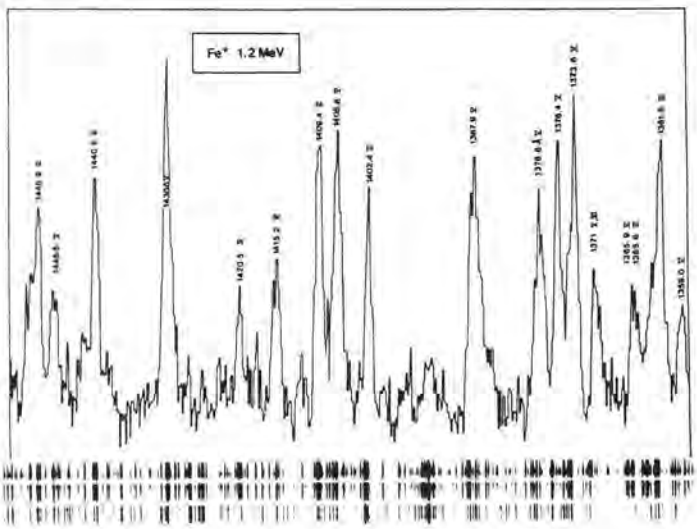

Fig. 2. Comparison of a beam-foil spectrum of Fe (Dumont et al., 1979) and three photographic recordings of spark spectra (Ekberg, 1975). Most lines belong to Fe V.

higher charge states. Studies of this kind may not appear as "trendy", but the data are badly needed by atomic theorists and astronomers.

Some experimental values are available for higher ionization stages of Fe. In these systems there are only a few valence electrons, and the spectra are easier to analyze. A very clean beam-foil spectrum of Fe in the VUV is depicted in fig. 3.

In one of the earlier beam-foil studies of highly stripped Fe, Träbert et al. (1982) measured decay times for some transitions in Fe XIII - Fe XVI. More recently, accurate beam-foil data have been obtained for the resonance lines in Fe XV and Fe XVI (Hutton et al., 1988a, 1988b). In these two papers, which also included some other ions, careful cascade corrections, using the ANDC method, were performed.

Nickel

It can be seen from Fuhr et al. (1988) that experimental data on f-values and lifetimes are rare for this element. Following some early beam-foil results, there has now appeared a paper on Ni II in which lifetimes of 12 levels were determined using the laser-induced fluorescence technique, the final uncertainties being about 6% (Lawler and Salih 1987). No experimental data seem to exist for Ni IV - Ni XIV, however.

However, a recent paper reports lifetimes for several levels belonging to the $3s3p^3$ and and $3s^2 3p3d$ configurations in Si-like Ni XV (Träbert et al., 1989). The experimental data agree with theoretical results. No rigorous corrections for cascading were possible, however, largely because the $3s3p^2 3d$ and $3p^4$ configurations, from which cascading can take place, have not been established for this ion. Biémont (1986) has calculated the decay rates and excitation energies of these levels and this data will be valuable in further spectroscopic work.

Intercombination lines

Intercombination lines are E1 transitions which violate the $\Delta S = 0$ selection rule. They are made possible by the spin-orbit interaction. Since these lines connect systems of different multiplicities, their wavelengths will be useful in placing the various term systems on an absolute scale. The importance of such lines for plasma diagnostics, for instance in determining electron densities, is well known.

Recently, intercombination lines in several highly charged iron-group elements have been experimentally studied. The results include Mg-like, Al-like and Si-like ions. In these systems there are metastable levels ($3s3p\ ^3P$, $3s3p^2\ ^4P$, $3s3p^3\ ^5S$, respectively) that decay to the various ground states by intersystem lines. These transitions are frequently very difficult to classify with certainty because the lines are fairly weak compared to other lines appearing in the same region. However, in "delayed" beam-foil spectra, recorded far downstream from the foil, these intersystem lines (which have markedly longer decay times than most other transitions in the same

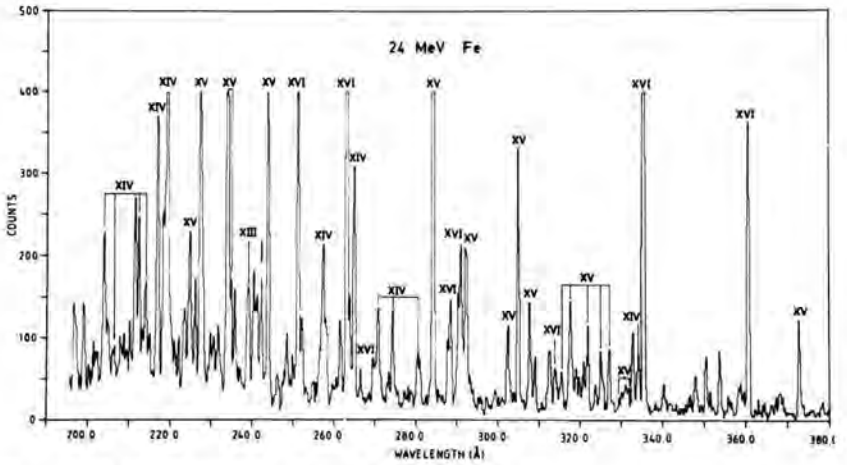

Fig. 3. A high-energy beam-foil spectrum of Fe, showing transitions in Fe XIII - Fe XVI (Hutton et al., 1988a).

wavelength range) appear as distinct peaks (Träbert et al., 1988). Following such line identifications, many experimental transition probabilities have been determined in recent years (Träbert et al., 1988, Ellis et al., 1988). The experimental results usually confirm theoretical predictions, in particular those based on relativistic treatments.

RARE EARTH IONS

In the early 1970's several solar astronomers emphasized the need for reliable gf-values for neutral and singly ionized rare earth elements. These data were necessary for establishing the solar abundances of these 4f-elements. In Aarhus and Stockholm the beam-foil method was therefore extended to such complex systems. A preliminary study of some Tm II lines (Curtis et al., 1973) showed that the gf-values given by Corliss and Bozman (1962) in their classic monograph were *too low* for this ion. Such a result was not expected at that time (because the trend was the opposite in most other cases), and the beam-foil data were initially doubted by solar astronomers (Ross and Aller 1974). However, in a more comprehensive beam-foil investigation, Andersen and Sørensen (1974) provided the necessary confirmation for Tm II, and they also showed that the differences between beam-foil data and the gf-values of Corliss and Bozman (1962) did not follow a simple general trend for the rare earths.

Nowadays beam-foil work on singly ionized rare-earth elements has been replaced by beam-laser studies which are here very much superior. Such results were already reviewed by Richter (1984). As a rather early example the work on Er II (Bentzen et al., 1982) deserves mentioning. Here the lifetimes were determined with about 10% uncertainties. It was also shown that a previous beam-foil study of Er II (Engman et al., 1976) had not resulted in correct lifetimes. Since the line spectrum of Er II is much more dense than that of Tm II, blends must have affected the beam-foil data. To paraphrase Crossley (1984) and Hibbert (1989), the beam-foil work was "over-ambitious". It is worth noting that for Er II the beam-laser data agree fairly well with the emission results (Corliss and Bozman, 1962). Recently, very accurate beam-laser lifetimes (1-3% uncertainties) were reported for Sm II (Vogel et al.,1988). Three of their decay curves are displayed in fig. 4.

For some levels previous lifetime data were available, but in these cases the new values represent marked improvements.

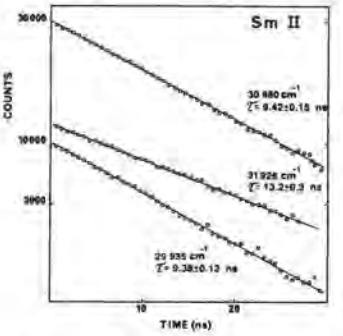

Fig. 4. Beam-laser decay data for three levels in Sm II (Vogel et al., 1988).

VERY ACCURATE DATA

At the symposium in Lund Crossley (1984) reviewed the developments in f-value calculations, thereby dividing the results into four categories, a) Very accurate calculations, b) Accurate calculations, c) Calculations for larger systems and d) Mass production. Recent theoretical studies have emphasized very accurate calculations of f-values, see e.g. Frose Fischer (1988). Among the motivations for such efforts is the existence of highly accurate (0.2%) beam-laser data, e.g. by Gaupp et al.(1984). Presently there seem to persist certain small differences between the "best" theoretical and experimental f-values in the case of Li I, Li II, Na I and K I (Froese Fischer 1988). On the other hand, an earlier beam-foil result for He I, which has a total uncertainty of 0.26% (Astner et al. 1976), agrees quite well with theory.

Very interesting results have recently appeared for the 3s - 3p resonance doublet in the Na I sequence. As noted, the value of Gaupp et al. (1984) for Na I deviates from that predicted by very "sophisticated" models wheras agreement is very good with the results of simpler theoretical approaches, such as the semiempirical Coulomb approximation. In recent beam-foil studies of Na-like Ti, Fe, Ni and Cu, Hutton et al. (1988b) also noted a small systematic shift from theoretical f-values. Quite recently this trend was established for Na-like Mg II for which Ansbacher et al.(1989) report an accurate beam-laser measurement. A new high-precision result has been meanwhile reported for Na I (Carlsson, 1989) which is in nearly perfect agreement with the lifetime of Gaupp et al. (1984). All these studies yield a consistent picture, i.e. there exists an admittedly small but persistent deviation from theoretical results based on *ab initio*

methods. However, a recent semiempirical calculation in which the central field Hartree-Slater approximation is combined with core polarization (Theodosiou and Curtis (1988) agrees quite closely with these recent experimental data.

CONCLUDING REMARKS

In this brief survey we have sketched some cases where progress has been made on the experimental side in recent years. With a few exceptions only beam-foil and beam-laser methods have been considered.

A number of experimental developments are expected for the future. For example, with short-wavelength lasers transitions in mutliply ionized atoms can be resonantly excited. Laser techniques have already been applied to such ions, in connection with Lamb shift and fine-structure measurements, see e.g. Silver (1988), but here "ordinary" lasers (gas or solid-state lasers) have been employed to induce transitions between excited levels in H-like and He-like ions. A particularly interesting novel idea involves the excitation of highly stripped ions with synchrotron radiation from a dedicated storage ring for electrons, see e.g. Jones et al. (1987).

ACKNOWLEDGEMENTS

This work has been supported by the Swedish Natural Science Research Council (NFR).

REFERENCES

Abbott, D.C., 1978 - J. Phys. B **11**, 3479-3497.
Andersen, T., and G. Sørensen, 1974 - Solar Phys. **38**, 343-350.
Andersen, T., P. Petersen and E. Biémont, 1977 - J. Quant. Spectrosc. Radiat. Transfer **17**, 389-392.
Andrä, H.J., A. Gaupp and W. Wittmann, 1973 - Phys. Rev. Lett. **31**, 501-504.
Ansbacher, W., Y. Li and E.H. Pinnington, 1989 - Phys. Lett. **A 139**, 165-169.
Astner, G., L.J. Curtis, L. Liljeby, S. Mannervik and I. Martinson, 1976 - Z. Physik **A 279**, 1-6.
Bashkin, S., ed., 1976 - Beam-Foil Spectroscopy, Berlin, Springer.
Becker, B., 1985 - Thesis, University of Münster.
Becker, B., and H.J. Andrä, 1985 - Nucl. Instr. Meth. **B9**, 650-654.
Bentzen, S.M., U. Nielsen and O. Poulsen, 1982 - J. Opt. Soc. Am. **72**, 1210-1212.
Biémont, E., 1986 - private communication.
Carlsson, J., 1989 - Phys. Scr. **39**, 442-446.
Corliss, C.H., and W.R. Bozman, 1962 - NBS Monograph 53, Washington, D.C.
Cowan, R.D., and I. Martinson, 1988 - Atomic Spectroscopy, University of Lund, pp 36-37 and unpublished data.
Crossley, R., 1984 - Phys. Scr. **T8**, 117-128.
Curtis, L.J., 1984 - Phys. Scr. **T8**, 77-83.
Curtis, L.J., H.G. Berry, and J. Bromander, 1971 - Phys. Lett. **34 A**, 169-170.
Curtis, L.J., I. Martinson and R. Buchta, 1973 - Nucl. Instr. Meth. **110**, 391-394.
Dolby, J.S., R.W.P. McWhirter and C.J. Sofield 1979 - J. Phys. B **12**, 187-201.
Dumont, P.D., Y. Baudinet-Robinet, H.P. Garnir E. Biémont and N. Grevesse, 1979 - Phys. Rev. **A 20**, 1347-1351.
Dumont, P.D., H.P. Garnir, Y. Baudinet-Robinet and M. Kapenyak, 1981 - J. Opt. Soc. Am. **71**, 502-503.
Ekberg, J.O., 1975 - Phys. Scr. **12**, 42-57, and private communication.
Ellis, D.G., I. Martinson and E. Träbert, 1989 - Comm. At. Mol. Phys. **22**, 241-262.
Emmoth, B., M. Braun, J. Bromander and I. Martinson, 1975 - Phys. Scr. **12**, 75-79.
Engman, B., J.O. Stoner, Jr., I. Martinson and N.E. Cerne, 1976 - Phys. Scr. **13**, 363-364.
Engström, L., 1989 - Phys. Scr. **40**, 17-24.
Fawcett, B.C., 1989 - At. Data Nucl. Data Tables **41**, 181-255.
Froese Fischer, C., 1988 - Nucl. Instr. Meth. **B31**, 265.
Fuhr, J.R., G.A. Martin and W.L. Wiese, 1988 - J. Phys. Chem. Ref. Data **17**, Suppl. No. 4.
Gaupp, A., P. Kuske and H.J. Andrä, 1984 - Phys. Rev. **A 26**, 3351.
Gosselin, R.N., E.H. Pinnington and W. Ansbacher, W., 1987 - Phys. Lett. **A 123**, 175-178.
Gosselin, R.N., E.H. Pinnington and W. Ansbacher, W., 1988 - Nucl. Instr. Meth. **B31**, 305-310.
Haar, R.R., 1989 - Thesis, University of Toledo..
Huber, M.C.E., and R.J. Sandeman, 1986 - Rep. Prog. Phys. **49**, 397-490.
Hibbert, A., 1989 - Phys. Scr. **39**, 574-580.
Hutton, R., L. Engström and E. Träbert, 1988a - Nucl. Instr. Meth. **B 31**, 294-299.
Hutton, R., L. Engström and E. Träbert, 1988b - Phys. Rev. Lett. **60**, 2469-2472.
Imhof, R.E., and F.H. Read, 1977 - Rep. Prog. Phys. **40**, 1-104.
Jones, K.W., B.M. Johnson, M. Meron, B. Crasemann, Y. Hahn, V.O. Kostroun, S.T. Manson and S.M. Younger, 1987 -

Comm. At. Mol. Phys. **20**, 1-18.
Lawler, J.E., and S. Salih, 1987 - Phys. Rev. **A 35**, 5046-5050.
Martin, G.A., J.R. Fuhr and W.L. Wiese, 1988 - J. Phys. Chem. Ref. Data **17**, Suppl. No. 3.
Martinson, I., 1988 - Rep. Prog. Phys. **52**, 157-225.
Masterson, K.D., and J.O. Stoner, Jr., 1973 - Nucl. Instr. Meth. **110**, 441-444.
Matthews, D.L., and M.D. Rosen, 1988 - Scientific American **259**, 60-65.
Richter, J., 1984 - Phys. Scr. **T8**, 70-76.
Roberts, J.R., T. Andersen and G. Sørensen, 1973 - Astrophys. J. **181**, 567-586.
Roberts, J.R., P.A. Voigt and A. Czernichwski, 1975 - Astrophys. J. **197**, 791-798.
Ross, J.E., and L.H. Aller, 1974 - Solar Phys. **36**, 21-23.
Silver, J.D., 1988 - Phys. Scr. **37**, 720-727.
Theodosiou, C.E., and L.J. Curtis, 1988 - Phys. Rev. **A 38**, 4435-4445.
Träbert, E., 1986 - Z. Physik D **1**, 283-286.
Träbert, E., K.W. Jones, B.M. Johnson, D.C. Gregory and T.H. Kruse, 1982 - Phys. Lett. **87A**, 336-340.
Träbert, E., P.H. Heckmann, R. Hutton and I. Martinson, 1988 - J. Opt. Soc. Am. **B5**, 2173-2182.
Träbert, E., N. Reistad, I. Martinson and R. Hutton, 1989 - Z. Phys. D **11**, 207-211.
Vogel, O., B. Edvardsson, A. Wännström, A. Arnesen and R. Hallin, 1988 - Phys. Scr. **38**, 567-572.
Wiese, W.L., 1987 - Phys. Scr. **35**, 846-850.

AUTHOR'S ADDRESS

Department of Physics, University of Lund, Sölvegatan 14, S-223 62 Lund, Sweden

D.E. Blackwell

An appraisal of the accuracy of furnace gf measurements: their extension by use of a hollow cathode source

ABSTRACT

The need for a reliable assessment of the accuracy of determined oscillator strengths is stressed. A discussion is given of the various sources of error and uncertainty in the furnace method for determining relative oscillator strengths. Experiments being made at Oxford with a hollow cathod source for extending furnace results to weaker and higher excitation lines are described.

NEED FOR A RELIABLE ASSESSMENT OF ACCURACY

Since 1960 there have been great advances in almost all areas of stellar spectroscopy. There has been a corresponding progress in the accuracy and range of available atomic data, as is clear from the proceedings of this meeting, but much remains to be done. Dr Petford and I started measurements in Oxford some 20 years ago, and I propose to speak first about accuracy in relation to what we have tried to do since then. A discussion of accuracy is important because a vital part of a determination of an oscillator strength is the assessment of a probable error. If this is not done reliably then, for example, an apparent detection of non-LTE in a stellar atmosphere might only be due to errors in the adopted oscillator strengths. There are some tests that can be applied to measured oscillator strengths, which will be mentioned later, but this is the basic requirement. The history of science contains many examples of experiments with stated accuracies subsequently found to have been too optimistic. I hope that our Oxford measurements using the furnace method will not suffer the same fate when more accurate methods are developed, but part of the purpose of this talk is to show that what began as a simple direct experiment is in practice a complex one, full of opportunities for small errors of measurement which are not easily assessed.

Supposing that it is possible, using a Fourier Transform spectrometer, to measure the equivalent width of a stellar absorption line to one per cent, then oscillator strengths are needed to at least this order of accuracy. They are needed for weak lines, high excitation lines, and of course for atoms of all degrees of ionisation. Our measurements of FeI lines were begun because we were interested in the determination of stellar masses by using strong lines in stellar spectra broadened by collision damping. Then the work developed into a general study of diagnostics for stellar atmospheres, and we added TiI, CrI and NiI, among other atoms, to the programme. The furnace method, which measures the ratios of oscillator strengths, was adopted because it was ostensibly capable of high accuracy, needing only measurements of the ratio of two equivalent widths and a temperature.

THE FURNACE METHOD

I want to say only enough about the appartus to discuss the many difficulties of the experiments, the precautions taken, and sources of error that are not apparent from published papers (e.g. Blackwell et al., 1982), and indeed were not apparent to ourselves when we started. The Oxford furnace has a carbon tube 1m long, heated to temperatures approaching 3000 K by a current of up to 5000 A. In practice, a three-pass optical system is used giving a 3m column of metal vapour. It is run in an atmosphere of argon. One purpose of this is to contain the metal vapour in the tube, while another is to ensure that there is a state of LTE in excitation there. The temperature is measured using a photoelectric pyrometer which compares the brightness of carbon blocks in the tube with the brightness of a standard source calibrated by the National Physical Laboratory. Pairs of lines are measured simultaneously using two high resolution photoelectric spectrometers. A high degree of simultaneity (i.e. to within about 3 seconds) is required to avoid difficulties due to minor eruptions of vapour at isolated places along the tube. The accuracy of comparison of oscillator strengths varies between 0.5 per cent for small differences in excitation, to 2 per cent for an excitation difference of 3 eV for apparently unblended lines of FeI.

This basic description conceals the many

minor details of the experiment and the uncertainties that go with them; for instance, at very high temperatures a correction should be made for the emission from the furnace of a line spectrum. A basic requirement is a high photometric accuracy because all iron lines, for example, must be compared ultimately with the resonance line FeI 3719.9, for which an accurate absolute oscillator strength is known. This is the strongest line in the furnace spectrum, and is stronger than a typical 3 eV line of comparable wavelength and log gf = -1, by a factor of about 10^7. This large ratio must be measured to good accuracy, but its determination is complicated by the need for a curve of growth correction, which is obtained theoretically. Such a calculated curve of growth must be approximate because there is only poor knowledge of collision damping, so the absorption lines must be kept weak and they then suffer from noise in the continuum. We were encouraged early in our experiments by a comparison between 0eV oscillator strengths obtained with the furnace and those of Huber & Tubbs (1972), who used the hook method, over a range of nearly 10^6:1. The ratios over the whole of this span, given by these two experiments using different methods, differ by less than one per cent. Both furnace spectrometers suffer from scattered light of the kind described by Griffin (1969). However, this has been allowed for through an examination of the solar spectrum obtained with each spectrometer and a comparison with the double-pass solar atlas of Delbouille et al. (1973), leading to a correction for scattered light. Such a procedure is only possible because the colour temperature of the high pressure xenon arc source used in the experiments approximates to the colour temperature of the sun.

An accurate measurement of temperature is crucial. An error of 1K at a temperature of 2500K gives an error of about 0.6 per cent for an excitation difference of 3eV. The standard temperature source used at Oxford has an accuracy of 0.9K at 1900K (3 sigma), and the furnace temperature measurements should be of comparable accuracy. A complication is that the use of radiation pyrometry depends on a negligible absorption by the metal vapour within the bandpass used by the detector. Any possible error has been reduced by choice of a suitable filter, but scans across its bandwidth are needed. A further complication is that the temperature varies along the tube. This affects the thermal excitation through the Boltzmann relation, but it also poses a problem about the change of number density along the tube. We assume this is proportional to the vapour pressure at the local temperature, but this assumption will be vitiated if there is a flow of carrier gas and vapour along the tube.

An important defect of the experiment is that, because of impurities in the carbon tube, the absorption spectrum at very high temperature is rich in weak lines of elements other than iron. If the lines are obvious they can be avoided, but their density is such that an impurity line may well fall, undetected, within the profile of a measured line. Line profiles are fitted to synthetic profiles so that an allowance can be made for blending lines, but I am doubtful if blends of one per cent can be detected in this way. One shield against them is the warning of possible blending from study of the large number of semi-empirical gf values calculated by Kurucz and Peytremann (1975).

TESTS FOR ACCURACY

The many imponderable sources of error discussed here make other tests of accuracy desirable. One arises automatically from the reduction process. In this, the lines under investigation are placed in a two-dimensional array of excitation and log gf (e.g. Blackwell et al., 1979). If the measures of Δlog gf were accurate, all routes between two well-separated spectrum lines on the diagram would give the same overall Δlog gf value. This condition is satisfied by making minimum alterations to all the measured values. In practice, the individual changes that have to be made are small, typically 0.25 per cent for 0.0eV/1.0eV FeI lines, and it is suggested that the average change is a measure of the photometric accuracy of the experiments. However, these changes increase with increasing temperature, to 0.53 per cent for 2.6eV lines, probably because of undetected blending.

Two other tests have been devised. In one we compare measured ratios of oscillator strengths of lines within multiplets with those calculated by Kurucz and Peytremann (1975). The average deviation can be large, but the standard deviation of the differences is usually small. This is especially true for TiII lines; for example, the five lines of multiplet 5 show a standard deviation of 0.003 dex (0.8 per cent). A similar test can be made using the solar spectrum. There are apparent changes of iron abundance with excitation, but the apparent abundances for lines within a multiplet can be closely

similar. As an example of this, four of the lines of TiI multiplet 104 show a standard deviation of 0.006 dex (1.5 per cent). These are encouraging tests, but they are not particularly informative because the lines being compared are always close in strength and excitation; hence they do not check for possible temperature errors. This check can only be made by comparing with the results of other, completely different methods of experiment.

LIMITATION OF FURNACE MEASUREMENTS

Because the furnace method depends on thermal excitation, it is limited to low excitations. For the Oxford furnace, with its effective tube length of 3m, the limit is about 3eV for 'weak' solar FeI lines having equivalent widths of about 80 mA at 6000 A. The limit for the strongest solar lines is about 3.5eV. The furnace cut-off in excitation cannot easily be extended. It would be useless to try to increase the temperature, for this would result in a rapid destruction of the tube. A doubling of the tube length, to 2m, would only increase the maximum excitation by 0.16eV for FeI, whereas we would like to increase it by nearly 2eV. However, it is desirable to measure FeI lines that are both weaker than these limits and of higher excitation. For example, it is not easy to measure 'weak' FeI lines in the Arcturus spectrum, where they are stronger than in the sun because of the smaller degree of ionisation. Also, stellar lines of higher excitation are of great interest. They can be expected to be formed closer to LTE in excitation, so that the corresponding stellar abundances should be more representative of true abundances. This is illustrated by the results we have found for TiI (Blackwell et al., 1987), where the low excitation lines show a somewhat erratic variation of derived abundance, but the high excitation lines show a levelling off to a more constant abundance value which we may suppose to be closer to the true abundance value. Also, the influence of collision damping on line profiles for cooler stars increases quite rapidly with excitation, so that even weak solar lines show extended damping wings. There is scope here for investigation of surface gravity using such lines.

MEASUREMENTS USING A HOLLOW CATHODE

In order to extend the furnace measurements, we started a programme of hollow cathode measurements some years ago. The use of this source for oscillator strength measurements is well known, and important and accurate work has been done with it, for example by Whaling and colleagues (Whaling et al., 1985). Our own application is linked to a continuing use of the furnace, and is illustrated by the schematic energy level diagram of Figure 1. In this, A represents a transition measured in absorption with the furnace. The corresponding transition in emission is represented by B, where log gf(B) = -log gf(A). Another transition C is compared with B to give log gf(C) by comparing the fluxes in B and C from the hollow cathode, for which of course an absolute calibration of flux is needed. As the two transitions B and C originate from the same upper level, no knowledge of excitation conditions in the lamp is needed. Now, if D is the absorption line corresponding to the emission line C, log gf(D) = -log gf(C). Line A might be a measured furnace line of excitation 3.3eV, say, so that D becomes a measured line of higher excitation. Of course, A is of shorter wavelength than D, but there is

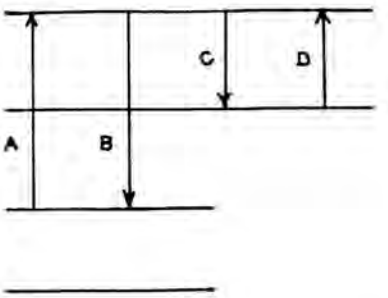

Fig. 1 Energy level diagram showing relation between furnace line A and final measured absorption line D

little disadvantage in this. The temperature measurement needed for the furnace is replaced here by an absolute flux measurement, using a standard lamp, which itself is based on the measurement of the temperature of a standard flux source. The same arrangement of two spectrometers used for the furnace work is adopted for the hollow cathode experiments. This enables a simultaneous comparison of the emission lines B and C to be made, followed by a measurement of the flux from a standard lamp using each

spectrometer. This technique has the advantage that very weak lines can be measured by using long integration periods.

USES OF THE HOLLOW CATHODE TECHNIQUE

Our use of this technique is based entirely on existing and future furnace results. We have used it to see how far its results follow those obtained using the furnace, although it is not clear whether we are testing the hollow cathode or furnace methods. We are also using it to check the temperature scale of the furnace results. An important application is to the measurement of weaker FeI, CrI, TiI and NiI lines, among others, than can be obtained with the furnace. We are making a particular effort to measure lines of high excitation, and have so far reached an excitation of 5.1eV for an FeI line that is apparently unblended in the solar spectrum.

BIBLIOGRAPHY

The furnace measurements published so far are listed in Table 1, together with the range of excitation potential studied.

Table 1. Furnace measurements of oscillator strengths

Atom	Excitation range	Reference
FeI	0.0 - 2.6	Andrews et al., 1979 Blackwell et al., 1979a, b; 1982a, b; 1986a
TiI	0.0 - 2.3	Blackwell et al., 1982c, d; 1983
TiII	0.0 - 0.1	Blackwell et al., 1982e
CrI	0.0 - 3.5	Blackwell et al., 1984, 1986b; 1986c
MnI	0.0 - 3.0	Booth et al., 1984
NiI	0.0 - 0.4	Blackwell et al., 1989
CaI	2.5 - 3.0	Smith & Raggett, 1981; Smith, 1988

Work is continuing on these and other elements.

REFERENCES

Andrews, J.W., Coates, P.B., Blackwell, D.E., A.D. & Shallis, M.J., 1979 - Mon. Not. R. astr. Soc., 186, 651

Blackwell, D.E., Ibbetson, P.A., Petford, A.D. & Shallis, M.J., 1979a - Mon. Not. R. astr. Soc., 186, 633

Blackwell, D.E., Petford, A.D., Shallis, M.J., 1979b - Mon. Not. R. astr. Soc., 186, 657

Blackwell, D.E., Petford, A.D., Shallis, M.J. & Simmons, G.J., 1980 - Mon. Not. R. astr. Soc., 191, 445

Blackwell, D.E., Petford, A.D., Shallis, M.J. & Simmons, G.J., 1982a - Mon. Not. R. astr. Soc., 199, 43

Blackwell, D.E., Petford, A.D. & Simmons, G.J., 1982b - Mon. Not. R. astr. Soc., 201, 595

Blackwell, D.E., Petford, A.D., Shallis, M.J. & Leggett, 1982c - Mon. Not. R. astr. Soc., 199, 21

Blackwell, D.E., Menon, S.L.R., Petford, A.D. & Shallis, M.J., 1982d - Mon. Not. R. astr. Soc., 201, 611

Blackwell, D.E., Menon, S.L.R.& Petford, A.D., 1982e - Mon. Not. R. astr. Soc., 201, 603

Blackwell, D.E., Menon, S.L.R. & Petford, A.D., 1983 - Mon. Not. R. astr. Soc., 204, 883

Blackwell, D.E., Menon, S.L.R. & Petford, A.D., 1984, Mon. Not. R. astr. Soc., 207, 533

Blackwell, D.E., Booth, A.J., Haddock, D.J. & Petford, A.D., 1986a - Mon. Not. R. astr. Soc., 220, 549

Blackwell, D.E., Booth, A.J., Menon, S.L.R. & Petford, A.D., 1986b - Mon. Not. R. astr. Soc., 220, 289

Blackwell, D.E., Booth, A.J., Menon, S.L.R. & Petford, A.D., 1986c - Mon. Not. R. astr. Soc., 220, 303

Blackwell, D.E., Booth, A.J., Menon, S.L.R. and Petford, A.D., 1987 - Astron. Astrophys., 180, 229

Blackwell, D.E., Booth, A.J., Petford, A.D. & Laming, J.M., 1989 - Mon. Not. R. astr. Soc., 236, 235

Booth, A.J., Blackwell, D.E., Petford, A.D. & Shallis, M.J., 1984 - Mon. Not. R. astr. Soc., 208, 147

Delbouille, L., Roland, G. & Neven, L., 1973 - Photometric Atlas of the Solar Spectrum from 3000 A to 10,000 A. Institut d'Astrophysique de l'Universite de Liege, Belgium

Griffin, R.F., 1969 - Mon. Not. R. astr. Soc., 143, 319

Huber, M.C.E. & Tubbs, E.F., 1972 - Astrophys. J., 177, 847

Kurucz, R. & Peytremann, E., 1975 - A table of semi-empirical gf values. Parts 1, 2, 3. Smithson. Astrophys. Obs. Spec. Rep., No. 362

Smith, G. & Raggett, D. St J., 1981 - Astron. Astrophys., 103, 231
Smith, G., 1988 - J. Phys. B: At. Mol. Opt. Phys., 21, 2827
Whaling, W., Hannaford, P., Lowe, R.M., Biemont, E. & Grevesse, N., 1985 - Astron. Astrophys., 153, 109

AUTHOR'S ADDRESS

Department of Astrophysics
Nuclear Physics and Astrophysics Building
Keble Road
Oxford OX1 3RH UK

I.S. Savanov

Oscillator strength catalogues for iron and titanium lines

ABSTRACT

In order to obtain data on chemical composition and physical conditions in the atmospheres of stars on the basis of spectral analysis, it is necessary to know atomic constants, and transition probabilities in particular. At the Crimean Observatory we have been collecting and reducing the data available in the literature concerning oscillator strengths for lines of the iron group elements (neutral and first stages of ionization).

DATA REDUCTION

While analysing the published data on the gf-values of these elements, we first considered the problem of the absolute scale of the gf-values and then the effects of systematic errors on the published oscillator strengths. The best accuracy in the determination of the absolute gf-value scale is provided by measurements of the lifetimes of the atoms in excited states. If such measurements are rather numerous for neutral iron, for other elements and ions of the iron group they are rather scarce, and the determination of the zero-point of the oscillator strengths system is less accurate.

The errors connected with the interpretation of the measured values in terms of observed quantities like the intensities of emission lines, equivalent widths of absorption lines, distances between hooks in experiments on anomalous dispersion, etc, we take to be systematic. The main goal of our reductions is to reveal the following errors:

1. Errors in the zero-point of the gf-value system.
2. Errors due to the wavelength range.
3. Errors in the line intensities.
4. Self-absorption effects.
5. Temperature errors.

At present the problem of comparison of oscillator strengths is simplified due to the existence of the precise measurements obtained by Blackwell and his group in Oxford. The high accuracy of the oxford data is confirmed by the measurements of other authors and by theoretical computations. Unfortunately, these measurements have been carried out only for a limited number of the numerous lines which have been observed in the spectra of stars. In our analysis we adopt the Oxford system as the basic one (for those elements where data are available) assuming it is free from systematic errors.

Reducing all published measurements to the Oxford system (for the lines of ionized iron we use a system of theoretical gf-values due to Kurucz), we assign a priority to the various contributing authors. While collecting the catalogue of oscillator strengths, we adopted the mean value from the group of references with highest priority as recommended gf-value, assuming that such a treatment will not affect the accuracy of good measurements.

A description of the oscillator strengths catalogues which have been prepared for iron and titanium lines is given in Table I.

Table I

Elem.	N of lines	Wavelength range, A	Range of E_i	Num. ref.	Notes
1.FeI	3420	2084-9889	0-5.1	20	a
2.FeII	798	2029-7711	0-8.6	11	b
3.TiI	795	2272-8778	0-4.3	17	c
4.TiII	419	2440-5416	0-4.3	10	d

Notes

a. Boyarchuk, A.A. and Savanov, I.S., 1985 Bull. Crim. Astrophys. Obs. 70, 57.
b. Boyarchuk, A.A. and Savanov, I.S., 1986 Bull. Crim. Astrophys. Obs. 74, 49.
c. Vaculenko D.A. and Savanov, I.S., 1990 Bull. Crim. Astrophys. Obs. 82 (in press)
d. Savanov I.S., 1990 (in press)

AUTHOR'S ADDRESS

Crimean Astrophysical Observatory
334413 p/o Nauchny, Crimea, USSR.

Table II: A portion of the Ti I catalogue (Ref. 3). The three quantities given are Wavelength (Å), Multiplet number and Recommended gf-value.

2272.61		-0.73	2735.61		-1.14	3214.240	27	-1.13
2273.330	15	-1.03	2739.81		-0.59	3217.942	179	-0.20
2276.750	15	-0.48	2742.32		-0.20	3219.212	179	-0.18
2280.000	15	-0.46	2749.06		-1.03	3221.151	26	-2.60
2299.860	14	-0.74	2757.40		-0.78	3221.381	179	-0.17
2302.750	14	-0.67	2758.08		-0.26	3222.741	26	-2.11
2305.690	14	-0.60	2802.50		-0.20	3223.519	179	0.18
2380.81		-1.24	2805.70		-0.87	3226.128	179	0.88
2384.520	12	-1.46	2809.17		-1.07	3226.240	27	-2.57
2418.370	11	-1.52	2812.98		-0.93	3243.803	26	-2.18
2421.310	11	-1.24	2817.40		-0.92	3292.078	62	-0.20
2424.260	11	-1.05	2817.84		-0.79	3299.413	61	-0.81
2428.240	10	-1.51	2828.07		-0.99	3306.879	190	0.09
2433.22		-1.66	2912.08		-0.03	3308.391	87	-0.49
2434.10		-1.97	2928.34		0.18	3309.501	87	-0.13
2440.980	10	-1.33	2933.526	1	-1.17	3309.730	190	-0.39
2504.54		-1.90	2937.301	1	-1.16	3312.690	190	-0.13
2519.010	8	-1.73	2941.995	1	-0.24	3314.422	87	0.11
2520.543	8	-1.11	2948.255	1	-0.14	3314.523	87	-0.52
2527.991	8	-1.51	2956.133	30	-0.06	3321.588	87	-0.60
2529.866	8	-0.89	2956.18		-0.01	3341.875	24	-0.14
2541.917	8	-0.68	2956.799	30	-1.07	3342.151	23	-1.38
2590.265	7	-1.65	2959.71		-1.39	3342.707	25	-2.39
2593.647	6	-1.41	2959.99		-1.22	3348.535	25	-2.49
2596.596	6	-1.35	2965.707	94	-0.37	3352.937	25	-2.05
2599.910	6	-0.60	2967.225	30	-1.12	3354.634	24	0.04
2605.163	6	-0.45	2968.231	29	-2.20	3360.990	24	-1.21
2611.287	6	-0.34	2970.384	29	-1.40	3361.263	25	-1.12
2611.468	6	-0.90	2974.934	94	-1.31	3361.835	23	-1.55
2619.942	6	-0.97	2981.448	29	-2.21	3370.436	24	-0.49
2631.550	5	-1.04	2983.29		-0.94	3371.447	24	0.14
2632.424	5	-0.99	2983.306	29	-1.11	3377.485	25	-0.36
2641.116	5	-0.36	3000.868	29	-0.92	3377.577	23	-0.26
2644.275	5	-0.23	3100.666	92	-0.46	3379.216	24	-1.08
2646.650	5	-0.05	3106.806	92	-0.98	3382.312	86	-0.50
2654.93		-2.30	3112.482	92	-1.17	3385.664	24	-1.27
2657.186	3	-1.79	3119.725	137	0.46	3385.944	23	-0.25
2661.966	2	-1.33	3123.074	67	-0.50	3390.682	86	-0.65
2669.610	2	-1.15	3141.537	66	-0.64	3392.713	136	-0.59
2679.949	2	-0.96	3141.670	192	-0.15	3398.634	86	-1.26
2685.14		-1.90	3186.451	27	-0.11	3439.305	120	-1.00
2725.07		-0.59	3191.994	27	0.04	3467.260	84	-1.06
2727.42		-0.67	3199.515	27	0.17	3478.918	84	-1.33
2731.13		-1.37	3203.828	27	-1.20	3480.525	84	-0.52
2731.58		-1.02	3204.870	90	-0.79	3485.689	84	-1.33
2733.26		-0.16	3205.168	26	-2.63	3493.280	22	-2.34
2735.28		-0.60	3205.848	26	-2.16	3495.754	84	-1.34

3499.099	84	-1.08	3798.276	115	-0.88	4005.952	187	-0.84
3506.643	22	-1.95	3818.22		-0.26	4008.046	187	-0.48
3511.626	22	-2.53	3822.026	189	-0.11	4008.926	12	-1.07
3547.029	133	-0.50	3828.180	189	0.08	4009.653	11	-1.84
3574.245	247	-0.49	3833.68		-0.34	4013.587	187	-0.26
3598.714	59	-1.02	3836.78		-0.08	4015.377	185	-0.42
3603.845	20	-2.82	3846.45		-0.31	4016.264	186	-0.82
3606.786	20	-2.41	3853.038	176	-0.23	4017.771	185	-0.26
3610.154	58	-0.43	3853.719	176	-0.22	4021.812	185	-0.17
3626.085	20	-2.41	3858.133	176	-0.01	4024.573	12	-0.99
3634.202	20	-1.92	3866.446	176	0.05	4026.539	185	-0.17
3635.46	19	0.04	3868.397	175	-0.12	4027.48		-0.03
3637.966	18	-1.97	3873.203	176	-0.27	4030.512	185	0.14
3642.675	19	0.14	3875.262	15	-1.64	4032.628	297	-0.92
3646.198	18	-1.65	3881.399	15	-2.30	4033.883	208	-0.70
3653.497	19	0.22	3882.147	175	-0.12	4034.884	208	-0.87
3654.592	18	-1.33	3882.313	176	-0.12	4035.828	208	-0.24
3658.097	19	-1.11	3882.892	176	0.37	4040.310	185	-0.79
3660.631	18	-1.43	3888.020	175	-0.60	4055.011	80	-0.65
3668.965	18	-1.31	3889.948	15	-2.32	4057.612	254	-0.26
3671.672	19	-1.10	3895.243	176	-0.08	4058.139	254	-0.26
3685.964	117	-0.84	3898.487	13	-2.28	4060.263	80	-0.64
3687.354	19	-2.20	3900.958	15	-1.69	4064.203	80	-0.86
3689.916	18	-1.30	3904.785	56	0.27	4065.094	80	-0.82
3694.445	117	-0.75	3911.185	175	-0.49	4071.2	254	-0.06
3698.183	222	-1.03	3914.334	15	-1.38	4076.37	9	-2.84
3698.43		-1.23	3914.751	14	-2.31	4078.471	80	-0.27
3700.08		-1.22	3919.822	130	-1.14	4079.708	207	-0.72
3702.291	83	-0.93	3921.423	14	-1.61	4082.456	80	-0.81
3704.295	117	-0.60	3924.527	13	-0.95	4099.166	207	-0.31
3707.549	177	-0.92	3926.319	292	0.13	4112.708	9	-1.76
3709.963	83	-0.45	3929.875	13	-1.07	4122.143	296	-0.16
3715.40		-1.64	3934.228	15	-2.21	4123.287	302	-0.22
3717.393	17	-1.26	3938.005	246	-0.23	4123.559	296	0.01
3722.568	17	-1.25	3947.770	14	-1.08	4127.531	296	-0.05
3724.59	131	0.25	3948.670	13	-0.47	4131.244	253	-0.50
3725.155	83	-0.34	3956.336	13	-0.45	4137.284	253	-0.07
3729.806	17	-0.35	3958.206	13	-0.16	4142.480	296	-1.04
3735.67		-0.43	3962.851	12	-1.17	4143.048	253	-0.10
3738.901	166	-0.95	3964.27	12	-1.17	4143.280	253	-0.09
3741.059	17	-0.21	3981.761	12	-0.34	4149.445	296	-1.10
3748.101	166	-0.45	3982.478	11	-1.33	4150.963	206	0.09
3752.860	17	-0.02	3984.313	188	-0.56	4154.865	221	-0.74
3753.623	17	-1.10	3985.25		-0.84	4159.634	163	-0.23
3766.445	82	-1.36	3985.580	188	-0.58	4166.314	163	-1.00
3771.652	17	-1.05	3989.758	12	-0.19	4169.330	163	-0.64
3774.331	16	-3.21	3994.683	188	-0.84	4171.018	206	-0.24
3786.043	57	-0.07	3998.635	12	-0.05	4183.294	220	-0.75
3788.80	16	-3.26	3999.336	188	-0.49	4186.119	129	-0.31
3789.293	115	-0.50	4002.466	188	-0.37	4188.694	220	-0.36
3795.903	115	-0.92	4003.789	188	-0.30	4200.752	220	-0.38

4203.465	220	-0.34	4404.276	219	0.17	4527.305	42	-0.51
4211.729	279	-0.52	4404.911	161	-0.76	4533.238	42	0.48
4224.795	301	-0.20	4405.694	78	-1.95	4534.782	42	0.28
4227.654	278	-0.46	4416.535	161	-0.75	4535.574	42	0.08
4237.889	284	0.15	4417.274	161	-0.13	4535.920	42	-0.16
4249.114	252	-0.40	4421.754	218	-0.12	4536.051	42	-0.24
4256.025	252	-0.12	4422.823	78	-1.15	4539.10		0.06
4258.523	252	-0.40	4424.401	243	-0.88	4544.688	42	-0.53
4261.609	252	-0.35	4425.840	78	-1.93	4548.764	42	-0.35
4263.134	162	0.23	4426.054	161	-0.41	4552.453	42	-0.30
4265.723	162	-0.75	4427.098	128	0.18	4555.069	266	-0.73
4266.827	252	-0.61	4430.023	267	-0.83	4555.486	42	-0.46
4270.139	251	-0.39	4430.366	113	-0.97	4557.857	270	-0.79
4272.440	44	-1.46	4431.284	218	-0.53	4558.092	262	-0.93
4274.584	44	-1.20	4432.60		-0.77	4559.920	112	-1.12
4276.441	148	-0.46	4433.578	267	-0.77	4562.637	7	-2.66
4278.231	200	0.32	4434.003	113	-0.62	4563.427	266	-0.50
4278.829	252	-0.75	4436.586	160	-0.67	4570.906		-0.53
4281.371	44	-1.36	4438.232	218	-0.78	4599.23		-0.17
4282.702	162	-0.09	4440.345	159	-0.41	4609.37		0.12
4284.988	148	-0.39	4441.272	160	-0.86	4617.269	145	0.39
4286.006	44	-0.33	4444.267	218	-0.92	4619.525	261	-0.79
4287.405	44	-0.44	4449.143	160	0.45	4623.098	145	0.11
4288.161	43	-2.20	4450.896	160	-0.21	4629.336	145	-0.39
4289.068	44	-0.28	4453.312	113	-0.05	4634.87		-0.46
4290.933	44	-0.40	4453.708	160	-0.01	4637.877	261	-0.31
4291.14		-0.11	4455.321	113	0.12	4639.369	145	-0.14
4295.751	44	-0.42	4457.428	113	0.26	4639.669	145	-0.19
4298.664	44	-0.07	4462.099	8	-3.11	4639.944	145	-0.22
4299.229	148	-0.31	4463.391	160	-0.66	4645.193	145	-0.56
4299.636	43	-0.93	4463.539	160	-0.50	4650.016	145	-0.64
4300.566	44	0.12	4465.807	146	-0.16	4656.048	145	-1.37
4301.089	44	0.25	4471.238	146	-0.15	4656.468	6	-1.35
4305.910	44	0.44	4474.852	113	-0.87	4667.585	6	-1.19
4308.514	79	-1.87	4479.724	146	-0.62	4675.118	77	-1.39
4311.654	205	-0.74	4480.600	146	-0.98	4681.908	6	-1.07
4314.356	45	-1.60	4481.261	146	0.15	4686.921	203	-1.04
4314.801	43	-0.30	4482.688	113	-0.84	4688.392	306	-0.32
4318.631	235	0.29	4489.089	146	-0.08	4690.827	76	-2.03
4321.655	235	-0.07	4492.540	184	-1.04	4691.336	75	-0.95
4325.134	235	0.11	4495.01		-0.57	4693.670	6	-2.72
4326.356	43	-1.13	4496.146	146	-0.08	4696.923	203	-0.96
4334.840	43	-2.20	4497.709	184	-1.03	4698.766	75	-1.04
4346.104	234	-0.40	4503.762	184	-0.71	4710.186	75	-1.34
4354.094	204	-0.77	4506.36		-0.78	4715.295	6	-2.69
4360.487	204	-0.45	4511.17		0.37	4722.603	75	-1.30
4368.941	245	-0.91	4512.734	42	-0.48	4723.171	75	-1.62
4369.682	290	-0.27	4515.610	184	-1.15	4731.172	202	0.08
4372.383	277	-0.32	4518.022	42	-0.33	4733.426	202	-0.61
4388.077	219	-0.80	4518.700	112	-0.89	4734.682	233	-0.75
4393.92		0.03	4522.798	42	-0.35	4742.129	202	-1.20

4742.791	233	-1.17	4973.051	173	-0.65	5186.61	215	-0.99
4747.680	233	-1.20	4975.344	283	0.07	5192.971	4	-1.01
4758.120	233	0.43	4977.731	173	-0.41	5194.043	183	-0.55
4758.913	41	-2.25	4978.191	173	-0.32	5201.096	183	-0.75
4759.272	233	0.51	4981.732	38	0.50	5206.059	276	0.79
4766.330	233	-0.67	4989.140	173	-0.22	5207.852	183	-0.63
4769.775	233	-0.93	4991.067	38	0.38	5210.386	4	-0.88
4771.103	41	-2.48	4995.062	216	-0.90	5212.271	215	-0.55
4778.259	232	-0.47	4997.099	5	-2.12	5219.697	4	-2.29
4781.718	41	-2.04	4999.504	38	0.25	5222.685	183	-0.62
4783.306	41	-2.92	5000.991	173	-0.03	5223.623	183	-0.56
4789.803	41	-2.91	5007.209	38	0.11	5224.301	183	-0.03
4792.482	26	-0.21	5009.652	5	-2.26	5224.558	183	-0.49
4796.210	260	-0.57	5013.284	173	-0.08	5224.928	183	-0.16
4797.983	260	-0.73	5014.185	5	-1.20	5238.560	37	-1.68
4799.797	242	-0.20	5014.277	38	-0.02	5246.143	282	-0.97
4805.416	260	-0.12	5016.162	38	-0.57	5246.574	37	-2.00
4808.531	305	-0.06	5020.028	38	-0.41	5247.293	183	-0.73
4811.074	158	-1.42	5022.871	38	-0.43	5250.95	37	-2.30
4812.240	260	-0.64	5024.842	38	-0.60	5252.185	4	-2.45
4812.906	41	-3.53	5025.570	173	0.08	5255.811	183	-0.64
4820.410	126	-0.44	5035.908	110	0.19	5259.976	298	-0.27
4825.445	250	-1.01	5036.468	110	0.13	5263.483	183	-0.79
4827.597	250	-0.62	5038.400	110	0.01	5265.967	156	-0.42
4836.125	241	-0.65	5039.959	5	-1.14	5266.49	36	-4.19
4840.874	53	-0.51	5040.642	38	-1.74	5282.378	74	-1.76
4848.487	201	-0.47	5043.578	38	-1.70	5283.441	156	-0.39
4856.012	231	0.46	5044.27		-0.91	5284.380	74	-1.89
4864.187	201	-0.86	5045.400	38	-1.98	5289.28	36	-2.96
4868.264	231	0.04	5048.208	199	-1.09	5295.781	74	-1.52
4870.129	231	0.13	5052.879	199	-0.33	5297.236	156	-0.47
4880.922	201	-1.03	5054.070	294	-0.71	5298.429	281	-0.35
4882.326	231	-0.66	5062.112	199	-0.46	5323.958	36	-3.11
4885.082	157	0.36	5064.068	294	-0.41	5328.72		-2.05
4899.910	157	0.13	5064.654	5	-0.99	5338.326	35	-1.94
4908.46	295	-0.68	5065.985	110	-1.07	5340.68	36	-3.26
4913.616	157	0.16	5068.332	294	-0.32	5341.50	316	0.49
4915.236	157	-1.02	5069.351	199	-0.58	5351.072	300	-0.14
4919.867	200	-0.25	5070.48		-0.87	5361.724	35	-3.13
4921.768	200	-0.11	5071.47	110	-1.06	5366.651	35	-2.63
4925.396	157	-0.92	5085.333	109	-2.89	5384.634	35	-2.75
4926.148	39	-2.29	5087.055	109	-0.99	5389.180	35	-2.21
4928.342	200	-0.14	5103.15		-0.94	5389.996	155	-1.09
4937.719	39	-2.31	5109.427	109	-1.39	5396.600	3	-3.18
4938.283	289	-0.01	5113.448	109	-0.78	5397.093	155	-0.83
4941.562	200	-1.00	5120.420	288	0.28	5401.32	35	-2.90
4948.183	200	-1.18	5145.465	109	-0.57	5404.023	259	-0.90
4958.26	52	-2.34	5147.483	4	-2.01	5408.940	3	-3.84
4964.713	173	-0.86	5152.105	4	-2.02	5409.609	155	-0.76
4966.04		-1.19	5173.742	4	-1.12	5426.256	3	-3.01
4968.566	173	-0.67	5186.329	183	-0.94	5429.139	259	-0.53

5436.703	51	-2.65	5774.037	309	0.40	6556.066	102	-1.07
5438.310	108	-2.23	5780.778	214	-1.08	6575.18	286	-0.11
5446.593	3	-3.32	5785.67	309	0.31	6599.112	49	-2.05
5446.593	259	-0.83	5785.979	309	0.28	6650.38		-2.90
5448.882	259	-1.00	5804.265	309	0.17	6657.03		-2.56
5449.155	107	-2.07	5812.827	309	-0.33	6666.548	101	-1.86
5453.646	108	-1.78	5823.679	239	-0.96	6677.25	274	-0.86
5460.502	3	-2.89	5832.470	309	-0.23	6716.679	273	-0.66
5471.198	106	-1.35	5866.453	72	-0.84	6743.124	48	-1.59
5472.696	107	-1.78	5903.317	71	-1.96	6745.56	226	-1.01
5473.517	259	-0.83	5818.548	71	-1.54	6861.47		-0.69
5474.228	108	-1.17	5922.112	72	-1.47	6873.92		-1.12
5474.449	259	-0.98	5937.806	72	-1.94	6913.19		-0.96
5477.695	265	-0.21	5941.755	72	-1.46	6933.15		-0.48
5481.426	265	-0.24	5953.162	154	-0.33	6943.70		-0.43
5481.862	106	-1.12	5965.828	154	-0.41	6996.63	256	-0.94
5488.210	265	-0.45	5978.543	154	-0.50	7004.60	256	-1.18
5490.151	107	-0.93	5999.003	198	0.08	7008.35	256	-1.22
5490.840	3	-3.42	5999.668		-0.68	7010.94	256	-1.22
5497.92	51	-2.93	6013.42		-3.18	7035.86	307	-0.45
5503.897	287	-0.14	6017.00		-3.73	7038.80	256	-0.63
5511.795	108	-1.69	6064.631	69	-1.68	7050.65	256	-1.21
5512.529	106	-0.46	6085.228	69	-1.39	7069.11	307	-0.12
5514.350	106	-0.39	6091.175	238	-0.42	7084.25	99	-3.32
5514.536	106	-0.32	6092.814	153	-1.38	7138.91	99	-1.61
5530.49		-0.09	6098.655	304	-0.13	7188.55	99	-1.87
5562.74		-2.95	6121.008	153	-1.33	7189.89	285	-0.22
5565.476	229	-0.42	6126.217	69	-1.35	7209.44	99	-0.57
5600.05		-3.43	6138.38	197	-1.37	7216.20	98	-1.29
5644.137	240	0.06	6146.225	153	-1.38	7244.86	99	-0.97
5648.570	269	-0.39	6149.743	197	1.29	7251.74	99	-0.82
5662.154	249	-0.11	6186.14	197	-0.96	7266.29	143	-1.67
5662.891	269	-0.39	6215.212	293	-0.24	7271.41	97	-2.34
5673.42		-0.47	6220.460	293	-0.23	7299.67	97	-2.01
5675.413	249	-0.20	6221.41	293	-0.49	7315.56		-1.39
5679.908	269	-0.90	6258.103	104	-0.36	7318.39	212	-1.00
5689.465	249	-0.47	6258.706	104	-0.27	7344.72	97	-1.04
5702.666	249	-0.65	6261.101	104	-0.48	7352.16	272	-1.26
5708.199	249	-0.98	6303.754	104	-1.57	7357.74	97	-1.12
5711.852	249	-0.04	6312.240	104	-1.55	7364.11	97	-1.21
5713.895	249	-0.94	6318.027	103	-1.89	7423.17	97	-2.79
5715.123	228	-0.49	6336.104	103	-1.73	7440.60	225	-1.04
5716.450	249	-0.75	6358.66		-2.57	7474.94	142	-2.12
5720.445	249	-1.09	6366.354	103	-1.57	7489.61	225	-1.04
5739.464	228	-0.18	6395.47		-2.73	7696.12	225	-1.24
5739.975	228	-0.33	6419.15	196	-1.50	7580.55	211	-1.53
5741.192	280	-1.16	6497.689	102	-1.94	7614.50	211	-1.39
5752.89	214	-1.35	6499.92		-4.19	7654.44	211	-1.16
5756.45	228	-1.39	6508.135	102	-1.89	7938.53	151	-2.48
5762.295	309	0.25	6546.276	102	-1.25	7949.17	125	-1.35
5766.330	309	0.26	6554.226	102	-1.22	7961.58	308	-0.17

7978.88	151	-1.17	8377.90	33	-2.03	8468.46	150	-1.51
7978.88	308	-0.77	8382.54	33	-2.04	8496.03	209	-1.80
7996.53	308	-0.10	8382.82	33	-2.38	8518.05	182	-1.80
8024.84	151	-1.17	8396.93	33	-2.22	8518.37	150	-1.64
8066.05	151	-2.60	8412.36	33	-1.94	8539.36	209	-1.90
8068.24	151	-1.17	8416.97	224	-1.61	8548.07	150	-1.65
8100.1		-2.59	8424.41	182	-1.88	8569.72	209	-2.18
8306.31		-0.54	8426.50	33	-1.25	8598.18	236	-2.17
8307.41	33	-2.86	8434.98	33	-1.14	8675.38	68	-2.10
8311.76		-0.82	8435.68	33	-1.02	8682.99	68	-2.51
8312.85		-0.88	8438.93	224	-1.19	8692.34	68	-2.87
8334.37	33	-3.20	8450.89	224	-1.21	8734.70	68	-3.04
8353.15	33	-3.13	8457.10	141	-2.55	8766.64	68	-2.93
8364.24	33	-2.16	8467.15	182	-1.77	8778.66	140	-2.53

W. Ansbacher, Y. Li and E.H. Pinnington

Lifetime measurements using pulsed laser excitation of fast ion beams

ABSTRACT

A review is presented of the Edmonton program of lifetime measurements using pulsed laser excitation of fast ion beams. Since 1985 measurements have been completed for the 3p and 4p levels of Mg II and Ca II respectively, the precision of these measurements being about 1%. Excellent agreement is found with the calculations of Theodosiou. Recently we have begun a more extensive study of some resonance levels in Fe II. Preliminary results for the levels of the z $^6G^o$ term show agreement with (less precise) previous experiments but differ significantly from the results of calculations by Fawcett and Kurucz.

INTRODUCTION

In 1985 we reported the first measurements using pulsed laser excitation of the 4p levels of Ca II. The precision of those measurements was about 5%, the major limitation being the high level of laser scattered light. Since then we have constructed a new chamber, designed both to minimize this problem and to increase the collection efficiency of the detection system. The lifetimes obtained using the new chamber had a precision of about 1.0%. They were in agreement with the earlier experiment but were significantly longer than all the calculations available at that time. Shortly after these results were published, a calculation by Theodosiou (1989) gave results in excellent agreement with our experiments. These results are summarized in Table 1.

Table 1. Summary of Beam-Laser Measurements of the Lifetimes (in ns) of the 4p Levels of Ca II. (Uncertainties shown in parentheses)

Reference	j=1/2	j=3/2
Ansbacher et al(1985)	6.96(.35)	6.71(.25)
Gosselin et al(1988)	7.07(.07)	6.87(.06)
Theodosiou (theory,1989)	7.045	6.852

STUDIES USING FREQUENCY-DOUBLED RADIATION

Following the success of our Ca II measurements, we decided to attempt a study of the 3p levels of Mg II. Here the excitation wavelengths (279.6 and 280.3nm) require the use of a frequency-doubling crystal and, prior to the experiment, it was not clear that our Lumonics EPD-330 dye laser system would deliver sufficient power for a useful signal. In the event, we were able to measure the lifetimes of the 3p levels to a precision of about 1%, these results showing agreement with the most recent calculation.

Table 2. Lifetimes of the Mg II 3p Levels(ns) (Uncertainties shown in parentheses.)

Reference	j=1/2	j=3/2
Ansbacher et al(1989)	3.854(.030)	3.810(.040)
Theodosiou and Curtis (theory, 1988)	3.872	3.842

The close coincidence of the 3s-3p and 3p-3d transition wavelengths in Mg II permits two further experiments. Firstly, two-step excitation of the 3d(3/2) level is possible by reflecting the laser beam back along its path through the chamber. The Doppler shifts are arranged so that the 3s-3p(1/2) transition is excited by the first passage of the laser beam and the 3p(1/2)-3d(3/2) transition is excited by the return passage. Secondly, direct two-photon excitation of the 3d(5/2) level is possible using a single passage of the laser having a wavelength which differs by only 0.13nm from that of the 3s-3p(3/2) transition. Further details of these two experiments are available elsewhere (Ansbacher et al, 1989). The important point here is that they are possible using our equipment, which provides strong evidence that we are still saturating the single-photon excitations at 280nm.

MEASUREMENTS FOR SINGLY-IONIZED IRON.

There are two main factors that make measurements in Fe II more difficult than those just discussed. Firstly, the excitation wavelengths are even shorter. Our preliminary measurements indicate that at these wavelengths we are not able to saturate the excitation transition completely. This has the serious consequence that the observed signal depends on the laser power, which is difficult to maintain constant over the million or so pulses required for one decay curve. Secondly, the lowest configuration of Fe II contains many levels within 1eV or so of the ground state. Since only a small fraction of the ion beam is in a given level, the background contribution from gas excitation and laser scattering is larger for a given signal level than in our previous experiments. The measurements we have made to date for the z $^6D^0$ levels are summarized in Table 3.

Table 3. Lifetimes of the Fe II z $^6D^0$ Levels. (Uncertainties shown in parentheses.)

J-Value	Lifetime (ns)				
	(1)	(2)	(3)	(4)	(5)
9/2	3.78(.05)	3.7(.2)	3.9(.2)	2.97	3.41
7/2	3.79(.06)	3.8(.3)	4.0(.2)	2.99	3.43
5/2	3.75(.07)	3.8(.3)	4.0(.2)	2.99	3.44
3/2	3.89(.08)	3.7(.2)	3.9(.3)	3.00	3.45
1/2	3.94(.08)	3.8(.3)	4.0(.3)	3.00	3.46

(1) Fast beam-laser excitation (This work).
(2) Laser-ind. fluor. (Schade et al, 1988).
(3) --------- (Hannaford and Lowe, 1983).
(4) RHF calculation (Fawcett, 1987).
(5) Semi-emp. calculation (Kurucz, 1981).

The higher uncertainties for lower j-values reflect the progressively smaller fraction of the ion beam that is in the lower state involved in the excitation. Even though these measurements are rather preliminary, it is clear that our technique gives results in agreement with previous, less precise, laser measurements. All the experiments differ significantly from the calculations by Fawcett and Kurucz.

REFERENCES

Ansbacher, W., A.S. Inamdar and E.H. Pinnington, 1985 - Pulsed laser measurements of the lifetimes of the 4p levels of Ca II. In: Phys. Lett. 110A, 383-386.

Ansbacher, W., Y. Li and E.H. Pinnington, 1989 - Precision lifetime measurements for the 3p levels of Mg II using frequency-doubled laser radiation to excite a fast ion beam. In: Phys. Lett. A. (in press).

Fawcett, B.C., 1987 - Computed f-values and energy levels for Fe II. In: At. Data Nucl. Data Tables 37, 333-364.

Gosselin, R.N., E.H. Pinnington and W. Ansbacher, 1988 - Measurements of the lifetimes of the 4p levels in Ca II using laser excitation of a fast beam. In: Phys. Rev. A. 38, 4887-4890.

Hannaford, P. and R.M. Lowe, 1983 - Radiative lifetimes in Fe II using selective laser excitation. In. J. Phys. B. 16, L43-L46.

Kurucz, R.L., 1981 - Semi-empirical calculation of gf-values, IV: Fe II. In: Smithsonian Astrophysical Observatory Special Report 390.

Schade, W., B. Mundt and V. Helbig, 1988 - Radiative lifetimes of Fe II levels. In: J. Phys. B. 21, 2691-2696.

Theodosiou, C.E., 1989 - Accurate calculation of the 4p lifetimes of Ca^+. In: Phys. Rev. A., 39, 4880-4883.

Theodosiou, C.E. and L.J. Curtis, 1988 - Accurate calculations of the 3p and 3d lifetimes in the Na sequence. In: Phys. Rev. A. 38, 4435-4445.

AUTHORS' ADDRESS

Department of Physics,
University of Alberta, Edmonton, Alberta,
Canada, T6G 2J1.

M.D. Davidson, E.P. Buurman,
A. Dönszelmann and C. Snoek

Renormalization of oscillator strengths in aluminum

ABSTRACT

Renormalization of the lifetime values and oscillator strengths of aluminum levels is necessary. The data available are not sufficiently reliable. Accurate values obtained until now are given; plans for future experiments are described.

DESCRIPTION

Aluminum is an important element in astronomical spectra. A large number of AlI lines are present in the solar spectrum. Moreover, the element is of physical interest: it demonstrates strong configuration interaction effects, especially the $3s^2nd\ ^2D$ series, which is perturbed by the $3s3p^2(^1D)\ ^2D$ term. The perturbing term without interaction is situated between the states n=4 and n=5. The interaction affects the whole series and its influence on lifetimes, level positions etc. can be observed up to the high n values (Buurman, 1989a).

For astronomical applications the oscillator strengths in the lowest part of the spectrum are of special interest. Penkin and Shabanova (1965) published experimental values of oscillator strengths of the sharp and diffuse series for n<12. The experimental values show a discontinuity between n=4 and n=5, which is in accordance with calculations of Weiss (1974) and others. Penkin and Shabanova's values for the oscillator strengths have been normalized by Wiese using one accurate lifetime value obtained by Buddick for the 3p-3d transition (Wiese, 1969 and references therein). As far as we know these are upto now, except for measurements by Buurman et al (1986,1989b), the only experimental data for the oscillator strengths of this series.

Jönsson et al (1984) have measured the lifetimes along the series upto n=12. The claimed accuracy is 10%. These lifetime values may be compared with the normalised values from Wiese. However, with the exception of n=4, the deviations are between +25 and +30 %.

A renormalization of the experimental data from Penkin and Shabanova based on new accurate lifetime measurements is therefore required. We are undertaking such a systematic study of the lifetime values of the lowest part of the nd ^2D and ns ^2S series together with a study of other observables for the higher members of these Rydberg series.

In the experiment aluminum atoms in an atomic beam are excited by a short pulse of dye laser radiation (pulse duration 6ns). Population of the levels of the ^2P series is achieved by non-resonant two step excitation. The levels of the ^2S and ^2D series are excited directly by frequency-doubled radiation from the dye laser.

The fluorescent light from the excited atoms is detected by a fast photomultiplier (risetime ~ 1 ns). By optical filtering corrections for cascades are made. The signals are recorded by a fast multichannel system coupled to a personal computer. Averaging over a large number of laserpulses increases the signal/noise ratio to an acceptable level.

Normal precautions are taken to prevent influence of multiple scattering, collisions, flight out of view and saturation of the photomultiplier tube and electronic devices.

Table 1. Lifetimes in AlI (in ns). Error limits are given in parentheses

	Buurman et al. (1986,1989b) experiment	theory	Jönsson (1984) experiment	Wiese (1969)
$4s^2S_{1/2}$	6.92 (7)	5.54		6.8
$5s^2S_{1/2}$	19.8 (5)	16.1	24 (4)	25
$4p^2P_{1/2}$	65 (2)	52.9		
$4p^2P_{3/2}$	60.5 (9)	52.9		
$5p^2P_{1/2,3/2}$	275 (8)	200		
$3d^2D_{3/2,5/2}$	14.0 (2)	12.0	16 (3)	13.7
$4d^2D_{3/2,5/2}$	29.5 (7)	26.4	29 (4)	37.9

Experimental and calculated values for the lifetimes of the lowest part of the spectrum obtained till now, are given in table 1.

REFERENCES

Buurman, E.P., A. Dönszelmann, J.E. Hansen and C. Snoek, 1986 - Oscillator Strengths of transitions between low-lying levels in the aluminum spectrum. In: Astronomy and Astrophys, 164, 224

Buurman, E.P., O.J. Koning and A. Dönszelmann, 1989a - Study of the ns ^2S and nd ^2D Rydberg series in aluminum. In: J. Phys. B., accepted for publication.

Buurman, E.P., A. Dönszelmann, 1989b - New determination of the radiative properties of the $4p\,^2P_{1/2,3/2}$ levels in aluminum and the $5p\,^2P_{1/2,3/2}$ levels in gallium. In: Astron. Astrophys., accepted for publication.

Jönsson, G., S. Kröll, H. Lundberg and S. Svanberg, 1984 - Natural radiative lifetimes in the $^2S_{1/2}$ and $^2D_{5/2,3/2}$ sequences of aluminum. In: Z. Phys. A316, 259

Penkin, N.P., L.N. Shabanova, 1965 - Absorption spectra of aluminum, gallium, indium, and thallium atoms. In: Opt. Spectr., 18, 896

Weiss, A.W., 1974 - Series perturbations in atomic spectra: Superposition-of-configurations calculations on AlI and AlII. In: Phys. Rev., 9, 1524

Wiese, A.W., M.W. Smith and B.M. Miles, 1969 - Transition probabilities, NSRDS-NBS 22, vol.2, 47

AUTHOR'S ADDRESS

Zeeman-Laboratorium,
Plantage Muidergracht 4,
1018 TV Amsterdam, The Netherlands.

W.E. v.d. Veer, D.Ph. v.d. Blonk,
A. Dönszelmann and C. Snoek

Lifetime measurements in neutral cadmium and copper

ABSTRACT

Lifetimes of energy levels in neutral atoms are discussed. Two different sources are used for the creation of free atoms. Results in Cd and Cu are given.

DESCRIPTION

Accurate lifetimes in neutral atoms can be obtained by several laserspectroscopical methods. The most direct way is by exciting (metastable) atoms in a beam with pulsed laserlight. The decay(s) are monitored by detecting the fluorescent light. The beam source can either be thermal or a hollow cathode.

Cd - The atomic beam as a source for neutral atoms. For lifetime measurements in Cd a resistively heated oven at a temperature of approximately 620 K was used to produce an atomic beam. A frequency-doubled, pulsed dye laser at a wavelength of 326 nm excites the atoms in the beam to the $3d^{10}5s5p\ ^3P_1$ level (fig. 1). The fluorescence signal is observed with a photomultiplier. Measured intensities as a function of time are fitted to an exponential giving the lifetime of the $^3P_1$ level. Special care was taken to remove Zeemanbeats from the signal.

A second pulsed laser at a wavelength of 479 nm populates the 5s6s $^3S_1$ level. With the same technique the lifetime of this level can be determined. The level however decays into the 5s5p $^3P_2$, $^3P_1$ and $^3P_0$ levels. The relative intensities of these lines are determined using interference filters. The fluorescence radiation of these three spectral lines are detected separately with one photomultiplier, while monitoring the total intensity with another photomultiplier. This allows us to calculate the branching ratios and hence the oscillator strengths. Results are given in table 1 and table 2.

Table 1. Lifetime values in ns.

level	this work	Lit. values
5s5p $^3P_1$	2420 ± 60	2390 ± 40 *)
5s6s $^3S_1$	10.2 ± .3	9.2 ± .3 **)
		10.6 ± .8 ***)

*) Byron, **) Laniepce, ***) Verolainen.

Table 2. Branching ratios and oscillator strengths from the 5s6s $^3S_1$ to the 5s5p ^3P levels:

transition	ratio	osc. strength
$^3S_1$ - $^3P_2$	.629 ± .038	.143 ± .010
$^3S_1$ - $^3P_1$	.249 ± .015	.084 ± .006
$^3S_1$ - $^3P_0$	.122 ± .011	.118 ± .011

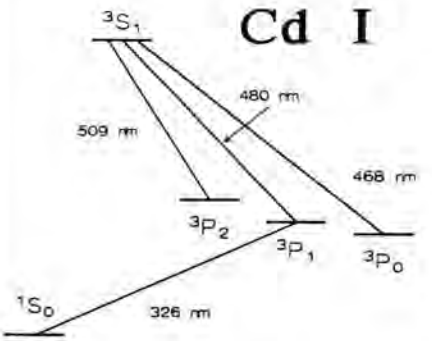

fig. 1. Termscheme of CdI.

Hollow cathode as a source for metastable Cu atoms. For lifetime measurements of highly excited levels a hollow cathode is applied. Metastable atoms produced in a pulsed hollow cathode discharge, diffuse through a hole in the cathode into the excitation region. A pulsed laser excites the atoms into the level under examination. The lifetime of this level is measured by analyzing the fluorescence radiation. Due to the large velocity of some of the sputtered atoms, the hollow cathode is less suited for the measurement of longer lifetimes (>100ns); the atoms or ions have left the detection region before decaying. Moreover straylight from the discharge causes a background which forms a severe disturbance.

The apparatus (Carlsson et al. 1987) consists of a water cooled, electrically insulated tube. A hollow target with a 1 mm hole in the centre is mounted at one side as a

cathode. A tungsten electrode at the other side of the tube is the anode. The tube is filled with Ar at pressures up to 1,5 mbar. A keep-alive current (I ≈ 20 mA) provides Ar^+ ions, needed to start the pulsed discharge. The maximum current of the main discharge is 1000 A. The pulse is switched by a thyristor. The minimal length of the discharge is 9 μs, limited by the characteristics of the thyristor. During the main discharge Ar^+ ions are accelerated to the cathode. Some of the target's atoms are sputtered directly into the orifice in the cathode. Others loose much of their velocity in collisions and diffuse through the hole. Consequently two clouds of metastable atoms, emerge with a time interval of approximately 20 μs. The first cloud consists of particles with a high velocity and is therefore only useful in case of short lifetimes. This cloud is more stable than the second one. The peak number of metastables atoms in the clouds is comparable. The amount of metastables produced by the discharge depends strongly on the discharge characteristics. Since these are not completely understood, an optimum has to be found experimentally.

A copper target was used to generate $3d^9\ 4s^2\ ^2D_{3/2,5/2}$ metastables (fig. 2). The metastable atoms are monitored by excitation to the $3d^{10}\ 4p\ ^2P_{1/2}$ level with a pulsed laser at a wavelength of 578 nm. This level decays radiative into the $3d^{10}\ 4s\ ^2S_{1/2}$ ground level. The amplitude of the fluorescence is a measure for the number of metastables. The lifetime measured 7.3 ±.3 ns, is in good agreement with values from literature (Carlsson et al. 1987).

Many CuI lines occurring in the solar spectrum are situated in the 300 nm region, starting from a metastable state. We will undertake a systematic study of these lines.

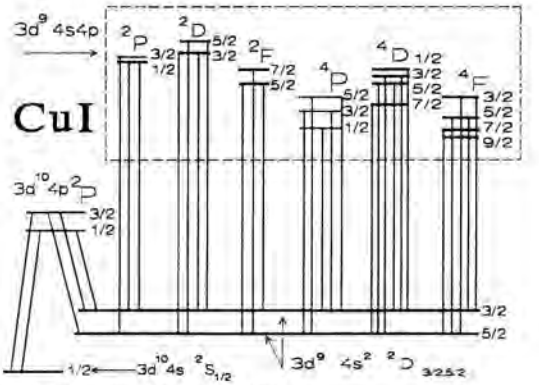

fig. 2. Termscheme of CuI.

REFERENCES

Byron,F.W., M.N. McDermott and R. Novick, 1964, Self broadening of optical double resonance lines in cadmium. In Phys. Rev. 134, A615.

Carlsson,J.,A. Dönszelmann,H. Lundberg,A. Persson,L. Sturesson, and S. Svanberg, 1987, Natural lifetimes in the $^2S_{1/2}$ and $^2D_{3/2,5/2}$ sequences in neutral copper (and references therein). In Z. Physik D6, 125.

Laniepce, B.,1968, Mesure de la duree de vie du niveau 6^3S_1 de cadmium et de section efficaces de collision de divers gaz pour ce niveau. In Journ. Physique, T29, 427.

Verolainen,Ya.F. and A.L. Osherovich, 1966, The lifetimes of certain levels of mercury and cadmium. In Opt. Spectr. XX,517.

AUTHOR'S ADDRESS

Zeeman-Laboratorium,Plantage Muidergracht 4, 1018 TV Amsterdam, the Netherlands.

R.R. Haar, T.J. Kvale, D.G. Ellis,
I. Martinson and L.J. Curtis

Lifetime measurements of core excited quintet levels in carbon I

ABSTRACT

J dependent lifetimes for the $2s2p^2 3s\ ^5P$ levels in C I have been studied by beam foil measurements and by multiconfiguration relativistic Hartree-Fock calculations. The experimental lifetimes $\tau(J=3)=2.5(5)$ ns and $\tau(J=1,2)=0.3(1)$ ns indicate the presence of differential autoionisation channels.

INTRODUCTION

Although the singlet and triplet spectra of C I have been comprehensively studied, only the $2s2p^3\ ^5S$ and $2s2p^2 3s\ ^5P$ terms have been established for the core-excited quintet system (Edlén 1947, Shenstone 1947). As shown in Fig.1, the ^5P levels lie above the first (doublet) ionisation limit, but well below its parent (quartet) ionisation limit. Thus autoionisation to the triplet continuum is energetically possible, but forbidden to Coulomb interactions in LS coupling by the $\Delta S=0$ selection rule. Intermediate coupling opens autoionisation channels through triplet-quintet mixing and leads to lifetimes that are strongly J-dependent. In order to investigate these radiative and autoionisation effects, we have performed a combined theoretical and experimental study of the lifetimes of the individual fine structure levels of the $2s2p^2 3s\ ^5P$ term. The experimental portion was carried out by beam foil excitation methods, and the theoretical calculations were made using the multiconfiguration Hartree-Fock program of Cowan, which includes both radiation and autoionisation.

Figure 1

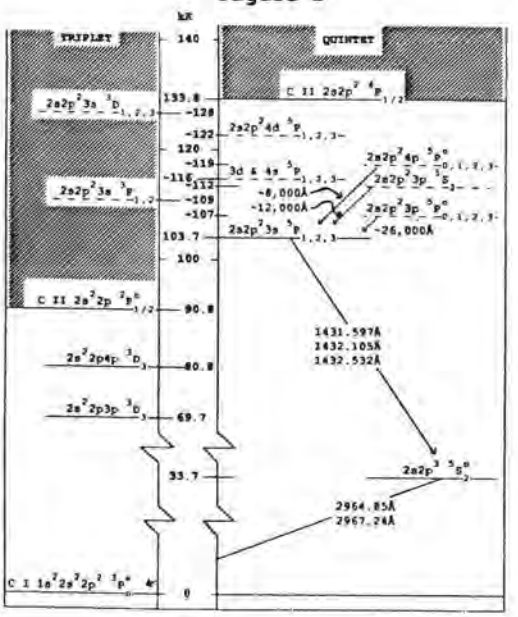

EXPERIMENT

Time resolved carbon spectra were obtained by directing beams of 100-200 keV C^+ ions from the University of Toledo 330 kV Danfysik heavy ion accelerator through a translatable 2 $\mu g/cm^2$ carbon foil. At these energies the beam loses approximately 3.5 keV in traversing the foil. The wavelength range 1150-1800 Å was studied, using an Acton 1 m normal incidence vacuum monochromator equipped with a solar blind EMI photomultiplier at the exit slit. The wavelength resolution used was 0.8 Å and the time window was set at 0.3 ns, values chosen to optimise the necessary compromises between resolution and signal intensity that are inherent in the beam-foil light source. Lifetimes were measured by recording the intensity of the spectral lines as a function of the distance from the foil. Many known lines from C I and C II were identified, and their relative intensities were used to select a beam energy that is well suited to the study of C I. Lifetime measurements of many of the singlet and triplet levels were also made. The results agreed well with earlier work, and served as an additional check of the determination of beam energy and energy loss in the foil.

TIME RESOLVED DEBLENDING

The wavelength separations of the lines are about 0.5 Å, which creates special problems. While the beam foil source copiously populates these excited core states, its inherent Doppler broadening precludes them

from being completely resolved spectroscopically. However, since these lines were found to be relatively free of cascades, blends, and backgrounds, it was possible to determine the lifetimes of the individual fine structure levels by performing a three dimensional array of intensity vs wavelength vs time measurements. Fig.2 shows a sample decay curve, indicating

Figure 2

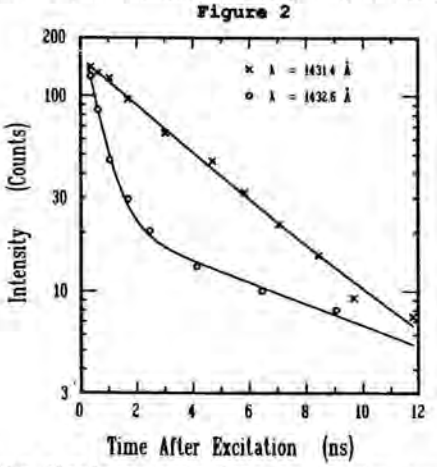

the distinct variation in lifetime content over the unresolved multiplet profile. The experimental lifetimes show a strong J-dependence with $\tau(J=3)=2.5(5)$ns and $\tau(J=1,2)=0.3(1)$ns. The radiative branch for each of these decays was measured in emission by Boldt (1963) using an intensity calibrated wall stablised arc. Assuming statistical populations, these measurements indicate that the radiative rates are essentially J independent . Combining the lifetime and emission measurements permits experimental determination of the J-dependent autoionisation rates.

THEORETICAL CALCULATIONS

In order to provide a theoretical comparison, the Cowan suite of programs RCN-RCG (Cowan 1981) was used to compute the autoionisation rates of the ^{5}P levels. The calculation included interactions among eight even and seven odd parity configurations. The autoionisation transition $2s2p^2 3s \rightarrow 2s^2 2p\varepsilon p$ was calculated using an outgoing electron energy of 0.116 Ry, computed from the observed position of the $2s2p^2 3s\ ^5P$ term and the ionisation potential. The autoionisation rate is J-dependent because the spin-orbit mixing with nearby triplet levels is J-dependent. This mixing is determined by the spin-orbit interaction strength and by the energy intervals between the ^{5}P and the other $2s2p^2 3s$ terms. The former can be determined empirically from the ^{5}P fine structure; the latter cannot because the energies of the other terms are not known.

In order to investigate the possibility of cascade repopulation from higher lying $2s2p^2 n\ell$ quintet levels, approximate calculations of some of these levels and their decay rates were made. These are indicated on Fig.1, but it should be emphasised that these are only order of magnitude estimates, and not of spectroscopic accuracy. The results indicated that, although $2s2p^2 3p$ quintet levels which have infrared transitions to the levels of interest do exist, they have very low ($<10^7$/s) radiative transition rates. Thus these theoretical results lend considerable support to our interpretation of the source of the J-dependent meanlives.

ACKNOWLEDGEMENTS

This work was supported by the US Department of Energy, Office of Basic Energy Sciences, Division of Chemical Sciences, under Grants DE-FG05-88ER13971 (TJK) and DE-FG05-88ER13958 (LJC).

REFERENCES

Boldt, G. 1963 Z.Naturforschung **18A**, 1107-

Cowan, R.D. 1981 *The Theory of Atomic Structure and Spectra*, Univ.Cal.Press, Berkeley

Edlén, B. 1947 Nature **159**, 129-130.

Shenstone, A.G. 1947 Phys.Rev. **72**, 411-414.

AUTHORS' ADDRESS

Department of Physics and Astronomy, University of Toledo, Toledo Ohio 43606 USA

E. Träbert, G. Möller, A.E. Livingston and P.H. Heckmann

Wavelength and lifetime measurements on intercombination lines of Ag XVIII, Ag XVII and Ag XVI (Zn I, Ga I, and Ge I-like)

ABSTRACT AND INTRODUCTION

Intercombination lines are frequently used in the diagnosis of solar and terrestrial plasmas. A number of recent review papers have been devoted to the subject (see Träbert et al. 1988, Ellis et al. 1989). Much of the more recent progress in the identification of $\Delta n=0$ intercombination transitions has been achieved by exploiting the time resolution inherent in the observation of foil-excited fast ion beams. The present study gives results of such work on Ag ions of the isoelectronic sequences of Zn, Ga and Ge. The results are compared with predictions from semi-empirically scaled and or ab-initio calculations.

EXPERIMENT

The experiment was done at the Bochum 4 MV Dynamitron tandem accelerator laboratory. Ag ions of energies of 19 MeV and of 25 MeV were excited by being passed through a thin carbon foil. A grazing-incidence spectrometer equipped with a low dark rate channeltron detector analyzed the light emitted by the ion beam at right angles. Further details of the experimental apparatus and procedures are given elsewhere (Träbert et al. 1988, Träbert 1989).

Spectra were recorded in the wavelength range λ = 18 - 70 nm, at various distances downstream of the foil. Decay curves were recorded at the positions of all sufficiently strong intercombination lines and were analyzed by multi-exponential computer fits. The results are listed in table 1.

DISCUSSION

A lifetime study of the Ag XVIII intercombination line (λ=35.1804nm, Churilov et al. 1988) has been reported by Träbert (1989) and corroborated by new decay curve data. The agreement with the results of an ab-initio MCRRPA calculation (Huang et al. 1985) is excellent. The results of a semi-empirically adjusted Hartree-Fock Relativistic calculation (Biémont et al. 1989) deviate considerably from these results, probably because of a non-optimum choice of the scaling parameters (Fig. 1). The low-Z trend of the latter, however, seems to be closer to experiment than that of the MCRRPA calculation.

The intercombination lines in Ga- and Ge-like Ag have been identified in the wavelength range λ = 32 - 40 nm, in rough agreement with various calculations. The lifetime of the Ag XVII 4 $^4P_{1/2}$ level has been established from decay curves recorded at the $^2P^o_{1/2}$ - $^4P_{1/2}$ transition at λ = 35.908 nm. The Ag XVII 4 $^4P_{3/2}$ level has two decay branches. The $^2P^o_{3/2}$ - $^4P_{3/2}$ line (at λ = 39.695 nm) is the stronger one and yielded a lifetime of 8.6 ns.

The Ga-like $^2P^o_{3/2}$ - $^4P_{5/2}$ line at 36.439 nm is blended with the Ge-like $^3P_1$ - $^5S^o_2$ at 36.551 nm. The predicted lifetimes of both levels involved (see table 1) differ by only about 60%. This makes it almost impossible to separate the two major decay components in the superimposed experimental decay curves. The observed effective decay time of 1.3 ns is compatible with a range of pairs of lifetimes of the two levels. This "time blend" can be partly disentangled by a lifetime measurement on the other decay branch of the Ge-like quintet level, $^3P_2$ - $^5S^o_2$, at 38.66 nm.

These are the first lifetime measurements on intercombination transitions in Ga- and Ge-like ions. The lifetimes of these levels as calculated by different codes scatter and also differ from the experimental findings by 10 to 30%. However, this present mismatch may be expected to decrease when dedicated calculations will be done.

ACKNOWLEDGMENT

E.T. presently enjoys financial support by the Max Kade Foundation and the Alexander von Humboldt Foundation (Feodor Lynen Program).

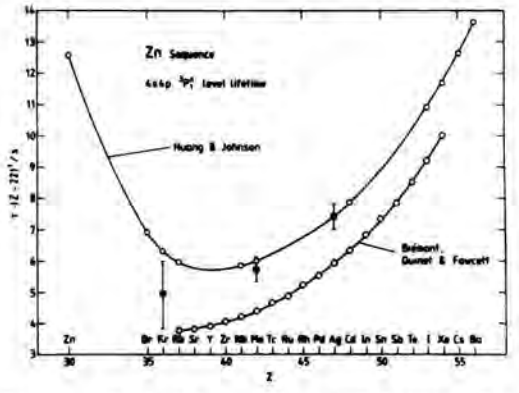

Fig. 1: Scaled transition probability of the intercombination transition in the Zn I sequence. Experimental data: Kr (Pinnington et al. 1984), Mo and Ag (Träbert 1989 and this work), Theoretical predictions: Huang et al. (1985), Biémont et al. (1989)

Table 1: Lifetimes of the lowest levels in the high-multiplicity term systems of Ag XVIII (Ag^{17+}), Ag XVII (Ag^{16+}) and Ag XVI (Ag^{15+}).

Spectrum	Level	Lifetime τ / ns Experiment	Theory
XVIII	$^3P^o_1$	1.20±0.06	1.224[a,b]
		1.18±0.08[c]	0.974[d]
XVII	$^4P_{1/2}$	1.05±0.10	1.277[b]
			0.905[e]
XVII	$^4P_{3/2}$	8.60±0.40	6.750[b]
			6.047[e]
XVII	$^4P_{5/2}$	1.13±0.15	0.999[b]
			0.941[e]
XVI	$^5S^o_2$	2.10±0.30	1.52[b]

a Huang et al. (1985)
b Fawcett (1988)
c Träbert (1989)
d Biémont et al. (1989)
e Kaufman (1988)

REFERENCES

Biémont, E., Quinet, P., and Fawcett, B.C., 1989 - Energy levels and transition probabilities along the zinc isoelectronic sequence, in Physica Scripta, 39, 562

Churilov, S.S., Ryabtsev, A.N., and Wyart, J.-F., 1988 - Identification of n=4, Δn=0 transitions in the spectra of nickel-like and zinc-like ions through tin, in Physica Scripta, 38, 31

Ellis, D.G., Martinson, I., and Träbert, E., 1989 - Intercombination transitions in heavy ions, in Comm. At. Mol. Phys., 22, 241

Fawcett, B.C., 1988 - (private communication, results from Hartree-Fock Relativistic calculations)

Huang, K.N. and Johnson, W.R., 1985 - Resonance transitions of Mg- and Zn-like ions from multiconfiguration relativistic random- phase approximation, in Nucl. Instrum. Meth., B9, 502 (1985)

Kaufman, V., 1988 - (private communication, results from Cowan code calculations)

Pinnington, E.H., Ansbacher, W., and Kernahan, J.A., 1984 - Energy level and lifetime measurements for Kr VII, in J. Opt. Soc. Am., B1, 30

Träbert, E., Heckmann, P.H., Hutton, R., and Martinson, I., 1988 - Intercombination lines in delayed beam-foil spectra, in J. Opt. Soc. Am., B5, 2173

Träbert, E., 1989 - Lifetime of the 4s4p $^3P^o_1$ level in foil-excited Mo^{12+} and Ag^{17+} ions, in Physica Scripta, 39, 592 (1989)

AUTHORS' ADDRESSES

E. Träbert*, G. Möller, P.H. Heckmann, Experimentalphysik III, Ruhr-Universität Bochum, D-4630 Bochum 1, FRG

A.E. Livingston, University of Notre Dame, Notre Dame, IN 46556, U.S.A.

* Present address (leave of absence): Harvard College Observatory, Mail Stop 50, 60 Garden Street, Cambridge, MA 02138, U.S.A.

P. van der Westhuizen, F.J. Coetzer and T.C. Kotzé

Cascade-corrected beam-foil lifetimes of levels in N III

ABSTRACT

Nitrogen ions from a 5.5 MV Van de Graaff accelerator have been used in beam-foil studies of nitrogen in the wavelength region 200.0 - 500.0 nm. The arbitrarily normalised decay curve (ANDC) method have been used to determine the cascade-corrected radiative lifetimes of the 3p $^4P_{5/2,3/2,1/2}$ levels. These results are compared with other experimental lifetimes.

INTRODUCTION

The beam-foil excitation technique has been used to study different levels in N III. It is essential to take into account the influence of all cascading levels on the population of the primary level. In the early beam-foil experiments, corrections for cascading were performed by fitting a sum of exponentials to the decay curve. It has been realized since that, although this method in some cases may produce surprising accurate results, it can lead to appreciable errors. The most successful cascade-correcting methods all involve measurements of the transitions from all the cascading levels and including these results explicitly in the analyses. In this investigation we account for repopulation of the primary levels by using the ANDC (Arbitrarily Normalized Decay Curve) technique (Curtis, 1971). The lifetimes of the 3p ^4P_J levels in N III have been the subject of several studies during the past two decades. The fact that these experiments were performed in the early days of beam-foil spectroscopy, when the effect of cascade repopulation was underestimated to a considerable extent, prompted this investigation.

EXPERIMENTAL

The experiments were performed at the National Accelerator Centre (NAC) at Faure using a 5.5 MV single ended vertical Van de Graaff (HVEC model CN) accelerator. A nitrogen ion beam, with a post-foil beam current of approximately 4 μA, was sent through carbon foils with typical areal densities of between 5 and 15 $\mu g.cm^{-2}$. In the case of obtaining intensity decay curves for primary and cascading levels we used foils with the same areal densities and we also changed the foils sufficiently often to prevent any possible effect due to thickening of the foils.

A spectrum was recorded between 200 and 500 nm at beam energies of 0.5, 1.0 and 2.0 MeV, using spectrometer slit widths of 100 μm. The spectrometer was then refocused and the spectra were rescanned in the regions of special interest to ensure the detection of possible blends.

RESULTS AND DISCUSSIONS

The identification of the observed spectra was accomplished with the aid of the tables of Striganov and Sventitskii (Striganov, 1968). As a first step in the data analyses the decay curves were analyzed via a curve-fitting technique using the computer program DISCRETE (Provencher, 1976), fitting a sum of exponentials to each curve. The decay parameters of the primary and cascading levels were then used as input data in the computer program CANDY (Engström, 1982), which was used to perform the ANDC analyses. The cascade-corrected lifetimes obtained from the ANDC analyses are given in Table 1. The uncertainty of the lifetimes quoted not only takes into account the uncertainty in the results given by CANDY, but also other effects such as the uncertainty in the beam velocity, etc.

Table 1: N III radiative lifetimes.

	Lifetimes (ns)	
Level	This work	Other experiments
3p $^4P_{5/2}$	5.26 ± 0.36	5.2[a] [5.4, 5.3][b] [5.4, 5.8][c]; [5.84, 5.71][d]
3p $^4P_{3/2}$	5.63 ± 0.36	7.3[b]; 9.8[e]; [5.67, 5.71][d]
3p $^4P_{1/2}$	5.54 ± 0.36	

(a) Denis, 1968; (b) Pinnington, 1970;
(c) Pinnington, 1969; (d) Lewis, 1967; (e) Fink, 1968.

Decays of the 3p ^4P_J levels occur via transitions to the 3s $^4P^0_J$ levels at 335.4 - 337.4 nm. The spectral analysis showed a few completely resolved lines and decays were therefore measured at 336.7, 337.4, 336.2 and 335.8 nm. A decay was also recorded at 335.5 nm corresponding to a blend between transitions from the J = 5/2 and J = 3/2 fine structure components of the 3p ^4P term at 335.38 and 335.43 nm. The curve-fitting results of all these levels were very similar, yielding a two component best fit with primary lifetimes between 5.2 and 5.7 ns and a growing-in component of approximately 0.8 ns. This short-lived growing-in component indicated that the 3p ^4P_J levels may be subjected to the influence of cascading levels with a short lifetime.

A partial energy level diagram indicating the relevant terms and transitions as well as the decay curves of the primary and cascade levels are shown in Fig. 1.

The possible cascading levels are transitions from the 3d $^4D^0_J$ and 3d $^4P^0_J$ levels. The 3d $^4D^0_J$ levels decay to the 3p ^4P_J levels via transitions between 644.5 and 648.8 nm but these transitions lie outside the de-

tection range of our spectrometer system. To obtain the decay constants of the 3d $^4D^0_J$ levels we therefore used the decay channel with the 3p $^4D_{5/2}$ lower level at 432.4 nm. This posed no problem as it is well known that any decay branch can be used in the ANDC treatment of cascading. The other cascading level i.e. the 3d $^4P^0_J$ levels decay to the 3p ^4P_J levels at 526.1 nm, but again this transition lies outside the detection range of the spectrometer. Therefore the decay of this cascading level was measured via the 3d $^4P^0_{5/2}$ - 3p $^4D_{7/2}$ transition at 379.3 nm. These cascading levels were used, one at a time as well as simultaneously as input to CANDY. The results when both cascading levels were included represented a good fit, satisfying all the criteria testing the validity of the ANDC result (Engström, 1982).

The 335.4 and 336.7 nm decay channels were used by Pinnington (Pinnington, 1970), Lewis et al. (Lewis, 1967) and Pinnington et al. (Pinnington, 1969) to measure the radiative lifetime of the 3p $^4P_{5/2}$ level, obtaining values of (5.3, 5.4 ns), (5.71, 5.84 ns) and (5.8, 5.4 ns) respectively. The values of Pinnington (Pinnington, 1970) are in good agreement with our curve-fitting results, obtained by measuring the decay of the J = 5/2 level via the same transitions. The value quoted by Denis et al.(Denis, 1968) are also in excellent agreement with our measurements. The beam-foil results of Lewis et al. (Lewis, 1967) are, for both transitions, about 10% higher than the lifetimes obtained in this investigation.

There are a rather wide spread in the lifetimes reported for the J = 3/2 level measured via the same 337.4 nm decay channel i.e. Pinnington (Pinnington, 1970) (τ = 7.3 ns), Fink et al. (Fink, 1968) (τ = 9.8 ns) and Lewis et al. (Lewis, 1967) (τ = 5.67 ns). Fink et al. (Fink, 1968) used the beam-foil technique, but recorded the decrease in intensity of a specific spectral line photographically. The difficulty involved in the interpretation of the analyses is obvious and is the reason why they estimated their listed decay times to be good to within ±50% and certainly to within a factor of two. At the time of their report very few measurements of mean lifetimes were available and they stated clearly that approximate values seem worthwhile.

REFERENCES

Curtis, L.J., Berry, H.G. and Bromander, J., 1971 - Phys. Lett. 34A, 169.

Denis, A., Desesquelles, J., Dufay, M., and Poulizac, M.-C., 1968 - Compt. Rend. 266, 64.

Engström, L., 1982 - Nucl. Instr. Methods 202, 369.

Fink, U., McIntite, G.N., and Bashkin, S., 1968 - J. Opt. Soc. Am. 58, 475.

Lewis, M.R., Marshall, T., Carnevale, E.H., Zimnoch, F.S., and Wares, G.W., 1967 - Phys. Rev. 164, 94.

Pinnington, E.H., and Lin, C.C., 1969 - J. Opt. Soc. Am., 59, 717.

Pinnington, E.H., 1970 - Nucl. Inst. Meth. 90, 93.

Provencher, S.W., 1976 - J. Chem. Phys., 64, 2772.

Striganov, A.R., and Sventitskii, N.S., 1968 - Tables of Spectral Lines of Neutral and Ionized Atoms (Plenum, New York).

AUTHOR'S ADDRESS

Department of Physics, University of Stellenbosch, Stellenbosch 7600, Republic of South Africa.

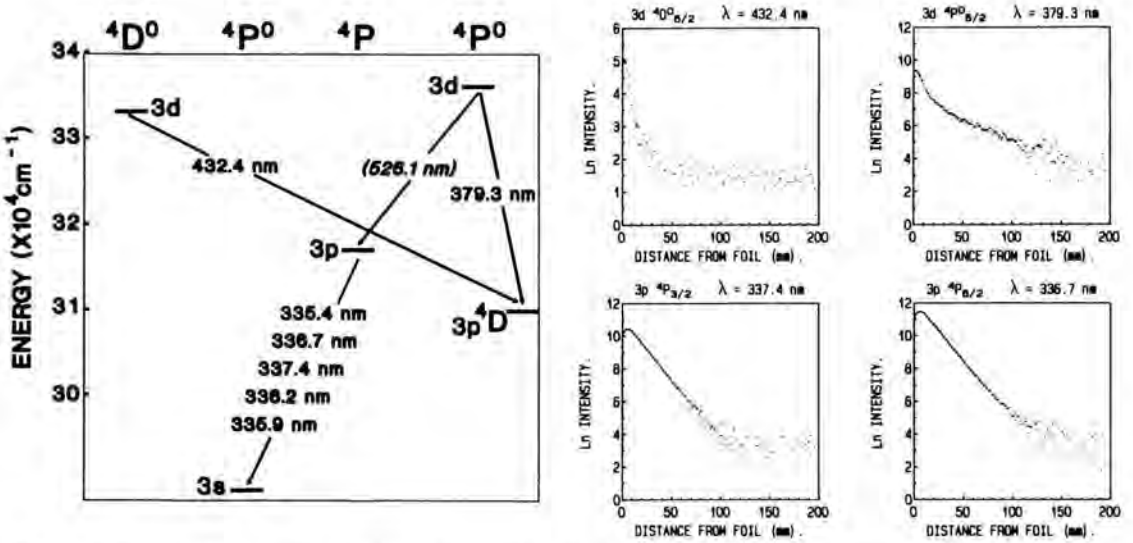

Fig. 1. Partial Grotrian diagram of levels involved in the 3p ^4P_J analyses. The inserts show the decay curves of the primary and cascading levels.

Jack Sugar

Spectroscopy of the $3s^2 3p^n$ shell from Cu to Mo

ABSTRACT

The $3s^2 3p^n$ isoelectronic sequences from Cu to Mo have been actively investigated in the past 15 years largely because of the importance of these spectra for tokamak plasma diagnostics. Many magnetic dipole transitions within these configurations were identified in tokamak plasmas even before anything was known of many of these ions. We give a brief review of the major spectroscopic studies that have been carried out with these ions. Revised tables of M1 lines for the isoelectronic sequences $3s^2 3p^2$ and $3s^2 3p^4$ from Cu to Mo are given.

This review will show how user needs (in this case tokamak research) stimulated spectroscopic research and led to a large body of new data for highly ionized atoms for the elements Cu to Mo and beyond where practically nothing was previously known. These data have found other uses as well, such as advancing the art of atomic structure calculations, providing internal wavelength standards for spectra of hot plasmas, and for extending spectral interpretation to even heavier ions.

Tokamak plasmas are "blessed" with many impurities: Cr, Fe, and Ni coming from the stainless steel interior walls and at various times W, Mo, C, and Ti from the aperture limiters. All these elements have been observed at the hot center of the plasma in highly stripped condition. To measure and interpret the consequent radiation from these as well as other elements intentionally injected into the plasma for diagnostic purposes has provided work for the last decade and one-half. The last generation of tokamaks such as the PLT at Princeton and the TEXT at the University of Texas are 1-2 keV machines and can ionize iron period elements down to the L-shell and heavier elements through Mo to the M-shell. The new generation of tokamaks such as TFTR, JET, and JT60 generate plasmas at 5-10 keV and can strip the heavier elements down to the L-shell.

Some of these impurity elements were eliminated early, such as W and Mo, because they held down the achievable temperature. Hinnov and Mattioli (1978) show two types of temperature profiles obtained in the PLT with a W limiter. The usual profile is peaked at the center but often the profile develops a central depression. After the Ag and Pd isoelectronic sequences were well understood it became clear that these features were mainly from these sequences. Limiters are now made of lighter elements, such as titanium-carbide coated graphite at TEXT, for example. When W and Mo were high priority elements a great deal of new data along isoelectronic sequences relevant to them were interpreted. Long isoelectronic extensions into the unknown territories resulted largely from the interests of magnetic fusion. They occur mainly along or near sequences of closed shells: $4f^{14}$ and $4d^{10}$ for interpreting W spectra, $3d^{10}$, and $2p^6$ for Mo. That Mo was a favored element is evident from the energy level compilation of Sugar and Musgrove (1988) that shows results for nearly every stage of ionization. For the $3s^2 3p^n$ sequences of Cu to Mo many magnetic dipole (M1) lines have been identified in tokamak plasmas, mainly by Hinnov and Suckewer and their colleagues at Princeton. These are included in the compilation of M1 lines and A-values by Kaufman and Sugar (1986). Today many electric dipole (E1) lines for nearly all of the ions of this group are accurately measured and securely interpreted. These are probably the first ions for which the classification of M1 lines preceded that of E1 lines. The next region of current interest is the $2p^n$ shell from Cu to Mo. These data are coming from high energy lasers and from the large tokamaks.

The importance of M1 lines of the 2p and 3p shells for plasma diagnostics has been reviewed in many publications, for example by Denne and Hinnov (1987) and by Doschek and Feldman (1976) who first suggested that M1 lines could be observed in a tokamak plasma. M1 lines are prominent in tokamak plasmas because the electron collision rate is about the same as the transition rate in this thin plasma of about 5×10^{13} electrons/cm^3. Their wavelengths are frequently longer than 2000 Å and their Doppler profiles are easily measured for determining ion temperatures. The first such line was observed with the PLT

tokamak by Suckewer and Hinnov (1978) at 2665 Å originating from Fe XX. The transition is $2s^2 2p^3 ({}^2D_{5/2} - {}^2D_{3/2})$. These M1 lines have had other diagnostic applications. Their Doppler shift has been used to measure the plasma rotation in tokamaks induced by unbalanced neutral beam injection (Suckewer et al., 1979). These lines have also proved convenient for mapping impurity transport in tokamaks (Suckewer et al. 1984). Recently, Wróblewski et al. (1988) measured the poloidal magnetic field in the TEXT tokamak by means of the circular polarization of the M1 line of Ti XVII at 3834 Å. The optics for this experiment requires a line above 2000 Å. To make a similar measurement in a high temperature tokamak may require a much heavier element in order that it not be too highly ionized. Ti in the TFTR would probably be totally stripped.

To assist in the program of M1 line identification Kaufman and I (1984) undertook to predict the wavelengths of all the M1 lines of the 3p-shell from Cu to Mo. This was done by fitting radial energy parameters to the known levels in the Fe period and extrapolating the ratios of these parameters to Hartree-Fock values for use in the heavier elements. The eigenvectors resulting from the matrix diagonalizations for Cu to Mo were then used to calculate the transition probabilities for all the M1 lines. The method was repeated by Biémont and Hansen (1985) who added correlation explicitly to the calculation. In our calculations correlation was absorbed by the scaling of the parameters and by the introduction of the "effective" configuration interaction parameter α. In general the A-values resulting from these two methods agreed to about 3%. These M1 wavelength predictions were sufficiently accurate to help in the discovery of many more lines. We have now refined the wavelength predictions by another method, that I will shortly describe, so that they are nearly as accurate as the measured lines.

I would like to review briefly the main spectroscopic studies that have been carried out in the range of ions of Cu to Mo for the isoelectronic sequences Na-like to K-like. For most of them the wavelength uncertainty is ±0.02 - ±0.05 Å. These estimates are based on comparison with our present measurements on the TEXT tokamak, which have an uncertainty of about ±0.007 Å. High energy laser-generated spectra are notoriously difficult to measure accurately because there are few internal impurities and no low ionization lines that have previously been measured. Five major papers appeared in the 1970's, beginning with Fawcett and Hayes (1975) who identified the strong lines of the elements Cu to Br. The motivation for most of this work was tokamak impurity spectra. Fawcett and Hayes remarked that their data could be used for accurate predictions of wavelengths of Mo.

Hinnov (1976) identified resonance lines of Na-like, Mg-like, Cu-like and Zn-like Kr and Mo in a tokamak plasma with an uncertainty of ±0.05 Å. Burkhalter et al. (1977) gave a fairly extensive spectrum of Na-like Mo and some lines of Mg-like with an uncertainty of ±0.06 Å. Mansfield et al. (1978) attempted to classify many lines of Mo, measured with an uncertainty of ±0.06 Å, from a large number of ionization stages. Kononov et al. (1979) renewed isoelectronic sequence studies with Na-like Cu to Br and with wavelength measurement uncertainties of ±0.01 Å. The 1980's brought a greatly increased flow of papers that continue to the present, making use of high powered lasers, tokamaks, a Z-pinch machine, and beam foil excitation. The Na sequence was extended to Se by Brown et al. (1986) with a wavelength uncertainty of ±0.04 Å and to Sr by Reader (1986) who achieved a wavelength uncertainty of ±0.005 Å. Kaufman and I measured the n=3-3 transitions of Na-like spectra for Cu to Mo with a wavelength uncertainty of ±0.007 Å. These were incorporated in a study of these transitions for Ar to Sn by Reader et al. (1987) who fit a simple function to the difference between observed and calculated wavelengths and used these fitted differences to obtain an overall accuracy of ±0.007 Å. A study of Al-like spectra for Zn, Ge, Se, Zr, Mo, and Ag was made by Hinnov et al. (1986) with the PLT tokamak. They obtained a wavelength uncertainty of about ±0.05 Å. Several studies of Kr have been made, one by Wyart and the TFR Group (1985) of K to Na-like and another by Stewart et al. (1987) of Al to Na-like, the latter with a Z-pinch device. The TFR Group and Wyart (1988) reported another study of Kr, Sr, Zr, and Rh for K to Na-like spectra. The wavelength uncertainty achieved by these groups was ±0.03 Å. Wyart et al. (1987) measured and interpreted 40 lines of Mg-like Sr. Using laser excitation they obtained the spectrum with a wavelength uncertainty of ±0.05 Å.

Beam-foil excitation was used by Hutton et al. (1987) to obtain the spectrum of P-like Cu with an uncertainty of ±0.03 Å. With a similar device, Träbert et al. (1988) observed intersystem transitions in Al-like and Si-like Cu and Zn and established the $3s3p^2\ {}^4P$ term and the $3s3p^3\ {}^5S$ term, respectively, of these sequences. Their

average measurement uncertainty is about ±0.04 Å.

Kaufman, Rowan, and I observed all the elements from Cu to Mo (except for Rb and Sr) with the TEXT tokamak at the University of Texas, Austin using a 2.2m grazing incidence spectrograph with a 1200 line/mm grating and photographic detection. These were supplemented by laser-generated plasmas of Cu to As, photographed at NIST with a 10.7m grazing incidence spectrograph. These light sources are complementary in some respects. Wavelengths of Fe and Ti suitable for standards were present in the TEXT exposures as impurities, so no wavelength shifts between standards and sample lines were present. Furthermore the lines observed in TEXT were sharp due to the low density of the plasma. These factors combined to provide accurate wavelengths from the tokamak exposures. The rms deviations of the standard lines from the dispersion curves were about ±0.005 Å. Thus we estimate the wavelength measurement uncertainty to be ±0.007 Å. The spectra obtained from the laser-generated plasmas, on the other hand, contained very few impurity or low ionization lines with which to detect shifts of the spectra from the standard wavelengths. Standards were exposed on a second track and from a different light source, usually a spark. However, measurements from TEXT served as internal standards for the laser spectra.

A drawback of the low electron density of TEXT is that it does not maintain the population of high-lying configurations, so that one is limited to observing mostly resonance lines and low configurations. However, M1 lines and strongly spin-forbidden transitions are not quenched. Laser-plasmas, on the other hand, provide more fully developed spectra but have the disadvantage of a lack of internal reference lines. A combination of the two light sources is ideal.

To interpret these data we used the methods successfully employed by Edlén in his analysis of the data for the n=2 shell in the Fe period (1984). We follow a transition along its isoelectronic sequence, each step of the way comparing it with its calculated value and plotting the difference. These plots are smooth and slowly varying with atomic number. The change per element is usually less than 0.1 Å and frequently only a few hundredths. This allows for an accurate prediction of the next unknown line in the sequence.

The first isoelectronic study incorporating our new data was on the Na sequence (Reader et al. 1987). Edlén (1978) treated the data of this sequence from S to Mo in a similar manner. For elements Cu to Mo the wavelength data available to him had measurement errors of ±0.05 Å. With our new data for Cu to Mo, with Y to Pd data from a 100 GW laser at Los Alamos, and with Ru to Sn from the 24 beam 2 TW OMEGA laser facility at Rochester we derived improved wavelengths for Ar to Sn with an uncertainty of ±0.007Å. Theoretical values were calculated with the Dirac-Fock code of Grant. The difference between measured and calculated wavenumbers was fit to the formula $\Delta\sigma=a+bZ+c(Z+d)^{-1}$ with a, b, c, and d as adjustable parameters.

We next carried out a study of the Al sequence (Sugar et al., 1988). Calculated wavelengths were published by Huang, who used the Dirac-Fock code of Desclaux. An earlier study of this sequence was carried out by Hinnov et al. (1986) for selected elements. Our improved wavelengths with an uncertainty of ±0.007 Å permitted a well defined observed-minus-calculated (O-C) curve to be fit to the new data. Interpolated values for the missing points were obtained with an uncertainty of ±0.01 Å. The energy levels of the ground configuration $3s^23p$ and the excited configurations $3s3p^2$ and $3s^23d$ were derived from the wavelength data.

Seven lines of the K-like transition array $3p^63d$ - $3p^53d^2$ were identified for Zn XII to Mo XXIV (Kaufman et al., 1989). This sequence illustrates a problem encountered in complicated cases where there are many levels and the eigenvectors for some of them change rapidly along the sequence. Kaufman et al. give two O-C curves. One of them shows a transition from a level that maintains its identity and the intensity of the transition throughout the sequence. The other represents a transition from a level whose designation is shifting to a new level along the sequence, as is the calculated intensity of the transition. The latter required the start of a new O-C curve after the theoretical crossing at Kr.

Our work on the Mg I isoelectronic sequence (Sugar et al., 1989) from Cu XVIII to Mo XXXI showed the great disparity between the amount of data that may be observed with a laser plasma compared with a tokamak plasma. For Cu to As obtained with a laser we observed transitions among the configurations 3s3p, 3s3d, $3p^2$, 3p3d and $3d^2$ with at most 53 lines of Zn XIX classified. With the tokamak the 3p3d and $3d^2$ configurations were not found and only 8 lines were observed in Se XXIII. For the theoretical wavelengths we carried out Dirac-Fock calculations. The resulting O-C curves showed a scatter of the experimental data of about 20 cm^{-1}, or well within our ±0.007 Å

uncertainty estimate. Values for Rb and Sr were read from the curves and have an estimated uncertainty of ±0.01 Å. For the spin-forbidden resonance line $3s^2\ {}^1S_0$ - $3s3p\ {}^3P_1$ the first points, Cu and Zn, are deduced from our E1 measurements. From As to Mo they were observed with TEXT.

For the Cl I isoelectronic sequence the $3s^23p^5\ {}^2P$ ground term splitting is known from observed M1 lines for the elements Cu to Se, Kr, Y, Zr, and Mo (see Kaufman and Sugar, 1986). Those of Br, Rb, Sr, and Nb were determined by Kaufman et al. (1989) from a plot of observed minus calculated values. Several transitions to the ^2P term from levels of the $3s^23p^43d$ configuration were also reported by them.

The remaining sequences S, P, and Si are much more complicated cases having $3p^4$, $3p^3$, and $3p^2$ ground configurations. The first step in treating them was to determine the energy levels of these ground configurations. Employing the method of the O-C curves we were able to derive these levels for Cu to Mo from the known M1 lines. For calculated values we used the Dirac-Fock calculations by Saloman and Kim (1988) for S, and by Huang (1984, 1985) for P and Si. The M1 data was taken from Kaufman and Sugar (1986).

Table 1 summarizes the new M1 predictions for the Si sequence. The starred values are the new predictions with indicated uncertainties about equal to the those of the observed data. Table 2 is a similar table for the S sequence. A large number of predicted values from the compilation are revised with much improved uncertainties. A table for the P sequence is in preparation. With these results all the levels of the ground configurations for the $3p^n$ sequences from Cu to Mo are now known.

Several applications of these data have been found. When the Na work was underway calculations were made with both the Desclaux and Grant Dirac-Fock codes and compared with the observed data (Reader et al., 1988). There was a significant difference; the Desclaux results were found to diverge from the observed values of the $3s\ {}^2S_{1/2}$-$3p\ {}^2P_{1/2}$ transition with increasing Z but the Grant code did not. The latter contained an approximation for the QED effects for the n=3 shell, namely $1/n^3$ scaling of the n=2 calculations. Kim et al. (1988) did the same test with the Al sequence data by calculating the ground term ^2P splitting with and without this correction. The difference between the observed splitting and the calculated value without n=3 shell QED diverges rapidly whereas with the QED correction for the n=3

Table 1. Complete M1 line-list (in Å) for transitions within the $3s^23p^2$ ground configuration of Si-like Fe through Mo. Wavelengths > 2000 Å are values in air. Newly predicted values are preceded by the symbol "*". The rest are observed values.

Spectrum	$3s^23p^2$ $({}^3P_0 - {}^3P_1)$	$({}^3P_1 - {}^3P_2)$	$({}^3P_1 - {}^1D_1)$	$({}^3P_2 - {}^1D_2)$	$({}^3P_1 - {}^1S_0)$
Fe XIII	10746.8(4)	10797.9(4)	2578.77(1)	3388.5(4)	1216.43(1)
Co XIV	*8440.8(4.0)	*9242.2(9.0)	2320.4(1.0)	3099.2(2.0)	*1120.6(3)
Ni XV	6701.7(4)	8024.1(4)	2085.51(5)	*2818.0(5)	*1033.2(3)
Cu XVI	5375.8(3)	*7067.7(5.0)	1871.2(2)	2544.7(5)	952.8(3)
Zn XVII	4355.0(3)	*6298.3(5.0)	1676.9(2)	2284.6(1)	* 878.7(3)
Ga XVIII	*3559.4(1.0)	*5676.1(4.0)	*1500.0(4)	*2038.4(1.0)	* 810.2(3)
Ge XIX	2933.7(2)	5170.3(3)	*1340.7(4)	1810.4(5)	746.9(3)
As XX	2438.0(3)	*4746.6(2.0)	*1197.6(4)	*1602.3(5)	* 688.2(3)
Se XXI	2042.3(3)	4396.5(3)	1069.2(5)	1414.2(5)	* 633.8(3)
Br XXII	*1722.4(3)	*4096.1(2.0)	* 955.5(5)	*1246.5(5)	583.6(1)
Kr XXIII	1462.65(3)	3840.9(3)	853.8(1.0)	*1098.5(5)	* 537.2(3)
Rb XXIV	*1249.8(3)	*3294.6(1.0)	* 764.0(4)	* 968.6(5)	* 494.4(3)
Sr XXV	*1074.5(3)	*3426.1(1.0)	* 684.3(3)	* 855.2(5)	* 455.3(3)
Y XXVI	* 928.9(3)	3254.8(1.0)	* 613.7(3)	* 756.4(3)	* 418.6(3)
Zr XXVII	807.1(3)	3101.1(3)	551.3(3)	670.8(3)	* 385.1(3)
Nb XXVIII	* 705.0(3)	*3055.7(1.0)	* 496.0(3)	* 595.6(3)	* 354.4(3)
Mo XXIX	618.5(3)	2841.1(2)	446.9(2)	530.3(3)	* 326.3(3)[k]

Table 2. Complete M1 line-list (in Å except where otherwise indicated) for transitions within the $3s^2 3p^4$ ground configuration of S-like Cu through Mo. Wavelength between 2000 Å and 5 μm are values in air. Newly predicted values are preceded by the symbol "*". The remainder are observed values.

$3s^2 3p^4$ Spectrum	$(^3P_0 - ^3P_1)$	$(^3P_2 - ^3P_1)$	$(^3P_1 - ^1D_2)$	$(^3P_2 - ^1D_2)$	$(^3P_1 - ^1S_0)$
Cu XIV	*14.18(12)μm	4183.4(3)	*3490.3(9)	*1903.3(4)	1190.4(5)
Zn XV	* 4.010(10)μm	3450.4(2)	*3360.0(8)	1702.8(2)	*1108.2(5)
Ga XVI	* 2.014(10)μm	*2870.7(5)	*3241.1(9)	*1522.8(3)	*1029.0(3)
Ge XVII	*12125(15)	2406.9(3)	3131.3(3)	*1361.3(3)	952.9(3)
As XVIII	* 8020(9)	2032.6(3)	*3030.8(1.3)	*1216.8(3)	* 880.0(3)
Se XIX	56450(3)	1727.7(3)	2935.8(3)	*1087.8(3)	810.3(3)
Br XX	* 4146(4)	*1477.8(4)	*2847(2)	* 973.0(3)	* 744.7(5)
Kr XXI	* 3147(3)	*1271.1(3)	*2765(2)	* 870.9(3)	* 682.9(5)
Rb XXII	* 2451(2)	*1099.3(3)	*2687(2)	* 780.2(3)	* 625.2(5)
Sr XXII	* 1950(2)	* 955.4(3)	*2613(2)	* 699.6(3)	* 571.7(5)
Y XXIV	* 1579.5(1.2)	* 834.3(3)	*2543(2)	* 628.3(3)	* 522.4(5)
Zr XXV	* 1298.4(9)	731.8(2)	2476(2)	564.9(3)	477.1(5)
Nb XXVI	* 1081.3(8)	* 644.5(3)	*2412(2)	* 508.6(3)	* 435.5(5)
Mo XXVII	* 910.9(5)	569.8(1)	2350.8(3)	458.6(2)	397.2(3)

shell it is nearly linear. It is due to the accuracy of the data that this test of the theory may be made.

Na-like spectra occur in many high-energy plasmas, including those generated to obtain Ne-like spectra for x-ray lasers. Eckart et al. (1988) obtained a spectrum of Se with a line focus of a high powered laser beam, looking down the axis of the line-focus where lasing is observed. Distributed among the lasing lines are Na-like lines, which provide wavelength standards to measure the lasing lines. Similar spectra of Ne-like Cu and Ge obtained by Lee et al. (1987) show a similar distribution of Na-like lines, and there is also a strong Mg-like line present. These lines were used by them as wavelength standards to measure the lasing lines. They note that "High precision wavelength measurements for the lasing lines are needed for comparison with theoretical predictions and atomic physics models."

ACKNOWLEDGEMENTS

This work was supported in part by the Office of Fusion Energy of the U. S. Department of Energy (DOE) and by the Innovative Science and Technology/Strategic Defense Initiative Organization under the direction of the Naval Research Laboratory.

REFERENCES

Biémont, E., and Hansen, J.E., 1985 - Radiative transition rates in the ground configuration of the phosphorus sequence from argon to ruthenium. In: Phys. Scr. 31, 509.

Brown, C.M., Seely, J.F., Feldman, U., Richardson, M.C., Behring, W.E., and Cohen, L., 1986 - Spectrum of sodiumlike selenium: Se XXIV. In: J. Opt. Soc. Am. B3, 701.

Burkhalter, P.G., Reader, J., and Cowan, R.D., 1977 - Spectra of Mo XXX, XXXI, and XXXII from a laser-produced plasma. In: J. Opt. Soc. Am. 67, 1521.

Denne, B., and Hinnov, E., 1987 - Spectral lines of highly-ionized atoms for the diagnostics of fusion plasmas. In: Phys. Scr. 35, 811.

Doschek, G.A., and Feldman, U., 1976 - Diagnostic forbidden lines of highly ionized elements for tokamak plasma. In: J. Appl. Phys. 47, 3083.

Eckart, M.J., Scofield, J.H., and Hazi, A.U., 1988 - XUV emission features from the Livermore soft x-ray laser experiments. In: J. Physique Coll. C1 Suppl. 3, 49, 361.

Edlén, B., 1978 - The transitions 3s-3p and 3p-3d, and the ionization energy in the Na I isoelectronic sequence. In: Phys. Scr. 17, 565.

Edlén, B., 1984 - Comparison of the theoretical and experimental level values

of the n=2 configurations in the nitrogen isoelectronic sequence. In: Phys. Scr. 30, 135.
Fawcett, B.C., and Hayes, R.W., 1975 - Spectra in the period between copper and bromine produced with the aid of a 4 GW laser. In: J. Opt. Soc. Am. 65, 623.
Hinnov, E., 1976 - Highly ionized atoms in tokamak discharges. In: Phys. Rev. A14, 1533.
Hinnov, E., and Mattioli, M., 1978 - Observations of multiply ionized tungsten radiation in the PLT discharge. In: Phys. Lett. 66A, 109.
Hinnov, E., Boody, F., Cohen, S., Feldman, U., Hosea, J., Sato, K., Schwob, J.L., Suckewer, S., and Wouters, A., 1986 - Spectrum lines of highly ionized zinc, germanium, selenium, zirconium, molybdenum, and silver injected into Princeton Large Torus Tokamak Fusion Test Reactor tokamak discharges. In: J. Opt. Soc. Am. B3, 1288.
Huang, K.-N., 1984 - Energy-level scheme and transition probabilities of P-like ions. In: At. Data Nucl. Data Tables 30, 313.
Huang, K.-N., 1985 - Energy-level scheme and transition probabilities of Si-like ions. In: At. Data Nucl. Data Tables 32, 503.
Hutton, R., Jupen, C., Träbert, E., and Heckmann, P.H., 1987 - Spectroscopy of highly ionized copper and nickel. In: Nucl. Instr. Meth. Phys. Res. B23, 297.
Kaufman, V., and Sugar J., 1986 - Forbidden Lines in ns^2np^k ground configurations and nsnp excited configurations of beryllium through molybdenum atoms and ions. In: J. Phys. Chem. Ref. Data 15, 321.
Kaufman, V., Sugar, J., and Rowan, W.L., 1989 - Wavelengths and energy levels of the K I isoelectronic sequence from copper to molybdenum. In: J. Opt. Soc. Am. B6, 142.
Kaufman, V., Sugar, J., and Rowan, W.L., 1989 - Chlorinelike spectra of copper to molybdenum. In: J. Opt. Soc. Am. B6, 1444.
Kim, Y.-K., Sugar, J., Kaufman, V., and Ali, M.A., 1988 - Quantum-electrodynamic contributions to the spin-orbit splitting in the ground state of aluminumlike ions. In: J. Opt. Soc. Am. B5, 2225.
Kononov, E. Ya., Ryabtsev, A.N., and Churilov, S.S., 1979 - Spectra of sodium-like ions Cu XIX-Br XXV. In: Phys. Scr. 19, 328.
Lee, T.N., McLean, E.A., and Elton, R.C., 1987 - Soft x-ray lasing in neonlike germanium and copper plasmas. In: Phys. Rev. Lett. 59, 1185.
Mansfield, M.W.D., Peacock, N.J., Smith, C.C., Hobby, M.G., and Cowan, R.D., 1978 - The XUV spectra of highly ionized molybdenum. In: J. Phys. B11, 1521.
Reader, J., 1986 - Spectrum and energy levels of the sodiumlike ion Sr^{27+}. In: J. Opt. Soc. Am. B3, 870.
Reader, J., Kaufman, V., Sugar, J., Ekberg, J.O., Feldman, U., Brown, C.M., Seely, J.F., and Rowan, W.L., 1987 - 3s-3p, 3p-3d, and 3d-4f transitions of sodiumlike ions. In: J. Opt. Soc. Am. B4, 1821.
Reader, J., Sugar, J., and Kaufman, V., 1988 - Recent progress on spectral data for x-ray lasers at the National Bureau of Standards. In: IEEE Trans. Plasma Sci. 16, 560.
Saloman, E.B., and Kim, Y.-K., 1989 - Energy levels and transition probabilities in the ground-state configuration of sulfur-like ions. In: At. Data Nucl. Data Tables 41, 339.
Stewart, R.E., Dietrich, D.D., Fortner, R.J., and Dukart, R., 1987 - Soft x-ray spectra of krypton XXIV-XXVII in gas puff Z-pinch plasmas. In: J. Opt. Soc. Am. B4, 396.
Suckewer, S., and Hinnov, E., 1978 - Observation of a forbidden line of Fe XX and its application for ion temperature measurements in the Princeton Large Torus Tokamak. In: Phys. Rev. Lett. 41, 756.
Suckewer, S., Eubank, H.P., Goldston, R.J., Hinnov, E., and Sauthoff, N.R., 1979 - Toroidal Plasma Rotation in the Princeton Large Torus induced by neutral beam injection. In: Phys. Rev. Lett, 43, 207.
Suckewer, S., Cavallo, A., Cohen, S., Daughney, C., Denne, B., Hinnov, E., Hosea, J., Hulse, R., Huang, D., Schilling, G., Stratton, B., and Wilson, R., 1984 - Ion transport studies in the PLT tokamak during neutral beam injection. In: Nucl. Fusion 24, 815.
Sugar, J., and Kaufman, V., 1984 - Predicted wavelengths and transition rates for the magnetic-dipole transitions within $3s^23p^n$ ground configurations of ionized Cu to Mo. In: J. Opt. Soc. Am. B1, 218.
Sugar, J., and Musgrove, A., 1988 - Energy Levels of molybdenum, Mo I through Mo XLII. In: J. Phys. Chem Ref. Data 17, 155.
Sugar, J., Kaufman, V., and Rowan, W.L., 1988 - Aluminumlike spectra of copper through molybdenum. In: J. Opt. Soc. Am. B5, 2183.
Sugar, J., Kaufman, V., Indelicato, P., and Rowan, W.L., 1989 - Analysis of magnesiumlike spectra from Cu XVIII to Mo XXXI. In: J. Opt. Soc. Am. B6, 1437.
TFR Group and Wyart, J.F., 1988 - On the spectra of highly ionized krypton strontium, zirconium, and rhodium excited in the plasma of the TFR tokamak. In: Phys. Scr. 37, 66.

Träbert, E., Heckmann, P.H., Hutton, R., and Martinson, I., 1988 - Intercombination lines in delayed beam-foil spectra. In: J. Opt. Soc. Am. B5, 2173.

Wróblewski, D., Huang, L.K., Moos, W., and Phillips, P.E., 1988 - Determination of the poloidal magnetic field profiles in a tokamak by polarization spectroscopy of an impurity ion line. In: Phys. Rev. Lett. 61, 1724.

Wyart, J.F., and TFR Group, 1985 - Identification of krypton Kr XVIII to Kr XXIX spectra excited in TFR tokamak plasmas. In: Phys. Scr. 31, 539.

Wyart, J.F., Gauthier, J.C., Geindre, J.P., Tragin, N., Monier, P. Klisnick, A., and Carillon, A., 1987 - Interpretation of a spectrum of laser irradiated strontium in the range 115 - 208 Å. In: Phys. Scr. 36, 227.

AUTHOR'S ADDRESS

National Institute of Standards and Technology, Atomic and Plasma Radiation Division, Bldg. 221, Room A167, Gaithersburg, MD 20899

A.P. Thorne and R.C.M. Learner

Wavelengths and branching ratios with an ultra-violet Fourier transform spectrometer

ABSTRACT

The advantages offered by Fourier transform spectroscopy over grating spectroscopy for the accurate measurement of wavelengths and intensity ratios in the visible and ultra-violet are discussed. The combination of very high resolution with high light throughput allows the wavenumbers of strong lines from a stable laboratory source to be measured with an absolute accuracy of .001 cm^{-1} and a precision about 20 times better. The resolving power can be varied up to a maximum of 1.5 to 2 million, so that the resolution of blends and hyperfine structure is limited only by true line widths. Good intensity measurements can be made over a wide spectral range because of the slow variation in response of the instrument with wavelength, allowing accurate determinations of branching ratios and hence of relative f-values.

INTRODUCTION

Fourier transform spectrometry (FTS) has several distinct advantages over grating spectrometry in the measurement of wavelengths and line intensities. FTS has been extended to the ultra-violet only rather recently, mainly because of the stringent optical and mechanical tolerances required at short wavelengths, and is not familiar to many astrophysicists. We therefore describe briefly the principal differences between the two types of instrument before showing how the characteristic features of FTS can be exploited to acquire very large quantities of high quality laboratory data relevant to the needs of astrophysics.

The first astronomical FTS observations were made by Connes in the 1960's in the near infra-red, where detector noise dominated and the FTS improved signal to noise ratios by many orders of magnitude. Large Fourier transform spectrometers have now been built at Orsay, at the National Solar Observatory (NSO) on Kitt Peak, and at Liege and the Jungfraujoch, and as a result of improvements in IR detectors these are photon noise limited from the near IR to the near UV, about 300 nm being the short wavelength limit of their useful ranges. The NSO instrument has been used about equally for solar and laboratory measurements. The quantity and quality of the data emanating from these instruments convinced us of the potential of UV FTS, and about 10 years ago we started to design and build at Imperial College an instrument to operate from the visible to 175 nm. This is now producing laboratory data - of higher quality than we had dared to hope - much of which is complementary to that from NSO. The shorter wavelength data has direct application not only to the Hubble space telescope programme but also to observations at longer wavelengths. Astrophysics is the science of blended lines, and better UV data, particularly for Iron and the other transition elements, is constantly required for improving the accuracy and reliability of line lists in the visible and IR. In addition, astrophysicists are well known for their insatiable demand for f-values, many of which are derived from branching ratios involving UV as well as visible transitions.

GRATING AND FOURIER TRANSFORM SPECTROMETRY COMPARED

The Imperial College UV FTS is a Michelson interferometer with catseye retroreflectors instead of plane mirrors. One of these is scanned through a distance $\pm L/2$ from zero path difference, introducing a maximum optical path difference of L between the two beams. The catseyes reduce tilt sensitivity during the scan and also allow us to use the complementary interference fringe pattern that is returned, laterally displaced, in the direction of the source. All the radiation admitted to the interferometer is incident on the detectors all of the time, but different wavelengths are distinguished by their different spatial modulation frequencies σ, where $\sigma = 1/\lambda$. The interferogram resulting from the superposition of all the sinusoidal signals is sampled at equal intervals of path difference Δx, as determined by a Helium-Neon laser following the same optical path as the signal, and the spectrum is recovered from the interferogram by means of a fast Fourier transform (FFT). The free spectral range $\Delta\sigma$ (cm^{-1}) of the spectrum, and hence also the wavenumber scale, are determined by the sampling step according to $\Delta\sigma = 1/(2\Delta x)$ whereas the resolution $\delta\sigma$ (cm^{-1}) depends on the maximum optical path difference: $\delta\sigma = 1/2L$. Note the contrast to a grating spectrometer where the sampling step determines the resolution and the scan length the spectral range.

The advantages of FTS over grating spectrometry follow from these properties. First, the axial symmetry of the interferometer, working with a circular entrance aperture instead of a slit, allows a light throughput greater by one to two orders of magnitude than that of a grating instrument of the same resolving power (the Jacquinot advantage). Second, the wavenumber precision and reproducibility relate directly to a laser standard and the wavenumber scale is accurately linear (the Connes advantage).

This scale does, however, require calibration as explained below if an absolute accuracy of better than about 1:10^7 is needed. Third, the resolution can be increased as much as is necessary to resolve the source line (i.e., to eliminate instrumental contributions to the line width) by increasing the scan length. Since $\delta\sigma$ is independent of wavelength, the resolving power as defined by $\sigma/\delta\sigma$ or $\lambda/\delta\lambda$, increases at shorter wavelengths, in contrast to the decrease shown by a grating spectrometer for which $\delta\lambda$ remains approximately constant. The multiplex advantage familiar in far IR FTS is not realised in the visible/UV where detector noise is normally negligible. There is, however, a fourth advantage in the complete spectral coverage and computer compatibility of FTS. Every single spectral element in the selected bandwidth is automatically stored for future access.

Learner and Thorne (1988) have compared the wavenumber accuracies attainable with FTS and grating spectrometry in some detail and have shown that FTS can achieve a wavenumber precision of about 6 parts per billion (ppb) on lines generated in a hollow cathode glow discharge lamp, which is a quiet, photon noise limited, source. Whereas precision is proportional to the width of the line divided by its signal to noise ratio (Brault,1988), the absolute accuracy with which any line can be measured depends also on the calibration constant of the instrument. In principle this can be obtained from a single reference wavelength, in contrast to the set of references that are essential to calibrate a grating instrument, and the variation of the calibration constant obtained from different reference lines is an excellent indicator of the quality of the data. Furthermore, the high resolution of FTS eliminates instrumental contributions to line width, and its high throughput maximises signal to noise ratio for any given resolution. An absolute accuracy of about 0.001 cm^{-1} for the stronger lines of Fe all the way from 5.4 μm to about 180 nm is an attainable goal.

Accurate measurement of transition probabilities requires data of high quality on the intensity axis. Laser spectroscopy has yielded a large number of lifetime measurements, and to obtain absolute transition probabilities from these one needs the relative intensities of all lines starting from the level concerned. These lines frequently extend over a wide wavelength range. FTS has two, perhaps three, advantages in this respect. First, if the optics have broadband coatings the spectral range is limited only by the detectors and any filters used, in contrast to the limited spectral range offered by a blazed grating; second, since all wavelengths are observed all of the time, errors from drifts of source intensity during scanning are reduced. A third advantage often arises from the superior resolution and line shape information, which allows blending of weaker lines and incipient self-absorption to be more readily detected.

3. APPLICATIONS TO ASTROPHYSICS

The high cosmic abundance and rich spectrum of Iron - and to a somewhat lesser extent the other transition elements - are largely responsible for the demands of astrophysicists for accurate wavelengths and unambiguous identification of weak lines of these atoms and their ions. The resolution, wavenumber and luminosity advantages of FTS can and should be exploited to improve systematically the data bases used by astrophysicists. As an example, work on Ti I at Lund (Forsberg, 1987) using FTS data has found roughly 100 new levels. Much more important, however, is that it has led to the rejection of 50 previously listed levels. By extending into the UV measurements made with the NSO FTS in the IR and visible, we are contributing to this improvement in four areas.

The first is in the compilation of extremely accurate wavelength standards. We have recently published a list of Fe I standards from the visible to the near UV with an absolute accuracy of 0.001 cm^{-1} (Learner and Thorne, 1988), and we are now in the process of extending this list down to 180 nm. The relative accuracy - that is, the accuracy of the calibration constant that puts all spectra on the same relative scale - is 2 ppb. This is illustrated in Figs.1 and 2, which show the scatter in this constant over two broad spectral bands, 4000 - 3000 Å and 2900 - 2400 Å respectively. It is remarkable that the data compared in Fig.1 were obtained in different continents with different operators using different spectrometers and different hollow cathode lamps running under different conditions, while the data in Fig.2 show the relative accuracy to be maintained in the more difficult shorter wavelength region.

The second area is the re-measurement of laboratory spectra of Fe and other astrophysically important atoms and ions to obtain better wavelengths for all lines, strong and weak, to make positive identifications of very weak lines, and to eliminate chance coincidences with impurities. The UV measurements on Fe, for example, have yielded nearly three times as many lines in the region 250-190 nm as were found by Crosswhite (1976) using a similar hollow cathode source and a grating spectrometer of similar resolution - clear evidence of the luminosity advantage (Thorne, Harris, Wynne-Jones, Learner and Cox, 1987). Johansson and Baschek (1988) found these same measurements to give an improvement of almost an order of magnitude in wavenumber accuracy over those from the 10 m. grating at the National Bureau of Standards. It is also interesting that Johansson and Learner (1989), using IR FTS data from NSO, have found the lowest 4s4f configuration in Fe I, accounting for nearly 50 new levels and more than 350 lines near 1.6 μm. These lines have intensity characteristics in the Sun that are systematically different from those of other Iron lines.

The third area is the disentangling of blends and the resolution of hyperfine structure and isotope shifts, exploiting the high resolution attainable. Work in progress

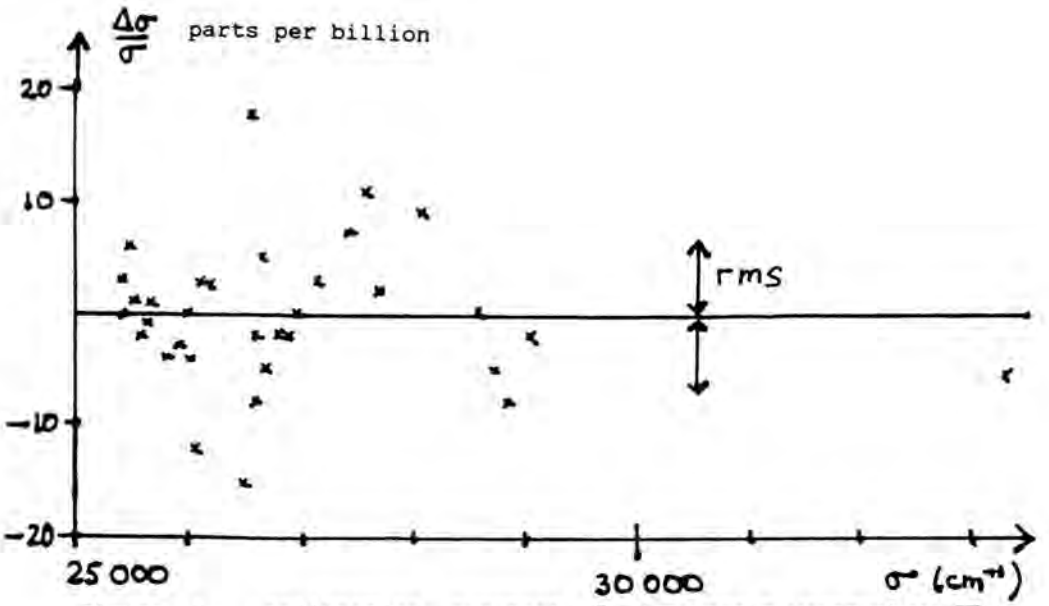

Figure 1. Calibration constant $\Delta\sigma/\sigma$ versus wavenumber σ : comparison of N.S.O. and I.C. data. The rms scatter is 7 parts per billion, or about 0.0002 cm^{-1}.

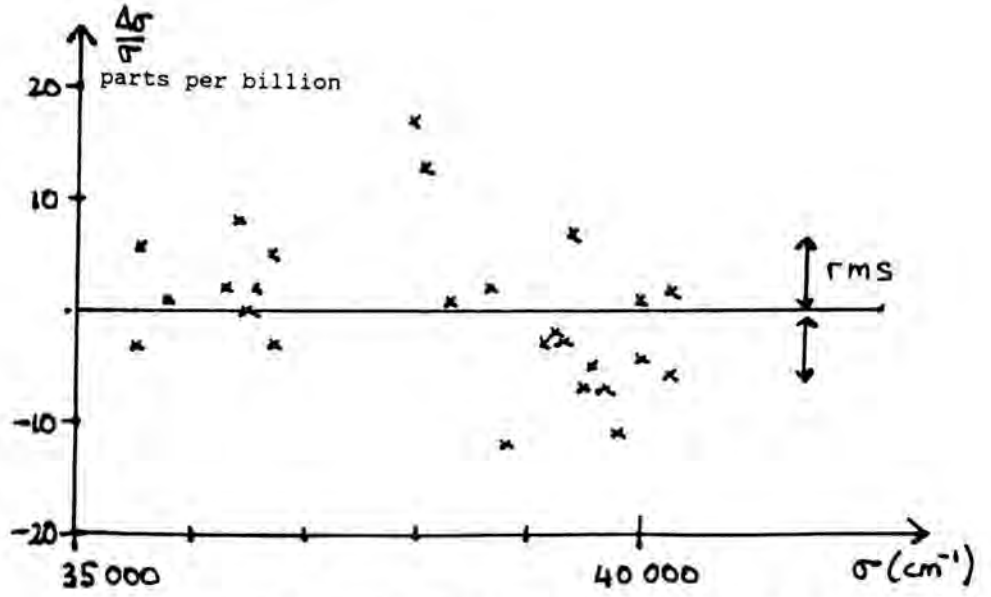

Figure 2. Calibration constant $\Delta\sigma/\sigma$ versus wavenumber σ : comparison of two different I.C.spectra in the UV. The rms scatter is 6.5 parts per billion, or about 0.0003 cm^{-1}.

on the spectrum of Pt II is reported in the poster paper by Learner, Thorne, Davies and Federmann in the present meeting.

Finally, the fourth area is the measurement of branching ratios for absolute f-values, as outlined in section 2. An example of the power of this technique is furnished by Whaling and Brault (1988), who used the NSO FTS to generate transition probabilities of more than 2800 lines in the spectrum of Mo I. The uncertainties for the stronger lines are typically 8%. A similar exercise on Mo II requires intensity measurements extending further into the UV, and we are in the process of providing these. It is worth noting that the completeness of their spectral information enabled Whaling and Brault, almost as a side issue, to find 27 new levels in Mo I and to eliminate as spurious about as many from the Atomic Energy Levels list.

Apart from the general programme to improve the data base, we have applied the UV FTS to a few particular problems, of which two examples may be given. The first of these was a fortuitous rather than deliberate use of the earliest data produced by the UV FTS: the analysis of the abundance of Boron in the Sun, called into question when the Boron line on which it was based appeared to coincide with a weak line in the spectrum of a laboratory Fe hollow cathode source, was confirmed when careful measurements of FTS wavelengths and intensity ratios tracked the weak "Fe" line down to a boron impurity in the source (Learner and Harris, 1987). The second example is among those presented in the poster paper by Learner et al. referred to above: the "stellar chronometer" of Butcher required absolute wavelength measurements on two very weak lines of Fe and Ni. The accuracy of better than 0.5 mÅ that we were able to achieve would simply not have been possible by grating or Fabry-Perot spectroscopy. The signal to noise ratio obtained was 30 for the weak Fe line involved and no less than 100,000 for the neighbouring strong line used as the transfer wavelength standard.

4.THE FUTURE OF UV FTS

Interest in UV FTS has increased significantly over the last few years. A multi-million dollar instrument at Los Alamos, designed for very high resolution from the IR to 200 nm, has been recently commissioned. Two commercial manufacturers, Bomem and Bruker, have extended the ranges of their instruments to the 200 nm region, and Chelsea Instruments have manufactured a commercial version of the Imperial College FTS. This last is the only one currently of proven high performance below 200 nm.

We are now working on extending the capabilities of our laboratory instrument in two respects. The first, on which we are just beginning, is to extend the spectral range below the spectrosil cut-off by substituting a magnesium fluoride beamsplitter and upgrading some of the mechanical adjustments to meet the tighter tolerances. This would open up the range from 200 nm to Lyman α, a range of great importance for solar spectroscopy from space. In this connection the European Space Agency has accepted in principle a proposal for an imaging UV FTS, using an array detector in the focal plane to add two-dimensional spatial information to the spectral information. The demands on data handling presented by the acquisition of up to 10000 simultaneous interferograms in 30 seconds have warranted a separate special study.

The second project, on which we have already achieved encouraging preliminary results, is to investigate the use of pulsed sources to allow us to excite higher stages of ionisation - Fe III, for example - and to obtain spectra from pinch discharges, laser induced fluorescence and laser ablation plasmas. Experiments with a small commercial hollow cathode have shown virtually no degradation of signal to noise ratio in going from dc to pulsed operation, with careful synchronisation of the pulses with the sampling steps in the interferogram. Pulsed UV FTS therefore seems a very real possibility for the near future.

This paper has emphasised the quality of FTS data, but its shear quantity should not be forgotten. A 10 minute run can give a million data points - 1000 Å bandwidth at a resolution of 1 mÅ, for example - and if several runs are co-added to improve the signal to noise ratio the acquisition time is still only an hour or two. In a rich line spectrum perhaps 1% of these data points contain useful information, but, even so, the analysis of the spectrum rather than its acquisition is the limiting factor on the ultimate data rate. This vast potential for gathering the data enthusiastically welcomed by astrophysicists is not enthusiastically supported by Atomic Physics funding bodies, to whom it smacks of large-scale stamp collecting. The flow of laboratory FTS data will have to be funded from astrophysical sources if it is not to dry up.

REFERENCES

Brault,J.W., 1987 - High precision Fourier transform spectrometry. In: Mikrochim. Acta (Wien) 1987 III, 215-227

Crosswhite,H.M., 1975 - The iron-neon hollow cathode spectrum. In: J.Res.NBS A 79, 17-69

Forsberg,P., 1987 - PhD. thesis, University of Lund

Johansson,S and Baschek,B., 1988 - Term analysis of complex spectra: new experimental data for Fe II. In: Nuclear Inst. & Methods B 31, 222-232

Johansson,S. and Learner,R.C.M., 1989 - The lowest 3d 4s4f subconfiguration of Fe I determined from laboratory and solar Fourier transform spectra in the infrared. Submitted to Astrophys.J.

Learner, R.C.M. and Harris,C.J., 1987 - The solar boron abundance. In: Astrophs.J. 320, 926-927

Learner,R.C.M. and Thorne,A.P., 1988 - Wavelength calibration of Fourier transform emission spectra with applications to

Fe I. In: J.Opt.Soc.Amer. B 5, 2045-2059
Learner,R.C.M., Thorne,A.P., Davies,J.W. and Federmann,F., 1989 - Astrophysical applications of high resolution laboratory FTS observations in the visible and ultraviolet. In these proceedings.
Thorne,A.P., Harris,C.J., Wynne-Jones,I., Learner,R.C.M. and Cox,G., 1987 - A Fourier transform spectrometer for the vacuum ultraviolet: design and performance. In: J.Phys.E 20, 54-60
Whaling,W. and Brault,J.W., 1988 - Comprehensive transition probabilities in Mo I. In: Physica Scripta 38, 707-718

AUTHORS' ADDRESS

Blackett Laboratory
Imperial College
London SW7 2BZ, U.K.

R.C.M. Learner, A.P. Thorne, J. Davies and F. Federmann

Astrophysical applications of high resolution laboratory FTS in the visible and ultra-violet

There are a large number of topics in which high resolution and/or high wavelength precision are required in the laboratory data that underwrite observational astrophysics. We consider three cases in which recent FTS data are of relevance.

The first is the stellar chronometer of Butcher (1987) In this case precise relative wavelengths are needed for four weak lines: two lines in the Thorium and Neodymium spectra that form the basis of the chronometer and two lines in the Iron & Nickel spectra that interfere and whose influence must be considered.

It is fundamental to a measurement of the wavelength that the precision of the measurement depends on the signal to noise ratio of the observation and the width of the line (Learner & Thorne, 1988). For the observations considered here, the noise is dominated by the photon noise) and can be minimised by co-adding several interferograms and by using narrow bandwidth optical filters. In the present case a filter of 490 cm^{-1} bandwidth and 40% peak transmission was used. Optimum line width is achieved by using sources with intrinsically narrow lines - low current (10 to 20 mA) Neon hollow cathode lamps - and by matching instrumental resolution to this line width. An instrumental line width one half that of the source is required for maximum signal to noise ratio and was employed for all lines studied except the Thorium line. The majority of the observations were taken using the Chelsea Instruments FT-500 FTS at UKAEA Harwell.

Because the lines being studied are weak a staged calibration procedure was used. Data taken with the low bandwidth filter were used to relate each weak line to a stronger line in the same spectrum. A second set of observations using a much wider filter then linked the strong line to the Neon line at 28937 cm^{-1}, which is of similar strength. One of this set of observations linked the Neon line to the Fe I line at 24709.9345 cm^{-1} which was used to set the data on an absolute scale. The errors of observation are dominated by the first stage, the observation of the weak lines.

The Fe I line proved too weak to observe under the above conditions and recourse was had to a very high current (750 mA) long observation time (1hr 40 min) spectrum taken using the IC FTS. This line can be directly related to the 24709 cm^{-1} FeI line, so Neon line shifts with current or pressure are irrelevant.

The final set of wavelengths with their errors are set out in Table I. Relative errors are relative to Fe I 24709, absolute errors include the uncertainty in the wave number of that line the error analysis includes all uncertainties in line-to-line transfers.

The second problem is concerned with the Pt I & II spectra. A Pt hollow cathode lamp has been developed as a wavelength and intensity standard for the Hubble telescope (Reader et al, 1988). Precise wavelengths depend on observations in the far UV and are influenced by hyperfine structure (Engleman, 1989). Observations with the FTS in the region 1750 - 3000 A show the hfs of many lines. So far the analysis has concentrated on lines relating to the lowest terms in the spectrum; once again a major gain in precision is evident.

The third problem is that of high class absolute wavelengths in Fe I & Fe II. Studies by Dravins et al (1981, 1986) on solar convection have shown that the principal source of error in that type of work is due to uncertainties in the laboratory wavelengths. We have published improved measurements of Fe I in the visible and report here the extension of those measurements to cover the ultra violet. The wavelengths observed with the IC FTS (Harris, 1986) were already known to be on a good relative scale (Johansson, 1988) but were not linked to the longer wavelength work.

In order to minimise photon noise a novel technique using different detectors in the two FTS output beams was employed. This permits simultaneous observation of both UV & visible regions without each being degraded by the photon noise from the other region. We have also made observations, using deliberate misalignments, to show that the Fe I & Fe II wavelengths are stable with respect to changes of illumination. One curiosity of the two detector technique arises from the fact that, due to absorption losses at the beam splitter, the computed phase correction is not of the standard form.

A comparison of the new data with that of Harris and of Learner & Thorne, using strong lines common to overlapping regions of the three spectra shows that the random errors of the calibration are $\pm$ 1.8 x 10^{-9} (typically 7 x 10^{-5} cm^{-1} or 6μA). We are confident that, using the many strong lines in the three data sets, we can establish UV wavelengths to better than $\pm$ 1 mK in Fe I and Fe II covering the region down to 2000 A. This represents a major improvement on older standards (Kaufman & Edlen, 1974; Norlen, 1987).

TABLE 1 WAVELENGTHS OF LINES USED IN THE BUTCHER CHRONOMETER

Element	cm^{-1}	Relative Error		Abs. Error		Å
		mK	mÅ	mK	mÅ	
Th	24873.9780	±0.82	±0.13	±1.3	±0.21	4019.1298
Ni	74.3670	2.0	0.32	2.2	0.36	9.0667
Fe	74.5141	2.5	0.40	2.7	0.43	9.0431
Nd	75.8576	2.7	0.44	2.9	0.47	8.8259

References

Butcher, H., 1987
Thorium in G-Dwarf Stars as a Chronometer for the Galaxy. Nature 328 127-131.

Dravins, D., Lindegren, L. & Nordlund, A., 1981
Solar Granulation: Influence of Convection on Spectral Line
Asymmetries & Wavelength Shifts. Astron Astrophys, 91 345-64

Dravins, D Larsson, B. & Nordlund A., 1986
Solar FeII Line Asymmetries and Wavelength Shifts.
Astron Astrophys 158 83-88

Engleman R., 1989
The Structure and Wavelength of Some Pt II Lines of Astrophysical Interest. Astrophys J 340 1140-1143

Harris, C.J., 1986, Ph.D. Thesis, London

Johansson, S & Baschek, B., 1988
New Experimental Data For Fe II
Nucl Instrum Methods Phys Res B31, 222-232

Kaufman, V. & Edlen, B., 1974
Reference Wavelengths from Atomic Spectra in the Range
15A to 25000A. J Phys Chem Ref Data 3 825-895

Learner, R.C.M., & Thorne, A.P., 1988
Wavelength Calibration of Fourier Transform Emission Spectra with Applications to Fe I.J Opt Soc Am B5, 2045-2059

Norlen G., 1987, Interferometric Measurements in Fe II. Private communication from S Johansson.

Reader J, Acquista, N., Sansonetti, C.J. & Engleman, R.,1988 Accurate Energy Levels for Singly Ionised Platinum (Pt II).
J Opt Soc Am B5 2106-2118

AUTHORS' ADDRESS

Blackett Laboratory
Imperial College
London SW7 2BZ, U.K.

Ulf Litzén

The Ni I spectrum and term system. A progress report

ABSTRACT

The Ni I spectrum is being analyzed in the region 1600 - 50 000 Å. The first results comprise the classification of 375 lines in the infrared region and the establishment of numerous new levels of high configurations.

INTRODUCTION

The most recent analysis of the Ni I spectrum was published by Russell in 1929, and no new levels have been reported since that work 60 years ago. Although Russell's analysis was very comprehensive, it is possible to extend and improve it today by extending the observed wavelength region in the infrared, by improving the wavelength accuracy, and by using theoretical methods for predictions and interpretation. Besides the interest inherent in the analysis of the complex structure of a system involving equivalent d electrons, increased knowledge of the Ni I spectrum is important for astrophysical work due to the high cosmic abundance of nickel.

NEW OBSERVATIONS

In the present investigation the nickel spectrum emitted from a hollow cathode has been recorded in the region 1600 - 4000 Å on the 10.7-m normal incidence spectrograph at the National Institute for Standards and Technology (NIST), Gaithersburg, and in the region 2900 - 55 000 Å on the Fourier transform spectrometer at the National Solar Observatory at Kitt Peak.

In the infrared region partly resolved isotope structure is observed for numerous lines connecting the two configuration types $3d^9nl$ and $3d^84snl$.

THE ENERGY LEVEL SYSTEM

From Russell's work the $3d^9nl$ system was well known as regards the configurations $3d^94s$, 5s, 6s, 4p, 5p, 3d, 4d and (partly) 5d. In the $3d^84snl$ system only $3d^84s^2$ was completely known. A number of levels from higher parents were missing in 4s4p, and only levels from the lower parents were reported in 4s5s and 4s4d.

In the present work the analysis was started in the infrared region, where only 17 lines were previously known (Fisher et al., 1959). The analysis has this far yielded levels of the configurations $3d^97s$, 6p, 4d, 4f, 5f, and 5g; and $3d^84s5p$. Furthermore, the accuracy of the relative energy values of the high levels has been considerably improved due to the identification of numerous ir lines connecting these levels. 375 observed lines in the region 11 150 - 55 000 Å have been identified this far.

The continued work will mainly lead to an extended knowledge of the $3d^84snl$ system, thus increasing the number of classified Ni I lines over the whole observed region.

Ni I IN THE INFRARED SOLAR SPECTRUM

By comparing nickel hollow cathode spectra with the infrared solar spectrum, Biémont et al. (1986) were able to identify some 200 solar lines in the region 11 130 - 41 500 Å as due to Ni I or Ni II. 130 of these lines have now been classified as transitions between high Ni I levels, i.e. transitions of the types 5s - 5p, 5p - 6s, 5p - 5d, 4d - 4f, 4d - 5f, and 4f - 5g. Increased knowledge of the configurations $3d^84snl$ will greatly increase the possibilities for further identifications in this region.

As an example of the solar identifications all the Ni I 4d - 4f, 4d - 5f, and 4f - 5g lines present in the solar spectrum are reported in Table 1.

REFERENCES

Biémont, E., Brault, J.W., Delbouille, L., and Roland, G., 1986 - The nickel spectrum in the infrared. Application to the solar spectrum. In: Astron. Astrophys. Suppl. Ser. 65, 21.

Fisher, R.A., Knopf Jr., W.C., and Kinney, F.E., 1959 - Laboratory wave lengths and intensities in the near infrared spectra of nine elements. In: Astrophys. J. 130, 683.

Russell, H.N., 1929 - The arc spectrum of nickel. In: Phys. Rev. 34, 821.

Table 1. Ni I lines in the infrared solar spectrum classified as 4d-4f, 4d-5f and 4f-5g. The laboratory data are preliminary.

Laboratory		Sun	
Intensity	σ(cm^{-1})	σ(cm^{-1})	Combination
84	2506.057	.054	4f(5/2)[11/2]$_6$ - 5g(5/2)[13/2]$_7$
79	2506.494	.491	4f(5/2)[11/2]$_5$ - 5g(5/2)[13/2]$_6$
154	5400.934	.956	4d f^3D_2 - 4f(5/2)[5/2]$_2$
380	5418.860	.845B	4d e^1F_3 - 4f(3/2)[7/2]$_4$
306	5484.603	.604	4d f^1D_2 - 4f(3/2)[5/2]$_3$
678	5519.013	8.986?	4d e^1G_4 - 4f(3/2)[9/2]$_5$
76	5540.043	.028	4d e^3P_2 - 4f(5/2)[1/2]$_1$
46	5540.735	.789B	4d e^3P_1 - 4f(5/2)[3/2]$_1$
1123	5541.465	.453B	4d e^3G_4 - 4f(5/2)[11/2]$_5$
155	5541.906	.907B	4d e^3P_1 - 4f(5/2)[3/2]$_2$
550	5549.511	.568B	4d e^3G_3 - 4f(3/2)[9/2]$_4$
206	5557.590	.588	4d e^3P_1 - 4f(5/2)[5/2]$_2$
39	5557.752	.744	4d e^3G_5 - 4f(5/2)[11/2]$_5$
1404	5558.192	.186	4d e^3G_5 - 4f(5/2)[11/2]$_6$
101	5567.385	B	4d e^3G_4 - 4f(5/2)[9/2]$_4$
300	5568.940	.930	4d e^3P_2 - 4f(5/2)[5/2]$_3$
68	5571.994	.993B	4d e^3G_3 - 4f(3/2)[7/2]$_3$
58	5678.769	.782B	4d e^1P_1 - 4f(3/2)[3/2]$_1$
116	5745.052	.040	4d e^3S_1 - 4f(5/2)[1/2]$_0$
218	5745.759	.752	4d e^3S_1 - 4f(5/2)[1/2]$_1$
195	5758.570	.562	4d e^3S_1 - 4f(5/2)[3/2]$_1$
60	8030.306	.303	4d e^3G_4 - 5f(5/2)[11/2]$_5$
17	8039.959	.967	4d e^3P_1 - 5f(5/2)[5/2]$_2$
78	8046.949	.945	4d e^3G_5 - 5f(5/2)[11/2]$_6$
19	8054.047	.023?	4d e^3P_2 - 5f(5/2)[5/2]$_3$

AUTHOR'S ADDRESS

Department of Physics, Lund University,
Sölvegatan 14, S-223 62 Lund, Sweden.

A.E. Nilsson and Se. Johansson

The 4d4f configuration in YII

ABSTRACT

Hollow-cathode spectra of yttrium have been registered in the wavelength region 1000Å - 28000Å. New high-lying levels, belonging to e.g. the 4dnf configurations (n = 4-8), have been established. The levels of the 4d4f configuration, which are reported here, give strong lines at 1600Å in transitions to the low even configurations $5s^2$, 5s4d and $4d^2$. This is due to a selective excitation by the charge-exchange reaction between Ar^+ and Y which effectively populates the 4d4f levels of YII when Ar is used as a carrier gas in the hollow-cathode lamp.

INTRODUCTION

Singly ionized yttrium is the second member of the SrI isoelectronic sequence. Alike SrI, YII has the groundconfiguration $5s^2$, while higher members of the sequence have the groundconfiguration $4d^2$. In YII the two lowest excited configurations 4d5s and $4d^2$ lie very close to $5s^2$. This structure makes the system a good example of the competition between 4d- and 5s-orbitals regarding the lowest energy.

The first analysis of Y was done by Meggers and Russel in 1929 (Meggers, 1929). They established 61 energy levels of YII and 145 levels of YI. In a later study of Y, (Palmer, 1977) improved level values of YI and YII were given together with 47 new levels of YI. However, no additions to the old analysis of YII were done. The present analysis of YII has improved the earlier known energy levels, and led to the establishment of 134 new high-lying levels.

This report describes parts of the analysis that can be of astrophysical interest e.g. the strong 4d-4f transitions.

EXPERIMENT

The UV spectra (1000Å-2400Å) were registered by use of the 10.7 m normal incidence spectrograph at NIST, Gaithersburg, Md. The strongest YII spectrum was obtained when the hollow-cathode was run in a continuous mode with Ar, at a pressure of 0.2 Torr, as a carrier gas. Spectra were also registered with Ne, at a pressure of 1.0 Torr, as a carrier gas. A comparison of the spectrograms from these different runs, shows that the YII lines appear much stronger in the hollow-cathode run with Ar. Figure 1, which shows the region 1580Å-1630Å with some of the strongest 4d-4f transitions, is a good illustration of this phenomenon which we refer to as charge-transfer (Johansson, 1978).

Fig.1. Hollow cathode spectra of Y run with a) Ar and b) Ne as a carrier gas.

In this case the charge-transfer process is evident, as the excitation potential for the 4d4f-levels is approximately 9 eV, which, together with the ionization energy for YI, well match the ionization energy for ArI (fig.2). The enhancement of the YII lines thus makes them easy to distinguish from YI, YIII and carrier gas lines in a comparison with Y-Ne spectra.

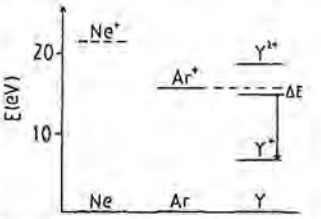

Fig.2. The charge-transfer reaction :

$Y + Ar^+ \rightarrow Y^{+*} + Ar + \Delta E$

The wavelength region 2100Å-28000Å has later been covered in order to enable a complete analysis of YII. (To be reported elsewhere.) Those spectra were registered by use of the 1 m Fourier Transform Spectrometer (FTS) at Kitt Peak National Observatory, Tucson, Az.

The hollow-cathode used in that experiment had a slightly different geometry than the one used at NIST. Unexpectedly, this meant that the hollow-cathode could not be run with

100% Ne as a carrier gas. The only way to make the light source burn with Ne, was to mix equal parts of Ne and Ar. Consequently, the easy method of distinguishing YII from YI and YIII, applied in the UV, is not so powerful here.

ANALYSIS

In this analysis, 82 lines in the wavelength region 1387Å-1849Å, have been identified. They connect the 19 new 4d4f levels with the $5s^2$, 4d5s and $4d^2$ levels. The missing 4d4f ^3P_o does only have two allowed transitions to the lowest even configurations. There are a number of plausible candidates for this level, which at this moment cannot be established unambiguously.

On the spectrograms, most of the strong 4d-4f transitions can clearly be seen to form a prominent group around 1600Å. The estimated error in the wavelengths is around ±0.002Å. Some of the strongest lines with very broad profiles have a somewhat larger error. This means that the energy levels established by use of UV-lines, have uncertainties as big as $\pm 0.3 cm^{-1}$.

The level values given in Table 1, have a much higher accuracy, which has been obtained by means of the FTS data. After being established by the $4d^2$-4d4f transitions in the UV, the 4d4f levels have been connected to the ground state via the 4d5d and 4d5p configurations through FTS measurements. The estimated error in the energies is less than $\pm 0.005 cm^{-1}$.

ACKNOWLEDGEMENTS

The help of Dr Victor Kaufman at NIST and Dr James Brault at KPNO is greatly acknowledged.

Table 1. The 4d4f configuration of YII

Term	J	Level(cm^{-1})
^1G	4	69746.436
^3F	2	69901.161
	3	69977.806
	4	70415.225
^3H	4	70081.961
	5	70285.156
	6	70786.579
^3G	3	70267.625
	4	70787.460
	5	70913.028
^1D	2	70594.407
^3D	1	70619.987
	2	70977.232
	3	70845.933
^1F	3	71178.484
^3P	0	
	1	71550.657
	2	71448.656
^1H	5	71635.626
^1P	1	72079.803

REFERENCES

Johansson, Se. and Litzén U., 1978 - Observations of charge-transfer reactions through enhancement of spectral lines. In: J. Phys. B, 11, L703-L706.

Meggers, W.F. and Russel, H.N., 1929 - An analysis of the arc and spark spectra of Yttrium (YI and YII). In: Bur. Std. J. Res., 2, 733-769.

Palmer, B.A., 1977 - The first spectrum of yttrium and an automatic comparator for its measurement. In: Thesis, Purdue Univ.

AUTHORS' ADDRESS

Atomic Spectroscopy, Department of Physics, Sölvegatan 14, S-223 62 Lund, Sweden.

A.J.J. Raassen*, A.A. van der Valk* and Y.N. Joshi**

Atomic data for the elements of the 5d-sequence

ABSTRACT

A review is given of the availability of atomic data for the elements of the 5d-sequence and of the reliability of these data.

AVAILABILITY OF DATA

Most of the data concerned were obtained in the thirties, and these investigations were limited to the lower stages of ionization, in which the ground configurations are $5d^{n-2}6s^2$ or $5d^{n-1}6s$. In these systems the lowest odd configurations are $5d^{n-2}6s6p$ and $5d^{n-1}6p$. For higher stages of ionization the $5d^n$ configuration ($0<n<10$) will be the lower one. These data were very carefully compiled by Charlotte E. Moore in the Circular of the National Bureau of Standards 467 (1958) but sometimes the data were of somewhat low quality. Initially in the 3d-sequence the situation was the same but in the sixties, seventies and early eighties very many spectra were (re)analysed. This revival was made possible by the introduction of large computer systems to calculate the complex structure of d^n-systems. The difference between the 3d- and 5d-elements, however, is that in 3d-systems the electrostatic interactions dominate the energy-level structure, while for 5d-systems the magnetic influence, which is more difficult to describe theoretically, is more important. This effect is due to the larger nuclear charge. For this reason there are considerably less data available for the 5d-elements than in the 3d-sequence. This is shown in tables I and II.

Those 5d-spectra that have been analysed thus far are the least complex. Only $5d^n$ configurations (starting to be the ground configuration from the III-spectra)with small n or n close to 10 were investigated. This is shown in table III.

RELIABILITY OF DATA

Reliability of data is difficult to prove without re-analysing or re-investigating the spectra. This, however, is seldom done. Sometimes there are suspicions about the correctness of an analysis on theoretical or other grounds. After calculations of the average energy of the d^9 and d^8s configurations by Edlén doubts were raised about the correctness of the published abalysis of Hg IV in which the ground term belongs to $5d^86s$, while in the calculations $5d^9$ definitely is the lowest one. A recent analysis by Joshi et al. (1989) shows that Edlén's doubts were justified. The earlier (faulty) and the new (completely revised) analysis of Hg IV are given in table IV.

After the analysis of Tl III and Pb IV by Gutmann and Crooker (1973) some revision was made by us in the spectrum of Bi V also (Raassen et al. 1989). The changes were, in this case, supported by the isoelectronic trend from Tl III to Bi V.

A new tool for proving the correctness will be parametric calculations along isoelectronic as well as isoionic sequences using the recently introduced complete sets of operators (Hansen et al. 1988a and 1988b) and (Uylings et al. 1989). Inclusion of the recently developed magnetic operators is essential for calculations in 5d-spectra. A simple example is given in table V. It shows the calculation of the d^9s configuration in the 3d- as well as in the 5d-sequence.

CONCLUSION

-Most of the spectra of higher stages of ionization and with more complex d^n ground configurations in the 5d-sequence are still unknown.
-Analyses done in the past need reinvestigation.
-Parametric treatment using a complete set of operators is helpful to find errors in former analyses and to analyse unknown spectra.

Table I Percentage of levels known in lowest even configurations.

	Ti	V	Cr	Mn	Fe	Co	Ni	Cu	Zn	Ga	Ge	As
I	>90	>75	>75	>75	>90	>90	100					
II	100	>90	>90	>90	100	>90	>90	100				
III	100	100	>90	>75	>90	100	100	100	100			
IV	100	100	100	>90	100	>90	100	100	>90	100		
V		100	100	100	100	100	>90	100	100	>90	100	
VI			100	100	100	100	100	>90	100	100	>90	100
VII				100	100	100	>90	100		100	100	100
VIII					>90	100	100					100

Table II Percentage of levels known in lowest even configurations.

	Hf	Ta	W	Re	Os	Ir	Pt	Au	Hg	Tl	Pb	Bi
I	>90	>90	>90	>90	>90	>90	100					
II	>90	>90	>90	>90	>75	>90	>90	100				
III	>90		>90*					>90	100			
IV	100	100	100						>90*	100		
V		100	100						>90*	>90*	100	
VI			100							>90*	>90*	100
VII				100							>90*	>90*
VIII					100							>90*

* = publication in preparation

Table III Number of configurations investigated.

	d^1	d^2	d^3	d^4	d^5	d^6	d^7	d^8	d^9	d^{10}
3d	5	6	6	5	5	4	4	6	5	4
5d	5	3	1	1				4	5	4

Table IV

Hg IV (old) Config.	Desig.	J	Level
$5d^8(^3F)6s$	$6s\ ^4F$	4½	0
		3½	7557
		2½	12084
		1½	15438
$5d^9$	$5d^9\ ^2D$	2½	2192
		1½	10376
$5d^7\ 6s^2$	$6s^2\ ^4F$	4½	5653
		3½	7897
		2½	9476
		1½	10592
$5d^8(^3P)6s$	$6s'\ ^4P$	2½	21011
		1½	23270
		0½	24564
$5d^7\ 6s^2$	$6s^2\ ^4P$	2½	24054
		1½	25001
		0½	25802
		4½	42131
		2½,3½	44599
		3½	53342
		3½	55664
		2½	57122
		3½	57270
		3½	59490
$5d^8(^3F)6p$	$6p\ ^4F^o$	4½	70567
		3½	75655
		2½	79688
		1½	82884
$5d^8(^3F)6p$	$6p\ ^4G^o$	5½	74419
		4½	81039
		3½	87825
		2½	92237
		3½	74702
		3½	75388
		2½	75772
		3½	77045
		3½	78556
		3½	79919
$5d^8(^3F)6p$	$6p\ ^4D^o$	3½	85056
		2½	88216
		1½	89513
		0½	90327
		2½	85091
		3½	86380
		1½,2½	87185
		2½	91752
		1½,2½	101826
		2½	102255
		2½	102353
		1½,2½	106210
		2½	106385
		1½	106748
		1½,2½	108798
		2½	113648
		2½	114508

Hg IV (new) Config.	J	Level
$5d^9$	5/2	0
	3/2	15685
$5d^86s$	9/2	60137
	7/2	66108
	5/2	69941
	3/2	71761
	5/2	77674
	7/2	78852
	1/2	82389
	3/2	83914
	5/2	86029
	3/2	88899
	9/2	92352
	7/2	93179
	1/2	93405
	3/2	100153
	5/2	100911
	1/2	-
$5d^86p$	7/2	130813
	9/2	133616
	3/2	138710
	5/2	139262
	5/2	146768
	7/2	147286
	1/2	-
	11/2	150231
	3/2	152092
	9/2	152492
	7/2	153354
	5/2	154125
	1/2	154238
	5/2	155956
	3/2	156773
	7/2	159698
	5/2	160553
	9/2	161406
	1/2	162542
	7/2	164146
	3/2	165069
	5/2	165172
	9/2	165900
	7/2	167726
	3/2	168415
	5/2	169343
	3/2	172765
	5/2	173046
	7/2	173307
	1/2	173589
	3/2	173841
	1/2	177882
	5/2	178025
	3/2	178149
	11/2	178694
	5/2	179890
	3/2	180159
	7/2	183308
	9/2	184942
	3/2	186779
	5/2	188791
	7/2	188868
	1/2	191225
	1/2	-
	3/2	-

Table V Experimental and calculated values in a $3d^9 4s$ and $5d^9 6s$ conf.

	$3d^9 4s$ (Ge V)			$5d^9 6s$ (Pb V)				
J	Exp.	Calc.		Exp.	Calc.		Calc.	
3	234231	234234	-3	110768	110845	-77	110764	4
2	235971	235966	5	114705	114592	113	114713	-8
1	238767	238767	0	132711	132577	134	132698	13
2	241947	241948	-1	135997	136083	-86	136003	-6
E_{av}		237275			121351		121351	
C_{ds}		2127			3141		3141	
Zeta		1813			8693		8693	
A_{mso}		0			0		81	
A_{ss}		0			0		0	

REFERENCES

Gutmann, F. and Crooker A.M., 1973 - Extensions in the Spark Spectra of Tl III and Pb IV. In: Ca. J. Phys., 51, 1823-1830.

Hansen, J.E., Uylings, P.H.M. and Raassen, A.J.J., 1988a - Parametric fitting with orthogonal operators. In: Physica Scripta, 37, 664-672.

Hansen, J.E., Raassen, A.J.J., Uylings, P.H.M. and Lister, G.M.S., 1988b - Parametric fitting to d^N configurations using orthogonal operators. In: Nucl. Instr. Methods Phys. Res._ B31, 134-138.

Joshi, Y.N., Raassen, A.J.J. and Arcimowicz, B., 1989 - Fourth spectrum of mercury: Hg IV. In: J. Opt. Soc. Am. B6, 534-538.

Raassen, A.J.J., Van der Valk, A.A. and Joshi, Y.N., 1989 - Revised and extended analysis of Bi V. In: J. Phys. B: At. Mol. Opt. Phys., 22, 13-20.

Uylings, P.H.M., Van het Hof, G.J. and Raassen, A.J.J., 1989 - Orthogonal operators for $d^N s$ configurations: definition and interpretation. In: J. Phys. B: At. Mol. Opt. Phys., 22, L1-L4.

AUTHOR'S ADDRESS *
Zeeman-Laboratorium
Plantage Muidergracht 4
1018 TV AMSTERDAM, The Netherlands.

AUTHOR'S ADDRESS **
Phys. Dept. St. Fr. X. University
P.O. Box 121
ANTIGONISH, N.S., Canada B2G 1C0.

E. Jannitti+, P. Nicolosi0 and G. Tondello0

Inner shell photoabsorption spectra of C ions

ABSTRACT

The absorption spectra of ionized and neutral carbon have been obtain in the soft X-ray range by using two laser produced plasmas. They correspond to the transitions of the 1s inner electron. The CIV and CIII spectra, in addition with the CV one already studied, are reported. Furthermore the absorption spectra of neutral carbon have been observed for the states: solid, vapour (clusters) and CI atoms.

THE EXPERIMENT AND THE RESULTS

Absorption spectra of moderately charged ions can be obtained with two laser produced plasmas, one acting as the background continuum source, the other as the absorbing medium. This technique has been widely used both in the normal and in the grazing incidence spectral regions (Jannitti, 1987 and references).

Here we report on the absorption measurements of the spectra of carbon ions (CI, III, IV) in the grazing incidence. In the same spectral region the spectra of graphite vapours and for comparison of an amorphous graphite film have been observed. The experimental technique has been described in detail in a previous paper (Jannitti, 1987). In fig. 1 the absorption of the CV, IV and III ions between 25 and 45 Å is reported. The CV spectrum is due almost to the optical electron and is shown here for comparison with the other spectra. It was obtained by focusing about 1.3 J of laser energy in a 1 mm diameter focal spot size on a graphite target and delaying the continuum irradiation of the absorbing plasma about 4.5 ns. Furthermore the absorbing plasma has been probed at y=0.5 mm from the target surface. The photoionization cross-section measurement

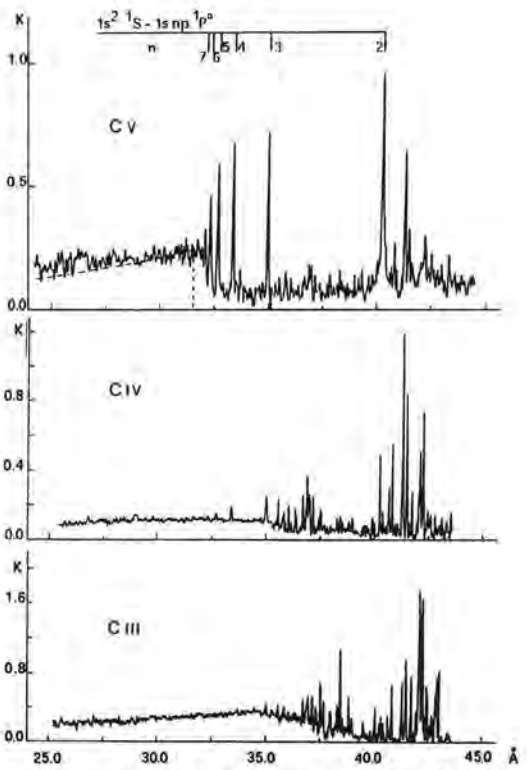

Fig. 1. Experimental absorption coefficient of the C III, IV, V ions.

has been already reported (Jannitti, 1988). The CIV spectrum has been produced with 0.7 J focused in a spot of 1.2 mm diameter and the absorbing plasma has been irradiated at y=1.1 mm with a delay of 30 ns. On the other hand the CIII spectrum has been produced by focusing 1.4 J in 0.3x16 mm^2 and the plasma has been probed at y=0.7 mm with a delay of 18 ns. The long wavelength portion of the two spectra showing the discrete transitions has been deconvoluted by applying a constrained deconvolution procedure to the absorptance (Jannitti, 1989). With respect to the CV spectrum there is apparent an increased mixing between the ionization stages. The main reasons can be: the range of the abundance ratio of the Li- and Be-like ions in an ionization balanced plasma, the duration of the background continuum emission (~ 20 ns) compared to the life time of the Li- and Be-like ions, the poor uniformity of the laser power density distribution in the focal spot on the graphite target. The CIII and CIV spectra are due to inner shell transitions of the 1s electron to np (and ϵp)

levels. A complete analysis of these spectra is in progress while a preliminary identification of the observed transitions has been already reported (Jannitti, 1989). The CIV transitions can be mostly attributed to the $1s^2 2s$-$1s2snp$ and $1s^2 2p$-$1s2pnp$ configurations.

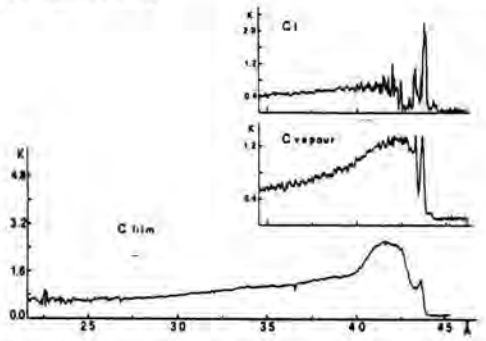

Fig. 2. Experimental absorption coefficient of neutral carbon.

The absorption spectra of neutral carbon are shown in fig. 2. Also the long wavelength portions of the CI and C vapour spectra have been deconvoluted. The experimental parameters were respectively for the CI case: 0.45 J laser energy, focal spot size 0.7x7 mm^2, y=1.5 mm and delay ~ 100 ns; for the C vapour: 0.07 J, 4.2x10mm^2, y=0.25 mm and delay ~ 100 ns.Finally the spectrum of amorphous graphite has been obtained by positioning a 30 $\mu g/cm^2$ graphite film in front of the spectrograph entrance slit and by using the laser produced plasma continuum. It is evident that by decreasing the laser power density on the graphite target the spectrum changes deeply. The CI photoionization spectrum extends down up to about 35 Å with the threshold at about 41.5 Å. It corresponds to the 1s photoionization from the $1s\ ^2 2s^2\ 2p^2\ ^3P, ^1D, ^1S$ states. Some preliminary wavelength measurements and the corresponding tentative assignments have been already reported (Jannitti, 1989). Work is in progress also on this spectrum. The C vapour spectrum looks like those corresponding to core level-valence state transitions of solid or clusters compounds. The graphite film spectrum has been recorded for comparison. It shows clearly a bulk absorption starting at about 43 Å. The shape at shorter wavelengths appears different from the clusters and CI cases while an absorption peak is present at wavelengths longer than the absorption edge in a perfect agreement with the high resolution spectra obtained with synchrotron radiation (Del Grande, 1988) It appears a true structure of carbon absorption and corresponds in wavelength to the peak observed in the cluster vapours spectrum. On the other hand there is not an immediate correspondence with the discrete lines of the CI spectrum. In conclusion these spectra show a smooth transition from the solid state to the atomic behaviour and once again confirm that in absorption spectroscopy LPP's compare favourably, as continuum source, with synchrotron radiation.

REFERENCES

Del Grande, N.K. and K.G. Tirsell, 1988 - A program to obtain reliable photoabsorption cross sections. In SPIE Conf. Proc., 911, 6-10.

Jannitti, E., P. Nicolosi and G. Tondello, 1988 - Photoionization Cross-section Measurement of the CV Ion. In Phys. Lett. A, 131, 186-189.

Jannitti, E., P. Nicolosi and G. Tondello, 1989 - Absorption spectra from the 1s inner shell electron of ionized and neutral carbon. To be published in Physica Scripta.

AUTHOR'S ADDRESS

(+) Istituto Gas Ionizzati, CNR and (o) Dipartimento di Elettronica e Informatica, Universitá di Padova, via Gradenigo 6/A, 35131 Padova, ITALY.

Fusion and other uses of atomic data

H.P. Summers, R. Giannella, M. von Hellermann, N.J. Peacock and members of Experimental Division II, JET and Diagnostic Group, UKAEA, Culham

JET spectra and their interpretation

ABSTRACT

The scope of spectroscopic diagnostic studies on the JET tokamak is summarised. The atomic data and modelling required to analyse JET spectral observations are illustrated by some case studies.

INTRODUCTION

Spectroscopy on JET is committed to interpretative diagnostics for fusion plasmas. The theoretical modelling necessary to achieve these ends requires extensive atomic data, including energy levels and oscillator strengths, but especially electron-ion, ion-ion and ion-atom collision cross-sections. In keeping with this meeting, however, it is atomic structure and the spectra themselves which are emphasised. It is intended to provide an overview of the areas of current excitement, an outline of the reduction methods used and of the atomic data exploited.

Within the constraints of the fusion objectives, a flood of spectroscopic data is available at JET which, in principle, can be accessed together with other extensive diagnostic information in the JET database. At this time, more than 20000 pulses each with about 12 Mbytes of information have been recorded and a rich phenomenology has been observed. It is apparent that many features of such large volume, strongly heated fusion plasmas of the JET type are somewhat different from those of the familiar/idealised high temperature low density plasmas of the astrophysical type. The reasons are evident, namely:- powerful influence from interactions with the limiting surfaces of the plasma; high neutral deuterium presence due to neutral heating beams and recycling from boundary surfaces; a confining magnetic field which can be configurated to create plasma zones of different diffusive character; transient perturbation of the plasma by pellet injection and gas puff; active feedback control of selected plasma parameters.

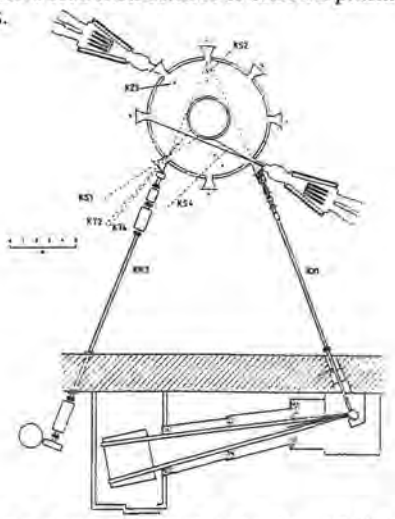

Fig. 1. A plan view of JET with the lines of sight of the principal spectrometers indicated. Note the two neutral deuterium beam injector (NBI) assemblies.

The characteristics of the various spectrometers are summarised in table 1. There are approximately fifty further diagnostics including various techniques for measuring the electron parameters $n_e(r)$ and $T_e(r)$ (LIDAR Thomson scattering, ECE , interferometry, reflectometry), infrared cameras, x-ray camera diode arrays allowing tomographic reconstruction in the poloidal section at very high time resolution etc.

Table 1. Characteristics of principal spectrometers.

Beam diagnostics		
KS4	4000-7000A	multi-chord
KS5	4000-7000A	multi-chord fibre optic link
Edge diagnostics		
KT3	4000-7000A	several lines
Spatial scan spectroscopy		
KT1	100-2500A	grating
KS2	1-24A	2-crystal
KT4(1,2)	10-340A, > 2000A	grazing incid.
Survey spectroscopy		
KS1	1-24A	
KT2	100-1700A	grating
High resolution spectroscopy		
KX1	1-3A	bent crystal
Other		
KH2	> 4kev	Pulse height
KZ3		laser ablat.

A more limited set of radiation protected spectrometers will be available in the active (deuterium / tritium) phase of JET operation.

NBI together with ion cyclotron resonance heating (ICRH) supplement the direct ohmic heating of the plasma by the induced toroidal current in the tokamak. Combinations of the plasma heating methods, control of the position and elongation of the plasma in the poloidal section, vessel conditioning, control of internal instabilities and X-point operation have achieved the plasma parameters in table 2. X-point refers to the operational mode in which a poloidal magnetic field null is created within the vessel so separating the plasma from material limiters. τ_E and τ_i are respectively the energy and particle confinement times. $Q_{D\text{-}T}$ is the predicted ratio of the total thermonuclear power output to the power input if the deuterium in the plasma were to be replaced by a fifty per cent mixture of deuterium and tritium.

Table 2. Selection of plasma parameters.

Param.	Achieved	Range
I_p	7 MA	< 5MA X-point, 7MA limiter
P_{tot}	35 MW	< 7 OH, < 18 ICRH, < 21.5 NBI
T_e	12 keV(centre)	< 12 keV
T_i	25 keV(centre)	< 25 keV
N_e	$2.8x10^{14}$ cm^{-3}(centre)	10^{12}-$2x10^{14}$
Zeff	1.3	1.5 - 6.0
τ_E	1.2 sec(global)	0.2-1.2 sec
τ_i		< 3.0 sec
$Q_{D\text{-}T}$	0.2-0.5 !	

The vessel, composed of the alloy Inconel, is protected at the inner wall of the torus by graphite tiles and at the outer wall by two graphite toroidal belt limiters. Further graphite tile protection is present especially at the top and bottom of the vessel for single and double null X-point operation. There has been a policy of carbonising the vessel interior by discharges in methane. This trend to light impurity contact materials is continuing. Presently beryllium evaporators are in use. The oxygen gettering effect of beryllium and other benefits of the beryllium coating appear quite marked and there is an intention to use beryllium as the material for limiters and antennae screens in the near future.

A general description is given in the JET Annual Reports (Keen, 1987) (see also Schumacher et al.,1989; Pasini et al.,1988; Bartirómo et al., 1989)

Table 3. Principal fractional impurities relative to n_e and their sources.

Impurity	Conc.	Source
He	arbitrary	initial gas fill
Be	< 0.01	evaporators--> walls & limiters.
C	0.05	limiters,inner wall, X-pt. strike pts.
O	0.01	walls, limiters
Ni	< 0.001	antennae screens, walls
Cl	< 0.007	uncertain
Ne,Ar,Kr	arbitrary	gas puff
Fe,Ni,Mo, etc.	arbitrary	laser ablation

SPECIFIC SPECTRA AND STUDIES

Table 4 itemises the various spectroscopic studies carried out, their fusion related objectives and the specific atomic data adopted. The purpose is to draw attention to the atomic data in use and to indicate the paths along which the JET spectroscopic studies are likely to evolve. It will be evident where particular weaknesses exist or new data will be required. Limitations in space allows illustrations in only three areas which have been particularly active in the recent JET program.

CXRS & ABAS - a new spectroscopy

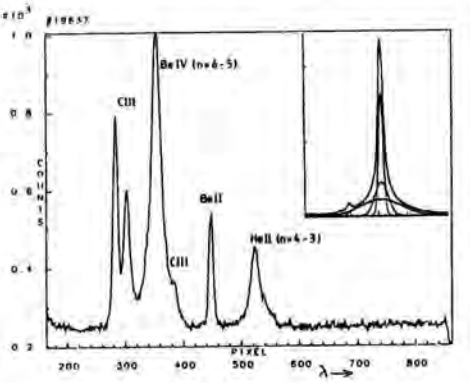

Fig. 2. Charge exchange signals from BeIV & HeII. Insert illustrates resolution of HeII line into hot (central) beam induced CX part and cold (edge) part

It is perhaps surprising to begin with observations of hydrogen (in fact deuterium in JET) and hydrogenic ions of low z, since from an atomic structure point of view, little has been added for many years. Nonetheless emission from such low z hydrogen-like ions has revolutionised the spectroscopic diagnostic capability for fusion

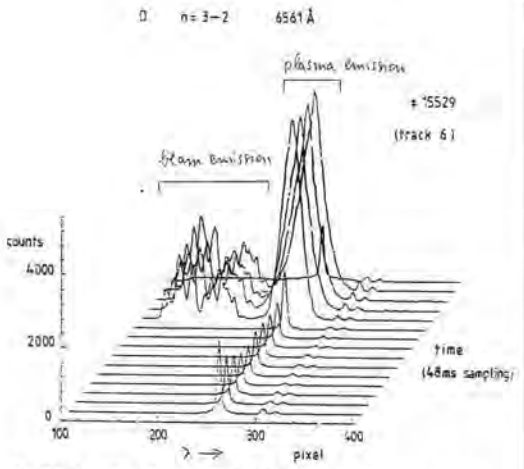

Fig. 3. D_α in the vicinity of 6561A showing plasma and beam emission.

plasmas. Strong O^{+7} emission is common in many plasmas, but not so common at temperatures of order 15keV and in the n=10-9 transition. The reason is of course neutral hydrogen beams. Figure 2 is a very recent spectrum from JET and illustrates spectra influenced by charge exchange from neutral deuterium (E=40keV/amu) in the heating beams. In the absence of beams, both HeII and BeIV show only narrow features similar to that of BeII and originating in the cold plasma periphery (T_e of order 100-500eV). The observed widths in figure 2 arise from hot component emission from the beam/viewing line intersection following capture by the corresponding bare nuclei. The hot feature separated from the cold 'edge features' allows diagnostics of light impurities in the plasma centre where they are normally fully ionised. Its width and displacement gives the ion temperature and plasma rotation. Exploitation depends on confident subtraction of the cold components and the bremsstrahlung background. For HeII, the cold feature arises from at least two populations which evolve during the neutral beam heating period. The shape of the hot feature at high plasma temperature is modified by the variation of the charge exchange cross-section with energy. Evidently the analysis procedures are improved by exploiting passive viewing lines (which do not intersect the beams), calibrating observations using the unviewed beam line and pulsed operation of the beams. Theoretical modelling of the effective emission coefficients allows reduction of the calibrated line of sight emissivities of the hot feature to an emission measure. The deduction of the effective coefficients is complicated by the n-shell distribution of charge exchange capture and its energy dependence, redistribution by collisions and Lorentz fields, cascade, fractional energy components in the beam and capture from excited states of deuterium. With the additional knowledge of the beam attenuation with path length, the emission measure of the observed volume can be resolved to a local impurity density. Such procedures termed 'charge exchange recombination spectroscopy' (CXRS) are practised at JET for He, Be, C and O -the primary light impurities (Boileau et al., 1989a,b).

Similar observation for deuterium itself is illustrated in figure 3 before and during beam injection. The Balmer alpha features become very complex during injection. Their exploitation has been termed 'active Balmer alpha spectroscopy' (ABAS). The hot and cold components at the unshifted wavelength have the same interpretation as before although the cold part is complicated by recycling deuterium from limiters which can penetrate quite deeply into the plasma and so have a relatively high temperature. The blue displaced emission is from the deuterium in the beam. The Doppler displacement follows from the beam/viewing line inclination. There are three components due to full, half and third energy fractions in the beam. Each of these is resolved into Stark components of π and σ polarisation by the large vxB electric field (of order 10^5 V/cm) arising from the cross-field motion of the beam particles. Because of the beam speed, the excitation is primarily by positive ion impact. These observations have huge diagnostic potential. Precise geometry is checked by the net Doppler displacements, the π and σ separations give the projected internal magnetic field. The variation of the signals along the beam path measures the beam attenuation and the differential attenuation with beam energy. The composition of the beams at source is also revealed. Zeff may be derived from the ratio of the Stark to main charge exchange feature ratio and is to an extent calibration independent. Clearly the interpretation is strongly dependent on accurate fundamental cross-section knowledge with particular sensitivity to beam stopping data (Boileau et al., 1989c).

On the other hand the transition probabilities and energy levels are well known. However the range of such observations is expanding rapidly. Similar high n-shell emission following charge transfer has been observed for He-like (Rice et al., 1987), Li-like, Na-like and K-like ions.(eg Si^{+13} n=11-10,..,15-14; Kr^{+25} n=16-15,..,23-22; Kr^{+17} n=15-14 - Hofmann (1989)). The Rice results followed capture from thermal hydrogen.

Table 4. Summary of energy and transition probability data usage at JET.

Primary area	Secondary area	Tertiary area	Study	Illustration	Energy & transition probability data	Sources & Comments
Edge plasma	Visible spectroscopy	Influx of light impurities from limiters	Deduction of suitable lines & S/XB ratios for BeI, BeII, CI, CII, CIII, OII, OIII	1. OII(4351A) & Dy relative intensities JET pulses #10353, #10354	n = 3-3 & 4-3 A-values; 2-electron transition probs. from n = 3; cascade paths from n < 7	mostly reasonably known - some exceptions
		Influx of metal. impur. from limiters	Deduction of suitable lines & S/XB ratios for CrI, CrII, FeI, FeII, NiI, NiII	2. CrII(2835-2862A multiplet) JET pulse #2470	Association of lines with metastables; A-values; branching to to different metastables; parent mixing	Kurucz(1972), Johannson(1987), Litzen(1987), Hibbert(1988) - uncertain!
		Fluxes of light & med. impur. in divertors	As (2) above, extended to include AlI, AlII, SiI, SiII Density dependent corrections	3. not available	not determined	probably available
		Fluxes of high z elements in divertors	As (2) above, extended to include MoI, MoII, WI, WII	4. not available	not determined	quite uncertain!
		Thermal deuterium	Evidence of CX from excited states of D to fully ionised and helium- like ions	5. Composition of CVI (5290A) cold feature (see refs.)	Energies of high nl levels of lithium-like ions in terms of polarisabilities	well known - Edlen.
		Molecular species	Direct evidence for chemical sputtering, states & kinetic energies of atomic/ionic constituents after dissociation Equivalent approach to S/XB ?	6. CII band spectrum (fig. 10.)	Suitable bands for CH_n, CH^+, OII, H_2, BeII etc; emission & dissociation probabilities - uncertain requirements	not investigated - uncertain
	VUV & EUV	Thermal hydrogen	Evidence of CX from ground & excited states of D to stripped impurities	7. CVI Lyman series, inner wall discharge JET pulse #13751	well known	
			Evidence of CX from ground & excited states of D to partially stripped light impurities	8. CIII disruption spectrum in KT4 JET pulse #11011	Radiative &/or Auger probabilities for 2snl & 2pnl ($2 < n < 6$); state selective dielectronic coeffts.	Mostly known; Badnell(1986) for Auger/diel
		Radiated power by heavy species in divertors	Stages, radiat. power, observable spectral features for 10-200 eV plasma. Shell group / pseudo - band structure approach ?	9. MoIII - MoXII transition arrays (fig. 9.)	Energies & A-values for describing integral emission of pseudobands and shell-shell ionis./recom. Mo, W	uncertain - Klapisch , Cowan ?
		ion/surface interaction	Secondary electron emission by impact of highly ionised ions on graphite & metal surfaces	10. not available	Radiat./Auger probs. & cascade paths for multi - spectator & strongly correl. neutralisation for He^{+4}, C^{+6} etc.	unknown

Primary area	Secondary area	Tertiary area	Study	Illustration	Energy & transition probability data	Sources & Comments
Bulk plasma	Visible spectroscopy	Bremsstrahlung emission	Deduction of local Zeff	11. Zeff variation radially across plasma many illust.	free-free hydrogenic Gaunt factors,	well known
		CX from neutral beam deuterium to stripped impurities	Deduction of local T_i for D, He, Be, C & O at radial pts. Deduction of local v_{rot} for plasma at radial pts.	12. OVIII n = 10-9 fitted line shape many illust.	well known	
			Deduction of local n_i for D, He, Be, C & O at radial pts.	13. C & O density evol. in JET pulse many illust.	well known	
		Radiation by D in the neutral beams	σ & π D measurements to obtain internal B-field; full, 1/2 and 1/3 energy beam attenuation measure; excited D content of beam; Zeff measure	14. D_α emission from the beam - Stark cpts. (fig. 2.)	well known	
	VUV & EUV	Ionisation balance & radiated power	Dielectronic coefficients for complex Cr, Fe & Ni ions (fluorine- like to magnesium-like); consistent metastable treatment; possible extension to Al, Si, Mo, Kr	15. Dielectronic coefficient for Ni^{+17} (see refs.)	Very high Rydberg state energy level separations - dipole polarisabilities with ground & metastable cores; A-values	various incomplete!
		Line ratio diagnostics	Deuterium dilution from boron-like line ratios in Ni^{+23} & Kr^{+31}	16. KT4 spectrum of NiXXIV at 118A & 138A JET pulse #13868	Ground term M1 fine structure transition probabilities and $2s^2 2p\ ^2P_{1/2,3/2}$; $2s\ 2p^2\ ^2D_{3/2,5/2}$ etc A-values.	reasonably known
	XUV & X-ray	Ionisation balance	Transport studies	17. Ni^{+27} & Ni^{+26} radial profiles		
		Ion temperature and plasma rotation	Plasma heating & electron-ion thermalisation	18. Ni^{+26} emission many illust.	Resonance, forbidden, intercomb. & satellite line parameters	reasonably known

In non-hydrogenic cases, the low l transition arrays diverge from the hydrogen-like transition energy and potentially cause a distorted n-n' profile. Essential for analysing this are precise high Rydberg state energy levels and a sub-shell direct capture and redistribution model which gives the lj relative populations. The redistribution within an n-shell is strongly sensitive to the precise level separations. n-shells up to about 40 need to be included. A most useful presentation of this extensive energy level data is as polarisabilities. Such polarisabilities are useful in an other context to be described later. An associated set of problems and data requirements occur with partially stripped species and thermal hydrogen (see table 4).

Influx of BeI and CrI contrasted

Deduction of the flux of an impurity from a localised surface from observed column emissivities along a line of sight directed at the surface can be inferred if the theoretical quantity termed the 'ionisation per photon' or 'S/XB' ratio for each observed line is known. The inference is valid from any low ionisation stage of an element provided it has not significantly spread from its source before being ionised. Fluxes of both light and metallic impurities have been measured systematically from limiters, inner wall RF antenna screens etc. by this means. The calculation of the 'ionisation per photon' is interesting for a number of reasons. Firstly an inflowing ion generally has ground and metastable states whose populations are not necessarily strongly coupled in the highly ionising environment of the plasma edge. It requires therefore separate line observations, from each spin system at least, to evaluate the total flux. The choice of lines is also governed by the wish to use visible spectroscopy. For light impurities, the most suitable lines therefore have upper levels with n = 3 or 4 shell electrons and no dipole decay to the n = 2 shell so as to give favourable branching. A comprehensive collisional radiative model with uncoupled metastables is used to evaluate the populations and thence the ionisation per photon for the selected lines. Essential ingredients are non-dipole excitation cross-sections for $\Delta n > 0$ transitions, two-electron transition probabilities which tend to compete with the observed lines and corrections for cascading from higher quantum shells not included directly in the collisional radiative model. Further checks are necessary that charge transfer from the co-located neutral recycling hydrogen cloud is negligible. A valuable and consistent picture appears to have been established at JET for influx of CII, CIII, OII and OIII using these methods. (Behringer et al., 1989)

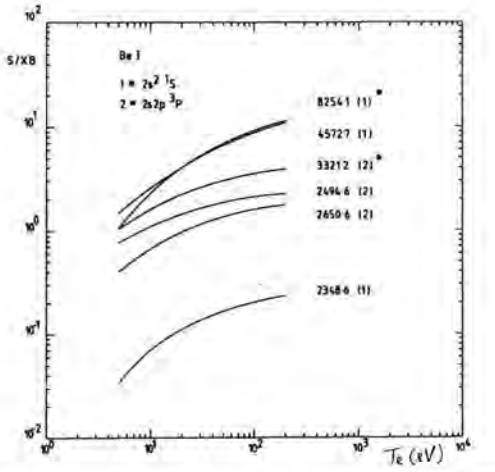

Fig. 4. S/XB ratios for BeI. * indicates preferred lines.

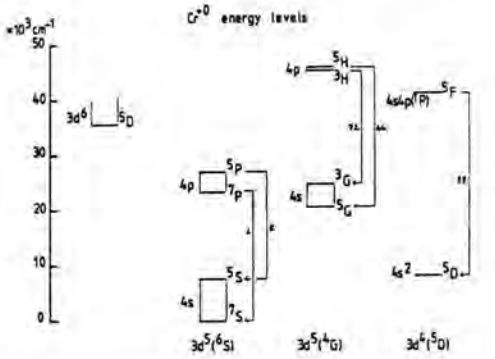

Fig. 5. Partial Grotrian diagram for CrI. (Behringer et al.,1989)

Consider however the situation for beryllium. This species has only been present in JET during 1989 and is under intense study. Clearly BeII with the 2s-2p resonance line at 3130A is the simplest ion for flux determination, but the wish to know more about release from the wall prompts study also of BeI. The atomic structure of BeI has been studied extensively. It displays strong configuration interaction, most notably the perturbation of the 2snd ¹D series by the 2p² ¹D term. Doubly excited states of the form 2pnl (n > 2) generally lie in the continuum. The very small oscillator strengths for 2s² ¹S - 2s3p ¹P and 2s² ¹S - 2s4p ¹P are of note as

is the large oscillator strength for $2s^2\,{}^1S$ - $2p3s\,{}^1P$ (a two electron transition with the upper state in the continuum. These complexities have created some anxiety and prompted us to select $2s2p\,{}^1P$ - $2s3s\,{}^1S$ at 8254A as a possible visible line for monitoring the singlet side. On the triplet side $2s2p\,{}^3P$ - $2s3s\,{}^3S$ at 3321A may just be usable. There does not appear to be a modern cross-section calculation available and so at present JET modelling uses fairly simple data. Preparatory studies on the UNITOR tokamak show a strong variation of metastable to ground population down to as low as 0.4 and with deviations of order 3 between theory and measurement for some lines. These are important issues for JET interpretation, but clearly the atomic data base must be made secure before proceeding much further (Forrest et al., 1989). Figure 4 shows S/XB ratios for BeI.

For the first and second ionisation stages of medium weight metals such as Cr, Fe and Ni the situation is rather different, partly because dipole allowed resonance transitions occur in the visible region, but mostly because of lack of detailed knowledge of energy level structure which allows association of lines with metastables (in practise, the best we can usually achieve is a linearly independent but non-orthogonal set of lines, so that a matrix equation must be solved for the metastable fluxes). A fortiori, good quality collision cross-section data is very limited. A detailed collisional radiative model cannot be supported. A partial Grotrian diagram for CrI is shown in figure 5. This indicates metastable states which might be important and spectrum lines which might be used to measure their fluxes. It is largely based on the work of Kurucz and Peytremann (1975). Measurements of metal influxes in JET are by far less complete than for light impurities. Furthermore a survey of limiter spectra based on different plasma pulses is unreliable because of the strongly varying metal coverage of the carbon tiles. Thus only the CrI 4254A (multiplet 1) line has been monitored routinely from the limiters and the quintet line 5208A (multiplet 8) has been measured on occasion. The chromium influxes for a strongly metal coated limiter case tend to indicate a small population for the ^5S state. In general no discrepancies have been encountered when asssuming the 4254A transition to be representative of the total neutral chromium flux. A capability for analysing metal influx is likely to become more important at JET in the light of possible divertor developments, as it is already in divertor machines such as ASDEX. For this reason we have a basic atomic physics study in progress on transition probabilities and collision cross-sections for CrI (Hibbert et al, 1988)

Line ratio diagnostics in JET

The powerful independent diagnostics for electron temperature and density profiles in the bulk plasma in JET have rendered line ratio methods for these quantities unnecessary. The dominant issues for spectroscopy are rather diffusion, impurity abundance and radiated power and so spectrum lines from different ionisation stages are compared with a view to infering ion transport. Large quantities of ionisation, recombination and line excitation data are used in the impurity transport codes and other global particle and power balance codes. The detailed interactive return to atomic physicists / spectroscopists from the use of their data has been rather low, partly because of calibration difficulties, partly because of the multiprocess dependence of most measurements, but mostly because of the complexity of the diffusion problem alone. The most direct information on ion diffusion is in fact obtained by transient injection of impurities either accidentally or intended by laser ablation. Such a system is in operation and a wide range of species have been used (Fe,Ni,Cu,Mo,Ag etc) (Magyar et al., 1988). Similarly rare gases have been introduced by gas puffing. The high plasma temperatures in JET have allowed spectra of very highly excited states to be acquired of interest for identification and precision wavelength studies as a by-product. Figure 6 shows such a molybdenum spectrum with the Li-like and Be-like resonance lines identified (Denne et al., 1989).
Experience on ion diffusion and particularly the identification of zones where there is confidence that ionisation balance exists suggests that it would be worthwhile to invert the problem and try afresh

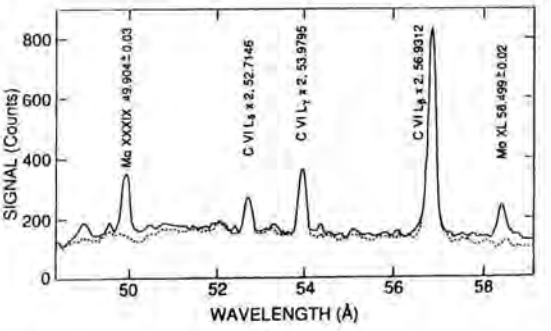

Fig. 6. Molybdenum spectrum following laser ablation.

to use line ratios from different ionisation stages to assess ionisation and recombination cross- sections. It is worth noting that dielectronic recombination of nickel ions around the Ne-like to Al-like stages is influenced by the finite plasma density in JET (factor of order 2) (Summers et al., 1987). Also it is desirable to adopt the more complete treatment of ionisation and recombination which handles metastables consistently in plasma modelling. High n-shell structure again plays a role (eg. dipole polarisabilities for metastable cores) Calibrated radial profiles from spectrometers such as KS2 (Table 1) with associated local densities and temperatures are very powerful for this. Also large statistical studies are possible exploiting the JET data base. For example, Ni^{+26} line ratios have been mapped and compared with theory for hundreds of samples over an electron temperature range from 3keV to 13 keV as illustrated in figure 7. (Zastrow et al., 1989)

The limited number of studies on single stage line ratios have tended to be primarily for cross-calibration or for simple checks on theoretical cross-sections. A possible exception may be highly ionised boron-like systems such as NiXXIV and KrXXXII where the forbidden line from the upper ground term fine structure level is observable and the competing collisional deexcitation is by ion impact. For NiXXIV in JET, it is more convenient to exploit the nearby lines at 118A and 138A (which arise from electron impact excitation from the ground and metastable to the $2s2p^2\ ^2D$ levels) rather than the forbidden line itself which occurs in a more remote wavelength region. At first impressions, this might be thought to be exploitable as an ion temperature indicator, but in practise, the ion tends to locate always at the same electron temperature. In circumstances when T_i and T_e are expected to be equal, the line ratio seems to be an indicator of 'dilution' (ie. the ratio of deuteron to electron density). Note this is most probably the dependence rather than Zeff because of the ion impact cross-sections' behaviour with energy. The preliminary study is promising and work is continuing.

FUTURE TRENDS

The active phase

Towards the end of JET, the machine will be prepared for deuterium/tritium operation in pursuit of one of its original goals, namely, plasma behaviour in the presence of significant heating by

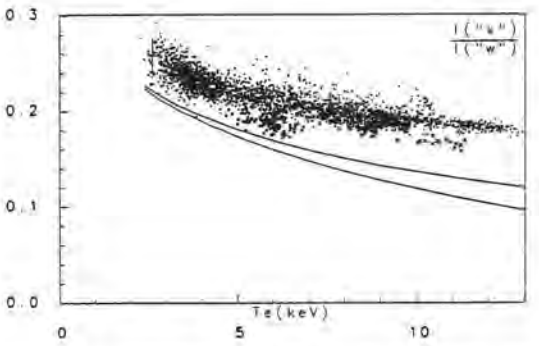

Fig. 7. Comparison of 'x' and 'w' line ratio for nickel. Solid curves show theoretical range.

fusion alpha particles. It will be necessary to measure these alpha particles, born at 3.5MeV and slowing by friction with electrons. It is possible that these cooling alpha particles might be detected spectroscopically following charge transfer from the neutral deuterium heating beams and the source function and parameters of the cooling distribution function determined. The HeII n = 4-3 spectral feature will have a finite width (of order 100A) because of the rapid fall of the charge exchange cross-section with relative speed above about 1.5 au. Figure 8 illustrates the form of the composite profile. Evidently the alpha particle feature must be detected against interfering species, which now include beryllium, the thermal helium feature and bremsstrahlung. The initial study for 80kev/amu beams suggests that detection will be possible at $Q_{D\text{-}T} = 1$.

The assessment of spectral features arising from non-thermal distributions is a problem at JET and is perhaps appropriately mentioned here. The

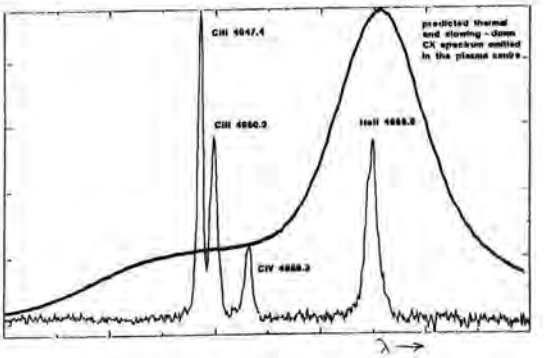

Fig. 8. Anticipated HeII (n = 4-3) profile (much amplified intensity) in the active phase.

alpha particle situation, in principal, is mimicked by ICRH heated helium minority species. A program is underway to seek evidence of such distorted features. Manifestly the whole cold and thermal feature emission must be isolated first with high confidence. High precision charge exchange data is essential, and JET is supported by AMOLF (Amsterdam) in this study.

Evidence for non-Maxwellian electron distributions, especially high energy tails in very high temperature fusion plasmas, is a perennial problem in which interest will increase again with the projected electron cyclotron resonance heating (ECRH). It must be admitted that there was some hope of obtaining clear evidence for a high energy electron tail from the Ni^{+26} KX1 study, but within the theoretical cross-section data errors this was not found. There is a further point, that kinematic relativistic corrections to electron impact rate coefficients is probably required.

Pumped divertors

It is certainly the case that any future large fusion machine will have a poloidal divertor designed to remove impurities and ash from the main plasma and seek to prevent (by efficient radiative cooling) sputtering of impurities and their migration back into the main plasma. It is possible that JET itself may be converted to a divertor machine at some stage. There is of course a substantial body of knowledge about divertors from the ASDEX tokamak, for example. It is within the relatively cool (10-150eV) divertor that the most pressing atomic and spectroscopic problems are expected. It is necessary to investigate the most suitable species for the target plates of the divertor and any other materials actively added to the divertor volume to achieve the required temperature and power shedding capability, and to assess by spectroscopic measurement whether the planned flows and inhibition of ion migration are produced. We anticipate making spectroscopic measurements on elements such as aluminium, silicon, nickel, copper, molybdenum and tungsten in the visible and uv/xuv. For example, molybdenum will be have to be studied as an inflowing species in stages Mo^{+0} and Mo^{+1} ,as a main radiating species in stages Mo^{+2} to Mo^{+11} and then on into high stages of ionisation to establish any link to the bulk plasma. It is anticipated that both spectral observation and transport modelling will require a pseudo-band structure approach base on shell groups of ions treated as a whole and evolving from one to another. We are planning on this basis at the present time using rudimentary atomic and spectroscopic data. Figure 9 shows the spectral locations of the transition arrays for some of the relevant molybdenum ions.

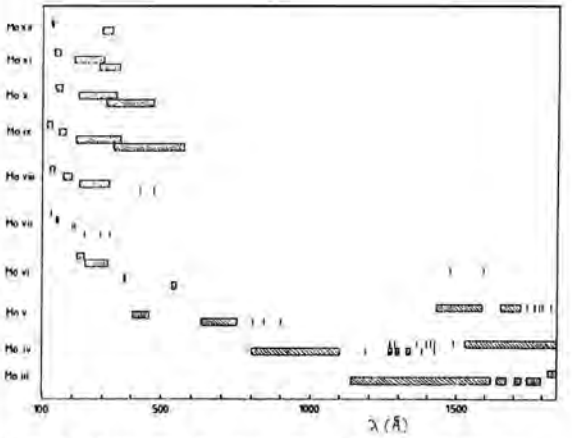

Fig. 9. Wavelength positions of transition arrays of MoIII - MoXII.

Surface interactions

It is at the bounding surface of the plasma that the greatest deficit of atomic/molecular/spectroscopic understanding appears to lie, at least in our awareness of it at JET. The release of impurites from surfaces clearly has a chemical dimension but as yet we have made no studies of molecular species and their catabolism in JET. Figure 10 identifies the CH band in a JET spectrum to demonstrate that the molecules do exist (Behringer et al., 1986). We wish to model molecular break-up and emission in the same manner as the collisional-radiative modelling for atomic ions in an effort to understand impurity release and the state and speeds of the inflowing atoms. We anticipate significant development of application of molecular spectroscopy and reaction kinetics to fusion plasma boundaries.

Energetic highly ionised ions striking surfaces are of course very effective also in releasing secondary electrons. There is at the present time no consistent model of the scrape-off-layer and the surface sheaths which incorporates an atomic description of this release, yet independent beam/surface experiments are successfully showing these effects and establishing a spectroscopic

signature of the emission associated with the cascade/Auger neutralising of the impacting ion.

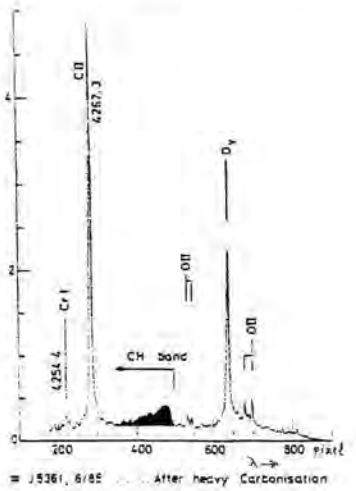

Fig.10. CH band in a JET spectrum

CONCLUSION

This paper has identified some main areas of activity in atomic physics and spectroscopy in JET and has speculated on where future activities may occur. It has been pointed out that there is an extensive and still developing spectroscopic capability on JET reinforced by a large diagnosic and computational infra-structure. It is hoped that the intriguing behaviour of the plasma will prove an incentive to atomic physicists and spectroscopists to support and become involved in some of these studies.

ACKNOWLEDGEMENTS

The work of K. Behringer, E. Kallne, K-D. Zastrow, J. Hackmann, J. Hofmann, A. Zinoviev, S. Bliman, and W. Dickson is specially acknowledged.

REFERENCES

R Bartiromo, F Bombarda, R Giannella et al. (1989) Rev Sci Instrum 60,237
K H Behringer, H P Summers, B Denne et al. (1989) Plasma Phys & Control. Fusion - in press.
K Behringer, W W Engelhardt, L Horton et al. (1986) Proc XIII Symposium on Physics of Ionised Gases , Yugoslavia.
A Boileau, M von Hellermann, L D Horton & H P Summers (1989a) Plasma Phys & Control. Fusion 31, 779
A Boileau, M von Hellermann, L D Horton et al.(1989b) Nuclear Fusion - in press.
A Boileau, M von Hellermann, W Mandl et al. (1989c) J Phys B 22, 1145.
B Denne, G Magyar & J Jacquinot (1989) Phys Rev A - to be published.
M J Forrest, J Hackmann, N J Peacock et al.(1989) - to be published.
A Hibbert, J H Tait, H P Summers & P G Burke (1988) Nucl. Inst. & Meth B 276, 279.
J V Hofmann (1989) Diplomarbeit, Max Planck Institut fur Plasmaphysik Garching, FRG.
B E Keen (1987) JET Progress Report, EUR 11579 EN, EUR-JET-PR5.
R L Kurucz & E Peytremann (1975) Smithsonian Astrophysical Observatory Special Report 362.
G Magyar, M R Barnes, S Cohen et al. (1988) JET Report JET-R(88)15.
D Pasini, R D Gill, J Holm & E van der Groot (1988) Rev Sci Instrum 59,693.
J E Rice, E S Marmor, E Kallne & J Kallne (1987) Phys Rev A 35, 3033.
U Schumacher, E Kallne, H W Morsi & G Rupprecht (1989) Rev Sci Instrum 60,562.
H P Summers, K H Behringer & L Wood (1987) Physica Scripta 35, 303.
K-D Zastrow, E Kallne & H P Summers (1989) Phys Rev A - in press.

AUTHOR'S ADDRESS

JET Joint Undertaking, Abingdon, Oxon.,U.K.

R. Hoekstra, F.J. de Heer and R. Morgenstern

The importance of transition probabilities in atomic collision experiments

ABSTRACT

The role of transition probabilities in Photon Emission Spectroscopy of charge changing collisions is discussed on the basis of collisions, like He^{2+}- and O^{3+} - H. For these systems an accurate knowledge of transition probabilities is essential to deduce state selective electron capture cross sections. In addition to these physical aspects, the practical aspect of calibrating the sensitivity of a vuv monochromator by the branching ratio method is discussed.

INTRODUCTION

Electron capture in collisions of multiply charged ions and neutral particles, especially atomic hydrogen is a subject of extensive theoretical and experimental studies (Janev and Winter, 1985). The interest in these charge transfer processes stems not only from fundamental aspects but also from their importance in fusion plasma research and astrophysics. We study these electron capture processes by means of Photon Emission Spectroscopy -PES- (Hoekstra et al, 1989a and Dijkkamp et al 1985). The process for single electron capture is schematically given by

$$A^{q+} + B \rightarrow \underline{A^{(q-1)+*}(nl)} + B^{+}$$
$$\hookrightarrow A^{(q-1)+}(n'l') + h\upsilon$$

In words: a multiply charged ion A^{q+} collides on a neutral target B and captures one of the target electrons into an excited state $A^{(q-1)+}(nl)$. This state will decay by emission of a photon, $h\upsilon$, and hence measurement of the photon emission gives direct information on the electron capture rate into $A^{(q-1)+}(nl)$.

The set-up used for this kind of measurements is shown schematically in fig. 1. Inside the collision chamber the multiply charged ions, produced by the Electron Cyclotron Resonance ion source installed at the KVI, cross a target beam. The photon emission is observed with two monochromators, one being sensitive in the "visible" spectral range (200 - 700 nm) and the other in the vuv range (10 - 80 nm). The monochromators can be positioned in such a way that there is no influence of polarization effects (Hoekstra et al 1989b). The absolute target beam density profiles are determined by electron impact induced radiation (Čirič et al, 1985). This radiation is measured with the spectrometer for "visible" light, which is equipped with an imaging lens system which enables measurements along the beam axis.

In this type of measurements there are three main applications of transition probabilities and the related quantities: branching ratio and lifetime, namely

I - Sensitivity calibration of the vuv monochromator

II - Identification of contributions from degenerate states in hydrogenic ions.

III - Determination of capture cross sections from complex emission spectra.

These three aspects will be discussed separately in the next sections on the basis of some collision systems of current interest.

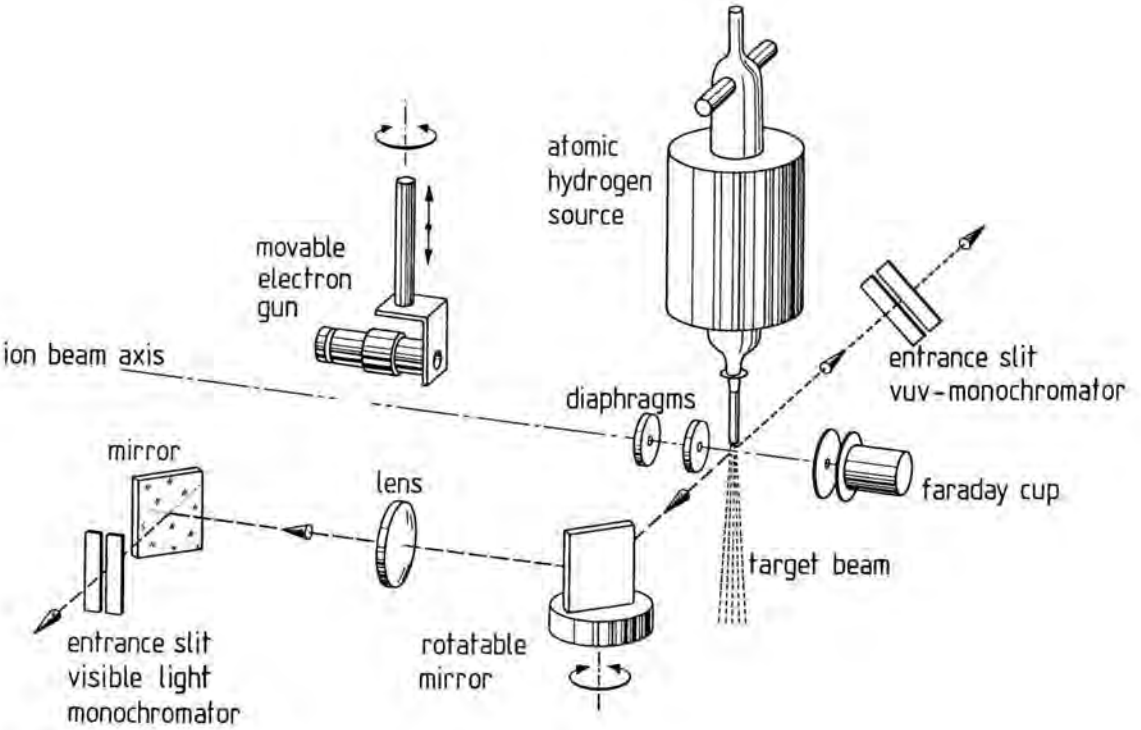

Figure 1. Schematical view of the experimental set-up.

I - SENSITIVITY CALIBRATION OF THE VUV MONOCHROMATOR

The vuv monochromator used is a grazing incidence vacuum spectrometer equipped with a position sensitive microchannelplate detector, enabling simultaneous detection of emission lines within ranges of about 20 nm. To determine the absolute sensitivity of this vuv monochromator, absolute emission cross sections for electron and ion impact processes are used. These cross sections are given in table 1. The wavelengths cover a range from 20 - 75 nm. If oscillator strengths are known, it is possible to get a few more calibration points in the range of 50 - 80 nm by measuring the intensity of resonance radiation after impact of electrons on noble gases (van Raan, 1973). In this range the sensitivity increases smoothly with decreasing wavelength (see fig. 2) and therefore an interpolation between the measured sensitivity points seems to be justified. However extrapolating to lower wavelengths is tricky since the sensitivity not only depends on the photon energy but also on the reflection coefficient of the grating. To extend the sensitivity calibration down to lower wavelengths we make use of branching ratios in Li-like ions (N^{4+}, O^{5+} and F^{6+}). For these ions the $4l \rightarrow 3l'$ transitions yield radiation in the range of 35 - 65 nm where the sensitivity is known, whereas the $4l \rightarrow 2l'$ transitions yield radiation in the range into which we want to extend the absolute

Table 1 Absolute emission cross sections (in 10^{-18}cm^2) used for the sensitivity calibration of the vuv monochromator (Dijkkamp et al, 1985 and references therein). Typical error: 20-25%

	wavelength in nm	
	20.8 + 21.3	30.4
system	Ne^{4+} + He	e + He
energy (keV)	60	0.2
transition		
ion	NeIV	HeII
upper level	$3s\ ^4P$ $3s\ ^2D$	$2p\ ^2P^o$
lower level	$2p^3\ ^4S^o$ $2p^3\ ^2D^o$	$2s\ ^2S$
cross section	470	0.56

	wavelength in nm	
	46.1	71.8 - 73.1
system	e + Ne	e + Ar
energy (keV)	0.20	0.20
transition		
ion	NeII	ArII
upper level	$2s2p^6\ ^2S$	$3p^4 4s\ ^2P$
lower level	$2s^2 2p^5\ ^2P^o$	$3p^5\ ^2P^o$
cross section	4.80	1.71

sensitivity calibration, namely 9 - 20 nm.

As an example of the branching ratio method we will discuss the case of NV($1s^2 4p$), which is shown in fig. 3. The branching ratios have been deduced from the transition probabilities calculated by Lindgård and Nielsen, 1977. The sensitivity at 16.3 nm, K(16.3) is related to the known sensitivity at 62.9 nm, K(62.9) by

$$K(16.3) = \frac{0.19}{0.77}\frac{S(16.3)}{S(62.9)} K(62.9)$$

with S(16.3) and S(62.9) the measured signals at 16.3 and 62.9 nm. Unfortunately the signal at 62.9 nm includes the third order of the $3p \rightarrow 2s$ transition (3*20.93 = 62.8nm). Since the excited N^{4+*} ions are produced in charge

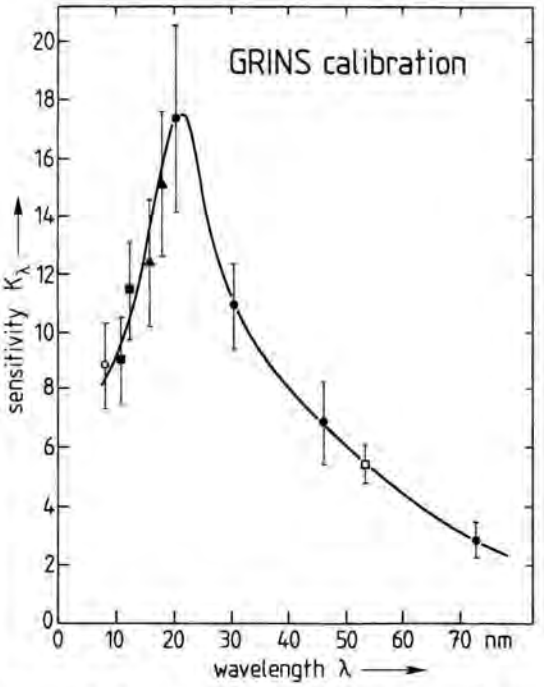

Figure 2. Sensitivity calibration curve of the vuv monochromator (GRINS). Branching ratio method: ○ - F^{6+}, ■ - O^{5+}, ▲ - N^{4+} and □ - He. ● - direct processes (table 1)

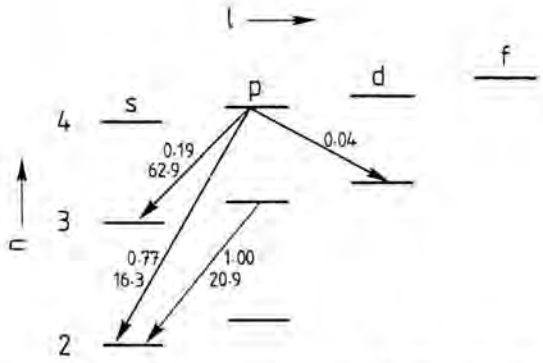

Figure 3. Schematic energy level diagram of NV. The relevant transitions have been indicated together with their branching ratios and wavelengths (in nm).

changing collisions of N^{5+} the excited state population can be steered by choosing an appropriate target. Charge transfer in collisions on H_2 populates $3l$ and $4l$ states, whereas collisions on He populate only $3l$ states (Dijkkamp et al, 1985). Hence collisions on He can be used to deduce the ratio between the first and third order of the $3p \rightarrow 2s$ line. Charge exchange between N^{5+} and H_2 is used to populate $N^{4+*}(1s^2 4p)$. It should be noted that at typical impact energies of 50 and 75 keV the contribution by the third order of the $3p \rightarrow 2s$ line to the signal at 62.9 nm is about 75 and 50%, respectively. Therefore the measurements have to be performed with optimal counting statistics. The results of this type of calibration procedures for Li-like ions are shown in fig. 2 together with the direct results of the processes given in table 1. Furthermore the figure includes the result of the branching ratio method for HeI($1s3p$) which has a branch in the visible spectral range (501.6 nm, $3p \rightarrow 3s$) and one in the vuv (53.7 nm, $3p \rightarrow 1s$), which links the sensitivity of the vuv monochromator to that of the spectrometer for visible light. The latter is calibrated on sensitivity (error 15%) by standard lamps and known electron impact emission cross sections.

Due to the accurate knowledge of branching ratios (ratio of transition probabilities) it has been possible to extend the sensitivity calibration of the vuv monochromator into the wavelength range of 9 - 20 nm.

II - IDENTIFICATION OF CONTRIBUTIONS FROM DEGENERATE STATES IN HYDROGENIC IONS

In hydrogenic ions the l levels are quasi-degenerate and therefore light emission from different l levels can not be resolved spectroscopically. So measurements of transitions in H-like ions have to be compared with the sum of the various theoretical contributions. Comparing in this way experiments for C^{6+} and O^{8+} - H collisions with the most elaborate calculations it was found that there is good agreement between theory and experiment for the dominant capture channels, whereas for the non-dominant high-n states there were considerable differences (Hoekstra et al, 1989a). Hovever these transitions between high-n states, yielding light in the visible spectral range are particularly important for future plasma diagnostics (Boileau et al, 1989). Due to the strong fields in a tokamak the l states are mixed (Fonck et al, 1984) and hence it is essential to know all the l state electron capture cross sections separately. For the case of He^{2+} colliding on atomic hydrogen we have deduced the separate $4l$ cross sections from the measurement of the $4 \rightarrow 3$ transition (Hoekstra et al, 1989c). To that end we have exploited the fact that the lifetimes of the states are different. For these HeII($4l$) states the lifetimes and branching ratios for transitions to $n = 3$ are given in table 2. Radiation from shortlived states, e.g. $4p$ is mainly concentrated on the target area, whereas radiation from longlived states, like $4s$ is still emitted downstream the ion beam axis (fig. 1). Therefore the measurement of the emission profiles along the ion beam gives information

Table 2 Lifetimes, τ_{4l}, branching ratios for decay to $n = 3$, $\beta(4l \rightarrow 3)$.

	state			
	$4s$	$4p$	$4d$	$4f$
τ_{4l}(nsec)	14.2	0.77	2.26	4.53
$\beta(4l \rightarrow 3)$	0.42	0.042	0.25	1.00

on the l state population. This method, often used in collision experiments on static targets and in beam foil experiments, has only once before been used in a beam experiment, namely by Aumayr et al 1984 for H^+ - Li collisions.

Neglecting cascades the emission profiles along the ion beam axis, P_{4l} are described by

$$P_{4l}(z) = \frac{1}{v\tau_{4l}} \int_0^z T(z') \, e^{-(z' - z)/v\tau_{4l}} \, dz'$$

with v the velocity of the ions and τ_{4l} the lifetime of state $4l$, z the position along the ion beam axis and T(z') the target density profile. The measured signals, S(z) are equal to

$$S(z) = K \sum_l \beta(4l \rightarrow 3) \, P_{4l}(z) \, \sigma_{4l}$$

with K an absolute calibration constant, $\beta(4l \rightarrow 3)$ the branching ratio for decay to $n = 3$ and σ_{4l} the electron capture cross sections. By measuring the signals at some 25-30 positions along the ion beam axis, it is possible to deduce the cross sections from a least squares fit. This is feasible since the emission profiles $P_{4l}(z)$ are well known, which also is due to the fact that the transition probabilities, lifetimes and branching ratios are accurately known. As a typical example of the experimental results obtained in this way fig. 4 shows the results for the $4f$ state, together with the theoretical predictions by Fritsch, 1988. It can be seen that the experimental results increase smoothly, whereas the theory shows a structure around 4 keV/amu.

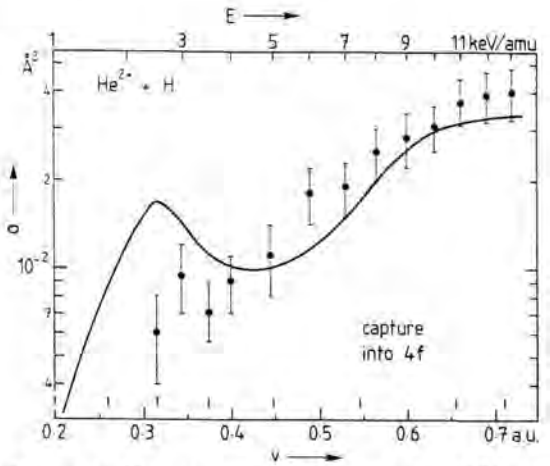

Figure 4. Electron capture into $He^+(4f)$ deduced from emission profile measurements. Solid curve - Atomic Orbital calculation by Fritsch, 1988

With knowledge of lifetimes and branching ratios of the HeII($4l$) states it has been possible to deduce for the first time high-n ($n = 4$ is a high-n level since the capture goes predominantly to the $n = 2$ level) state selective cross sections in He^{2+}-H collisions.

III - DETERMINATION OF CAPTURE CROSS SECTIONS FROM COMPLEX EMISSION SPECTRA

Photon emission following electron capture in O^{3+}- H ($O^{3+}(1s^2 2s^2 2p) \rightarrow O^{2+}(1s^2 2s^2 2pnl)$ plays an important role in astrophysical studies (Heil, 1987). Therefore fully quantal calculations have been performed (Heil et al, 1983 and Bienstock et al, 1983), which predicted that the $3p$ SL states are dominantly populated. However translational energy spectroscopy (Wilson et al, 1988) and PES (Hoekstra et al, 1989d) showed that the $3s$ SL are dominantly populated.

A useful evaluation of the PES measurements is only possible with a fair knowledge of transition probabilities, since a considerable number of emission lines falls outside the wavelength ranges covered by the spectrometers. Since a complete set of transition probabilities was not available, - especially two electron transitions of the type $2s^2 2p3p \rightarrow 2s2p^3$ were lacking - calcula-

tions have been performed (Hansen, 1989). The importance of these two electron transitions can be shown from measurements on the $3p\ ^1P$ and $3p\ ^3D$ states. Fig. 5 shows the emission profile for the $3p\ ^1P$ state. The solid curve is a least squares fit with a lifetime of 10 nsec, the dashed curve is a profile with a lifetime of 27 nsec, which is the lifetime deduced from the transition probability given by Wiese et al, 1966 for one-electron transition to $2s^2 2p3s\ ^1P^o$. The lifetime calculated (Hansen, 1989) is 11.8 nsec, which is in fair agreement with the measurement. His

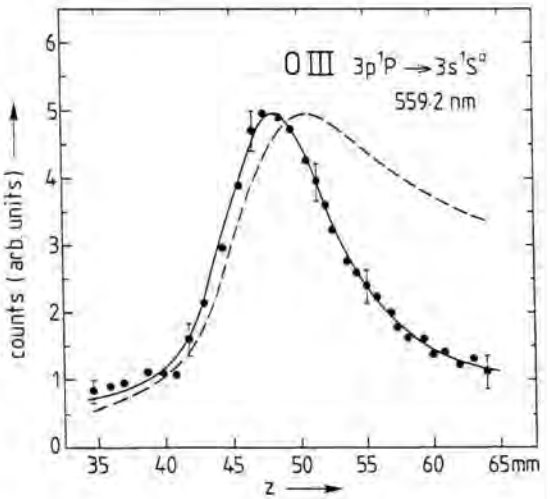

Figure 5. Emission profile along the ion beam axis of the $2s^2 2p3p\ ^1P \rightarrow 2s^2 2p3s\ ^1P^o$ transition. Solid curve least squares fit and dashed curve profile calculated with the lifetime deduced from Wiese et al, 1966 see text.

calculations show that for all the 6 $2s^2 2p3p$ states some 25-45% of the population decays via two-electron transitions to $2s2p^3$ states. We have measured the ratio between one- and two- electron transitions for $3p\ ^3D$ and found it to be 1.8 ± 0.4 which is in agreement with the calculated value of 2.1 (Hansen, 1989). More details will be given in a forthcoming article. Knowledge about these two-electron transitions is essential for determining level populations and interpreting the measured emission spectra.

CONCLUSION

It has been shown that an accurate knowledge of transition probabilities is important for photon emission spectroscopy of charge transferring collisions. With this knowledge it has been possible to extend the sensitivity calibration of a vuv monochromator. Furthermore it has been possible to resolve contributions from degenerate states in hydrogenic ions and to determine capture cross sections from complex emission spectra.

ACKNOWLEDGEMENTS

This work is part of the research program of the Stichting voor Fundamenteel Onderzoek der Materie (FOM) with financial support from the Nederlandse Organisatie voor Wetenschappelijk Onderzoek (NWO).

REFERENCES

Aumayr, F., M. Fehringer and H. Winter, 1984 - Inelastic H^+-Li($2s$) collisions (2-20keV): II. Electron capture into H($2p$) and H($3l$). In: J. Phys. B: At. Mol. Phys., 17, 4201-4211.

Bienstock, S., T.G. Heil and A. Dalgarno, 1983 Charge transfer of O^{3+} ions in collisions with atomic hydrogen. In: Phys. Rev. A., 27, 2741-2743.

Boileau, A., M. von Hellermann, L. D. Horton, J. Spence and H. P. Summers, 1989 - The de-

duction of low-Z ion temperature and densities in the JET tokamak using charge exchange recombination spectroscopy. In: Plasma Phys. Controlled Fusion, 31, 779

Čirič, D., D. Dijkkamp, E. Vlieg and F.J. de Heer, 1985 - Selective electron capture into HeII(n,l) subshells in collisions of He^{2+} with atomic and molecular hydrogen. In: J. Phys. B: At. Mol. Phys., 18, 4745-4762

Dijkkamp, D., D. Čirič, E. Vlieg, A. de Boer and F.J. de Heer, 1985 - Subshell-selective electron capture in collisions of C^{4+}, N^{5+}, O^{6+} with H, H_2 and He. In: J. Phys. B: At. Mol. Phys., 18, 4763-4793.

Fonck, R.J., D.S. Darrow and K.P. Jähnig, 1984 - Determination of plasma-ion velocity distribution via charge-exchange recombination spectroscopy. In: Phys. Rev. A., 29, 3288-3309.

Fritsch, W., 1988 - Calculation of partial electron-transfer cross sections in 1 - 84 keV/amu He^{2+}+ H collisions. In: Phys. Rev. A., 38, 2664-2667.

Hansen, J., 1989 - private communication.

Heil, T.G., 1987 - Multiply charged ions in astrophysics. In: Nucl. Instrum. Methods., B23, 222-225.

Heil, T.G., S.E. Butler and A. Dalgarno, 1983 Charge transfer of doubly charged and trebly charged ions with atomic hydrogen at thermal energy. In: Phys. Rev. A., 27, 2365-2383.

Hoekstra, R., D. Čirič, F.J. de Heer and R. Morgenstern, 1989a - State selective electron capture in collisions of C^{6+} and O^{8+} on atomic and molecular hydrogen studied by Photon Emission Spectroscopy. In: Phys. Scr., T28, 81-90.

Hoekstra, R., M.G. Suraud, F.J. de Heer and R. Morgenstern, 1989b - Alignment of p- and d- states of three electron carbon ions produced in collisions of $C^{4+}(1s^2)$ with H_2. In: J. Physique Coll., 50, 387-392.

Hoekstra, R., F.J. de Heer and R. Morgenstern, 1989c - l state selective charge exchange cross sections for collisions of He^{2+} on atomic and molecular hydrogen. In: Invited Papers XVI ICPEAC, New York, in press.

Hoekstra, R., K. Boorsma, F.J. de Heer and R. Morgenstern, 1989d - Photons shedding light upon charge exchange processes in collisions of 24 keV O^{3+} with atomic hydrogen. In: J. Physique Coll., 50, 349-352.

Janev, R.K. and H. Winter, 1985 - State selective electron capture in atom - highly charged ion collisions. In: Phys. Rep., 117, 265-387.

Lindgård, A. and S.E. Nielsen, 1977 - Transition probabilities for the alkali isoelectronic sequences LiI, NaI, KI, RbI, CsI, FrI. In: At. Nucl. Data Tables, 19, 533-633.

Raan, A.F.J. van, 1973 - An absolute intensity calibration method for vacuum ultra-violet spectrometry based on electron impact excitation. In: Physica, 65, 566-578

Wiese, W.L., M.W. Smith and B.M. Glennon, 1966 Atomic transition probabilities NSDRS-NBS4 vol 1 (Washington DC: US Govt Printing Office)

Wilson, S., R.W. McCullough and H.B. Gilbody, 1988 - State selective electron capture by slow O^{3+} and Ne^{3+} ions in H. In: J. Phys. B: At. Mol. Opt., 21, 1027-1037.

AUTHORS' ADDRESSES

K.V.I., Zernikelaan 25, 9747 AA Groningen, The Netherlands.

F.O.M. Institute for Atomic and Molecular Physics, P.O. Box 41883, 1009 DB Amsterdam, The Netherlands.

P.W.J.M. Boumans

A view at the needs of and activities in the analytical atomic spectroscopy community with respect to fundamental reference data

ABSTRACT

This paper discusses why analytical atomic spectroscopists need fundamental reference data, which data they need, and which actions have been undertaken in the recent past to establish the needs, to improve communication about fundamental data, and to expand the databases. As examples of new compilations the paper refers to work in Philips Research Laboratories dealing with the measurement of the physical widths of 350 prominent lines of 65 elements emitted from an inductively coupled plasma (ICP) and "pseudo physically resolved" spectra of rare earth elements (REE), covering 80-pm wide spectral windows about prominent REE lines, also emitted from an ICP. In that context the paper refers to a spectrum simulation program with, *inter alia*, spectral bandwidth as parameter, operational on a personal computer. Finally, the paper discusses the potentials of electronic publications in general and a proposal to start with an electronic supplement of *Spectrochimica Acta*.

INTRODUCTION

The purpose of this paper is to provide information about the needs of fundamental reference data in the analytical spectroscopy community and about some activities aimed at improving a situation, which, needless to say, is not as rosy as one might wish. Analytical atomic spectroscopists use and study plasmas, and therefore we have many interests in common with atomic physicists and astrophysicists. Although our goals, scope, and approaches are different, it appears useful to intensify the contacts between the various communities of scientists concerned with the compilation or application of spectroscopic data. This may at least increase the awareness of shared needs, on the one hand, and improve access to available, but apparently hidden data, on the other hand.

GOALS AND CHARACTERIZATION OF ANALYTICAL ATOMIC SPECTROSCOPY

The umbrella "analytical atomic spectroscopy" might cover all spectroscopic methods at present used for material characterization, as to both bulk chemical composition and structure. I shall limit the term, however, to spectroscopic methods for elemental analysis covering trace, minor, and major constituents, in solid, liquid, or gaseous samples. I thus exclude from discussion techniques for surface, interface and thin layer characterization.

Main types of spectroscopy used for elemental analysis

- *Classical* optical spectroscopy:
  - atomic emission spectroscopy (AES)
  - atomic absorption spectroscopy (AAS)
  - atomic fluorescence spectroscopy (AFS)
- *Mass* spectroscopy (MS) for inorganic analysis
- *Laser* spectroscopy for inorganic analysis:
  - laser enhanced ionization spectroscopy (LEIS)
  - laser enhanced atomic fluorescence spectroscopy (LEAFS)
  - resonance ionization spectroscopy (RIS)
  - resonance ionization mass spectroscopy (RIMS)
- *X-ray* spectroscopy, such as X-ray fluorescence spectroscopy (XRFS)

Common feature of optical, mass and laser spectroscopies

- Analysis of solids and liquids requires *atomizers:*
  - emission sources (AES)
  - atom reservoirs (AAS, AFS)
  - ion sources (MS)

Global characterization of sources and atom reservoirs

• Gas temperature	2,500 — 10,000 K
• Electron temperature	2,500 — 50,000 K (?)
• Pressure	1 torr — 1 atm
• Gaseous atmosphere	Ar He N_2 O_2 air
• λ-region used	160 — 800 nm
• Atomic species used	I II (III)

Atom reservoirs and sources

• Carbon furnace	AAS LEAFS	
• Flame	AAS LEIS	AES
• Arc	AES	
• Spark	AES	
• Inductively coupled plasma (ICP)	AES	MS
• Microwave induced plasma (MIP)	AES	
• DC plasma (DCP)	AES	
• Laser induced plasma (LIP)	AES	MS
• Glow discharge (GD)	AES	MS
• Hollow cathode discharge (HCD)	AES	
• Hybrid sources (*e.g.*, ICP + LIP)	AES	MS

Basic requirement in analytical atomic spectroscopy

- Control of:
  - sample evaporation/ablation
  - sample introduction into source or atom reservoir
  - sample atomization
  - the interaction of the sample components with the source or atom reservoir
  - the conditions in the source or reservoir (temporal and spatial stability, reproducibility of transients)

Ultimate analytical requirement

- Optimization of all parameters to achieve
  - low detection limits: $\mu g\ g^{-1} \rightarrow ng\ g^{-1}$ †
  - high precision (= reproducibility): 0.3%
  - high accuracy (= correctness) ‡
  - multielement capability
  - high speed and reliability
  - low cost

† Optimization of detection limits implies minimization of the noise (*i.e.*, the relative standard deviation of the background) and maximization of signal-to-background ratios.

‡ Generally an analysis is not made in an absolute way, but is based on empirical calibration functions obtained with standards of known composition. A major problem is that standards and samples should behave entirely identically, which, in general, is not so: differences in both chemical composition and physical structure may give rise to differences in the analysis signals between standards and samples for similar concentrations of the elements to be determined (termed "analytes"). The associated potential errors are designated "interferences" and the responsible components "interferents".

Fundamental knowledge needed for rational "analytical" optimization

- Overall plasma characterization: LTE, pLTE, non-LTE, T, T_e, n_e
- Spatial distributions of T, T_e, n_e, and heavy particle densities
- Atomization, ionization–recombination, and excitation mechanisms
- Particle transport mechanisms
- Accurate composition of the atomic spectra and the background [resolution: physical; dynamic range: $> 10^6$]

Eventually, "analytical plasmas" are always complex chemical systems, because we have to contaminate them with the samples, and these samples usually exert a major influence on the plasma characteristics and the spectra.

Conclusion

On the whole, if we want to approach our problems in a rational, systematic way, we are basically concerned with

- diagnosis of sample conversion,
- plasma diagnostics, and
- spectrum analysis.

Therefore we need fundamental reference data in the same way as other scientists dealing with plasmas.
What did we do with respect to these needs and what are we trying to do?

NEEDS FOR FUNDAMENTAL REFERENCE DATA FOR ANALYTICAL ATOMIC SPECTROSCOPY

Actions organized in the past three years

- Organizers:
  - Prof. Alexander Scheeline, Department of Chemistry, University of Illinois
  - Prof. Paul Boumans, Philips Research Laboratories and Spectrochimica Acta, Part B, Atomic Spectroscopy
- Flags:
  - National Research Council Committee on Line Spectra of the Elements
  - *Titre personnel*

- *Spectrochimica Acta, Part B* (SAB)

- Specification of actions:
  - Worldwide circulated questionnaire (1986)
  - Workshop in Scarborough, Ontario (1987)
  - Edited Workshop Proceedings (including reports of questionnaire and transcribed discussions) published in SAB (No. 1, 1988)
  - Column "News on Fundamental Reference Data", with cooperation of the National Institute of Standards and Technology (NIST), formerly NBS, started in SAB (1989)
  - Symposium on Fundamental Reference Data at the XVIth Meeting (Oct 1989) of the Federation of Analytical Chemistry and Spectroscopy Societies (FACSS) in Chicago, with cooperation of NIST
  - Proposal for starting an electronic supplement of *Spectrochimica Acta*

The questionnaire was circulated to help establish the scope of the workshop. Approximately 100 responses from laboratories worldwide were received. These responses ranged from requests for retabulation of data which have been known for many years, to requests for impossibly huge amounts of information.

The results of the questionnaire are summarized in the first two papers of the Proceedings of the Workshop (Boumans, 1988; Scheeline, 1988b), which have have been published as a special issue of *Spectrochimica Acta B* (Boumans and Scheeline, 1988); the conclusions have been summarized in the Preface (Scheeline, 1988a).

Discussion during the Workshop did not emphasize new work. Rather, it focused on problems which could not be adequately solved using currently available fundamental data tables of line wavelengths, line shapes, transition probabilities, energy exchange cross-sections, and assorted reaction rate constants. The diversity of the spectrochemical community can be seen from the range of points of view expressed. Some people desire source-specific information. Others want source-independent data. Still others are as concerned with the storage and retrieval of data as with the actual data values. It became clear that the individuals and organizations collecting reference data have been oblivious to the concern of analytical spectroscopists and *vice versa*. One effect of the workshop was to start a dialogue concerning reference data which can only benefit both the producers and consumers of such information.

The start of a column "News on fundamental reference data" in *Spectrochimica Acta B* is a direct and permanent follow-up of the Workshop (Scheeline and Boumans, 1989; Scheeline, 1989). Important is that we now have established some type of hot line with NIST via Dr. Wiese. The first result is that we can rapidly inform the analytical community about new data compilations and also make them aware of older compilations that may have escaped their attention. Evidently, this initial step primarily concerns an improvement in the access to existing and forthcoming information. In the next stage we hope to be able to exert some influence on the filling of the gaps in the data and on the way in which data are disseminated.

Categorization of needs

- Fundamental analytical spectroscopy
- Reference information for fundamental studies of emission sources and excitation processes:

  Wavelengths, Transition Probabilities, Fine Structure Data, Cross Sections

- Applied analytical spectroscopy
- Data on spectral interferences, notably to predict line overlap, for at least 50-pm wide spectral windows centred about 300-400 prominent analysis lines:

  Wavelengths, Sensitivities, Line Shapes and Widths, Fine Structures

With respect to fundamental analytical spectroscopy the the following detailed recommendations from the Workshop should be mentioned.

(i) From 180 to 600 nm, all emission lines of He I, Ar I, and either Fe I or Mo I should be observed and tabulated as to wavelength, fine structure, and transition moment. Any properties of continua and line broadening within this range which can be determined should be accurately measured. This will provide reference information for fundamental studies of emission sources and excitation processes. Implicit in this recommendation is further consultation between physicists, astrophysicists, and analytical spectroscopists so that all agree on the quality of the collected data.

Jack Sugar of NIST pointed out that the accuracy of the *known* Fe I transition probabilities is high, and that an additional reference, more or less equivalent to Fe I, may well be the Mo I spectrum, which recently has been investigated with considerable care by Whaling and his co-workers at the California Institute of Technology, Pasadena, CA, using an inductively coupled radio frequency argon plasma (ICP), which also is one of main excitation sources at present used in spectrochemical analysis (*cf.* Scheeline, 1989).

(ii) A clearinghouse, perhaps at NIST, should be established for the collection, confirmation, and

dissemination of atomic reference data. Discrepancies between published and observed data, undocumented spectral lines, and other experimental data would be submitted to this clearinghouse to aid in resolution of conflicting data, confirmation of unexpected results, and notification of the scientific community of significant improvements in measurement. The Office of Standard Reference Data at NIST may already offer such a forum, but the use of the Office as a routine clearinghouse for data is not part of the community's *modus operandi*. Should it be desirable to make it such, means of access should be widely publicized.

(iii) Currently, data are available from NIST, the Joint Institute for Laboratory Astrophysics (JILA), Oak Ridge National Laboratory (ORNL), and individual researchers. A single, central facilty should perpetually maintain a list of current data. NIST's Bibliographies of reference data form a solid basis for this central effort. This is a corollary of the need for a data clearinghouse.

Symposium at 1989 FACCS Meeting

The symposium during the forthcoming FACSS Meeting in Chicago, organized by Boumans and Scheeline, lists the following speakers and topics.

- W.C. Martin (NIST): Atomic wavelengths, energy levels, transition probabilities.
- J.W. Gallagher (NIST): Atomic collisions cross-sections.
- J.E. Lawler (Univ. Wisconsin): Laser and Fourier transform techniques for measurement of atomic transition probabilities.
- P.W.J.M. Boumans (Philips): Measurement and simulation of atomic spectra: towards an electronic publication.

MEASUREMENT AND SIMULATION OF ATOMIC SPECTRA

Detection limits

Obviously, in spectrochemical analysis, detection limits form an important issue. In AES, detection limits are dictated by the following factors:

- Intrinsic properties of the lines
  → prominent lines
- Source characteristics
  → optimization of source conditions
- Structure of background spectrum as dictated by the sample composition → *line interference*
  → remedies:
    → high-resolution spectroscopy
    → mathematical (chemometric) techniques

However, part of the problems connected with line interference stem from

(a) the lack of quantitative spectral data appropriate to each of the common excitation sources, and
(b) the intransferability of available data between different spectrometers.

Spectrum simulation: ab initio approach

The absolute ideal would be to have available the transition probabilities of "all" spectral lines as well as quantitative models for calculating the spectral emission distributions for the various sources. An interesting attempt to spectrum simulation using this approach has been made by Burton and Blades (1986, 1987) for spectra emitted from an ICP. The approach is currently limited by both the lack of accuracy and the limited availability of transition probabilities for all elements. The simulated spectra are only as complete and accurate as the gA-values used to generate them.

Spectrum simulation: compilation of new data

In Philips Research Laboratories we also made an approach to spectrum simulation (Boumans *et al.*, 1988b, 1989). We measured high-resolution spectra in 80-pm wide spectral windows about prominent analysis lines, deconvoluted the spectra, stored the physically resolved spectral data in the computer, and simulate spectral scans by convoluting the physical spectra with the instrument function.

To cover a maximum of pitfalls during the design and development of the measuring and simulation procedures we chose the complex spectra of rare earth elements (REE) for the exploration of the approach, which is further specified as follows.

- Excitation source: inductively coupled plasma
- Prominent lines: 26 lines of the most abundant rare earths: Ce, La, Nd, Pr, Sm
- Interferents: all rare earths
- Dynamic range: 6 orders of magnitude
- Number of lines of interferents: 1100

To cover also very weak lines we exploited a dynamic range as large as 10^6, but this demanded some sacrifice from the resolution, so that we

eventually obtained what we called "pseudo physically resolved spectral data", which for the time being are entirely adequate and can be treated in convolutions as truly physically resolved data, except at very small spectral bandwidths. This approach was feasible as a result of exploiting the basic outcomes of the measurement of the shapes and physical widths of 350 prominent lines of 65 elements emitted from an ICP (Boumans and Vrakking, 1986).

The publications (Boumans *et al.*, 1988b, 1989) describe the approach and cover assessments of the results for internal consistency and vis-à-vis classical data compilations (Gatterer and Junkes, 1945; Norris, 1960; Harrison, 1969; Meggers, Corliss, and Scribner, 1969) and a recent compilation for an other ICP (Tielrooy, 1987; Boumans *et al.*, 1988a). This asssessment demonstrates the poverty and, in fact, the definitive bankruptcy of the classical tables!

ELECTRONIC PUBLISHING IN SPECTROSCOPY

The publications on spectrum simulation (Boumans *et al.*, 1988b, 1989) describe the approach and its evaluation, show examples, and cover the underlying data. The only shortcoming is that the reader is doomed to passiveness whereas the subject urges him to activity! The reader would absorb the quintessence of the approach far more easily if he could himself specify parameters, choose examples from the infinite variety of possibilities, and watch the outcome on the computer screen. Not only would this facilitate his job as a reader, it could also fruitfully contribute to the development of new ideas and induce cross-fertilization.

Recognizing that this wealth of spectroscopic data including the simulation program may be important for the spectroscopy community as a benchmark and milestone as well as for its didactical value, we have redesigned and extended the program and data to make it operational on personal computers (PC) using a compiled version on diskette.

These are the main features of this potential "electronic publication":

- *Compiled program:* operational directly from "floppy" on IBM compatibles.
- *Simulates* about 240 REE spectra (80-pm) centred about 26 wavelengths.
- *Parameters:* Doppler temperature, *a*-parameter of Voigt profile, spectral bandwidth, interferent concentration.
- Covers simulation of interferent *plus* analyte spectra.
- Covers *superposition* of spectra of various interferents without or with analyte.
- Provides a muliplicity of *numerical data,* either appended to the graphics or in separate tables.

Obviously, the simulation program is only one example out of a plethora of potential electronic publications in spectroscopy. Generally speaking, I believe that there should be established adequate and "well structured" ways for readers to obtain programs and data on electronic media in order that they can explore published approaches more efficiently and incorporate them effectively in their own research work.

As Editor-in-Chief of *Spectrochimica Acta B,* I'm therefore considering the feasibility of starting with an electronic supplement of *Spectrochimica Acta:* SAE, *Spectrochimica Acta Electronica* (Boumans, 1989). A prerequisite for such a proposal is to establish the market of attractable electronic manuscripts in the authors' domain and the market of subscriptions in the readers' domain.

I do not see an electronic publication as a replacement of classical journal publications, but as an extension (Boumans, 1989), and I am not the first to consider such a possibility. One example is: *Tetrahedron Computer Methodology,* TCM (Wipke, 1988), which may be featured as follows.

- TCM focuses on new computer methods for handling chemical information, representing chemical entities, designing algorithms, and solving problems relating to organic chemistry.
- TCM is published and distributed as hardcopy journal plus floppy disks.
- The disks contain texts and, where possible, graphics of the printed version, and also additional key information such as executable programs, source code, data files, and parameter sets.
- Readers can reproduce published computer chemistry "experiments", apply a new algorithm to their own data, or use their own three-dimensional display software to view a molecular model, published in TCM, in ways not pictured in the printed article.
- The electronic version of TCM *text* offers the reader on a PC full text search capability.
- The readers can easily transfer references, molecules, reactions, and figures into their own personal documents or databases.

A major problem for research workers in an industrial organization may be the odium that sticks on "making software available to third parties", where the sting is in the term "software". Making a clear distinction between "electronic publication" and "software" appears indispensable to pull down possible "psychological and political barriers". The following definitions and explanations may be helpful to settle this point.

- *Software* is a commercial product, which is brought onto the market with the purpose of making money.
- Software should fulfil a particular specification and the vendor should guarantee the customer that the software does what the specification promises.
- The "power" of the software package and the degree of development are reflected in the price.
- An *electronic publication* is *not* the author's commercial product, but an extension and partial replacement of a classical publication, having the purpose to provide the "reader" (*not* the "customer" or "user") with information that may or may not be communicated in printed form, but can be far more effectively or even exclusively disseminated in electronic form to enable the reader picking up the thread of the work immediately and manipulating the author's data in the way described by the author.
- The reader gets the electronic publication as part of his subscription to the journal.
- The reader gets the same guarantees as a classical publication provides him: the author did his best to perform the research work in a scientifically correct and reliable way and the editor consulted reviewers to separate the wheat from the chaff.

Types of information that might be covered by a possible electronic supplement of *Spectrochimica Acta:*

- Programs with data that enable the reader to become actively involved in the communicated work, with a minimum of additional programming.
- Data such as transition probabilities, tables of normal-coordinate calculations, and whatever atomic or molecular spectral data in either numerical or graphical form.
- A gradually built, efficient subject index for *Spectrochimica Acta*, with text search capability, possibly extended to other Pergamon journals, such as *Progress in Analytical Spectroscopy* (rebaptized as *Spectrochimica Acta Reviews*) and *Journal of Quantitative Spectroscopy and Radiative Transfer.*

An important issue is that the leading scientists of the various Spectroscopy Communities seriously reflect about the proposal and help defining concrete examples where this approach could enrich scientific commmunication.

CONCLUSION

We need more, and more accurate data, we should communicate better about the existing data and the needs for new data, and we should more and more exploit the media that befit communication in the Electronocento (Boumans, 1989).

REFERENCES

Boumans, P.W.J.M., 1988 — *Spectrochim. Acta*, **43B**, 5–13.

Boumans, P.W.J.M., 1989 — The dissemination of the results of scientific research in the era of electronic media. In *"Future Trends in Spectroscopy"*, eds Paul Boumans, Sidney Kettle, Walter Slavin, and Jeffrey Steinfeld, *Spectrochim. Acta*, **44**, Golden Jubilee Supplement.

Boumans, P.W.J.M., and A. Scheeline, eds, 1988 — Needs for Fundamental Reference Data in Analytical Atomic Spectroscopy, Proceedings of a Workshop held in Scarborough, Ontario, Canada, 19–21 June 1987. *Spectrochim. Acta*, **43B**, 1–127.

Boumans, P.W.J.M., and J.J.A.M. Vrakking, 1986 — *Spectrochim. Acta*, **42B**, 1235–1275.

Boumans, P.W.J.M., J.A. Tielrooy and F.J.M.J. Maessen, 1988a — *Spectrochim. Acta*, **43B**, 173–199.

Boumans, P.W.J.M., J.J.A.M. Vrakking and A.H.M. Heijms, 1988b — *Spectrochim. Acta*, **43B**, 1365–1404.

Boumans, P.W.J.M., He ZhiZhuang, J.J.A.M. Vrakking, J.A. Tielrooy and F.J.M.J. Maessen, 1989 — *Spectrochim. Acta*, **44B**, 31–93.

Burton, L.L., and M.W. Blades, 1986 — *Spectrochim. Acta*, **41B**, 1063–1074.

Burton, L.L., and M.W. Blades, 1987 — *Spectrochim. Acta*, **42B**, 513–519.

Gatterer, A., and J. Junkes, 1945 — *Atlas der Restlinien*, Vol. II, *Spektren der seltenen Erden*. Specola Vaticana, Vatican City.

Harrison, G.R., 1969 — *M.I.T. Wavelength Tables.* The M.I.T. Press, Cambridge, MA / London.
Meggers, W.F., C.H. Corliss, and B.F.Scribner, 1975 — *Tables of Spectral-Line Intensities,* N.B.S. Monograph 145. U.S. Government Printing Office, Washington, DC.
Norris, J.E., 1960 — *Wavelength Tables of Rare-Earth Elements and Associated Elements.* Oak Ridge National Laboratory, Oak Ridge, TN, ORNL-2774.
Scheeline, A., 1988a — *Spectrochim. Acta,* 1—4.
Scheeline, A., 1988b — *Spectrochim. Acta,* 15—20.
Scheeline, A., 1989 — *Spectrochim. Acta,* 129—130, 427—430, 725—728.
Scheeline, A., and P.W.J.M. Boumans, 1989 — *Spectrochim. Acta,* 125—126.
Tielrooy, J.A., 1987 — *Ph.D. Thesis,* University of Amsterdam.
Wipke, W.T., editor-in-chief, 1988 — *Tetrahedron Computer Methodology* (Pergamon Press, Oxford). Thimann Laboratories, University of California, Santa Cruz, CA 95064.

AUTHOR'S ADDRESS

Philips Research Laboratories, P.O. Box 80.000, 5600 JA Eindhoven, The Netherlands.

André Heck and Fionn Murtagh (*)

How can artificial intelligence help spectral classification?

ABSTRACT

Spectral classifications have been carried out up to now basically through morphological approaches based on visual inspections of spectra from specific wavelength ranges. Automatic and statistical methodologies have been developed and have proved their effectiveness in dealing with huge amounts of data and newly explored spectral ranges. Artificial intelligence (AI) techniques can allow further progress in this direction and can facilitate classifications based on data of different spectral ranges. The reasoning examplified here in a case dealing with IUE low-resolution spectra could also be of application in other fields of (astro)physics.

SPECTRAL CLASSIFICATIONS

Stellar spectral classifications are more than taxonomical exercises aiming just at labelling stars and putting them into boxes, through comparison with standards. They are used for describing fundamental physical parameters in the outer stellar atmospheres, for discriminating peculiar objects, and for other subsidiary applications like distance determinations, interstellar extinction and population synthesis studies.

It is important to bear in mind that the classification systems are built independently of the stellar physics in the sense that they are defined completely by spectral features in a given wavelength range in selected standards (see e.g. Morgan, 1984). If the schemes are based on a sufficiently large number of objects, it is clear that they are intimately linked with physics, but not necessarily of the same stellar layers if the classification schemes refer to different wavelength ranges.

The example we shall follow in this paper deals with stellar low-resolution spectra collected by the International Ultraviolet Explorer (IUE). The original independent classification, proper to the ultraviolet (UV) domain, covered by IUE was carried out through a classical morphological approach (Jaschek & Jaschek, 1984) and led to a reference atlas (Heck *et al.*, 1984) including reference sequences and standard stars. Refer also to the review in Heck (1987).

AUTOMATIC & STATISTICAL CLASSIFICATIONS

Because of discrepancies arising between the MK spectral classifications (derived from the visible range) and the UV IUE ones, it was felt necessary to confirm independently the latter ones. A statistical approach was selected because it would essentially be free from any *a priori* bias arising from existing schemes, either in the visible or the ultraviolet ranges. An additional advantage of statistical methodology lies in the fact that it is able to work at will in a multidimensional parameter space, while classical morphological classifications can rarely go beyond two dimensions.

The results of this statistical study (Heck *et al.*, 1986) confirmed the correctness of the IUE UV classification and the lack of one-to-one correspondence between the results from the visual and the UV ranges. A detailed description of various statistical methodologies at hand (and applicable of course to a wide variety of data) can be found in Murtagh & Heck (1987). The codes of the algorithms are listed in this book and are also available on floppy disks.

Classification in itself has made significant progress over the past years, not only for dealing with spectra, but with objects and all kinds of data in general. Refer to the review paper by Kurtz (1983) and other contributions in the field gathered in Murtagh & Heck (1988). With new algorithms and new machines, astronomy is heading towards the challenge it will face with the huge accumulation of data expected for the next decades from space and ground instruments, ever more numerous, more powerful and more diversified.

ARTIFICIAL INTELLIGENCE TECHNIQUES

Because of the name, one should not be mistaken and consider – as in the first years of the computer age – artificial intelligence (AI) techniques as a panacea to be used as a black box for everything. One could simply say that applying AI, expert systems, or knowledge-based systems to astronomical problems is just programming by other means. AI techniques however emulate more closely the behaviour of human experts compare to traditional computing.

A compilation of what is done currently in astronomical AI has been published recently (Heck & Murtagh, 1989). Most of the chapters contain extensive bibliographies that can be used as reference for further reading. Refer also to the proceedings of the first dedicated meeting on AI techniques in astronomy held this Spring in Strasbourg (Heck, 1989).

Following the applications to IUE low-resolution stellar spectra described above, a *rule-based classifier* was devised (Rampazzo *et al.*, 1988) from a commercially avail-

able expert system shell. It required the development of a basic user interface and of a knowledge base, as well as tests on a set of well classified spectra. The system was linked to ESO's image processing system MIDAS, used for obtaining rough measurements of the spectral features necessary for the analysis.

Important justifications for using rule–based expert systems for classification purposes relate to the user interface, to the close relation between rules and physical interpretation, and to the facility offered by rules for expressing an expert's knowledge.

The user interface can always be modified as the system expands. Rules can also be meaningfully related to the physics involved in the problem under investigation. Knowledge capture may be problematic in the context of many expert–system designs, but was not too complex in this specific application to IUE spectra.

One can legitimately expect that systems will be *intelligent* enough to detect new classes and classification criteria to be added to the scheme residing in their knowledge base as they are fed with new data.

Ultimately it will be possible to build a procedure tackling all kind of data (continuous such as fluxes, binary such as presence or absence of lines, qualitative such as noise estimate, etc.) from various spectral regions, and even non–spectral information, in order to obtain the most general possible classification scheme of objects.

CONCLUSION

AI techniques are a logical further step in dealing with ever more sophisticated methodologies for spectral or object classification. The approach outlined in this paper can easily be extrapolated as a more genèral philosophy applicable to other fields and to the determination or refinement of other basic astrophysical quantities.

REFERENCES

Heck, A. 1987, UV stellar spectral classification, in *Scientific Accomplishments of the IUE*, eds. Y. Kondo *et al.*, D. Reidel Publ. Co., Dordrecht, 121–137

Heck, A. (ed.) 1989, *Artificial Intelligence Techniques for Astronomy*, Obs. Astron. Strasbourg, viii + 80p.

Heck, A., Egret, D., Jaschek, M. & Jaschek, C. 1984, *IUE Low-Resolution Spectra Reference Atlas - Part 1: Normal Stars*, European Space Agency Special Publication **ESA SP–1052**, 476p. + 34 plates

Heck, A., Egret, D., Nobelis, Ph. & Turlot, J.C. 1986, Statistical confirmation of the UV stellar spectral classification system based on IUE low–dispersion spectra, *Astrophys. Sp. Sc.* **120**, 223–237

Heck, A. & Murtagh, F. (eds.) 1989, *Knowledge–Based Systems in Astronomy*, Springer–Verlag, Heidelberg, iv + 280p.

Jaschek, M. & Jaschek, C. 1984, Classification of ultraviolet spectra, in *The MK Process and Stellar Classification*, ed. R.F. Garrison, David Dunlap Obs., Toronto, 290–301

Kurtz, M.J. 1983, Classification methods: an introductory survey, in *Statistical Methods in Astronomy*, ed. E. Rolfe, European Space Agency Special Publication **SP–201**, 47–58

Morgan, W.W. 1984, The MK system and the MK process, in *The MK Process and Stellar Classification*, ed. R.F. Garrison, David Dunlap Obs., Toronto, 18–23

Murtagh, F. & Heck, A. 1987, *Multivariate Data Analysis*, D. Reidel Publ. Co., Dordrecht, xvi + 210p.

Murtagh, F. & Heck, A. (eds.) 1988, *Astronomy from Large Databases – Scientific Objectives and Methodological Approaches*, ESO Conf. & Workshop Proc. **28**, xiv + 512p.

Rampazzo, R., Murtagh, F. & Heck, A. 1988, Classification of IUE spectra: a rule–based approach, *ESA Journal* **12**, 385–394

AUTHORS' ADDRESSES

Observatoire Astronomique, 11 rue de l'Université, F-67000 Strasbourg, France. (AH)

Space Telescope - European Coordinating Facility, European Southern Observatory, Karl-Schwarzschild-Straße 2, D-8046 Garching bei München, F.R. Germany. (FM)

(*) Affiliated to the Astrophysics Division, Space Science Department, European Space Agency.

List of participants

Dr. M.-C. Artru
Ecole Normale Supérieure de Lyon
46 Allée d'Italie, F-69364 LYON Cedex 07
France

Prof. B. Baschek
Institut für Theoretische Astrophysik
Im Neuenheimer Feld 561, D-6900 HEIDELBERG
W. Germany

Dr. S.R. Becker
Institut für Astronomie und Astrophysik
Scheinerstrasse 1, D-8000 MÜNCHEN 80
W.Germany

Dr. E. Biémont
Institut d'Astrophysique
Universite de Liège, B-4200 COINTE-LIEGE
Belgium

Dr. A. Bizzarri
Space Science Department
ESA/ESTEC, P.O. Box 299, 2200 AG NOORDWIJK
Netherlands

Prof. D.E. Blackwell
Department of Astrophysics
University of Oxford, South Parks Road,
OXFORD OX1 3RQ
U.K.

Dr. H. Blanke
Department of Physics
University of Kassel, KASSEL
W. Germany

Dr. P. Bonifacio
SISSA
Via Beirut 9, 34014 TRIESTE
Italy

Prof. P.W.J.M. Boumans
Philips Research Laboratories
P.O. Box 80.000, 5600 JA EINDHOVEN
Netherlands

Dr. J.H.M.J. Bruls
Sterrekundig Instituut
Postbus 80 000, 3508 TA UTRECHT
Netherlands

Dr. H.H. Bukow
Ruhr-Universität Bochum
Fakultät für Physik und Astronomie
Postfach 10 21 48, D-4630 BOCHUM 1
W. Germany

Prof. H. Butcher
Sterrenwacht Rijksuniversiteit Groningen
Mensingheweg 20, 9301 KA RODEN
Netherlands

Dr. K. Butler
Institut für Astronomie und Astrophysik
Universität München,
Scheinerstrasse 1, D-8000 MÜNCHEN 80
W. Germany

Dr. F. Castelli
Osservatorio Astronomico
Via G.B. Tiepolo 11, I-34131 TRIESTE
Italy

Prof. L.J. Curtis
Department of Physics and Astronomy
University of Toledo
2801 W. Bancroft Street, TOLEDO, Ohio 43606
U.S.A.

M.D. Davidson
Zeeman Laboratorium
Universiteit van Amsterdam
Plantage Muidergracht 4, 1018 TV AMSTERDAM
Netherlands

Dr. A. Dönszelmann
Zeeman Laboratorium
Universiteit van Amsterdam
Plantage Muidergracht 4, 1018 TV AMSTERDAM
Netherlands

Dr. W. Eissner
Department of Applied Mathematics and
Theoretical Physics
The Queen's University, BELFAST BT7 1NN
Northern Ireland

Prof. C. Froese Fischer
Vanderbilt University
Department of Computer Science
P.O. Box 1679 Station B, NASHVILLE, TN 37235
U.S.A.

Dr. M. Godefroid
Laboratoire de Chimie Physique Moléculaire
Université Libre de Bruxelles
Code Postal 160, B-1050 BRUXELLES
Belgium

Dr. W. Goldstein
L-45, Livermore National Laboratory
P.O. Box 808, LIVERMORE, Ca. 94550
U.S.A.

Dr. J.E. Hansen
Zeeman Laboratorium
Universiteit van Amsterdam
Plantage Muidergracht 4, 1018 TV AMSTERDAM
Netherlands

Dr. F. de Heer
FOM-Instituut voor Atoom- en Molecuulfysica
Kruislaan 407, 1098 SJ AMSTERDAM
Netherlands

Prof. A. Heck
Observatoire Astronomique
11, Rue de l'Université, F-67000 STRASBOURG
France

Dr. H.F. Henrichs
Sterrenkundig Instituut 'Anton Pannekoek'
Universiteit van Amsterdam
Roetersstraat 15, 1018 WB AMSTERDAM
Netherlands

Dr. A. Hibbert
Department of Applied Mathematics and Theoretical Physics
Queen's University of Belfast, BELFAST BT7 1NN
Northern Ireland

R. Hoekstra
K.V.I.
Rijksuniversiteit Groningen
Zernikelaan 25, 9747 AA GRONINGEN
Netherlands

G.J. van het Hof
Zeeman Laboratorium
Universiteit van Amsterdam
Plantage Muidergracht 4, 1018 TV AMSTERDAM
Netherlands

Dr. Se. Johansson
Fysiska Institutionen
Lunds Universitet
Sölvegatan 14, S-223 62 LUND
Sweden

Prof. C. Jordan
Department of Theoretical Physics
Oxford University
1 Keble Road, OXFORD OX1 3NP
U.K.

Dr. F.P. Keenan
Department of Pure and Applied Physics
Queen's University of Belfast, BELFAST BT7 1NN
Northern Ireland

Prof. P.F.A. Klinkenberg
Zeeman Laboratorium
Universiteit van Amsterdam
Plantage Muidergracht 4, 1018 TV AMSTERDAM
Netherlands

Prof. R.L. Kurucz
Smithsonian Astrophysical Observatory
60 Garden Street, CAMBRIDGE, MA 02138
U.S.A.

M. Landtman
Zeeman Laboratorium
Universiteit van Amsterdam
Plantage Muidergracht 4, 1018 TV AMSTERDAM
Netherlands

Dr. C. Laughlin
Department of Mathematics
The University of Nottingham,
NOTTINGHAM NG7 2RD
U.K.

Dr. R.C.M. Learner
Blackett Laboratory
Imperial College
Prince Consort Road, LONDON SW7 2BZ
U.K.

Dr. D.S. Leckrone
Code 681 NASA
Goddard Space Flight Center
GREENBELT, MD 20771
U.S.A.

Dr. U. Litzén
Physics Department
University of Lund
Sölvegatan 14, S-223 62 LUND
Sweden

Dr. T.M. Luke
Department of Applied Mathematics
University of Western Ontario
LONDON, Ontario N6A 5B9
Canada

Prof. I. Martinson
Fysiska Institutionen
Lunds Universitet
Sölvegatan 14, S-223 62 LUND
Sweden

Dr. C. Mendoza
IBM Venezuela Scientific Center
P.O. Box 64778, CARACAS 1060A
Venezuela

Dr. R. Mewe
Laboratorium voor Ruimteonderzoek
Beneluxlaan 21, 3527 HS UTRECHT
Netherlands

Dr. F.G. Meijer
Zeeman Laboratorium
Universiteit van Amsterdam
Plantage Muidergracht 4, 1018 TV AMSTERDAM
Netherlands

Prof. D.C. Morton
Herzberg Institute of Astrophysics
National Research Council
OTTAWA, Ontario K1A 0R6,
Canada

Dr. P. Nicolosi
Dipartimento di Elettronica e Informatica
Università di Padova
Via Gradenigo 6/A, 35131 PADOVA
Italy

A.E. Nilsson
Department of Physics
University of Lund
Sölvegatan 14, S-223 62 LUND
Sweden

Prof. E.H. Pinnington
Physics Department
University of Alberta
EDMONTON, Alberta, T6G 2J1
Canada

P. Quinet
Astrophysique et Spectroscopie
Université de l'Etat à Mons
Rue de la Halle 15, B-7000 MONS
Belgium

Dr. A.J.J. Raassen
Zeeman Laboratorium
Universiteit van Amsterdam
Plantage Muidergracht 4, 1018 TV AMSTERDAM
Netherlands

Dr. M. Rosa
ST-ECF
European Southern Observatory
Karl-Schwarzschildstrasse 2, D-8046 GARCHING
W. Germany

Dr. R.J. Rutten
Sterrekundig Instituut
Postbus 80 000, 3508 TA UTRECHT
Netherlands

Dr. H.E. Saraph
Department of Physics and Astronomy
University College London, LONDON WC1E 6BT
U.K.

Dr. I. Savanov
Crimea Astrophysics Observatory
p/o NAUCHNY, 334413 CRIMEA
U.S.S.R.

Dr. J. Schrijver
Laboratorium voor Ruimteonderzoek
Beneluxlaan 21, 3527 HS UTRECHT
Netherlands

Prof. M. J. Seaton
Department of Physics and Astronomy
University College London,
Gower Street, LONDON WC1E 6BT
U.K.

Dr. P. Selvelli
Osservatorio Astronomico di Trieste
Via Tiepolo 11, I-34131 TRIESTE
Italy

Dr. Y.-T. Shen
Zeeman Laboratorium
Universiteit van Amsterdam
Plantage Muidergracht 4, 1018 TV Amsterdam
Netherlands

Dr. C. Snoek
Zeeman Laboratorium
Universiteit van Amsterdam
Plantage Muidergracht 4, 1018 TV AMSTERDAM
Netherlands

Dr. J. Sugar
Plasma Spectroscopy
National Institute of Standards and Technology
Physics Building A-167, Gaithersburg, Md 20899
U.S.A.

Dr. H.P. Summers
JET Joint Undertaking
ABINGDON, Oxfordshire OX13 3EA
U.K.

Dr. K. T. Taylor
Department of Mathematics
Royal Holloway and Bedford New College
University of London
EGHAM, Surrey TW20 OEX
U.K.

Dr. A.P. Thorne
Blackett Laboratory
Imperial College
Prince Consort Road, London SW7 2BZ
U.K.

Dr. E. Träbert
Harvard College Observatory
Mail Stop 50
60, Garden Street, CAMBRIDGE. Ma. 02138
U.S.A.

Dr. P.H.M. Uylings
Zeeman Laboratorium
Universiteit van Amsterdam
Plantage Muidergracht 4, 1018 TV AMSTERDAM
Netherlands

N. Vaeck
Laboratoire de Chimie Physique Moléculaire
Université Libre de Bruxelles
Code Postal 160, B-1050 BRUXELLES
Belgium

A.A. van der Valk
Zeeman Laboratorium
Universiteit van Amsterdam
Plantage Muidergracht 4, 1018 TV AMSTERDAM
Netherlands

W.E. van der Veer
Zeeman Laboratorium
Universiteit van Amsterdam
Plantage Muidergracht 4, 1018 TV AMSTERDAM
Netherlands

Dr. P. van der Westhuizen
Department of Physics
University of Stellenbosch, STELLENBOSCH 7600
Republic of South Africa

Dr. M. Wilson
Physics Department
Royal Holloway and Bedford New College
University of London
EGHAM, Surrey TW20 OEX
U.K.

Dr. C.J. Zeippen
Observatoire de Paris
DAMAP
F-92190 MEUDON
France

Dr. G. Žukauskas
Institute of Physics
Lithuanian Academy of Sciences
Požela 54, 232600, VILNIUS
U.S.S.R.

Author index